LOCAL IMMUNE MODULATION OF MACROPHAGES AND DENDRITIC CELLS

EDITED BY: Felix Bock, Daniel Saban and Alexander Steinkasserer
PUBLISHED IN: Frontiers in Immunology

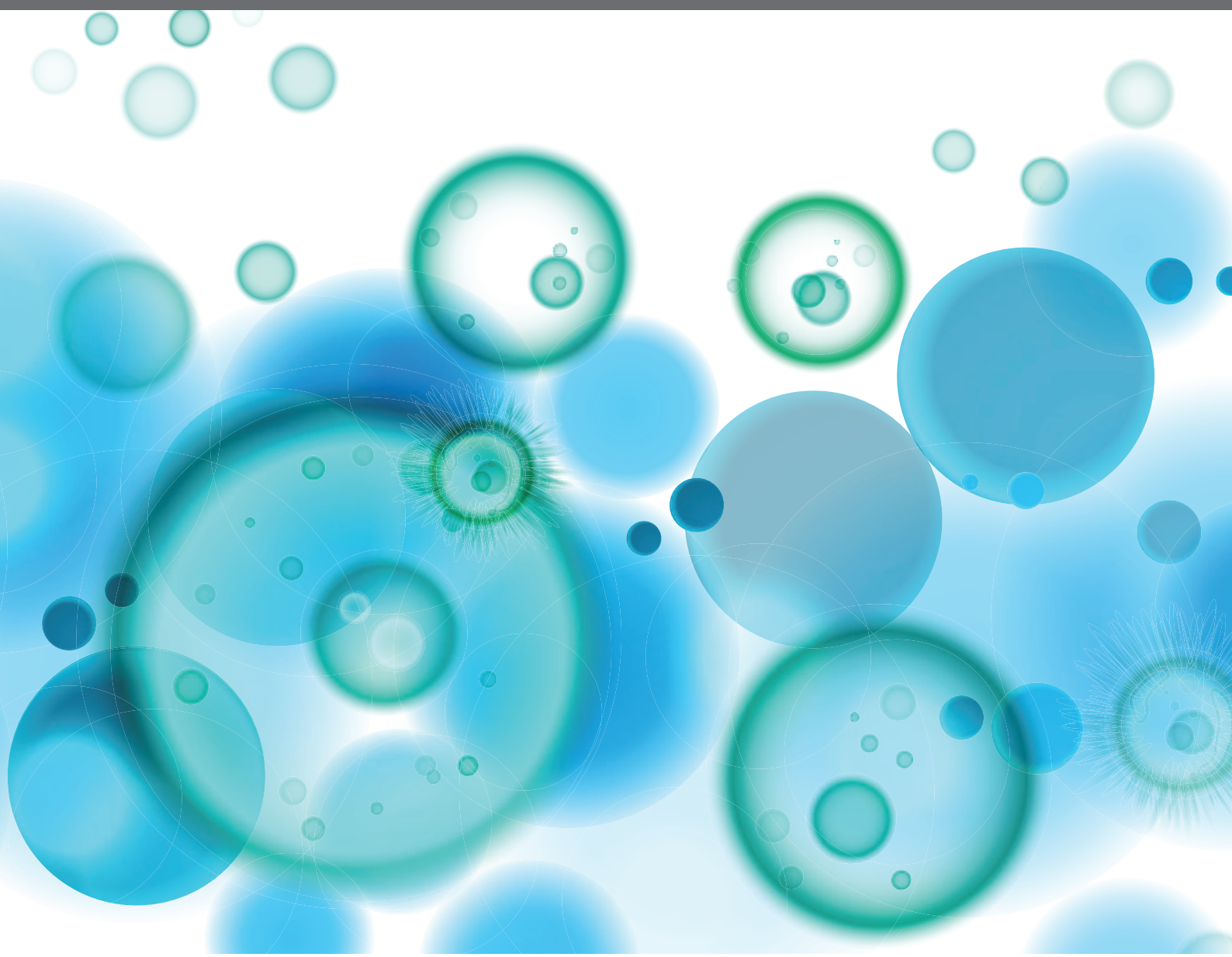

frontiers Research Topics

Frontiers eBook Copyright Statement

The copyright in the text of individual articles in this eBook is the property of their respective authors or their respective institutions or funders. The copyright in graphics and images within each article may be subject to copyright of other parties. In both cases this is subject to a license granted to Frontiers.

The compilation of articles constituting this eBook is the property of Frontiers.

Each article within this eBook, and the eBook itself, are published under the most recent version of the Creative Commons CC-BY licence. The version current at the date of publication of this eBook is CC-BY 4.0. If the CC-BY licence is updated, the licence granted by Frontiers is automatically updated to the new version.

When exercising any right under the CC-BY licence, Frontiers must be attributed as the original publisher of the article or eBook, as applicable.

Authors have the responsibility of ensuring that any graphics or other materials which are the property of others may be included in the CC-BY licence, but this should be checked before relying on the CC-BY licence to reproduce those materials. Any copyright notices relating to those materials must be complied with.

Copyright and source acknowledgement notices may not be removed and must be displayed in any copy, derivative work or partial copy which includes the elements in question.

All copyright, and all rights therein, are protected by national and international copyright laws. The above represents a summary only. For further information please read Frontiers' Conditions for Website Use and Copyright Statement, and the applicable CC-BY licence.

ISSN 1664-8714
ISBN 978-2-88976-615-4
DOI 10.3389/978-2-88976-615-4

About Frontiers

Frontiers is more than just an open-access publisher of scholarly articles: it is a pioneering approach to the world of academia, radically improving the way scholarly research is managed. The grand vision of Frontiers is a world where all people have an equal opportunity to seek, share and generate knowledge. Frontiers provides immediate and permanent online open access to all its publications, but this alone is not enough to realize our grand goals.

Frontiers Journal Series

The Frontiers Journal Series is a multi-tier and interdisciplinary set of open-access, online journals, promising a paradigm shift from the current review, selection and dissemination processes in academic publishing. All Frontiers journals are driven by researchers for researchers; therefore, they constitute a service to the scholarly community. At the same time, the Frontiers Journal Series operates on a revolutionary invention, the tiered publishing system, initially addressing specific communities of scholars, and gradually climbing up to broader public understanding, thus serving the interests of the lay society, too.

Dedication to Quality

Each Frontiers article is a landmark of the highest quality, thanks to genuinely collaborative interactions between authors and review editors, who include some of the world's best academicians. Research must be certified by peers before entering a stream of knowledge that may eventually reach the public - and shape society; therefore, Frontiers only applies the most rigorous and unbiased reviews.
Frontiers revolutionizes research publishing by freely delivering the most outstanding research, evaluated with no bias from both the academic and social point of view. By applying the most advanced information technologies, Frontiers is catapulting scholarly publishing into a new generation.

What are Frontiers Research Topics?

Frontiers Research Topics are very popular trademarks of the Frontiers Journals Series: they are collections of at least ten articles, all centered on a particular subject. With their unique mix of varied contributions from Original Research to Review Articles, Frontiers Research Topics unify the most influential researchers, the latest key findings and historical advances in a hot research area! Find out more on how to host your own Frontiers Research Topic or contribute to one as an author by contacting the Frontiers Editorial Office: frontiersin.org/about/contact

LOCAL IMMUNE MODULATION OF MACROPHAGES AND DENDRITIC CELLS

Topic Editors:
Felix Bock, Zentrum für Augenheilkunde, Uniklinik Köln, Germany
Daniel Saban, Duke University, United States
Alexander Steinkasserer, University Hospital Erlangen, Germany

Citation: Bock, F., Saban, D., Steinkasserer, A., eds. (2022). Local Immune Modulation of Macrophages and Dendritic Cells. Lausanne: Frontiers Media SA. doi: 10.3389/978-2-88976-615-4

Table of Contents

frontiers | Frontiers in Immunology

EDITORIAL
published: 27 June 2022
doi: 10.3389/fimmu.2022.957104

Editorial: Local Immune Modulation of Macrophages and Dendritic Cells - Local Matters

Felix Bock[1]*, *Daniel Saban*[2] *and Alexander Steinkasserer*[3]

[1] Department of Experimental Ophthalmology, University of Cologne, Cologne, Germany, [2] Department of Ophthalmology, Duke University, Durham, NC, United States, [3] Department of Immune Modulation, University Hospital Erlangen, Erlangen, Germany

Keywords: microenviroment, cornea, dendritic cells, macrophages, immune modulation, transplantation

Editorial on the Research Topic

Local Immune Modulation of Macrophages and Dendritic Cells

The microenvironment plays an important role in regulating immune reactions in many different diseases like ocular surface inflammation, autoimmune diseases or transplant immunology.

The eye is an example for a highly specialized microenvironment. As reviewed by Niederkorn and Taylor et al., in this Research Topic, the eye, is an immune privileged organ, which controls immune responses to injury or against pathogens very tightly to prevent irreversible damage in limited regenerative tissues, like the cornea or the retina. The maintenance of this immune privilege involves the regulation of macrophages and dendritic cells.

The ocular surface is the first frontline against environmental insults of the eye. Logeswaran et al., analyze in their study in depth the interplay between conjunctival goblet cells and dendritic cells. This study describes the micro–environmental interaction between tissue specific cells types and the immune system:goblet cells are mainly known as producers of the mucin layer of the ocular surface providing an adhesive ground for the aqueous phase of the tear film. Logeswaran et al., show that goblet cells furthermore can sense pathogens *via* the TLR 5 and subsequently locally suspend the immune regulation of adjacent dendritic cells by increasing the expression of IL6 and less activation of TGFβ.

The eye in general provides an ideal model to modulate the local immune system. Recently, it could be shown that the local application of the immune modulatory molecule sCD83, *via* preincubation of the corneal graft, induces a local as well as systemic shift of dendritic cells and macrophages towards tolerance (1).

The eye consists of macrophages from distinct ontogenies (2). Macrophages play a major role in the regulation of immune responses and therefore many contributions in this special issue focus on these cells. Hadrian et al. make a highly interesting comparison between the corneal and the skin regarding the contribution of macrophages in tissue vascularisation. Although both tissues constitute the outer barrier of our body, their properties are distinct. Both contain dendritic cells and macrophages, but whereas in the skin these cells are part of a dense vascular network, the cornea proper is free of blood and lymphatic vessels. Whereas in the skin macrophages are involved in the maintenance of the physiological blood and lymphatic vessels, corneal macrophages contribute heavily to the invasion of pathological blood and lymphatic vessels in certain inflammatory settings, but can also support the formation of lymphatic vessels only to drain corneal oedema. Therefore, the

OPEN ACCESS

Edited and reviewed by:
Florent Ginhoux,
*Singapore Immunology Network (A*STAR), Singapore*

***Correspondence:**
Felix Bock
felix.bock@uk-koeln.de

Specialty section:
This article was submitted to Antigen Presenting Cell Biology, a section of the journal Frontiers in Immunology

Received: *30 May 2022*
Accepted: *10 June 2022*
Published: *27 June 2022*

Citation:
Bock F, Saban D and Steinkasserer A (2022) Editorial: Local Immune Modulation of Macrophages and Dendritic Cells - Local Matters. Front. Immunol. 13:957104. doi: 10.3389/fimmu.2022.957104

macrophages change their M1-like phenotype into M2-like phenotype with an increased expression of VEGF-C, a pro-lymphangiogenic growth factor.

The polarization of macrophages plays also an important role in other parts of the nervous system. Muhammad et al. describe in this issue how vascular macrophages contribute to formation and rupture of intracranial aneurysm (ICA). Highly interesting, also for other disciplines, is the overview of experimental M2-like polarizing agents. Our group observed recently, that a local blockade of VEGF-A in the inflamed cornea prior to transplantation increases the expression of macrophage attracting cytokines like Rantes, MCP-1, MIP-1α, MIP-1β, or GM-CSF in the corneal microenvironment (3). In the review from Muhammad et al. inhibitors such as MCP-1 are shown to reduce ICA. So, therapeutic polarization of macrophages might be a promising strategy, not only for aneurysm, but also for inflammatory or chronic diseases of the cornea, retina or skin.

Modulation of macrophage activity is not only a strategy to dampen overshooting immune responses but is also a well-known escape strategy of pathogens, e.g. *Leishmania*. Frick et al., show that not only tumors but also *Leishmania* can create an acidic microenvironment to suppress NO production and thereby the leishmanicidal activity of macrophages. Leishmaniasis can also involve the eye – the so called ocular leishmaniasis – and can cause severe damage to the ocular tissue, like corneal melting or uveitis. Other pathogens, like *Pseudomonas aeruginosa*, where recently shown to modulate the local immune response, by e.g. inducing the production of CGRP by neurons inhibiting the bactericidal activity of neutrophils (4). However, pathogens not only induce immunosuppression but also induce effective defence mechanisms. Du et al., decipher such an antibacterial mechanism induced by *Staphylococcus aureus* (*S. aureus*) in macrophages. They show how *S. aureus* induced expression of activating transcription factor 3 (ATF3) in macrophages modifies the actin-filament and thereby the motility of macrophages, resulting in an effective recruitment of antibacterial macrophages to the site of infection. In other studies ATF3 was shown to negatively regulate the activation of *NFκB* and thereby functioning as an immune regulatory factor (5). This shows how important the micro-environmental context is for shaping the local immune response.

Dendritic cells are also highly involved in local immune responses since they surveil the tissue environment. Thereby, DCs can be divided into different subtypes as described by Hongo et al. They herein described that cells from the cDC1 subtype play a role in the protection against post-ischemic acute kidney injury, a phenomenon often observed after kidney transplantation. Li et al. show that the loss of the CD1c subtype in the kidney leads to an increased Th1 response. This work demonstrates how the microenvironment is fine-tuned to avoid overshooting immune responses and on the other hand to protect from massive damage. We could recently show that the migration of dendritic cells, from the graft into lymphatic vessels, is regulated by ALCAM and how local blockade of ALCAM can inhibit this migration and consequently improve graft survival (6). Also here, fine tuning of the microenvironment could change the immune response.

In conclusion, this Research Topic demonstrates how complex local immune responses are regulated and offers a great platform to share our knowledge in respect to the immunological microenvironment on an interdisciplinary level. New therapeutic ideas as well as hypotheses will hopefully arise from the contributions of different disciplines mentioned above.

AUTHOR CONTRIBUTIONS

FB draft and wrote the paper. DS revised and wrote the paper. AS revised and wrote the paper. All authors contributed to the article and approved the submitted version.

REFERENCES

1. Peckert-Maier K, Schonberg A, Wild AB, Royzman D, Braun G, Stich L, et al. Pre-Incubation of Corneal Donor Tissue With Scd83 Improves Graft Survival *via* the Induction of Alternatively Activated Macrophages and Tolerogenic Dendritic Cells. *Am J Transplant* (2022) 22(2):438–54. doi: 10.1111/ajt.16824
2. O'Koren EG, Yu C, Klingeborn M, Wong AYW, Prigge CL, Mathew R, et al. Microglial Function Is Distinct in Different Anatomical Locations During Retinal Homeostasis and Degeneration. *Immunity* (2019) 50(3):723–37 e7. doi: 10.1016/j.immuni.2019.02.007
3. Salabarria AC, Braun G, Heykants M, Koch M, Reuten R, Mahabir E, et al. Local VEGF-A Blockade Modulates the Microenvironment of the Corneal Graft Bed. *Am J Transplant* (2019) 19(9):2446–56. doi: 10.1111/ajt.15331
4. Lin T, Quellier D, Lamb J, Voisin T, Baral P, Bock F, et al. Pseudomonas Aeruginosa-Induced Nociceptor Activation Increases Susceptibility to Infection. *PloS Pathog* (2021) 17(5):e1009557. doi: 10.1371/journal.ppat.1009557
5. Jadhav K, Zhang Y. Activating Transcription Factor 3 in Immune Response and Metabolic Regulation. *Liver Res* (2017) 1(2):96–102. doi: 10.1016/j.livres.2017.08.001
6. Willrodt AH, Salabarria AC, Schineis P, Ignatova D, Hunter MC, Vranova M, et al. ALCAM Mediates DC Migration Through Afferent Lymphatics and Promotes Allospecific Immune Reactions. *Front Immunol* (2019) 10:759. doi: 10.3389/fimmu.2019.00759

Conflict of Interest: The authors declare that the research was conducted in the absence of any commercial or financial relationships that could be construed as a potential conflict of interest.

Publisher's Note: All claims expressed in this article are solely those of the authors and do not necessarily represent those of their affiliated organizations, or those of the publisher, the editors and the reviewers. Any product that may be evaluated in this article, or claim that may be made by its manufacturer, is not guaranteed or endorsed by the publisher.

Copyright © 2022 Bock, Saban and Steinkasserer. This is an open-access article distributed under the terms of the Creative Commons Attribution License (CC BY). The use, distribution or reproduction in other forums is permitted, provided the original author(s) and the copyright owner(s) are credited and that the original publication in this journal is cited, in accordance with accepted academic practice. No use, distribution or reproduction is permitted which does not comply with these terms.

frontiers in Immunology

MINI REVIEW
published: 08 March 2021
doi: 10.3389/fimmu.2021.630381

Vascular Macrophages as Therapeutic Targets to Treat Intracranial Aneurysms

Sajjad Muhammad[1,2,3], Shafqat Rasul Chaudhry[4], Gergana Dobreva[3], Michael T. Lawton[5], Mika Niemelä[2] and Daniel Hänggi[1]*

[1] Department of Neurosurgery, Faculty of Medicine, Heinrich-Heine-University, Düsseldorf, Germany, [2] Department of Neurosurgery, Helsinki University Hospital, University of Helsinki, Helsinki, Finland, [3] Department of Anatomy and Developmental Biology, Medical Faculty Mannheim and European Center for Angioscience (ECAS), University of Heidelberg, Mannheim, Germany, [4] Shifa College of Pharmaceutical Sciences, Shifa Tameer-e-Millat University, Islamabad, Pakistan, [5] Department of Neurosurgery, Barrow Brain and Spine, Barrow Neurological Institute, Phoenix, AZ, United States

Aneurysmal subarachnoid hemorrhage (aSAH) is a highly fatal and morbid type of hemorrhagic strokes. Intracranial aneurysms (ICAs) rupture cause subarachnoid hemorrhage. ICAs formation, growth and rupture involves cellular and molecular inflammation. Macrophages orchestrate inflammation in the wall of ICAs. Macrophages generally polarize either into classical inflammatory (M1) or alternatively-activated anti-inflammatory (M2)-phenotype. Macrophage infiltration and polarization toward M1-phenotype increases the risk of aneurysm rupture. Strategies that deplete, inhibit infiltration, ameliorate macrophage inflammation or polarize to M2-type protect against ICAs rupture. However, clinical translational data is still lacking. This review summarizes the contribution of macrophage led inflammation in the aneurysm wall and discuss pharmacological strategies to modulate the macrophageal response during ICAs formation and rupture.

Keywords: intracranial aneurysms, monocytes, macrophages, inflammation, subarachnoid hemorrhage, stroke, macrophage polarization

OPEN ACCESS

Edited by:
Alexander Steinkasserer, University Hospital Erlangen, Germany

Reviewed by:
Angel L. Corbi, Consejo Superior de Investigaciones Científicas (CSIC), Spain
Osamu Takeuchi, Kyoto University, Japan

****Correspondence:***
Sajjad Muhammad
sajjad.muhammad@med.uni-duesseldorf.de

Specialty section:
This article was submitted to Antigen Presenting Cell Biology, a section of the journal Frontiers in Immunology

Received: *17 November 2020*
Accepted: *11 January 2021*
Published: *08 March 2021*

Citation:
Muhammad S, Chaudhry SR, Dobreva G, Lawton MT, Niemelä M and Hänggi D (2021) Vascular Macrophages as Therapeutic Targets to Treat Intracranial Aneurysms. Front. Immunol. 12:630381. doi: 10.3389/fimmu.2021.630381

INTRODUCTION

Aneurysmal subarachnoid hemorrhage (aSAH) is a devastating subtype of hemorrhagic strokes and it accounts for 5% of all strokes. The worldwide incidence of aSAH is approximately 700000 person-years; the mortality of aSAH is approximately 40% despite appropriate surgical and medical care (1, 2). aSAH has a poor prognosis with significant lifelong morbidity and cognitive deficits for those who survive. Moreover, aSAH has a significant impact on society, as it often affects young people at the peak of their productive life (1, 2). This highly fatal and morbid type of intracranial hemorrhage is due to intracranial aneurysm (ICA) rupture in nearly 85% of SAH cases (3).

ICAs are weak ballooning, bulging, or abnormal dilatations that tend to form at arterial bifurcations due to chronic hemodynamic stress and inflammation (4). Intracranial aneurysms are usually found in 3% to 5% of the population and are slightly more prevalent among females (5).

The risk factors for aneurysm development are arterial hypertension, smoking, chronic alcohol consumption, aging, female gender, and family history of aSAH in first-degree relatives (6). Some genetic disorders such as autosomal dominant polycystic kidney disease, Marfan syndrome, Ehlers-Danlos syndrome type IV, neurofibromatosis type 1, and fibromuscular dysplasia are associated with ICA formation (6). Moreover, single nucleotide gene polymorphisms (SNPs) in or near the genes *CDKN2B-AS1*, *SOX17* transcription regulator gene, endothelin receptor gene, *HDAC9*, and the gene encoding elastin have been revealed in genome-wide association studies (GWAS). Linkage analysis suggests that these genes are strongly associated with intracranial aneurysms (5). An exome-wide association study identified a SNP of the collagen type XVIIα1 chain gene to be significantly associated with aSAH (7). Most ICAs are found incidentally and need preventive care to prevent enlargement and rupture. Prevention of growth and rupture is necessary, as the current treatment modalities, such as surgical clipping and endovascular modalities (coiling, with or without stent and flow diverter placement) are associated with some risks.

Patient factors (age, sex, comorbidities, family history, previous history of SAH, hypertension and smoking) and aneurysm characteristics (size, location, wall irregularity, presence of secondary pouches) are key factors that aid in deciding upon treatment for an unruptured ICA. It is challenging to predict exactly the rupture risk based on aneurysm characteristics and patient risk factors. It is thus, unclear which ICAs require active treatment.

A better understanding of the pathobiology of ICA is important to clarify when active treatment is needed and may facilitate development of pharmacological treatments with no or minimal risk.

Recent evidence from human and animal studies revealed that macrophage-mediated cellular and molecular inflammation is the key player in aneurysm formation and rupture. Here, we briefly review the current knowledge on the role of macrophages in aneurysm formation and their rupture.

INFLAMMATION IN INTRACRANIAL ANEURYSMS

The hallmarks of ICAs include endothelial cell dysfunction, smooth muscle cell phenotypic switch, matrix metalloproteinase secretion, and innate immune cell activation leading to vascular remodeling and vessel wall weakening (8–10). Histopathological analysis of aneurysm wall biopsies has revealed an upregulation of inflammatory mediators, disruption of lamina elastic interna, and thinning of media including mural cell death (11). Both cellular and molecular inflammation are crucial in aneurysm formation and rupture. Infiltration of inflammatory cells (especially macrophages) has been observed in the biopsies of ICAs, which shows a possible involvement of macrophages in aneurysm formation. NF-κB is a key transcription factor and is a major known regulator of important pro-inflammatory genes, including TNF, IL-1β, and COX-2. A genetic deletion of NF-κB has been shown to reduce ICA formation and growth (12). Moreover, pro-inflammatory genes regulated by NF-κB, including IL-1β (13), COX-2 (14), iNOS (15), and matrix metalloproteinase-9 (16) contribute to ICA formation. Furthermore, macrophage specific deletion of the prostaglandin E (PGE) receptor subtype 2 (EP2) (Ptger2), an upstream signaling receptor for NF-κB activation, significantly suppresses the development of ICAs in mice, indicating that prostaglandin E2-EP2-NF-κB signaling in macrophages plays a crucial role in ICA development (12). Intriguingly, macrophage-specific expression of a variant of IκBα, which abrogates the translocation of NF-κB, prevents ICA formation (17).

Transcriptomic analysis of ICAs revealed upregulation of pro-inflammatory cytokine genes associated with leukocyte infiltration (18–23). For instance, Nakaoka, Tajima (19) have shown an upregulation of genes related to inflammation, immune response and phagocytosis, whereas anti-inflammatory genes were downregulated. Similarly, upregulation of TNF-α and pro-apoptotic gene expression was shown along with suppressed IL-10 expression in ruptured ICAs. Moreover, SNPs in the IL-10 gene are associated with formation of ICAs (24, 25). Similar, transcriptomic and bioinformatic analyses of ruptured and unruptured ICAs have revealed enhanced expression and upregulation of inflammatory pathways such as TLR signaling, cytokine-cytokine receptor interaction, leukocyte trans-endothelial migration, NF-κB signaling, and many other inflammation-related gene ontology categories (18). Activation and involvement of the complement system has also been observed in ICAs and suggests that chronic inflammation underlies the pathogenesis of ICAs (10, 26). Further, shear stress due to disturbed blood flow at arterial branching points (which contributes to ICA development) upregulates inflammatory pathways such as NF-κB, promotes monocyte recruitment, and triggers sterile inflammation (27, 28). Inflammation in ICA walls is characterized by immune cell infiltration and altered composition of the immune cell populations such as natural killer cells, mast cells, lymphocytes, and importantly macrophages (29).

MONOCYTES/MACROPHAGES IN INTRACRANIAL ANEURYSMS

Monocytes/macrophages are among the main components of innate immunity and represent important members of the mononuclear phagocyte system comprised of myeloid-derived cells (30). Data from human and animal studies has revealed an increased infiltration of immune cells in the aneurysm wall (24, 25, 31, 32). Several lines of evidence have shown increased infiltration of T and B lymphocytes and macrophages along with increased pro-inflammatory molecular expression in clinical resections of ICAs (24, 31, 32).

Studies have clearly demonstrated that monocyte/macrophage infiltration in the wall of ruptured aneurysms is not only found

after aneurysmal rupture, but contributes to aneurysm formation and rupture (33). Increased monocyte/macrophage marker CD68 expression has been observed in mice carrying negative mutations of PPARγ in smooth muscle cells of cerebral arteries along with CXCL1, MCP-1, TNF-α expression upregulation. These mice have an increased incidence of aneurysm formation and rupture (34). Aoki, Frösen (12) demonstrated that macrophage infiltration driven by MCP-1 and activation of NF-κB involving PGE_2-PGEP2 (PGE receptor subtype 2) signaling in the macrophages of arterial wall leads to aneurysm formation, suggesting that inflammation is not only present after aneurysm rupture, but also drives aneurysm formation. As intracranial arteries lack vasa vasorum in the arterial wall, the macrophages may infiltrate through endothelial cell junctions. Sphingosine-1-phosphate (S1P) receptor type 1 signaling activation strengthens the endothelial barrier. Interestingly, activation of S1P receptor type 1 reduced the number of infiltrated macrophages and enlargement of ICAs (35).

MACROPHAGE POLARIZATION AND INTRACRANIAL ANEURYSMS

Mills, Kincaid (36) described for the first time the M1/M2 paradigm, where M1 represents classically activated pro-inflammatory monocytes/macrophages, whereas M2 represents alternatively activated anti-inflammatory monocytes/macrophages. A very brief and simplistic overview of M1/M2 biology is represented in **Figure 1**. However, there is a considerable heterogeneity in macrophage phenotypes and several subtypes have been described such as M1, M2a, M2b, M2c, M2d, Mhem, Mox, M4 (37–40). This over simplistic representation of M1 as pro-inflammatory and M2 as anti-inflammatory macrophages is considered here to recognize different functional states of these polarized phenotypes to assign pro-inflammatory and anti-inflammatory role. Macrophage polarization has implications in aneurysm formation and rupture (**Figure 2**). Aortic aneurysms formation has been shown to be promoted by inflammatory M1

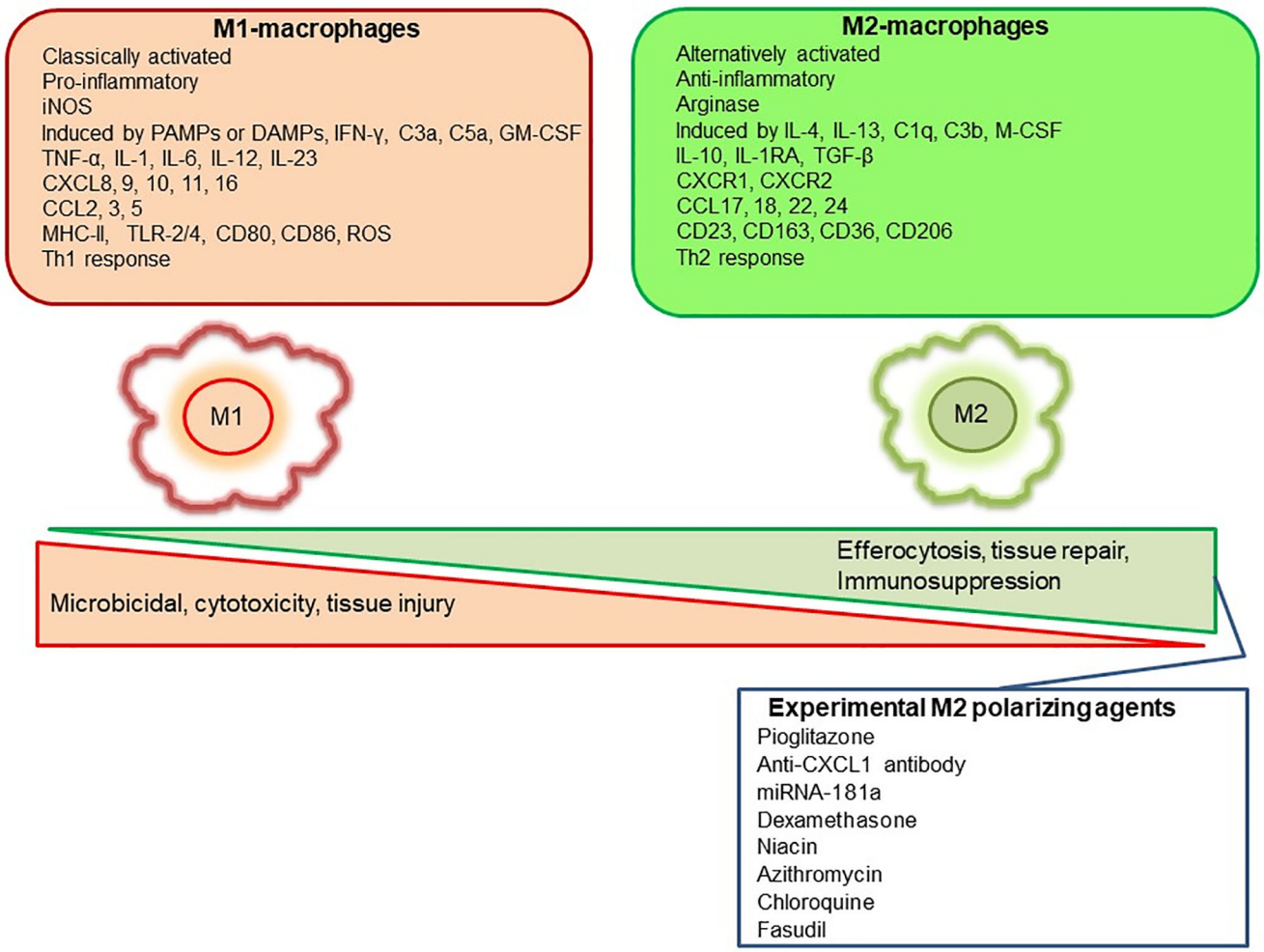

FIGURE 1 | Representation of M1 and M2 distinguishing features and some of the pharmacological agents employed experimentally to polarize macrophages to M2-anti-inflammatory subtype.

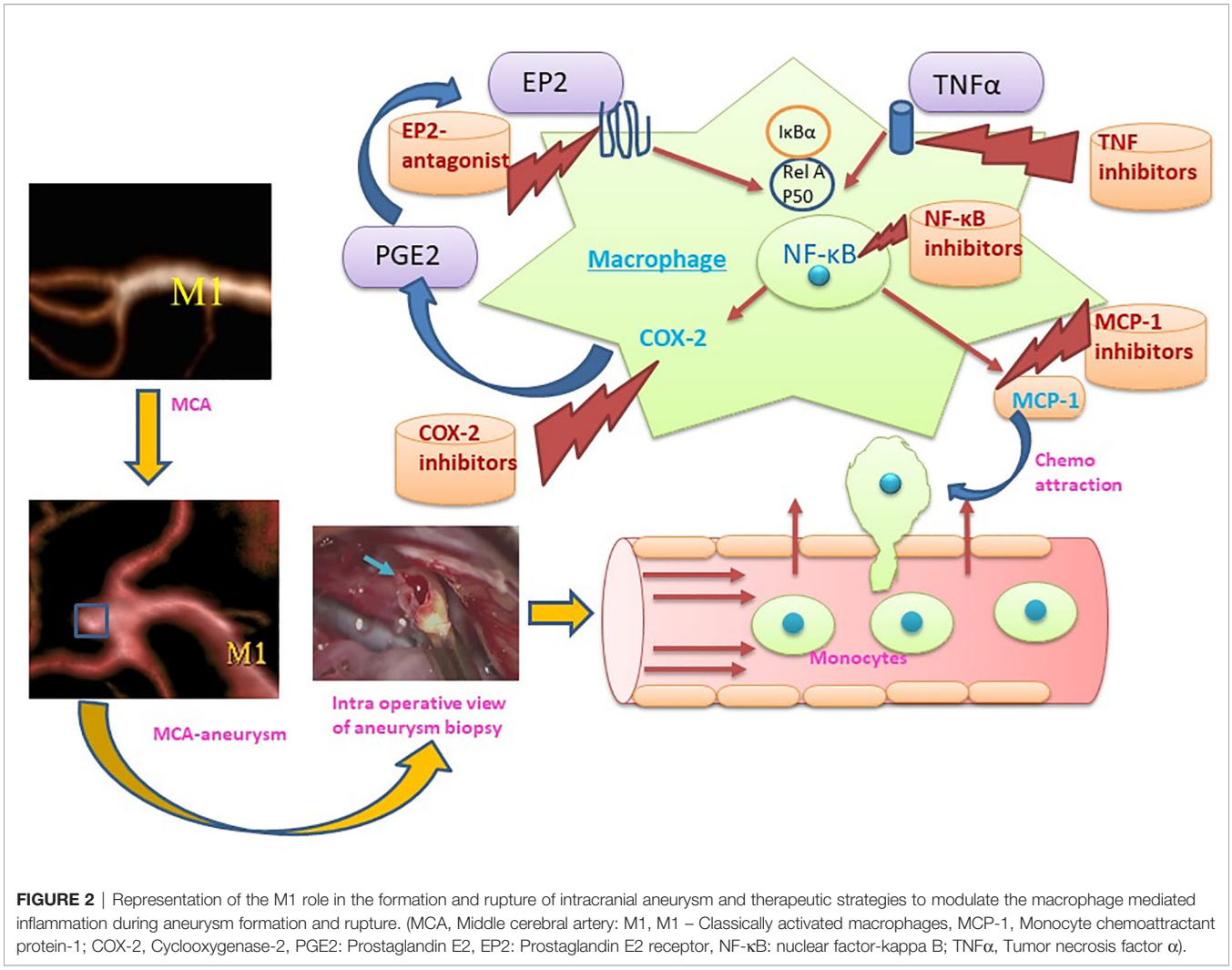

FIGURE 2 | Representation of the M1 role in the formation and rupture of intracranial aneurysm and therapeutic strategies to modulate the macrophage mediated inflammation during aneurysm formation and rupture. (MCA, Middle cerebral artery: M1, M1 – Classically activated macrophages, MCP-1, Monocyte chemoattractant protein-1; COX-2, Cyclooxygenase-2, PGE2: Prostaglandin E2, EP2: Prostaglandin E2 receptor, NF-κB: nuclear factor-kappa B; TNFα, Tumor necrosis factor α).

macrophages, whereas reparative M2 polarization prevents the formation, development and progression of aortic aneurysms (38, 41). It has been shown that GM-CSF contributes toward M1 polarization and M-CSF favors an M2 response (42). Intriguingly, GM-CSF has been shown to promote aortic aneurysm formation (43) and the levels of GM-CSF measured in plasma and lumen of the intracranial aneurysms have also shown a direct correlation with the size of intracranial aneurysms, highlighting a common inflammatory process upregulated by M1 macrophages underlie the development of both aortic and intracranial aneurysms (44). Consequently, immunohistochemical analysis of intracranial aneurysm dome resections have revealed that ruptured intracranial aneurysms from patients possess increased M1 (HLA-DR$^+$) cells opposed to M2 (CD163$^+$) cells (45). These findings suggest that a balance shift toward M2 may prevent aneurysm rupture. Previously, Froesen and colleagues demonstrated differences in CD68+ and CD163+ macrophages in human ruptured and unruptured ICAs (29). Intriguingly, CD68+ and CD163+ (hemoglobin-haptoglobin scavenger receptor) macrophages, mostly HLA-DR-, co-localize with glycophorin A (a component of the erythrocyte membrane) and infiltrate ICAs as a response to a luminal thrombus trapped and lysed erythrocytes, and may promote degenerative arterial wall remodeling (46). In a mouse model of ICAs, M1 (F4/80+ iNOS+) dominate over M2 (F4/80+ Arg1+) during aneurysm development (47). Interestingly, M1 dominance leading to aneurysm development is dependent on neutrophil infiltration, which when blocked led to an increased M2 polarization with reduced aneurysm formation (47). Shimada, Furukawa (48) employed different macrophage markers to assess the polarization of macrophages in ICAs. The authors employed CD68 as a macrophage marker and IL-12p40 and CD206 as M1 and M2 markers, respectively. They observed significant impairment in the M1/M2 ratio in ICAs associated with upregulation of M1-related gene expression (48).

MACROPHAGE MODULATION AS A TREATMENT STRATEGY FOR INTRACRANIAL ANEURYSMS

Recent case-control studies have shown that the use of statins and non-steroidal anti-inflammatory drugs (NSAIDs) is

inversely associated with SAH by affecting rupture of ICAs (49–52), supporting the notion that rupture of ICAs can be prevented by pharmacological therapy.

Aspirin protects against ICA rupture through modulation of inflammatory pathways (COX-2 and microsomal PGE_2 synthase-1 inhibition) and macrophage burden in ICAs (53–55). A prospective cohort study revealed that usage of atorvastatin in secondary prevention for ischemic stroke increases the incidence of hemorrhagic stroke (hazard ratio 1.66) (29). Therefore, statin usage to prevent aneurysm rupture should be approached with caution. Due to hemorrhagic diathesis by the antiplatelet effect, the use of NSAIDs as a pre-emptive medication to prevent SAH also requires caution. Thus, drugs with highly specific targets with minimal or no side effects should be explored for long-term prophylaxis.

Given the fact that macrophages are key players in orchestrating the inflammatory response during ICA formation and rupture, they may represent vital therapeutic targets to modulate and inhibit inflammation (48). Multiple targets at the level of macrophages and macrophage-mediated inflammation have been explored recently (**Figure 2**). Inhibition of a key chemoattractant molecule, monocyte chemotactic protein-1 (MCP-1) and depletion of macrophages are associated with reduced ICAs in animal models (8, 33) demonstrating that reducing macrophage burden with both strategies effectively prevented aneurysm formation and rupture. In contrast, CXCL1 (neutrophil chemoattractant) blockade reduced neutrophil infiltration and prevented aneurysm formation without modifying the macrophage burden in a mouse model of ICAs (47), which suggests that other molecular and cellular mechanisms may be involved. Interestingly, inhibition of neutrophil infiltration with CXCL1 inhibition is associated with a shift toward M2 macrophages from a M1 phenotype (47). Activation of PPARγ by Pioglitazone has also been shown to effectively reduce the rupture of ICAs through a reduction in infiltrating macrophages and the M1/M2 ratio (48). Clodronate liposome-mediated depletion of macrophages also reduced the rupture of ICAs similar to that shown with pioglitazone, which was associated with a decrease in M1-phenotype related gene expression (48).

In addition to cellular targets, molecular targets have also been successful in experimental models. Anagliptin, a dipeptidyl peptidase-4 inhibitor, suppresses ICA growth through inhibition of macrophage infiltration and activation *via* ERK-5-mediated suppression of NF-κB (56). Moreover, Eplerenone, a mineralocorticoid receptor blocker, has been shown to reduce ICA formation, in part *via* reduction in MCP-1, MMP-9 expression and CD68+ macrophage infiltration in a rat model of ICAs (57). A pilot clinical study showed the beneficial effects of Eplerenone in preventing growth and rupture of ICAs (58). Employment of NF-κB p50 decoy oligodeoxynucleotide (ODN) has been shown to downregulate the expression of macrophage related inflammatory genes and reduced macrophage infiltration with a decline in ICAs growth in a rat model (59). Nifedipine, the drug known to be associated with better outcomes after aSAH, has been shown to prevent the enlargement and degenerative ICAs wall changes through reduced macrophage infiltration, MCP-1, and MMP-2 expression probably by modulating the DNA binding capacity of NF-κB (60).

Macrophage polarization as a therapeutic venture has been studied across various disease models. For instance, tumor associated macrophages (TAMs) represent primarily M2 like macrophages promoting tumors and their polarization toward M1 phenotype through the application of various agents such as CSF-1R inhibitor BLZ945, anti-CSF-1 mAb, Zoledronic acid, Histidine-rich glycoprotein, Hydrazinocurcumin, vadimezan (5,6-dimethylxanthenone-4-acetic acid; DMXAA), flavone glycoside Baicalin, IL10R mAb, CD40 mAb, corosolic acid, N-(2-hydroxy acetophenone) glycinate (CuNG), imiquimod, etc. have been investigated as potential tumoricidal drugs (61, 62). Interestingly, certain pieces of evidence support the antagonism of M-CSF as a beneficial tumor therapy leading to M1 polarization of macrophages from M2 tumor associated macrophage phenotype (42). Similarly, in rheumatoid arthritis with a predominance of M1 response, an opposite approach polarizing macrophages from M1 to M2 type has been shown to reduce inflammation and disease severity (63). Several M1 to M2 polarizing agents such as gene therapy by using IL-10 DNA plasmid incorporated in nanoparticles carrying tuftsin protein to target synovial tissue macrophages, Withaferin-A incorporated in manosylated liposomes, paeoniflorin-6′-O-benzene sulfonate (CP-25), sSiglec-9, fucose/galactose analog 2-D-gal and JWH133 have been shown to reduce disease severity in experimental arthritis models and polarize macrophages to anti-inflammatory M2 type (63). Similar, approaches to modulate macrophage polarization from M1 to M2 may prevent the rupture of ICAs. For instance, molecular genetic approaches leading to polarization toward M2 macrophages using miRNAs such as miRNA-181a (64) could be of great potential. Aptamer based enrichment of M2 polarized macrophages in ICAs may also be developed (65). Epigenetic control of macrophage polarization could also be exploited to abrogate the chronic inflammation leading to ICAs formation (66). Egress of macrophages may also be promoted to decrease macrophage burden (67). Berberine, an alkaloid from *Coptis chinensis*, has been shown to inhibit macrophage activation and infiltration in ICAs by modulation of the phospho-focal adhesion kinase (pFAK)/Grp78/unfolded protein response signaling pathway and reduced the elaboration of inflammatory factors from macrophages such as MCP-1, IL-1β, IL-6, TNF-α, and MMPs (68). Intriguingly, cutaneous non-invasive vagus nerve stimulation has been shown to reduce aneurysm rupture rates and improve outcomes after aneurysm rupture, and may implicate reduced MMP-9 expression as a potential mechanism of action (69). Suppression of MMP-9 expression in macrophages and polarization of macrophages/microglia to the M2 phenotype has already been shown to stem from vagus nerve stimulation-mediated modulation of inflammatory pathways (69, 70). Taken together, there are multiple strategies at the level of inflammation and macrophage modulation that have translational potential in human disease. However, the heterogeneity and the complexity of macrophageal response

TABLE 1 | A brief summary of macrophage modulation studies for prevention of intracranial aneurysms (ICAs) formation and rupture.

Study Type	Model	Intervention	Macrophage markers	Main Findings	References
Clinical	–	No intervention	CD68+, CD163+, HLA-DR+	CD68+, CD163+, HLA-DR- macrophages infiltrate ICAs and correlate with GPA[f], loss of α-SMA, wall degeneration, rupture	Ollikainen et al. (46)
Clinical	–	No intervention	CD68+, CD163+, CD11b+	CD68+, CD163+, CD11b+ macrophages increased in ruptured than unruptured ICAs	Froesen et al. (29)
Clinical	–	No intervention	HLA-DR+ (M1), CD163+ (M2)	M1 macrophages were dominant compared to M2 macrophages in ruptured ICAs	Hasan et al. (45)
Clinical	–	ferumoxytol enhanced MRI	CD68+	Increased macrophage infiltration in ICAs wall assessed by enhanced uptake of ferumoxytol and CD68+ expression	Hasan et al. (45)
Clinical	–	Aspirin 81 mg for 3 months, ferumoxytol enhanced MRI		Decreased inflammation in ICAs due to macrophages with daily intake of Aspirin	Hasan et al. (54)
Preclinical	C57BL/6J mice, Elastase & Ang.II[g] induced HTN[c]	Clodronate MCP-1 KO[a], MMP-12 KO	CD68+	Increased CD68+ macrophage infiltration in ICAs, macrophage depletion and MCP-1 KO reduced ICAs formation	Kanematsu et al. (33)
Preclinical	Male Sprague Dawley rats, left internal carotid artery ligation, elastase and high salt diet	Berberine 200mg/kg/d for 35 days	CD68+	CD68+ macrophages infiltration in ICAs was decreased by berberine through suppressed expression of MMP-9 and secretion of MCP-1, IL-1β, TNF-α, and IL-6 *via* down regulation of pFAK/Grp78/UPR signaling pathway	Quan et al. (68)
Preclinical	C57BL/6J mice, ligation of left CCA and right renal artery, Ang. II, elastase, 8% NaCl, 0.12% β-aminopropionitrile	anti-CXCL1/GRO-α/KC/CINC-1 antibody	F4/80+, iNOS + (M1), Arg1+ (M2)	M1/M2 ratio increased in ICAs formation over time, CXCL1 blocked of neutrophils shifted the polarization toward M2 macrophages and reduced aneurysm formation	Nowicki et al. (47)
Preclinical	Deoxycorticosterone acetate-salt HTN, elastase	Pioglitazone 10 mg/kg/d[b], GW9662 2 mg/kg/d for 3 weeks, macrophage PPRγKO, clodronate liposome depletion of macrophages	CD68+, IL-12 p40 (M1), CD206 (M2), CD36	Pioglitazone reduced the incidence and rupture of ICAs *via* reduced infiltration of M1 and M1/M2 ratio in cerebral arteries. Pioglitazone effect was lost in macrophage specific PPRγKO. Pioglitazone also reduced expression of MCP-1, IL-1 and IL-6.	Shimada et al. (48)
Preclinical	Male Sprague Dawley rats, left renal and common carotid arteries ligation, 8% sodium chloride and 0.12% 3-aminopropionitrile,	Anagliptin 300 mg/kg	Iba-1+, MCP-1+	Anagliptin prevented the growth of ICAs, inhibited the infiltration and activation of macrophages through reduced MCP-1 expression and suppressed p65 phosphorylation through ERK5 activation.	Ikedo et al. (56)
Preclinical	Female Sprague-Dawley rats, Ligation of right common carotid artery and renal artery, 1% saline administration and bilateral oophorectomy	Eplerenone30 or 100 mg/kg/d	CD68+, MCP-1+	Increased infiltration of CD68+ macrophages in ICAs walls with upregulation of MCP-1 and MMP-9, which was prevented by Eplerenone administration associated with reduced incidence of ICAs.	Tada et al. (57)
Preclinical	Sprague-Dawley rats, unilateral ligation of common carotid artery along with β-aminopropionitrile	NF-κB p50 KO, NF-κB decoy ODN[d] 40 μg/60 μl every 2 weeks	CD68+, MCP-1+	Activated NF-κB (p65) colocalized with CD68+ macrophages in ICAs and also with MCP-1 and VCAM-1. Gene expression of MCP-1, VCAM-1, MMP-2, MMP-9, IL-1β, and iNOS along with reduced infiltration of CD68 + macrophages was observed in NF-κB p50 KO mice associated with decreased incidence of ICAs formation. Macrophage infiltration, expression of downstream genes, and ICAs formation were dramatically inhibited by NF-κB decoy ODN.	Aoki et al. (16)
Preclinical	Sprague-Dawley rats, ligation of left common carotid artery and posterior branches of bilateral renal arteries, 8% sodium chloride and 0.12% β-aminopropionitrile	Nifedipine 10mg/kg/d for 2 months i.p[e].	CD68+, MCP-1+	Nifedipine prevented the enlargement and degeneration of the walls of preexisting ICAs. Nifedinpine led to reduced macrophage infiltration, MCP-1, MMP-2 expression and NF-κB DNA binding.	Aoki et al. (60)
Preclinical	Sprague-Dawley rats C57BL/6NCrSlc, Ligation	Macrophage-specific deletion of Ptger2	CD68+	EP2 and COX-2 correlated with ICAs macrophage infiltration. NF-κB activated in macrophages in the adventitia and in endothelial cells and,	Aoki et al. (12)

(Continued)

TABLE 1 | Continued

Study Type	Model	Intervention	Macrophage markers	Main Findings	References
	of the left common carotid artery and left renal artery along with a salt loading dose (8% 0.12% 3-aminopropionitrile	(which encodes EP2) or macrophage-specific expression of an IκBα mutant that restricts NF-κB activation, EP2 antagonist		subsequently, in the entire arterial wall. Upregulation of proinflammatory genes, including Ptgs2 (encoding COX-2). EP2 signaling also stabilized CCL2 (encoding MCP-1). Rats administered an EP2 antagonist had reduced macrophage infiltration and ICAs formation and progression	

[a]*KO, Knock out;* [b]*d, day;* [c]*HTN, Hypertension;* [d]*ODN, oligodeoxynucleotide;* [e]*i.p, intraperitoneally;* [f]*GPA, Glycophorin A;* [g]*Ang. II, Angiotensin II.*

should be cautiously considered in future studies aiming at characterizing the role of these main sentinel cells of ICAs inflammation (39, 40). A recent study revealed that during Ang-II induced inflammation of the aorta, primarily adventitial macrophage population expanded due to the infiltration of the bone marrow derived macrophages, whereas the residential embryonic macrophages do show local proliferation, but retain their homeostatic roles (40). Similar, studies utilizing fate mapping, mass cytometry, single cell transcriptomics and proteomics may be required to unveil the complexity and heterogeneity of ICAs macrophages, which may be helpful to design better therapeutic strategies. A summary of various clinical and preclinical observations and interventions aiming to prevent macrophage mediated inflammation in ICAs is represented in **Table 1**. Clinical trials are needed to confirm the efficacy observed in animal studies.

CONCLUSION

Inflammation and macrophages represent the cornerstones of ICAs development and rupture. Macrophage modulation seems to represent an important therapeutic target and may lead to treatments against ICAs growth and rupture.

AUTHOR CONTRIBUTIONS

SM conceived the idea, contributed to the initial manuscript draft, and reviewed and edited it. SC significantly contributed to the initial manuscript draft. GD, ML, MN, and DH critically reviewed the final draft of the manuscript for the intellectual content. All authors contributed to the article and approved the submitted version.

REFERENCES

1. Hackenberg Katharina AM, Hänggi D, Etminan N. Unruptured Intracranial Aneurysms. *Stroke* (2018) 49(9):2268–75. doi: 10.1161/STROKEAHA.118.021030
2. Macdonald RL. Delayed neurological deterioration after subarachnoid haemorrhage. *Nat Rev Neurol* (2014) 10(1):44–58. doi: 10.1038/nrneurol.2013.246
3. Macdonald RL, Schweizer TA. Spontaneous subarachnoid haemorrhage. *Lancet* (2017) 389(10069):655–66. doi: 10.1016/S0140-6736(16)30668-7
4. Lawton MT, Vates GE. Subarachnoid Hemorrhage. *New Engl J Med* (2017) 377(3):257–66. doi: 10.1056/NEJMcp1605827
5. Etminan N, Rinkel GJ. Unruptured intracranial aneurysms: development, rupture and preventive management. *Nat Rev Neurol* (2016) 12(12):699–713. doi: 10.1038/nrneurol.2016.150
6. D'Souza S. Aneurysmal Subarachnoid Hemorrhage. *J Neurosurg Anesthesiol* (2015) 27(3):222–40. doi: 10.1097/ANA.0000000000000130
7. Yamada Y, Sakuma J, Takeuchi I, Yasukochi Y, Kato K, Oguri M, et al. Identification of six polymorphisms as novel susceptibility loci for ischemic or hemorrhagic stroke by exome-wide association studies. *Int J Mol Med* (2017) 39(6):1477–91. doi: 10.3892/ijmm.2017.2972
8. Aoki T, Kataoka H, Ishibashi R, Nozaki K, Egashira K, Hashimoto N. Impact of monocyte chemoattractant protein-1 deficiency on cerebral aneurysm formation. *Stroke* (2009) 40(3):942–51. doi: 10.1161/STROKEAHA.108.532556
9. Strong MJ, Amenta PS, Dumont AS, Medel R. The role of leukocytes in the formation and rupture of intracranial aneurysms. *Neuroimmunol Neuroinflamm* (2015) 2:107–14. doi: 10.4103/2347-8659.153972
10. Tulamo R, Frosen J, Junnikkala S, Paetau A, Kangasniemi M, Pelaez J, et al. Complement system becomes activated by the classical pathway in intracranial aneurysm walls. *Lab Invest* (2010) 90(2):168–79. doi: 10.1038/labinvest.2009.133
11. Frosen J, Tulamo R, Paetau A, Laaksamo E, Korja M, Laakso A, et al. Saccular intracranial aneurysm: pathology and mechanisms. *Acta Neuropathol* (2012) 123(6):773–86. doi: 10.1007/s00401-011-0939-3
12. Aoki T, Frösen J, Fukuda M, Bando K, Shioi G, Tsuji K, et al. Prostaglandin E_2–EP2–NF-κB signaling in macrophages as a potential therapeutic target for intracranial aneurysms. *Sci Signaling* (2017) 10(465):eaah6037. doi: 10.1126/scisignal.aah6037
13. Moriwaki T, Takagi Y, Sadamasa N, Aoki T, Nozaki K, Hashimoto N. Impaired progression of cerebral aneurysms in interleukin-1beta-deficient mice. *Stroke* (2006) 37(3):900–5. doi: 10.1161/01.STR.0000204028.39783.d9
14. Aoki T, Nishimura M, Matsuoka T, Yamamoto K, Furuyashiki T, Kataoka H, et al. PGE2-EP2 signalling in endothelium is activated by haemodynamic stress and induces cerebral aneurysm through an amplifying loop via NF-κB. *Br J Pharmacol* (2011) 163(6):1237–49. doi: 10.1111/j.1476-5381.2011.01358.x
15. Sadamasa N, Nozaki K, Hashimoto N. Disruption of gene for inducible nitric oxide synthase reduces progression of cerebral aneurysms. *Stroke* (2003) 34(12):2980–4. doi: 10.1161/01.str.0000102556.55600.3b
16. Aoki T, Kataoka H, Morimoto M, Nozaki K, Hashimoto N. Macrophage-derived matrix metalloproteinase-2 and -9 promote the progression of cerebral aneurysms in rats. *Stroke* (2007) 38(1):162–9. doi: 10.1161/01.STR.0000252129.18605.c8
17. Shimizu K, Kushamae M, Mizutani T, Aoki T. Intracranial Aneurysm as a Macrophage-mediated Inflammatory Disease. *Neurol Med-Chirurg* (2019) 59(4):126–32. doi: 10.2176/nmc.st.2018-0326
18. Kurki MI, Hakkinen SK, Frosen J, Tulamo R, von und zu Fraunberg M, Wong G, et al. Upregulated signaling pathways in ruptured human saccular intracranial aneurysm wall: an emerging regulative role of Toll-like receptor signaling and nuclear factor-kappaB, hypoxia-inducible factor-1A, and ETS transcription factors. *Neurosurgery* (2011) 68(6):1667–75; discussion 75-6. doi: 10.1227/NEU.0b013e318210f001
19. Nakaoka H, Tajima A, Yoneyama T, Hosomichi K, Kasuya H, Mizutani T, et al. Gene expression profiling reveals distinct molecular signatures

associated with the rupture of intracranial aneurysm. *Stroke* (2014) 45 (8):2239–45. doi: 10.1161/strokeaha.114.005851
20. Pera J, Korostynski M, Krzyszkowski T, Czopek J, Slowik A, Dziedzic T, et al. Gene expression profiles in human ruptured and unruptured intracranial aneurysms: what is the role of inflammation? *Stroke* (2010) 41(2):224–31. doi: 10.1161/strokeaha.109.562009
21. Shi C, Awad IA, Jafari N, Lin S, Du P, Hage ZA, et al. Genomics of human intracranial aneurysm wall. *Stroke* (2009) 40(4):1252–61. doi: 10.1161/strokeaha.108.532036
22. Weinsheimer S, Lenk GM, van der Voet M, Land S, Ronkainen A, Alafuzoff I, et al. Integration of expression profiles and genetic mapping data to identify candidate genes in intracranial aneurysm. *Physiol Genomics* (2007) 32(1):45–57. doi: 10.1152/physiolgenomics.00015.2007
23. Krischek B, Kasuya H, Tajima A, Akagawa H, Sasaki T, Yoneyama T, et al. Network-based gene expression analysis of intracranial aneurysm tissue reveals role of antigen presenting cells. *Neuroscience* (2008) 154(4):1398–407. doi: 10.1016/j.neuroscience.2008.04.049
24. Jayaraman T, Berenstein V, Li X, Mayer J, Silane M, Shin YS, et al. Tumor Necrosis Factor α is a Key Modulator of Inflammation in Cerebral Aneurysms. *Neurosurgery* (2005) 57(3):558–64. doi: 10.1227/01.NEU.0000170439.89041.D6
25. Sathyan S, Koshy LV, Srinivas L, Easwer HV, Premkumar S, Nair S, et al. Pathogenesis of intracranial aneurysm is mediated by proinflammatory cytokine TNFA and IFNG and through stochastic regulation of IL10 and TGFB1 by comorbid factors. *J Neuroinflamm* (2015) 12(1):1–10. doi: 10.1186/s12974-015-0354-0
26. Tulamo R, Frosen J, Junnikkala S, Paetau A, Pitkaniemi J, Kangasniemi M, et al. Complement activation associates with saccular cerebral artery aneurysm wall degeneration and rupture. *Neurosurgery* (2006) 59(5):1069–76; discussion 76-7. Epub 2006/10/04. doi: 10.1227/01.NEU.0000245598.84698.26
27. Baeriswyl DC, Prionisti I, Peach T, Tsolkas G, Chooi KY, Vardakis J, et al. Disturbed flow induces a sustained, stochastic NF-κB activation which may support intracranial aneurysm growth in vivo. *Sci Rep* (2019) 9(1):4738. doi: 10.1038/s41598-019-40959-y
28. Cuhlmann S, Van der Heiden K, Saliba D, Tremoleda JL, Khalil M, Zakkar M, et al. Disturbed blood flow induces RelA expression via c-Jun N-terminal kinase 1: a novel mode of NF-kappaB regulation that promotes arterial inflammation. *Circ Res* (2011) 108(8):950–9. doi: 10.1161/circresaha.110.233841
29. Frosen J, Piippo A, Paetau A, Kangasniemi M, Niemela M, Hernesniemi J, et al. Remodeling of saccular cerebral artery aneurysm wall is associated with rupture: histological analysis of 24 unruptured and 42 ruptured cases. *Stroke* (2004) 35(10):2287–93. doi: 10.1161/01.STR.0000140636.30204.da
30. Jakubzick CV, Randolph GJ, Henson PM. Monocyte differentiation and antigen-presenting functions. *Nat Rev Immunol* (2017) 17(6):349–62. doi: 10.1038/nri.2017.28
31. Kataoka K, Taneda M, Asai T, Kinoshita A, Ito M, Kuroda R. Structural fragility and inflammatory response of ruptured cerebral aneurysms. A comparative study between ruptured and unruptured cerebral aneurysms. *Stroke* (1999) 30(7):1396–401. doi: 10.1161/01.str.30.7.1396
32. Chyatte D, Bruno G, Desai S, Todor DR. Inflammation and intracranial aneurysms. *Neurosurgery* (1999) 45(5):1137–46; discussion 46-7. doi: 10.1097/00006123-199911000-00024
33. Kanematsu Y, Kanematsu M, Kurihara C, Tada Y, Tsou TL, van Rooijen N, et al. Critical roles of macrophages in the formation of intracranial aneurysm. *Stroke* (2011) 42(1):173–8. doi: 10.1161/strokeaha.110.590976
34. Hasan DM, Starke RM, Gu H, Wilson K, Chu Y, Chalouhi N, et al. Smooth Muscle Peroxisome Proliferator-Activated Receptor gamma Plays a Critical Role in Formation and Rupture of Cerebral Aneurysms in Mice In Vivo. *Hypertens (Dallas Tex 1979)* (2015) 66(1):211–20. doi: 10.1161/hypertensionaha.115.05332
35. Yamamoto R, Aoki T, Koseki H, Fukuda M, Hirose J, Tsuji K, et al. A sphingosine-1-phosphate receptor type 1 agonist, ASP4058, suppresses intracranial aneurysm through promoting endothelial integrity and blocking macrophage transmigration. *Br J Pharmacol* (2017) 174(13):2085–101. doi: 10.1111/bph.13820
36. Mills CD, Kincaid K, Alt JM, Heilman MJ, Hill AM. M-1/M-2 macrophages and the Th1/Th2 paradigm. *J Immunol* (2000) 164(12):6166–73. doi: 10.4049/jimmunol.164.12.6166
37. Boyle JJ, Johns M, Kampfer T, Nguyen AT, Game L, Schaer DJ, et al. Activating transcription factor 1 directs Mhem atheroprotective macrophages through coordinated iron handling and foam cell protection. *Circ Res* (2012) 110(1):20–33. doi: 10.1161/circresaha.111.247577
38. Cheng Z, Zhou Y-Z, Wu Y, Wu Q-Y, Liao X-B, Fu X-M, et al. Diverse roles of macrophage polarization in aortic aneurysm: destruction and repair. *J Trans Med* (2018) 16(1):354. doi: 10.1186/s12967-018-1731-0
39. Murray PJ, Allen JE, Biswas SK, Fisher EA, Gilroy DW, Goerdt S, et al. Macrophage activation and polarization: nomenclature and experimental guidelines. *Immunity* (2014) 41(1):14–20. doi: 10.1016/j.immuni.2014.06.008
40. Weinberger T, Esfandyari D, Messerer D, Percin G, Schleifer C, Thaler R, et al. Ontogeny of arterial macrophages defines their functions in homeostasis and inflammation. *Nat Commun* (2020) 11(1):4549. doi: 10.1038/s41467-020-18287-x
41. Li H, Bai S, Ao Q, Wang X, Tian X, Li X, et al. Modulation of Immune-Inflammatory Responses in Abdominal Aortic Aneurysm: Emerging Molecular Targets. *J Immunol Res* (2018) 2018:7213760. doi: 10.1155/2018/7213760
42. Hamilton TA, Zhao C, Pavicic PG, Datta S. Myeloid Colony-Stimulating Factors as Regulators of Macrophage Polarization. *Front Immunol* (2014) 5:554. doi: 10.3389/fimmu.2014.00554
43. Ye P, Chen W, Wu J, Huang X, Li J, Wang S, et al. GM-CSF contributes to aortic aneurysms resulting from SMAD3 deficiency. *J Clin Invest* (2013) 123 (5):2317–31. doi: 10.1172/JCI67356
44. Chalouhi N, Theofanis T, Starke RM, Zanaty M, Jabbour P, Dooley SA, et al. Potential role of granulocyte-monocyte colony-stimulating factor in the progression of intracranial aneurysms. *DNA Cell Biol* (2015) 34(1):78–81. doi: 10.1089/dna.2014.2618
45. Hasan D, Chalouhi N, Jabbour P, Hashimoto T. Macrophage imbalance (M1 vs. M2) and upregulation of mast cells in wall of ruptured human cerebral aneurysms: preliminary results. *J Neuroinflamm* (2012) 9(1):1–7. doi: 10.1186/1742-2094-9-222
46. Ollikainen E, Tulamo R, Kaitainen S, Honkanen P, Lehti S, Liimatainen T, et al. Macrophage Infiltration in the Saccular Intracranial Aneurysm Wall as a Response to Locally Lysed Erythrocytes That Promote Degeneration. *J Neuropathol Exp Neurol* (2018) 77(10):890–903. doi: 10.1093/jnen/nly068
47. Nowicki KW, Hosaka K, Walch FJ, Scott EW, Hoh BL. M1 macrophages are required for murine cerebral aneurysm formation. *J Neurointervent Surg* (2018) 10(1):93–7. doi: 10.1136/neurintsurg-2016-012911
48. Shimada K, Furukawa H, Wada K, Korai M, Wei Y, Tada Y, et al. Protective Role of Peroxisome Proliferator-Activated Receptor-gamma in the Development of Intracranial Aneurysm Rupture. *Stroke* (2015) 46(6):1664–72. doi: 10.1161/strokeaha.114.007722
49. Hasan DM, Mahaney KB, Brown RD Jr, Meissner I, Piepgras DG, Huston J, et al. Aspirin as a promising agent for decreasing incidence of cerebral aneurysm rupture. *Stroke* (2011) 42(11):3156–62. doi: 10.1161/STROKEAHA.111.619411
50. Can A, Castro VM, Dligach D, Finan S, Yu S, Gainer V, et al. Lipid-Lowering Agents and High HDL (High-Density Lipoprotein) Are Inversely Associated With Intracranial Aneurysm Rupture. *Stroke* (2018) 49(5):1148–54. doi: 10.1161/strokeaha.117.019972
51. Yoshimura Y, Murakami Y, Saitoh M, Yokoi T, Aoki T, Miura K, et al. Statin Use and Risk of Cerebral Aneurysm Rupture: A Hospital-based Case–control Study in Japan. *J Stroke Cerebrovasc Dis* (2014) 23(2):343–8. doi: 10.1016/j.jstrokecerebrovasdis.2013.04.022
52. Can A, Rudy RF, Castro VM, Yu S, Dligach D, Finan S, et al. Association between aspirin dose and subarachnoid hemorrhage from saccular aneurysms: A case-control study. *Neurology* (2018) 91(12):e1175–81. doi: 10.1212/wnl.0000000000006200
53. Chalouhi N, Atallah E, Jabbour P, Patel PD, Starke RM, Hasan D. Aspirin for the Prevention of Intracranial Aneurysm Rupture. *Neurosurgery* (2017) 64 (CN_suppl_1):114–8. doi: 10.1093/neuros/nyx299
54. Hasan DM, Chalouhi N, Jabbour P, Dumont AS, Kung DK, Magnotta VA, et al. Evidence that acetylsalicylic acid attenuates inflammation in the walls of human cerebral aneurysms: preliminary results. *J Am Heart Assoc* (2013) 2(1): e000019. doi: 10.1161/jaha.112.000019
55. Hasan DM, Chalouhi N, Jabbour P, Magnotta VA, Kung DK, Young WL. Imaging aspirin effect on macrophages in the wall of human cerebral

aneurysms using ferumoxytol-enhanced MRI: preliminary results. *J Neuroradiol J Neuroradiol* (2013) 40(3):187–91. doi: 10.1016/j.neurad.2012.09.002
56. Ikedo T, Minami M, Kataoka H, Hayashi K, Nagata M, Fujikawa R, et al. Dipeptidyl Peptidase-4 Inhibitor Anagliptin Prevents Intracranial Aneurysm Growth by Suppressing Macrophage Infiltration and Activation. *J Am Heart Assoc* (2017) 6(6):e004777. doi: 10.1161/jaha.116.004777
57. Tada Y, Kitazato KT, Tamura T, Yagi K, Shimada K, Kinouchi T, et al. Role of Mineralocorticoid Receptor on Experimental Cerebral Aneurysms in Rats. *Hypertens (Dallas Tex 1979)* (2009) 54(3):552–7. doi: 10.1161/HYPERTENSIONAHA.109.134130
58. Nagahiro S, Tada Y, Satomi J, Kinouchi T, Kuwayama K, Yagi K, et al. Treatment of Unruptured Cerebral Aneurysms with the Mineralocorticoid Receptor Blocker Eplerenone—Pilot Study. *J Stroke Cerebrovasc Dis* (2018) 27(8):2134–40. doi: 10.1016/j.jstrokecerebrovasdis.2018.03.008
59. Aoki T, Kataoka H, Shimamura M, Nakagami H, Wakayama K, Moriwaki T, et al. NF-κB Is a Key Mediator of Cerebral Aneurysm Formation. *Circulation* (2007) 116(24):2830–40. doi: 10.1161/CIRCULATIONAHA.107.728303
60. Aoki T, Kataoka H, Ishibashi R, Nozaki K, Hashimoto N. Nifedipine inhibits the progression of an experimentally induced cerebral aneurysm in rats with associated down-regulation of NF-kappa B transcriptional activity. *Curr Neurovasc Res* (2008) 5(1):37–45. doi: 10.2174/156720208783565663
61. Zheng X, Turkowski K, Mora J, Brüne B, Seeger W, Weigert A, et al. Redirecting TAMs to become tumoricidal effectors as a novel strategy for cancer therapy. *Oncotarget* (2017) 8(29):48436–52. doi: 10.18632/oncotarget.17061
62. Genard G, Lucas S, Michiels C. Reprogramming of Tumor-Associated Macrophages with Anticancer Therapies: Radiotherapy versus Chemo- and Immunotherapies. *Front Immunol* (2017) 8:828. doi: 10.3389/fimmu.2017.00828
63. Tardito S, Martinelli G, Soldano S, Paolino S, Pacini G, Patane M, et al. Macrophage M1/M2 polarization and rheumatoid arthritis: A systematic review. *Autoimmun Rev* (2019) 18(11):102397. doi: 10.1016/j.autrev.2019.102397
64. Bi J, Zeng X, Zhao L, Wei Q, Yu L, Wang X, et al. miR-181a Induces Macrophage Polarized to M2 Phenotype and Promotes M2 Macrophage-mediated Tumor Cell Metastasis by Targeting KLF6 and C/EBPalpha. *Mol Ther Nucleic Acids* (2016) 5(9):e368. doi: 10.1038/mtna.2016.71
65. Enam SF, Bellamkonda RV. FKN-aptamer functionalized hydrogels for local enrichment of M2 macrophages after traumatic brain injury. *Front Bioeng Biotechnol.* (2016) 4. doi: 10.3389/conf.FBIOE.2016.01.00132
66. de Groot AE, Pienta KJ. Epigenetic control of macrophage polarization: implications for targeting tumor-associated macrophages. *Oncotarget* (2018) 9(29):20908–27. doi: 10.18632/oncotarget.24556
67. Randolph GJ. Mechanisms that regulate macrophage burden in atherosclerosis. *Circ Res* (2014) 114(11):1757–71. doi: 10.1161/circresaha.114.301174
68. Quan K, Li S, Wang D, Shi Y, Yang Z, Song J, et al. Berberine Attenuates Macrophages Infiltration in Intracranial Aneurysms Potentially Through FAK/Grp78/UPR Axis. *Front Pharmacol* (2018) 9:565. doi: 10.3389/fphar.2018.00565
69. Suzuki T, Takizawa T, Kamio Y, Qin T, Hashimoto T, Fujii Y, et al. Noninvasive Vagus Nerve Stimulation Prevents Ruptures and Improves Outcomes in a Model of Intracranial Aneurysm in Mice. *Stroke* (2019) 50(5):Strokeaha118023928. doi: 10.1161/strokeaha.118.023928
70. Zhao XP, Zhao Y, Qin XY, Wan LY, Fan XX. Non-invasive Vagus Nerve Stimulation Protects Against Cerebral Ischemia/Reperfusion Injury and Promotes Microglial M2 Polarization Via Interleukin-17A Inhibition. *J Mol Neurosci MN* (2019) 67(2):217–26. doi: 10.1007/s12031-018-1227-7

Conflict of Interest: The authors declare that the research was conducted in the absence of any commercial or financial relationships that could be construed as a potential conflict of interest.

Copyright © 2021 Muhammad, Chaudhry, Dobreva, Lawton, Niemelä and Hänggi. This is an open-access article distributed under the terms of the Creative Commons Attribution License (CC BY). The use, distribution or reproduction in other forums is permitted, provided the original author(s) and the copyright owner(s) are credited and that the original publication in this journal is cited, in accordance with accepted academic practice. No use, distribution or reproduction is permitted which does not comply with these terms.

frontiers in Immunology

REVIEW
published: 07 April 2021
doi: 10.3389/fimmu.2021.667830

Macrophage-Mediated Tissue Vascularization: Similarities and Differences Between Cornea and Skin

Karina Hadrian[1], *Sebastian Willenborg*[2], *Felix Bock*[1], *Claus Cursiefen*[1,3], *Sabine A. Eming*[2,3,4,5*] *and Deniz Hos*[1,3*]

[1] Department of Ophthalmology, University of Cologne, Faculty of Medicine and University Hospital Cologne, Cologne, Germany, [2] Department of Dermatology, University of Cologne, Cologne, Germany, [3] Center for Molecular Medicine Cologne (CMMC), University of Cologne, Cologne, Germany, [4] Cologne Excellence Cluster on Cellular Stress Responses in Aging-Associated Diseases (CECAD), University of Cologne, Cologne, Germany, [5] Developmental Biology Unit, Institute of Zoology, University of Cologne, Cologne, Germany

OPEN ACCESS

Edited by:
Elodie Segura,
Institut Curie, France

Reviewed by:
Gabriel Courties,
INSERM U1183 Cellules Souches, Plasticité Cellulaire, Médecine Régénératrice Et Immunothérapies, France
Carlos Minutti,
Francis Crick Institute, United Kingdom

***Correspondence:**
Deniz Hos
deniz.hos@uk-koeln.de
Sabine A. Eming
sabine.eming@uni-koeln.de

Specialty section:
This article was submitted to Antigen Presenting Cell Biology, a section of the journal Frontiers in Immunology

Received: 14 February 2021
Accepted: 19 March 2021
Published: 07 April 2021

Citation:
Hadrian K, Willenborg S, Bock F, Cursiefen C, Eming SA and Hos D (2021) Macrophage-Mediated Tissue Vascularization: Similarities and Differences Between Cornea and Skin. Front. Immunol. 12:667830. doi: 10.3389/fimmu.2021.667830

Macrophages are critical mediators of tissue vascularization both in health and disease. In multiple tissues, macrophages have been identified as important regulators of both blood and lymphatic vessel growth, specifically following tissue injury and in pathological inflammatory responses. In development, macrophages have also been implicated in limiting vascular growth. Hence, macrophages provide an important therapeutic target to modulate tissue vascularization in the clinic. However, the molecular mechanisms how macrophages mediate tissue vascularization are still not entirely resolved. Furthermore, mechanisms might also vary among different tissues. Here we review the role of macrophages in tissue vascularization with a focus on their role in blood and lymphatic vessel formation in the barrier tissues cornea and skin. Comparing mechanisms of macrophage-mediated hem- and lymphangiogenesis in the angiogenically privileged cornea and the physiologically vascularized skin provides an opportunity to highlight similarities but also tissue-specific differences, and to understand how macrophage-mediated hem- and lymphangiogenesis can be exploited for the treatment of disease, including corneal wound healing after injury, graft rejection after corneal transplantation or pathological vascularization of the skin.

Keywords: macrophages, monocytes, angiogenesis, cornea, skin, lymphangiogenesis

INTRODUCTION

Macrophages represent highly plastic cells of the hematopoietic system and are found in all tissues (1). Macrophages exert multiple functions including important roles in tissue development, homeostasis, repair and host defense. Several pieces of evidence indicate a critical role of macrophages as mediators of neovascularization (2–4). Furthermore, macrophages have also been shown to mediate repair of damaged vascular tissue (5). Neovascularization occurs very diversly in different tissues. Here we review the role of macrophages in tissue vascularization with a

focus on blood and lymphatic vessel formation in cornea and skin. Furthermore, a recent study showed the mediation of vascular tissue repair by macrophages (5).

The cornea is the outer barrier of the eye and is, under healthy conditions, transparent and the major refractive element in the eye. The cornea belongs to the few immune-privileged tissues of the organism and is, unlike the skin, avascular in its healthy state. After severe injury or chronic inflammation, however, corneal avascularity is abrogated as blood and lymphatic vessels can sprout from the adjacent vascularized tissues into the cornea, leading to reduced visual acuity and undesired immune responses (6, 7). However, on the other side previous studies also reported on beneficial roles of lymphatic vessels in the cornea under certain disease conditions (8–10). Corneal macrophages have been shown to be critical mediators of corneal hem- and lymphangiogenesis (2, 11). Similar to the cornea, the skin is an important barrier tissue protecting the body from harmful insults of the environment. In contrast to the avascular cornea, the skin contains a tight network of blood and lymphatic vessels and also several resident immune cell types, including macrophages, which have been shown to be important mediators of skin vascularization. Comparing angiogenesis in both tissues provides an opportunity to highlight molecular principles of macrophage-mediated tissue vascularization.

MONOCYTE AND MACROPHAGE HETEROGENEITY

Origin and Development of Monocytes and Macrophages

Until recently, it was thought that macrophages exclusively originate from hematopoietic stem cell (HSC)-derived monocytes in the bone marrow and are released into the peripheral blood circulation (12). The egression of monocytes from bone marrow into blood requires the expression of the C-C chemokine receptor type 2 (CCR2) (13, 14). Blood monocytes can be subdivided into two subtypes: classical and non-classical monocytes. Classical monocytes are circulating for several days in the blood before leaving the circulation by diapedesis and entering tissues in steady state to replenish the tissue macrophage populations under inflammatory conditions. Non-classical monocytes predominantly remain in the circulation (13) and engage in long-term migration along the endothelium with or against the flow, a process termed patrolling (14). These monocyte subpopulations are reviewed in detail in section 2.2, including their various expression of surface markers.

However, besides macrophages originating and renewing from HSCs, some macrophages develop in the early embryo before the development of HSCs. These cells are termed erythromyeloid progenitors (EMP) (15). It was shown in mice, that macrophages develop in the yolk sac beginning from embryonic day 8.5 (E8.5) (16, 17). Further, the transcription factor myeloblastosis (Myb) is required for the development of HSCs in the bone marrow as well as for the development of all $CD11b^{high}$ monocytes and $CD11b^{high}$ macrophages. For the development of yolk sac-derived $F4/80^{+}$ macrophages in several tissues, including liver Kupffer cells, epidermal Langerhans cells as well as microglia cell populations, Myb was dispensable. In adult mice, these populations can persist independently of HSCs, suggesting that a lineage of tissue macrophages is derived from the yolk sac and is genetically distinct from HSC progeny (18). Additionally, it was shown in mice, that the majority of adult tissue-resident macrophages in various organs like liver, brain, lung and skin originates from an Angiopoietin-1 $receptor^{+}$ (Tie2) cellular pathway generating Colony stimulating factor 1 $receptor^{+}$ (Csf1r) EMPs, which are distinct from HSCs (19, 20). It has been shown that during inflammation there is an expansion of both HSC- and EMP-derived macrophages, presumably performing different functions at different stages of the inflammatory process.

In the cornea, the $CCR2^{-}$ population is already is present in the cornea at E12.5, which are similar to yolk sac-derived macrophages, whereas the $CCR2^{+}$ population does not appear in the cornea until E17.5. Besides the different phenotype and gene expression profile, the role of these populations in corneal wound healing is different. Whereas $CCR2^{+}$ macrophages seem to act pro-inflammatory in an early stage of corneal wound healing, $CCR2^{-}$ macrophages seem to act anti-inflammatory during the later stage of wound healing (21).

Subpopulations of Murine Monocytes and Macrophages

In mice, the antigenic differentiation of two monocyte subsets was first achieved after the observation that monocytes could be subdivided according to their expression of CCR2, L-selectin (CD62L) and CX3C chemokine receptor 1 (CX3CR1) (13, 22–25). $CCR2^{+}CD62L^{+}CX3CR1^{low}$ expressing monocytes have pro-inflammatory characteristics and are recruited into the tissue during inflammation, e.g., for host defense, whereas $CCR2^{-}CD62L^{-}CX3CR1^{high}$ monocytes/macrophages have anti-inflammatory properties and replenish the tissue resident macrophage population, mediate wound healing and patrol the vasculature (13, 26–28). $CCR2^{+}CD62L^{+}CX3CR1^{low}$ expressing monocytes are known to be the "inflammatory" subset, whereas $CCR2^{-}CX3CR1^{high}$ expressing monocytes are considered as the "resident" subset. Besides CCR2 as a marker for monocytes/macrophages, Geissmann et al. identified an additional marker, lymphocyte antigen 6C (Ly6C), for $CCR2^{+}$ monocytes/macrophages (13). In particular, $CCR2^{+}CD62L^{+}CX3CR1^{low}$ $Ly6C^{+}$ monocytes seem to have an outstanding importance for the infiltration into inflamed tissues (29). These cells produce pro-inflammatory cytokines and chemokines, including tumor necrosis factor (TNF)-α, Interleukin (IL)-1β, IL-6, IL-12, IL-23, and C-C motif chemokine 11 (CCL11) (30, 31). Additionally, cells express high levels of Triggering receptor expressed on myeloid cells 1 (TREM1), which can potently amplify pro-inflammatory responses (32).

Fate-mapping studies as well as single cell analyses were recently able to provide major insights into the heterogeneity of macrophages. In this context, a study performed by Yona et al. demonstrated, that tissue resident macrophage populations, including peritoneal, splenic and lung macrophages, as well as liver Kupffer cells, are established prior to birth and are

disconnected from monocyte input in adult steady state (27). Furthermore, this study demonstrated that in steady state monocytes with a CX3CR1^{int}Ly6C^{+} expression form a short-lived obligatory precursor intermediate for the generation of Ly6C^{-} monocytes, which dynamically control the lifespan of their progenitors (27). A very recent study from Wieghofer et al., provided further insight into the heterogeneity of macrophages in various tissues of the eye, including the cornea (33). In this study, a combination of three techniques, single-cell RNA sequencing, embryonic and adult cell fate mapping and parabiosis with the use of reporter mouse lines was deployed to compare the transcriptional profiles, origin and turnover characteristics of retinal microglia, and resident macrophages in the ciliary body as well as in the cornea (33). Out of 17 different clusters containing CD45^{+}CD3^{-}CD19^{-}Ly6G^{-} cells, five clusters were significantly enriched in the cornea. Furthermore, this study showed, that all investigated compartments of the adult murine eye contained macrophages of prenatal origin that derive either from the yolk sac and/or the fetal liver to various degrees. However, in the cornea of adult mice, macrophages are continuously replaced with cells derived from the definitive hematopoiesis with a short turnover (33).

A number of markers that are expressed by macrophages can be used for characterization and localization during experimental set ups, including F4/80, CD11b and CD68 (34–36). Besides macrophages, F4/80 is also a marker for microglial cells (37). Additionally, myeloid dendritic cells, blood monocytes and eosinophilic granulocytes also express low levels of F4/80 (38), whereas CD11b is also expressed on neutrophils, peritoneal B1 cells, CD8^{+} dendritic cells (DCs), natural killer cells (NK) and a subset of CD8^{+} T cells (39–41). CD11b is also highly expressed in CD4^{+} conventional DCs and in conventional DCs type 2 regardless of their CD4 expression (42). CD68 is also present on basophils, dendritic cells, fibroblasts, Langerhans cells, mast cells, CD34^{+} progenitor cells, neutrophils, osteoclasts, activated platelets and B and T cells (43, 44). Additional markers widely used for the characterization of tissue resident macrophages are CD64 and Mer tyrosine kinase (MerTK). A combination of different markers including CD11b, F4/80, CD64, MerTK and CD68 for flow cytometry is commonly used to characterize tissue-resident macrophages (45). Furthermore, the characterization of macrophages is also possible using immunofluorescence. For example, Saylor et al. developed an automated, multiplexed staining approach including anti-CD68, -CD163, -CD206, -CD11b, and -CD11c antibodies to identify macrophages in tumor tissue (46).

Interestingly, macrophages share the marker Lymphatic Vascular Endothelial Hyaluronan Receptor 1 (LYVE-1) with lymphatic endothelial cells (LECs) (47). Therefore, these cell types also have to be discriminated, e.g. by using further specific markers for LECs such as the transcription factor Prospero homeobox protein (Prox-1) (48) and the membrane glycoprotein Podoplanin (6, 49, 50). Besides lymphatic vascular endothelium, LYVE-1 serves for both, macrophages and LECs as receptor during hyaluronate metabolism and angiogenesis (2, 3, 6, 51–53). Intriguingly, a recent study of Chakarov et al. has shown that two independent monocyte-derived tissue resident macrophage populations exist across various tissues with specific niche-dependent phenotypes and functional programming, distinguished by their LYVE-1, MHC II and CX3CR1 expression pattern (54). LYVE-1^{low}MHC II^{high}CX3CR1^{high} macrophages are preferentially located, but conserved, in sub tissular niches located adjacent to nerve fibers, whereas LYVE-1^{high}MHC II^{low}CX3CR1^{low} macrophages are preferentially located adjacent to blood vessels (54). LYVE-1^{low}MHC II^{high}CX3CR1^{high} macrophages exhibit potent immune-regulatory potential, while LYVE-1^{high}MHC II^{low}CX3CR1^{low} macrophages are able to express higher levels of genes which are involved in wound healing, repair, and fibrosis, as well as blood vessel morphology and leukocyte migration (54).

Activation Phenotypes of Macrophages

A plethora of functional macrophage phenotypes exist. For a long time, macrophage phenotypes were classified into two polarized macrophage subtypes, depending on their activation state. The "classical" activation of macrophages occurs *via* stimulation by pro-inflammatory mediators, e.g. Interferon (IFN)-γ, TNF-α or lipopolysaccharides (LPS). These macrophages show an increased expression of pro-inflammatory cytokines such as TNF-α, IL-6 and IL-12, increased antigen presentation and production of nitrogen and oxygen radicals as well as increased microbicidal activity (55). This macrophage phenotype occurs primarily in early phases of inflammatory responses. In contrast, "alternative" activation of macrophages is mediated by the Type 2 cytokines IL-4 and IL-13 which induce the expression of hallmark genes such as *Retnla* (resistin-like molecule alpha), *Chil3* (chitinase-like 3), and *Arg1* (arginase 1) (55, 56). IL-4/IL-13-activated macrophages show an increased activity in signaling pathways that are important for the termination of an immune response, leading to an increase of the expression of prophagocytic, antioxidant and motility-enhancing factors, while the expression of pro-inflammatory factors is decreased (55). Furthermore, IL-4Rα-activated macrophages are crucially involved in tissue repair, evidenced by defective skin wound healing in *Il4ra*$^{fl/-}$*Lyz2-cre* mice (57). In this study, IL-4Rα-activated macrophages were shown to have a major impact on the collagen-modifying function of fibroblasts and thereby on scar formation (57). Macrophages in *Il4ra*$^{fl/-}$*Lyz2-cre* mice fail to initiate an essential repair program rather than an unrestrained pro-inflammatory response which was reported in prior studies by Chen et al. (58). It is clear, however, that this subdivision is an oversimplification and only reflects two extremes of polarization and that in tissues a wide range of activation states exist in parallel (56).

CORNEAL MACROPHAGES

Previous studies have demonstrated that resident tissue macrophages and antigen-presenting cells (APCs) are present in various tissues of the eye, including the iris, ciliary body, uvea, retina, conjunctiva, and cornea (59–63). It was also shown that macrophages express low levels of MHC II and further costimulatory molecules, which enables them to act as APCs,

although working less efficiently than dendritic cells due to their relatively reduced ability to migrate and prime naïve T cells (42, 64–67). In this regard, it should be noted that there are several lines of evidence that Langerhans cells are not DCs but rather a population of specialized macrophages (42, 68). Furthermore, it was demonstrated that a high number of $CD45^+$ cells (leucocytes) with pleomorphic and dendriform morphology were found within the pericentral and central region of the corneal stroma (69). It was demonstrated, that all $CD45^+$ cells in the corneal stroma are also $CD11b^+$ and around 50% of the $CD45^+$ cells were also $F4/80^+$. Approximately 30% of all $CD45^+$ cells and 50% of $F4/80^+$ cells co-expressed MHC II, whereas only a very small number of the $CD45^+$ cells were positive for CD11c (dendritic cells) or Ly6G (granulocytes) (69). In short, this study shows that two different subsets of $F4/80^+$ macrophages exist in the cornea, discriminated based on their MHC II expression. No T cells and NK cell markers were found in the naïve corneal stroma, indicating that all cells identified in the stroma were of the myeloid lineage (69).

Early experiments from Streilein and colleagues indicated that the cornea has no MHC II^+ cells capable of stimulating acute allogeneic rejection (70). Subsequently, two independent studies described a network of $CD11b^+$ macrophage-like cells as well as a significant number of $CD45^+$ leukocytes in the stroma and $CD11c^+$ DCs in the corneal epithelium of normal mouse corneas (69, 71). MHC II^+ cells were typically located in the periphery of the corneal epithelium with a dendritic morphology in various species, including mice (72) and humans (72–74). It was also shown, that $CCR2^-$ macrophages, which already exist in the cornea at E12.5, may be derived from progenitors originating in the fetal liver or earlier yolk sac (17), as yolk sac progenitors seem to express only low levels of CCR2. The $CCR2^+$ population does not appear in the cornea until E17.5 (21). It was also demonstrated that $CCR2^-$ macrophages in the cornea were mainly maintained through local proliferation and were rarely replaced by blood monocytes, whereas $CCR2^+$ macrophages with a lower ability to proliferate were replaced by blood monocytes (21). It was proposed that the turnover rate of bone marrow-derived $CX3CR1^+$ cells in the cornea is fast (approximately 40% in 4 weeks) compared to other non-lymphoid tissues (75), including lung, liver and brain [turnover of less than 5% in 4 weeks (76)]. This study also proposed, that the higher turnover rate in the peripheral cornea is a reflection of the close location to the vascular limbus (75).

Taken together, macrophages are also present in the immune-privileged cornea, preferable in the periphery of the corneal stroma. However, macrophages are also found occasionally in the central cornea, with a possible origin in the bone marrow as well as in the yolk sac. Nonetheless, the normal central cornea is devoid of MHC II^+ cells (70, 77).

CORNEAL HEM- AND LYMPHANGIOGENIC PRIVILEGE

In most tissues and organs, blood and lymphatic vascular systems are essential to supply organs and tissues with oxygen and nutrients, to drain redundant fluid and metabolites and to support the immune system to protect the body against foreign organisms (78, 79). However, there are some tissues that do not rely on the presence of blood and/or lymphatic vessels to maintain their unique structure and fulfill their function. The cornea is one of these rare tissues that actively maintains an avascular state, which is called "corneal (lymph)angiogenic privilege" (80) (**Figure 1A**). In general, it seems that the maintenance of corneal avascularity does not only occur as a result of the upregulation of anti-angiogenic factors, but also from the downregulation of pro-angiogenic factors in the healthy cornea (81). It has been shown in this context, that the balance between angiogenic and anti-angiogenic factors especially in the corneal epithelium plays an important role in corneal avascularity (82–84). This includes the pro-angiogenic factors fibroblast growth factor-2 (FGF-2), vascular endothelial growth factor (VEGF) and the transforming growth factor-α (TGF-α) (85, 86), as well as the anti-angiogenic factors including endostain (87), thyrosinase (88), semaphorin 3F (89), angiostatin (90) and thrombospondin (TSP-1) (91–96). TSP-1, an anti-angiogenic, multifunctional extracellular matrix protein, plays an interesting role in the lymphangiogenic privilege of the cornea. It was shown that aged (6-month-old) TSP $1^{-/-}$ mice develop a spontaneous ingrowth of lymphatic vessels into the cornea, which was also shown in mice lacking the TSP-1 receptor CD36 (95). Mechanistically, it was demonstrated that TSP-1 down-regulates the expression of VEGF-C *via* CD36 in macrophages, proposing that macrophages are involved in the maintenance of the lymphangiogenic privilege of the cornea (95). Additionally, factors which can act pro- as well as anti-angiogenic are also present in the cornea, including TGF-β (97–99). It was further demonstrated that corneal avascularity is dependent on the expression of soluble VEGF receptor 1 (sVEGFR-1) in the corneal epithelium (100). The lack of sVEGFR-1, which serves as an endogenous VEGF−A trap (101), abolishes corneal avascularity in mice (100). A further crucial regulator of lymphatic vessel growth is sVEGFR-2, which inhibits lymphangiogenesis by blocking VEGF−C function (102). Further studies showed that also sVEGFR-3 is expressed in the cornea and is essential for corneal alymphaticity (103). This protein binds and sequesters VEGF-C, thereby blocking signaling through VEGFR-3 and suppressing lymphangiogenesis induced by VEGF-C. The knockdown of sVEGFR-3 leads to neovascularization in the mouse cornea. In contrast, the overexpression of sVEGFR-3 inhibits neovascularization in a murine suture injury model (103). Membrane-bound VEGFR-3 is also strongly constitutively expressed by the corneal epithelium and is mechanistically responsible for suppressing inflammatory corneal hem- and lymphangiogenesis (104).

Additionally, the corneal (lymph)angiogenic privilege is provided by the special anatomy of the cornea, which ensures a constant dehydration, resulting in periodically ordered, tightly packed collagen lamellae and a compact keratocyte network. The periodicity is highly dependent on the state of stromal hydration. In case of stromal edema, the compactness of the stroma is disturbed and therefore vessels can easier grow in-between the

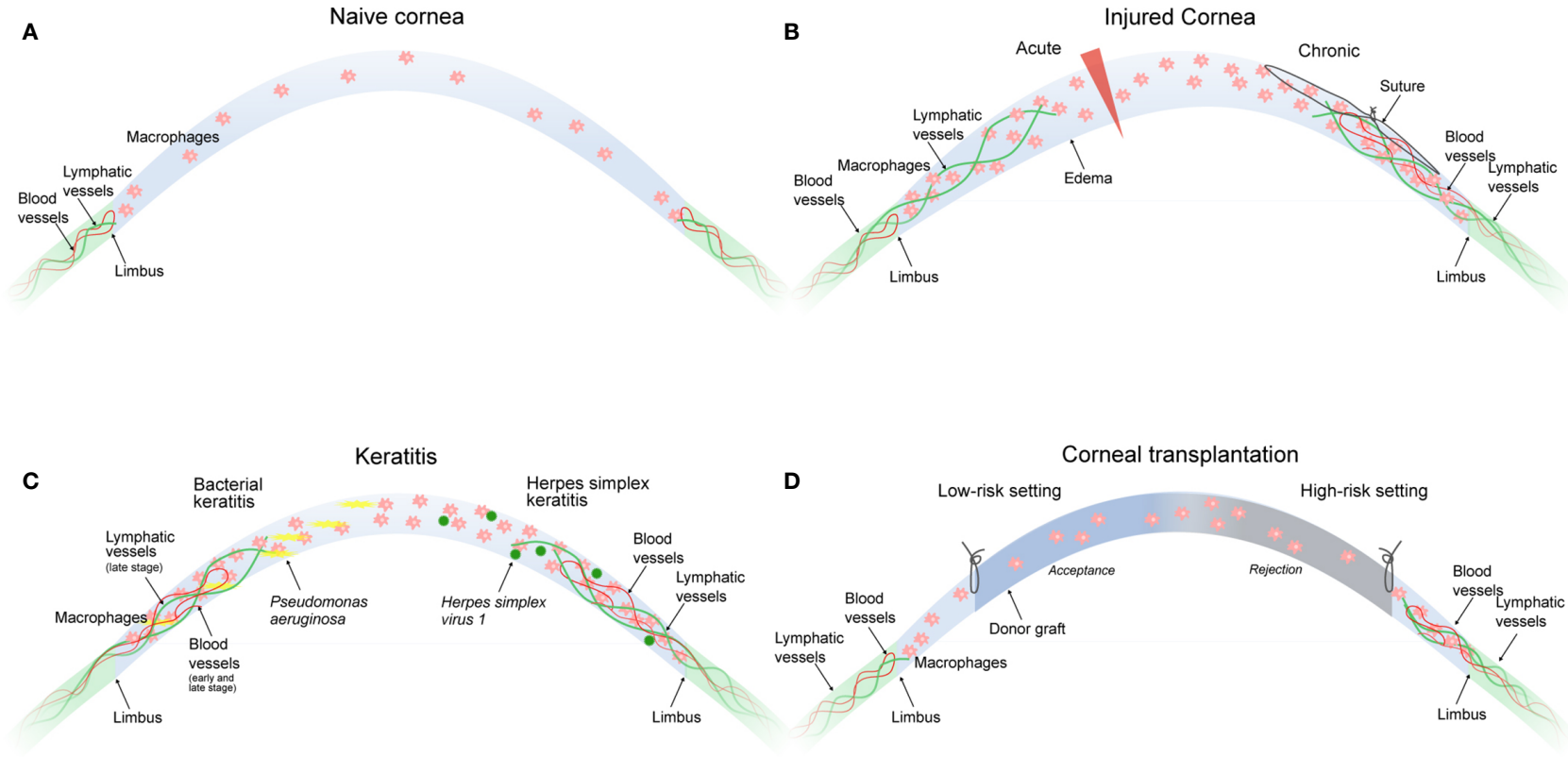

FIGURE 1 | Macrophages in corneal neovascular disease. **(A)** The naive cornea is devoid of blood and lymphatic vessels. Few immune cells including macrophages are present in the peripheral cornea and to a lesser extent in the central cornea. **(B)** An acute incisional injury (left) leads to the ingrowth of lymphatic, but not blood vessels. A chronic injury (suture placement, right) leads to the ingrowth of blood and lymphatic vessels. Corneal neovascularization in both injury models critically depends on the presence of corneal macrophages. **(C)** Bacterial keratitis (left) leads to ingrowth of blood vessels in the early and late stage of infection, whereas lymphatic vessels only appear in the late stage of infection. Both are critically dependent on the presence of corneal macrophages. HSV-1 keratitis (right) leads to the ingrowth of blood and lymphatic vessels independently of the presence of corneal macrophages. **(D)** The low-risk corneal transplantation setting (left) without pre-existent corneal neovascularization usually does not result in graft rejection, whereas the high-risk corneal transplantation setting (right) with pre-existent blood and lymphatic vessels is likely to result in graft rejection. Macrophage depletion significantly improves graft survival. All settings **(B–D)** result in the accumulation of corneal macrophages.

lamellae (105, 106). However, in early studies it was shown, that corneal swelling can occur without vascularization (107). Currently, it is thought that also the limbus may act as a physical and physiological barrier to invading vessels in the immediate vicinity and might also prevent an overgrowth of the cornea with conjunctival epithelial cells (108–112). Disturbances of limbal stem cells for example by UV-light may also deregulate the (lymph)angiogenic privilege of the cornea (113). However, other studies question the concept of the limbal barrier to corneal vascularization as the basis of corneal angiogenic privilege (81, 114).

Besides being a (lymph)angiogenic privileged tissue, it is well established that the cornea is also an immune-privileged tissue (115). Anterior chamber-associated immune deviation (ACAID) is an example for this immune privilege, which partially depends on an eye-derived, suppressor-inducing macrophage subset that acts through NK cells (116, 117) and suppresses antigen-specific, delayed-type hypersensitivity (DTH) (118). It was shown that corneal immune privilege is co-responsible for the (lymph) angiogenic privilege of the cornea (119). Interestingly, several molecules are involved in maintaining both corneal angiogenic and immune privilege such as the thrombospondins (95, 96).

Due to the here described (lymph)angiogenic privilege, corneal wound healing after (minor) injury usually takes place without any neovascularization. However, after severe injury, e.g. as a result of trauma, infection, and inflammatory or degenerative disorders, the (lymph) angiogenic privilege of the cornea might be overwhelmed ("threshold concept"), leading to the invasion of blood and/or lymphatic vessels into the cornea (corneal neovascularization).

CORNEAL NEOVASCULARIZATION IN PATHOLOGY AND DISEASE

Breakdown of Corneal (Lymph) Angiogenic Privilege

Corneal avascularity is highly important for the maintenance of corneal transparency, ensuring the basis of good visual acuity. However, a variety of diseases and surgical manipulations can lead to the breakdown of the hem- and lymphangiogenic privilege of the cornea resulting in pathological corneal hem- and lymphangiogenesis. Diseases that can be associated with corneal neovascularization include inflammatory disorders, corneal graft rejection after transplantation, infectious keratitis, contact lens-related hypoxia, alkali burns, stromal ulceration, or limbal stem cell deficiency. In these conditions, the balance between pro-angiogenic and anti-angiogenic factors is disturbed and leads to an upregulation of pro-angiogenic factors, and a downregulation of anti-angiogenic factors followed by neovascularization (120–122). Blood vessels directly reduce corneal transparency if growing into the optical zone or due to secondary effects such as hemorrhage and lipid exudation through immature and leaky capillaries. Unlike blood vessels, clinically invisible lymphatic vessels do not reduce the transparency of the cornea. However, they contribute to various inflammatory diseases of the ocular surface, including corneal transplant rejection, dry eye disease (DED) and ocular allergy (7, 123). In those diseases, the corneal lymphatic vessels facilitate the migration of APC from the ocular surface to the regional lymph nodes, which induces undesired immune responses (124–126). On the other hand, lymphatics may also be involved in draining excess tissue fluid thus contributing to corneal transparency and vision (9).

Role of Macrophages in Corneal Neovascularization

Macrophages play a pivotal role in corneal neovascularization. Macrophages are able to secrete paracrine factors, such as VEGF-A, which promotes hem- and lymphangiogenesis by binding on VEGFR-2 (2), and VEGF-C and VEGF-D, which promote lymphangiogenesis by binding to VEGFR-3 (127, 128). In addition, macrophages also express VEGFR-1 and VEGFR-3 which both may mediate chemotactic effects in myeloid cells and thereby perpetuate an inflammatory hem- and lymphangiogenic response ("immune amplification") (2). Notably, so far it is not reported in the literature whether macrophage-derived VEGF-A is critical for corneal vascularization, and it is unclear by which other mediator macrophages precisely might mediate corneal vascularization. Besides secreting lymphangiogenic and angiogenic growth factors (2), macrophages also directly contribute to corneal lymph vessel formation by integrating into newly formed corneal lymphatic vessels (3). That means macrophages have a dual important role in mediating corneal lymphangiogenesis (129). Furthermore, macrophages seem to be essential also for maintenance of (corneal) lymphatics (130). It was shown that depletion of macrophages significantly reduces corneal hem- and lymphangiogenesis (2, 131, 132). Recent studies have also identified distinct functions of early- versus late-phase corneal wound macrophages in hem- and lymphangiogenesis: whereas early-phase wound macrophages are essential for the initiation and progression of injury-mediated corneal hem- and lymphangiogenesis, late-phase wound macrophages control the maintenance of established corneal lymphatic vessels, but not blood vessels (10, 11). Furthermore, studies indicate that the type of corneal damage controls the hem- and lymphangiogenic potential of corneal macrophages: whereas an acute perforating incision injury induced wound macrophages with lymphangiogenic, but not hemangiogenic potential with an increased expression of VEGF-C and D, suture placement into the corneal stroma provoked wound macrophages with hem- and lymphangiogenic potential (**Figure 1B**). Interestingly, in a model of *Pseudomonas aeruginosa*-induced bacterial keratitis, corneal hemangiogenesis was induced in early as well as late stages, whereas lymphangiogenesis was induced solely in late stages, which was strongly dependent on corneal macrophages (**Figure 1C**) (10). Taken together, the hem- and lymphangiogenic potential of corneal wound macrophages is determined by the type of the corneal damage and the phase of corneal injury (11). However, based on currently available data, it seems not possible to speculate or conclude whether different macrophage populations or different

activation phenotypes are separately regulating corneal hem- and/or lymphangiogenesis.

Another possibility of macrophages promoting hemangiogenesis is VEGF-independent, as macrophages might act as bridge cells on the tips of sprouting lymphatics guiding the cells into finding and anastomosing with tip cells from other sprouting lymphatics (133, 134). However, this pathway has not been shown for corneal neovascularization so far.

It should be noted that corneal neovascularization might also occur independent of macrophages. An example is corneal lymphangiogenesis induced by Herpes simplex virus 1 (HSV-1) (135). It was shown in this context that lymphangiogenesis depends on VEGF-A/VEGFR-2 signaling but not on VEGFR-3 ligands. Importantly, macrophages were not the source of VEGF-A and did not play a role in the induction of the lymphangiogenic response. Infected epithelial cells were discovered as the primary source of VEGF-A in this model, suggesting that HSV-1 directly induces vascularization of the cornea through up-regulation of epithelial VEGF-A expression and not *via* macrophages (**Figure 1C**).

We have recently demonstrated an important role of Interleukin-10 (IL-10)-activated macrophages in inflammatory corneal neovascularization. In particular, we could show that the multifunctional cytokine IL-10, which acts anti-inflammatory as well as immune-regulatory, controls the corneal lymphangiogenesis and the resolution of corneal inflammation *via* macrophages (8). In healthy corneas, the expression of IL-10 was unverifiable, however macrophages which infiltrated inflamed corneas after corneal injury showed a strong increase in IL-10 expression. *In vitro* stimulation of macrophages with IL-10 led to an anti-inflammatory, but surprisingly pro-lymphangiogenic phenotype, characterized by an upregulation of VEGF-C. In IL-10 deficient mice, corneal injury resulted in both reduced expression of VEGF-C and reduced corneal lymphangiogenesis. However, the loss of IL-10 had no effect on corneal hemangiogenesis (8). The deletion of the central mediator of IL-10 signaling, Signal transducer and activator of transcription 3 (Stat3), specifically in myeloid cells resulted in reduced corneal lymphangiogenesis and persistent corneal inflammation in injured corneas, reinforcing the critical role of IL-10^{+} macrophages in the regulation of corneal lymphangiogenesis and inflammation (8). These findings indicate that IL-10 leads to an anti-inflammatory but pro-lymphangiogenic VEGF-C secreting macrophage phenotype during an inflammatory corneal response. These macrophages can induce the activation and growth of lymphatic vessels, leading to an egress of inflammatory cells and the termination of the local inflammatory response (8).

Role of Specific Macrophage Subpopulations in Corneal Neovascularization

Not much is known about the role of specific macrophage subpopulations during corneal neovascularization. In a mouse model with either a knockout of CCR2 or CX3CR1, or a macrophage depletion model, corneal neovascularization was induced by alkali injury (136). It was shown in this model that CCR2-deficient mice exhibited reduced corneal neovascularization with reduced macrophage infiltration, whereas corneal neovascularization in CX3CR1-deficient mice was increased with reduced macrophage infiltration. Macrophage depletion did not affect corneal neovascularization, which is in contrast to other studies showing that macrophage depletion inhibits corneal neovascularization (2, 11). It should also be noted that this study only assessed corneal hemangiogenesis and did not analyze corneal lymphangiogenesis (136).

Corneal Transplantation and the Role of Macrophages in Transplant Rejection

Corneal transplantation (keratoplasty) is the most frequently performed form of transplantation worldwide, with more than 100.000 transplants per year (137). Due to the immunological privilege of the cornea, keratoplasty usually results in good transplantation outcomes (138, 139).

This immunological privilege of the cornea actively suppresses immune responses against the allograft, enabling the transplantation of HLA-mismatched corneal grafts without the need of systemic immunosuppression (119, 140). However, the immunological privilege of the cornea is not invulnerable. In this regard, it has been shown that e.g. severe inflammation can overcome the immunosuppressive mechanisms of the cornea and results in an immunological scenario similar to solid organ transplantation, where e.g. HLA-matching and systemic immunosuppression are necessary to avoid immune-mediated allograft rejection (140–142). Thus, in eyes with compromised immunological privilege graft failure caused by immune rejection continues to be a major barrier to transplantation success. Keratoplasty can thus be divided into two risk categories dependent on the immunological status of the host cornea. In the so-called low-risk setting, the immunological privilege of the cornea is intact and graft rejection is unlikely. In contrast, in the high-risk setting, the immunological privilege of the cornea is lost, and the risk of graft rejection is significantly increased (**Figure 1D**) (141, 143). It is now widely accepted that the vascularization status of the cornea is the most important factor defining the low- or high-risk status of the host. Avascular hosts are generally considered as low-risk hosts, whereas vascularized hosts are generally considered as high-risk hosts. In this regard, it has been demonstrated that preexistent pathological lymphatic vessels facilitate trafficking of APCs from the graft site to regional draining lymphoid tissues where APCs can then present alloantigens to host T cells. In fact, in the murine model of corneal transplantation it was clearly shown that lymphatic and not blood vessels determine the high-risk state of neovascularized recipient beds (124). Pathological preexistent blood vessels then facilitate the homing of primed effector T cells to the graft site where allorejection is mediated (141).

Early research in rat eyes have demonstrated reduced rejection rates of corneal transplants after depletion of macrophages, demonstrating the crucial role of macrophages in corneal transplantation (131, 144). In this study, all transplants in the control group were rejected within 17 days,

whereas the transplants in macrophage-depleted eyes were not rejected during the entire follow-up period over 100 days post transplantation. Additionally, a reduced vascular response in clodronate-treated recipient corneas was observed, indicating that a positive graft outcome might (indirectly) depend on corneal vessels (145). In a pre-vascularized high-risk transplantation model, depletion of macrophages did not fully prevent, but significantly delayed graft rejection (146). Additionally, corneal neovascularization was significantly reduced after macrophage depletion in this model (131). It was also shown that the depletion of macrophages results in a strongly downregulated local and systemic immune response after transplantation (144). Additionally, large numbers of $CD11b^+$, $F4/80^+$ and $iNOS^+$ (inducible nitrous oxide synthase) macrophages infiltrated corneal allografts during rejection in mice, indicating that these cells might directly contribute to corneal graft rejection (147). As the use of clodronate liposomes to deplete macrophages may also affect APCs like DCs (148, 149), the conclusions regarding the role of macrophages indicated by these experiments have to be drawn with caution, because the findings may also be indirectly caused by the affection of other cell types.

The gold standard to prevent or treat corneal graft rejection is the application of glucocorticosteroids (150, 151). The treatment with glucocorticosteroids leads to decreased corneal infiltration of macrophages and reduced expression of pro-inflammatory cytokines, such as TNF-α and IL-1β (152). Furthermore, glucocorticosteroids also significantly reduce progressive corneal hem- and lymphangiogenesis, which likely contributes to reduced rejection rates (152). A recent study showed that the topical application of VEGF-C and VEGF-C prevents the in growth of lymphatic vessels into the murine cornea after suture-placement in a high-risk corneal transplantation model (153). Further it was shown that the topical application of VEGF-C and VEGF-D increases the number of macrophages, together with a decreased expression of the anti-inflammatory macrophage marker Arginase-1, as well as of the immune modulatory cytokine TGF-β (153). Moreover, it was shown, that corneal crosslinking with UVA light together with riboflavin leads to a regression of preexisting blood and lymphatic vessels significantly *via* induction of apoptosis in vascular endothelial cells with a reduced number of macrophages and $CD45^+$ cells (154).

In summary, modulation of corneal macrophages does not only alter the inflammatory and cellular milieu in transplanted corneas, but also affects corneal neovascularization (131). Thus, the beneficial effect of macrophage depletion on graft survival may be attributable to diminished corneal neovascularization. The effect of a modulation of macrophage function without altering the corneal vascular response in the context of transplantation was not shown yet.

Novel Beneficial Functions of Macrophage-Mediated Corneal Lymphangiogenesis in the Regulation of Corneal Edema and Transparency

Outside the eye, e.g. in the skin, it is well-established that lymphatic vessels regulate tissue pressure, allow fluid drainage and prevent the development of edema (155). However, so far it remained elusive, whether lymphatic vessels have similar functions in the cornea and are involved in the regulation of edema and transparency. Recently, we have therefore investigated whether an incisional corneal injury that leads to acute corneal edema and transparency loss is accompanied by the ingrowth of lymphatic vessels into the cornea and whether corneal lymphangiogenesis potentially contributes to the healing response. This type of corneal injury indeed resulted in a transient ingrowth of lymphatic vessels into the cornea (9). Importantly, blockade of lymphangiogenesis resulted in increased corneal thickness, arguably due to delayed drainage of corneal edema, and a trend towards prolonged corneal opacification (9). Corneal lymphangiogenesis after this type of corneal injury was dependent on the presence of macrophages, as macrophage depletion using clodronate liposomes significantly reduced corneal lymphangiogenesis (11). This study indicates that corneal lymphangiogenesis plays an important role in the regulation of corneal edema and transparency, and is also in line with the finding that corneal lymphangiogenesis may be beneficial in bacterial keratitis by improving corneal edema in later disease stages (10). Whether this holds true also for chronic forms of (mild) corneal edema needs to be studied. That would open completely new therapeutic options for common diseases leading to corneal transplantation.

SIMILARITIES AND DIFFERENCES OF MACROPHAGE-MEDIATED NEOVASCULARIZATION IN CORNEA AND SKIN

Both cornea and skin are protective barrier organs that shield the body from harmful insults of the environment. The skin consists of the epidermis, the dermis and the dermal white adipose tissue. In contrast to the avascular cornea, skin contains in the steady state an interwoven network of blood and lymphatic vessels, in which diverse leukocyte subsets such as dermal dendritic cells, T cells, and macrophages are embedded (156). Studies in *PU.1*$^{-/-}$ mice, in which the myeloid cell lineage is severely impaired and which lack skin resident $F4/80^+$ myeloid cells, revealed that macrophages are dispensable in developing skin vasculature (157, 158). However, macrophages critically regulate pericyte development in the skin and the dermal lymphatic vessel caliber, as shown in both, macrophage deficient *PU.1*$^{-/-}$ and *Csf1r*$^{-/-}$ mice (158, 159)

Based on their spatial relationship to dermal vessels, skin-resident macrophages were defined as perivascular (direct contact with vessel or < 15 μm from vessel) or interstitial macrophages (> 15 μm from vessel) (156, 160). In human skin the proportion of perivascular macrophages (PVMs) increases from the apical towards the deep dermis (156). PVMs are considered to have maintenance functions in steady state tissues, such as regulating vascular permeability and scavenging blood-derived pathogens (160). Under inflammatory conditions

PVMs have been shown to guide neutrophils during extravasation into infected dermis and to regulate dendritic cell clustering in perivascular areas (161, 162). Interestingly, a subset of skin PVMs has been identified, which protrudes across endothelial junctions into microvessels in order to take up macromolecules from the blood stream (163).

Comparable to the inflamed cornea, macrophages have a critical function in regulating neovascularization in skin under inflammatory conditions. Vascularization upon skin injury and during the wound healing response is a useful experimental model to study the molecular basis of neovascularization (164). Upon skin injury a high number of myeloid cells is recruited from the blood and forms together with mainly fibroblasts, myofibroblasts and endothelial cells a highly vascularized granulation tissue within several days (165). In this model, angiogenesis is at the core of an efficient repair response and critical for timely wound closure. With time, inflammation declines, and the granulation tissue matures into scar tissue, characterized by regression of blood and lymph vessels (29, 166). By using mouse models of diphtheria toxin-inducible cell depletion, several groups provided evidence that angiogenesis in the developing granulation tissue requires myeloid cells (167–169). Similar to the cornea, early-phase wound macrophages in skin wounds were shown to be essential for the initiation of wound vascularization (11, 167). Specifically, myeloid cell–derived VEGF–A was shown to be critical for the induction of wound angiogenesis and tissue growth during the early phase of skin repair (29). While the role of specific macrophage populations in corneal neovascularization is not entirely resolved, blood-derived inflammatory $CCR2^{+}Ly6C^{high}$ monocytes/macrophages were identified as the critical source of VEGF–A in skin wounds (29).

The Role of HIF During Macrophage-Mediated Vascularization in Skin and Cornea

A major transcription factor, which is stabilized during physiological skin wound healing and which is required for the induction of *Vegfa*, is Hypoxia-Inducible Factor 1 α (HIF-1α) (170, 171). Stabilization of HIF-1α is impaired in a diabetic environment and in aged mice, conditions with a typically impaired wound healing response. Interestingly, angiogenesis and wound closure are improved in diabetic mice when HIF-1α is stabilized (170–174). Up to date, in classic repair models in the cornea (e.g. corneal incision injury, suture-induced corneal neovascularization) a functional impact of HIF-1α stabilization on neovascularization and repair has not been described. Of note, in a mouse model of corneal HSV−1 infection, hypoxia in the cornea and subsequent stabilization of HIF-1α in immune cells has been shown (175). However, whether HIF-1α is activated specifically in macrophages and whether this has a functional impact in this infection model, remains open. Chen et al. could show an inhibition of VEGF expression and corneal neovascularization by shRNA targeting HIF-1α in a mouse model of closed eye contact lens wear (176). In skin, wound healing studies using mouse models with cell type-specific *Hif1a* gene deletion revealed that endothelial cell-, fibroblast-, and epidermis-specific HIF-1α are critical for *Vegfa* expression, angiogenesis, and timely wound closure (177–179). However, direct evidence that myeloid cell-derived *Vegfa* expression depends on HIF-1α activation in early phase wound macrophages is lacking. Yet, the critical role of HIF-1α in regulating *Vegfa* expression in macrophages and the inflammatory phenotype of skin macrophages is well documented (180), proposing that HIF-1α might regulate *Vegfa* expression in early phase wound macrophages. Both, hypoxia and inflammatory stimuli such as TNF-α, IL-1β, and bacterial products have been shown to stabilize HIF-1α in a NF-κB (nuclear factor kappa-light-chain-enhancer of activated B cells)-dependent manner (181, 182). Interestingly, by day 1 after injury the wound tissue was shown to be normoxic, while macrophages already expressed *Vegfa* (183), indicating that in the very early phase of healing other signals than hypoxia might induce an angiogenic phenotype in macrophages. Recently, mitochondrial metabolism has been identified as critical regulator of HIF-1α activation in macrophages *in vitro*. Under inflammatory conditions, macrophages repurpose their mitochondria from ATP production towards production of mitochondrial reactive oxygen species (mtROS), which stabilize HIF-1α independently of hypoxia (184). In future studies it will be interesting to understand whether mtROS operate in wound macrophages to mediate the wound angiogenic response.

Macrophage-Mediated Lymphangiogenesis in the Skin

As revealed by imaging of lymphatic vessels in Vegfr3 reporter mice (*Vegfr3*^{EGFPLuc}), lymphangiogenesis is a transient process during skin wound healing, peaking in the mid-phase of healing and returning back to basal levels after re-epithelialization is completed (166). In experimental mouse models of skin wound healing and contact hypersensitivity, treatment with the synthetic glucocorticoid dexamethasone blocks lymphangiogenesis, showing that lymphangiogenesis is tightly connected with the inflammatory response in the skin (166). A similar finding was reported in corneal repair; after suture placement in the cornea corticosteroids were identified as strong inhibitors of corneal lymphangiogenesis (152). Furthermore, by phase-specific macrophage depletion our group has shown that in the injured cornea early-phase macrophages are essential for initiation of lymphangiogenesis (11). Yet, the assessment of lymphangiogenesis in skin wounds upon diphtheria toxin-mediated macrophage ablation is lacking (11, 167–169). However, similar to the inflamed cornea, independent groups identified $F4/80^{+}$/LYVE-1^{+} lymphatic structures in early granulation tissue after excisional punch injury, indicating that macrophages contribute to lymphatic vessels during physiological skin repair (185, 186). The crucial function of macrophages in regulating lymphangiogenesis in skin wounds was further demonstrated by treating wounds of diabetic mice with IL-1β-activated macrophages, which resulted in the formation of granulation tissue and of new $F4/80^{+}$/LYVE-1^{+} lymphatic vessel structures (186). Further,

macrophages are well-known sources of lymphangiogenic paracrine factors. The critical impact of macrophage-derived VEGF-A, VEGF-C, and VEGF-D on lymphangiogenesis was shown by Kataru et al. in an ear skin inflammation model (187). Following the intradermal injection of Toll-like receptor (TLR) ligands, depletion of macrophages by clodronate or blockade of VEGF−A or VEGF−C/D resulted in significantly attenuated lymphangiogenesis in the inflamed skin and impaired inflammation resolution (187). Expression of *Vegfc* in skin macrophages has been shown to be controlled by the transcription factor tonicity-responsive enhancer-binding protein (TonEBP, also known as NFAT5) (188). In this study, deletion of *Nfat5* specifically in myeloid cells prevented high salt diet-induced *Vegfc* expression and subsequently lymphangiogenesis in the skin (188). Interestingly, in a mouse model of bacterial skin infection it was found that salt accumulated at the site of the skin lesion drives inflammatory macrophage activation *via* TonEBP to facilitate pathogen removal (189). Whether myeloid cell-specific TonEBP has a function during skin and corneal repair is unknown. It will be interesting to study in the future the interrelationship between salt concentrations, TonEBP activation, lymphangiogenesis, and macrophage activation in both tissues.

CONCLUSIONS AND PERSPECTIVES

Macrophages originating either from HSCs or the yolk sack, can act inflammatory as well as anti-inflammatory, characterized by their surface marker expression. In the eye, several studies have demonstrated, that resident tissue macrophages as well as APCs are present in most tissues of the eye, including the corneal limbus. Although, the cornea is an immune-privileged tissue, macrophages are also present in the cornea, preferable in the periphery of the corneal stroma. However, macrophages are also found occasionally in the central cornea, with a possible origin in the bone marrow as well as in the yolk sac. Nonetheless, the normal central cornea is devoid of MHC II^+ cells.

The healthy cornea is one of the rare avascular tissues of the organism, following the "corneal (lymph)angiogenic privilege", which is actively maintained by the balanced expression of pro- and anti-angiogenic factors. Is this equilibrium somehow disturbed (e.g. in infectious keratitis, stromal ulceration, or limbal stem cell deficiency), the imbalance of these factors leads to a pathological vascularization of the cornea, often mediated by macrophages that secrete paracrine factors, such as VEGF-A promoting hem- and lymphangiogenesis, and VEGF-C and VEGF-D specifically promoting lymphangiogenesis. Additionally, the expression of VEGFR-1 and VEGFR-3 mediates chemotactic effects and perpetuates an inflammatory hem- and lymphangiogenic response. However, not much is known about the role of specific macrophage subpopulations during corneal neovascularization and the available data is still ambiguous. Recently, factors like IL-10 found their way into corneal neovascularization research by acting anti-inflammatory as well as immune-regulatory and by controlling corneal lymphangiogenesis and the resolution of corneal inflammation *via* macrophages. In corneal transplantation, graft survival can be increased by depleting corneal macrophages, which may also be attributable to diminished corneal neovascularization.

Outside the eye, e.g. in the skin, it is well-established that lymphatic vessels regulate tissue pressure, allow fluid drainage and prevent the development of edema. Not much is known about a similar concept in the cornea, but we recently demonstrated increased corneal thickness after blockade of lymphangiogenesis in an acute corneal wound model. If this might also be true for chronic forms of (milder) corneal edema, it would open new therapeutic options for common edematous corneal diseases necessitating corneal transplantation.

In contrast to the avascular cornea, the skin contains in the steady state an interwoven network of blood and lymphatic vessels containing various types of immune cells, including macrophages. Under inflammatory conditions, macrophages have a comparable, critical function in regulating neovascularization in skin and cornea. Similar to the cornea, early-phase wound macrophages in skin wounds were shown to be essential for the initiation of wound vascularization. In contrast to the role of specific macrophage populations in corneal neovascularization, it was shown, that blood-derived inflammatory $CCR2^+Ly6C^{high}$ monocytes/macrophages act as the critical source of VEGF−A in skin wounds. In contrast to corneal wound healing, in skin HIF-1α is an important transcription factor which is required for the induction of *Vegfa*. However, it should be mentioned, that stabilization of HIF-1α in immune cells has been shown in a mouse model of corneal HSV−1 infection. The use of glucocorticoids blocks lymphangiogenesis, which is similar in the skin and the cornea. Phase-specific macrophage depletion studies have shown that in the injured cornea early-phase macrophages are essential for initiation of lymphangiogenesis. By now, this information for skin is lacking, whereas it is known, that macrophages play a crucial role in lymphangiogenesis during skin repair by the expression of VEGF-C. One transcription factor acting as an inducer for VEGF-C in macrophages is TonEBP. However, whether TonEBP plays also a crucial role during lymphangiogenesis during corneal wound repair is still unknown.

AUTHOR CONTRIBUTIONS

Writing—original draft preparation, KH, SW. Writing—review and editing, FB, CC, SE, DH. Funding acquisition, FB, CC, SE, DH. All authors contributed to the article and approved the submitted version.

FUNDING

Financial Support: German Research Foundation (DFG): FOR2240 "(Lymph)angiogenesis and Cellular Immunity in Inflammatory Diseases of the Eye", Cu 47/4-2 (CC), Cu 47/6-1

(CC), Cu 47/9-1 (CC), Cu 47/12-2 (CC), HO 5556/1-2 (DH), EM 48/5-2 (SAE), BO4489/1-1 (FB), BO4489/1-2 (FB), BO4489/3-1 (FB) (www.for2240.de); CRC829 project ID 73111208 (SAE), CRC1403 project ID 1403–414786233 (SAE), FOR2599 project ID 3927 49992 (SAE), Germany's Excellence Strategy – CECAD, EXC 2030 - 390661388 (SAE). Center for Molecular Medicine Cologne (SAE, DH, CC). EU COST CA18116 (CC; www.aniridia-net.eu).

REFERENCES

1. Gordon S, Pluddemann A. Tissue macrophages: heterogeneity and functions. *BMC Biol* (2017) 15(1):53. doi: 10.1186/s12915-017-0392-4
2. Cursiefen C, Chen L, Borges LP, Jackson D, Cao J, Radziejewski C, et al. VEGF-A stimulates lymphangiogenesis and hemangiogenesis in inflammatory neovascularization via macrophage recruitment. *J Clin Invest* (2004) 113(7):1040–50. doi: 10.1172/JCI20465
3. Maruyama K, Ii M, Cursiefen C, DG J, Keino H, Tomita M, et al. Inflammation-induced lymphangiogenesis in the cornea arises from CD11b-positive macrophages. *J Clin Invest* (2005) 115(9):2363–72. doi: 10.1172/JCI23874
4. Chung ES, Chauhan SK, Jin Y, Nakao S, Hafezi-Moghadam A, van Rooijen N, et al. Contribution of macrophages to angiogenesis induced by vascular endothelial growth factor receptor-3-specific ligands. *Am J Pathol* (2009) 175(5):1984–92. doi: 10.2353/ajpath.2009.080515
5. Minutti CM, Modak RV, Macdonald F, Li F, Smyth DJ, Dorward DA, et al. A Macrophage-Pericyte Axis Directs Tissue Restoration via Amphiregulin-Induced Transforming Growth Factor Beta Activation. *Immunity* (2019) 50 (3):645–54 e6. doi: 10.1016/j.immuni.2019.01.008
6. Cursiefen C, Schlotzer-Schrehardt U, Kuchle M, Sorokin L, Breiteneder-Geleff S, Alitalo K, et al. Lymphatic vessels in vascularized human corneas: immunohistochemical investigation using LYVE-1 and podoplanin. *Invest Ophthalmol Vis Sci* (2002) 43(7):2127–35.
7. Bock F, Maruyama K, Regenfuss B, Hos D, Steven P, Heindl LM, et al. Novel anti(lymph)angiogenic treatment strategies for corneal and ocular surface diseases. *Prog Retin Eye Res* (2013) 34:89–124. doi: 10.1016/j.preteyeres.2013.01.001
8. Hos D, Bucher F, Regenfuss B, Dreisow ML, Bock F, Heindl LM, et al. IL-10 Indirectly Regulates Corneal Lymphangiogenesis and Resolution of Inflammation via Macrophages. *Am J Pathol* (2016) 186(1):159–71. doi: 10.1016/j.ajpath.2015.09.012
9. Hos D, Bukowiecki A, Horstmann J, Bock F, Bucher F, Heindl LM, et al. Transient Ingrowth of Lymphatic Vessels into the Physiologically Avascular Cornea Regulates Corneal Edema and Transparency. *Sci Rep* (2017) 7 (1):7227. doi: 10.1038/s41598-017-07806-4
10. Narimatsu A, Hattori T, Koike N, Tajima K, Nakagawa H, Yamakawa N, et al. Corneal lymphangiogenesis ameliorates corneal inflammation and edema in late stage of bacterial keratitis. *Sci Rep* (2019) 9(1):2984. doi: 10.1038/s41598-019-39876-x
11. Kiesewetter A, Cursiefen C, Eming SA, Hos D. Phase-specific functions of macrophages determine injury-mediated corneal hem- and lymphangiogenesis. *Sci Rep* (2019) 9(1):308. doi: 10.1038/s41598-018-36526-6
12. van Furth R, Sluiter W. Distribution of blood monocytes between a marginating and a circulating pool. *J Exp Med* (1986) 163(2):474–9. doi: 10.1084/jem.163.2.474
13. Geissmann F, Jung S, Littman DR. Blood monocytes consist of two principal subsets with distinct migratory properties. *Immunity* (2003) 19(1):71–82. doi: 10.1016/s1074-7613(03)00174-2
14. Auffray C, Sieweke MH, Geissmann F. Blood monocytes: development, heterogeneity, and relationship with dendritic cells. *Annu Rev Immunol* (2009) 27:669–92. doi: 10.1146/annurev.immunol.021908.132557
15. Bertrand JY, Kim AD, Violette EP, Stachura DL, Cisson JL, Traver D. Definitive hematopoiesis initiates through a committed erythromyeloid progenitor in the zebrafish embryo. *Development* (2007) 134(23):4147–56. doi: 10.1242/dev.012385
16. Bertrand JY, Jalil A, Klaine M, Jung S, Cumano A, Godin I. Three pathways to mature macrophages in the early mouse yolk sac. *Blood* (2005) 106 (9):3004–11. doi: 10.1182/blood-2005-02-0461
17. Stremmel C, Schuchert R, Wagner F, Thaler R, Weinberger T, Pick R, et al. Yolk sac macrophage progenitors traffic to the embryo during defined stages of development. *Nat Commun* (2018) 9(1):75. doi: 10.1038/s41467-017-02492-2
18. Schulz C, Gomez Perdiguero E, Chorro L, Szabo-Rogers H, Cagnard N, Kierdorf K, et al. A lineage of myeloid cells independent of Myb and hematopoietic stem cells. *Science* (2012) 336(6077):86–90. doi: 10.1126/science.1219179
19. Gomez Perdiguero E, Klapproth K, Schulz C, Busch K, Azzoni E, Crozet L, et al. Tissue-resident macrophages originate from yolk-sac-derived erythro-myeloid progenitors. *Nature* (2015) 518(7540):547–51. doi: 10.1038/nature13989
20. Hoeffel G, Chen J, Lavin Y, Low D, Almeida FF, See P, et al. C-Myb(+) erythro-myeloid progenitor-derived fetal monocytes give rise to adult tissue-resident macrophages. *Immunity* (2015) 42(4):665–78. doi: 10.1016/j.immuni.2015.03.011
21. Liu J, Xue Y, Dong D, Xiao C, Lin C, Wang H, et al. CCR2(-) and CCR2(+) corneal macrophages exhibit distinct characteristics and balance inflammatory responses after epithelial abrasion. *Mucosal Immunol* (2017) 10(5):1145–59. doi: 10.1038/mi.2016.139
22. Mantovani A, Sica A, Sozzani S, Allavena P, Vecchi A, Locati M. The chemokine system in diverse forms of macrophage activation and polarization. *Trends Immunol* (2004) 25(12):677–86. doi: 10.1016/j.it.2004.09.015
23. Landsman L, Varol C, Jung S. Distinct differentiation potential of blood monocyte subsets in the lung. *J Immunol* (2007) 178(4):2000–7. doi: 10.4049/jimmunol.178.4.2000
24. Yrlid U, Jenkins CD, MacPherson GG. Relationships between distinct blood monocyte subsets and migrating intestinal lymph dendritic cells in vivo under steady-state conditions. *J Immunol* (2006) 176(7):4155–62. doi: 10.4049/jimmunol.176.7.4155
25. Tacke F, Alvarez D, Kaplan TJ, Jakubzick C, Spanbroek R, Llodra J, et al. Monocyte subsets differentially employ CCR2, CCR5, and CX3CR1 to accumulate within atherosclerotic plaques. *J Clin Invest* (2007) 117 (1):185–94. doi: 10.1172/JCI28549
26. Auffray C, Fogg D, Garfa M, Elain G, Join-Lambert O, Kayal S, et al. Monitoring of blood vessels and tissues by a population of monocytes with patrolling behavior. *Science* (2007) 317(5838):666–70. doi: 10.1126/science.1142883
27. Yona S, Kim KW, Wolf Y, Mildner A, Varol D, Breker M, et al. Fate mapping reveals origins and dynamics of monocytes and tissue macrophages under homeostasis. *Immunity* (2013) 38(1):79–91. doi: 10.1016/j.immuni.2012.12.001
28. Thomas G, Tacke R, Hedrick CC, Hanna RN. Nonclassical patrolling monocyte function in the vasculature. *Arterioscler Thromb Vasc Biol* (2015) 35(6):1306–16. doi: 10.1161/ATVBAHA.114.304650
29. Willenborg S, Lucas T, van Loo G, Knipper JA, Krieg T, Haase I, et al. CCR2 recruits an inflammatory macrophage subpopulation critical for angiogenesis in tissue repair. *Blood* (2012) 120(3):613–25. doi: 10.1182/blood-2012-01-403386
30. Kamada N, Hisamatsu T, Okamoto S, Chinen H, Kobayashi T, Sato T, et al. Unique CD14 intestinal macrophages contribute to the pathogenesis of Crohn disease via IL-23/IFN-gamma axis. *J Clin Invest* (2008) 118(6):2269–80. doi: 10.1172/JCI34610
31. Lampinen M, Waddell A, Ahrens R, Carlson M, Hogan SP. CD14+CD33+ myeloid cell-CCL11-eosinophil signature in ulcerative colitis. *J Leukoc Biol* (2013) 94(5):1061–70. doi: 10.1189/jlb.1212640
32. Schenk M, Bouchon A, Seibold F, Mueller C. TREM-1–expressing intestinal macrophages crucially amplify chronic inflammation in experimental colitis and inflammatory bowel diseases. *J Clin Invest* (2007) 117(10):3097–106. doi: 10.1172/JCI30602

33. Wieghofer P, Hagemeyer N, Sankowski R, Schlecht A, Staszewski O, Amann L, et al. Mapping the origin and fate of myeloid cells in distinct compartments of the eye by single-cell profiling. *EMBO J* (2021) 40:e105123. doi: 10.15252/embj.2020105123
34. Lewis CE, Pollard JW. Distinct role of macrophages in different tumor microenvironments. *Cancer Res* (2006) 66(2):605–12. doi: 10.1158/0008-5472.CAN-05-4005
35. Ahn GO, Tseng D, Liao CH, Dorie MJ, Czechowicz A, Brown JM. Inhibition of Mac-1 (CD11b/CD18) enhances tumor response to radiation by reducing myeloid cell recruitment. *Proc Natl Acad Sci U S A* (2010) 107(18):8363–8. doi: 10.1073/pnas.0911378107
36. Holness CL, Simmons DL. Molecular cloning of CD68, a human macrophage marker related to lysosomal glycoproteins. *Blood* (1993) 81 (6):1607–13. doi: 10.1182/blood.V81.6.1607.1607
37. Perry VH, Hume DA, Gordon S. Immunohistochemical localization of macrophages and microglia in the adult and developing mouse brain. *Neuroscience* (1985) 15(2):313–26. doi: 10.1016/0306-4522(85)90215-5
38. Hamann J, Koning N, Pouwels W, Ulfman LH, van Eijk M, Stacey M, et al. EMR1, the human homolog of F4/80, is an eosinophil-specific receptor. *Eur J Immunol* (2007) 37(10):2797–802. doi: 10.1002/eji.200737553
39. Springer TA. Adhesion receptors of the immune system. *Nature* (1990) 346 (6283):425–34. doi: 10.1038/346425a0
40. Nielsen HV, Christensen JP, Andersson EC, Marker O, Thomsen AR. Expression of type 3 complement receptor on activated CD8+ T cells facilitates homing to inflammatory sites. *J Immunol* (1994) 153(5):2021–8.
41. Kawai K, Tsuno NH, Matsuhashi M, Kitayama J, Osada T, Yamada J, et al. CD11b-mediated migratory property of peripheral blood B cells. *J Allergy Clin Immunol* (2005) 116(1):192–7. doi: 10.1016/j.jaci.2005.03.021
42. Cabeza-Cabrerizo M, Cardoso A, Minutti CM, Pereira da Costa M, Reis ESC. Dendritic Cells Revisited. *Annu Rev Immunol* (2021) 39. doi: 10.1146/annurev-immunol-061020-053707
43. Kunz-Schughart LA, Weber A, Rehli M, Gottfried E, Brockhoff G, Krause SW, et al. [The "classical" macrophage marker CD68 is strongly expressed in primary human fibroblasts]. *Verh Dtsch Ges Pathol* (2003) 87:215–23.
44. Kunisch E, Fuhrmann R, Roth A, Winter R, Lungershausen W, Kinne RW. Macrophage specificity of three anti-CD68 monoclonal antibodies (KP1, EBM11, and PGM1) widely used for immunohistochemistry and flow cytometry. *Ann Rheum Dis* (2004) 63(7):774–84. doi: 10.1136/ard.2003.013029
45. Misharin AV, Morales-Nebreda L, Mutlu GM, Budinger GR, Perlman H. Flow cytometric analysis of macrophages and dendritic cell subsets in the mouse lung. *Am J Respir Cell Mol Biol* (2013) 49(4):503–10. doi: 10.1165/rcmb.2013-0086MA
46. Saylor J, Ma Z, Goodridge HS, Huang F, Cress AE, Pandol SJ, et al. Spatial Mapping of Myeloid Cells and Macrophages by Multiplexed Tissue Staining. *Front Immunol* (2018) 9:2925:2925. doi: 10.3389/fimmu.2018.02925
47. Kaipainen A, Korhonen J, Mustonen T, van Hinsbergh VW, Fang GH, Dumont D, et al. Expression of the fms-like tyrosine kinase 4 gene becomes restricted to lymphatic endothelium during development. *Proc Natl Acad Sci U S A* (1995) 92(8):3566–70. doi: 10.1073/pnas.92.8.3566
48. Wigle JT, Oliver G. Prox1 function is required for the development of the murine lymphatic system. *Cell* (1999) 98(6):769–78. doi: 10.1016/s0092-8674(00)81511-1
49. Breiteneder-Geleff S, Soleiman A, Kowalski H, Horvat R, Amann G, Kriehuber E, et al. Angiosarcomas express mixed endothelial phenotypes of blood and lymphatic capillaries: podoplanin as a specific marker for lymphatic endothelium. *Am J Pathol* (1999) 154(2):385–94. doi: 10.1016/S0002-9440(10)65285-6
50. Schacht V, Ramirez MI, Hong YK, Hirakawa S, Feng D, Harvey N, et al. T1alpha/podoplanin deficiency disrupts normal lymphatic vasculature formation and causes lymphedema. *EMBO J* (2003) 22(14):3546–56. doi: 10.1093/emboj/cdg342
51. Cho CH, Koh YJ, Han J, Sung HK, Jong Lee H, Morisada T, et al. Angiogenic role of LYVE-1-positive macrophages in adipose tissue. *Circ Res* (2007) 100 (4):e47–57. doi: 10.1161/01.RES.0000259564.92792.93
52. Xu H, Chen M, Reid DM, Forrester JV. LYVE-1-positive macrophages are present in normal murine eyes. *Invest Ophthalmol Vis Sci* (2007) 48 (5):2162–71. doi: 10.1167/iovs.06-0783
53. Schroedl F, Kaser-Eichberger A, Schlereth SL, Bock F, Regenfuss B, Reitsamer HA, et al. Consensus statement on the immunohistochemical detection of ocular lymphatic vessels. *Invest Ophthalmol Vis Sci* (2014) 55 (10):6440–2. doi: 10.1167/iovs.14-15638
54. Chakarov S, Lim HY, Tan L, Lim SY, See P, Lum J, et al. Two distinct interstitial macrophage populations coexist across tissues in specific subtissular niches. *Science* (2019) 363(6432). doi: 10.1126/science.aau0964
55. Gordon S, Taylor PR. Monocyte and macrophage heterogeneity. *Nat Rev Immunol* (2005) 5(12):953–64. doi: 10.1038/nri1733
56. Murray PJ, Allen JE, Biswas SK, Fisher EA, Gilroy DW, Goerdt S, et al. Macrophage activation and polarization: nomenclature and experimental guidelines. *Immunity* (2014) 41(1):14–20. doi: 10.1016/j.immuni.2014.06.008
57. Knipper JA, Willenborg S, Brinckmann J, Bloch W, Maass T, Wagener R, et al. Interleukin-4 Receptor alpha Signaling in Myeloid Cells Controls Collagen Fibril Assembly in Skin Repair. *Immunity* (2015) 43(4):803–16. doi: 10.1016/j.immuni.2015.09.005
58. Chen F, Liu Z, Wu W, Rozo C, Bowdridge S, Millman A, et al. An essential role for TH2-type responses in limiting acute tissue damage during experimental helminth infection. *Nat Med* (2012) 18(2):260–6. doi: 10.1038/nm.2628
59. Forrester JV, McMenamin PG, Holthouse I, Lumsden L, Liversidge J. Localization and characterization of major histocompatibility complex class II-positive cells in the posterior segment of the eye: implications for induction of autoimmune uveoretinitis. *Invest Ophthalmol Vis Sci* (1994) 35 (1):64–77.
60. McMenamin PG, Crewe J, Morrison S, Holt PG. Immunomorphologic studies of macrophages and MHC class II-positive dendritic cells in the iris and ciliary body of the rat, mouse, and human eye. *Invest Ophthalmol Vis Sci* (1994) 35(8):3234–50.
61. Gomes JA, Jindal VK, Gormley PD, Dua HS. Phenotypic analysis of resident lymphoid cells in the conjunctiva and adnexal tissues of rat. *Exp Eye Res* (1997) 64(6):991–7. doi: 10.1006/exer.1997.0297
62. McMenamin PG. Dendritic cells and macrophages in the uveal tract of the normal mouse eye. *Br J Ophthalmol* (1999) 83(5):598–604. doi: 10.1136/bjo.83.5.598
63. Schroedl F, Brehmer A, Neuhuber WL, Kruse FE, May CA, Cursiefen C. The normal human choroid is endowed with a significant number of lymphatic vessel endothelial hyaluronate receptor 1 (LYVE-1)-positive macrophages. *Invest Ophthalmol Vis Sci* (2008) 49(12):5222–9. doi: 10.1167/iovs.08-1721
64. van Rooijen N, Wijburg OL, van den Dobbelsteen GP, Sanders A. Macrophages in host defense mechanisms. *Curr Top Microbiol Immunol* (1996) 210:159–65. doi: 10.1007/978-3-642-85226-8_16
65. van Vugt E, Verdaasdonk MA, Kamperdijk EW, Beelen RH. Antigen presenting capacity of peritoneal macrophages and dendritic cells. *Adv Exp Med Biol* (1993) 329:129–34. doi: 10.1007/978-1-4615-2930-9_22
66. Morrissette N, Gold E, Aderem A. The macrophage–a cell for all seasons. *Trends Cell Biol* (1999) 9(5):199–201. doi: 10.1016/s0962-8924(99)01540-8
67. De Becker G, Moulin V, Van Mechelen M, Tielemans F, Urbain J, Leo O, et al. Dendritic cells and macrophages induce the development of distinct T helper cell populations in vivo. *Adv Exp Med Biol* (1997) 417:369–73. doi: 10.1007/978-1-4757-9966-8_60
68. Doebel T, Voisin B, Nagao K. Langerhans Cells - The Macrophage in Dendritic Cell Clothing. *Trends Immunol* (2017) 38(11):817–28. doi: 10.1016/j.it.2017.06.008
69. Brissette-Storkus CS, Reynolds SM, Lepisto AJ, Hendricks RL. Identification of a novel macrophage population in the normal mouse corneal stroma. *Invest Ophthalmol Vis Sci* (2002) 43(7):2264–71.
70. Streilein JW, Toews GB, Bergstresser PR. Corneal allografts fail to express Ia antigens. *Nature* (5736) 1979) 282:326–7. doi: 10.1038/282326a0
71. Hamrah P, Liu Y, Zhang Q, Dana MR. The corneal stroma is endowed with a significant number of resident dendritic cells. *Invest Ophthalmol Vis Sci* (2003) 44(2):581–9. doi: 10.1167/iovs.02-0838
72. Rodrigues MM, Rowden G, Hackett J, Bakos I. Langerhans cells in the normal conjunctiva and peripheral cornea of selected species. *Invest Ophthalmol Vis Sci* (1981) 21(5):759–65.
73. Gillette TE, Chandler JW, Greiner JV. Langerhans cells of the ocular surface. *Ophthalmology* (1982) 89(6):700–11. doi: 10.1016/s0161-6420(82)34737-5

74. Treseler PA, Foulks GN, Sanfilippo F. The expression of HLA antigens by cells in the human cornea. *Am J Ophthalmol* (1984) 98(6):763–72. doi: 10.1016/0002-9394(84)90696-2
75. Chinnery HR, Humphries T, Clare A, Dixon AE, Howes K, Moran CB, et al. Turnover of bone marrow-derived cells in the irradiated mouse cornea. *Immunology* (2008) 125(4):541–8. doi: 10.1111/j.1365-2567.2008.02868.x
76. Kennedy DW, Abkowitz JL. Kinetics of central nervous system microglial and macrophage engraftment: analysis using a transgenic bone marrow transplantation model. *Blood* (1997) 90(3):986–93. doi: 10.1182/blood.V90.3.986.986_986_993
77. Hamrah P, Zhang Q, Liu Y, Dana MR. Novel characterization of MHC class II-negative population of resident corneal Langerhans cell-type dendritic cells. *Invest Ophthalmol Vis Sci* (2002) 43(3):639–46.
78. Potente M, Gerhardt H, Carmeliet P. Basic and therapeutic aspects of angiogenesis. *Cell* (2011) 146(6):873–87. doi: 10.1016/j.cell.2011.08.039
79. Rovenska E, Rovensky J. Lymphatic vessels: structure and function. *Isr Med Assoc J* (2011) 13(12):762–8.
80. Cursiefen C, Chen L, Dana MR, Streilein JW. Corneal lymphangiogenesis: evidence, mechanisms, and implications for corneal transplant immunology. *Cornea* (2003) 22(3):273–81. doi: 10.1097/00003226-200304000-00021
81. Azar DT. Corneal angiogenic privilege: angiogenic and antiangiogenic factors in corneal avascularity, vasculogenesis, and wound healing (an American Ophthalmological Society thesis). *Trans Am Ophthalmol Soc* (2006) 104:264–302.
82. Ma DH, Tsai RJ, Chu WK, Kao CH, Chen JK. Inhibition of vascular endothelial cell morphogenesis in cultures by limbal epithelial cells. *Invest Ophthalmol Vis Sci* (1999) 40(8):1822–8.
83. Eliason JA, Elliott JP. Proliferation of vascular endothelial cells stimulated in vitro by corneal epithelium. *Invest Ophthalmol Vis Sci* (1987) 28(12):1963–9.
84. Kaminski M, Kaminska G. Inhibition of lymphocyte-induced angiogenesis by enzymatically isolated rabbit cornea cells. *Arch Immunol Ther Exp (Warsz)* (1978) 26(1-6):1079–82.
85. Yamamoto T, Terada N, Nishizawa Y, Petrow V. Angiostatic activities of medroxyprogesterone acetate and its analogues. *Int J Cancer* (1994) 56 (3):393–9. doi: 10.1002/ijc.2910560318
86. Cursiefen C, Rummelt C, Kuchle M. Immunohistochemical localization of vascular endothelial growth factor, transforming growth factor alpha, and transforming growth factor beta1 in human corneas with neovascularization. *Cornea* (2000) 19(4):526–33. doi: 10.1097/00003226-200007000-00025
87. Lai LJ, Xiao X, Wu JH. Inhibition of corneal neovascularization with endostatin delivered by adeno-associated viral (AAV) vector in a mouse corneal injury model. *J BioMed Sci* (2007) 14(3):313–22. doi: 10.1007/s11373-007-9153-7
88. Buttner C, Clahsen T, Regenfuss B, Dreisow ML, Steiber Z, Bock F, et al. Tyrosinase Is a Novel Endogenous Regulator of Developmental and Inflammatory Lymphangiogenesis. *Am J Pathol* (2019) 189(2):440–8. doi: 10.1016/j.ajpath.2018.10.014
89. Reuer T, Schneider AC, Cakir B, Buhler AD, Walz JM, Lapp T, et al. Semaphorin 3F Modulates Corneal Lymphangiogenesis and Promotes Corneal Graft Survival. *Invest Ophthalmol Vis Sci* (2018) 59(12):5277–84. doi: 10.1167/iovs.18-24287
90. Cheng HC, Yeh SI, Tsao YP, Kuo PC. Subconjunctival injection of recombinant AAV-angiostatin ameliorates alkali burn induced corneal angiogenesis. *Mol Vis* (2007) 13:2344–52.
91. Armstrong LC, Bornstein P. Thrombospondins 1 and 2 function as inhibitors of angiogenesis. *Matrix Biol* (2003) 22(1):63–71. doi: 10.1016/s0945-053x(03)00005-2
92. Lawler J. The functions of thrombospondin-1 and-2. *Curr Opin Cell Biol* (2000) 12(5):634–40. doi: 10.1016/s0955-0674(00)00143-5
93. Lawler J. Thrombospondin-1 as an endogenous inhibitor of angiogenesis and tumor growth. *J Cell Mol Med* (2002) 6(1):1–12. doi: 10.1111/j.1582-4934.2002.tb00307.x
94. Panigrahy D, Kaipainen A, Huang S, Butterfield CE, Barnes CM, Fannon M, et al. PPARalpha agonist fenofibrate suppresses tumor growth through direct and indirect angiogenesis inhibition. *Proc Natl Acad Sci U S A* (2008) 105(3):985–90. doi: 10.1073/pnas.0711281105
95. Cursiefen C, Maruyama K, Bock F, Saban D, Sadrai Z, Lawler J, et al. Thrombospondin 1 inhibits inflammatory lymphangiogenesis by CD36 ligation on monocytes. *J Exp Med* (2011) 208(5):1083–92. doi: 10.1084/jem.20092277
96. Cursiefen C, Masli S, Ng TF, Dana MR, Bornstein P, Lawler J, et al. Roles of thrombospondin-1 and -2 in regulating corneal and iris angiogenesis. *Invest Ophthalmol Vis Sci* (2004) 45(4):1117–24. doi: 10.1167/iovs.03-0940
97. Friling R, Yassur Y, Levy R, Kost J, Schwartz B, Mikhailowsky R, et al. A role of transforming growth factor-beta 1 in the control of corneal neovascularization. *In Vivo* (1996) 10(1):59–64.
98. Sakamoto T, Ueno H, Sonoda K, Hisatomi T, Shimizu K, Ohashi H, et al. Blockade of TGF-beta by in vivo gene transfer of a soluble TGF-beta type II receptor in the muscle inhibits corneal opacification, edema and angiogenesis. *Gene Ther* (2000) 7(22):1915–24. doi: 10.1038/sj.gt.3301320
99. Ferrari G, Cook BD, Terushkin V, Pintucci G, Mignatti P. Transforming growth factor-beta 1 (TGF-beta1) induces angiogenesis through vascular endothelial growth factor (VEGF)-mediated apoptosis. *J Cell Physiol* (2009) 219(2):449–58. doi: 10.1002/jcp.21706
100. Ambati BK, Nozaki M, Singh N, Takeda A, Jani PD, Suthar T, et al. Corneal avascularity is due to soluble VEGF receptor-1. *Nature* (2006) 443 (7114):993–7. doi: 10.1038/nature05249
101. Kendall RL, Thomas KA. Inhibition of vascular endothelial cell growth factor activity by an endogenously encoded soluble receptor. *Proc Natl Acad Sci U.S.A.* (1993) 90(22):10705–9. doi: 10.1073/pnas.90.22.10705
102. Albuquerque RJ, Hayashi T, Cho WG, Kleinman ME, Dridi S, Takeda A, et al. Alternatively spliced vascular endothelial growth factor receptor-2 is an essential endogenous inhibitor of lymphatic vessel growth. *Nat Med* (2009) 15(9):1023–30. doi: 10.1038/nm.2018
103. Singh N, Tiem M, Watkins R, Cho YK, Wang Y, Olsen T, et al. Soluble vascular endothelial growth factor receptor 3 is essential for corneal alymphaticity. *Blood* (2013) 121(20):4242–9. doi: 10.1182/blood-2012-08-453043
104. Cursiefen C, Chen L, Saint-Geniez M, Hamrah P, Jin Y, Rashid S, et al. Nonvascular VEGF receptor 3 expression by corneal epithelium maintains avascularity and vision. *Proc Natl Acad Sci U.S.A.* (2006) 103(30):11405–10. doi: 10.1073/pnas.0506112103
105. Cogan DG. Vascularization of the Cornea. Its Experimental Induction by Small Lesions and a New Theory of Its Pathogenesis. *Trans Am Ophthalmol Soc* (1948) 46:457–71.
106. Langham M. Observations on the growth of blood vessels into the cornea; application of a new experimental technique. *Br J Ophthalmol* (1953) 37 (4):210–22. doi: 10.1136/bjo.37.4.210
107. Levene R, Shapiro A, Baum J. Experimental Corneal Vascularization. *Arch Ophthalmol* (1963) 70:242–9. doi: 10.1001/archopht.1963.00960050244017
108. Kruse FE. Stem cells and corneal epithelial regeneration. *Eye (Lond)* (1994) 8 (Pt 2):170–83. doi: 10.1038/eye.1994.42
109. Schlotzer-Schrehardt U, Kruse FE. Identification and characterization of limbal stem cells. *Exp Eye Res* (2005) 81(3):247–64. doi: 10.1016/j.exer.2005.02.016
110. Zieske JD. Perpetuation of stem cells in the eye. *Eye (Lond)* (1994) 8(Pt 2):163–9. doi: 10.1038/eye.1994.41
111. Yoon JJ, Ismail S, Sherwin T. Limbal stem cells: Central concepts of corneal epithelial homeostasis. *World J Stem Cells* (2014) 6(4):391–403. doi: 10.4252/wjsc.v6.i4.391
112. Friedenwald JS. Growth pressure and metaplasia of conjunctival and corneal epithelium. *Doc Ophthalmol* (1951) 5-6:184–92. doi: 10.1007/bf00143661
113. Notara M, Lentzsch A, Coroneo M, Cursiefen C. The Role of Limbal Epithelial Stem Cells in Regulating Corneal (Lymph)angiogenic Privilege and the Micromilieu of the Limbal Niche following UV Exposure. *Stem Cells Int* (2018) 2018:8620172. doi: 10.1155/2018/8620172
114. Gao X, Guo K, Santosa SM, Montana M, Yamakawa M, Hallak JA, et al. Application of corneal injury models in dual fluorescent reporter transgenic mice to understand the roles of the cornea and limbus in angiogenic and lymphangiogenic privilege. *Sci Rep* (2019) 9(1):12331. doi: 10.1038/s41598-019-48811-z
115. Medawar PB. Immunity to homologous grafted skin; the fate of skin homografts transplanted to the brain, to subcutaneous tissue, and to the anterior chamber of the eye. *Br J Exp Pathol* (1948) 29(1):58–69.
116. Stein-Streilein J, Sonoda KH, Faunce D, Zhang-Hoover J. Regulation of adaptive immune responses by innate cells expressing NK markers and

antigen-transporting macrophages. *J Leukoc Biol* (2000) 67(4):488–94. doi: 10.1002/jlb.67.4.488
117. Wilbanks GA, Mammolenti M, Streilein JW. Studies on the induction of anterior chamber-associated immune deviation (ACAID). II. Eye-derived cells participate in generating blood-borne signals that induce ACAID. *J Immunol* (1991) 146(9):3018–24.
118. Stein-Streilein J, Streilein JW. Anterior chamber associated immune deviation (ACAID): regulation, biological relevance, and implications for therapy. *Int Rev Immunol* (2002) 21(2-3):123–52. doi: 10.1080/08830180212066
119. Cursiefen C. Immune privilege and angiogenic privilege of the cornea. *Chem Immunol Allergy* (2007) 92:50–7. doi: 10.1159/000099253
120. Folkman J, Shing Y. Angiogenesis. *J Biol Chem* (1992) 267(16):10931–4. doi: 10.1016/S0021-9258(19)49853-0
121. Kato T, Kure T, Chang JH, Gabison EE, Itoh T, Itohara S, et al. Diminished corneal angiogenesis in gelatinase A-deficient mice. *FEBS Lett* (2001) 508 (2):187–SS90. doi: 10.1016/s0014-5793(01)02897-6
122. Beck LJr., D'Amore PA. Vascular development: cellular and molecular regulation. *FASEB J* (1997) 11(5):365–73. doi: 10.1096/fasebj.11.5.9141503
123. Hos D, Schlereth SL, Bock F, Heindl LM, Cursiefen C. Antilymphangiogenic therapy to promote transplant survival and to reduce cancer metastasis: what can we learn from the eye? *Semin Cell Dev Biol* (2015) 38:117–30. doi: 10.1016/j.semcdb.2014.11.003
124. Dietrich T, Bock F, Yuen D, Hos D, Bachmann BO, Zahn G, et al. Cutting edge: lymphatic vessels, not blood vessels, primarily mediate immune rejections after transplantation. *J Immunol* (2010) 184(2):535–9. doi: 10.4049/jimmunol.0903180
125. Goyal S, Chauhan SK, El Annan J, Nallasamy N, Zhang Q, Dana R. Evidence of corneal lymphangiogenesis in dry eye disease: a potential link to adaptive immunity? *Arch Ophthalmol* (2010) 128(7):819–24. doi: 10.1001/archophthalmol.2010.124
126. Lee HS, Hos D, Blanco T, Bock F, Reyes NJ, Mathew R, et al. Involvement of corneal lymphangiogenesis in a mouse model of allergic eye disease. *Invest Ophthalmol Vis Sci* (2015) 56(5):3140–8. doi: 10.1167/iovs.14-16186
127. Karpanen T, Alitalo K. Molecular biology and pathology of lymphangiogenesis. *Annu Rev Pathol* (2008) 3:367–97. doi: 10.1146/annurev.pathmechdis.3.121806.151515
128. Makinen T, Veikkola T, Mustjoki S, Karpanen T, Catimel B, Nice EC, et al. Isolated lymphatic endothelial cells transduce growth, survival and migratory signals via the VEGF-C/D receptor VEGFR-3. *EMBO J* (2001) 20(17):4762–73. doi: 10.1093/emboj/20.17.4762
129. Kerjaschki D. The crucial role of macrophages in lymphangiogenesis. *J Clin Invest* (2005) 115(9):2316–9. doi: 10.1172/JCI26354
130. Maruyama K, Nakazawa T, Cursiefen C, Maruyama Y, Van Rooijen N, D'Amore PA, et al. The maintenance of lymphatic vessels in the cornea is dependent on the presence of macrophages. *Invest Ophthalmol Vis Sci* (2012) 53(6):3145–53. doi: 10.1167/iovs.11-8010
131. Van der Veen G, Broersma L, Dijkstra CD, Van Rooijen N, Van Rij G, Van der Gaag R. Prevention of corneal allograft rejection in rats treated with subconjunctival injections of liposomes containing dichloromethylene diphosphonate. *Invest Ophthalmol Vis Sci* (1994) 35(9):3505–15.
132. Nakao S, Kuwano T, Tsutsumi-Miyahara C, Ueda S, Kimura YN, Hamano S, et al. Infiltration of COX-2-expressing macrophages is a prerequisite for IL-1 beta-induced neovascularization and tumor growth. *J Clin Invest* (2005) 115 (11):2979–91. doi: 10.1172/JCI23298
133. Fantin A, Vieira JM, Gestri G, Denti L, Schwarz Q, Prykhozhij S, et al. Tissue macrophages act as cellular chaperones for vascular anastomosis downstream of VEGF-mediated endothelial tip cell induction. *Blood* (2010) 116(5):829–40. doi: 10.1182/blood-2009-12-257832
134. Schmidt T, Carmeliet P. Blood-vessel formation: Bridges that guide and unite. *Nature* (7299) 2010) 465:697–9. doi: 10.1038/465697a
135. Wuest TR, Carr DJ. VEGF-A expression by HSV-1-infected cells drives corneal lymphangiogenesis. *J Exp Med* (2010) 207(1):101–15. doi: 10.1084/jem.20091385
136. Lu P, Li L, Liu G, van Rooijen N, Mukaida N, Zhang X. Opposite roles of CCR2 and CX3CR1 macrophages in alkali-induced corneal neovascularization. *Cornea* (2009) 28(5):562–9. doi: 10.1097/ICO.0b013e3181930bcd
137. Gain P, Jullienne R, He Z, Aldossary M, Acquart S, Cognasse F, et al. Global Survey of Corneal Transplantation and Eye Banking. *JAMA Ophthalmol* (2016) 134(2):167–73. doi: 10.1001/jamaophthalmol.2015.4776
138. Niederkorn JY. The immune privilege of corneal allografts. *Transplantation* (1999) 67(12):1503–8. doi: 10.1097/00007890-199906270-00001
139. Hos D, Matthaei M, Bock F, Maruyama K, Notara M, Clahsen T, et al. Immune reactions after modern lamellar (DALK, DSAEK, DMEK) versus conventional penetrating corneal transplantation. *Prog retinal eye Res* (2019) 73:100768. doi: 10.1016/j.preteyeres.2019.07.001
140. Hori J, Yamaguchi T, Keino H, Hamrah P, Maruyama K. Immune privilege in corneal transplantation. *Prog retinal eye Res* (2019) 72:100758. doi: 10.1016/j.preteyeres.2019.04.002
141. Niederkorn JY. High-risk corneal allografts and why they lose their immune privilege. *Curr Opin Allergy Clin Immunol* (2010) 10(5):493–7. doi: 10.1097/ACI.0b013e32833dfa11
142. Di Zazzo A, Kheirkhah A, Abud TB, Goyal S, Dana R. Management of high-risk corneal transplantation. *Survey Ophthalmol* (2017) 62(6):816–27. doi: 10.1016/j.survophthal.2016.12.010
143. Dana MR, Streilein JW. Loss and restoration of immune privilege in eyes with corneal neovascularization. *Invest Ophthalmol Vis Sci* (1996) 37 (12):2485–94.
144. Slegers TP, Torres PF, Broersma L, van Rooijen N, van Rij G, van der Gaag R. Effect of macrophage depletion on immune effector mechanisms during corneal allograft rejection in rats. *Invest Ophthalmol Vis Sci* (2000) 41 (8):2239–47.
145. Torres PF, Slegers TP, Peek R, van Rooijen N, van der Gaag R, Kijlstra A, et al. Changes in cytokine mRNA levels in experimental corneal allografts after local clodronate-liposome treatment. *Invest Ophthalmol Vis Sci* (1999) 40(13):3194–201.
146. Slegers TP, van Rooijen N, van Rij G, van der Gaag R. Delayed graft rejection in pre-vascularised corneas after subconjunctival injection of clodronate liposomes. *Curr Eye Res* (2000) 20(4):322–4. doi: 10.1076/0271-3683(200004)2041-5FT322
147. Oh JY, Lee HJ, Ko AY, Ko JH, Kim MK, Wee WR. Analysis of macrophage phenotype in rejected corneal allografts. *Invest Ophthalmol Vis Sci* (2013) 54 (12):7779–84. doi: 10.1167/iovs.13-12650
148. Ward NL, Loyd CM, Wolfram JA, Diaconu D, Michaels CM, McCormick TS. Depletion of antigen-presenting cells by clodronate liposomes reverses the psoriatic skin phenotype in KC-Tie2 mice. *Br J Dermatol* (2011) 164 (4):750–8. doi: 10.1111/j.1365-2133.2010.10129.x
149. Konig S, Nitzki F, Uhmann A, Dittmann K, Theiss-Suennemann J, Herrmann M, et al. Depletion of cutaneous macrophages and dendritic cells promotes growth of basal cell carcinoma in mice. *PloS One* (2014) 9(4): e93555. doi: 10.1371/journal.pone.0093555
150. Tabbara KF. Pharmacologic strategies in the prevention and treatment of corneal transplant rejection. *Int Ophthalmol* (2008) 28(3):223–32. doi: 10.1007/s10792-007-9100-7
151. Randleman JB, Stulting RD. Prevention and treatment of corneal graft rejection: current practice patterns (2004). *Cornea* (2006) 25(3):286–90. doi: 10.1097/01.ico.0000178731.42187.46
152. Hos D, Saban DR, Bock F, Regenfuss B, Onderka J, Masli S, et al. Suppression of inflammatory corneal lymphangiogenesis by application of topical corticosteroids. *Arch Ophthalmol* (2011) 129(4):445–52. doi: 10.1001/archophthalmol.2011.42
153. Salabarria AC, Koch M, Schonberg A, Zinser E, Hos D, Hamdorf M, et al. Topical VEGF-C/D Inhibition Prevents Lymphatic Vessel Ingrowth into Cornea but Does Not Improve Corneal Graft Survival. *J Clin Med* (2020) 9 (5). doi: 10.3390/jcm9051270
154. Hou Y, Le VNH, Toth G, Siebelmann S, Horstmann J, Gabriel T, et al. UV light crosslinking regresses mature corneal blood and lymphatic vessels and promotes subsequent high-risk corneal transplant survival. *Am J Transplant* (2018) 18(12):2873–84. doi: 10.1111/ajt.14874
155. Alitalo K. The lymphatic vasculature in disease. *Nat Med* (2011) 17 (11):1371–80. doi: 10.1038/nm.2545
156. Wang XN, McGovern N, Gunawan M, Richardson C, Windebank M, Siah TW, et al. A three-dimensional atlas of human dermal leukocytes, lymphatics, and blood vessels. *J Invest Dermatol* (2014) 134(4):965–74. doi: 10.1038/jid.2013.481

157. Scott EW, Simon MC, Anastasi J, Singh H. Requirement of transcription factor PU.1 in the development of multiple hematopoietic lineages. *Science* (5178) 1994) 265:1573–7. doi: 10.1126/science.8079170
158. Yamazaki T, Nalbandian A, Uchida Y, Li W, Arnold TD, Kubota Y, et al. Tissue Myeloid Progenitors Differentiate into Pericytes through TGF-beta Signaling in Developing Skin Vasculature. *Cell Rep* (2017) 18(12):2991–3004. doi: 10.1016/j.celrep.2017.02.069
159. Gordon EJ, Rao S, Pollard JW, Nutt SL, Lang RA, Harvey NL. Macrophages define dermal lymphatic vessel calibre during development by regulating lymphatic endothelial cell proliferation. *Development* (2010) 137(22):3899–910. doi: 10.1242/dev.050021
160. Lapenna A, De Palma M, Lewis CE. Perivascular macrophages in health and disease. *Nat Rev Immunol* (2018) 18(11):689–702. doi: 10.1038/s41577-018-0056-9
161. Abtin A, Jain R, Mitchell AJ, Roediger B, Brzoska AJ, Tikoo S, et al. Perivascular macrophages mediate neutrophil recruitment during bacterial skin infection. *Nat Immunol* (2014) 15(1):45–53. doi: 10.1038/ni.2769
162. Natsuaki Y, Egawa G, Nakamizo S, Ono S, Hanakawa S, Okada T, et al. Perivascular leukocyte clusters are essential for efficient activation of effector T cells in the skin. *Nat Immunol* (2014) 15(11):1064–9. doi: 10.1038/ni.2992
163. Barreiro O, Cibrian D, Clemente C, Alvarez D, Moreno V, Valiente I, et al. Pivotal role for skin transendothelial radio-resistant anti-inflammatory macrophages in tissue repair. *Elife* (2016) 5. doi: 10.7554/eLife.15251
164. Eming SA, Brachvogel B, Odorisio T, Koch M. Regulation of angiogenesis: wound healing as a model. *Prog Histochem Cytochem* (2007) 42(3):115–70. doi: 10.1016/j.proghi.2007.06.001
165. Gurtner GC, Werner S, Barrandon Y, Longaker MT. Wound repair and regeneration. *Nature* (7193) 2008) 453:314–21. doi: 10.1038/nature07039
166. Martinez-Corral I, Olmeda D, Dieguez-Hurtado R, Tammela T, Alitalo K, Ortega S. In vivo imaging of lymphatic vessels in development, wound healing, inflammation, and tumor metastasis. *Proc Natl Acad Sci U S A* (2012) 109(16):6223–8. doi: 10.1073/pnas.1115542109
167. Lucas T, Waisman A, Ranjan R, Roes J, Krieg T, Muller W, et al. Differential roles of macrophages in diverse phases of skin repair. *J Immunol* (2010) 184 (7):3964–77. doi: 10.4049/jimmunol.0903356
168. Mirza R, DiPietro LA, Koh TJ. Selective and specific macrophage ablation is detrimental to wound healing in mice. *Am J Pathol* (2009) 175(6):2454–62. doi: 10.2353/ajpath.2009.090248
169. Goren I, Allmann N, Yogev N, Schurmann C, Linke A, Holdener M, et al. A transgenic mouse model of inducible macrophage depletion: effects of diphtheria toxin-driven lysozyme M-specific cell lineage ablation on wound inflammatory, angiogenic, and contractive processes. *Am J Pathol* (2009) 175(1):132–47. doi: 10.2353/ajpath.2009.081002
170. Mace KA, Yu DH, Paydar KZ, Boudreau N, Young DM. Sustained expression of Hif-1alpha in the diabetic environment promotes angiogenesis and cutaneous wound repair. *Wound Repair Regener* (2007) 15(5):636–45. doi: 10.1111/j.1524-475X.2007.00278.x
171. Botusan IR, Sunkari VG, Savu O, Catrina AI, Grunler J, Lindberg S, et al. Stabilization of HIF-1alpha is critical to improve wound healing in diabetic mice. *Proc Natl Acad Sci U S A* (2008) 105(49):19426–31. doi: 10.1073/pnas.0805230105
172. Liu L, Marti GP, Wei X, Zhang X, Zhang H, Liu YV, et al. Age-dependent impairment of HIF-1alpha expression in diabetic mice: Correction with electroporation-facilitated gene therapy increases wound healing, angiogenesis, and circulating angiogenic cells. *J Cell Physiol* (2008) 217 (2):319–27. doi: 10.1002/jcp.21503
173. Loh SA, Chang EI, Galvez MG, Thangarajah H, El-ftesi S, Vial IN, et al. SDF-1 alpha expression during wound healing in the aged is HIF dependent. *Plast Reconstr Surg* (2009) 123(2 Suppl):65S–75S. doi: 10.1097/PRS.0b013e318191bdf4
174. Thangarajah H, Yao D, Chang EI, Shi Y, Jazayeri L, Vial IN, et al. The molecular basis for impaired hypoxia-induced VEGF expression in diabetic tissues. *Proc Natl Acad Sci U.S.A.* (2009) 106(32):13505–10. doi: 10.1073/pnas.0906670106
175. Rao P, Suvas S. Development of Inflammatory Hypoxia and Prevalence of Glycolytic Metabolism in Progressing Herpes Stromal Keratitis Lesions. *J Immunol* (2019) 202(2):514–26. doi: 10.4049/jimmunol.1800422
176. Chen P, Yin H, Wang Y, Wang Y, Xie L. Inhibition of VEGF expression and corneal neovascularization by shRNA targeting HIF-1alpha in a mouse model of closed eye contact lens wear. *Mol Vis* (2012) 18:864–73.
177. Tang N, Wang L, Esko J, Giordano FJ, Huang Y, Gerber HP, et al. Loss of HIF-1alpha in endothelial cells disrupts a hypoxia-driven VEGF autocrine loop necessary for tumorigenesis. *Cancer Cell* (2004) 6(5):485–95. doi: 10.1016/j.ccr.2004.09.026
178. Rezvani HR, Ali N, Serrano-Sanchez M, Dubus P, Varon C, Ged C, et al. Loss of epidermal hypoxia-inducible factor-1alpha accelerates epidermal aging and affects re-epithelialization in human and mouse. *J Cell Sci* (2011) 124 (Pt 24):4172–83. doi: 10.1242/jcs.082370
179. Duscher D, Maan ZN, Whittam AJ, Sorkin M, Hu MS, Walmsley GG, et al. Fibroblast-Specific Deletion of Hypoxia Inducible Factor-1 Critically Impairs Murine Cutaneous Neovascularization and Wound Healing. *Plast Reconstr Surg* (2015) 136(5):1004–13. doi: 10.1097/PRS.0000000000001699
180. Cramer T, Yamanishi Y, Clausen BE, Forster I, Pawlinski R, Mackman N, et al. HIF-1alpha is essential for myeloid cell-mediated inflammation. *Cell* (2003) 112(5):645–57. doi: 10.1016/s0092-8674(03)00154-5
181. Crowther M, Brown NJ, Bishop ET, Lewis CE. Microenvironmental influence on macrophage regulation of angiogenesis in wounds and malignant tumors. *J Leukoc Biol* (2001) 70(4):478–90. doi: 10.1189/jlb.70.4.478
182. Lin N, Simon MC. Hypoxia-inducible factors: key regulators of myeloid cells during inflammation. *J Clin Invest* (2016) 126(10):3661–71. doi: 10.1172/JCI84426
183. Haroon ZA, Raleigh JA, Greenberg CS, Dewhirst MW. Early wound healing exhibits cytokine surge without evidence of hypoxia. *Ann Surg* (2000) 231 (1):137–47. doi: 10.1097/00000658-200001000-00020
184. Mills EL, Kelly B, Logan A, Costa ASH, Varma M, Bryant CE, et al. Succinate Dehydrogenase Supports Metabolic Repurposing of Mitochondria to Drive Inflammatory Macrophages. *Cell* (2016) 167(2):457–70 e13. doi: 10.1016/j.cell.2016.08.064
185. Schledzewski K, Falkowski M, Moldenhauer G, Metharom P, Kzhyshkowska J, Ganss R, et al. Lymphatic endothelium-specific hyaluronan receptor LYVE-1 is expressed by stabilin-1+, F4/80+, CD11b+ macrophages in malignant tumours and wound healing tissue in vivo and in bone marrow cultures in vitro: implications for the assessment of lymphangiogenesis. *J Pathol* (2006) 209(1):67–77. doi: 10.1002/path.1942
186. Maruyama K, Asai J, Ii M, Thorne T, Losordo DW, D'Amore PA. Decreased macrophage number and activation lead to reduced lymphatic vessel formation and contribute to impaired diabetic wound healing. *Am J Pathol* (2007) 170(4):1178–91. doi: 10.2353/ajpath.2007.060018
187. Kataru RP, Jung K, Jang C, Yang H, Schwendener RA, Baik JE, et al. Critical role of CD11b+ macrophages and VEGF in inflammatory lymphangiogenesis, antigen clearance, and inflammation resolution. *Blood* (2009) 113(22):5650–9. doi: 10.1182/blood-2008-09-176776
188. Wiig H, Schroder A, Neuhofer W, Jantsch J, Kopp C, Karlsen TV, et al. Immune cells control skin lymphatic electrolyte homeostasis and blood pressure. *J Clin Invest* (2013) 123(7):2803–15. doi: 10.1172/JCI60113
189. Jantsch J, Schatz V, Friedrich D, Schroder A, Kopp C, Siegert I, et al. Cutaneous Na+ storage strengthens the antimicrobial barrier function of the skin and boosts macrophage-driven host defense. *Cell Metab* (2015) 21 (3):493–501. doi: 10.1016/j.cmet.2015.02.003

Conflict of Interest: The authors declare that the research was conducted in the absence of any commercial or financial relationships that could be construed as a potential conflict of interest.

Copyright © 2021 Hadrian, Willenborg, Bock, Cursiefen, Eming and Hos. This is an open-access article distributed under the terms of the Creative Commons Attribution License (CC BY). The use, distribution or reproduction in other forums is permitted, provided the original author(s) and the copyright owner(s) are credited and that the original publication in this journal is cited, in accordance with accepted academic practice. No use, distribution or reproduction is permitted which does not comply with these terms.

frontiers in Immunology

REVIEW
published: 17 June 2021
doi: 10.3389/fimmu.2021.700790

The Role of Ageing and Parenchymal Senescence on Macrophage Function and Fibrosis

Ross A. Campbell[1*], *Marie-Helena Docherty*[1,2], *David A. Ferenbach*[1,2†] *and Katie J. Mylonas*[1†]

[1] Centre for Inflammation Research, Queen's Medical Research Institute, University of Edinburgh, Edinburgh, United Kingdom, [2] Department of Renal Medicine, Royal Infirmary of Edinburgh, Edinburgh, United Kingdom

In this review, we examine senescent cells and the overlap between the direct biological impact of senescence and the indirect impact senescence has *via* its effects on other cell types, particularly the macrophage. The canonical roles of macrophages in cell clearance and in other physiological functions are discussed with reference to their functions in diseases of the kidney and other organs. We also explore the translational potential of different approaches based around the macrophage in future interventions to target senescent cells, with the goal of preventing or reversing pathologies driven or contributed to in part by senescent cell load *in vivo.*

Keywords: macrophage, senescence, ageing, fibrosis, immunoageing, immunevasion, senolytic, senescence-associated secretory phenotype

OPEN ACCESS

Edited by:
Alexander Steinkasserer, University Hospital Erlangen, Germany

Reviewed by:
Victor J. Thannickal, University of Alabama at Birmingham, United States
Yasutaka Okabe, Osaka University, Japan

****Correspondence:***
Ross A. Campbell
ross.campbell@ed.ac.uk

†These authors have contributed equally to this work

Specialty section:
This article was submitted to Antigen Presenting Cell Biology, a section of the journal Frontiers in Immunology

Received: *26 April 2021*
Accepted: *07 June 2021*
Published: *17 June 2021*

Citation:
Campbell RA, Docherty M-H, Ferenbach DA and Mylonas KJ (2021) The Role of Ageing and Parenchymal Senescence on Macrophage Function and Fibrosis. Front. Immunol. 12:700790. doi: 10.3389/fimmu.2021.700790

INTRODUCTION

Ageing in humans is marked by a decrease in fitness over time with a simultaneous increase in mortality (1). With increasing age, the functions of key biological systems begin to decline, as shown by decreased nutrient sensing, stem cell exhaustion and cellular senescence (1). Due to advances in healthcare, human life expectancy has increased worldwide, with estimates of the average global population placing 1 in 9 people over 60, which is expected to rise to 1 in 5 by 2050 (2). As we age, the incidence of physiological dysfunction increases as well, and thus the risk of age-associated diseases such as chronic kidney disease (CKD), cardiovascular disease and type II diabetes (3) also increases. These diseases predispose individuals to developing additional pathologies and increase both morbidity and mortality. This calls for polypharmaceutical treatments and interventions to maintain quality of life (2), which come with the caveats of side-effects and cross-reactions and are therefore potentially detrimental to patient welfare. Because of these drawbacks, novel treatments need to be developed to target the causes of these co-morbidities to reduce the need for large amounts of medication.

This review aims to summarize the current understanding of the functions of senescent cells and macrophages, and their combined effect on fibrosis within tissues. Focus will be given to the kidney, supplemented by other relevant organ systems. Finally, we will summarize the challenges for future research, and potential avenues for translating research studies into therapeutic advances.

AGEING AND DISEASE

The trans-NIH Geroscience Interest Group (GSIG) held a summit in 2016, focusing on the seven pillars of ageing, expanding on previously assessed hallmarks (1). These seven factors include metabolic changes, macromolecular damage, epigenetic changes, inflammation, adaptation to stress, stem cells and regeneration and changes to proteostasis (4), all of which share interconnected relationships (**Figure 1**).

Ageing is associated with progressive decline in function of multiple organ systems. Bone loss has long been associated with advancing age, with a reduced capacity to heal fractures (5), which is marked by a decrease in osteocytes with increasing age (6). The consequences of this are seen in the increase of non-traumatic bone fractures, with the frequency of these fractures increasing for persons aged over 60 (5).

Cardiovascular function is negatively impacted by age, as the arterial tree can thicken and stiffen (7). This trend, seen in both genders, and as measured by carotid-femoral pulse wave velocity (PWV), diverges at age 50 for men and women, with men having a steeper increase of PWV (7). This has key implications for certain diseases such as end-stage renal disease, as significantly higher 'pulse-wave velocity' (PWV) has been used to predict mortality in patients (8). This indicates certain aspects of ageing differ based on gender, suggesting a hormonal role contributes to the phenotype, however this is beyond the focus of this review and will not be discussed.

Chronic kidney disease (CKD) is relevant in ageing studies as it has been found that there are signs of premature ageing in CKD patients such as osteoporosis, poor wound healing and inflammation, leading to the proposal that CKD be included as a disease that displays traits usually associated with advanced ageing (9). The aged kidney is marked by up to 40% less renal blood flow in old *vs.* young male patients (10). Increasing donor age is associated with reduced transplant function after donation, even in the context of well-preserved pre-donation function (11). Overcoming these problems requires investigating the links between ageing and physiological dysfunction, which is the greatest risk factor for the diseases listed previously.

Ageing is associated with decline in cellular functions, including the phagocytic clearance of cells. This has been shown using *in vitro* mouse models in which serum from aged mice (24 months old) was added to cultures of macrophages, which resulted in decreased levels of phagocytosis (12). In addition to this, direct studies of clearance of apoptotic skin cells (induced by UV B irradiation) showed a higher level of apoptotic keratinocytes compared to younger mice indicating reduced phagocytic activity. Of note, in aged mice with reduced phagocytosis of apoptotic cells, renal autoantibodies developed along with complement deposition within the kidney, findings consistent with the development of autoimmunity (12). Macrophage numbers were not significantly reduced or increased in older mice compared to younger mice in these studies and therefore, a decrease of macrophage phagocytic activity is implicated. This shows that the persistence of apoptotic cells has a detrimental effect on normal tissue function, particularly the kidney (13). However, when macrophage phagocytosis was assessed *in vitro*, there was no difference between young and old derived, indicating systemic factors may modulate the potency of macrophage phagocytosis (13).

'Gerontology' focuses on ageing and older adults, whereas 'geroscience' emphasizes the overlap of normal ageing and chronic disease. The geroscience hypothesis predicts that the targeting of the suspected drivers of ageing will also mitigate the main risk factors of multiple chronic diseases (4). This would have the potential to increase the health span of individuals. An example of this is caloric restriction (CR), and has long been known to have pro-longevity properties as first seen in

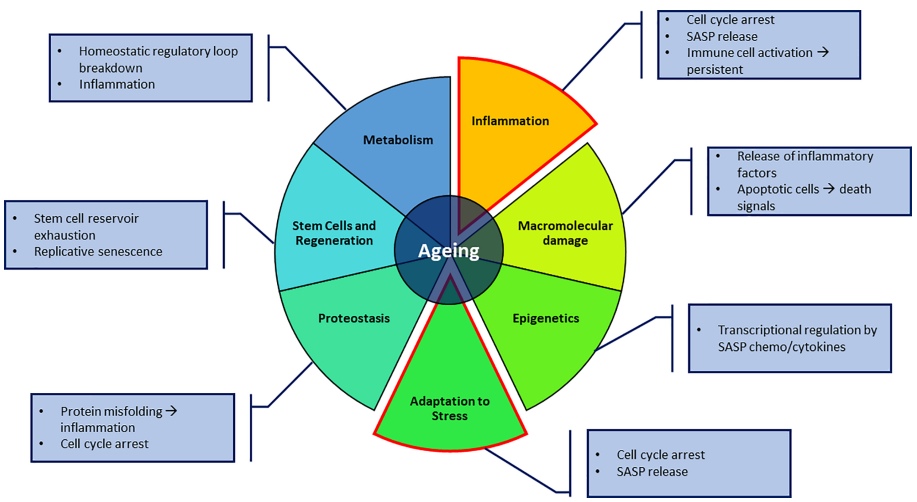

FIGURE 1 | The seven pillars of ageing proposed by Kennedy et al. (4). Key aspects in this review focus on the adaptation to stressful environments in the form of senescence and macrophages, and the inflammatory effect it can have on its surroundings. Annotations to each pillar highlight possible contributions to direct senescence or producing a senescence-promoting environment.

C.elegans (14). This has since been investigated in mouse models, which showed an increase in longevity, decreased cancer incidence and a rejuvenated immune system through intermittent fasting (15). Data for controlled calorie consumption in humans showed a limited impact from calorie restriction (16). However, a meta-analysis of clinical studies indicated increases of fibrinolytic activity, to degrade fibrin deposits, improving prognosis for cardiovascular disease patients (17). This indicates at least partial benefits when applied to humans. However, this may come at a cost, as recent studies in grey mouse lemurs (*Microcebus murinus*) indicated that moderate caloric restriction (30%), accelerated grey matter atrophy (18). Despite this, lifespan was increased (50% median increase), with a decrease in nephritis as cause of death and cognitive function comparable to controls. Further studies are warranted to make comparisons to humans who have higher-level reasoning capacities that may not be properly assessed with animal models.

SENESCENCE

Senescence involves irreversible arrest of the cell cycle (19) and was first observed by Hayflick and Moorhead (20). Multiple factors can stimulate senescence in a cell, including DNA damage, chronological ageing in the form of telomere shortening and cell stress from chronic conditions (19, 21, 22). This is marked by increased expression of cyclin dependent kinase inhibitors $p21^{CIP1}$ and $p16^{INK4a}$ (23, 24) that drive cell-cycle arrest. Despite the impact of external stress, senescent cells remain metabolically active with an altered secretome of cytokines, chemokines and proteases that have the capacity to modulate the activity and functionality of surrounding cells. This is called the senescence-associated secretory phenotype (SASP) (25). These include, but are not limited to, interleukin-8 (IL-8) (26), TNF-α (27), IL-6 (28) and IL-1α (29). Alone, none of these markers are definitive for senescence. Combinations of other markers such as senescence-associated β galactosidase (SA-β-Gal), a marker of increased lysosomal activity, γH2AX which is a marker of double DNA strand breaks and the DNA damage response, along with markers for cell-cycle checkpoints ($p21^{CIP1}$, $p16^{INK4a}$) (30) are used to infer senescence of cells.

Acute *vs* Chronic Senescence

Acute senescence is a tightly regulated process seen during wound healing (31, 32), in embryogenesis (33, 34), and in protection from cancer (35). Wound healing is a tightly regulated process of inflammation, infiltration, and proliferation, with specific proteins driving senescence of particular cells. The CCN1/CYR61 matricellular protein, is involved in this process and can induce senescence in the fibroblasts at site of wound repair (32). Mouse studies in which the CCN1 locus was replaced a mutated sequence showed that mice lacking the active form of this gene had faster wound healing but greater levels of fibrosis (scarring) and lower levels of senescence markers including SA-β-Gal and $p16^{INK4a}$ (32) compared to WT. As the exogenous addition of CCN1 to cutaneous wounds of mutated mice resulted in the increase of *Mmp2*, *Mmp3*, and *Mmp9*, and reduced expression of *Col1a1* and *Tgfb1* (32), this indicates a role of senescence in limiting excessive fibrosis in wound healing, where fibrosis could become detrimental. The beneficial role of senescence in acute wound healing is supported by studies using genetically-mediated depletion of senescent cells - where senescent cell removal resulted in a delay in skin wound closure (31).

Chronic senescence is marked by senescent cells that accumulate with age and chronic diseases, such as pre-cirrhotic fibrosis of livers (36, 37) and chronic kidney disease in which senescent cell accumulation correlates to increased disease severity (38) Accumulation of senescent cells also contributes to radiation toxicity from radiotherapy (39, 40) and chemotherapy (39). It is believed that chronically senescent cells become problematic when they are not destroyed and cleared by immune cells, such natural killer (NK) cells and macrophages (41), and continue to generate signaling molecules that systemically and locally affect the normal function of cell (19).

Senescent cells that accumulate with age, and their associated SASP, can alter the functions of other cells of an organism (42–44). This ties in closely with the geroscience hypothesis (4). If ageing is viewed as a disease, certain drivers have been identified. For example, the expression of $p16^{INK4a}$ has both short and long term impacts, as it prevents cancer by triggering senescence, the cost of which is that ageing is promoted (45). Selective $p16^{INK4a}$ ablation ameliorates some ageing phenotypes, increasing production of T-cells and increases antigen-specific immune responses, but causes an increased risk of cancers such as high-grade B-cell neoplasms (45). Defense against cancer initiation is one of the key roles of senescence, with oncogenes such as RAF or BRAF causing oncogene-induced senescence (35). The advantage of senescence in this case would be the continued survival of an organism with gradual decline from ageing versus the more imminent death of the organism due to increase in cancer incidence, an example of antagonistic pleiotropy. This highlights the need for senescence as a protection mechanism, but a need to remove senescent cells after they have fulfilled their protective role, to prevent the detrimental impact of exposure of the SASP to healthy tissues and organs.

SENESCENCE IN THE KIDNEY

Senescence With Age/Injury

When the kidney undergoes damage, the resident cells including renal tubular epithelial cells, endothelial cells, podocytes, T-cells (46) and macrophages (47) produce paracrine signaling factors that affect resident tissues, termed the chronic kidney disease (CKD)-associated secretory phenotype (CASP) (48). The parallels between the CASP and the commonly accepted SASP may be due to the presence of senescent cells within the dysfunctional kidney, as many cytokines of the SASP are also found in the CASP such as IL-8, TNF-α and IL-6 (48). This would suggest that any comparisons of the secretory phenotypes

should be separated between senescent cells and the other cell types of the renal system as this may reveal other cell targets for therapeutics. This would help determine if SASP is driving the cell behaviors in the tissue or if they are independent.

Age has been shown to be a key contributor to progression of acute kidney injury (AKI) into chronic kidney disease (CKD) due to an inability to fully recover from an acute insult (49–51). Age can also be detrimental to transplantations, including kidneys, in which mice deficient in $p16^{INK4a}$ displayed fewer senescent cells, with an increase in proliferative rates of tubular cells, all leading to significantly better survival of donor mice (52). Studies using bilateral renal ischemia-reperfusion to induce AKI in young (8-10 weeks) and ageing (46-49 weeks) mice showed an increase in fibrosis by picrosirius red staining and immunolocalization of cellular fibronectin, collagen III and collagen IV in the older mice (49). This correlates to higher levels of p53 and $p21^{CIP1}$ expression as well as SA-β-Gal staining in the older mice. Less fibrosis and tubular atrophy was seen in $p16^{INK4a}$ knock-out mice after ischemia-reperfusion injury (52) and in addition to this, the deletion of senescent cells in old (18 – 24 months) and prematurely aged mice, resulted in a better prognosis (53). Whilst activation and proliferation of fibroblasts can be a key wound-healing response to injury, excessive fibrosis can also be detrimental to physiological functions across multiple organs including the heart, kidney, and liver.

Senescence in Other Organs

Liver pathologies can also be made worse by the presence of senescent cells as has been reviewed (54). Chronic injuries in the liver can lead to fibrosis, and may develop into cirrhosis, but may be resolved by several endogenous mechanisms, one of which is the CCN1 protein which induces senescence of hepatic myofibroblasts (55). However, this has also been shown to activate DNA damage response (DDR) pathways and p53 by engaging integrin $\alpha_6\beta_1$ which generates the production of reactive oxygen species (ROS) which stimulates the DDR, activating the p53-$p21^{CIP1}$ dependent pathway of cellular senescence (32, 55, 56). These acutely senescent cells display anti-fibrotic transcriptional programs, resolving potentially dangerous fibrosis of the liver (55). This also demonstrates the complex and contextually significant role of senescent cells in the body, which can be beneficial in injury resolution and wound healing, and must be taken into consideration with any systemic therapies that target senescent cells.

Senescent cells are found in multiple tissues of the body, including the bones and brain. For example, an increase in the number of senescent astrocytes are found in cadaveric Parkinson's disease patients compared to normal control tissues, along with an increase in SASP markers IL-6, IL-1α and IL-8 (29). In mice, clearance of senescent [glial] cells of the brain has been shown to reduce the accumulation of hyperphosphorylated tau aggregates in the dentate gyrus (responsible for memory formation and cognition), that has been linked to cognitive decline (57) and Alzheimer's (58). Similarly, clearance of senescent cells that accumulate in osteoarthritis produced a pro-regenerative environment as marked by subchondral sclerosis and osteophyte formation similar to controls (59). Inhibition of SASP factors generated by senescent cells, such as the profibrotic TGF-β, has also been shown to improve regeneration in the liver (60).

CLEARANCE OF SENESCENT CELLS BY THE IMMUNE SYSTEM

When senescence is induced, these cells need to be cleared from tissues to prevent damage to the surrounding cells. The SASP generated by senescent cells is able to promote immune clearance of the senescent cells (61). The SASP potency can be modulated by the epigenetic regulator BRD4 (Bromodomain-containing protein 4), as when this was knocked down, secreted SASP factors in *in vitro* cultures were reduced (62). *In vitro* experiments also showed that conditioned medium from senescent cell cultures induced senescence in naïve cells, halting proliferation and upregulating SA-β-Gal activity, whereas conditioned medium from BRD4-inhibited cultures had significantly reduced capacity to transmit senescence to naïve cells (62).

Senescent cell destruction within tissues can be carried out by natural killer (NK cells). One of the first instances in which this was reported was in a study in which p53 was activated in liver carcinomas using RNAi, resulting in rapid tumor regression, and inhibition of NK cells showing significantly delayed tumor regression compared to controls (63, 64). By Day 8 of p53 senescence induction, infiltration of leukocytes including NK cells was observed in mouse kidneys by immunohistochemistry, with detection of NK-specific transcripts (*Klrb1* and *Klrd1*) upregulated in tumors suggesting NK infiltration because of the presence of senescent tumor cells (63).

NK cells are not the only immune cell involved in the clearance of senescent cells. Macrophages can be recruited by numerous factors, including SASP factors and the secretome of NK cells. NK cells can produce interferon gamma (IFN-γ) upon interaction with senescent cells (65) which acts to recruit macrophages (66). In addition to this the induction of tumor senescence can lead to an increase in oxidative stress, as shown in breast cancer due to protein acetyltransferase dysregulation (67). This led to an increase in chemoattractants CCL2, CXCL1, CXCL16 and IL-8, which recruit NK cells and macrophages, causing clearance of senescent tumors (67). This is matched in other organs; for example the liver where senescent hepatic myofibroblasts, produce CCL2, attracting $CCR2^{+}$ macrophages to the liver to clear pre-cancerous cells, demonstrating a protective role for senescence in the liver (68). Together this shows the orchestration of immune cells by signaling of senescent cells to exert a protective anti-cancerous role, with the roles of macrophages in senescence being explored later.

MACROPHAGES

Functions

Macrophages have a diverse range of functions, including tissue homeostasis, immune surveillance, resolving cutaneous wound

healing (69), clearance of red blood cells (70, 71) and even supporting embryogenesis (72). One of their primary functions as 'big eaters' is to phagocytose cells, such as apoptotic cells [efferocytosis (73)] and senescent cells (33). One component of the macrophage lysosome is DNase II which degrades the DNA of engulfed cells (74). Mouse experiments in which DNase II was knocked out, showed undigested DNA within the lysosomal compartment of macrophages, leading to activation of the immune system as marked by increases in IFN-γ and more moderately, TNF-α (74). This indicates that incomplete phagocytosis can be pro-inflammatory. During inflammation of the body, macrophages can be recruited by chemotactic factors secreted by neutrophils to aid in inflammation resolution. This is useful in host defense against pathogens in which macrophages phagocytose apoptotic neutrophils (75) which promotes inflammation resolution (76).

The ability of macrophages to robustly clear senescent cells from the tissues of the body diminishes with age (77). One proposed explanation for this is for macrophages to be able to acquire senescent-like properties, termed "senescent associated macrophages (SAMs)". A possible cause of this may be due to the ability of the SASP of senescent cells to induce senescent features in macrophages such as SA-β-Gal positivity (28, 78). However, as there is inherent β-galactosidase activity in macrophages due to their lysosomes (79), this cannot be an accurate marker to definitively class macrophages as senescent.

Macrophages in the Kidney and Models to Dissect Senescent Cell–Macrophage Interactions

Resident macrophages of the kidney arise from three separate sources, the C-Myb independent yolk-sac EMP-derived, fetal liver C-Myb dependent EMP-derived and finally, hematopoietic stem cells (HSC) as comprehensively summarized (80). Macrophages in the adult kidney can be separated by markers into distinct populations, which may result in them displaying differing responses to stimuli.

Circulating monocytes can populate the kidney and mature to macrophages to continue to provide immune and injury response, but these are not precise analogues to the long-lived kidney resident macrophages (KRM) (81). Models have been developed to study the effect of senescent cells in the kidneys of young mice (82). These models utilize *Pax8* which is a transcription factor involved in the formation of the kidney tissues in mice, with human homologues (83). Conditional excision of *mdm2* is driven by *Pax8*; *mdm2* codes for MDM2 which negatively regulates p53, promoting stabilization and degradation by ubiquitination, promoting senescence induction (84). The $Csf1r^{\Delta FIRE/\Delta FIRE}$ (FIRE) mouse has recently been developed, and shows robust elimination of resident F4/80^{high} macrophages in multiple tissues of interest including the kidney (85). This was achieved by the removing the super enhancer (*fms*-intronic regulatory element) located in the second intron of the *Csf1r* gene (85). This improves on the limitations of the $Csfr1^{-/-}$ macrophage deficient mouse model which showed lack of bone remodeling (osteopetrosis), resulting in deformities during development, and reproductive defects, resulting in lower pregnancy rates (86). In addition to this, the niche population is not repopulated by circulating monocytes (85), which suggest the alteration of the niche-cell interaction by the removal of the CSF-1 receptor from F4/80^{+} cells (85).

These models will provide information of the effects of senescent cells in young animals and their effects on macrophages in an *in vivo* setting. These two models may provide insight into how different macrophage populations interact with senescent cells of the kidney, for instance in the absence of resident F4/80^{high} renal macrophages, and in mice exposed to chronically senescent cells from an early age.

MACROPHAGE PLASTICITY

Macrophages display phenotypes adapted to their various roles and can be classified very simply as M1 (pro-inflammatory) or M2 (pro-regenerative) states based upon cell surface markers, synthesis of specific factors and biological activities. This was first suggested by Mills and colleagues, based upon the Th1/Th2 paradigm (87) and represents extremes of a spectrum of polarization states (88) (**Figure 2**). M1 macrophages generate inflammatory cytokines (89) in response to microbial infection or inflammation, such as IL-6 (90), nitric oxide (NO) (91, 92), TNF-α, IL-1β, IL-12 and IL-23 (93, 94). Inflammatory monocytes are recruited to sites of acute and chronic kidney injury, with the SASP-associated CCL2 promoting the accumulation of cytotoxic and pro-inflammatory M1 (classically activated) macrophages (95, 96).

After injury, pro-reparative or 'alternatively activated' M2 macrophages can be induced by exposure to Th2 type cytokines, such as IL-4 and IL-13 (97, 98) or phagocytosis of apoptotic cells, with transition from M1 to M2 polarization seen in successful resolution of inflammation by the production of mitogenic and pro-survival signals that promote renal repair (88, 99, 100). Failure of macrophages to switch from a pro-inflammatory state to the pro-reparative state has been implicated in chronic diseases, including chronic kidney disease due to the excessive fibrosis caused by the presence of a proinflammatory environment (49). M2 macrophages have anti-inflammatory roles, secreting cytokines such as IL-10, and express markers such as CD206, Ym1, CD163, CCL1, CCL18, FIZZ1, arginase1 (Arg1) and chitotriosidase genes (101–103). In the lungs it has been shown that M2 macrophages are able to suppress inflammation secretion of factors that affect the behavior of surrounding cells (103).

M2 macrophages are crucial to wound healing, with their functions including clearance of debris, activation of regulatory T-Cells, suppression of inflammation, reduction of neutrophil infiltration and antagonism of M1 macrophage functions (104). M2 macrophages can be further subdivided into M2a,b,c and d types (**Figure 2**), with M2a being the most commonly described and referred to as alternatively activated (IL-4 induced) (100). M2a are activated by IL-4 and IL-13 while M2c are activated by IL-10 and TGF-β, and glucocorticoids (105). M2a (wound-

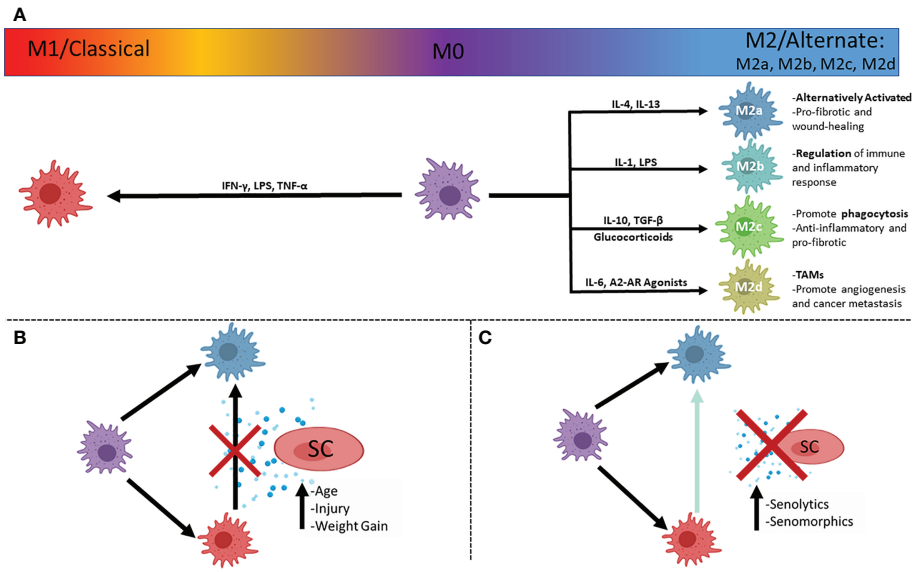

FIGURE 2 | The simplified polarizations of macrophages and potential interactions with senescent cells. **(A)** Macrophages can be in an unpolarized M0 state, and polarize to the classical inflammatory M1 state, or the alternately activated, pro-reparative M2 state, with subcategories of M2 activation that dictates function, with prominent drivers listed. **(B)** Plasticity of macrophages allows a shift in polarized states from M1 to M2 that can be inhibited by the secretosome of senescent cells (SASP), associated with injuries to organs and increasing age. **(C)** Inhibition of polarization shift can be ameliorated with pharmaceutical compounds ultimately minimizing the effect of the SASP. SC, Senescent cell; TAMs, Tumor Associated Macrophages.

healing macrophages) are profibrotic, secreting TGF-β, insulin-like growth factor (IGF) and fibronectin (106). M2c potently induce regulatory T-cells, which aid in protection from renal injury (104, 107). It has been shown, using mouse renal models, that both M2a and M2c polarizations can be robustly induced in aged mononuclear cells *in vitro*, whereas polarization was limited *in vivo* in IRI models when compared to young mice (108). This suggests that the intrarenal microenvironment of aged mice after IRI has a greater negative impact on macrophage polarization than the ageing of the bone-marrow derived monocytes (108). M2c subtypes also have strong anti-inflammatory and pro-fibrotic functions due to the production of IL-10 and TGF-β, respectively, with high expression of Mer receptor tyrosine kinase (MerTK) for efficient phagocytosis of apoptotic cells (104, 106). M2b (regulatory macrophages) are activated by IL-1, LPS (105) and secrete both pro-inflammatory factors (IL-1β, IL-6, and TNF-α) as well as the potent anti-inflammatory IL-10, due to their roles in the regulation of inflammation and immune response (88, 106). M2d (tumor-associated macrophages – TAMs) are activated by IL-6 and A2 adenosine receptor (AR) agonists (105, 106), and represent a more detrimental class of M2 macrophage as they contribute to angiogenesis (by release of vascular endothelial growth factor – VEGF) and cancer metastasis (109, 110).

As with M1 macrophages, niche context can also influence M2 functions, as increased fibrosis (collagen I, II and III deposition) is seen in injured kidneys due to the signaling effects of macrophages on resident kidney fibroblasts (111). To some extent, macrophage origin can also affect polarization capacity, as the M2a subtype derived from bone marrow was more likely to switch to an inflammatory phenotype, than M2a cells derived from the spleen (104). Macrophages are not terminally differentiated and retain the ability to switch to other phenotypes. As well as M1 macrophages having the ability to switch to a more pro-repair phenotype (99), M2 macrophages can be induced to adopt proinflammatory features to enable microbial killing (112).

Macrophages and Fibrosis

In the kidney, with increased ageing, fibrosis can be driven by the upregulation of the Wnt/β-catenin signaling and renin-angiotensin system (RAS) pathways, shown by an increase of fibronectin and picrosirius red staining (113). This was validated by the experimental overexpression of Klotho which acts as an antagonist of Wnt/β-catenin, resulting in diminished renal fibrosis, preservation of mitochondrial mass and reduced production of reactive oxygen species (ROS) (113). Levels of Klotho decrease with age in mice (over 12 months), correlating to increase in fibrosis and aging markers. This indicates that potent and selective inhibitors of the Wnt/β-catenin pathway could provide a useful therapeutic for age-related fibrosis as well as fibrosis caused by the presence of senescent cells due to injury in the kidney.

However, fibrosis may be caused by other mechanisms, such as macrophages. Pro-reparative ("M2") macrophages have the potential to accelerate tissue repair, but if they remain persistently activated, or are continually recruited, they may contribute to chronic fibrosis (114). This is due to secreted cytokines from macrophages, such as TGF-β which simultaneously has anti-inflammatory and profibrotic activity (114).

Tissue fibrosis may be impacted by the effect of ageing on macrophages, which undergo changes in secretory production. Importantly the anti-inflammatory IL-10 cytokine is decreased (115). This has important implications for tissue function as IL-10 is also anti-fibrotic by inhibition of pro-fibrotic molecules such as TGF-β (116). Recent therapeutic research has focused on the potential of utilizing IL-10 for its potent antifibrotic properties (117). This highlights an important decline in a key M2 macrophage signaling molecule, demonstrating a decrease in potency with host age and leading to tissue environments more permissive to fibrosis.

Macrophages in Kidney Injury

When the kidney is injured, proliferative monocytes are recruited and infiltrate the kidney to the site of tissue damage (118). This occurs after IRI (119) along an IL-6 chemotaxis (120), among other signaling factors. Monocyte infiltration begins early after injury, as shown by increased F4/80 staining at day 1. These monocytes migrate towards injured tubules of the outer medulla and mature to macrophages (121). Macrophages enhance pro-inflammatory damage caused by injury, as depletion of macrophages can be beneficial at early timepoints, as marked by a decrease in in blood urea nitrogen (BUN). However, they are also needed for resolution of inflammation and tissue repair, as their depletion (by liposomal clodronate) is detrimental at later (72 hour) timepoints at which recovery begins (13). This affect appeared to be due to the inflammatory environment of the kidney and how it changes over the first 72 hours of injury, in which pro-inflammatory cytokines such as CCL2 were upregulated in the first 24 hours, and anti-inflammatory IL-10 rose in later stages (13). This indicates that macrophages involved in kidney injury have functions that are dependent on the local cytokine signals, which affect their polarization, and show a beneficial effect when depleted at early inflammatory timepoints and a beneficial effect when re-administered at later timepoints. Depletion of macrophages by clodronate liposomes has been shown in other studies, delivering functional protection and reduced acute tubular necrosis (122). Genetic diphtheria toxin (DT)-mediated depletion of CD11b-DTR mouse macrophages did not give a protective effect compared to controls, possibly due to clodronate having a minimal effect on resident $CD11b^+$ populations (122). This suggests that partial depletion of mononuclear phagocytes at earlier timepoints has a cytoprotective effect.

After renal IRI, M2 macrophages are present at later timepoints of injury repair (~day 3), coinciding with peak cell division of tubular cells (121). Gene expression assays by qPCR showed that macrophages (fluorescence associated cell sorted for $F4/80^+$) in the injured kidneys displayed a concurrent decrease of iNOS and increase of Arg1, markers of pro-inflammatory/classical and alternatively activated macrophages respectively (121). To verify a transition of macrophage states from M1 to M2, and not polarization of infiltrating monocytes, bone marrow monocytes were labelled with PKH26 and exposed to interferon gamma (Ifn-γ) to stimulate iNOS-positive, pro-inflammatory M1 polarization, and injected 3 days post-IRI. PKH26 labelled cells collected at day 5 displayed downregulated iNOS expression and increased CD206 (mannose receptor), a marker for M2 polarization, suggesting their polarization altered in response to their environment (121).

Most of these studies have been carried out on young mice. However, the presence of senescent cells can impact macrophage phenotype. For instance, inhibition of the SASP cytokine TNF-α in human macrophages derived from peripheral blood mononuclear cells (PBMCs) induced a shift in polarization of macrophages to an M2 phenotype from an M1 phenotype and decreases the secretion of pro-inflammatory cytokines (TNF-α, IL-6 and IL-12) (123). Further experiments showed an increase in phagocytosis of M1 macrophages. Taken together, this indicates that through SASP signaling, senescent cells can reduce phagocytic activity of macrophages and inhibit the transition to pro-reparative M2 macrophages, leading to a persistence of pro-inflammatory M1 macrophages. How the presence of senescent cells with ageing might affect the roles of macrophages in inflammation and tissue repair after injury of the kidney and other organs warrants further experimental investigation.

SENESCENCE INDUCTION IN MACROPHAGES

The concept of "macrophageing" was first introduced in 2000 (78, 124, 125) and suggests that macrophages are induced into becoming senescent in response to signaling from surrounding cells. This has been a controversial subject in previous years, as although macrophages may display upregulation of senescence associated markers such as $p16^{INK4a}$ and SA-β-Gal (126) they remain proliferative indicating that they have not acquired "true" senescence (127). Evidence indicates that these markers that emerge are contextual in macrophages and may in fact be indicative of their polarization (128). Recent research has provided more evidence for senescent macrophages, as shown by significant upregulation of both $p16^{INK4a}$ and $p21^{CIP1}$ cell-cycle checkpoints in a mouse model of DNA damage repair deficiency (129). In addition to this, macrophages as sorted by $F4/80^+$ and $CD11b^+$ markers showed significant upregulation of SASP components, including TNF-α, IL-6 and IL-1β as compared to littermates, in which the coding sequence for DNA repair protein ERCC1 is not excised (129). This is matched by significant increases in $p16^{INK4a}$ and $p21^{CIP1}$ in the bone marrow compartment of the transgenic mice, compared to 2 year old wild-type control mice and un-induced controls, with an increase in the pro-inflammatory IL-6 accompanying this. This field is constantly being re-interpreted as new evidence is produced, and it is beyond the scope of this review to advocate for or against senescent macrophages, and will focus on the role(s) of senescent cells upon macrophages and their ability to function.

IMMUNOAGEING AND IMMUNEVASION

Ageing of the immune system is marked by a chronic level of systemic inflammation, which contributes to the pathogenesis of

age-related diseases called 'inflammaging' (124, 125). This can be seen in monocyte/macrophage populations of the body. The peripheral blood monocytes that in some cases invade tissues and supplement resident macrophages are reduced with age (130). The macrophages of the lungs (alveolar macrophages) have shown lower levels of phagocytosis of apoptotic neutrophils (75). This can lead to increased susceptibility to infections such as influenza, resulting in a higher mortality in mouse studies (75). In the brain, phagocytosis of amyloid-beta is reduced in multiple populations of blood monocytes (131).

The dysregulation of macrophage functions with age may be linked to low levels of innate immune activation as marked by sCD163 and CXCL10 (132). It was also found that age resulted in higher levels of inflammation as shown by an increase in TNF-α of aged monocytes compared to young human peripheral blood monocytes (132). Higher levels of inflammation are also seen in kidney macrophages of aged mice, with aged $CD73^+$ kidney mesenchymal stromal cells upregulating *Ccl2* with a higher proportion of $CCR2^+$ macrophages detected (95). This indicates an increase in pro-inflammatory macrophages with age. This is made more detrimental by the presence of senescent cells (**Figure 2**) that can cause macrophages to show 'senescent traits' (78), losing potency as shown by the decrease of IL-10 synthesis by "M2" macrophages (115) and a significant reduction in their capacity to phagocytose (133).

Macrophages of the spleen upregulate $p16^{INK4a}$ expression up to 20-fold in response to ionizing radiation, which is in stark contrast to the 4-fold upregulation seen in T-cells (134). This indicates a higher sensitivity of macrophages to ionizing radiation, as shown by a sharp decrease in absolute cell number, which is rescued by targeted depletion of $p16^{INK4a}$ cells. This would also indicate that immunosenescence induced by the SASP of splenic cells partially models the decline of immune system potency with age explained by inflammaging (78) and demonstrated by a decrease in phagocytosis with age (133). Given the key roles of macrophages in tissue repair, this higher sensitivity to the SASP components could be an explanation as to why senescent cell burden is such a detrimental component of the ageing soma and the role of decreased immune function has been shown to accelerate senescent burden (135). Despite rescue of cell number by $p16^{INK4a}$ cell depletion, phagocytic activity measured by uptake of a fluorescent substrate, was diminished. It remains possible that there exists a spectrum of senescence due to the multiple components that can contribute to the phenotype, as senescence markers such as $p16^{INK4a}$, $p21^{CIP1}$, and SASP components (IL-6, IL-1α) can be present but well-established markers such as SA-β-Gal can be absent (134).

CD47 is a membrane protein recognized as an inhibitory signal of phagocytosis or a "don't eat me" signal, first discovered in mice injected with red blood cells from CD47-null mice, in which the CD47 deficient red blood cells were rapidly cleared by splenic macrophages (136). As macrophages abundantly express the SIRP1α receptor, which binds to CD47, and depletion of splenic macrophages protected $CD47^{-/-}$ red blood cells when injected into wild-type mice, this suggests the CD47-SIRP1α axis represents a method of evasion of immune clearance and CD47 as a "marker of self" (136). CD47 is overexpressed in cancers (137), and senescent cells upregulate expression of CD47 (138), including in human renal proximal tubular epithelial cells. This may allow cancers and senescent cells to appear as "self" to the immune system and escape clearance. As previously mentioned, senescent cells have roles in development (72), and it is possible that their ability to upregulate CD47 is an example of antagonistic pleiotropy (139), in which senescent cells need to avoid clearance during development and therefore upregulate CD47, an ability that becomes detrimental in later life as senescent cells persist and generate SASP.

Other immune cells are affected by age. The number of activated, $CD56^{bright}$ NK cells that produce cytokines decreases with age in humans (>60 years) (140). *In vitro* studies have shown that senescent cells are able to escape by NK cell cytotoxicity by upregulation of HLA-E (MHC I) which can bind inhibitory receptors on NK cells (41). In addition, activating ligands for the NKG2D receptor such as MICA can be cleaved from the surfaces of senescent cells by matrix metalloproteases (MMPs) (141). These free MICA ligands are able to bind to the NKG2A of NK cells and inhibit binding to target cells, with a reversal of this evasion shown by a broad-spectrum MMP inhibitor (141).

THERAPEUTIC INTERVENTIONS TO TACKLE DETRIMENTAL EFFECTS OF CHRONIC SENESCENT CELLS

Macrophage Therapeutics

As macrophages have been shown to be involved in kidney injury, with their removal at early timepoints appearing beneficial (13, 122), controlled depletion of macrophages may be of therapeutic interest. However, the methods used in these mice studies may not effectively translate to humans, and there may be off-target effects, depleting other macrophage populations. This could be deleterious in some settings, for instance if a patient was to suffer a myocardial event (142), and could disrupt normal homeostasis of red blood cell turnover by depletion of splenic macrophages (136).

Tailored genetic therapies are another possible option. Macrophages that have had their SIRPα receptor knocked out by CRISPr-Cas9, caused an increase of phagocytosis of human osteosarcoma cells by a factor of 4 (143). This study did not investigate phagocytic capacity of senescent cells, but logically as the macrophages are the cells being edited, senescent cells would also be more likely to be phagocytosed due to the lack of the SIRPα on the macrophages. Again, this is limited by its proof-of-principle in experimental settings, using human cell lines.

An alternative to time-consuming tailored healthcare, is the administration of humanized anti-CD47 antibodies (144). This study showed that the AO-176 antibody bound to human CD47, resulting in increased tumor cell death. An advantage of this is that the AO-176 antibody had minimal affinity for red blood cells, a common drawback of previous CD47 antibodies (144).

Further investigation of whether this anti-CD47 antibody has any anti-senescent properties is warranted.

Interventions to Improve Macrophage/ Senescent Cell Clearance

Klotho

The kidney accumulates senescent cells with age, with mouse studies in which targeted depletion of senescent cells led to a decrease in age-associated pathologies in the kidney (43). Senescence is regulated internally by different mechanisms, one of which is the *Klotho* gene. ICGN ('Institute of Cancer Research'- derived glomerulonephritis) mice transgenic for the *Klotho* gene had an average survival of 70% compared to ICGN controls (30%) (145). This overexpression of *Klotho* also led to a decrease in senescence associated SA-β-Gal, an established marker of senescence. Together, these indicate that *Klotho* positively affects survival, possibly by reducing senescent burden. *Klotho* knock-out mice have an increased number senescent cells (146), and as human levels of *Klotho* decline with CKD (147) it may be beneficial to increase soluble KLOTHO levels in patients. This repression of accelerated senescence, which is found with glomerulonephritis, preserves renal function and improves survival (145).

Senolytics and Senomorphics

Senescent cells have been shown to accumulate in age and in disease in both human and animal tissue and crucially, their clearance in animal models is safe and has been shown to improve health span (43) and organ function (39, 53). It has become of therapeutic interest to remove senescent cells, operating under the hypothesis that removal of chronically senescent cells will have a positive impact on local and systemic tissues (**Figure 3**). Drugs that accomplish this are called senolytics and treatments that target senescent cells are called senotherapies.

Recent studies have focused on small molecular compounds to inhibit the pro-survival mechanisms of senescent cells, such as ABT-263 (Navitoclax) and ABT-737 (148) which inhibit Bcl2/w/xL (39). ATB-263-induced elimination of senescent cells improves prognosis after IRI injury in mice as seen by decrease in fibrosis and ongoing injury, with increased levels of regeneration and better kidney function (53). Human trials of ABT-263 have revealed that the onset of thrombocytopenia (abnormally low platelet counts) may limit the dose/timing of ABT-263 administration to patients (149). Further research is required to determine if ABT-263 can be used as a senolytic in different settings, such as organ rejuvenation in transplants.

It has been shown that the senolytics, dasatinib and quercetin (D+Q) can be safely used in humans (150, 151). D+Q have a different target to ABT-263, and cause depletion of macrophages, with early studies showing a decrease of macrophage number per adipocyte by 28% (150). The control of senescent cell clearance by pharmaceuticals proves crucial, as inhibition of acute senescence present in wound healing (31, 32), could be disruptive to natural wound-healing processes that animal models/patients may be undergoing. This same study demonstrated that common markers for senescent cells, namely $p16^{INK4a}$/$p21^{CIP1}$ expression and β-galactosidase activity at pH 6.0, were decreased post senolytic treatment, but this can't be attributed to Langerhans cell clearance or macrophage recruitment (150).

It has been proposed that noncoding RNAs (ncRNAs) may have a role in the regulation of SASP factors generated by senescent cells (152). Exogenous administration of ncRNAs

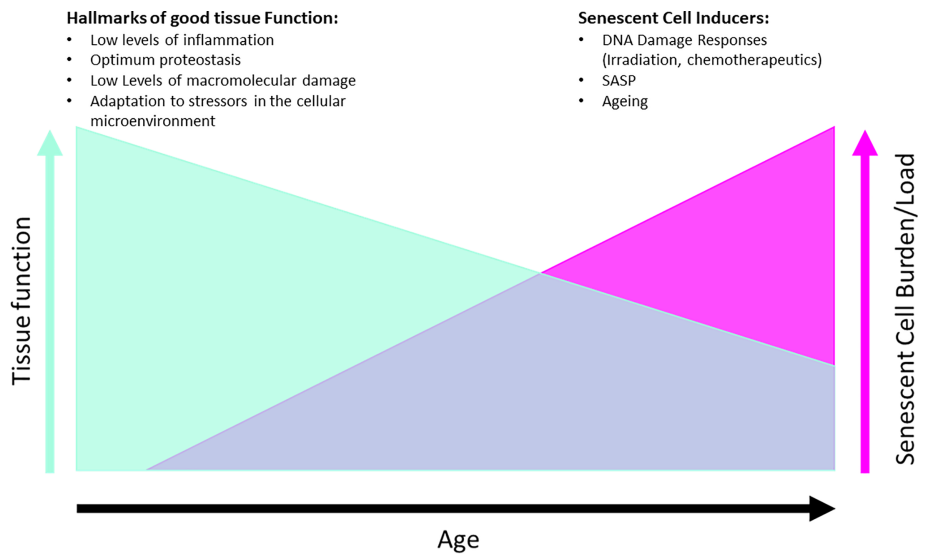

FIGURE 3 | Hypothesis of effects of senescent cell removal therapies on tissue function, with examples of each of different hallmarks and drivers listed for both conditions. Graphs are not directly proportional as mitigating factors can alter the tissue functionality such as diet, exercise, disease.

capable of downregulating SASP factors (senomorphics) may provide a complimentary approach to senescence therapeutics such as senolytics and lifestyle adaptations.

Exposure to chemotherapeutic drugs such as Actinomycin D (ActD) can induce senescence in human mesenchymal stem cells (hMSCs) (153). Whilst the resident cells may be prevented from becoming cancerous, the effect of the SASP-generating senescent cells on the hMSC niche may be detrimental over time. Therefore, it is important that be able to target the induced senescent cell populations for removal, to give more tailored treatments.

Studies in which senescent cells were transplanted into healthy young mice, showed an increase in mortality as a result of senescent cell burden, which was subsequently reversed by intermittent administration of dasatinib and quercetin (154). This reduction of senescent cell burden has also been replicated in humans with diabetic kidney disease, however effects on mortality remain to be assessed (150). Elimination of senescent cells relieved persistent physiological dysfunctions including the secretion of frailty-related pro-inflammatory cytokines, as demonstrated by human adipose tissue explants (154). This and other methods are outlined in **Table 1**, adapted with permission (160).

Lifestyle

Hall and colleagues showed that many $p16^{INK4a}$ and SA-β-gal positive cells in the adipose tissue of mice may have been SAMs (senescent associated macrophages), attracted by senescent cells, and displaying pro-inflammatory ("M1") phenotype (126) which has been shown to create a sterile inflammatory environment associated with obesity, as reviewed comprehensively (161). If adiposity affects senescent cell numbers, this could indicate that life-style choices (i.e. weight loss by calorie restriction and exercise) may successfully reduce numbers of macrophages secreting pro-inflammatory cytokines, by minimizing excess adipose tissue in response to exercise, showing positive feedback by reducing leptin (satiety hormone) (162) and minimizing adipose tissue – which is reported to contain large numbers of senescent cells (3) – and cause inflammation (126, 154). As briefly reviewed, by Xu and colleagues (163) pro-inflammatory mediators can also be reduced by CR. This may

TABLE 1 | Experimental models of senescent cell deficiency/induction/depletion in the kidney and their effects on renal outcomes.

Reference	Model	Modulation of Senescence	Outcome	Effect of Any Intervention
(43)	Natural aging In INK-ATTAC mice	INK-ATTAC +AP20187 or vehicle administration to deplete $p16^{ink4a}$+ cells	↑Glomerulosclerosis ↑ ß-gal positivity	↓Glomerulosclerosis ↓ß-gal positivity
(155)	Natural aging p16-3MR mice and fast aging Xpd TTD/TTD mice	FOXO4-DRI agent causes p53 nuclear exclusion. Ganciclovir Rx to p16-3MR mice causes $p16^{ink4a}$+ restricted cell death	↑Serum Urea ↓Lmnb1 expression ↑SASP expression (both $Xpd^{TTD/TTD}$ and aged p16-3MR)	FOXO4-DRI or GCV to p16-3MR admin: ↓Serum Urea ↑Lmnb1 expression ↓SASP expression (both $Xpd^{TTD/TTD}$ and aged p16-3MR)
(34)	Nephrogenesis	WT *vs* $P21^{cip1}$ KO mice with deficient growth arrest in nephrogenesis	↓ ß-gal positivity in $P21^{cip1}$ KO mice utero. ↑Ki67 expression but ↑Apoptosis maintains development	Use of PI3K inhibitor augments developmental senescence in WT mice
(156)	UUO	WT *vs* $p16^{ink4a}$ KO mice with impaired cell cycle arrest	UUO induces ß-gal positivity, apoptosis, and collagen deposition in WT mice	↓ ß-gal positivity ↓Apoptosis ↑Collagen, ↑proliferation after UUO in $p16^{ink4a}$ KO
(157)	Renal IRI	WT *vs* $P21^{cip1}$ KO mice with impaired cell cycle arrest	WT mice show tubular injury and raised blood urea levels after IRI	↑proliferation ↓Renal function ↑Mortality in $P21^{cip1}$ KO
(156)	Renal IRI	WT *vs* $p16^{ink4a}$/$p19^{ARF}$ Double KO mice with impaired cell cycle arrest	WT mice show marked $p16^{ink4a}$ and $p19^{ARF}$ induction 28d after IRI, with apoptosis and reduced tubular density	$p16^{ink4a}$ and $p19^{ARF}$ deficient mice show improved epithelial and microvascular repair, with increased myeloid cell recruitment
(158)	Diabetic	WT *vs* $p21^{cip1}$ KO	WT mice develop albuminuria and glomerular hypertrophy	Both $p27^{kip1}$ KO and $p21^{Cip1}$ KO mice were protected from proteinuria and glomerular expansion
(159)	Nephropathy	WT *vs* $p27^{kip1}$ KO		
(52)	Renal Transplant	$p16^{ink4a}$ KO mice with impaired cell cycle arrest	WT mice develop interstitial fibrosis and tubular atrophy	$p16^{ink4a}$ KO mice develop less atrophy and fibrosis after Tx
(154)	Senescent cell transplant (young and older mice)	Dasatinib and Quercetin (D +Q) - senolytic administration	↑ Frailty ↑ Mortality ↑ Senescent burden	↓In frailty-related + pro-inflammatory cytokines (IL-6, IL-8, CCL2, PAI-1, GM-CSF) ↑ Survival
(150)	Diabetic Kidney Disease (Human)	Dasatinib and Quercetin (D +Q) - senolytic administration	↑ ↑ Probability of end-stage kidney failure ↑ Senescent burden	↓ $p16^{INK4A}$ and $p21^{CIP1}$ positive cells ↓ SASP (IL-1α, IL-2, IL-6, IL-9, MMP-2, MMP-9, MMP-12) ↓ $CD68^{+}$ macrophages

Transgenic and genetic knockout mice have been used to study the impact of 1) deficiencies in the induction of senescence or 2) depletion of established senescent cells. Several of these models are summarized in this table, with description of the experimental model of renal disease used, the alteration in senescence induction employed and any alterations in renal disease outcomes. TTD/TTD, trichothiodystrophy/trichothiodystrophy; GCV, ganciclovir; WT, wild-type; KO, knock-out; UUO, unilateral ureteric obstruction; IRI, ischemia-reperfusion injury; Tx, Transplant; PAI-1, plasminogen activator inhibitor-1; GM-CSF, granulocyte macrophage colony-stimulating factor; IL-, Interleukin-; MMP-, Matrix Metalloprotease. Adapted with permission (160).

be a relevant therapeutic intervention due to the oxidative damage in response to transplantation procedures, caused by ischemia-reperfusion injury, which may lead to an increase in senescent burden and therefore premature ageing of the transplant and surrounding tissues (164). However, as previously mentioned this could lead to accelerated grey matter atrophy (18), meaning cost-benefit analysis needs to be considered for administration to patients.

THERAPEUTICS – CONCLUSIONS

The presence of senescent cells may be the most relevant case of the antagonistic pleiotropy theory of ageing (139), in that the key genes involved in senescence are beneficial in early life, promoting healthy embryogenesis (33) and rapid wound repair whilst protecting from cancer formation/progression (35). However, as senescent burden increases with age, SASP generating cells comprise a larger proportion of non-regenerating cell populations in tissues, negatively affecting homeostasis (42, 126, 165). This would suggest that certain therapeutic interventions, such as pharmaceutical treatment (senolytics/senomorphics) or lifestyle changes [regular aerobic exercise (3, 162)] may only show a significant impact when administered to patients of a certain age, who have accumulated enough senescent cell burden, and pharmaceutical interventions may be preventative. Senescence has wide-reaching effects and the elective administration of appropriate senolytics has the potential to improve the quality of life for patients with chronic conditions and age-associated morbidity, and further clinical trials are warranted.

CHALLENGES FOR FUTURE RESEARCH INTO AGEING-ASSOCIATED FIBROSIS

Ageing is difficult to model in a translationally significant manner using genetically close models, due to the marked expense and timescale limitations of non-human primate (NHP) models such as rhesus monkeys that live three to four decades. Although uncommon, these studies have been performed, pooling non-human primates (gorilla, rhesus monkey, baboon and others) to identify conservation of certain ageing phenotypes across species, such as arterial thickening correlated to increased age (166). The trans-NIH GSIG summit identified the induction of pathologies in young mice precludes analysis of interactions with other aspects of ageing seen in chronic diseases, requiring longer term studies to recapitulate the ageing phenotype before pathology induction (4). To overcome the limitations of relatively long-lived animals used for ageing, other vertebrate models have been assessed for use, for example the African turquoise killifish (*Nothobranchius furzeri*) has been assessed as a model for aging against the "Hallmarks of Ageing" (1) and has begun to be genetically altered and separate lines bred to provide a genetic toolkit to investigate ageing (167, 168).

FINAL CONCLUSIONS

Senescent cells are attractive candidates as drivers of age-related organ dysfunction. They are consistently seen in diseased and older tissues when compared with healthy age-matched controls, actively secreting pro-inflammatory and pro-fibrotic molecules (90–92) capable of driving further (paracrine) senescence and propagating on-going tissue damage (78, 125). This is potentially because they secrete pro-inflammatory cytokines in the SASP which modify the surrounding environment (169).

Macrophages contribute to clearance of senescent cells by phagocytosis (73). This activity declines with age in multiple organ systems (115), including the kidney, as macrophages polarize from M1 to M2 in response to exogenous growth factors (170), and can potentially become 'senescent-associated' (78, 125, 133) and possibly senescent themselves (129). This is followed by a concurrent increase in fibrosis with age, which negatively affects organ function.

New therapy strategies have been developed, both pharmaceutical (39, 150) and lifestyle changes (126, 162) that aim at reducing the burden of senescent cells and the SASP they generate, and reducing inflammation, aimed at removing blockades for macrophage polarity transitions essential for response to injuries. This research is slowed by the feasibility of ageing models currently utilized, however efforts by researchers have brought new animals more relevant to ageing research into mainstream use, as is the case with the African Killifish (167, 168).

Ageing is a complex interaction of different physiological responses that can be influenced by multiple factors from genetics to the environment, but current research has and is investigating these interactions and different factors for therapeutic benefit in humans.

AUTHOR CONTRIBUTIONS

RC: First author and primary writer. M-HD: Content contributor. DF: Content contributor and editor. KJM: Content contributor, editor, and last author. All authors contributed to the article and approved the submitted version.

FUNDING

RC is supported by the Wellcome Trust [108906/Z/15/Z]. M-HD is supported by a MRC Clinical Training Research Fellowship (CRTF) [MR/T008253/1]. DF is supported by Intermediate Clinical Fellowship 1243 [WT100171MA] from the Wellcome Trust. KJM is supported by a Chief Scientist Office/Kidney Research UK Fellowship [CSO_PDF/2018/1].

REFERENCES

1. López-Otín C, Blasco MA, Partridge L, Serrano M, Kroemer G. The Hallmarks of Aging. *Cell* (2013) 153(6):1194–217. doi: 10.1016/j.cell.2013.05.039
2. Dagli RJ, Sharma A. Polypharmacy: A Global Risk Factor for Elderly People. *J Int Oral Health* (2014) 6(6):i–ii.
3. Palmer AK, Gustafson B, Kirkland JL, Smith U. Cellular Senescence: At the Nexus Between Ageing and Diabetes. *Diabetologia* (2019) 62(10):1835–41. doi: 10.1007/s00125-019-4934-x
4. Kennedy BK, Berger SL, Brunet A, Campisi J, Cuervo AM, Epel ES, et al. Geroscience: Linking Aging to Chronic Disease. *Cell* (2014) 159(4):709–13. doi: 10.1016/j.cell.2014.10.039
5. Hui SL, Slemenda CW, Johnston CC. Age and Bone Mass as Predictors of Fracture in a Prospective Study. *J Clin Invest* (1988) 81(6):1804–9. doi: 10.1172/JCI113523
6. Farr JN, Xu M, Weivoda MM, Monroe DG, Fraser DG, Onken JL, et al. Targeting Cellular Senescence Prevents Age-Related Bone Loss in Mice. *Nat Med* (2017) 23(9):1072–9. doi: 10.1038/nm.4385
7. Alghatrif M, Strait JB, Morrell C, Canepa M, Ferrucci L, Lakatta EG. Longitudinal Trajectories of Arterial Stiffness and the Role of Blood Pressure: The Baltimore Longitudinal Study of Aging. *Hypertension* (2014) 62(5):1–16. doi: 10.1161/HYPERTENSIONAHA.113.01445
8. Blacher J, Guerin AP, Pannier B, Marchais SJ, Safar ME, London GM. Impact of Aortic Stiffness on Survival in End-Stage Renal Disease. *Circulation* (1999) 99(18):2434–9. doi: 10.1161/01.CIR.99.18.2434
9. Stenvinkel P, Larsson TE. Chronic Kidney Disease: A Clinical Model of Premature Aging. *Am J Kidney Dis* (2013) 62(2):339–51. doi: 10.1053/j.ajkd.2012.11.051
10. Kanasaki K, Kitada M, Koya D. Pathophysiology of the Aging Kidney and Therapeutic Interventions. *Hypertens Res* (2012) 35(12):1121–8. doi: 10.1038/hr.2012.159
11. Summers DM, Johnson RJ, Hudson A, Collett D, Watson CJ, Bradley JA. Effect of Donor Age and Cold Storage Time on Outcome in Recipients of Kidneys Donated After Circulatory Death in the UK: A Cohort Study. *Lancet* (2013) 381(9868):727–34. doi: 10.1016/S0140-6736(12)61685-7
12. Aprahamian T, Takemura Y, Goukassian D, Walsh K. Ageing is Associated With Diminished Apoptotic Cell Clearance *In Vivo*. *Clin Exp Immunol* (2008) 152(3):448–55. doi: 10.1111/j.1365-2249.2008.03658.x
13. Vinuesa E, Hotter G, Jung M, Herrero-Fresneda I, Torras J, Sola A. Macrophage Involvement in the Kidney Repair Phase After Ischaemia/Reperfusion Injury. *J Pathol* (2007) 214(1):104–13. doi: 10.1002/path.2259
14. Lakowski B, Hekimi S. The Genetics of Caloric Restriction in Caenorhabditis Elegans. *Proc Natl Acad Sci U S A* (1998) 95(22):13091–6. doi: 10.1073/pnas.95.22.13091
15. Brandhorst S, Choi IY, Wei M, Cheng CW, Sedrakyan S, Navarrete G, et al. A Periodic Diet That Mimics Fasting Promotes Multi-System Regeneration, Enhanced Cognitive Performance, and Healthspan. *Cell Metab* (2015) 22(1):86–99. doi: 10.1016/j.cmet.2015.05.012
16. Fontana L, Villareal DT, Das SK, Smith SR, Meydani SN, Pittas AG, et al. Effects of 2-Year Calorie Restriction on Circulating Levels of IGF-1, IGF-Binding Proteins and Cortisol in Nonobese Men and Women: A Randomized Clinical Trial. *Aging Cell* (2015) 15(1):22–7. doi: 10.1111/acel.12400
17. Most J, Tosti V, Redman LM, Fontana L. Calorie Restriction in Humans: An Update. *Ageing Res Rev* (2016) 39:36–45. doi: 10.1016/j.arr.2016.08.005
18. Pifferi F, Terrien J, Marchal J, Dal-Pan A, Djelti F, Hardy I, et al. Caloric Restriction Increases Lifespan But Affects Brain Integrity in Grey Mouse Lemur Primates. *Commun Biol* (2018) 1(1):30. doi: 10.1038/s42003-018-0024-8
19. Burton DGA, Stolzing A. Cellular Senescence: Immunosurveillance and Future Immunotherapy. *Ageing Res Rev* (2018) 43(February):17–25. doi: 10.1016/j.arr.2018.02.001
20. Hayflick L, Moorhead PS. The Serial Cultivation of Human Diploid Cell Strains. *Exp Cell Res* (1961) 25(3):585–621. doi: 10.1016/0014-4827(61)90192-6
21. Campisi J, Kapahi P, Lithgow GJ, Melov S, Newman JC, Verdin E. From Discoveries in Ageing Research to Therapeutics for Healthy Ageing. *Nature* (2019) 571(7764):183–92. doi: 10.1038/s41586-019-1365-2
22. Gorgoulis V, Adams PD, Alimonti A, Bennett DC, Bischof O, Bishop C, et al. Cellular Senescence: Defining a Path Forward. *Cell* (2019) 179(4):813–27. doi: 10.1016/j.cell.2019.10.005
23. Megyesi J, Price PM, Tamayo E, Safirstein RL. The Lack of a Functional p21WAF1/CIP1 Gene Ameliorates Progression to Chronic Renal Failure. *Proc Natl Acad Sci U S A* (1999) 96(19):10830–5. doi: 10.1073/pnas.96.19.10830
24. Melk A, Schmidt BMW, Takeuchi O, Sawitzki B, Rayner DC, Halloran PF. Expression of p16INK4a and Other Cell Cycle Regulator and Senescence Associated Genes in Aging Human Kidney. *Kidney Int* (2004) 65(2):510–20. doi: 10.1111/j.1523-1755.2004.00438.x
25. Coppé JP, Patil CK, Rodier F, Sun Y, Muñoz DP, Goldstein J, et al. Senescence-Associated Secretory Phenotypes Reveal Cell-Nonautonomous Functions of Oncogenic RAS and the p53 Tumor Suppressor. *PloS Biol* (2008) 6(12):2853–68. doi: 10.1371/journal.pbio.0060301
26. Andriani GA, Almeida VP, Faggioli F, Mauro M, Li Tsai W, Santambrogio L, et al. Whole Chromosome Instability Induces Senescence and Promotes SASP. *Sci Rep* (2016) 6(September):1–17. doi: 10.1038/srep35218
27. Wiley CD, Velarde MC, Lecot P, Liu S, Sarnoski EA, Freund A, et al. Mitochondrial Dysfunction Induces Senescence With a Distinct Secretory Phenotype. *Cell Metab* (2016) 23(2):303–14. doi: 10.1016/j.cmet.2015.11.011
28. Acosta JC, Banito A, Wuestefeld T, Georgilis A, Janich P, Morton JP, et al. A Complex Secretory Program Orchestrated by the Inflammasome Controls Paracrine Senescence. *Nat Cell Biol* (2013) 15(8):978–90. doi: 10.1038/ncb2784
29. Chinta SJ, Woods G, Demaria M, Rane A, Zou Y, McQuade A, et al. Cellular Senescence is Induced by the Environmental Neurotoxin Paraquat and Contributes to Neuropathology Linked to Parkinson's Disease. *Cell Rep* (2018) 22(4):930–40. doi: 10.1016/j.celrep.2017.12.092
30. Knoppert SN, Valentijn FA, Nguyen TQ, Goldschmeding R, Falke LL. Cellular Senescence and the Kidney: Potential Therapeutic Targets and Tools. *Front Pharmacol* (2019) 10(July):1–18. doi: 10.3389/fphar.2019.00770
31. Demaria M, Ohtani N, Youssef SA, Rodier F, Toussaint W, Mitchell JR, et al. An Essential Role for Senescent Cells in Optimal Wound Healing Through Secretion of PDGF-AA. *Dev Cell* (2014) 31(6):722–33. doi: 10.1016/j.devcel.2014.11.012
32. Jun J, Lau LF. The Matricellular Protein CCN1 Induces Fibroblast Senescence and Restricts Fibrosis in Cutaneous Wound Healing. *Nat Cell Biol* (2010) 12(7):676–85. doi: 10.1038/ncb2070
33. Storer M, Mas A, Robert-Moreno A, Pecoraro M, Ortells MC, Di Giacomo V, et al. Senescence is a Developmental Mechanism That Contributes to Embryonic Growth and Patterning. *Cell* (2013) 155(5):1119. doi: 10.1016/j.cell.2013.10.041
34. Muñoz-Espín D, Cañamero M, Maraver A, Gómez-López G, Contreras J, Murillo-Cuesta S, et al. Programmed Cell Senescence During Mammalian Embryonic Development. *Cell* (2013) 155(5):1104. doi: 10.1016/j.cell.2013.10.019
35. Muñoz-Espín D, Serrano M. Cellular Senescence: From Physiology to Pathology. *Nat Rev Mol Cell Biol* (2014) 15(7):482–96. doi: 10.1038/nrm3823
36. Krizhanovsky V, Yon M, Dickins RA, Hearn S, Simon J, Miething C, et al. Senescence of Activated Stellate Cells Limits Liver Fibrosis. *Cell* (2008) 134(4):657–67. doi: 10.1016/j.cell.2008.06.049
37. Kang TW, Yevsa T, Woller N, Hoenicke L, Wuestefeld T, Dauch D, et al. Senescence Surveillance of Pre-Malignant Hepatocytes Limits Liver Cancer Development. *Nature* (2011) 479(7374):547–51. doi: 10.1038/nature10599
38. Liu J, Yang JR, He YN, Cai GY, Zhang JG, Lin LR, et al. Accelerated Senescence of Renal Tubular Epithelial Cells is Associated With Disease Progression of Patients With Immunoglobulin A (IgA) Nephropathy. *Transl Res* (2012) 159(6):454–63. doi: 10.1016/j.trsl.2011.11.008
39. Chang J, Wang Y, Shao L, Laberge RM, Demaria M, Campisi J, et al. Clearance of Senescent Cells by ABT263 Rejuvenates Aged Hematopoietic Stem Cells in Mice. *Nat Med* (2016) 22(1):78–83. doi: 10.1038/nm.4010
40. Citrin DE, Shankavaram U, Horton JA, Shield W, Zhao S, Asano H, et al. Role of Type II Pneumocyte Senescence in Radiation-Induced Lung Fibrosis. *J Natl Cancer Inst* (2013) 105(19):1474–84. doi: 10.1093/jnci/djt212
41. Pereira BI, Devine OP, Vukmanovic-Stejic M, Chambers ES, Subramanian P, Patel N, et al. Senescent Cells Evade Immune Clearance Via HLA-E-mediated NK and CD8+ T Cell Inhibition. *Nat Commun* (2019) 10(1):2387. doi: 10.1038/s41467-019-10335-5

42. Nelson G, Wordsworth J, Wang C, Jurk D, Lawless C, Martin-Ruiz C, et al. A Senescent Cell Bystander Effect: Senescence-Induced Senescence. *Aging Cell* (2012) 11(2):345–9. doi: 10.1111/j.1474-9726.2012.00795.x
43. Baker DJ, Childs BG, Durik M, Wijers ME, Sieben CJ, Zhong J, et al. Naturally Occurring P16 Ink4a-Positive Cells Shorten Healthy Lifespan. *Nature* (2016) 530(7589):184–9. doi: 10.1038/nature16932
44. Hoyer FF, Naxerova K, Schloss MJ, Hulsmans M, Nair AV, Dutta P, et al. Tissue-Specific Macrophage Responses to Remote Injury Impact the Outcome of Subsequent Local Immune Challenge. *Immunity* (2019) 51 (5):899–914.e7. doi: 10.1016/j.immuni.2019.10.010
45. Liu Y, Johnson SM, Fedoriw Y, Rogers AB, Yuan H, Krishnamurthy J, et al. Expression of p16INK4a Prevents Cancer and Promotes Aging in Lymphocytes. *Blood* (2011) 117(12):3257–67. doi: 10.1182/blood-2010-09-304402
46. Betjes MGH, Langerak AW, van der Spek A, De Wit EA, Litjens NHR. Premature Aging of Circulating T Cells in Patients With End-Stage Renal Disease. *Kidney Int* (2011) 80(2):208–17. doi: 10.1038/ki.2011.110
47. Rodriguez-Menocal L, Faridi MH, Martinez L, Shehadeh LA, Duque JC, Wei Y, et al. Macrophage-Derived IL-18 and Increased Fibrinogen Deposition are Age-Related Inflammatory Signatures of Vascular Remodeling. *Am J Physiol Heart Circ Physiol* (2014) 306(5):641–53. doi: 10.1152/ajpheart.00641.2013
48. Wang W, Cai G, Chen X. Senescence , Phenotype , and Chronic Kidney Disease Secretory. *Oncotarget* (2017) 8(38):64520–33. doi: 10.18632/oncotarget.17327
49. Clements ME, Chaber CJ, Ledbetter SR, Zuk A. Increased Cellular Senescence and Vascular Rarefaction Exacerbate the Progression of Kidney Fibrosis in Aged Mice Following Transient Ischemic Injury. *PloS One* (2013) 8(8):e70464. doi: 10.1371/journal.pone.0070464
50. Coca SG, Singanamala S, Parikh CR. Chronic Kidney Disease After Acute Kidney Injury: A Systematic Review and Meta-Analysis. *Kidney Int* (2012) 81(5):442–8. doi: 10.1038/ki.2011.379
51. Ferenbach DA, Bonventre JV. Mechanisms of Maladaptive Repair After AKI Leading to Accelerated Kidney Ageing and CKD. *Nat Rev Nephrol* (2015) 11 (5):264–76. doi: 10.1038/nrneph.2015.3
52. Braun H, Schmidt BMW, Raiss M, Baisantry A, Mircea-Constantin D, Wang S, et al. Cellular Senescence Limits Regenerative Capacity and Allograft Survival. *J Am Soc Nephrol* (2012) 23(9):1467–73. doi: 10.1681/ASN.2011100967
53. Mylonas KJ, O'Sullivan ED, Humphries D, Baird DP, Docherty M, Neely SA, et al. Cellular Senescence Inhibits Renal Regeneration After Injury in Mice, With Senolytic Treatment Promoting Repair. *Sci Transl Med* (2021) 13(594): eabb0203. doi: 10.1126/scitranslmed.abb0203
54. Papatheodoridi AM, Chrysavgis L, Koutsilieris M, Chatzigeorgiou A. The Role of Senescence in the Development of Nonalcoholic Fatty Liver Disease and Progression to Nonalcoholic Steatohepatitis. *Hepatology* (2020) 71 (1):363–74. doi: 10.1002/hep.30834
55. Kim K-H, Chen C-C, Monzon RI, Lau LF. Matricellular Protein CCN1 Promotes Regression of Liver Fibrosis Through Induction of Cellular Senescence in Hepatic Myofibroblasts. *Mol Cell Biol* (2013) 33(10):2078–90. doi: 10.1128/MCB.00049-13
56. Collado M, Blasco MA, Serrano M. Cellular Senescence in Cancer and Aging. *Cell* (2007) 130(2):223–33. doi: 10.1016/j.cell.2007.07.003
57. Bussian TJ, Aziz A, Meyer CF, Swenson BL, van Deursen JM, Baker DJ. Clearance of Senescent Glial Cells Prevents Tau-Dependent Pathology and Cognitive Decline. *Nature* (2018) 562(7728):578–82. doi: 10.1038/s41586-018-0543-y
58. Musi N, Valentine JM, Sickora KR, Baeuerle E, Thompson CS, Shen Q, et al. Tau Protein Aggregation is Associated With Cellular Senescence in the Brain. *Aging Cell* (2018) 17(6):e12840. doi: 10.1111/acel.12840
59. Jeon OH, Kim C, Laberge RM, Demaria M, Rathod S, Vasserot AP, et al. Local Clearance of Senescent Cells Attenuates the Development of Post-Traumatic Osteoarthritis and Creates a Pro-Regenerative Environment. *Nat Med* (2017) 23(6):775–81. doi: 10.1038/nm.4324
60. Ferreira-Gonzalez S, Lu WY, Raven A, Dwyer B, Man TY, O'Duibhir E, et al. Paracrine Cellular Senescence Exacerbates Biliary Injury and Impairs Regeneration. *Nat Commun* (2018) 9(1):1–15. doi: 10.1038/s41467-018-03299-5
61. Kale A, Sharma A, Stolzing A, Stolzing A, Desprez PY, Desprez PY, et al. Role of Immune Cells in the Removal of Deleterious Senescent Cells. *Immun Ageing* (2020) 17(1):1–9. doi: 10.1186/s12979-020-00187-9
62. Tasdemir N, Banito A, Roe JS, Alonso-Curbelo D, Camiolo M, Tschaharganeh DF, et al. BRD4 Connects Enhancer Remodeling to Senescence Immune Surveillance. *Cancer Discov* (2016) 6(6):613–29. doi: 10.1158/2159-8290.CD-16-0217
63. Xue W, Zender L, Miething C, Dickins RA, Hernando E, Krizhanovsky V, et al. Senescence and Tumour Clearance is Triggered by p53 Restoration in Murine Liver Carcinomas. *Nature* (2007) 445(7128):656–60. doi: 10.1038/nature05529
64. Iannello A, Thompson TW, Ardolino M, Lowe SW, Raulet DH. p53-dependent Chemokine Production by Senescent Tumor Cells Supports NKG2D-dependent Tumor Elimination by Natural Killer Cells. *J Exp Med* (2013) 210(10):2057–69. doi: 10.1084/jem.20130783
65. Soriani A, Iannitto ML, Ricci B, Fionda C, Malgarini G, Morrone S, et al. Reactive Oxygen Species– and DNA Damage Response–Dependent NK Cell Activating Ligand Upregulation Occurs at Transcriptional Levels and Requires the Transcriptional Factor E2F1. *J Immunol* (2014) 193(2):950–60. doi: 10.4049/jimmunol.1400271
66. Corbera-Bellalta M, Planas-Rigol E, Lozano E, Terrades-García N, Alba MA, Prieto-González S, et al. Blocking Interferon γ Reduces Expression of Chemokines CXCL9, CXCL10 and CXCL11 and Decreases Macrophage Infiltration in *Ex Vivo* Cultured Arteries From Patients With Giant Cell Arteritis. *Ann Rheum Dis* (2015) 75(6):1177–86. doi: 10.1136/annrheumdis-2015-208371
67. Sharma C, Wang H-X, Li Q, Knoblich K, Reisenbichler ES, Richardson AL, et al. Protein Acyltransferase DHHC3 Regulates Breast Tumor Growth, Oxidative Stress, and Senescence. *Cancer Res* (2017) 77(24):6880–90. doi: 10.1158/0008-5472.CAN-17-1536
68. Eggert T, Wolter K, Ji J, Ma C, Yevsa T, Klotz S, et al. Distinct Functions of Senescence-Associated Immune Responses in Liver Tumor Surveillance and Tumor Progression. *Cancer Cell* (2016) 30(4):533–47. doi: 10.1016/j.ccell.2016.09.003
69. Delavary BM, van der Veer WM, van Egmond M, Niessen FB, Beelen RHJ. Macrophages in Skin Injury and Repair. *Immunobiology* (2011) 216(7):753–62. doi: 10.1016/j.imbio.2011.01.001
70. de Back DZ, Kostova EB, van Kraaij M, van den Berg TK, van Bruggen R. Of Macrophages and Red Blood Cells; A Complex Love Story. *Front Physiol* (2014) 5:9. doi: 10.3389/fphys.2014.00009
71. Kay MMB. Mechanism of Removal of Senescent Cells by Human Macrophages in Situ. *Proc Natl Acad Sci U S A* (1975) 72(9):3521–5. doi: 10.1073/pnas.72.9.3521
72. Egashira M, Hirota Y, Shimizu-Hirota R, Saito-Fujita T, Haraguchi H, Matsumoto L, et al. F4/80+ Macrophages Contribute to Clearance of Senescent Cells in the Mouse Postpartum Uterus. *Endocrinology* (2017) 158(7):2344–53. doi: 10.1210/en.2016-1886
73. Dimitrijević M, Stanojević S, Blagojević V, Ćuruvija I, Vujnović I, Petrović R, et al. Aging Affects the Responsiveness of Rat Peritoneal Macrophages to GM-CSF and IL-4. *Biogerontology* (2016) 17(2):359–71. doi: 10.1007/s10522-015-9620-x
74. Kawane K, Fukuyama H, Yoshida H, Nagase H, Ohsawa Y, Uchiyama Y, et al. Impaired Thymic Development in Mouse Embryos Deficient in Apoptotic DNA Degradation. *Nat Immunol* (2003) 4(2):138–44. doi: 10.1038/ni881
75. Wong CK, Smith CA, Sakamoto K, Kaminski N, Koff JL, Goldstein DR. Aging Impairs Alveolar Macrophage Phagocytosis and Increases Influenza-Induced Mortality in Mice. *J Immunol* (2017) 199(3):1060–8. doi: 10.4049/jimmunol.1700397
76. Serhan CN, Chiang N, Dalli J, Levy BD. Lipid Mediators in the Resolution of Inflammation. *Cold Spring Harb Perspect Biol* (2015) 7(2):a016311. doi: 10.1101/cshperspect.a016311
77. Lloberas J, Tur J, Vico T, Celada A. Molecular and Cellular Aspects of Macrophage Aging. In: T Fulop, C Franceschi, K Hirokawa and G Pawelec, editors. *Handbook of Immunosenescence: Basic Understanding and Clinical Implications*. Cham: Springer International Publishing (2019). p. 1631–63. doi: 10.1007/978-3-319-99375-1_46

78. Prattichizzo F, Bonafè M, Olivieri F, Franceschi C. Senescence Associated Macrophages and "Macroph-Aging": Are They Pieces of the Same Puzzle? *Aging (Albany NY)* (2016) 8(12):3159–60. doi: 10.18632/aging.101133
79. Lee BY, Han JA, Im JS, Morrone A, Johung K, Goodwin EC, et al. Senescence-Associated β-Galactosidase is Lysosomal β-Galactosidase. *Aging Cell* (2006) 5(2):187–95. doi: 10.1111/j.1474-9726.2006.00199.x
80. Munro DAD, Hughes J. The Origins and Functions of Tissue-Resident Macrophages in Kidney Development. *Front Physiol* (2017) 8(OCT):1–13. doi: 10.3389/fphys.2017.00837
81. Puranik AS, Leaf IA, Jensen MA, Hedayat AF, Saad A, Kim KW, et al. Kidney-Resident Macrophages Promote a Proangiogenic Environment in the Normal and Chronically Ischemic Mouse Kidney. *Sci Rep* (2018) 8(1):1–15. doi: 10.1038/s41598-018-31887-4
82. Thomasova D, Ebrahim M, Fleckinger K, Li M, Molnar J, Popper B, et al. MDM2 Prevents Spontaneous Tubular Epithelial Cell Death and Acute Kidney Injury. *Cell Death Dis* (2016) 7(11):e2482–14. doi: 10.1038/cddis.2016.390
83. Sharma R, Sanchez-Ferras O, Bouchard M. Pax Genes in Renal Development, Disease and Regeneration. *Semin Cell Dev Biol* (2015) 44:97–106. doi: 10.1016/j.semcdb.2015.09.016
84. Bond G, Hu W, Levine A. MDM2 is a Central Node in the P53 Pathway: 12 Years and Counting. *Curr Cancer Drug Targets* (2005) 5(1):3–8. doi: 10.2174/1568009053332627
85. Rojo R, Raper A, Ozdemir DD, Lefevre L, Grabert K, Wollscheid-Lengeling E, et al. Deletion of a CSF1R Enhancer Selectively Impacts CSF1R Expression and Development of Tissue Macrophage Populations. *Nat Commun* (2019) 10(1):1–17. doi: 10.1038/s41467-019-11053-8
86. Dai XM, Ryan GR, Hapel AJ, Dominguez MG, Russell RG, Kapp S, et al. Targeted Disruption of the Mouse Colony-Stimulating Factor 1 Receptor Gene Results in Osteopetrosis, Mononuclear Phagocyte Deficiency, Increased Primitive Progenitor Cell Frequencies, and Reproductive Defects. *Blood* (2002) 99(1):111–20. doi: 10.1182/blood.V99.1.111
87. Mills CD, Kincaid K, Alt JM, Heilman MJ, Hill AM. M-1/M-2 Macrophages and the Th1/Th2 Paradigm. *J Immunol* (2000) 164(12):6166–73. doi: 10.4049/jimmunol.164.12.6166
88. Mosser DM, Edwards JP. Exploring the Full Spectrum of Macrophage Activation. *Nat Rev Immunol* (2008) 8(12):958–69. doi: 10.1038/nri2448
89. Ramello MC, Tosello Boari J, Canale FP, Mena HA, Negrotto S, Gastman B, et al. Tumor-Induced Senescent T Cells Promote the Secretion of Pro-Inflammatory Cytokines and Angiogenic Factors by Human Monocytes/Macrophages Through a Mechanism That Involves Tim-3 and CD40L. *Cell Death Dis* (2014) 5(11):1–10. doi: 10.1038/cddis.2014.451
90. Chang H, Wang X, Yang S. miR-350-3p Contributes to Age-Associated Impairment of IL-6 Production by Macrophages. *Immunol Invest* (2018) 47(8):790–800. doi: 10.1080/08820139.2018.1508227
91. Daigneault M, Preston JA, Marriott HM, Whyte MKB, Dockrell DH. The Identification of Markers of Macrophage Differentiation in PMA-stimulated THP-1 Cells and Monocyte-Derived Macrophages. *PloS One* (2010) 5(1):e8668. doi: 10.1371/journal.pone.0008668
92. MacMicking J, Xie QW, Nathan C. Nitric Oxide and Macrophage Function. *Annu Rev Immunol* (1997) 15(1):323–50. doi: 10.1146/annurev.immunol.15.1.323
93. Goerdt S, Politz O, Schledzewski K, Birk R, Gratchev A, Guillot P, et al. Alternative Versus Classical Activation of Macrophages. *Pathobiology* (1999) 67(5–6):222–6. doi: 10.1159/000028096
94. Hao NB, Lü MH, Fan YH, Cao YL, Zhang ZR, Yang SM. Macrophages in Tumor Microenvironments and the Progression of Tumors. *Clin Dev Immunol* (2012) 2012:948098. doi: 10.1155/2012/948098
95. Lefèvre L, Iacovoni JS, Martini H, Bellière J, Maggiorani D, Dutaur M, et al. Kidney Inflammaging is Promoted by CCR2+ Macrophages and Tissue-Derived Micro-Environmental Factors. *Cell Mol Life Sci* (2020) 78(7):3485–501. doi: 10.1007/s00018-020-03719-0
96. Fujiu K, Manabe I, Nagai R. Renal Collecting Duct Epithelial Cells Regulate Inflammation in Tubulointerstitial Damage in Mice. *J Clin Invest* (2011) 121(9):3425–41. doi: 10.1172/JCI57582
97. Orihuela R, McPherson CA, Harry GJ. Microglial M1/M2 Polarization and Metabolic States. *Br J Pharmacol* (2016) 173(4):649–65. doi: 10.1111/bph.13139
98. Zhang MZ, Wang X, Wang Y, Niu A, Wang S, Zou C, et al. IL-4/IL-13–Mediated Polarization of Renal Macrophages/Dendritic Cells to an M2a Phenotype is Essential for Recovery From Acute Kidney Injury. *Kidney Int* (2017) 91(2):375–86. doi: 10.1016/j.kint.2016.08.020
99. Wynn TA, Vannella KM. Macrophages in Tissue Repair, Regeneration, and Fibrosis. *Immunity* (2016) 44(3):450–62. doi: 10.1016/j.immuni.2016.02.015
100. Mantovani A, Sica A, Sozzani S, Allavena P, Vecchi A, Locati M. The Chemokine System in Diverse Forms of Macrophage Activation and Polarization. *Trends Immunol* (2004) 25(12):677–86. doi: 10.1016/j.it.2004.09.015
101. Bohlson SS, O'Conner SD, Hulsebus HJ, Ho MM, Fraser DA. Complement, C1Q, and C1q-related Molecules Regulate Macrophage Polarization. *Front Immunol* (2014) 5(AUG):1–7. doi: 10.3389/fimmu.2014.00402
102. Maresz K, Ponomarev ED, Barteneva N, Tan Y, Mann MK, Dittel BN. IL-13 Induces the Expression of the Alternative Activation Marker Ym1 in a Subset of Testicular Macrophages. *J Reprod Immunol* (2008) 78(2):140–8. doi: 10.1016/j.jri.2008.01.001
103. Nair MG, Du Y, Perrigoue JG, Zaph C, Taylor JJ, Goldschmidt M, et al. Alternatively Activated Macrophage-Derived RELM-α is a Negative Regulator of Type 2 Inflammation in the Lung. *J Exp Med* (2009) 206(4):937–52. doi: 10.1084/jem.20082048
104. Chen T, Cao Q, Wang Y, Harris DCH. M2 Macrophages in Kidney Disease: Biology, Therapies, and Perspectives. *Kidney Int* (2019) 95(4):760–73. doi: 10.1016/j.kint.2018.10.041
105. Rőszer T. Understanding the Mysterious M2 Macrophage Through Activation Markers and Effector Mechanisms. *Mediators Inflamm* (2015) 2015:816460. doi: 10.1155/2015/816460. Keisari Y, Editor.
106. Wang Lx, Zhang S, Wu Hj, Rong X, Guo J. M2b Macrophage Polarization and its Roles in Diseases. *J Leukoc Biol* (2019) 106(2):345–58. doi: 10.1002/JLB.3RU1018-378RR
107. Lu J, Cao Q, Zheng D, Sun Y, Wang C, Yu X, et al. Discrete Functions of M2a and M2c Macrophage Subsets Determine Their Relative Efficacy in Treating Chronic Kidney Disease. *Kidney Int* (2013) 84(4):745–55. doi: 10.1038/ki.2013.135
108. Kim MG, Yang J, Ko YS, Lee HY, Oh SW, Cho WY, et al. Impact of Aging on Transition of Acute Kidney Injury to Chronic Kidney Disease. *Sci Rep* (2019) 9(1):1–11. doi: 10.1038/s41598-019-54585-1
109. Duluc D, Delneste Y, Tan F, Moles MP, Grimaud L, Lenoir J, et al. Tumor-Associated Leukemia Inhibitory Factor and IL-6 Skew Monocyte Differentiation Into Tumor-Associated Macrophage-Like Cells. *Blood* (2007) 110(13):4319–30. doi: 10.1182/blood-2007-02-072587
110. Wang Q, Ni H, Lan L, Wei X, Xiang R, Wang Y. Fra-1 Protooncogene Regulates IL-6 Expression in Macrophages and Promotes the Generation of M2d Macrophages. *Cell Res* (2010) 20(6):701–12. doi: 10.1038/cr.2010.52
111. Lin SL, Castaño AP, Nowlin BT, Lupher ML, Duffield JS. Bone Marrow Ly6C High Monocytes are Selectively Recruited to Injured Kidney and Differentiate Into Functionally Distinct Populations. *J Immunol* (2009) 183(10):6733–43. doi: 10.4049/jimmunol.0901473
112. Mylonas KJ, Nair MG, Prieto-Lafuente L, Paape D, Allen JE. Alternatively Activated Macrophages Elicited by Helminth Infection Can be Reprogrammed to Enable Microbial Killing. *J Immunol* (2009) 182(5):3084–94. doi: 10.4049/jimmunol.0803463
113. Miao J, Liu J, Niu J, Zhang Y, Shen W, Luo C, et al. Wnt/β-Catenin/RAS Signaling Mediates Age-Related Renal Fibrosis and is Associated With Mitochondrial Dysfunction. *Aging Cell* (2019) 18(5):1–21. doi: 10.1111/acel.13004
114. Wynn TA, Ramalingam TR. Mechanisms of Fibrosis: Therapeutic Translation for Fibrotic Disease. *Nat Med* (2012) 18(7):1028–40. doi: 10.1038/nm.2807
115. Zhang B, Bailey WM, Braun KJ, Gensel JC. Age Decreases Macrophage IL-10 Expression: Implications for Functional Recovery and Tissue Repair in Spinal Cord Injury. *Exp Neurol* (2015) 273:83–91. doi: 10.1016/j.expneurol.2015.08.001
116. Shamskhou EA, Kratochvil MJ, Orcholski ME, Nagy N, Kaber G, Steen E, et al. Hydrogel-Based Delivery of Il-10 Improves Treatment of Bleomycin-Induced Lung Fibrosis in Mice. *Biomaterials* (2019) 203(September 2018):52–62. doi: 10.1016/j.biomaterials.2019.02.017

117. Steen EH, Wang X, Balaji S, Butte MJ, Bollyky PL, Keswani SG. The Role of the Anti-Inflammatory Cytokine Interleukin-10 in Tissue Fibrosis. *Adv Wound Care* (2020) 9(4):184–98. doi: 10.1089/wound.2019.1032
118. Yang N, Isbel NM, Nikolic-Paterson DJ, Li Y, Ye R, Atkins RC, et al. Local Macrophage Proliferation in Human Glomerulonephritis. *Kidney Int* (1998) 54(1):143–51. doi: 10.1046/j.1523-1755.1998.00978.x
119. Ysebaert DK, De Greef KE, De Beuf A, Van Rompay AR, Vercauteren S, Persy VP, et al. T Cells as Mediators in Renal Ischemia/Reperfusion Injury. *Kidney Int* (2004) 66(2):491–6. doi: 10.1111/j.1523-1755.2004.761_4.x
120. Scheller J, Chalaris A, Schmidt-Arras D, Rose-John S. The Pro- and Anti-Inflammatory Properties of the Cytokine Interleukin-6. *Biochim Biophys Acta Mol Cell Res* (2011) 1813(5):878–88. doi: 10.1016/j.bbamcr.2011.01.034
121. Lee S, Huen S, Nishio H, Nishio S, Lee HK, Choi BS, et al. Distinct Macrophage Phenotypes Contribute to Kidney Injury and Repair. *J Am Soc Nephrol* (2011) 22(2):317–26. doi: 10.1681/ASN.2009060615
122. Ferenbach DA, Sheldrake TA, Dhaliwal K, Kipari TMJ, Marson LP, Kluth DC, et al. Macrophage/Monocyte Depletion by Clodronate, But Not Diphtheria Toxin, Improves Renal Ischemia/Reperfusion Injury in Mice. *Kidney Int* (2012) 82(8):928–33. doi: 10.1038/ki.2012.207
123. Degboé Y, Rauwel B, Baron M, Boyer JF, Ruyssen-Witrand A, Constantin A, et al. Polarization of Rheumatoid Macrophages by TNF Targeting Through an IL-10/STAT3 Mechanism. *Front Immunol* (2019) 10(JAN):1–14. doi: 10.3389/fimmu.2019.00003
124. Franceschi C, Garagnani P, Parini P, Giuliani C, Santoro A. Inflammaging: A New Immune–Metabolic Viewpoint for Age-Related Diseases. *Nat Rev Endocrinol* (2018) 14(10):576–90. doi: 10.1038/s41574-018-0059-4
125. Franceschi C, Bonafè M, Valensin S, Olivieri F, De Luca M, Ottaviani E, et al. Inflamm-Aging. An Evolutionary Perspective on Immunosenescence. *Ann N Y Acad Sci* (2000) 908:244–54. doi: 10.1111/j.1749-6632.2000.tb06651.x
126. Hall BM, Balan V, Gleiberman AS, Strom E, Krasnov P, Virtuoso LP, et al. Aging of Mice is Associated With p16(Ink4a)- and β-Galactosidasepositive Macrophage Accumulation That can be Induced in Young Mice by Senescent Cells. *Aging (Albany NY)* (2016) 8(7):1294–315. doi: 10.18632/aging.100991
127. Liu JY, Souroullas GP, Diekman BO, Krishnamurthy J, Hall BM, Sorrentino JA, et al. Cells Exhibiting Strong P16 INK4a Promoter Activation *In Vivo* Display Features of Senescence. *Proc Natl Acad Sci U S A* (2019) 116(7):2603–11. doi: 10.1073/pnas.1818313116
128. Hall BM, Balan V, Gleiberman AS, Strom E, Krasnov P, Virtuoso P, et al. p16 and SAbetaGal can be Induced in Macrophages as Part of a Reversible Response to Physiological Stimuli. *Aging (Albany NY)* (2017) 9(8):1867–84. doi: 10.18632/aging.101268
129. Yousefzadeh MJ, Flores RR, Zhu Y, Schmiechen ZC, Brooks RW, Trussoni CE, et al. An Aged Immune System Drives Senescence and Ageing of Solid Organs. *Nature* (2021) 594:100–5. doi: 10.1038/s41586-021-03547-7
130. Nyugen J, Agrawal S, Gollapudi S, Gupta S. Impaired Functions of Peripheral Blood Monocyte Subpopulations in Aged Humans. *J Clin Immunol* (2010) 30(6):806–13. doi: 10.1007/s10875-010-9448-8
131. Chen SH, Tian DY, Shen YY, Cheng Y, Fan DY, Sun HL, et al. Amyloid-Beta Uptake by Blood Monocytes is Reduced With Ageing and Alzheimer's Disease. *Transl Psychiatry* (2020) 10(1):423. doi: 10.1038/s41398-020-01113-9
132. Hearps AC, Martin GE, Angelovich TA, Cheng WJ, Maisa A, Landay AL, et al. Aging is Associated With Chronic Innate Immune Activation and Dysregulation of Monocyte Phenotype and Function. *Aging Cell* (2012) 11(5):867–75. doi: 10.1111/j.1474-9726.2012.00851.x
133. Holt DJ, Grainger DW. Senescence and Quiescence Induced Compromised Function in Cultured Macrophages. *Biomaterials* (2012) 33(30):7497–507. doi: 10.1016/j.biomaterials.2012.06.099
134. Palacio L, Goyer ML, Maggiorani D, Espinosa A, Villeneuve N, Bourbonnais S, et al. Restored Immune Cell Functions Upon Clearance of Senescence in the Irradiated Splenic Environment. *Aging Cell* (2019) 18(4):1–11. doi: 10.1111/acel.12971
135. Ovadya Y, Landsberger T, Leins H, Vadai E, Gal H, Biran A, et al. Impaired Immune Surveillance Accelerates Accumulation of Senescent Cells and Aging. *Nat Commun* (2018) 9(1):5435. doi: 10.1038/s41467-018-07825-3
136. Oldenborg PA, Zheleznyak A, Fang YF, Lagenaur CF, Gresham HD, Lindberg FP. Role of CD47 as a Marker of Self on Red Blood Cells. *Science (80-)* (2000) 288(5473):2051–4. doi: 10.1126/science.288.5473.2051
137. Majeti R, Chao MP, Alizadeh AA, Pang WW, Jaiswal S, Gibbs KDJr., et al. CD47 Is an Adverse Prognostic Factor and Therapeutic Antibody Target on Human Acute Myeloid Leukemia Stem Cells. *Cell* (2009) 138(2):286–99. doi: 10.1016/j.cell.2009.05.045
138. Lo J, Lau EYT, Ching RHH, Cheng BYL, Ma MKF, Ng IOL, et al. Nuclear Factor Kappa B-Mediated CD47 Up-Regulation Promotes Sorafenib Resistance and its Blockade Synergizes the Effect of Sorafenib in Hepatocellular Carcinoma in Mice. *Hepatology* (2015) 62(2):534–45. doi: 10.1002/hep.27859
139. Schmitt R, Melk A. New Insights on Molecular Mechanisms of Renal Aging. *Am J Transplant* (2012) 12(11):2892–900. doi: 10.1111/j.1600-6143.2012.04214.x
140. Chidrawar SM, Khan N, Chan YLT, Nayak L, Moss PAH. Ageing is Associated With a Decline in Peripheral Blood CD56bright NK Cells. *Immun Ageing* (2006) 3:1–8. doi: 10.1186/1742-4933-3-10
141. Muñoz DP, Yannone SM, Daemen A, Sun Y, Vakar-Lopez F, Kawahara M, et al. Targetable Mechanisms Driving Immunoevasion of Persistent Senescent Cells Link Chemotherapy-Resistant Cancer to Aging. *JCI Insight* (2019) 4(14):1–22. doi: 10.1172/jci.insight.124716
142. Van Amerongen MJ, Harmsen MC, Van Rooijen N, Petersen AH, Van Luyn MJA. Macrophage Depletion Impairs Wound Healing and Increases Left Ventricular Remodeling After Myocardial Injury in Mice. *Am J Pathol* (2007) 170(3):818–29. doi: 10.2353/ajpath.2007.060547
143. Ray M, Lee YW, Hardie J, Mout R, Yeşilbag Tonga G, Farkas ME, et al. Crispred Macrophages for Cell-Based Cancer Immunotherapy. *Bioconjug Chem* (2018) 29(2):445–50. doi: 10.1021/acs.bioconjchem.7b00768
144. Puro RJ, Bouchlaka MN, Hiebsch RR, Capoccia BJ, Donio MJ, Manning PT, et al. Development of AO-176, a Next-Generation Humanized Anti-CD47 Antibody With Novel Anticancer Properties and Negligible Red Blood Cell Binding. *Mol Cancer Ther* (2020) 19(3):835–46. doi: 10.1158/1535-7163.MCT-19-1079
145. Haruna Y, Kashihara N, Satoh M, Tomita N, Namikoshi T, Sasaki T, et al. Amelioration of Progressive Renal Injury by Genetic Manipulation of Klotho Gene. *Proc Natl Acad Sci U S A* (2007) 104(7):2331–6. doi: 10.1073/pnas.0611079104
146. Liu H, Fergusson MM, Castilho RM, Liu J, Cao L, Chen J, et al. Augmented Wnt Signaling in a Mammalian Model of Accelerated Aging. *Science (80-)* (2007) 317(5839):803–6. doi: 10.1126/science.1143578
147. Hu MC, Kuro- OM, Moe OW. Klotho and Chronic Kidney Disease. *Contrib Nephrol* (2013) 180:47–63. doi: 10.1159/000346778
148. Yosef R, Pilpel N, Tokarsky-Amiel R, Biran A, Ovadya Y, Cohen S, et al. Directed Elimination of Senescent Cells by Inhibition of BCL-W and BCL-XL. *Nat Commun* (2016) 7:11190. doi: 10.1038/ncomms11190
149. Kaefer A, Yang J, Noertersheuser P, Mensing S, Humerickhouse R, Awni W, et al. Mechanism-Based Pharmacokinetic/Pharmacodynamic Meta-Analysis of Navitoclax (ABT-263) Induced Thrombocytopenia. *Cancer Chemother Pharmacol* (2014) 74(3):593–602. doi: 10.1007/s00280-014-2530-9
150. Hickson LTJ, Langhi Prata LGP, Bobart SA, Evans TK, Giorgadze N, Hashmi SK, et al. Senolytics Decrease Senescent Cells in Humans: Preliminary Report From a Clinical Trial of Dasatinib Plus Quercetin in Individuals With Diabetic Kidney Disease. *EBioMedicine* (2019) 47:446–56. doi: 10.1016/j.ebiom.2019.08.069
151. Justice JN, Nambiar AM, Tchkonia T, LeBrasseur NK, Pascual R, Hashmi SK, et al. Senolytics in Idiopathic Pulmonary Fibrosis: Results From a First-in-Human, Open-Label, Pilot Study. *EBioMedicine* (2019) 40:554–63. doi: 10.1016/j.ebiom.2018.12.052
152. Panda AC, Abdelmohsen K, Gorospe M. SASP Regulation by Noncoding RNA. *Mech Ageing Dev* (2017) 168(April):37–43. doi: 10.1016/j.mad.2017.05.004
153. Minieri V, Saviozzi S, Gambarotta G, Lo Iacono M, Accomasso L, Cibrario Rocchietti E, et al. Persistent DNA Damage-Induced Premature Senescence Alters the Functional Features of Human Bone Marrow Mesenchymal Stem Cells. *J Cell Mol Med* (2015) 19(4):734–43. doi: 10.1111/jcmm.12387
154. Xu M, Pirtskhalava T, Farr JN, Weigand BM, Palmer AK, Weivoda MM, et al. Senolytics Improve Physical Function and Increase Lifespan in Old Age. *Nat Med* (2018) 24(8):1246–56. doi: 10.1038/s41591-018-0092-9

155. Baar MP, Brandt RMC, Putavet DA, Klein JDD, Derks KWJ, Bourgeois BRM, et al. Targeted Apoptosis of Senescent Cells Restores Tissue Homeostasis in Response to Chemotoxicity and Aging. *Cell* (2017) 169 (1):132–147.e16. doi: 10.1016/j.cell.2017.02.031
156. Wolstein JM, Lee DH, Michaud J, Buot V, Stefanchik B, Plotkin MD. INK4a Knockout Mice Exhibit Increased Fibrosis Under Normal Conditions and in Response to Unilateral Ureteral Obstruction. *Am J Physiol Renal Physiol* (2010) 299(6):1486–95. doi: 10.1152/ajprenal.00378.2010
157. Megyesi J, Andrade L, Vieira JM, Safirstein RL, Price PM. Positive Effect of the Induction of p21WAF1/CIP1 on the Course of Ischemic Acute Renal Failure. *Kidney Int* (2001) 60(6):2164–72. doi: 10.1046/j.1523-1755.2001.00044.x
158. Al-Douahji M, Brugarolas J, Brown PAJ, Stehman-Breen CO, Alpers CE, Shankland SJ. The Cyclin Kinase Inhibitor p21(WAF1/CIP1) is Required for Glomerular Hypertrophy in Experimental Diabetic Nephropathy. *Kidney Int* (1999) 56(5):1691–9. doi: 10.1046/j.1523-1755.1999.00728.x
159. Wolf G, Schanze A, Stahl RAK, Shankland SJ, Amann K. p27Kip1 Knockout Mice are Protected From Diabetic Nephropathy: Evidence for p27Kip1 Haplotype Insufficiency. *Kidney Int* (2005) 68(4):1583–9. doi: 10.1111/j.1523-1755.2005.00570.x
160. Docherty MH, O'Sullivan ED, Bonventre JV, Ferenbach DA. Cellular Senescence in the Kidney. *J Am Soc Nephrol* (2019) 30(5):726–36. doi: 10.1681/ASN.2018121251
161. Suganami T, Ogawa Y. Adipose Tissue Macrophages: Their Role in Adipose Tissue Remodeling. *J Leukoc Biol* (2010) 88(1):33–9. doi: 10.1189/jlb.0210072
162. Frodermann V, Rohde D, Courties G, Severe N, Schloss MJ, Amatullah H, et al. Exercise Reduces Inflammatory Cell Production and Cardiovascular Inflammation Via Instruction of Hematopoietic Progenitor Cells. *Nat Med* (2019) 25(11):1761–71. doi: 10.1038/s41591-019-0633-x
163. Xu XM, Ning YC, Wang WJ, Liu JQ, Bai XY, Sun XF, et al. Anti-Inflamm-Aging Effects of Long-Term Caloric Restriction Via Overexpression of SIGIRR to Inhibit NF-κB Signaling Pathway. *Cell Physiol Biochem* (2015) 37(4):1257–70. doi: 10.1159/000430248
164. van Willigenburg H, de Keizer PLJ, de Bruin RWF. Cellular Senescence as a Therapeutic Target to Improve Renal Transplantation Outcome. *Pharmacol Res* (2018) 130:322–30. doi: 10.1016/j.phrs.2018.02.015
165. Irvine KM, Skoien R, Bokil NJ, Melino M, Thomas GP, Loo D, et al. Senescent Human Hepatocytes Express a Unique Secretory Phenotype and Promote Macrophage Migration. *World J Gastroenterol* (2014) 20 (47):17851–62. doi: 10.3748/wjg.v20.i47.17851
166. Stout LC, Whorton EB, Vaghela M. Pathogenesis of Diffuse Intimal Thickening (DIT) in Non-Human Primate Thoracic Aortas. *Atherosclerosis* (1983) 47(1):1–6. doi: 10.1016/0021-9150(83)90065-5
167. Harel I, Benayoun BA, Machado B, Singh PP, Hu CK, Pech MF, et al. A Platform for Rapid Exploration of Aging and Diseases in a Naturally Short-Lived Vertebrate. *Cell* (2015) 160(5):1013–26. doi: 10.1016/j.cell.2015.01.038
168. Kim Y, Nam HG, Valenzano DR. The Short-Lived African Turquoise Killifish: An Emerging Experimental Model for Ageing. *Dis Model Mech* (2016) 9(2):115–29. doi: 10.1242/dmm.023226
169. Baker DJ, Wijshake T, Tchkonia T, Lebrasseur NK, Childs BG, Van De Sluis B, et al. Clearance of P16 Ink4a-Positive Senescent Cells Delays Ageing-Associated Disorders. *Nature* (2011) 479(7372):232–6. doi: 10.1038/nature10600
170. Xu W, Zhao X, Daha MR, van Kooten C. Reversible Differentiation of Pro- and Anti-Inflammatory Macrophages. *Mol Immunol* (2013) 53(3):179–86. doi: 10.1016/j.molimm.2012.07.005

Conflict of Interest: The authors declare that the research was conducted in the absence of any commercial or financial relationships that could be construed as a potential conflict of interest.

Copyright © 2021 Campbell, Docherty, Ferenbach and Mylonas. This is an open-access article distributed under the terms of the Creative Commons Attribution License (CC BY). The use, distribution or reproduction in other forums is permitted, provided the original author(s) and the copyright owner(s) are credited and that the original publication in this journal is cited, in accordance with accepted academic practice. No use, distribution or reproduction is permitted which does not comply with these terms.

frontiers in Immunology

REVIEW
published: 18 June 2021
doi: 10.3389/fimmu.2021.701935

"Corneal Nerves, CD11c$^+$ Dendritic Cells and Their Impact on Ocular Immune Privilege"

Jerry Y. Niederkorn *

Department of Ophthalmology, University of Texas Southwestern Medical Center, Dallas, TX, United States

The eye and the brain have limited capacities for regeneration and as such, immune-mediated inflammation can produce devastating consequences in the form of neurodegenerative diseases of the central nervous system or blindness as a result of ocular inflammatory diseases such as uveitis. Accordingly, both the eye and the brain are designed to limit immune responses and inflammation – a condition known as "immune privilege". Immune privilege is sustained by physiological, anatomical, and regulatory processes that conspire to restrict both adaptive and innate immune responses.

Keywords: contrasuppressor cells, nerves, dendritic cells, immune privilege, cornea

OPEN ACCESS

Edited by:
Daniel Saban,
Duke University, United States

Reviewed by:
Darren James Lee,
University of Oklahoma Health Sciences Center, United States
Luc Van Kaer,
Vanderbilt University, United States

****Correspondence:***
Jerry Y. Niederkorn
jerry.niederkorn@utsouthwestern.edu

Specialty section:
This article was submitted to Antigen Presenting Cell Biology, a section of the journal Frontiers in Immunology

Received: *28 April 2021*
Accepted: *19 May 2021*
Published: *18 June 2021*

Citation:
Niederkorn JY (2021) "Corneal Nerves, CD11c$^+$ Dendritic Cells and Their Impact on Ocular Immune Privilege". Front. Immunol. 12:701935. doi: 10.3389/fimmu.2021.701935

INTRODUCTION

A striking example of immune privilege was reported by Abel who treated an 8-year old boy who had a 10 week history of ocular pain (1). Examination of the painful eye revealed the presence of a vermiform foreign body in the anterior chamber. The foreign body was removed and it was found not to be a helminth but rather, it was a seedling of a dicotyledonous plant of the Compositae family that had germinated in the anterior chamber (**Figure 1**). Two noteworthy features of this case bear noting. The "foreign body" had eluded the immune system and persisted in the eye for over two months. The second and equally astonishing finding was the conspicuous absence of inflammation in the anterior chamber of the eye in which the seedling had germinated. These two observations are in keeping with the principles of immune privilege: 1) the prolonged survival of a foreign tissue that would normally be rejected in conventional body sites and 2) the local quenching of inflammation. A more commonly recognized example of ocular immune privilege is the remarkable success of corneal allografts, which in uncomplicated cases enjoy a survival rate of 90% even though histocompatibility matching is not routinely practiced and the only immunosuppressive drugs are topically applied corticosteroids (2–4).

IMMUNE PRIVILEGE IS A DYNAMIC PROCESS THAT INVOLVES ANATOMICAL, PHYSIOLOGICAL, AND IMMUNOREGULATORY ELEMENTS

Although the concept of immune privilege is widely recognized it is often over-simplified and misunderstood. Two common misconceptions about immune privilege are that corneal transplants

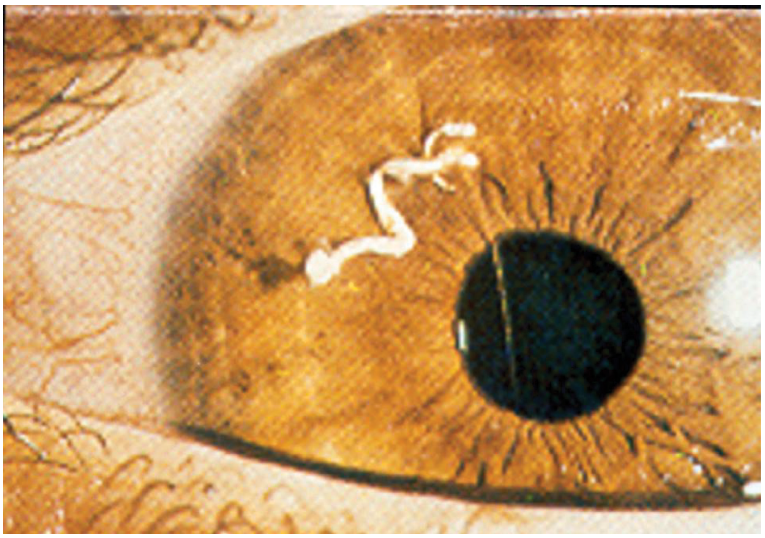

FIGURE 1 | Germinating seedling in the anterior chamber of an eight year-old boy following 10 weeks of ocular pain. The vermiform object was extirpated and identified by a botanist to be a seedling of a dicotyledonous plant. Reproduced from Abel (1) with permission from Archives Ophthalmology.

are exempt from immune rejection and that the anterior chamber (AC) of the eye is devoid of lymphatic drainage, which presumably isolates the interior of the eye from the systemic immune apparatus. Although corneal transplants enjoy a survival that is unrivaled in the field of transplantation, they can occasionally undergo immune rejection, which remains the leading cause of corneal graft failure. The notion that the AC of the eye is devoid of lymphatic drainage was proposed by Medawar over a half-century ago (5) and persisted until the late 20th century when it was discovered that although lymphatic vessels were invisible to most anatomical observations, antigens introduced into the AC could reach the ipsilateral cervical lymph nodes (6), however the majority of antigens injected into the AC enter the venous circulation and reach the lymph nodes *via* the blood vascular pathway (7).

Over the past 50 years it has become clear that immune privilege in the AC and the success of corneal allografts are due to a combination of anatomical, physiological, and dynamic immunoregulatory processes that restrict the expression of both innate and adaptive immune responses (8, 9). In addition, many of the blood vessels within the eye are non-fenestrated and the tight junctions between the cells lining the blood vessels restrict the diapedesis of leukocytes and the extravasation of macromolecules into the interior of the eye (10). This "blood-ocular barrier" is imperfect and in certain conditions leukocytes can extravasate and enter the eye, a condition that occurs in uveitis.

The aqueous humor that fills the AC of the eye is a potpourri of anti-inflammatory and immunosuppressive molecules including: a) transforming growth factor-β(TGF-β), b) α-melanocyte stimulating hormone (α-MSH), c) complement regulatory proteins (CRP), d) calcitonin gene-related protein (CGRP), e) somatostatin (SOM), f) macrophage migration inhibitory factor (MIF), and g) vasoactive intestinal peptide (VIP) (11–16). These humoral molecules act to quench inflammation and to buffer the deleterious effects of activation of the complement cascade. The cells lining the inside of the eye are decorated with a panoply of cell membrane-bound molecules that induce apoptosis of immune cells that enter the eye thereby eliminating immune attack. These include: a) FasL, b) tumor necrosis factor-related apoptosis-inducing ligand (TRAIL), c) PD-L1, d) CRP, and e) galectin-9 (17–19).

In addition to the anatomical and physiological properties of the eye, dynamic immunoregulatory processes contribute to ocular immune privilege. Antigens entering the eye including histocompatibility antigens sloughed from the corneal endothelium of corneal transplants induce a dynamic form of immune deviation in which cell-mediated immune responses such as delayed-type hypersensitive (DTH) and cytotoxic T lymphocyte (CTL) responses are suppressed by T regulatory cells (Tregs) – a phenomenon termed anterior chamber-associated immune deviation (ACAID) (8). Not only does ACAID suppress Th1 type immune responses but it also blunts Th2-mediated inflammatory disease (20). ACAID also culminates in a deviation of the antibody responses from complement fixing isotypes to a preferential production of non-complement-fixing antibodies. This deviation reduces the likelihood of antibody-mediated injury to ocular tissues as activation of the complement cascade can produce deleterious effects of granulocytic inflammation that occurs in response to complement byproducts.

ROLE OF ANTIGEN-PRESENTING CELLS IN CORNEAL ALLOGRAFT SURVIVAL AND ACAID

The induction of ACAID is an extraordinarily complex process that involves four organ systems: a) eye, b) spleen, c) thymus, and

d) sympathetic nervous system. Removal of the eye, thymus, or spleen within three days of introducing antigens into the AC abrogates the induction of ACAID. Likewise chemical sympathectomy prior to AC injection of antigens blocks the induction of ACAID. The contributions of these organ systems in the induction of ACAID are complex and are discussed in detail elsewhere (8) (**Figure 2**).

The eye-dependent stage of ACAID is widely believed to involve the participation of antigen-presenting cells (APC), which under the influence of soluble molecules in the AC, induce the generation of Tregs. Antigens are captured by resident F4/80$^+$ APC that are bathed in TGF-β, which in turn preferentially produce IL-10. The production of IL-10 by ocular APC is pivotal to induction of ACAID as shown by the inability of ocular APC from IL-10 knockout mice to induce ACAID (21). Ocular APC exposed to TGF-β that is present in the AC preferentially produce macrophage inflammatory protein-2 (MIP-2), which is crucial for the induction of T regs in the spleen (22). The role of F4/80$^+$ APC in the induction of ACAID is strengthened by the observation that ACAID cannot be induced in F4/80 KO mice (23).

ACAID is intimately associated with corneal allograft survival (9, 24) Maneuvers that block the induction of ACAID, such as splenectomy or deletion of IL-10, invariably result in the immune rejection of corneal allografts. Likewise, induction of ACAID through the intracameral injection of corneal graft donor alloantigens prior to corneal transplantation significantly enhances corneal allograft survival and dramatically reduces the incidence of immune rejection (25).

ROLE OF CD11C$^+$ DC IN THE ABROGATION OF ACAID AND INDUCTION OF CORNEAL ALLOGRAFT REJECTION

The remarkable success of corneal allografts defies the laws of transplantation immunology. Studies in animal models

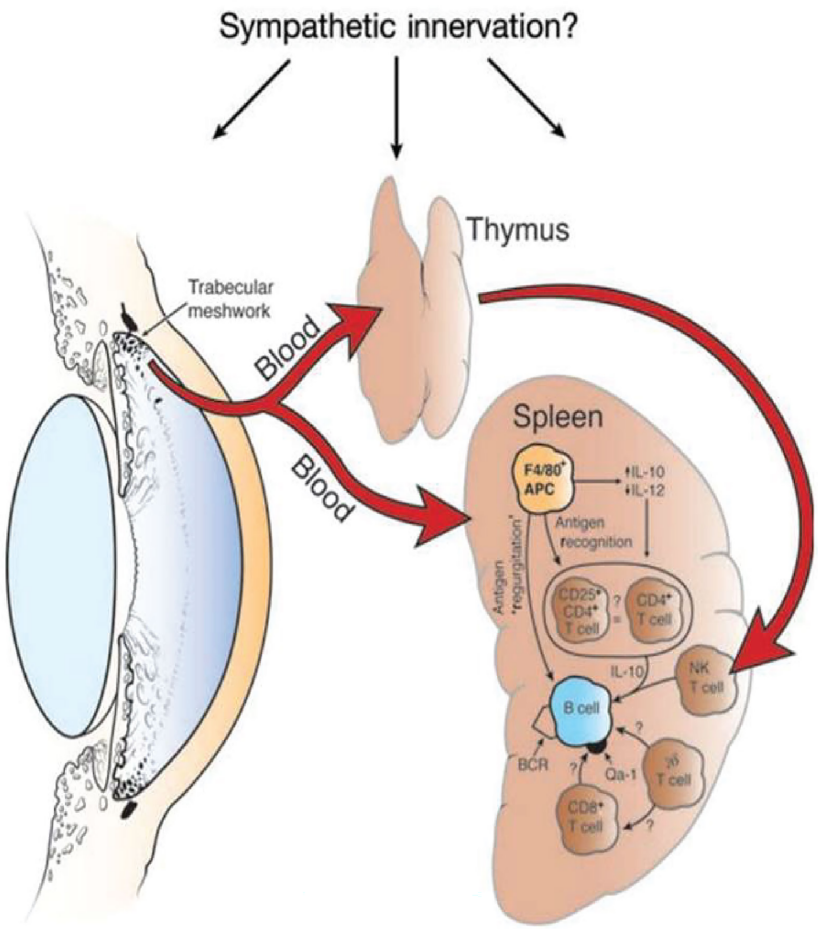

FIGURE 2 | Four organ systems are required for the induction of ACAID. Removal of the eye, spleen, or thymus within 3 days of injecting antigen into the anterior chamber prevents the induction of ACAIDS. Chemical sympathectomy prior to injecting antigens into the anterior chamber also prevents ACAID. BCR, B cell receptor. Reproduced from Niederkorn (9) with permission from Nature Publishing Group.

of penetrating keratoplasty demonstrate that in the absence of any form of immunosuppressive agents corneal allografts mismatched with the recipient at all known MHC and minor histocompatibility gene loci routinely enjoy a 50% acceptance rate (4). By contrast orthotopic skin allografts transplanted under similar conditions undergo rejection in 100% of the hosts. As mentioned earlier, immune privilege is not absolute and corneal allografts can undergo immune rejection. Virtually any condition that provokes inflammation at the ocular surface, such as herpes simplex virus keratitis (HSVK), abolishes ocular immune privilege and invariably leads to corneal allograft rejection (4, 26).

The leading risk factor for corneal allograft failure in human subjects is the rejection of a previous graft. The incidence of corneal allograft rejection rises three-fold in patients receiving a second corneal transplant (27). On first blush one might reasonably conclude that such patients were sensitized to the donor alloantigens expressed on the first transplant and the heightened incidence of rejection was simply a recall or memory immune response elicited by the second transplant. However, this conclusion is flawed. Under normal conditions corneal buttons are selected for transplantation based on the quality of the tissue and the corneas suitability for surgery. Histocompatibility matching is not employed and accordingly the array of MHC and minor histocompatibility antigens expressed on the first and second grafts is random and the likelihood of shared antigenic epitopes on the first and second grafts is remote. Moreover, second corneal allografts can occur in patients with a long-standing clear transplant in the opposite eye suggesting that the immune system was "unaware" of the alloantigens expressed on the first transplant (28).

In an attempt to unravel this paradox we employed a mouse model of penetrating keratoplasty and recapitulated experiments in which patients receive two corneal transplants from unrelated donors. For these experiments we employed a widely utilized mouse model in which C57BL/6 corneal allografts are transplanted to BALB/c recipients. These two mouse strains differ at all known major and minor histocompatibility gene loci, yet only 50% of the corneal allografts undergo immune rejection even though no immunosuppressive drugs are employed. To evaluate the effect of a first corneal transplant on the survival of subsequent corneal grafts we transplanted corneas from C3H mice to the right eyes of BALB/c recipients. Sixty days later we transplanted C57BL/6 corneas to the opposite eye (i.e., left eye) of these mice. Instead of the expected 50% incidence of rejection for initial C57BL/6 corneal allografts in naïve hosts, we observed 100% graft rejection (29). Importantly C3H and C57BL/6 mice differ at all known MHC and minor histocompatibility gene loci and thus the C3H corneal allografts were incapable of immunizing the BALB/c recipients to C57BL/6 alloantigens thereby removing the possibility that the profound increased incidence of rejection in the BALB/c mice was a result of "cross-immunization" or prior allosensitization. Thus, corneal surgery itself robbed the second eye of its immune privilege. To confirm that the surgery and not the rejection of a previous corneal graft abolished immune privilege, syngeneic BALB/c corneal grafts were placed onto the right eyes of BALB/c mice 60 days prior to transplanting C57BL/6 corneal allograft to the opposite eyes. As expected, the BALB/c syngrafts remained clear and healthy throughout the entire course of these experiments, yet 100% of the C57BL/6 corneal allografts applied to the opposite eye underwent immune rejection even though the expected incidence of rejection was 50%. These results recapitulated the previously reported cases in human subjects in which second corneal transplants underwent rejection in hosts having long-standing clear first corneal transplants in the opposite eye (28). Additional experiments revealed that this loss of immune privilege was due to the severing of corneal nerves that occurs during the penetrating keratoplasty procedure. Simply cutting the superficial corneal nerves with a circular trephine in one eye abolished immune privilege in the opposite eye and thus represented a "sympathetic loss of immune privilege" (SLIP) (29). SLIP did not require complex surgical procedures and could be induced by simply making a shallow circular incision in the corneal epithelium (**Figure 3**).

It is important to note that SLIP should not be confused with a similar condition called sympathetic ophthalmia (SO) that sometimes occurs in individuals following a penetrating traumatic injury to one eye that is subsequently followed by intense inflammation in the opposite eye (30). The inflammation in the "sympathizing" eye led to the moniker sympathetic ophthalmia. Although SO is still poorly understood, it is widely believed that the penetrating injury to one eye leads to the release of ocular antigens, especially those sequestered from the immune apparatus in the retina, and culminates in the generation of an immune response to the ocular antigens and the appearance of immune inflammation in both eyes. By contrast, SLIP is not the direct initiation of an antigen-specific immune response, instead it is the antigen non-specific disabling of Tregs and can be induced by a single bolus injection of 0.1 pg of substance P (SP) and thus, occurs in the absence of traumatic injury to eye (see below).

The impact of neuropeptides on immune responses has long been recognized. Neuropeptides exert an important effect on immune privilege in the eye (11). Interestingly, one neuropeptide stands apart from the rest. The expression of SP and its receptor NK1-R increases over 300% in both eyes following circular corneal incisions in one eye (29). Blocking NK1-R with the SP receptor antagonist Spantide II, restores immune privilege in mice subjected to corneal nerve injury and results in 50% corneal allograft acceptance, which is identical to the incidence of graft survival in naïve mice. Moreover, simply injecting as little as 0.1 pg of SP intravenously abrogates immune ocular immune privilege and results in 100% corneal allograft rejection.

Severing corneal nerves also adversely affects ACAID. Placing a shallow corneal incision in one eye prevents the induction of ACAID in both eyes (31, 32). These results are remarkably similar to earlier finding by Lucas and co-workers who observed that retinal laser burns (RLB) to one eye prevented the induction of ACAID in the opposite eye that was not subjected to RLB (33). Moreover, the loss of ACAID produced by RLB coincided with a steep upregulation in the SP receptor

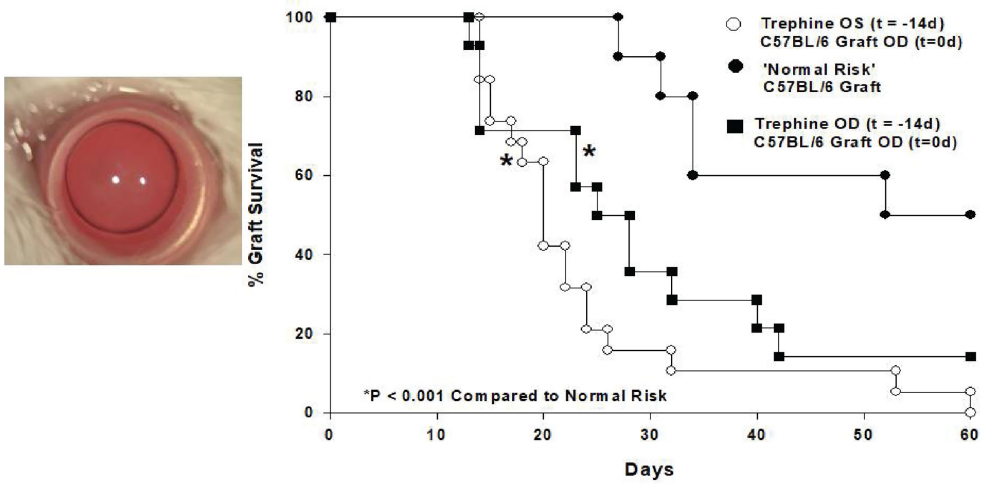

FIGURE 3 | Shallow circular incisions of the cornea in one eye abolishes ACAID in both eyes. 360° corneal incisions were placed in left (OS) eyes of BALB/c mice 14 days prior to application of C57BL/6 corneal allografts to the right (OD) eyes. (Modified from Paunicka et al. (29).

NK1-R in the opposite non-manipulated eye. Studies by Guzman and co-workers found a similar association between corneal nerve injury and the induction of ocular immune tolerance (34). These investigators found that placing 180° incisions in the cornea of one eye prevented the induction of mucosal tolerance following topical application of ovalbumin (OVA) to the opposite eye. This abrogation of mucosal tolerance, like SLIP, could be reversed by the application of a SP receptor antagonist.

SP has emerged as the end stage effector molecule in SLIP. Although the SP receptor, NK1-R is expressed on numerous cell types including antigen-presenting DCs, we were intrigued by the juxtaposition of $CD11c^+$ ocular surface DCs to the area where we placed circular incisions in the cornea. When stimulated *via* their NK1-R, $CD11c^+$ DCs inhibit IL-10 production and promote the generation of Th1 immune responses (35). Both of these conditions are associated with the abrogation of ACAID and corneal allograft rejection (4, 9).

We explored the potential role of $CD11c^+$ DCs in the development of SLIP and the loss of ocular immune privilege by isolating $CD11c^+$ CS from mice subjected to corneal nerve injury (i.e., trephining) and adoptively transferring them to naïve recipients. ACAID could not be induced in these recipients but was induced in recipients of $CD11c^+$ DCs from donors that had not been subjected to corneal nerve injury (31). Additional experiments revealed that $CD11c^+$ DCs isolated from trephined donors blocked the suppressive activity of Tregs *in vivo*. Accordingly, we categorized these $CD11c^+$ cells as contrasuppressor (CS) cells based on their capacity to suppress Tregs and their similarity to "contrasuppressor" cells described over four decades ago (36). Although the concept of "suppressor cells" was hotly debated for over a decade, the suppressor cell concept vindicated by the elegant investigations of Sakaguchi who now referred to these cells by the euphemistic moniker "T regulatory cells" (37). CS cells have also enjoyed a renewed appreciation and have been demonstrated in multiple models of immune regulation (38).

INDUCTION OF $CD11C^+$ CS CELLS AND THEIR MODE OF ACTION

The weight of evidence suggests that there is an axis involving ocular surface $CD11c^+$ cells, corneal nerve injury, and the elaboration of SP that conspires to rob both eyes of their immune privilege (**Figure 4**). SP is clearly involved in the generation of CS cells as *in vitro* treatment of $CD11c^+$ cells with SP licenses them to block Treg activity *in vivo* (31). Moreover, corneal nerve injury fails to induce CS cells in $SP^{-/-}$ mice (31). A single bolus intravenous injection of 1.0 pg prevents the induction of ACAID and 0.1 pg of SP culminates in 100% corneal allograft rejection (29, 31). The pivotal role of SP in the generation of CS cells was confirmed by briefly exposing naïve $CD11c^+$ DC to SP *in vitro* and infusing these cells into naïve recipients. Mice that received SP-conditioned $CD11c^+$ DC resisted the development of ACAID, while neither naïve $CD11c^+$ DC nor $CD11c^+$ cells conditioned in saline adversely affected the generation of ACAID T regs (32). We are attracted to the hypothesis that SP elaborated in response to corneal nerve injury converts resident $CD11c^+$ DC at the graft/host margin to become CS cells. If this scenario is correct then it should be possible to prevent the generation of CS cells by purging ocular $CD11c^+$ DCs prior to corneal nerve injury. This hypothesis was confirmed in experiments in which clodronate-containing liposomes were injected into the conjunctiva prior to trephining the ocular surface (32). Subconjunctival injection of clodronate-containing liposomes specifically depletes ocular surface APC including $CD11c^+$ DC (40). Corneal nerve injury blocks ACAID, however depletion of ocular surface $CD1c^+$ DC

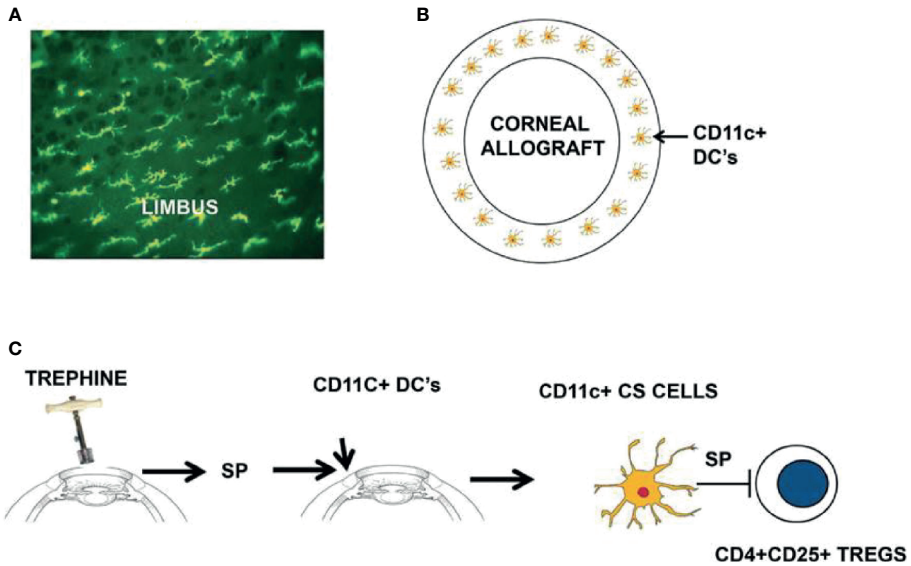

FIGURE 4 | Sympathetic loss of immune privilege is the result of an axis involving ocular surface $CD11c^+$ DCs, corneal nerves, and the elaboration of substance P (SP). **(A, B)** MHC class II^+ DCs (including $CD11c^+$ DCs) reside at the interface between the corneal allograft and the graft bed. **(C)** Severing corneal nerves with a trephine elicits the release of SP that converts resident $CD11c^+$ DCs to contrasuppressor (CS) cells that disable $CD4^+CD25^+$ Tregs. Reproduced from Niederkorn (39) with permission from Invest Ophthalmol Vis Sci.

through the injection of clodronate-containing liposomes prior to AC injection of antigens restores ACAID and allows the development of Tregs (32). The crucial role of SP signaling in the generation of $CD11c^+$ CS cells was also supported by experiments in which administration of the SP receptor antagonist Spantide II prevented the generation of CS cells and restored immune privilege of corneal allografts in hosts subjected to trephining and simultaneously injected with Spantide II (29, 31).

CS cells disable two distinct categories of T regulatory cells that are involved in ocular immune privilege: a) $CD8^+$ ACAID T regs and b) $CD4^+CD25^+$ corneal allograft-induced Tregs. In both cases the CS cells exert their effect in an antigen-non-specific manner. The molecular mechanisms involved in Treg suppression are still under investigation, but at least one molecule has emerged as a crucial player. Microarray analysis on 12,000 genes expressed on $CD8^+$ ACAID T regs revealed an 85-fold increase in the expression of CD103 (41). The finding that ACAID cannot be induced in $CD103^{-/-}$ mice supports the notion that CD103 is critical for the induction of $CD8^+$ ACAID T regs (41). It bears noting that CD103 is also expressed on $CD4^+CD25^+$ T regs (41–45). With this in mind we examined the role of CD103 in CS cell blockade of Treg activity. Co-culturing $CD8^+$ ACAID T regs with CS cells resulted in a 66% reduction in CD103 expression on ACAID T regs (46). The down-regulation of CD103 on $CD8^+$ ACAID Tregs was directly attributed to SP and could be mimicked by co-culturing $CD8^+$ T regs with SP *in vitro* (46). CD103 is a cell-adhesion molecule that binds to E-cadherin, which is expressed on numerous cell types including APCs (47, 48). TGF-β is necessary for conditioning ocular APC for the induction of ACAID presumably by upregulating E-cadherin. CD103/E-cadherin interactions are enhanced when T cell-receptor signaling occurs (49). These interactions would stabilize the interaction between $CD8^+$ ACAID Tregs and effector T cells that occurs during the suppression of T cell responses and it would also explain the requirement for CD103 expression on $CD8^+$ ACAID Tregs for their capacity to directly suppress T cells during DTH responses.

CONUNDRUMS AND PUZZLING PROPERTIES OF SLIP

On the surface, the induction of SLIP and the generation of CS cells seem straightforward and logical. However, closer analysis reveals conundrums that are difficult to reconcile. A single intravenous bolus injection of as little as 0.1 pg of SP abolishes the immune privilege of corneal allografts (29). This loss of immune privilege persists for at least 100 days even though only a single injection of SP was administered and the serum half-life of SP is less than two minutes (50). The nature of the corneal nerve injury involved in the development of SLIP is also puzzling. Circular corneal incisions induce $CD11c^+$ CS cells yet "X" shaped corneal incisions of similar linear dimensions do not adversely affect corneal allograft survival or ocular immune privilege (29). Equally perplexing is the observation that blocking the SP receptor with Spantide II prevents SLIP but does not enhance corneal allograft survival beyond the 50% acceptance that is found in naïve mice. That is, blocking SP restores immune privilege, but does not enhance it. DC are recognized for their remarkable capacity to amplify immune responses and as few as 10 allogeneic DC can elicit allospecific

T cell responses (51) and as little as 1,000 $CD11c^+$ CS cells can abolish immune privilege and ablate the suppressive activity of ACAID Tregs (32).

Corneal nerve ablation or a single intravenous injection of SP abolishes immune privilege for corneal allografts for at least 100 days, which suggests that $CD11c^+$ CS cell populations are long-lived. However, whole body ionizing irradiation 14 days after corneal nerve injury abolishes CS cell activity, which suggests that the initial CS cell population is radiosensitive (32). Studies in bone marrow (BM) chimeric mice revealed that lethally irradiated $CD45.2^+$ congenic mice that were reconstituted with BM from $CD45.1^+$ congenic donors failed to display CS cell activity in either $CD45.1^+$ or $CD45.2^+$ cells populations following corneal nerve injury. This finding suggests that naïve BM-derived cells introduced into mice 14 days after corneal nerve injury are not converted to CS cells. This also indicates that the generation of CS cells is complete within 14 days or corneal nerve injury and that CS cells themselves are not long-lived even though SLIP persists for at least 100 days following trephining of the cornea (32).

WHAT IS THE MEANING OF SLIP?

On first blush SLIP seems to represent a flaw in ocular immune privilege. The time-honored view of ocular immune privilege proposes that the eye is endowed with a highly redundant system that dampens immune-mediated inflammation in order to preserve ocular tissues that have little or no regenerative capacities. Why then does the simple severing of corneal nerves abolish ocular immune privilege and why are both eyes affected? We favor the hypothesis that under certain circumstances terminating immune privilege is an adaptation to restore immune defense mechanisms at the ocular surface to protect the host against life-threatening infections. Under normal circumstances nominal non-infectious agents that pose no threat to survival are either ignored or they induce immune tolerance that reduces the risk of unwittingly provoking inflammation that might damage ocular tissues. By contrast, infectious agents that are potentially lethal transmit "danger signals" that lead to the termination of immune privilege. In mainstream immunology "danger signals" are in the form of pathogen-associated molecular patterns (PAMP that are recognized by toll-like receptors (TLRs) and other pathogen recognition receptors (PRRs). Although TLRs are expressed on cells comprising the ocular surface, other danger signals also originate at the ocular surface. Corneal nerve injury, alkali burns, and infectious agents can terminate immune privilege by a process that involves the release of SP, which represents another "danger signal" (39). It is noteworthy that two of the most common causes of infectious blindness, *Pseudomonas aeruginosa* and herpes simplex virus (HSV) are closely associated with the release of SP and the termination of ocular immune privilege (52–55). It is reasonable to assume that a corneal infection in one eye has a high likelihood to also occur in the opposite eye. As a result, the immune system anticipates that both eyes are at risk for life-threatening infections. A similar condition has been reported with cutaneous infections with *Candida* and *Staphylococcus* (56). Pain signals transmitted by neuropeptides during cutaneous infections with either of these microorganisms activates $TRPV1^+$ sensory nerves and activates innate Th17 responses in affected tissues and in adjacent non-involved tissues in anticipation of the infections spreading. The authors of this study use the term "anticipatory immunity", which is conceptually similar to SLIP. However, unlike "anticipatory immunity" in the skin, terminating immune privilege in the eye imposes more serious consequences. Even though life is preserved, the cost can be blindness.

AUTHOR CONTRIBUTIONS

The author confirms being the sole contributor of this work and has approved it for publication.

FUNDING

Supported in part by P30-EY030413 and an unrestricted grant from Research to Prevent Blindness.

REFERENCES

1. Abel S. Germinating Seed in Anterior Chamber. *Rep an unusual case. Arch Ophthalmol* (1979) 97:1651. doi: 10.1001/archopht.1979.01020020219005
2. Niederkorn JY. The Immunology of Corneal Transplantation. *Dev Ophthalmol* (1999) 30:129–40. doi: 10.1159/000060740
3. Niederkorn JY. The Immune Privilege of Corneal Grafts. *J Leukoc Biol* (2003) 74:167–71. doi: 10.1189/jlb.1102543
4. Niederkorn JY, Larkin DF. Immune Privilege of Corneal Allografts. *Ocular Immunol Inflammation* (2010) 18:162–71. doi: 10.3109/09273948.2010.486100
5. Medawar PB. Immunity to Homologous Grafted Skin. III. The Fate of Skin Homografts Transplanted to the Brain, to Subcutaneous Tissue, and to the Anterior Chamber of the Eye. *Br J Exp Pathol* (1948) 29:58–69.
6. Egan RM, Yorkey C, Black R, Loh WK, Stevens JL, Woodward JG. Peptide-Specific T Cell Clonal Expansion *In Vivo* Following Immunization in the Eye, An Immune-Privileged Site. *J Immunol* (1996) 157:2262–71.
7. Camelo S, Kezic J, Shanley A, Rigby P, McMenamin PG. Antigen From the Anterior Chamber of the Eye Travels in a Soluble Form to Secondary Lymphoid Organs Via Lymphatic and Vascular Routes. *Invest Ophthalmol Vis Sci* (2006) 47:1039–46. doi: 10.1167/iovs.05-1041
8. Niederkorn JY. See No Evil, Hear No Evil, Do No Evil: The Lessons of Immune Privilege. *Nat Immunol* (2006) 7:354–9. doi: 10.1038/ni1328
9. Niederkorn JY. Anterior Chamber-Associated Immune Deviation and Its Impact on Corneal Allograft Survival. *Curr Opin Organ Transplant* (2006) 11:360–5. doi: 10.1097/01.mot.0000236697.07092.ac
10. Bill A. The Blood-Aqueous Barrier. *Trans Ophthalmol Soc U K* (1986) 105(Pt 2):149–55.
11. Taylor AW. Ocular Immunosuppressive Microenvironment. *Chem Immunol* (2007) 92:71–85. doi: 10.1159/000099255
12. Taylor AW, Alard P, Yee DG, Streilein JW. Aqueous Humor Induces Transforming Growth Factor-Beta (TGF-Beta)- Producing Regulatory T-Cells. *Curr Eye Res* (1997) 16:900–8. doi: 10.1076/ceyr.16.9.900.5043

13. Taylor AW, Streilein JW, Cousins SW. Identification of Alpha-Melanocyte Stimulating Hormone as a Potential Immunosuppressive Factor in Aqueous Humor. *Curr Eye Res* (1992) 11:1199–206. doi: 10.3109/02713689208999545
14. Taylor AW, Streilein JW, Cousins SW. Alpha-Melanocyte-Stimulating Hormone Suppresses Antigen-Stimulated T Cell Production of Gamma-Interferon. *Neuroimmunomodulation* (1994) 1:188–94. doi: 10.1159/000097167
15. Taylor AW, Streilein JW, Cousins SW. Immunoreactive Vasoactive Intestinal Peptide Contributes to the Immunosuppressive Activity of Normal Aqueous Humor. *J Immunol* (1994) 153:1080–6.
16. Taylor AW, Yee DG. Somatostatin is an Immunosuppressive Factor in Aqueous Humor. *Invest Ophthalmol Vis Sci* (2003) 44:2644–9. doi: 10.1167/iovs.02-1216
17. Griffith TS, Brunner T, Fletcher SM, Green DR, Ferguson TA. Fas Ligand-Induced Apoptosis as a Mechanism of Immune Privilege. *Science* (1995) 270:1189–92. doi: 10.1126/science.270.5239.1189
18. Hori J, Wang M, Miyashita M, Tanemoto K, Takahashi H, Takemori T, et al. B7-H1-Induced Apoptosis as a Mechanism of Immune Privilege of Corneal Allografts. *J Immunol* (2006) 177:5928–35. doi: 10.4049/jimmunol.177.9.5928
19. Wang S, Boonman ZF, Li HC, He Y, Jager MJ, Toes RE, et al. Role of TRAIL and IFN-Gamma in CD4+ T Cell-Dependent Tumor Rejection in the Anterior Chamber of the Eye. *J Immunol* (2003) 171:2789–96. doi: 10.4049/jimmunol.171.6.2789
20. Katagiri K, Zhang-Hoover J, Mo JS, Stein-Streilein J, Streilein JW. Using Tolerance Induced *Via* the Anterior Chamber of the Eye to Inhibit Th2-Dependent Pulmonary Pathology. *J Immunol* (2002) 169:84–9. doi: 10.4049/jimmunol.169.1.84
21. D'Orazio TJ, Niederkorn JY. A Novel Role for TGF-Beta and IL-10 in the Induction of Immune Privilege. *J Immunol* (1998) 160:2089–98.
22. Faunce DE, Sonoda KH, Stein-Streilein J. MIP-2 Recruits NKT Cells to the Spleen During Tolerance Induction. *J Immunol* (2001) 166:313–21. doi: 10.4049/jimmunol.166.1.313
23. Lin HH, Faunce DE, Stacey M, Terajewicz A, Nakamura T, Zhang-Hoover J, et al. The Macrophage F4/80 Receptor Is Required for the Induction of Antigen-Specific Efferent Regulatory T Cells in Peripheral Tolerance. *J Exp Med* (2005) 201:1615–25. doi: 10.1084/jem.20042307
24. Niederkorn JY. Corneal Transplantation and Immune Privilege. *Int Rev Immunol* (2013) 32:57–67. doi: 10.3109/08830185.2012.737877
25. Niederkorn JY, Mellon J. Anterior Chamber-Associated Immune Deviation Promotes Corneal Allograft Survival. *Invest Ophthalmol Vis Sci* (1996) 37:2700–7.
26. Niederkorn JY. High-Risk Corneal Allografts and Why They Lose Their Immune Privilege. *Curr Opin Allergy Clin Immunol* (2010) 10:493–7. doi: 10.1097/ACI.0b013e32833dfa11
27. Coster DJ, Williams KA. The Impact of Corneal Allograft Rejection on the Long-Term Outcome of Corneal Transplantation. *Am J Ophthalmol* (2005) 140:1112–22. doi: 10.1016/j.ajo.2005.07.024
28. Williams KA, Kelly TL, Lowe MT, Coster DJ. All Contributors to the Australian Corneal Graft R. The Influence of Rejection Episodes in Recipients of Bilateral Corneal Grafts. *Am J Transplant* (2010) 10:921–30. doi: 10.1111/j.1600-6143.2009.03002.x
29. Paunicka KJ, Mellon J, Robertson D, Petroll M, Brown JR, Niederkorn JY. Severing Corneal Nerves in One Eye Induces Sympathetic Loss of Immune Privilege and Promotes Rejection of Future Corneal Allografts Placed in Either Eye. *Am J Transplant* (2015) 15:1490–501. doi: 10.1111/ajt.13240
30. Castiblanco CP, Adelman RA. Sympathetic Ophthalmia. *Graefes Arch Clin Exp Ophthalmol* (2009) 247:289–302. doi: 10.1007/s00417-008-0939-8
31. Mo J, Neelam S, Mellon J, Brown JR, Niederkorn JY. Effect of Corneal Nerve Ablation on Immune Tolerance Induced by Corneal Allografts, Oral Immunization, or Anterior Chamber Injection of Antigens. *Invest Ophthalmol Vis Sci* (2017) 58:137–48. doi: 10.1167/iovs.16-20601
32. Neelam S, Mellon J, Wilkerson A, Niederkorn JY. Induction of Contrasuppressor Cells and Loss of Immune Privilege Produced by Corneal Nerve Ablation. *Invest Ophthalmol Vis Sci* (2018) 59:4738–47. doi: 10.1167/iovs.18-24894
33. Lucas K, Karamichos D, Mathew R, Zieske JD, Stein-Streilein J. Retinal Laser Burn-Induced Neuropathy Leads to Substance P-dependent Loss of Ocular Immune Privilege. *J Immunol* (2012) 189:1237–42. doi: 10.4049/jimmunol.1103264
34. Guzman M, Miglio MS, Zgajnar NR, Colado A, Almejun MB, Keitelman IA, et al. The Mucosal Surfaces of Both Eyes Are Immunologically Linked by a Neurogenic Inflammatory Reflex Involving TRPV1 and Substance P. *Mucosal Immunol* (2018) 11:1441–53. doi: 10.1038/s41385-018-0040-5
35. Janelsins BM, Sumpter TL, Tkacheva OA, Rojas-Canales DM, Erdos G, Mathers AR, et al. Neurokinin-1 Receptor Agonists Bias Therapeutic Dendritic Cells to Induce Type 1 Immunity by Licensing Host Dendritic Cells to Produce IL-12. *Blood* (2013) 121:2923–33. doi: 10.1182/blood-2012-07-446054
36. Gershon RK, Eardley DD, Durum S, Green DR, Shen FW, Yamauchi K, et al. Contrasuppression. A Novel Immunoregulatory Activity. *J Exp Med* (1981) 153:1533–46. doi: 10.1084/jem.153.6.1533
37. Sakaguchi S, Sakaguchi N, Asano M, Itoh M, Toda M. Immunologic Self-Tolerance Maintained by Activated T Cells Expressing IL-2 Receptor Alpha-Chains (CD25). Breakdown of a Single Mechanism of Self-Tolerance Causes Various Autoimmune Diseases. *J Immunol* (1995) 155:1151–64.
38. Lehner T. Special Regulatory T Cell Review: The Resurgence of the Concept of Contrasuppression in Immunoregulation. *Immunology* (2008) 123:40–4. doi: 10.1111/j.1365-2567.2007.02780.x
39. Niederkorn JY. The Eye Sees Eye to Eye With the Immune System: The 2019 Proctor Lecture. *Invest Ophthalmol Vis Sci* (2019) 60:4489–95. doi: 10.1167/iovs.19-28632
40. Schaumburg CS, Siemasko KF, De Paiva CS, Wheeler LA, Niederkorn JY, Pflugfelder SC, et al. Ocular Surface APCs Are Necessary for Autoreactive T Cell-Mediated Experimental Autoimmune Lacrimal Keratoconjunctivitis. *J Immunol* (2011) 187:3653–62. doi: 10.4049/jimmunol.1101442
41. Keino H, Masli S, Sasaki S, Streilein JW, Stein-Streilein J. CD8+ T Regulatory Cells Use A Novel Genetic Program That Includes CD103 to Suppress Th1 Immunity in Eye-Derived Tolerance. *Invest Ophthalmol Vis Sci* (2006) 47:1533–42. doi: 10.1167/iovs.04-1454
42. Andrew DP, Rott LS, Kilshaw PJ, Butcher EC. Distribution of Alpha 4 Beta 7 and Alpha E Beta 7 Integrins on Thymocytes, Intestinal Epithelial Lymphocytes and Peripheral Lymphocytes. *Eur J Immunol* (1996) 26:897–905. doi: 10.1002/eji.1830260427
43. Myers L, Croft M, Kwon BS, Mittler RS, Vella AT. Peptide-Specific CD8 T Regulatory Cells Use IFN-Gamma to Elaborate TGF-Beta-Based Suppression. *J Immunol* (2005) 174:7625–32. doi: 10.4049/jimmunol.174.12.7625
44. Suffia I, Reckling SK, Salay G, Belkaid Y. A Role for CD103 in the Retention of CD4+CD25+ Treg and Control of Leishmania Major Infection. *J Immunol* (2005) 174:5444–55. doi: 10.4049/jimmunol.174.9.5444
45. Uss E, Rowshani AT, Hooibrink B, Lardy NM, van Lier RA, ten Berge IJ. CD103 Is a Marker for Alloantigen-Induced Regulatory CD8+ T Cells. *J Immunol* (2006) 177:2775–83. doi: 10.4049/jimmunol.177.5.2775
46. Neelam S, Niederkorn JY. Corneal Nerve Ablation Abolishes Ocular Immune Privilege by Downregulating CD103 on T Regulatory Cells. *Invest Ophthalmol Vis Sci* (2020) 61:25. doi: 10.1167/iovs.61.4.25
47. Geiger B, Ayalon O. Cadherins. *Annu Rev Cell Biol* (1992) 8:307–32. doi: 10.1146/annurev.cb.08.110192.001515
48. Tang A, Amagai M, Granger LG, Stanley JR, Udey MC. Adhesion of Epidermal Langerhans Cells to Keratinocytes Mediated by E-Cadherin. *Nature* (1993) 361:82–5. doi: 10.1038/361082a0
49. Higgins JM, Mandlebrot DA, Shaw SK, Russell GJ, Murphy EA, Chen YT, et al. Direct and Regulated Interaction of Integrin $\alpha e\beta 7$ With E-Cadherin. *J Cell Biol* (1998) 140:197–210. doi: 10.1083/jcb.140.1.197
50. Schaffalitzky De Muckadell OB, Aggestrup S, Stentoft P. Flushing and Plasma Substance P Concentration During Infusion of Synthetic Substance P in Normal Man. *Scand J Gastroenterol* (1986) 21:498–502. doi: 10.3109/00365528609015169
51. McKinney EC, Streilein JW. On the Extraordinary Capacity of Allogeneic Epidermal Langerhans Cells to Prime Cytotoxic T Cells *In Vivo*. *J Immunol* (1989) 143:1560–4. doi: 10.1167/iovs.19-28632
52. Foldenauer ME, McClellan SA, Barrett RP, Zhang Y, Hazlett LD. Substance P Affects Growth Factors in Pseudomonas Aeruginosa-Infected Mouse Cornea. *Cornea* (2012) 31:1176–88. doi: 10.1097/ICO.0b013e31824d6ffd
53. Hazlett LD, McClellan SA, Barrett RP, Liu J, Zhang Y, Lighvani S. Spantide I Decreases Type I Cytokines, Enhances IL-10, and Reduces Corneal Perforation in Susceptible Mice After Pseudomonas Aeruginosa Infection. *Invest Ophthalmol Vis Sci* (2007) 48:797–807. doi: 10.1167/iovs.06-0882

54. McClellan SA, Zhang Y, Barrett RP, Hazlett LD. Substance P Promotes Susceptibility to Pseudomonas Aeruginosa Keratitis in Resistant Mice: Anti-Inflammatory Mediators Downregulated. *Invest Ophthalmol Vis Sci* (2008) 49:1502–11. doi: 10.1167/iovs.07-1369
55. Twardy BS, Channappanavar R, Suvas S. Substance P in the Corneal Stroma Regulates the Severity of Herpetic Stromal Keratitis Lesions. *Invest Ophthalmol Vis Sci* (2011) 52:8604–13. doi: 10.1167/iovs.11-8089
56. Cohen JA, Edwards TN, Liu AW, Hirai T, Jones MR, Wu J, et al. Cutaneous TRPV1(+) Neurons Trigger Protective Innate Type 17 Anticipatory Immunity. *Cell* (2019) 178:919–32.e14. doi: 10.1016/j.cell.2019.06.022

Conflict of Interest: The author declares that the research was conducted in the absence of any commercial or financial relationships that could be construed as a potential conflict of interest.

Copyright © 2021 Niederkorn. This is an open-access article distributed under the terms of the Creative Commons Attribution License (CC BY). The use, distribution or reproduction in other forums is permitted, provided the original author(s) and the copyright owner(s) are credited and that the original publication in this journal is cited, in accordance with accepted academic practice. No use, distribution or reproduction is permitted which does not comply with these terms.

frontiers in Immunology

ORIGINAL RESEARCH
published: 21 June 2021
doi: 10.3389/fimmu.2021.685559

IRF8-Dependent Type I Conventional Dendritic Cells (cDC1s) Control Post-Ischemic Inflammation and Mildly Protect Against Post-Ischemic Acute Kidney Injury and Disease

Na Li[1,2], Stefanie Steiger[2], Lingyan Fei[1], Chenyu Li[2], Chongxu Shi[2], Natallia Salei[3,4], Barbara U. Schraml[3,4], Zhihua Zheng[1], Hans-Joachim Anders[2*] and Julia Lichtnekert[2*]*

[1] Department of Nephrology, Center of Kidney and Urology, The Seventh Affiliated Hospital, Sun Yat-sen University, Shen Zhen, China, [2] Division of Nephrology, Department of Medicine IV, University Hospital, Ludwig Maximilian University of Munich, Munich, Germany, [3] Walter-Brendel-Centre of Experimental Medicine, University Hospital, LMU Munich, Munich, Germany, [4] Institute for Cardiovascular Physiology and Pathophysiology, Biomedical Center, Faculty of Medicine, LMU Munich, Munich, Germany

OPEN ACCESS

Edited by:
Daniel Saban, Duke University, United States

Reviewed by:
Ehud Zigmond, Tel Aviv Sourasky Medical Center, Israel
George Bertsias, University of Crete, Greece

***Correspondence:**
Julia Lichtnekert julia.lichtnekert@med.uni-muenchen.de
Hans-Joachim Anders hjanders@med.uni-muenchen.de
Zhihua Zheng zhzhihua@mail.sysu.edu.cn

Specialty section:
This article was submitted to Antigen Presenting Cell Biology, a section of the journal Frontiers in Immunology

Received: *25 March 2021*
Accepted: *26 May 2021*
Published: *21 June 2021*

Citation:
Li N, Steiger S, Fei L, Li C, Shi C, Salei N, Schraml BU, Zheng Z, Anders H-J and Lichtnekert J (2021) IRF8-Dependent Type I Conventional Dendritic Cells (cDC1s) Control Post-Ischemic Inflammation and Mildly Protect Against Post-Ischemic Acute Kidney Injury and Disease. Front. Immunol. 12:685559. doi: 10.3389/fimmu.2021.685559

Post-ischemic acute kidney injury and disease (AKI/AKD) involve acute tubular necrosis and irreversible nephron loss. Mononuclear phagocytes including conventional dendritic cells (cDCs) are present during different phases of injury and repair, but the functional contribution of this subset remains controversial. Transcription factor interferon regulatory factor 8 (IRF8) is required for the development of type I conventional dendritic cells (cDC1s) lineage and helps to define distinct cDC1 subsets. We identified one distinct subset among mononuclear phagocyte subsets according to the expression patterns of CD11b and CD11c in healthy kidney and lymphoid organs, of which IRF8 was significantly expressed in the $CD11b^{low}CD11c^{high}$ subset that mainly comprised cDC1s. Next, we applied a *Irf8*-deficient mouse line (*Irf8*$^{fl/fl}$*Clec9a*^{cre} mice) to specifically target *Clec9a*-expressing cDC1s *in vivo*. During post-ischemic AKI/AKD, these mice lacked cDC1s in the kidney without affecting cDC2s. The absence of cDC1s mildly aggravated the loss of living primary tubule and decline of kidney function, which was associated with decreased anti-inflammatory Tregs-related immune responses, but increased T helper type 1 (T_{H1})-related and pro-inflammatory cytokines, infiltrating neutrophils and acute tubular cell death, while we also observed a reduced number of cytotoxic $CD8^+$ T cells in the kidney when cDC1s were absent. Together, our data show that IRF8 is indispensable for kidney cDC1s. Kidney cDC1s mildly protect against post-ischemic AKI/AKD, probably *via* suppressing tissue inflammation and damage, which implies an immunoregulatory role for cDC1s.

Keywords: interferon regulatory factor 8, type I conventional dendritic cells, dendritic cells, ischemia reperfusion, acute kidney injury

INTRODUCTION

Ischemia-reperfusion injury (IRI) is a frequent clinical complication following kidney transplantation, volume depletion, heart failure, or major trauma, presenting as acute kidney injury (AKI). Severe IRI induced tubular necrosis implies a longer period of kidney dysfunction referred to as acute kidney disease (AKD) and, if persistent, can lead to chronic kidney disease (CKD) (1). IRI involves acute tubular epithelial cell (TEC) necrosis accompanied by a crescendo and decrescendo of sterile inflammation, referred to as "necroinflammation" (2). Necroinflammation in AKI is associated with the release of pathogen- or danger-associated molecular patterns (PAMPs or DAMPs) and the activation of kidney mononuclear phagocytes, including dendritic cells (DCs) (3, 4). Of note, the specific roles of kidney DCs and subsets in AKI/AKD remain controversial (3, 5–8).

DCs play a sentinel role between innate and adaptive immune responses. Upon kidney injury, some DCs primarily produce tumor necrosis factor-α (TNF-α) to recruit other inflammatory cells (9, 10). The antigen cross-presentation capacity of DCs can also be enhanced by PAMPs and DAMPs (10), which consequently drives naïve T cell differentiation towards cytotoxic $CD8^+$ T cells or naïve $CD4^+$ T cells (11, 12). Activated $CD4^+$ T cells differentiate towards pro-inflammatory T_{H1} and T_{H17} cells, which stimulate macrophages, neutrophils, and other immune effectors (11–14). This avenue supports a pro-inflammatory function of kidney DCs. On the other hand, more functional studies reported protective effects of kidney DCs (15–20). This could be linked to the anti-inflammatory functions of certain DC subsets by priming naïve $CD4^+$ T cells towards regulatory T cells (Tregs) to suppress inflammation (16–18, 20, 21) or enhancing cytokine pathways to improve kidney repair, including interleukin (IL)-10, IL-22, and single Ig IL-1-related receptor (3, 5, 22).

One explanation for the discrepancies on the functional role of kidney DCs may be associated with the plasticity of DCs, depending on various diseases (3, 23, 24). Kidney DCs are mixed subsets and consist of four cell subsets, namely type I conventional dendritic cells (cDC1s), type II conventional dendritic cells (cDC2s), $CD64^+F4/80^{high}$, and $CD64^+CD11b^{high}$ DCs, that differ ontogenetically, functionally, and transcriptionally (25). cDC1s derive exclusively from a single cDC precursor, whereas other DC subsets are heterogeneous (26). $CD64^+F4/80^{high}$ DCs are transcriptionally similar to macrophages, while $CD64^+CD11b^{high}$ DCs resemble cDC2s. However, the phenotype of $CD64^+$ DCs still remains unclear (25). Lymphoid cDC2s consist of two subtypes with distinct functions, including the anti-inflammatory cDC2A and the pro-inflammatory cDC2B subset (27, 28). Under virus infection, cDC2s commonly share the function and gene expression with cDC1s and macrophages, collaboratively boosting $CD4^+$ and $CD8^+$ T cell immunity (29). This suggests that cDC1s are more homogenous than other DC subsets. In addition, the spatially and temporarily different microenvironments in diseases are responsible for the plasticity of intrarenal M1/M2 macrophages as well as DCs (8, 24). Consistently, kidney DCs are found to either play a pro-inflammatory role in adriamycin-induced nephropathy, diabetic and hypertensive nephropathy, or to be anti-inflammatory in kidney graft rejection, crescent and immune complex glomerulonephritis (3). The temporal appearance of each phenotype in different phases of single disease also varies (24).

DCs are most abundant in the interstitial compartment of the kidney and fewer than 5% of these subsets are cDC1s (25, 30). cDC1s and few plasmacytoid DCs (pDCs) exclusively arise from the C-type lectin receptor DNGR-1-expressing common DC progenitors (CDP) (31, 32). DNGR-1 is encoded by the gene *Clec9a*. In addition, cDC1s require the transcription factor *Irf8*, basic leucine zipper transcription factor ATF-like 3 (*Batf3*) and WD repeat and FYVE Domain Containing 3 (*Wdfy3*) and are marked by XCR-1, DNGR-1, and integrin CD103 (25, 26, 32, 33). DC migration also depends on chemokines and their receptors, such as C-C chemokine receptor type 7 (CCR7) (34). Functionally, cDC1s evoke IL-10-expressing Tregs to antagonize inflammatory cDC2s in crescent nephritis, or to suppress cell apoptosis in ischemic reperfusion-induced hepatic injury (18, 20, 21, 35). Furthermore, cDC1s are known for their cross-presentation capacity of antigens on MHC class I molecules to activate $CD8^+$ cytotoxic T cells (36, 37). Kidney cDC1s are small subsets and the functional role of cDC1s in AKI/AKD are not well understood. Although *Xcr1*-cre, *Batf3* KO, Langerin-DTR, and *Flt3L* KO mouse lines were generated to track cDC1s, the efficiency and specificity of cDC1s reduction among these mice still need more understanding (20, 37). We generated a mouse line with *Irf8*-deficiency in *Clec9a*-expressing progenitors and hypothesized that *Irf8*-deficiency would deplete cDC1s, which may promote a pro-inflammatory immune response and consequently drive AKI/AKD progression.

MATERIALS AND METHODS

Animals

All animal experiments were performed according to the European protection law of animal welfare and upon approval by the local government authorities Regierung von Oberbayern (Az 55.2-1-54-2532-175-2014) based on the European directive for the Protection of Animals Used for Scientific Purposes (2010/63/EU) and reported according to the ARRIVE guidelines (38). Mice were housed in groups of five under SPF condition with free access to food and water, and a 12-h light circle. Six- to eight-week-old male mice were used for experiments. The following mouse lines were used: wildtype C57BL/6 mice, *Irf8*-deficient mice ($Irf8^{fl/fl}Clec9a^{cre}$ mice) as experimental group and littermates ($Irf8^{fl/fl}Clec9a^{wt}$ mice) as control group (**Table S1**).

Ischemic Reperfusion Injury (IRI Surgery)

IRI surgery was performed as previously described (39). Briefly, groups of age-matched littermate mice ($n \geq 3$) were anesthetized to achieve analgesia, amnesia, and hypnosis prior to unilateral left kidney pedicle clamping (25 min). Body temperature was monitored by online rectal temperature recording during the whole surgery process. Following kidney pedicle clamping and

clamping removal, successful reperfusion was assessed by color change from pale (ischemia) to the original color. Afterwards, wounds were closed (Ethicon, Belgium) and 500 µl saline applied to balance fluid loss. Anesthesia was antagonized as previously described (38). Mice were sacrificed on day 1 and 7 days after IRI. Left kidneys spleen and left kidney draining lymph nodes were collected for further analysis.

Glomerular Filtration Rate (GFR) Measurement

We measured GFR in conscious mice before IR surgery as well as on days 1 and 7 after IR surgery ($n \geq 3$ mice/group) as described (39). Briefly, mice were anesthetized with isoflurane and the shaved neck was covered with a miniaturized image device built from two light-emitting diodes, a photodiode, and a battery (MediBeacon™ Inc., Mannheim, Germany). The whole recording period lasted 1.5–2 h after a single injection of FITC-sinistrin (i.v., 150 mg/kg body weight) (MediBeacon™Inc., Mannheim, Germany). Prior to the injection of FITC-sinistrin, the skins' background signal was recorded for 5 min. Recorded mice were conscious and unrestrained in a single cage. After removing the image device, data were analyzed using the imaging device MPD Studio software (MediBeacon™Inc., Mannheim, Germany). GFR (µl/min per 100 g body weight) was calculated from the decrease of fluorescence intensity of FITC-sinistrin over time using a three-compartment model with linear correction (injection, plasma, and interstitial compartment, t1/2 of FITC- sinistrin), body weight of the mouse, and an empirical conversion factor (40).

Cell Isolation

Kidneys were mashed gently and digested with 2 ml fresh D-PBS solution containing collagenase V (2 mg/ml, Sigma-Aldrich) and DNase I (500 Units/ml, Roche). Suspension was kept at 37°C for 45 min followed by homogenizing three to four times. Cold FACS buffer (D-PBS, 1% BSA, 0.1% NaN_3) was added to stop tissue digestion. Digested tissues were homogenized and gently pressed through a 70 µm cell strainer (MACS® SmartStrainers). Cell pellets were washed twice with D-PBS and kept on ice. Kidney leukocytes and tubular epithelial cells were enriched using a 30–70% Percoll (Sigma-Aldrich) gradient by centrifugation (2,000 rpm, 30 min, room temperature [RT]). Leukocytes were washed once with D-PBS, resuspended in 500 µl FACS buffer, and placed on ice for further analysis. Spleen and lymph nodes (25, 41) were gently pressed through a 70 µm cell strainer by using a 1 ml syringe and washed with FACS buffer. Erythrocytes in spleen were lysed with 2 ml red blood cell (RBC) lysis buffer (MilliQ water, 0.15 M NH_4Cl) at RT for 10 min. After lysis, 8 ml D-PBS was added to stop lysis. Cell pellet was resuspended in 1,000 µl FACS buffer and stored on ice. Tubular epithelial cells were washed once with D-PBS and resuspended in lysis buffer for further RNA isolation.

FACS Analysis of Leukocytes

Cell suspensions from the left kidney, spleen, and left kidney draining lymph node were used for FACS analysis. Cells were blocked with anti-mouse CD16/CD32 antibody (Fcγ III/II, 1 mg/ml, BD Biosciences) for 10 min on ice. After blocking, cells were stained with the fluorescent surface anti-mouse antibodies for 20 min at 4°C in the dark (**Table S2**). For intracellular staining of transcription factors, the fixation/permeabilization kit was performed according to manufacturer instruction (Foxp3/transcription factor staining buffer set, eBioscience™) and cells stained with the intracellular fluorescent-labeled anti-mouse antibodies using the indicated concentrations for 20 min at 4°C in the dark (**Table S2**). The cytometric acquisition was performed on FACSCanto™ II or LSRFortessa™ (BD Biosciences). Cell analysis, dot plots, and raw data export were completed using FlowJo software.

Histology

Kidney tissues were embedded in paraffin and 2-µm kidney sections for periodic acid-Schiff (PAS) staining as described (40, 42). Representative images of kidney sections (cortex and outer medulla) are shown to illustrate tubular injury that displayed cast formation and tubular dilation. Injured tubular index was scored by the percentage of tubules in the corticomedullary junction that displayed cell necrosis, loss of brush border, cast formation, edema, and tubular dilation as follows: 0, none; 1, ≤10%; 2, 11–25%; 3, 26–45%; 4, 46–75%; 5, >76%. For immunostaining, we used biotinylated *L. tetragonolobus* lectin stain (Vector Labs), Tamm-Horsfall protein (THP) stain (Santa Cruz Biotechnology), anti-mouse IRF8 (Abcam), rabbit anti-mouse CD3 (Abcam), rat anti-mouse Ly6B.2 (Serotec, UK), and rat anti-mouse MHCII (I-A/I-E) (eBioscience™) (**Table S2**). All results were quantified by Image J software. To count interstitial cells, 10 cortical high-power fields (HPF) (400×). All assessments were performed by two blinded observers (CL and CS).

Quantitative Real-Time PCR (qRT-PCR)

RNA was extracted from kidney tissue or isolated tubular epithelial cells using Pure Link RNA Mini Kit (Invitrogen™, Germany) according to the manufacturer's protocol (40, 41). cDNA was synthesized from 2 µg of total RNA using the transcript kit (Invitrogen™, Germany). Quantitative real-time PCR (qRT-PCR) from cDNA was performed using SYBR Green dye detection system on a Light Cycler 480 (Roche, Germany). All samples were normalized to 18s rRNA. The sequences of gene-specific primers (300 nM; Metabion, Martinsried, Germany) are listed (**Table S3**).

Blood Urea Nitrogen (BUN) Measurement

Serum BUN (DiaSys, Holzheim, Germany) was measured according to manufacturer's protocol (40).

Statistical Analysis

All data were given means ± SD. Statistical analysis of data were performed using GraphPad Prism 8 software. Data normality was checked using Shapiro-Wilk test. Comparative statistics between two unpaired groups were performed using *t-test* for parametric data and Mann Whitney test or Wilcoxon test for non-parametric data. Comparative statistics between multiple groups were performed using One-way ANOVA with Tukey's *post-hoc* test for parametric data or Two-way ANOVA with Dunnett test for non-parametric data under Bonferroni correction. A *P*-value less than 0.05 indicated statistical

significance (shown as $^{*}P < 0.05$, $^{**}P < 0.01$, $^{***}P < 0.001$, $^{****}P < 0.0001$).

RESULTS

Mononuclear Phagocyte Cell Such as CD11b^{low}CD11c^{high} Subset Accumulates in Kidney During Post-Ischemic AKI/AKD

To characterize mononuclear phagocytes in lymphoid organs (spleen, kidney draining lymph node [LN]) and non-lymphoid organs (kidney), we used established multi-flow cytometric analysis as previously demonstrated (43). Mononuclear phagocytes of C57BL/6 mice were identified by gating on CD45$^+$ leukocytes and singlets, while excluding T cells, B cells, natural killer cells (NK cells), and neutrophils (**Figure 1A**). We classified one distinct subset of mononuclear phagocytes according to the expression levels of CD11b and CD11c as followed: R1 subset (CD11b^{low}CD11c^{high}), which commonly exists in healthy organs, including the kidney (**Figure 1B**).

To identify the dynamic changes of the intrarenal R1 subset (CD11b^{low}CD11c^{high}) during AKI/AKD, wild type C57BL/6 mice underwent IRI surgery and flow cytometric analysis was performed on days 1 and 7 after IRI (**Figure 1C**). Post-ischemic AKI/AKD was associated with a significant drop in GFR on day 1 and 7 as compared to healthy mice (**Figure S1B**). The absolute number of intrarenal CD11b^{low}CD11c^{high} (R1 subset) increased during the early acute injury phase (IRI-1D) and the recovery phase (IRI-7D) (**Figures 1D, E**), suggesting that the R1 subset accumulates in the kidney during post-ischemic AKI/AKD.

R1 Subset (CD11b^{low}CD11c^{high}) Corresponds to Type I Conventional Dendritic Cell (cDC1)-Like Cells

To confirm the phenotype characteristic of the R1 subset (CD11b^{low}CD11c^{high}), we further subdivided CD45$^+$CD3e$^-$CD19$^-$CD49b$^-$Ly6g$^-$ mononuclear phagocytes into CD64$^-$F4/80$^-$ cells to exclude macrophages and MHCII$^+$ cells independent of CD11c expression (**Figure S1A**). We found similar surface marker expression pattern between kidney CD103$^+$ cDC1s and the R1 subset (CD11b^{low}CD11c^{high}) (**Figures 1F** and **S1A**), suggesting that the R1 subset (CD11b^{low}CD11c^{high}) shares similar phenotypic characteristics with cDC1s. Immunohistochemistry staining confirmed that the number of intrarenal MHCII$^+$ cells and mRNA expression levels of *Ccr7*, *Cd40*, *Cd80*, and *Cd86* increased over time after IRI (**Figures 1G** and **S2**). Taken together, post-ischemic AKI/AKD triggered the accumulation of mononuclear phagocytes including the R1 subset (CD11b^{low}CD11c^{high}), which we identified as cDC1-like cells.

cDC1s Express Transcription Factor IRF8 in Post-Ischemic AKI/AKD

IRF8 is terminally expressed in cDC1s and important for the development of cDC1s lineage in the bone marrow (43–45). However, the expression pattern of IRF8 in intrarenal DCs in health and AKI/AKD still remains unknown. To investigate this, we first determined the mRNA expression levels of *Irf8* in lymphoid and non-lymphoid organs of healthy wild type C57BL/6 mice, and found higher *Irf8* mRNA expression levels in spleen, bone marrow, thymus, small intestine, and lung, while the *Irf8* mRNA level in the kidney was lower and comparable to that in liver and heart (**Figure 2A**). Upon IRI, the number of IRF8$^+$ cells significantly increased in the tubulointerstitium (**Figures 2B, C**). This was consistent with increased *Irf8* mRNA expression levels within total kidneys after IRI, but not in isolated TECs (**Figure 2D**). Flow cytometry revealed that the MFI of IRF8 among cDC1-like R1 cells (CD11b^{low}CD11c^{high}) as well as monocytes significantly increased over time after IRI (**Figures 2E** and **S3A, B**). We also found that the MFI of IRF8 in cDC1-like R1 cells (CD11b^{low}CD11c^{high}) was significantly higher than that in monocytes. Thus, kidney cDC1-like cells express and require IRF8 during post-ischemic AKI/AKD.

Fewer cDC1s Accumulate in Post-Ischemic *Irf8*-Deficient Mice

To confirm whether the specific depletion of *Irf8* could reduce the accumulation of kidney cDC1s in AKI/AKD, we generated a *Irf8*-deficient model using *Irf8*$^{flox/flox}$*Clec9a*^{cre} mice (briefly called *Irf8*$^{fl/fl}$*Clec9a*^{cre}) with a cre-lox recombination system. We identified the DC subsets according to various surface makers by established flow cytometric analysis (25). In detail, MHCII$^+$ cells were divided into cDCs and CD64$^+$ DCs according to the surface markers CD11c and CD64, while XCR-1 was used to classify cDC1s and CD11b to classify cDC2s (**Figure 3A**) (25). Under healthy condition, we observed that the absolute number of cDC1s was significantly reduced in the kidney of *Irf8*-deficient mice (*Irf8*$^{fl/fl}$*Clec9a*^{cre}), but not that of cDC2s, CD64$^+$ DCs and monocytes (**Figures 3B** and **S3C**). However, the absolute number of cDC1s remained significantly reduced (70–80%) even after IRI on days 1 and 7. While no difference was observed in the number of cDC2s, CD64$^+$ DCs were reduced after IRI on day 7 (**Figure 3B**). Immunostaining revealed less infiltrating MHCII$^+$ cells in kidney and spleen in *Irf8*-deficient mice compared to control mice after IRI, especially on day 7 (**Figures 3C, D**). The data suggest that the deficiency of *Irf8* in *Clec9a*-expressing progenitors could deplete intrarenal accumulation of cDC1s after IRI. Of note, the absolute number and percentage of infiltrating monocytes in the kidney significantly increased in *Irf8*-deficient mice after IRI on day 1 due to the inflammatory response after IRI (**Figure S3D**). Together, in the *Irf8*$^{fl/fl}$*Clec9a*^{cre} mouse line, cDC1s are significantly depleted in steady state and after IRI. Additionally, we observed a partial reduction of CD64+DCs 7 days after IRI (25, 29).

cDC1s Are Mildly Protective in Post-Ischemic AKI/AKD

The function of cDC1s was proved controversy under crescent nephritis and adriamycin nephropathy (20, 46). To clarify the role of cDC1s in post-ischemic AKI/AKD, we applied this *Irf8*-deficient mouse model, which conditionally lacks cDC1s (**Figures 3A, B**). IRI was induced in *Irf8*-deficient mice as well

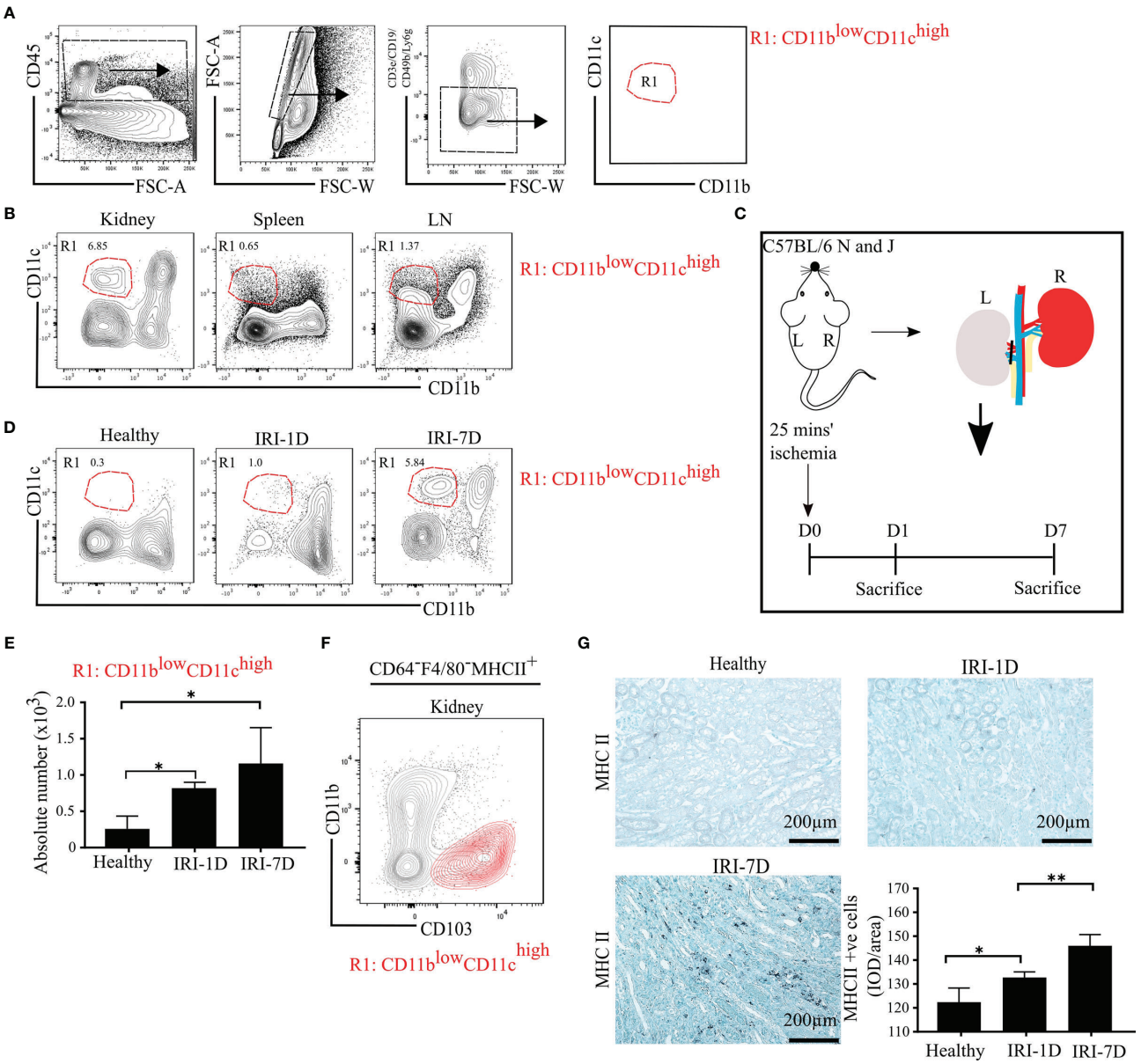

FIGURE 1 | Mononuclear phagocytes, including type I conventional dendritic cells (cDC1s), accumulate in kidney during post-ischemic AKI/AKD. **(A)** Representative gating strategy of mononuclear phagocytes of adult C57BL/6 mice. Of the CD45$^+$ cells and singlets FSC-W/A, mononuclear phagocytes were identified by excluding T cells/natural killer cells/neutrophils/B cells. Mononuclear phagocytes contain one distinct subset according to the expression levels of CD11b and CD11c and was named as R1 subset CD11b^{low}CD11c^{high} (red). **(B)** Identification of the mononuclear phagocyte R1 subset in healthy kidney, spleen, and kidney draining lymphoid node (LN). **(C)** Schematic of experimental set-up. Unilateral IRI was induced in C57BL/6 mice by 25 min kidney pedicle clamping. Organ harvest was taken from healthy state, day 1 (IRI-1D) and day 7 (IRI-7D) after IRI. Time point D0 represents healthy state. **(D)** Dot plots displaying phenotypic change of kidney R1 subset on healthy state, IRI-1D, and IRI-7D. **(E)** Absolute cell number of R1 subset per kidney (n = 4–5 mice/group). **(A–E)** Representative data of three independent experiments. **(F)** Similarity between CD103$^+$ cDC1s (black contour plot) and R1 subset (CD11b^{low}CD11c^{high}, red contour plot) in kidney (Gating strategy is shown in **Figure S1A**). **(G)** Representative immunostaining of kidney major histocompatibility complex class II (MHCII) positive cells and quantitative analysis indicated by integrated optical density (IOD)/area (n = 3–4 mice/group). Bars = 200 μm. Data are means ± SD. One-way ANOVA. *P < 0.05; **P < 0.01.

as control mice. We observed a significant increase of serum BUN levels, a marker of kidney excretory function (**Figure 4A**), but no significance was observed in GFR between *Irf8*-deficient mice and control mice (**Figure 4B**). Macroscopic analysis likely revealed more tubular atrophy and injury in *Irf8*-deficient mice, as indicated by a higher value of delta kidney weights (Delta kidney weight = KW_R – KW_L) (**Figures 4C, D**), more tubular cast formation and dilation in PAS-stained kidney

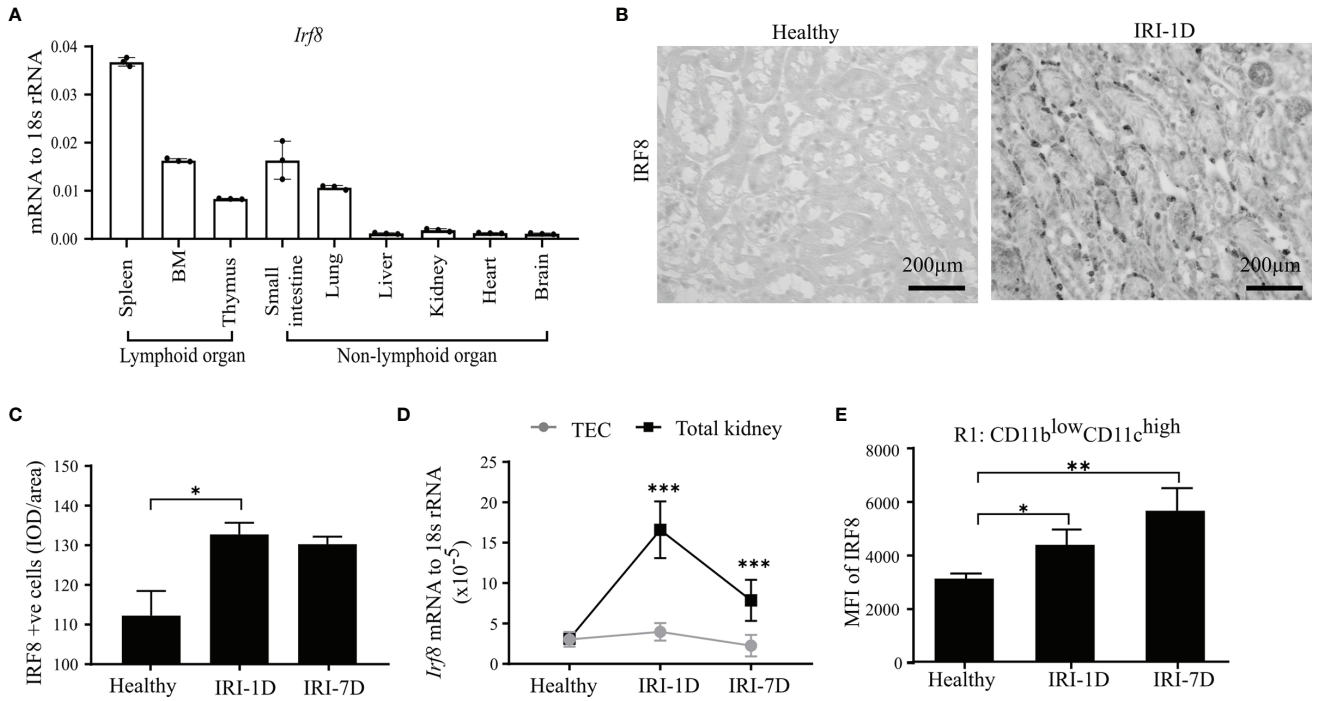

FIGURE 2 | Kidney type I conventional dendritic cells (cDC1s) require transcription factor IRF8. **(A)** mRNA expression of *Irf8* in lymphoid and non-lymphoid organs from healthy C57BL/6 mice and expression level were normalized to 18s rRNA (n = 3 mice/group). **(B)** Representative image of IRF8 positive cells in kidney in healthy state and day 1 after IRI (IRI-1D). Bars = 200 μm. **(C)** Quantitative analysis of IRF8 positive cells by integrated optical density (IOD)/area (n = 5 mice/group). **(D)** Normalized mRNA expression level of *Irf8* in terms of whole kidney or isolated primary tubular epithelial cells (TECs) from mice in healthy state, IRI-1D, and IRI-7D (n = 5 mice/group). **(E)** Mean fluorescence intensity (MFI) of IRF8 in R1 subset (n = 3–5 mice/group). **(E)** Representative data of three independent experiments. Data are means ± SD. One-way ANOVA. $^*P < 0.05$; $^{**}P < 0.01$; $^{***}P < 0.001$.

sections as well as a significant higher value of injured tubular index (**Figure 4E**).

Intrarenal DCs also accelerate tubular regeneration and recovery by secreting IL-22 or upregulating the expression of IL-10 in AKI (5, 20). Consistent with that, we found decreased mRNA expression levels of *Il-22* and *Il-10* in *Irf8*-deficient mice after IRI as compared to control mice (**Figure 5A**). To investigate tubular recovery, immunohistochemistry staining for living proximal or distal tubules was performed during the recovery phase 7 days after IRI. We found less living proximal tubules, as indicated by reduced lectin positivity in *Irf8*-deficient mice (**Figure 5B**) and no difference in living distal tubules, as indicated by quantification of Tamm-Horsfall protein (uromodulin, THP) positive area (**Figure 5C**). Thus, our data suggest that cDC1s probably protect against tissue damage structurally but play a mild protective role on kidney function.

Reduced Anti-Inflammatory Tregs as well as Pro-Inflammatory CD8$^+$ T in Post-Ischemic *Irf8*-Deficient Mice

Kidney DCs are known for their migratory ability to activate T cells in the kidney draining lymph node *via* chemokine receptors and co-stimulatory molecules (3). In kidneys from *Irf8*-deficient mice, while the mRNA expression level of *Ccl-20* did not change on day 1 after IRI (**Figure 6B**), we observed decreased mRNA expression levels of *Ccr7*, *Ccr9*, *Cd40*, *Cd80*, and *Cd86* as compared to control mice after IRI (**Figures 6A–C**). We also found that the number of kidney CD3$^+$ T cells increased with time upon AKI in sections from control mice, while *Irf8*-deficient mice had significantly less CD3$^+$ T cells after IRI on day 7 as compared to control mice (**Figures 6D, E**). However, no difference of CD3$^+$ T cells was observed in spleen between the two groups of mice (data not shown). This suggests an impaired T cell-related adaptive immune response in *Irf8*-deficient mice upon post-ischemic AKI/AKD.

Among T cells, aortic cDC1s preferably activate the accumulation of pro-atherogenic CD4$^+$ T and CD8$^+$ T cells *via* the application of *Irf8*-deficient mice (43). In adriamycin nephropathy, CD103$^+$ cDC1s elicit CD8$^+$ T cells aggravate tissue injury, which imply that CD8$^+$ T cells were pathogenic (46). To address this in AKI/AKD, our flow cytometric analysis showed that the number of kidney CD4$^-$CD8$^+$ T cells was selectively reduced in *Irf8*-deficient mice overtime after IRI (**Figures 6F, H**), without differences in the numbers of infiltrating kidney CD4$^-$CD8$^-$, CD4$^+$CD8$^+$, and CD4$^+$CD8$^-$ T cells after IRI. Similar results were obtained with splenic CD4$^-$CD8$^+$ T cells (**Figures S4A, C**), suggesting that cDC1s

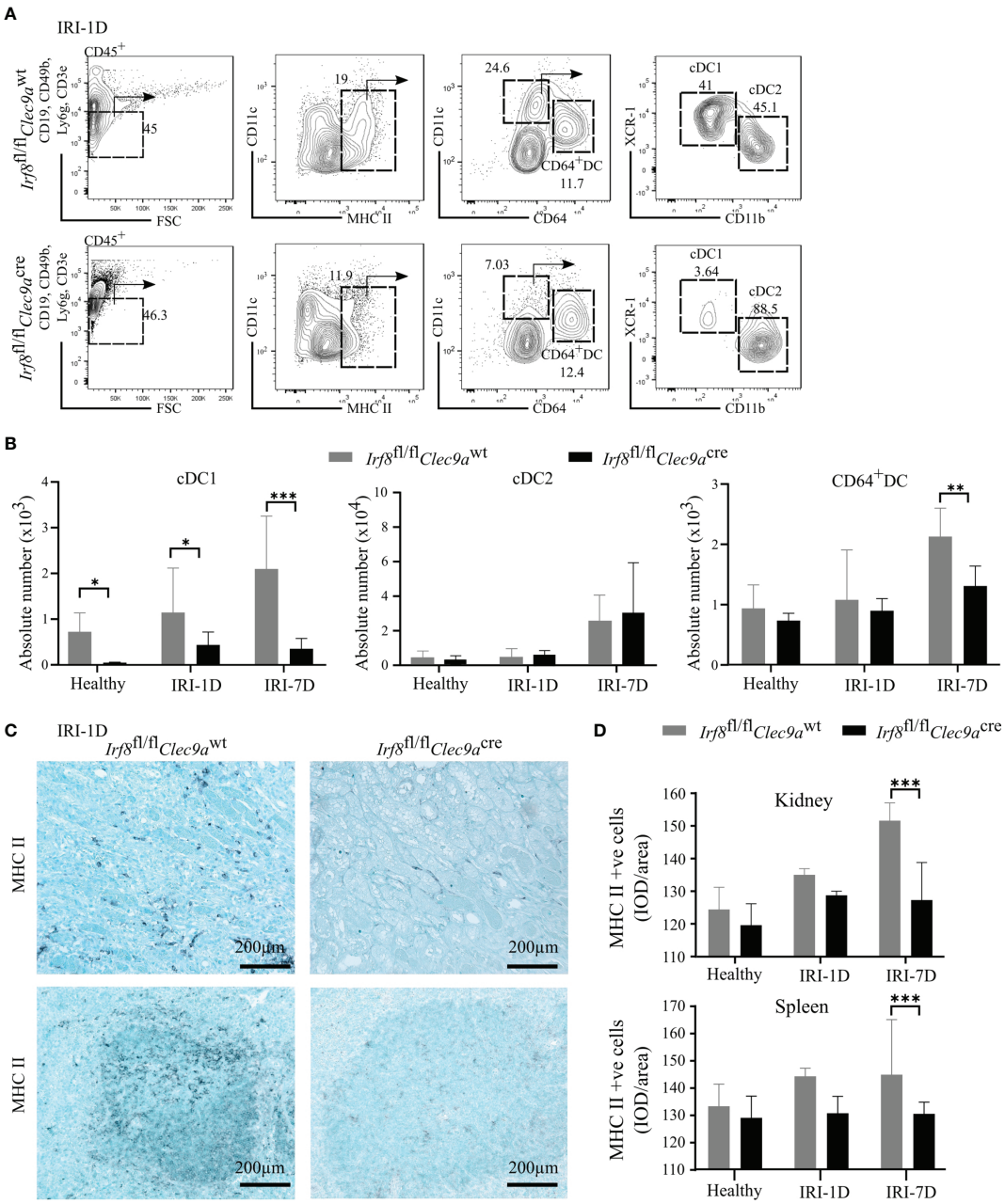

FIGURE 3 | Impaired accumulation of type I conventional dendritic cells (cDC1s) in *Irf8*-deficient mice after IRI. IRI was induced in *Irf8*-deficient mice (*Irf8*$^{fl/fl}$*Clec9a*^{cre} mice) and control mice (*Irf8*$^{fl/fl}$*Clec9a*^{wt} mice). **(A)** Representative gating strategy of kidney DC subsets on day 1 after IRI (IRI-1D) (gated on live CD45$^+$CD19$^-$CD49b$^-$CD3e$^-$Ly6g$^-$MHCII$^+$ cells). cDCs (such as cDC1s and cDC2s) and CD64$^+$ DCs were identified according to specific markers (CD11c, CD64, XCR-1, and CD11b). **(B)** Absolute cell numbers of cDC1, cDC2, and CD64$^+$ DCs per kidney in healthy mice and mice after IRI. **(C)** Representative images of MHCII positive cells distributing in kidney sections (upper row) and splenic sections (bottom row) on IRI-1D. Bars = 200 μm. **(D)** Quantitative analysis of MHCII positive cells in mice in healthy state and after IRI (n = 3–5 mice/group). Data are means ± SD. Two-way ANOVA. *P < 0.05; **P < 0.01; ***P < 0.001.

likely prime pathogenic CD8$^+$ T cells upon post-ischemic AKI/AKD.

CD103$^+$ cDC1s can foster the accumulation of intrarenal Tregs to protect against crescent glomerulonephritis and ischemic reperfusion-induced hepatic injury (18, 20). Since we demonstrated the efficient depletion of cDC1s and impaired expression levels of co-stimulatory molecules and chemokine receptors in *Irf8*-deficient mice on day 1 after IRI, Tregs were found to be present at the same timepoint. However, in *Irf8*-deficient mice, the numbers of CD4$^+$CD25$^+$ Tregs including

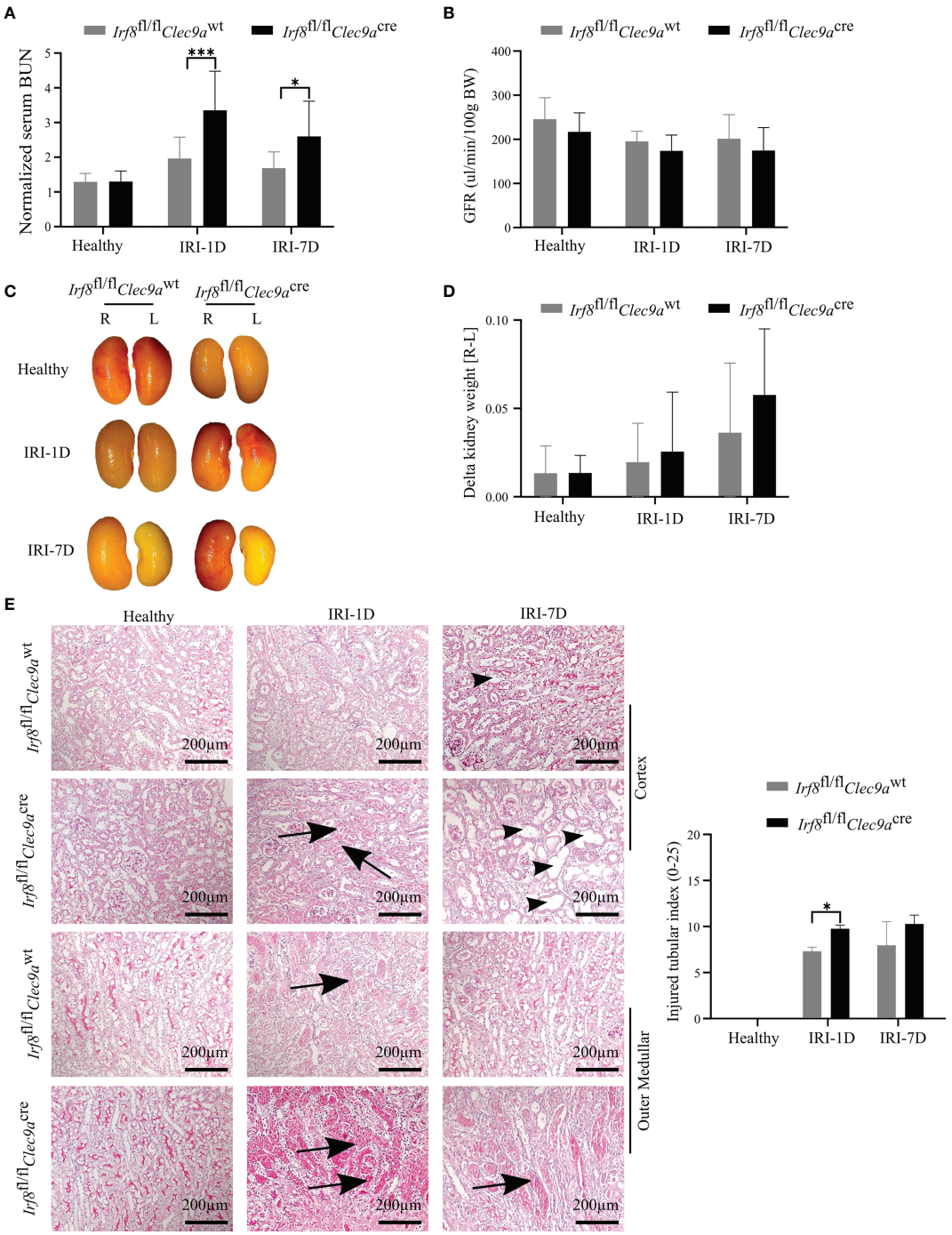

FIGURE 4 | Absence of type I conventional dendritic cells (cDC1s) aggravates kidney injury during post-ischemic AKI/AKD. IRI was applied in left kidneys from *Irf8*-deficient mice (*Irf8*$^{fl/fl}$*Clec9a*^{cre} mice) and control mice (*Irf8*$^{fl/fl}$*Clec9a*^{wt} mice). **(A)** Representative values of serum blood urea nitrogen (BUN) in mice on healthy state and after IRI and normalized to respective baseline level in healthy state (n = 3–10 mice/group). Data were repeated twice. **(B)** GFR of *Irf8*-deficient mice and control mice from healthy state, day 1, and day 7 after IRI (n = 3–14 mice/group). **(C)** Representative macroscopic images of kidney atrophy. **(D)** Weight loss of left kidney [L] compared to right sham kidney [R] as illustrated as "delta kidney weight = KW_R-KW_L" (n = 3–6 mice/group). **(E)** Representative images with periodic acid-Schiff (PAS)-stained kidney sections. Tubular injury was illustrated in cortex and outer medullar and labeled with cast formation (black arrow) and tubular dilation (black arrowhead). Semiquantitative morphometry of tubular injury was shown (n = 3–5 mice/group). Bars = 200 μm. Data are means ± SD. Two-way ANOVA test. *P < 0.05; ***P < 0.001.

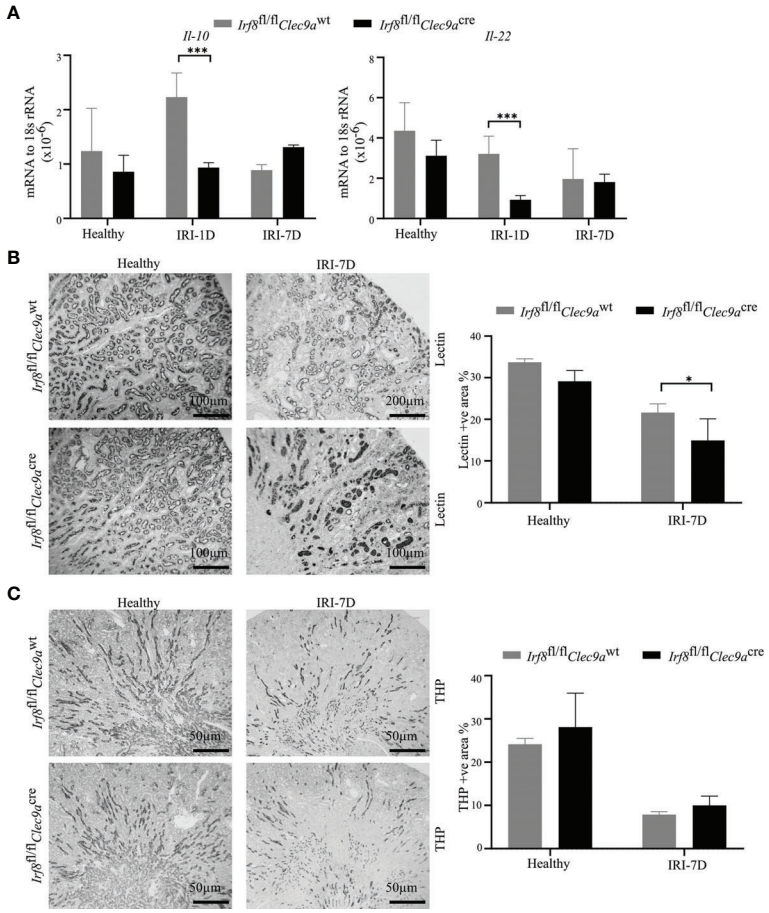

FIGURE 5 | Absence of type I conventional dendritic cells (cDC1s) delays tubular recovery after IRI. IRI was induced in *Irf8*-deficient mice (*Irf8*$^{fl/fl}$*Clec9a*^{cre} mice) and control mice (*Irf8*$^{fl/fl}$*Clec9a*^{wt} mice). **(A)** Intrarenal mRNA expression of the regeneration genes interleukin-10 (*Il-10*) and *Il-22* in mice in healthy state and after IRI (n = 3–6 mice/group). Representative pictures of **(B)** *Lotus tetragonolobus lectin* (Lectin)-stained kidney sections for proximal tubule (Bars = 100 μm) and **(C)** Tamm-Horsfall protein (THP)-stained kidney sections for distal tubule (Bars = 50 μm) in healthy mice and 7 days after IRI. Quantitative assessment of living tubule per kidney (n = 3–5 mice/group). Data are means ± SD. Two-way ANOVA test. *P < 0.05; ***P < 0.001.

Foxp3$^+$ Tregs and IL-10$^+$ Tregs were reduced in kidney and spleen (**Figures 6G, I** and **S4B, D**). Together, cDC1s are required for maintaining anti-inflammatory Tregs upon post-ischemic AKI/AKD.

Enhanced Pro-Inflammatory T_{H1}-Related Response in Post-Ischemic *Irf8*-Deficient Mice

T_{H1} cells are classically associated with IFN-γ secretion. Their differentiation and activity are promoted by IL-12, IL-18, and IFN-γ. IFN-γ is a cytokine, which can impair cell proliferation or activate inflammatory cell death pathways. In the kidney from *Irf8*-deficient mice, we also observed increased mRNA expression levels of T_{H1}-related cytokines, including *Il-12p35*, *Il-12p40*, *Il-18*, and *Ifn-γ* after IRI on day 1 (**Figure 6J**). In summary, this indicates that cDC1s probably antagonize the pro-inflammatory T_{H1} immune response to reduce kidney injury upon post-ischemic AKI/AKD.

Increased Neutrophils and Necroinflammation in Post-Ischemic *Irf8*-Deficient Mice

Ischemic tubular necrosis involves neutrophil-related necroinflammation (2). To investigate whether the deficiency of cDC1s affects neutrophil infiltration, we performed immunohistochemistry staining of kidney sections and found a significant increased number of Ly6B.2$^+$ neutrophils after IRI on day 1 in *Irf8*-deficient mice as compared to control mice (**Figures 7A, B**). This was in line with the flow cytometric analysis, which showed an increased cell number of Ly6g$^+$ neutrophils in *Irf8*-deficient mice after IRI on day 1 (**Figures 7C, D**). In addition, we observed increased mRNA expression levels of neutrophil-related chemokines (*Cxcl1*, *Cxcl8*) and pro-inflammatory cytokines (*Tnf-α*, *Il-6*, *Tgf-β*, *pro-Il-1β*) as well as cell death-related genes (*Caspase8*, *Mlkl*, *Ripk1*, *Ripk3*) in *Irf8*-deficient mice (**Figures 7E–I**). Thus, the absence of cDC1s enhances the recruitment of neutrophils and inflammatory cell death in IRI-induced AKI/AKD.

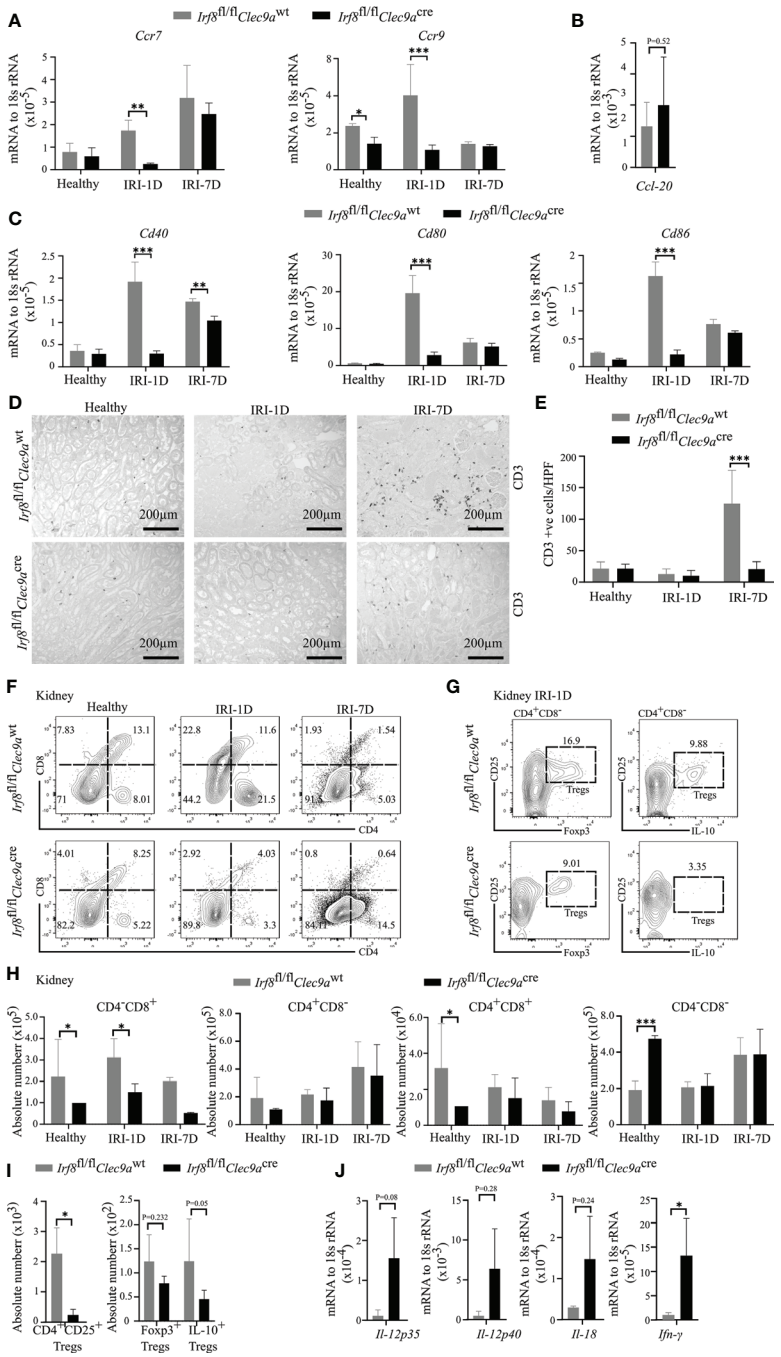

FIGURE 6 | Altered T cell-related adaptive response in kidney from *Irf8*-deficient mice after IRI. IRI was induced in *Irf8*-deficient mice (*Irf8*$^{fl/fl}$*Clec9a*^{cre} mice) and control mice (*Irf8*$^{fl/fl}$*Clec9a*^{wt} mice). **(A)** mRNA expression of chemokine receptors *C-C chemokine receptor type 7* (*Ccr7*) and *Ccr9* in kidney tissues from mice in healthy state and after IRI normalized to 18s rRNA. **(B)** mRNA expression of CC-chemokine ligand-20 (*Ccl-20*) in kidney tissues on day 1 after IRI (IRI-1D) and normalized to 18s rRNA. **(C)** mRNA expression of co-stimulatory molecules *Cd40*, *Cd80*, and *Cd86* in kidney tissues from mice in healthy state and after IRI and normalized to 18s rRNA. **(A–C)** n = 3–5 mice/group. **(D)** Representative CD3$^+$ T cell immunostaining from paraffin-embedded kidneys in mice on healthy state, IRI-1D, and IRI-7D. Bars = 200 μm. **(E)** Number of kidney CD3$^+$ T cells manually counted per HPF (n = 3–5 mice/group). **(F)** Gating strategy of kidney T cells (gated on live CD45$^+$CD19$^-$CD49b$^-$Ly6g$^-$CD3$^+$ cells) and their subsets according to CD4/CD8 expression on healthy state, IRI-1D, and IRI-7D. **(G)** Gating strategy of kidney Tregs (gated on live CD45$^+$CD19$^-$CD49b$^-$Ly6g$^-$CD3$^+$CD4$^+$CD8$^-$CD25$^+$ cells) on IRI-1D. **(H)** Absolute cell number of kidney T cell subsets (n = 3–8 mice/group). **(I)** Absolute cell numbers of kidney CD4$^+$CD25$^+$ Tregs, Foxp3$^+$ Tregs, and Interlukin-10 (IL-10)$^+$ Tregs on IRI-1D (n = 3–4 mice/group). **(J)** Gene expression of T_{H1} related cytokines on IRI-1D and normalized to 18s rRNA. See full term for each gene abbreviation in **Table S3**. n = 3–5 mice/group. Data are means ± SD. *t-test* or two-way ANOVA. *$P < 0.05$; ***$P < 0.001$.

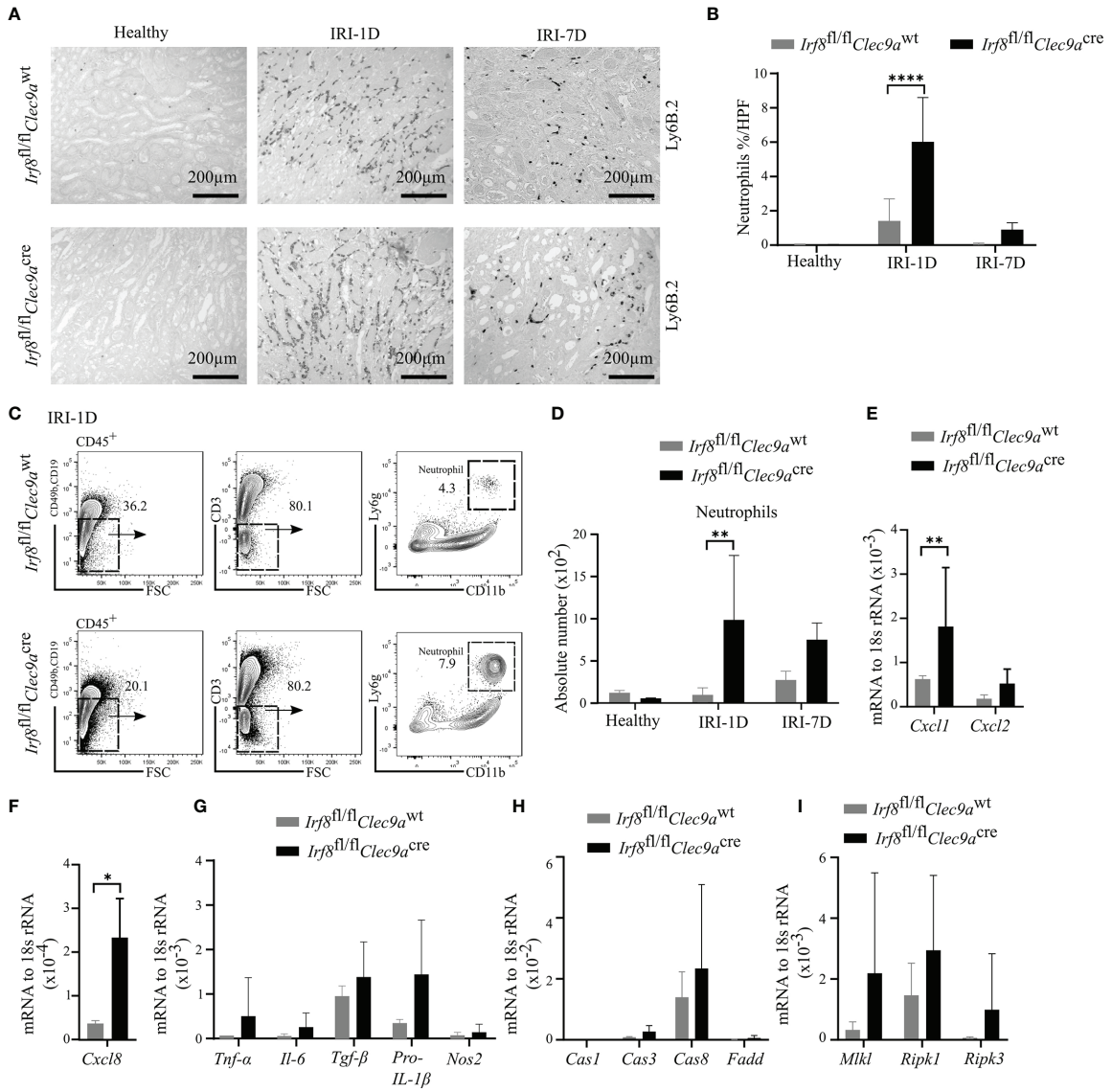

FIGURE 7 | Enhanced neutrophil-related necroinflammation in *Irf8*-deficient mice after IRI. IRI was induced in *Irf8*-deficient mice (*Irf8*$^{fl/fl}$*Clec9a*^{cre} mice) and control mice (*Irf8*$^{fl/fl}$*Clec9a*^{wt} mice). **(A)** Representative images of Ly6B.2$^+$ neutrophils in kidney sections from healthy mice and mice after IRI. Bars = 200 μm. **(B)** Quantification of Ly6B.2-stained neutrophils in kidney sections (n = 3–10 mice/group). **(C)** Gating strategy of kidney Ly6g$^+$ neutrophils (gated on live CD45$^+$CD19$^-$CD49b$^-$CD3$^-$ cells) on IRI-1D by flow cytometry. **(D)** Absolute cell numbers of Ly6g$^+$ neutrophils per kidney (n = 3–4 mice/group). **(E, F)** Normalized mRNA expression of neutrophil recruitment related, **(G)** proinflammatory, and **(H, I)** cell death-related cytokines/chemokines by qRT-PCR on IRI-1D (see full term for each gene abbreviation in **Table S3**, n = 3–6 mice/group). **(E–I)** Representative data repeated three times. Cas1, Caspase1; Cas3, Caspase3; Cas8, Caspase8. Data are means ± SD. *t-test* or two-way ANOVA test. *P < 0.05; **P < 0.01; ****P < 0.0001.

DISCUSSION

We hypothesized that kidney cDC1s accumulate in post-ischemic kidneys upon AKI/AKD and that deletion of kidney cDC1s promotes a pro-inflammatory immune response and consequently drives AKI/AKD progression, all confirmed by using *Irf8*-deficient mice in our *in vivo* studies. Thus, IRF8 is an important transcription factor for differentiation and survival of kidney cDC1s, in which cDC1s and the cDC1-related immune response probably antagonize tissue injury and contribute to the recovery after post-ischemic AKI/AKD.

Previous experiments on kidney mononuclear phagocytes are confounded by the lack of specific surface markers as well as gene- and cell-specific transgenic mice to clarify the overlapping functions of cDCs with monocytes/macrophages (20, 32). So far, the surface markers CD11b and CD11c in conjunction with other markers discriminate five mononuclear phagocytes in healthy kidney (34, 47–49), of which the CD11b^{low}CD11c^{high}

(R1) subset matches cDC1s (34). cDC1s require the transcription factor IRF8 for their development. Thus, targeting IRF8 in DCs represents a valid strategy to clarify the role of cDC1s in homeostasis and disease. For example, deletion of *Irf8* in $CD11c^+$ cells leads to a marked reduction of aortic $CD11b^-$ $CD103^+$ DCs (cDC1s) without affecting $CD11b^+CD103^-$DCs (cDC2s) or macrophages. But CD11c is not exclusively restricted to DCs so that mouse line also affects IRF8 expression in other immune cells (29, 43, 44). In particular, monocytes require IRF8 for their transition from common monocyte progenitors (cMoP) to monocytes in the bone marrow and pDCs rely on IRF8 for cell function (44). cDCs arise from CDP, which are known to specifically express *Clec9a*. Therefore, combining *Clec9a*Cre with IRF8 floxed mice provides an improved strategy to target IRF8 in cDCs, although some pDCs are also targeted (25, 26, 32). Importantly though, *Clec9a*Cre remains restricted to DCs and is not induced on monocytes or other leukocytes in the kidney on day 3 of IRI (25). Mice lacking *Irf8* in *Clec9a*-expressing progenitors showed reduced cDC1s in steady state kidney and after IRI, indicating that IRF8 is necessary for the development of cDC1s both at steady state and upon inflammation. This is consistent with highest expression of this transcription factor in cDC1s compared to other renal DCs and macrophages (25 and **Figure 3B**). Of note, we observed a reduction of $CD64^+$ DCs in *Irf8*-deficient on day 7 after IRI. It is possible that this reduction is secondary to the lack of cDC1s in this mouse model, however, since Clec9a also targets this subset, we cannot exclude a function of IRF8 in maintaining $CD64^+$ DCs in IRI at this point. The use of additional mouse models, that specifically target cDC1s, such as XCR-1-diptheria toxin receptor, *Xcr1*-Cre, Langerin-Cre, or *Karma*-Cre mice may help resolve this question in future studies. Thus, we cannot exclude a contribution of *Irf8*-dependent $CD64^+$ DCs on the observed effects in this context.

DCs are known for their functional contribution on T cells during AKI/AKD. For example, during kidney injury, cDCs release PAMP/DAMP-associated mediators that selectively determine the differentiation of T cells and the recruitment of these cells to the site of injury (3, 46). Our data now imply that a loss of cDC1s was associated with a lower number of T cells, including $CD8^+$ T and Tregs in kidney and spleen, as well as a decrease in the expression of chemokine receptors and co-stimulatory molecules. This is in line with previous reports showing that a loss of chemokine receptors and co-stimulatory molecules ultimately impairs the migration of DCs to the kidney lymph nodes and reduces the antigen presentation capacity of DCs to T cells, e.g., $CD8^+$ T and partially $CD4^+$ T cells (3, 42, 50).

The protective function of cDC1s is mostly demonstrated *via* sustaining Tregs. For examples, cDC1s can drive the recruitment of IL-10-expressing $CD25^+Foxp3^+$ Tregs in nephrotoxic AKD (17), liver IRI (18), crescent glomerulonephritis (20), as well as atherosclerosis (43). The cytokine IL-22 is a member of the IL-10 family and can directly stimulate TEC regeneration following kidney injury (5, 50, 51). Consistent with previous reports, our study shows that lack of cDC1s decreased the number of $Foxp3^+$ Tregs and IL-10^+ Tregs as well as the mRNA expression of *Il-10* and *Il-22* after AKI/AKD. For their recruitment, Tregs require the chemokine receptor CCR6 and the production of CCL-20, a known CCR6 ligand (52–54). However, we did not find changes in the gene expression of *Ccl-20* in *Irf8*-deficient mice after post-ischemic AKI/AKD. Adversely, *Irf8*-deficient mice had a profound T_{H1} immune response, which promoted the conversion of naïve T into T_{H1} cells (55). Activated T_{H1} cells can also secrete CXCL8 to recruit neutrophils or IFN-γ to induce necroinflammation (55). This enhanced pro-inflammatory T_{H1} immune response was probably due to the missing immunosuppressive response of Tregs in mice (45). cDC1s excel at cross-presentation of antigens to cytotoxic $CD8^+$ T cells and promote a pro-inflammatory response in lung and skin virus studies (56, 57) or adriamycin nephropathy (46). Our results showed that a reduced accumulation of kidney $CD8^+$ T cells may counterbalance the interaction with protective Tregs. However, further studies are needed to address the contribution of cDC1s on Tregs and $CD8^+$ T cell function.

cDCs can restrain innate immune responses (58–61). For example, DNGR-1 (encoded by gene *Clec9a*) deficiency increases neutrophilia and CXCL2 production, and consequently aggravates caerulein-induced sterile necrotizing pancreatitis during the acute phase (60). Consistently, depletion of kidney cDC1s displayed enhanced neutrophil recruitment, pro-inflammatory cytokine release, and moderate cell death, implying a role for cDC1s to regulate neutrophil-related inflammatory responses in post-ischemic AKI/AKD.

One should mention that similar to that observed in macrophage biology (61, 62), the microenvironment determines the phenotype of cDCs and the outcomes in AKI/AKD. For example, during different phases of nephrotoxic or post-ischemic AKI, $MHCII^{high}F4/80^{high}$ cells differentiate into $MHCII^{neg}F4/80^{high}$ cells, in which both may originate from DC precursor but are transcriptionally comparable to anti-inflammatory macrophages (25, 63). In post-ischemic AKI/AKD, cDC1s could contribute to an anti-inflammatory response, whereas monocyte-derived DCs differentiate into inflammatory cDC2s during infection (29). As we show herein, cDC1s comprise a small cell subset as compared to other DCs. It is possible that these cell subsets collaboratively contribute to the observed outcomes after AKI/AKD. Thus, further studies are needed to dissect the functional role of other cDC subsets and to characterize the crosstalk between cDC1s and other DC subpopulations in AKI/AKD. Meanwhile, different local microenvironment also determines the function of cDC1s. In lung and skin virus studies or adriamycin nephropathy, cDC1s dominated the MHC class I-restricted cross-presentation of both viral and self-antigens (35, 36, 46, 56, 57). In sterile kidney diseases including crescent nephritis, cDC1s most likely regulate Tregs to induce anti-inflammatory response (17, 18, 20, 21). We showed that the cDC1s-related immune response has protective effects on the outcomes after AKI/AKD. Further studies are needed to investigate the direct mechanism between cDC1s and related immune responses *in vivo*, e.g., by applying interventional studies.

In conclusion, we found that kidney cDC1s protect against post-ischemic AKI/AKD, because 1) cDC1s prime protective

Tregs; 2) cDC1s enhance the expression of reparative cytokines such as IL-10 and IL-22; 3) cDC1s can antagonize the pro-inflammatory T_{H1} immune response, recruitment of neutrophils, and necroinflammation, thus leading to less kidney injury; and 4) kidney cDC1s recruit cytotoxic $CD8^+$ T cells, an effect that might be counterbalanced by other anti-inflammatory cells. These findings would help to identify a functional role for intrarenal cDC1s upon AKI/AKD onset. Boosting the accumulation of cDC1s may not only potentially improve the long-term outcomes in AKI/AKD but also in other inflammatory conditions.

DATA AVAILABILITY STATEMENT

The original contributions presented in the study are included in the article/**Supplementary Material**. Further inquiries can be directed to the corresponding authors.

ETHICS STATEMENT

The animal study was reviewed and approved by Local government authorities Regierung von Oberbayern (Az 55.2-1-54-2532-175-2014).

AUTHOR CONTRIBUTIONS

JL, H-JA, and ZZ designed the study and experiments. NL conducted experiments, acquired and analyzed data. SS gave suggestions for experiments design and assisted with flow cytometry. ZZ and LF provided histology samples and related data analysis. NS and BS provided *Irf8*$^{fl/fl}$*Clec9a*^{cre} mice and helped with experimental design. CL and CS performed microscopy of mouse tissue sections and related data analysis. NL, H-JA, SS, and JL wrote the manuscript. All authors contributed to the article and approved the submitted version.

FUNDING

This study is supported by the Deutsche Forschungsgemeinschaft (DFG) (AN372/14-3 and AN372/24-1 to H-JA, STE2437/2-1 and STE2437/2-2 to SS, the International Program Fund for doctoral students, Sun Yat-sen University, and China Scholarship Council (CSC) 201906380147 to NL, CSC 201603250047 to CS and CSC 202008080076 to CL. Work in the Schraml lab is funded by the DFG [Emmy Noether grant: Schr 1444/1-1 and Project-ID 360372040 – SFB 1335 (project 8)] and the European Research Council (ERC-2016-STG-715182).

ACKNOWLEDGMENTS

The authors acknowledge Jana Mandelbaum and Anna Anfimiadou for technical assistance with histology.

SUPPLEMENTARY MATERIAL

The Supplementary Material for this article can be found online at: https://www.frontiersin.org/articles/10.3389/fimmu.2021.685559/full#supplementary-material

REFERENCES

1. Zhao H, Alam A, Soo AP, George AJT, Ma D. Ischemia-Reperfusion Injury Reduces Long Term Renal Graft Survival: Mechanism and Beyond. *EBioMedicine* (2018) 28:31–42. doi: 10.1016/j.ebiom.2018.01.025
2. Mulay SR, Linkermann A, Anders HJ. Necroinflammation in Kidney Disease. *J Am Soc Nephrol* (2016) 27(1):27–39. doi: 10.1681/ASN.2015040405
3. Kurts C, Ginhoux F, Panzer U. Kidney Dendritic Cells: Fundamental Biology and Functional Roles in Health and Disease. *Nat Rev Nephrol* (2020) 16 (7):391–407. doi: 10.1038/s41581-020-0272-y
4. Nakazawa D, Kumar SV, Marschner J, Desai J, Holderied A, Rath L, et al. Histones and Neutrophil Extracellular Traps Enhance Tubular Necrosis and Remote Organ Injury in Ischemic AKI. *J Am Soc Nephrol* (2017) 28(6):1753–68. doi: 10.1681/ASN.2016080925
5. Kulkarni OP, Hartter I, Mulay SR, Hagemann J, Darisipudi MN, Kumar Vr S, et al. Toll-Like Receptor 4-Induced IL-22 Accelerates Kidney Regeneration. *J Am Soc Nephrol* (2014) 25(5):978–89. doi: 10.1681/ASN.2013050528
6. Lassen S, Lech M, Römmele C, Mittruecker H-W, Mak TW, Anders H-J. Ischemia Reperfusion Induces IFN Regulatory Factor 4 in Renal Dendritic Cells, Which Suppresses Postischemic Inflammation and Prevents Acute Renal Failure. *J Immunol* (2010) 185(3):1976–83. doi: 10.4049/jimmunol.0904207
7. Lech M, Avila-Ferrufino A, Allam R, Segerer S, Khandoga A, Krombach F, et al. Resident Dendritic Cells Prevent Postischemic Acute Renal Failure by Help of Single Ig IL-1 Receptor-Related Protein. *J Immunol* (2009) 183 (6):4109–18. doi: 10.4049/jimmunol.0900118
8. Lech M, Gröbmayr R, Weidenbusch M, Anders HJ. Tissues Use Resident Dendritic Cells and Macrophages to Maintain Homeostasis and to Regain Homeostasis Upon Tissue Injury: The Immunoregulatory Role of Changing Tissue Environments. *Mediators Inflamm* (2012) 2012:951390. doi: 10.1155/2012/951390
9. Dong X, Swaminathan S, Bachman LA, Croatt AJ, Nath KA, Griffin MD. Resident Dendritic Cells are the Predominant TNF-Secreting Cell in Early Renal Ischemia-Reperfusion Injury. *Kidney Int* (2007) 71(7):619–28. doi: 10.1038/sj.ki.5002132
10. Rogers NM, Matthews TJ, Kausman JY, Kitching RA, Coates PTH. Review Article: Kidney Dendritic Cells: Their Role in Homeostasis, Inflammation and Transplantation. *Nephrology* (2009) 14(7):625–35. doi: 10.1111/j.1440-1797.2009.01200
11. Dong X, Swaminathan S, Bachman LA, Croatt AJ, Nath KA, Griffin MD. Antigen Presentation by Dendritic Cells in Renal Lymph Nodes Is Linked to Systemic and Local Injury to the Kidney. *Kidney Int* (2005) 68(3):1096–108. doi: 10.1111/j.1523-1755.2005.00502
12. Edgtton KL, Kausman JY, Li M, O'Sullivan K, Lo C, Hutchinson P, et al. Intrarenal Antigens Activate CD4+ Cells *Via* Co-Stimulatory Signals From Dendritic Cells. *J Am Soc Nephrol* (2008) 19(3):515–26. doi: 10.1681/ASN.2007030386
13. Riedel JH, Paust HJ, Turner JE, Tittel AP, Krebs C, Disteldorf E, et al. Immature Renal Dendritic Cells Recruit Regulatory CXCR6+ Invariant Natural Killer T Cells to Attenuate Crescentic GN. *J Am Soc Nephrol* (2012) 23(12):1987–2000. doi: 10.1681/ASN.2012040394
14. Breda PC, Wiech T, Meyer-Schwesinger C, Grahammer F, Huber T, Panzer U, et al. Renal Proximal Tubular Epithelial Cells Exert Immunomodulatory

Function by Driving Inflammatory CD4+ T Cell Responses. *Am J Physiol Renal Physiol* (2019) 317(1):F77–89. doi: 10.1152/ajprenal.00427.2018
15. Tadagavadi RK, Gao G, Wang WW, Gonzalez MR, Reeves WB. Dendritic Cell Protection From Cisplatin Nephrotoxicity Is Independent of Neutrophils. *Toxins* (2015) 7(8):3245–56. doi: 10.3390/toxins7083245
16. Kim MG, Su Boo C, Sook Ko Y, Young Lee H, Yong Cho W, Kyu Kim H, et al. Depletion of Kidney CD11c+ F4/80+ Cells Impairs the Recovery Process in Ischaemia/Reperfusion-Induced Acute Kidney Injury. *Nephrol Dialysis Transplant* (2010) 25(9):2908–21. doi: 10.1093/ndt/gfq183
17. Tadagavadi RK, Reeves WB. Endogenous IL-10 Attenuates Cisplatin Nephrotoxicity: Role of Dendritic Cells. *J Immunol* (2010) 185(8):4904–11. doi: 10.4049/jimmunol.1000383
18. Sfevdf PT, Jtdifnjb M, Bamboat ZM, Ocuin LM, Balachandran VP, Obaid H, et al. Conventional DCs Reduce Liver Ischemia/ Reperfusion Injury in Mice Via IL-10 Secretion. *Conflict* (2010) 120(2):559–69. doi: 10.1172/JCI40008DS1
19. Li L, Huang L, Ye H, Song SP, Bajwa A, Lee SJ, et al. Dendritic Cells Tolerized With Adenosine A2AR Agonist Attenuate Acute Kidney Injury. *J Clin Invest* (2012) 122(11):3931–42. doi: 10.1172/JCI63170
20. Evers BDG, Engel DR, Böhner AMC, Tittel AP, Krause TA, Heuser C, et al. CD103+ Kidney Dendritic Cells Protect Against Crescentic GN by Maintaining IL-10-producing Regulatory T Cells. *J Am Soc Nephrol* (2016) 27(11):3368–82. doi: 10.1681/ASN.2015080873
21. Zhou CZ, Wang RF, Cheng DL, Zhu YJ, Cao Q, Lv WF. FLT3/FLT3L-Mediated CD103+ Dendritic Cells Alleviates Hepatic Ischemia-Reperfusion Injury in Mice *Via* Activation of Treg Cells. *Biomed Pharmacother* (2019) 118:109031. doi: 10.1016/j.biopha.2019.109031
22. Gandolfo MT, Jang HR, Bagnasco SM, Ko GJ, Agreda P, Satpute SR, et al. Foxp3+ Regulatory T Cells Participate in Repair of Ischemic Acute Kidney Injury. *Kidney Int* (2009) 76(7):717–29. doi: 10.1038/ki.2009.259
23. Weisheit CK, Engel DR, Kurts C. Dendritic Cells and Macrophages: Sentinels in the Kidney. *Clin J Am Soc Nephrol* (2015) 10(10):1841–51. doi: 10.2215/CJN.07100714
24. Okusa MD, Li L. Dendritic Cells in Acute Kidney Injury: Cues From the Microenvironment. *Trans Am Clin Climatol Assoc* (2012) 123:54–63.
25. Salei N, Rambichler S, Salvermoser J, Papaioannou NE, Schuchert R, Pakalniškyte D, et al. The Kidney Contains Ontogenetically Distinct Dendritic Cell and Macrophage Subtypes Throughout Development That Differ in Their Inflammatory Properties. *J Am Soc Nephrol* (2020) 31(2):257–78. doi: 10.1681/ASN.2019040419
26. Ginhoux F, Liu K, Helft J, Bogunovic M, Greter M, Hashimoto D, et al. The Origin and Development of Nonlymphoid Tissue CD103+ DCs. *J Exp Med* (2009) 206(13):3115–30. doi: 10.1084/jem.20091756
27. Shin JY, Wang CY, Lin CC, Chu CL. A Recently Described Type 2 Conventional Dendritic Cell (cDC2) Subset Mediates Inflammation. *Cell Mol Immunol* (2020) 17(12):1215–1217. doi: 10.1038/s41423-020-0511-y
28. Brown CC, Gudjonson H, Pritykin Y, Deep D, Lavallée VP, Mendoza A, et al. Transcriptional Basis of Mouse and Human Dendritic Cell Heterogeneity. *Cell* (2019) 179(4):846–63.e24. doi: 10.1016/j.cell.2019.09.035
29. Bosteels C, Neyt K, Vanheerswynghels M, van Helden MJ, Sichien D, Debeuf N, et al. Inflammatory Type 2 cDCs Acquire Features of cDC1s and Macrophages to Orchestrate Immunity to Respiratory Virus Infection. *Immunity* (2020) 52(6):1039–1056.e9. doi: 10.1016/j.immuni.2020.04.005
30. Sedin J, Giraud A, Steiner SE, Ahl D, Persson AEG, Melican K, et al. High Resolution Intravital Imaging of the Renal Immune Response to Injury and Infection in Mice. *Front Immunol* (2019) 10:2744(November). doi: 10.3389/fimmu.2019.02744
31. Schraml BU, Reis e Sousa C. Defining Dendritic Cells. *Curr Opin Immunol* (2015) 32:13–20. doi: 10.1016/j.coi.2014.11.001
32. Salvermoser J, van Blijswijk J, Papaioannou NE, Rambichler S, Pasztoi M, Pakalniškyte D, et al. Clec9a-Mediated Ablation of Conventional Dendritic Cells Suggests a Lymphoid Path to Generating Dendritic Cells In Vivo. *Front Immunol* (2018) 9:699. doi: 10.3389/fimmu.2018.00699
33. Günthner R, Anders HJ. PMID: 24379524: Interferon-Regulatory Factors Determine Macrophage Phenotype Polarization. *Mediators Inflamm* (2013) 2013:731023. doi: 10.1155/2013/731023
34. Kawakami T, Lichtnekert J, Thompson LJ, Karna P, Bouabe H, Hohl TM, et al. Resident Renal Mononuclear Phagocytes Comprise Five Discrete Populations With Distinct Phenotypes and Functions. *J Immunol* (2013) 191(6):3358–72. doi: 10.4049/jimmunol.1300342
35. Yamazaki S, Dudziak D, Heidkamp GF, Fiorese C, Bonito AJ, Inaba K, et al. CD8+ CD205+ Splenic Dendritic Cells Are Specialized to Induce Foxp3+ Regulatory T Cells. *J Immunol* (2008) 181(10):6923–33. doi: 10.4049/jimmunol.181.10.6923
36. Heath WR, Carbone FR. Dendritic Cell Subsets in Primary and Secondary T Cell Responses at Body Surfaces. *Nat Immunol* (2009) 10(12):1237–44. doi: 10.1038/ni.1822
37. Ferris ST, Durai V, Wu R, Theisen DJ, Ward JP, Bern MD, et al. cDC1 Prime and are Licensed by CD4+ T Cells to Induce Anti-Tumour Immunity. *Nature* (2020) 584(7822):624–9. doi: 10.1038/s41586-020-2611-3
38. Kilkenny C, Browne WJ, Cuthill IC, Emerson M, Altman DG. Improving Bioscience Research Reporting: The Arrive Guidelines for Reporting Animal Research. *PloS Biol* (2010) 8(6):6–10. doi: 10.1371/journal.pbio.1000412
39. Marschner JA, Schäfer H, Holderied A, Anders H-J. Optimizing Mouse Surgery With Online Rectal Temperature Monitoring and Preoperative Heat Supply. Effects on Post-Ischemic Acute Kidney Injury. *PloS One* (2016) 11(2):e0149489. doi: 10.1371/journal.pone.0149489
40. Shi C, Kim T, Steiger S, Mulay SR, Klinkhammer BM, Bäuerle T, et al. Crystal Clots as Therapeutic Target in Cholesterol Crystal Embolism. *Circ Res* (2020) 126(8):e37–52. doi: 10.1161/circresaha.119.315625
41. Krüger T, Benke D, Eitner F, Lang A, Wirtz M, Hamilton-Williams EE, et al. Identification and Functional Characterization of Dendritic Cells in the Healthy Murine Kidney and in Experimental Glomerulonephritis. *J Am Soc Nephrol* (2004) 15(3):613–21. doi: 10.1097/01.ASN.0000114553.36258.91
42. Li N, He Y, Yang G, Yu Q, Li M. Role of TRPC1 Channels in Pressure-Mediated Activation of Airway Remodeling. *Respir Res* (2019) 20(1):91. doi: 10.1186/s12931-019-1050-x
43. Clément M, Haddad Y, Raffort J, Lareyre F, Newland SA, Master L, et al. Deletion of IRF8 (Interferon Regulatory Factor 8)-Dependent Dendritic Cells Abrogates Proatherogenic Adaptive Immunity. *Circ Res* (2018) 122(6):813–20. doi: 10.1161/CIRCRESAHA.118.312713
44. Sichien D, Scott CL, Martens L, Vanderkerken M, Van Gassen S, Plantinga M, et al. IRF8 Transcription Factor Controls Survival and Function of Terminally Differentiated Conventional and Plasmacytoid Dendritic Cells, Respectively. *Immunity* (2016) 45(3):626–40. doi: 10.1016/j.immuni.2016.08.013
45. Paust HJ, Ostmann A, Erhardt A, Turner JE, Velden J, Mittrücker HW, et al. Regulatory T Cells Control the Th1 Immune Response in Murine Crescentic Glomerulonephritis. *Kidney Int* (2011) 80(2):154–64. doi: 10.1038/ki.2011.108
46. Cao Q, Lu J, Li Q, Wang C, Wang XM, Lee VWS, et al. CD103+ Dendritic Cells Elicit CD8+ T Cell Responses to Accelerate Kidney Injury in Adriamycin Nephropathy. *J Am Soc Nephrol* (2016) 27(5):1344–60. doi: 10.1681/ASN.2015030229
47. George JF, Lever JM, Agarwal A. Mononuclear Phagocyte Subpopulations in the Mouse Kidney. *Am J Physiol Renal Physiol* (2017) 312(4):F640–6. doi: 10.1152/ajprenal.00369.2016
48. Li L, Huang L, Sung SSJ, Vergis AL, Rosin DL, Rose CE, et al. The Chemokine Receptors CCR2 and CX3CR1 Mediate Monocyte/Macrophage Trafficking in Kidney Ischemia-Reperfusion Injury. *Kidney Int* (2008) 74(12):1526–37. doi: 10.1038/ki.2008.500
49. Cao Q, Wang Y, Wang XM, Lu J, Lee VWS, Ye Q, et al. Renal F4/80 + CD11c + Mononuclear Phagocytes Display Phenotypic and Functional Characteristics of Macrophages in Health and in Adriamycin Nephropathy. *J Am Soc Nephrol* (2015) 26(2):349–63. doi: 10.1681/ASN.2013121336
50. Weidenbusch M, Song S, Iwakura T, Shi C, Rodler S, Kobold S, et al. IL-22 Sustains Epithelial Integrity in Progressive Kidney Remodeling and Fibrosis. *Physiol Rep* (2018) 6(16):e13817. doi: 10.14814/phy2.13817
51. Weidenbusch M, Rodler S, Anders HJ. Interleukin-22 in Kidney Injury and Regeneration. *Am J Physiol Renal Physiol* (2015) 308(10):F1041–6. doi: 10.1152/ajprenal.00005.2015
52. Kurts C, Panzer U, Anders HJ, Rees AJ. The Immune System and Kidney Disease: Basic Concepts and Clinical Implications. *Nat Rev Immunol* (2013) 13(10):738–53. doi: 10.1038/nri3523
53. Villares R, Cadenas V, Lozano M, Almonacid L, Zaballos A, Martínez-A C, et al. CCR6 Regulates EAE Pathogenesis by Controlling Regulatory CD4+ T-Cell Recruitment to Target Tissues. *Eur J Immunol* (2009) 39(6):1671–81. doi: 10.1002/eji.200839123

54. Elhofy A, DePaolo RW, Lira SA, Lukacs NW, Karpus WJ. Mice Deficient for CCR6 Fail to Control Chronic Experimental Autoimmune Encephalomyelitis. *J Neuroimmunol* (2009) 213(1–2):91–9. doi: 10.1016/j.jneuroim.2009.05.011
55. Dellepiane S, Leventhal JS, Cravedi P. T Cells and Acute Kidney Injury: A Two-Way Relationship. *Front Immunol* (2020) 17(11):1546. doi: 10.3389/fimmu.2020.01546
56. del Rio M-L, Rodriguez-Barbosa J-I, Kremmer E, Förster R. CD103 – and CD103 + Bronchial Lymph Node Dendritic Cells Are Specialized in Presenting and Cross-Presenting Innocuous Antigen to CD4 + and CD8 + T Cells. *J Immunol* (2007) 178(11):6861–6. doi: 10.4049/jimmunol.178.11.6861
57. Bedoui S, Whitney PG, Waithman J, Eidsmo L, Wakim L, Caminschi I, et al. Cross-Presentation of Viral And Self Antigens by Skin-Derived CD103+ Dendritic Cells. *Nat Immunol* (2009) 10(5):488–95. doi: 10.1038/ni.1724
58. Ahrens S, Zelenay S, Sancho D, Hanč P, Kjær S, Feest C, et al. F-Actin Is An Evolutionarily Conserved Damage-Associated Molecular Pattern Recognized by DNGR-1, A Receptor for Dead Cells. *Immunity* (2012) 36(4):635–45. doi: 10.1016/j.immuni.2012.03.008
59. Zhang JG, Czabotar PE, Policheni AN, Caminschi I, San Wan S, Kitsoulis S, et al. The Dendritic Cell Receptor Clec9a Binds Damaged Cells *Via* Exposed Actin Filaments. *Immunity* (2012) 36(4):646–57. doi: 10.1016/j.immuni.2012.03.009
60. Del Fresno C, Saz-Leal P, Enamorado M, Wculek SK, Martínez-Cano S, Blanco-Menéndez N, et al. DNGR-1 in Dendritic Cells Limits Tissue Damage by Dampening Neutrophil Recruitment. *Science* (2018) 362(6412):351–6. doi: 10.1126/science.aan8423
61. Anders H-J, Wilkens L, Schraml B, Marschner J. One Concept Does Not Fit All: The Immune System in Different Forms of Acute Kidney Injury. *Nephrol Dialysis Transplant* (2020) 36(1):1–10. doi: 10.1093/ndt/gfaa056
62. Anders HJ, Ryu M. Renal Microenvironments and Macrophage Phenotypes Determine Progression or Resolution of Renal Inflammation and Fibrosis. *Kidney Int* (2011) 80(9):915–25. doi: 10.1038/ki.2011.217
63. Lever JM, Hull TD, Boddu R, Pepin ME, Black LM, Adedoyin OO, et al. Resident Macrophages Reprogram Toward a Developmental State After Acute Kidney Injury. *JCI Insight* (2019) 4(2):e125503. doi: 10.1172/jci.insight.125503

Conflict of Interest: The authors declare that the research was conducted in the absence of any commercial or financial relationships that could be construed as a potential conflict of interest.

Copyright © 2021 Li, Steiger, Fei, Li, Shi, Salei, Schraml, Zheng, Anders and Lichtnekert. This is an open-access article distributed under the terms of the Creative Commons Attribution License (CC BY). The use, distribution or reproduction in other forums is permitted, provided the original author(s) and the copyright owner(s) are credited and that the original publication in this journal is cited, in accordance with accepted academic practice. No use, distribution or reproduction is permitted which does not comply with these terms.

frontiers in Immunology

ORIGINAL RESEARCH
published: 09 August 2021
doi: 10.3389/fimmu.2021.716939

Conjunctival Goblet Cell Responses to TLR5 Engagement Promote Activation of Local Antigen-Presenting Cells

*Abiramy Logeswaran, Laura Contreras-Ruiz and Sharmila Masli**

Department of Ophthalmology, Boston University School of Medicine, Boston, MA, United States

Conjunctival epithelium forms a barrier between the ocular surface microbial flora and the ocular mucosa. In addition to secreting gel-forming mucins, goblet cells, located in the conjunctival epithelium, help maintain local immune homeostasis by secreting active TGFβ2 and promoting tolerogenic phenotype of dendritic cells in the vicinity. Although dendritic cell subsets, characteristic of mucosal tissues, are found in the conjunctiva, previous studies provided limited information about their location within the tissue. In this study, we examine immunostained conjunctiva explants to determine the location of CD11c-positive dendritic cells in the context of MUC5AC-positive goblet cells. Considering that conjunctival goblet cells are responsive to signaling induced by pathogen recognition receptors, we also assess if their responses to microbial product, flagellin, can contribute to the disruption of ocular mucosal homeostasis that promotes activation of dendritic cells and results in chronic ocular surface inflammation. We find that dendritic cells in the conjunctiva with an increased microbial colonization are located adjacent to goblet cells. While their cell bodies in the stromal layer are immediately below the epithelial layer, several extensions of dendritic cells are projected across the epithelium towards the ocular surface. Such trans-epithelial dendrites are not detectable in healthy ocular mucosa. In response to topically applied flagellin, increased proportion of CD11c-positive cells in the conjunctiva strongly express MHC class II relative to the untreated conjunctiva. This change is accompanied by reduced immunoreactivity to TGFβ-activating Thrombospondin-1 in the conjunctival epithelium. These findings are supported by *in vitro* observations in primary cultures of goblet cells that respond to the TLR5 stimulation with an increased expression of IL-6 and reduced level of active TGFβ. The observed changes in the conjunctiva after flagellin application correspond with the development of clinical signs of chronic ocular mucosal inflammation including corneal epitheliopathy. Collectively, these findings demonstrate the ability of ocular mucosal dendritic cells to extend trans-epithelial dendrites in response to increased microbial colonization at the ocular surface. Moreover, this study provides key insight into how goblet cell responses to microbial stimuli may contribute to the disruption of ocular mucosal homeostasis and chronic ocular mucosal inflammation.

Keywords: conjunctiva, ocular mucosa, goblet cells, homeostasis, dendritic cells

OPEN ACCESS

Edited by:
Daniel Saban,
Duke University, United States

Reviewed by:
Giulio Ferrari,
San Raffaele Hospital (IRCCS), Italy
Adriana Mantegazza,
Thomas Jefferson University, United States

***Correspondence:**
Sharmila Masli
smasli@bu.edu

Specialty section:
This article was submitted to Antigen Presenting Cell Biology, a section of the journal Frontiers in Immunology

Received: *29 May 2021*
Accepted: *15 July 2021*
Published: *09 August 2021*

Citation:
Logeswaran A, Contreras-Ruiz L and Masli S (2021) Conjunctival Goblet Cell Responses to TLR5 Engagement Promote Activation of Local Antigen-Presenting Cells. Front. Immunol. 12:716939. doi: 10.3389/fimmu.2021.716939

INTRODUCTION

Ocular mucosa is persistently exposed to environmental factors including microbes. The epithelial layer of the ocular mucosa is composed of stratified columnar epithelial cells that are interspersed with goblet cells (GC) capable of secreting gel-forming mucins to form a physical barrier between the environment and host cells. At steady state, similar to other mucosal surfaces, it is critical that the ocular mucosal tissue environment supports immunologic tolerance to harmless microbes and protective immunity against pathogens to facilitate their rapid clearance. In addition to secreting mucins, conjunctival GC are found capable of contributing to maintaining a homeostatic balance between tolerogenic and protective immune responses. Several studies support such function of conjunctival GC. These include observations of GC loss in chronic ocular surface inflammatory conditions, their ability to secrete immunomodulatory factors, and loss of immunologic tolerance in mice deficient in GC (1–4). These reports and evidence from other mucosal surfaces suggest GC to be multi-faceted players in mucosal immunity (5).

In colonic mucosa, microbial sensing by GC is reported to limit the exposure of the colonic mucosal immune system to harmful antigens (6). Conjunctival GC are also known to be responsive to microbial products. Studies have reported their ability to secrete pro-inflammatory IL-1β in response to stimulation by toxigenic *S. aureus* (7) and anti-inflammatory TGFβ2 in response to LPS-mediated stimulation (8). Although these studies implicate their ability to modulate the tissue environment, it is not known if their responses can contribute to chronic ocular surface inflammation.

Previously, we have reported that conjunctival GC predominantly express TGFβ2 isoform and mediate its activation by their endogenously expressed thrombospondin-1 (TSP-1) (8). Consistently, TSP-1 deficiency in mice results in the spontaneous development of chronic ocular surface inflammation as seen in patients with Sjögren's syndrome (9). In these mice as well as in Sjögren's syndrome patients, increased microbial colonization is detected at the ocular surface (10, 11). Together, these studies point to TSP-1-mediated mechanisms as potential contributors to ocular mucosal homeostasis. In this study, we examine if GC responses to microbial products can alter the ocular mucosal tissue environment to disruption of homeostasis and whether such disruption can lead to the development of chronic ocular surface inflammation.

Under steady-state conditions, professional antigen-presenting cells like dendritic cells (DC) located in tissues are maintained in an immature tolerogenic phenotype characterized by low expression of MHC class II and co-stimulatory molecules. These cells function as sentinels capable of transporting captured antigens to draining lymph nodes to initiate an antigen-specific adaptive immune response. While in our previous studies we demonstrated the ability of GC-derived TGFβ2 to maintain immature DC phenotype *in vitro* (8), in this study, we examine if GC–microbial interaction-driven changes in ocular mucosal homeostasis alter DC phenotype *in vivo* that supports the development of chronic ocular surface inflammation.

Our results demonstrate that TLR5 engagement on GC downregulates their expression of TSP-1 both *in vitro* and *in vivo*. Resultant decline in GC-derived active TGFβ along with increased expression of IL-6 contribute to a disruption of ocular mucosal homeostasis. Such altered tissue environment supports the activated phenotype of DC in the conjunctiva and subsequent development of chronic ocular surface inflammation characterized by corneal epitheliopathy and tissue infiltrates.

MATERIALS AND METHODS

Mice

Wild-type (C57BL/6) mice were purchased from Charles River Laboratories (Wilmington, MA). TSP-$1^{-/-}$ mice were purchased from Jackson Laboratories (Bar Harbor, ME). They were then bred in-house at a pathogen-free facility at Boston University School of Medicine, Boston, MA. The experimental protocols strictly followed the ARVO Statement for the Use of Animals in Ophthalmic and Vision Research and were in accordance with the institution's guidelines.

Flagellin Treatment of Mice

Wild-type mice were treated topically with 10 ng flagellin (InvivoGen, San Diego, CA) bilaterally (5 μl/eye) for 7 days. Corneal barrier integrity was monitored for 4 weeks by fluorescein staining as described previously (12). Briefly, 1% sodium fluorescein (Sigma-Aldrich, St. Louis, MO, USA) was applied to each eye. Three minutes later, eyes were flushed with PBS to remove excess fluorescein, and corneal staining was evaluated using the slit-lamp microscope (Haag-Streit, USA) with cobalt blue light. Punctate staining was scored according to the standardized National Eye Institute grading system of 0–3 for each of the five areas of the cornea (13).

Immunostaining and Microscopy

To prepare frozen sections of conjunctiva, eyes were enucleated with the lids intact, fixed in 4% formaldehyde in phosphate buffered saline (PBS) for 48 h, followed by cryoprotection in 10%–30% sucrose for 72 h before embedding in OCT. Tissue sections 7 μm in thickness were cut using a microtome and placed on slides to be stored at – 20°C until ready to use. Conjunctival explants were fixed in 4% formaldehyde before staining. Tissue sections and explants were blocked by PBS that contained normal goat, hamster, or donkey serum, 0.3%–1% Triton X-100 at RT for 1 h, and incubated overnight at RT with primary specific antibodies for CD11c (Biolegend, Dedham, MA), MUC5AC (Abcam, Cambridge, MA), MHC class II (BD Biosciences, San Jose, CA), or TSP-1 (Santa Cruz Biotech, Santa Cruz, CA). After a PBS rinse, fluorescence-conjugated secondary antibodies (Invitrogen, Thermo Fisher Scientific, Waltham, MA) were applied for 1 h in RT. Cell nuclei were counterstained with DAPI dye. Fluorescent staining in tissue sections was visualized using the FSX100 Olympus fluorescence microscope. Staining in conjunctival explants was visualized using a Zeiss LSM 700 confocal microscope equipped with a 63× oil objective. Images (z-stacks) were captured using the Zeiss ZEN software.

Microscopic images were analyzed using NIH ImageJ software (14).

Primary Cultures of Conjunctival Goblet Cells

Goblet cells were obtained from mouse conjunctival pieces and grown in an organ culture as described previously (15). Briefly, conjunctival tissues were removed from 4- to 12-week-old male mice and kept in Hank's based salt solution (Lonza, Walkersville, MD). Small pieces of conjunctival tissue were anchored onto a scratch at the bottom of a well in a 24-well plate. Culture medium (RPMI-1640) supplemented with 10% heat-inactivated fetal bovine serum, 10 mM HEPES, 100 µg/ml penicillin/streptomycin, 1 mM sodium pyruvate, and 1× nonessential amino acid mixture (Lonza, Walkersville, MD) was added to submerge the tissue pieces. These explants were fed every other day with RPMI-1640 medium and grown for 2 weeks at 37°C and 5% CO_2 to reach 85% confluence. Explants were later discarded, and goblet cell phenotype was confirmed by positive immunostaining for cytokeratin-7 and MUC5AC and negative staining for cytokeratin-4 (15). Goblet cells were cultured with heat-killed pathogenic *Pseudomonas aeruginosa* strain PA14 (kindly provided by Dr. Mihaela Gadjeva, Brigham and Women's Hospital, Harvard Medical School, Boston, MA) at a MOI of 60 or flagellin-PA (InvivoGen, San Diego, CA) at different concentrations (0–10 µg/ml) for a period of 24 h. No significant effect on cell viability was detected as determined using CCK-8 kit (Dojindo Molecular Technologies, Inc., Rockville, MD). Culture supernatants were collected to determine cytokine content and cells were used to harvest RNA.

Flow Cytometry

Cultured goblet cells were stained with Fixable viability dye (eBioscience, San Diego, CA) and cells were immunostained with Alexa-647-conjugated anti-TLR5 antibody (Clone ACT5, Biolegend, Dedham, MA). Specificity of TLR5 staining was validated by confirming negative staining in RAW 264.7 cell line consistent with their minimal TLR5 transcript levels and functional responses to TLR5 agonist (16, 17). Fluorescence-labeled cells were analyzed using BD LSRII Flow Cytometer (BD Bioscience, San Jose, CA) at Boston University Flow Cytometry Core Facility. Further analysis of the data was performed using FlowJo software (Tree Star, Inc., Ashland, OR).

TGFβ Bioassay

Active TGFβ content of culture supernatants was determined using fibroblast cell line, MFB-11, derived from TGFβ knockout mice and stably transfected with SBE-SEAP reporter (18). Cells in complete DMEM were seeded into flat-bottomed 96-well plates (3×10^4 per well) and incubated overnight at 37°C, 5% CO_2. Cells were then washed twice with PBS and incubated with 50 µl of serum-free DMEM for 2 h before adding culture supernatants. Standard curve was set up using recombinant TGFβ2 (R&D Systems, Minneapolis, MN). After 24 h incubation, culture supernatants from each well were tested for SEAP activity using Great EscApe SEAP Reporter system 3 (Clontech, Mountain View, CA) according to the manufacturer's instructions. Absorbance was measured using a Synergy H1 microplate reader (Biotek, Winooski, VT). Each sample was analyzed in triplicate.

Real-Time PCR

Total RNA was isolated using TRIzol Reagent (Life Technologies, Carlsbad, CA) according to the manufacturer's directions and reverse transcribed to generate cDNA using the Superscript VILO cDNA kit (Life Technologies, Carlsbad, CA). Real-time PCR was performed to determine relative quantitative expression levels of TSP-1, TGFβ2, and IL-6 on 7200 Real-Time System (Applied Biosystems, Carlsbad, CA) using SYBR Green PCR Master Mix (Life Technologies, Carlsbad, CA). Amplification reactions were set up in quadruplicate using specific primer sets with the thermal profile of 95°C for 3 min, 40 cycles of 95°C for 20 s, 55°C for 30 s, and 72°C for 40 s. A melting curve analysis was performed to verify the specificity of amplification reactions. Analysis of fluorescence signal generated at each cycle with system software generated threshold cycle values, and quantification of gene expression was determined relative to that of the reference gene Glyceraldehyde-3-phosphate dehydrogenase. Primer sequences used were TGFβ2 (F-5'-AGGCGAGATTTGCAGGTATTGA-3' and R-5'-GTAGGAGGGCAACAACATTAGCAG-3'), TSP-1 (F-5'-AAG AGG ACC GGG CTC AAC TCT ACA and R-5'-CTC CGC GCT CTC CAT CTT ATC AC), IL-6 (F-5'-AGT CAA TTC CAG AAA CCG CTA TGA and R-5'-TAG GGA AGG CCG TGG TTG T), and GAPDH (F-5'-CGA GAA TGG GAA GCT TGT CA and R-5'-AGA CAC CAG TAG ACT CCA CGA CAT).

Statistical Analysis

Differences between mean values were compared using Student's *t*-test. A difference with $p < 0.05$ is considered statistically significant. The standard error of the mean is represented with error bars in figures. For corneal fluorescein staining scores, normal distribution of the pooled data for independent groups from a series of experiments was confirmed using D'Agostino and Pearson test supporting the assumption that data in this study are drawn from a normally distributed population. Homogeneity of variances among experimental and control groups are confirmed using *F*-test. Data analysis was performed using Excel (Microsoft Office) and GraphPad Prism software (GraphPad software Inc., San Diego, CA).

RESULTS

Dendritic Cells in the Conjunctiva With Increased Microbial Frequency Are Located in Close Proximity of Goblet Cells and Extend Dendrites to Access Ocular Surface

Similar to other mucosal surfaces, the presence of CD11c+ DC subsets have been reported in mouse ocular mucosa (19). These were identified by flow cytometry. In the intestinal mucosa, DC in the lamina propria extend trans-epithelial dendrites in response to epithelial cell TLR engagement (20). To evaluate

the location and morphology of DC in the context of GC in the ocular mucosa, we evaluated conjunctiva explants from TSP-$1^{-/-}$ mice, previously reported to harbor increased microbial frequency at the ocular surface (11), and from C57BL/6 mice as controls. A representative 3D reconstruction of confocal images of immunostained conjunctiva from TSP-$1^{-/-}$ mice is shown in **Figure 1**. Positively stained cell bodies of DC were detected below the epithelial layer containing MUC5AC+ GC (**Figure 1A**). While several DC were located in close proximity of GC, many DC extensions were visible on the ocular surface side of the tissue (**Figure 1B**). Some of these extensions had globular structure at the tip similar to that described by others in trans-epithelial dendrites (TEDs) of DC subsets in intestinal mucosa (20–22). In C57BL/6 conjunctiva, very few positively stained DC were located in the subepithelial region without clearly detectable trans-epithelial projections (**Supplemental Figure 1**). The presence of TEDs in TSP-$1^{-/-}$, but not C57BL/6, conjunctiva correlates with the known increased microbial colonization of the ocular surface in TSP-$1^{-/-}$ mice. These results demonstrate that DC in ocular mucosa can be located in close proximity of GC and extend trans-epithelial dendrites towards the ocular surface presumably to sample microbes.

Goblet Cells Express Functional TLR5, Which Mediates Reduced Secretion of Active TGFβ

Microbial keratitis caused by *P. aeruginosa* is the most common vision-threatening infection among contact lens wearers (23) and a relatively common but potentially serious cause of conjunctivitis in hospitalized preterm infants with significant morbidity and in some cases death due to systemic complications (24). Potential complications of keratitis include chronic inflammation and corneal scarring. To determine if GC responses may contribute to these complications, we examined their responses to pathogenic strain of *P. aeruginosa* (PA14). We stimulated primary GC cultures, derived from C57BL/6 conjunctiva explants, with heat-inactivated PA14 and detected significantly increased levels of IL-6 in culture supernatants (**Figure 2A**). As GC respond to LPS (TLR4 ligand) by increasing their secretion of active TGFβ, we determined if PA14 induces a similar response in GC. As shown in **Figure 2B**, GC stimulated with PA14 produced significantly reduced levels of active TGFβ as detected in a bioassay described in Materials and Methods.

Conjunctival GC are known to respond to TLR2- and TLR4-mediated signals (7, 8). To determine their TLR5 expression, cells from primary GC cultures were stained with anti-TLR5 antibody and analyzed by flow cytometry. Consistent with reported expression of TLR5 in human conjunctival epithelial cells (25, 26), GC expressed TLR5 (**Figure 2C**). To determine if reduced TGFβ secretion induced by PA14 resulted from combined TLR4/5 signaling or if it can be attributed to TLR5-mediated signaling in GC, we stimulated these cells with different concentrations of TLR5 ligand, flagellin derived from *P. aeruginosa*. As shown in **Figure 3**, we detected dose-dependent increased expression of IL-6 message by real-time PCR (**Figure 3A**) in flagellin-stimulated GC that was accompanied by increased IL-6 protein detected in culture supernatants by ELISA (**Figure 3B**). Similarly, flagellin also reduced secretion of active TGFβ by GC in a dose-dependent manner (**Figure 3C**). Together, these results confirm the expression of functional TLR5 on conjunctival GC that, in contrast to TLR4-mediated signals, reduces GC-derived active TGFβ.

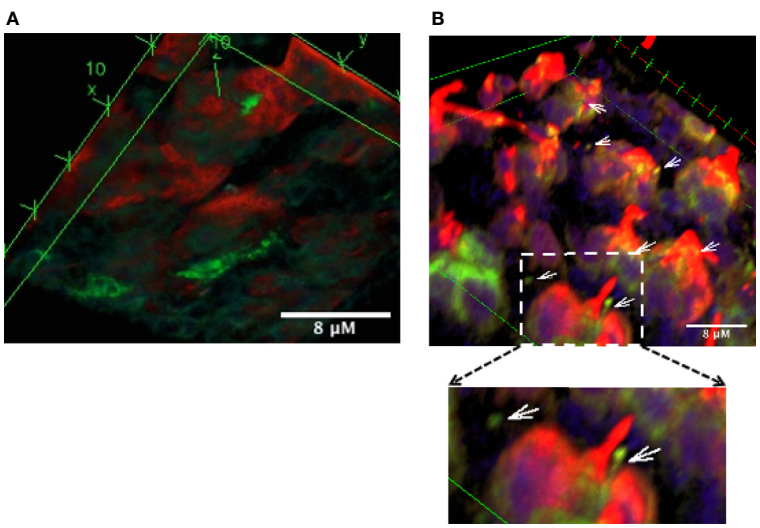

FIGURE 1 | Dendritic cells are located in close proximity of conjunctival goblet cells and extend trans-epithelial dendrites towards the ocular surface. Confocal microscopy images of the conjunctival explant from TSP-$1^{-/-}$ mice with increased microbial frequency at the ocular surface. Tissue was stained for MUC5AC (red) to label GCs and CD11c (green) to label DCs. Images show three-dimensional view of 63 z-stack images captured using laser-scanning confocal microscope. **(A)** Bottom view of the explant shows sub-epithelial location of some DCs (green), **(B)** In the top view, extensions of DCs (arrows) and their proximity of GCs (red) can be observed. Digital magnification of the boxed region in the top panel is shown to better illustrate DC extension with a globular tip protruding towards the ocular surface.

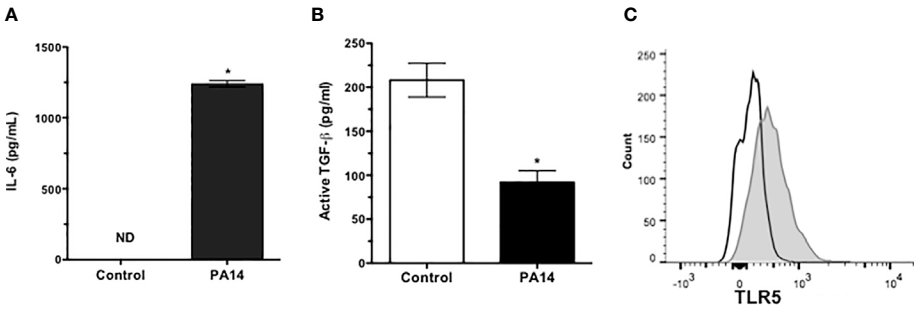

FIGURE 2 | Goblet cells express functional TLR5 and respond to pathogenic strain of *P. aeruginosa* by reducing active TGFβ secretion. Levels of **(A)** IL-6 and **(B)** active TGFβ in culture supernatants of GCs stimulated with heat-inactivated PA14 for 24 h. ND, Not Detected. Data are expressed as mean ± SEM, $n = 4$, $^*p < 0.05$. **(C)** Flow cytometric detection of surface expression of TLR5 in primary cultures of GCs. Filled histogram shows positively stained GCs and empty histogram represents isotype staining control.

Flagellin-Mediated Modulation of Goblet Cell TGFβ Secretion Contributes to the Development of Chronic Ocular Surface Inflammation

The ability of GC to secrete TGFβ and modulate DC phenotype implicates a potential role of GC in maintenance of immune homeostasis (8). To determine if flagellin-mediated reduced secretion of active TGFβ and increased secretion of IL-6 by GC disrupt ocular mucosal homeostasis and lead to the development of chronic ocular surface inflammation, we topically administered flagellin (10 ng/mouse) in mice daily for 1 week. Chronic inflammation of the conjunctiva is associated with the development of corneal epitheliopathy resulting from a disrupted corneal barrier. Therefore, we assessed corneal barrier integrity by determining corneal fluorescein staining score before initiating flagellin application (baseline) and comparing it to scores determined up to 4 weeks post-flagellin application. As shown in **Figure 4A**, a gradual increase in corneal fluorescein score led to a significant increase by 4 weeks after completion of flagellin application as compared to the baseline score. Consistent with this result, clinical signs of conjunctival inflammation were noted in mice. These included edema and hair loss around the eye caused by excessive grooming (**Figure 4B**). **Figure 4C** shows representative corneal

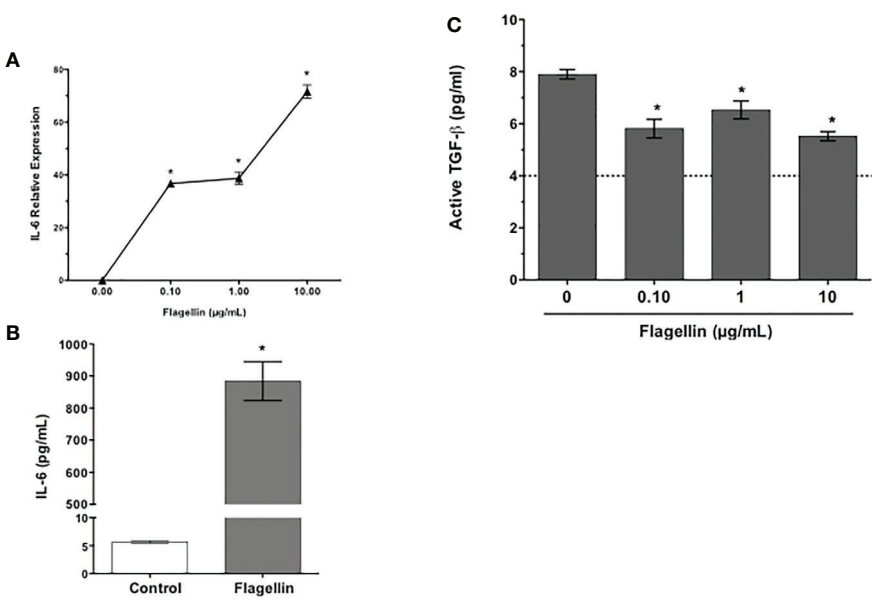

FIGURE 3 | Flagellin, a TLR5 ligand, reduces GC secretion of active TGFβ. Cultures of GCs were stimulated with indicated concentrations of flagellin for 24 h. The expression of IL-6 message **(A)** was detected by real-time PCR and IL-6 protein levels were determined by ELISA **(B)** in culture supernatants of GCs stimulated with 1 µg/ml flagellin. Culture supernatants were also evaluated for their content of active TGFβ **(C)** in a bioassay. The dotted line represents assay limit of detection. Data are expressed as mean ± SEM, $n = 4$, $^*p < 0.05$.

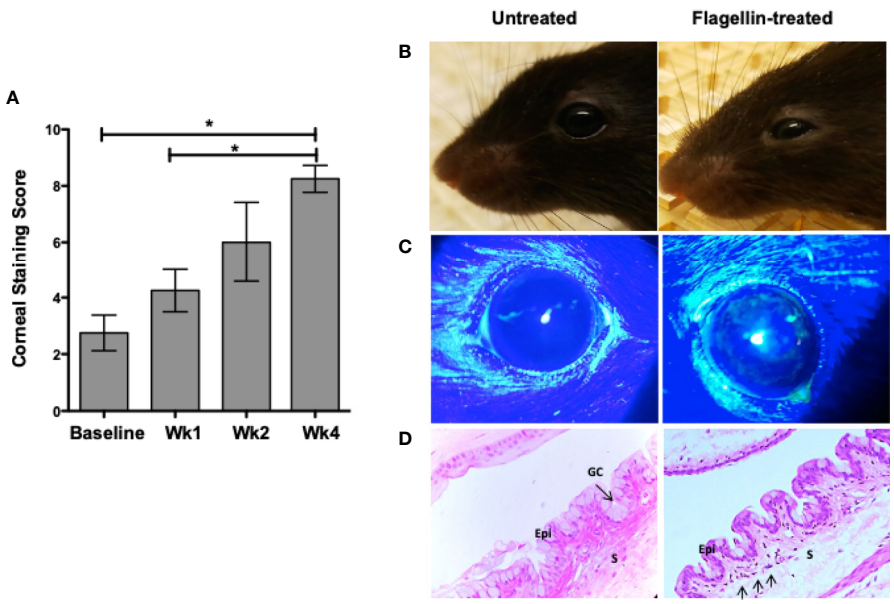

FIGURE 4 | Topical application of flagellin results in chronic ocular surface inflammation. Flagellin (10 ng/day) was applied topically in C57BL/6 mice for 7 days. Development of ocular surface inflammation was monitored by assessing corneal barrier integrity, clinical signs, and conjunctiva histology. Corneas were evaluated for punctate epitheliopathy before and up to 4 weeks post-flagellin application using 1% sodium fluorescein application followed by slit lamp exam using cobalt blue light. Staining was scored according to standardized NEI grading system **(A)**. Representative photographs of untreated and flagellin-treated mice **(B)**; their corneal fluorescein staining **(C)**; and H&E-stained sections of conjunctiva at 4 weeks. **(D)** Epithelium (Epi), Stroma (S), and Goblet cells (GC) are marked, and arrows in the conjunctiva from flagellin-treated mouse point to inflammatory infiltrates. Data expressed as mean ± SEM, $n = 4$, $^*p < 0.05$ wk4 *vs.* baseline.

fluorescein staining in untreated and flagellin-treated mice. These clinical signs correlated with inflammatory infiltrates observed in histological evaluation of conjunctiva from flagellin-treated mice (**Figure 4D**). Also, GC density appeared to be lower in flagellin-treated conjunctiva relative to that seen in untreated tissue. Together, these findings indicate development of chronic ocular surface inflammation in mice treated with topical application of flagellin.

Flagellin Stimulation of Goblet Cells Is Associated With Reduced Expression of TGFβ-Activator TSP-1 and Altered Ocular Mucosal Homeostasis

We have reported previously that GC depend on their endogenously expressed TSP-1 to activate their latent TGFβ (8). Moreover, TSP-1 deficiency in mice results in spontaneous development of chronic ocular surface inflammation (9). Therefore, we evaluated change in TSP-1 expression in primary cultures of GC exposed to different concentrations of flagellin. As shown in **Figure 5A**, significantly reduced levels of TSP-1 message were detected by real-time PCR in flagellin-treated GC. This *in vitro* finding was also confirmed *in vivo*, by assessing TSP-1 immunostaining in conjunctiva from flagellin-treated mice. **Figure 5B** shows reduced TSP-1 immunoreactivity in conjunctival epithelium after flagellin application.

Immature or tolerogenic state of DCs in tissues under steady-state homeostatic conditions is characterized by their low expression of MHC class II. To determine if flagellin-induced reduced TSP-1 and active TGFβ expression by GC alter ocular mucosal homeostasis, we examined MHC class II expression of CD11c+ DC in flagellin-treated conjunctiva. As seen in **Figure 6**, while CD11c+ DC are detectable in untreated conjunctiva, MHC class II expression of these cells was stronger in flagellin-treated conjunctiva. These results indicate loss of homeostasis in flagellin-exposed conjunctiva is consistent with reduced TSP-1 expression in this tissue.

DISCUSSION

As a mucosal surface persistently exposed to microbes, the steady-state homeostasis in the conjunctiva is central to ensuring immunologic tolerance induction while preventing excessive inflammatory damage to the tissue. Our results in this study demonstrate that DC in the conjunctiva can be located in close proximity of GC and can extend TEDs similar to those observed in other mucosal surfaces. Considering the location of DC, responses of GC to microbial stimuli have the potential to directly influence their functional phenotype. Notably, GC responses to the pathogenic strain of *P. aeruginosa* or TLR5-mediated signaling included altered balance in the expression of immunomodulatory TGFβ and pro-inflammatory IL-6. The decline in GC-derived active TGFβ induced by TLR5 stimulation correlated with their

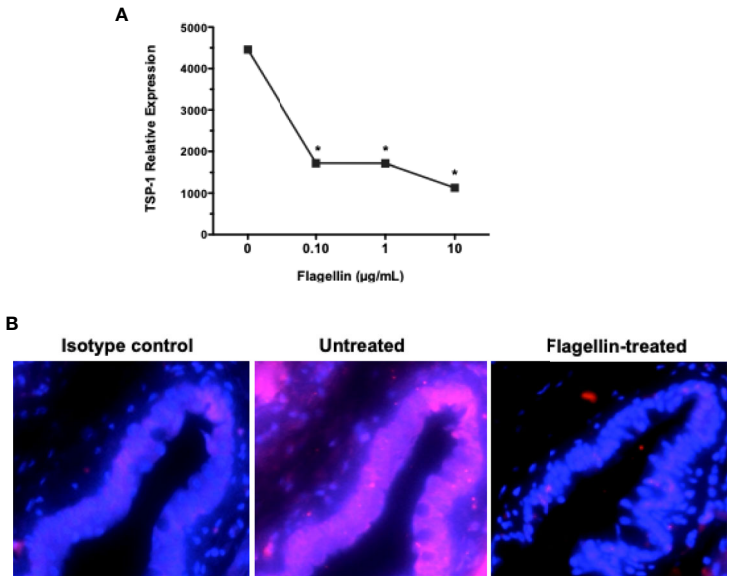

FIGURE 5 | Flagellin stimulation is associated with reduced expression of TGFβ-activator TSP-1. **(A)** The expression of TSP-1 in GC cultures stimulated with indicated concentrations of flagellin was determined by real-time PCR. Data are expressed as mean ± SEM, $n = 4$, $^*p < 0.05$. **(B)** Immunostaining of TSP-1 (magenta) in frozen sections of conjunctiva tissue harvested from C57BL/6 mice 4 weeks after topical application of flagellin (10 ng/day for 7 days). Nuclei were stained with DAPI (blue). Magnification ×20.

reduced expression of TGFβ-activator TSP-1. In mice, TLR5 agonist-induced altered tissue environment led to activated phenotype of DC indicated by their increased MHC class II expression and chronic ocular surface inflammation with corneal epitheliopathy.

Our results highlight the significance of GC–microbial interactions in maintaining homeostasis in the ocular mucosa. These findings implicate GC responses in altering tissue microenvironment in a way that promotes development of chronic inflammation. Although expression of TLR5 is reported in conjunctival epithelial cells (26), our data not only demonstrate its specific expression on GC but confirm flagellin-induced inflammatory IL-6 secretion in GC. In mice, macrophages and bone marrow-derived DC do not express TLR5, ruling out chronic inflammation resulting from systemic stimulation of DC (27). However, CD11c+ DC in intestinal mucosa express high levels of TLR5 in addition to intestinal epithelial cells. While normal conjunctiva in mice harbors CD11c+ DC, it is not known if these cells express TLR5 (19). Due to its size (>10 kDa), topically applied flagellin in our *in vivo* experiments is not expected to have crossed the epithelium through paracellular leak or GC-associated passages (GAPs), limiting the possibility of direct activation of conjunctival DC. Also, in normal conjunctiva, we did not observe TED formation (**Supplementary Figure 1**) in DC that could give them direct access to topically applied flagellin. However, TED formation induced by flagellin-stimulated GC or stratified epithelial cells cannot be ruled out. Regardless of cells targeted *in vivo* by flagellin, our experiments clearly support its ability to disrupt ocular mucosal homeostasis. Furthermore, the detection of corneal epitheliopathy over a prolonged period after stopping topical flagellin administration highlights the chronic nature of the ocular surface inflammation.

Conjunctival epithelium and GC predominantly express TGFβ2 isoform (8). The integral role of TGFβ in regulating immune response is well-documented and activation of its latent form is known to provide a crucial layer of regulation that controls TGFβ function (28). Conjunctival GC depend on TSP-1 to activate their latent TGFβ2 as, unlike other isoforms, latency-associated peptide (LAP) of TGFβ2 does not contain RGD sequence and therefore cannot be activated by integrins (8, 28, 29). In our experiment, flagellin stimulation of GC did not result in significant change in TGFβ2 message at lower concentrations tested with only increase detected at the highest concentration (**Supplementary Figure 2**). However, flagellin stimulation resulted in reduced expression of TSP-1 both *in vitro* and *in vivo* that is consistent with reduced levels of active TGFβ detected in culture supernatants of flagellin-stimulated GC. Moreover, the observed correlation of the reduced expression of TSP-1 in conjunctival epithelium with the development of chronic ocular surface inflammation in this study is consistent with our previously reported observations in human subjects (1). In individuals carrying single-nucleotide polymorphism in TSP-1-encoding gene, TSP-1 expression in conjunctival epithelial cells is reduced and correlates with their developing chronic ocular surface inflammation. Together, these findings confirm the significance of TSP-1 mediated TGFβ activation in maintaining homeostasis in ocular mucosa.

Environmental factors are considered possible contributors to the induction of autoimmunity. The relevance of microbes to chronic ocular surface inflammation associated with Sjögren's syndrome is supported by reports of altered microbial colonization at the ocular surface in patients as well as in the

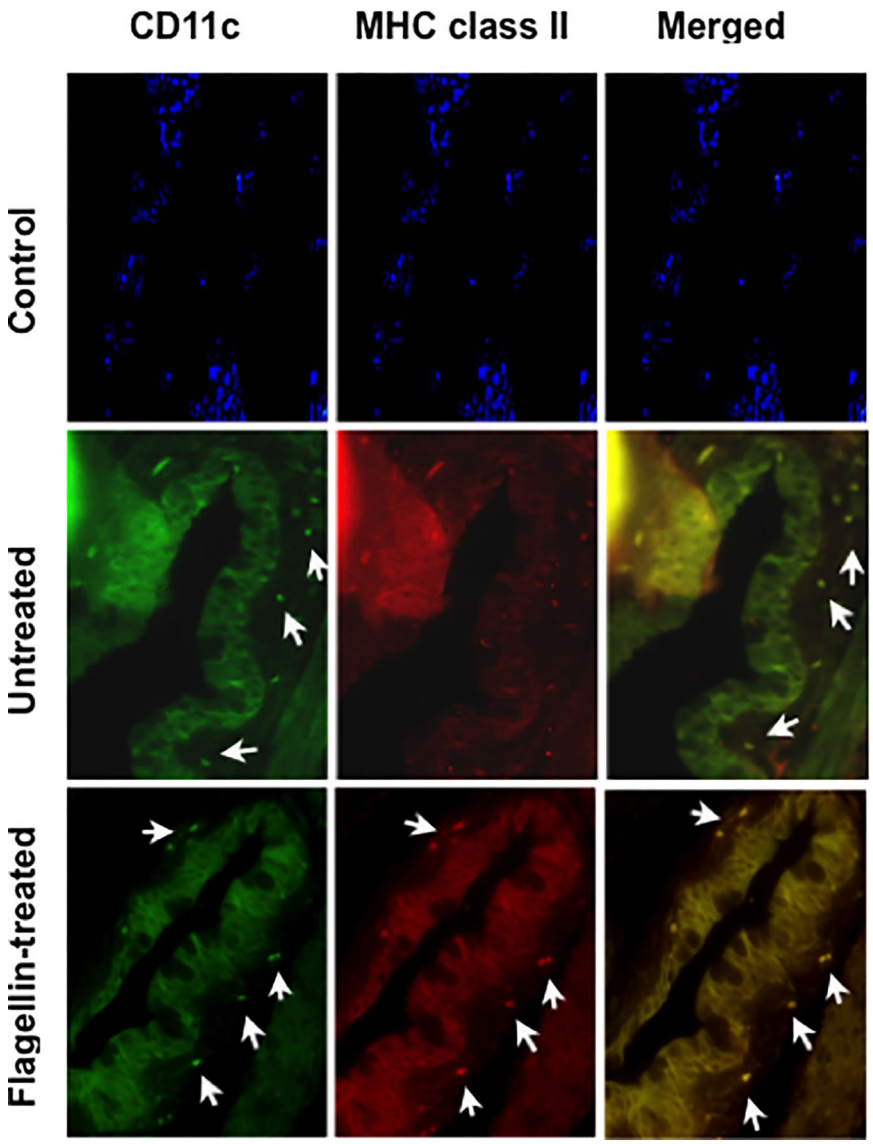

FIGURE 6 | Topically applied flagellin increases proportion of MHC class II expressing DCs in the conjunctiva. Frozen sections of conjunctiva harvested from either untreated or flagellin-treated mice (10 ng/day for 7 days) were immunostained for dendritic cell marker CD11c and their activation marker MHC class II. Nuclei were stained with DAPI (blue). White arrows indicate positively stained cells. Magnification ×20.

mouse model of the disease (10, 11). However, it is not known how ocular surface microbes may contribute to chronic inflammation. Our study provides the first evidence of TEDs in ocular mucosa that has been described as a mechanism of microbial sampling in intestinal and respiratory mucosa (5, 30). Considering that TEDs are observed in conjunctiva with increased microbial colonization, they are likely regulated by epithelial responses to microbial stimuli as noted in intestinal mucosa (20). Our focus on GC in this study is based on their previously reported immunomodulatory function (8) and critical role in induction of immune tolerance related to the ocular mucosa (2). However, responses of stratified epithelial cells to microbes and their contribution to overall tissue homeostasis and TED formation need further investigation. The proximity of DC to GC in our study does suggest a potential role of GC responses to microbial stimulation in inducing TED formation. Furthermore, our failure to detect TEDs in normal conjunctiva tissue indicates their relevance to inflammation. Particularly, pre-existing TSP-1 deficiency in the conjunctiva with increased microbial colonization suggests that altered tissue homeostasis may drive TED formation in DC. Therefore, it is quite possible that DC in the ocular mucosa capture ocular surface antigens *via* TED formation to induce an inflammatory adaptive immune response. Their ability to migrate to draining lymph nodes and characterization of inflammatory effectors induced remain to be determined in future studies.

Our findings may appear to contradict the previously reported protective effect of topically applied flagellin on the development of microbial keratitis (31). However, there are several differences between the two studies. A major difference being that microbial keratitis represents acute inflammation, while our study addresses development of chronic ocular surface inflammation. Moreover, induction of microbial keratitis involves prior disruption of corneal barrier and much higher concentration of flagellin (500 ng *vs.* 10 ng in our study) was applied to the corneal barrier disrupted with needle injury. Thus, while the microbial keratitis study focuses on responses of damaged corneal epithelial cells typically targeted by the causative pathogen, our study highlights responses of healthy conjunctival epithelial cells.

In conclusion, we demonstrate in this report that conjunctival GC express functional TLR5 that mediates signaling leading to disrupted ocular mucosal homeostasis. The TLR5-mediated changes to the tissue environment activate local antigen-presenting cells and result in the development of chronic ocular surface inflammation. Thus, GC response to ocular surface microbes represents an important regulator in the maintenance of ocular mucosal homeostasis.

DATA AVAILABILITY STATEMENT

The raw data supporting the conclusions of this article will be made available by the authors, without undue reservation.

ETHICS STATEMENT

The animal study was reviewed and approved by Boston University Institutional Animal Care and Use Committee.

AUTHOR CONTRIBUTIONS

Conceptualization, funding acquisition, resources and supervision, SM. Investigation and formal analysis, AL and LC-R. Writing—original draft preparation, AL and SM. Writing—review and editing, AL, LC-R, and SM. All authors contributed to the article and approved the submitted version.

FUNDING

This research was funded in part by National Eye Institute Grant EY015472, Massachusetts Lions Eye Research Fund (MLERF) and and Sjögren's Foundation.

SUPPLEMENTARY MATERIAL

The Supplementary Material for this article can be found online at: https://www.frontiersin.org/articles/10.3389/fimmu.2021.716939/full#supplementary-material

Supplementary Figure 1 | Trans-epithelial dendrites are not detected in mice with normal or low microbial frequency at the ocular surface. Confocal microscopy images of the conjunctival explant from WT (C57BL/6) mice stained for MUC5AC (red) to label GCs and CD11c (green) to label DCs. Images show three-dimensional view of 63 z-stack images captured using laser-scanning confocal microscope. **(A)** Bottom view of the explant shows sub-epithelial location of some DCs (green), **(B)** In the top view extensions of DCs (green) and their proximity of GCs (red) is not observed. Digital magnification of the boxed region in the top panel is shown to better illustrate the absence of a DC extension.

Supplementary Figure 2 | Changes in TGFb2 transcript levels after flagellin stimulation of GC cultures. The expression of TGFb2 after stimulation with indicated concentrations of flagellin was determined by real-time PCR, Data are expressed as Mean + SEM, n=4, *p < 0.05.

REFERENCES

1. Contreras-Ruiz L, Ryan DS, Sia RK, Bower KS, Dartt DA, Masli S. Polymorphism in THBS1 Gene Is Associated With Post-Refractive Surgery Chronic Ocular Surface Inflammation. *Ophthalmology* (2014) 121(7):1389–97. doi: 10.1016/j.ophtha.2014.01.033
2. Ko BY, Xiao Y, Barbosa FL, de Paiva CS, Pflugfelder SC. Goblet Cell Loss Abrogates Ocular Surface Immune Tolerance. *JCI Insight* (2018) 3(3):e98222. doi: 10.1172/jci.insight.98222
3. Pflugfelder SC, De Paiva CS, Moore QL, Volpe EA, Li DQ, Gumus K, et al. Aqueous Tear Deficiency Increases Conjunctival Interferon-Gamma (IFN-Gamma) Expression and Goblet Cell Loss. *Invest Ophthalmol Vis Sci* (2015) 56(12):7545–50. doi: 10.1167/iovs.15-17627
4. Xiao Y, de Paiva CS, Yu Z, de Souza RG, Li DQ, Pflugfelder SC. Goblet Cell-Produced Retinoic Acid Suppresses CD86 Expression and IL-12 Production in Bone Marrow-Derived Cells. *Int Immunol* (2018) 30(10):457–70. doi: 10.1093/intimm/dxy045
5. Knoop KA, Newberry RD. Goblet Cells: Multifaceted Players in Immunity at Mucosal Surfaces. *Mucosal Immunol* (2018) 11(6):1551–7. doi: 10.1038/s41385-018-0039-y
6. Knoop KA, McDonald KG, McCrate S, McDole JR, Newberry RD. Microbial Sensing by Goblet Cells Controls Immune Surveillance of Luminal Antigens in the Colon. *Mucosal Immunol* (2015) 8(1):198–210. doi: 10.1038/mi.2014.58
7. Li D, Hodges RR, Bispo P, Gilmore MS, Gregory-Ksander M, Dartt DA. Neither Non-Toxigenic Staphylococcus Aureus Nor Commensal S. epidermidi Activates NLRP3 Inflammasomes in Human Conjunctival Goblet Cells. *BMJ Open Ophthalmol* (2017) 2(1):e000101. doi: 10.1136/bmjophth-2017-000101
8. Contreras-Ruiz L, Masli S. Immunomodulatory Cross-Talk Between Conjunctival Goblet Cells and Dendritic Cells. *PLoS One* (2015) 10(3):e0120284. doi: 10.1371/journal.pone.0120284
9. Contreras-Ruiz L, Regenfuss B, Mir FA, Kearns J, Masli S. Conjunctival Inflammation in Thrombospondin-1 Deficient Mouse Model of Sjogren's Syndrome. *PLoS One* (2013) 8(9):e75937. doi: 10.1371/journal.pone.0075937
10. Hori Y, Maeda N, Sakamoto M, Koh S, Inoue T, Tano Y. Bacteriologic Profile of the Conjunctiva in the Patients With Dry Eye. *Am J Ophthalmol* (2008) 146(5):729–34. doi: 10.1016/j.ajo.2008.06.003
11. Terzulli M, Contreras-Ruiz L, Kugadas A, Masli S, Gadjeva M. TSP-1 Deficiency Alters Ocular Microbiota: Implications for Sjogren's Syndrome Pathogenesis. *J Ocul Pharmacol Ther* (2015) 31(7):413–8. doi: 10.1089/jop.2015.0017
12. Turpie B, Yoshimura T, Gulati A, Rios JD, Dartt DA, Masli S. Sjogren's Syndrome-Like Ocular Surface Disease in Thrombospondin-1 Deficient Mice. *Am J Pathol* (2009) 175(3):1136–47. doi: 10.2353/ajpath.2009.081058
13. Lemp MA. Report of the National Eye Institute/Industry Workshop on Clinical Trials in Dry Eyes. *CLAO J* (1995) 21(4):221–32.
14. Schneider CA, Rasband WS, Eliceiri KW. NIH Image to ImageJ: 25 Years of Image Analysis. *Nat Methods* (2012) 9(7):671–5. doi: 10.1038/nmeth.2089
15. Contreras-Ruiz L, Ghosh-Mitra A, Shatos MA, Dartt DA, Masli S. Modulation of Conjunctival Goblet Cell Function by Inflammatory Cytokines. *Mediators Inflamm* (2013) 2013:636812. doi: 10.1155/2013/636812

16. Applequist SE, Wallin RP, Ljunggren HG. Variable Expression of Toll-Like Receptor in Murine Innate and Adaptive Immune Cell Lines. *Int Immunol* (2002) 14(9):1065–74. doi: 10.1093/intimm/dxf069
17. Sigola LB, Fuentes AL, Millis LM, Vapenik J, Murira A. Effects of Toll-Like Receptor Ligands on RAW 264.7 Macrophage Morphology and Zymosan Phagocytosis. *Tissue Cell* (2016) 48(4):389–96. doi: 10.1016/j.tice.2016.04.002
18. Tesseur I, Zou K, Berber E, Zhang H, Wyss-Coray T. Highly Sensitive and Specific Bioassay for Measuring Bioactive TGF-Beta. *BMC Cell Biol* (2006) 7:15. doi: 10.1186/1471-2121-7-15
19. Khandelwal P, Blanco-Mezquita T, Emami P, Lee HS, Reyes NJ, Mathew R, et al. Ocular Mucosal CD11b+ and CD103+ Mouse Dendritic Cells Under Normal Conditions and in Allergic Immune Responses. *PLoS One* (2013) 8(5): e64193. doi: 10.1371/journal.pone.0064193
20. Chieppa M, Rescigno M, Huang AY, Germain RN. Dynamic Imaging of Dendritic Cell Extension Into the Small Bowel Lumen in Response to Epithelial Cell TLR Engagement. *J Exp Med* (2006) 203(13):2841–52. doi: 10.1084/jem.20061884
21. Niess JH, Brand S, Gu X, Landsman L, Jung S, McCormick BA, et al. CX3CR1-Mediated Dendritic Cell Access to the Intestinal Lumen and Bacterial Clearance. *Science* (2005) 307(5707):254–8. doi: 10.1126/science.1102901
22. Vallon-Eberhard A, Landsman L, Yogev N, Verrier B, Jung S. Transepithelial Pathogen Uptake Into the Small Intestinal Lamina Propria. *J Immunol* (2006) 176(4):2465–9. doi: 10.4049/jimmunol.176.4.2465
23. Willcox MD, Holden BA. Contact Lens Related Corneal Infections. *Biosci Rep* (2001) 21(4):445–61. doi: 10.1023/a:1017991709846
24. Shah SS, Gloor P, Gallagher PG. Bacteremia, Meningitis, and Brain Abscesses in a Hospitalized Infant: Complications of Pseudomonas Aeruginosa Conjunctivitis. *J Perinatol* (1999) 19(6 Pt 1):462–5. doi: 10.1038/sj.jp.7200247
25. Li J, Shen J, Beuerman RW. Expression of Toll-Like Receptors in Human Limbal and Conjunctival Epithelial Cells. *Mol Vis* (2007) 13:813–22.
26. Redfern RL, Barabino S, Baxter J, Lema C, McDermott AM. Dry Eye Modulates the Expression of Toll-Like Receptors on the Ocular Surface. *Exp Eye Res* (2015) 134:80–9. doi: 10.1016/j.exer.2015.03.018
27. Uematsu S, Jang MH, Chevrier N, Guo Z, Kumagai Y, Yamamoto M, et al. Detection of Pathogenic Intestinal Bacteria by Toll-Like Receptor 5 on Intestinal CD11c+ Lamina Propria Cells. *Nat Immunol* (2006) 7(8):868–74. doi: 10.1038/ni1362
28. Travis MA, Sheppard D. TGF-Beta Activation and Function in Immunity. *Annu Rev Immunol* (2014) 32:51–82. doi: 10.1146/annurev-immunol-032713-120257
29. Annes JP, Munger JS, Rifkin DB. Making Sense of Latent TGFbeta Activation. *J Cell Sci* (2003) 116(Pt 2):217–24. doi: 10.1242/jcs.00229
30. Denney L, Ho LP. The Role of Respiratory Epithelium in Host Defence Against Influenza Virus Infection. *BioMed J* (2018) 41(4):218–33. doi: 10.1016/j.bj.2018.08.004
31. Kumar A, Gao N, Standiford TJ, Gallo RL, Yu FS. Topical Flagellin Protects the Injured Corneas From Pseudomonas Aeruginosa Infection. *Microbes Infect* (2010) 12(12-13):978–89. doi: 10.1016/j.micinf.2010.06.007

Conflict of Interest: The authors declare that the research was conducted in the absence of any commercial or financial relationships that could be construed as a potential conflict of interest.

Publisher's Note: All claims expressed in this article are solely those of the authors and do not necessarily represent those of their affiliated organizations, or those of the publisher, the editors and the reviewers. Any product that may be evaluated in this article, or claim that may be made by its manufacturer, is not guaranteed or endorsed by the publisher.

Copyright © 2021 Logeswaran, Contreras-Ruiz and Masli. This is an open-access article distributed under the terms of the Creative Commons Attribution License (CC BY). The use, distribution or reproduction in other forums is permitted, provided the original author(s) and the copyright owner(s) are credited and that the original publication in this journal is cited, in accordance with accepted academic practice. No use, distribution or reproduction is permitted which does not comply with these terms.

frontiers in Immunology

ORIGINAL RESEARCH
published: 13 August 2021
doi: 10.3389/fimmu.2021.718841

Interleukin 23 Produced by Hepatic Monocyte-Derived Macrophages Is Essential for the Development of Murine Primary Biliary Cholangitis

Debby Reuveni[1,2], *Miriam R. Brezis*[1,2], *Eli Brazowski*[2,3], *Philip Vinestock*[1], *Patrick S. C. Leung*[4], *Paresh Thakker*[5], *M. Eric Gershwin*[4] *and Ehud Zigmond*[1,2,6*]

[1] The Research Center for Digestive Tract and Liver Diseases, Tel Aviv Sourasky Medical Center, Tel Aviv, Israel, [2] Sackler Faculty of Medicine, Tel Aviv University, Tel Aviv, Israel, [3] Department of Pathology, Tel Aviv Sourasky Medical Center, Tel Aviv, Israel, [4] Division of Rheumatology, Allergy and Clinical Immunology, University of California, Davis, Davis, CA, United States, [5] Regeneron Pharmaceuticals, Inc., Tarrytown, NY, United States, [6] Center for Autoimmune Liver Diseases, Tel Aviv Sourasky Medical Center, Tel Aviv, Israel

OPEN ACCESS

Edited by:
Daniel Saban,
Duke University, United States

Reviewed by:
Joana Dias,
Vaccine Research Center (NIAID), United States
Luc Van Kaer,
Vanderbilt University, United States

Correspondence:
Ehud Zigmond
zigmond@tlvmc.gov.il

Specialty section:
This article was submitted to Antigen Presenting Cell Biology, a section of the journal Frontiers in Immunology

Received: 01 June 2021
Accepted: 29 July 2021
Published: 13 August 2021

Citation:
Reuveni D, Brezis MR, Brazowski E, Vinestock P, Leung PSC, Thakker P, Gershwin ME and Zigmond E (2021) Interleukin 23 Produced by Hepatic Monocyte-Derived Macrophages Is Essential for the Development of Murine Primary Biliary Cholangitis. Front. Immunol. 12:718841. doi: 10.3389/fimmu.2021.718841

Background and Aims: Primary Biliary Cholangitis (PBC) is an organ-specific autoimmune liver disease. Mononuclear phagocytes (MNPs), comprise of monocyte, dendritic cells and monocyte-derived macrophages, constitute major arm of the innate immune system known to be involved in the pathogenesis of autoimmune disorders. MNPs were shown to accumulate around intra-hepatic bile ducts in livers of PBC patients. Interleukin 23 (IL-23) is a pro-inflammatory cytokine. IL-23-positive cells were detected in livers of patients with advanced stage PBC and IL-23 serum levels found to be in correlation with PBC disease severity. Our overall goal was to assess the importance of IL-23 derived from MNPs in PBC pathogenesis.

Methods: We utilized an inducible murine model of PBC and took advantage of transgenic mice targeting expression of IL-23 by specific MNP populations. Analysis included liver histology assessment, flow cytometry of hepatic immune cells and hepatic cytokine profile evaluation. Specific MNPs sub-populations were sorted and assessed for IL-23 expression levels.

Results: Flow cytometry analysis of non-parenchymal liver cells in autoimmune cholangitis revealed massive infiltration of the liver by MNPs and neutrophils and a decrease in Kupffer cells numbers. In addition, a 4-fold increase in the incidence of hepatic IL-17A producing $CD4^+$ T cells was found to be associated with an increase in hepatic IL23-p19 and IL17A expression levels. Disease severity was significantly ameliorated in both $CD11c^{cre}P19^{flox/flox}$ and $CX_3CR1^{cre}P19^{flox/flox}$ mice as assessed by reduced portal inflammation and decreased hepatic expression of various inflammatory cytokines. Amelioration of disease severity was associated with reduction in IL-17A producing $CD4^+$ T cells percentages and decreased hepatic IL23-p19 and IL17A expression levels. qRT-PCR analysis of sorted hepatic MNPs demonstrated high

expression levels of IL-23 mRNA specifically by $CX_3CR1^{hi}CD11c^+$ monocyte-derived macrophages.

Conclusion: Our results indicate a major role for IL-23 produced by hepatic monocyte-derived macrophages in the pathogenesis of PBC. These results may pave the road for the development of new immune-based and cell specific therapeutic modalities for PBC patients not responding to current therapies.

Keywords: primary biliary cholangitis, monocytes, macrophages, cytokines, interleukin-23

INTRODUCTION

Primary Biliary Cholangitis (PBC) is a chronic cholestatic liver disease characterized by progressive destruction of the intrahepatic bile ducts, leading to cholestasis, portal inflammation, fibrosis and potentially cirrhosis and liver failure (1). Mononuclear phagocytes (MNPs) are myeloid immune cells comprised of monocytes, macrophages (MFs) and dendritic cells (DCs). These cells are strategically positioned throughout the body tissues where they ingest and degrade dead cells, debris, and foreign material, and orchestrate inflammatory processes (2, 3). Studies in PBC patients, demonstrated accumulation of MNPs in the liver as well as impaired function of these cells. Mononuclear cells expressing the low-density lipoprotein binding glycoprotein CD68 were detected in the biliary epithelial layer of PBC patients, whereas in viral hepatitis these cells were scattered, and in normal livers were rarely seen around bile ducts (4). We have recently revealed a major role for $Ly6C^{hi}$ monocytes in PBC pathogenesis and demonstrated significant amelioration of disease development by inhibiting the recruitment of these cells into the liver (5). Interleukin 23 (IL-23) is a pro-inflammatory cytokine belonging to the IL-12 family of heterodimeric cytokines (6). IL-12 and IL-23 share a common p40 chain as well as a common IL-12RB1 chain in their respective cognate receptors. IL-23 consists of two subunits, p19 and the shared p40 chain (6) and signals through a heterodimeric receptor consisting of the IL-23R chain and the shared IL- 12RB1 (6). IL-23 was shown to be essential for disease development in several models of autoimmune diseases, including psoriasis, inflammatory bowel disease and experimental autoimmune encephalomyelitis (7). The mechanism by which IL-23 exerts its pathogenic role has been mostly scrutinized in the context of Th17 cells, which were thought to mediate autoimmunity by secretion of IL-17 family cytokines. Studies in PBC patients showed higher IL-23p19 mRNA expression levels in PBMC's from PBC patients that were correlated with PBC disease stages. Moreover, serum levels of IL-23 and IL-17 were positively correlated with serum GGT levels (8) and immunohistochemistry studies revealed expression of IL-23p19 in portal tracts of patients with advance disease (9). Mice deficient for IL-23 in all cells were found to be protected from PBC development (10), however the mechanisms involved and the cellular source of IL-23 has not been investigated. Of note, it has been suggested that IL-23 is expressed specifically by inflamed portal hepatocytes in PBC patients (9). Exposure to xenobiotics have been shown to be associated with break of immune tolerance in PBC (11). Xenobiotic modified PDC-E2 peptides mimic lipoic acid in a way that anti-PDC-E2 antibodies from PBC patients recognize them and results in higher titer reactivity than the native autoantigen. Notably, quantitative structure–activity relationship analysis identified 2-octynoic acid (2OA) as a xenobiotic candidate for antigenic modification of the PDC-E2 peptide (12–14). Thus, we have established a murine model for PBC based on immunization of mice with 2OA conjugated to bovine serum albumin (2OA-BSA) resulting in the appearance of anti-PDCE2 antibodies and histological lesions typical of autoimmune cholangitis 8 weeks following 2OA-BSA immunization (15).

By taking advantage of the 2OA-BSA inducible murine PBC model and transgenic mice that enabled targeting of IL-23 specifically in MNPs, we explored the importance of this cytokine expression uniquely by these cells, in the pathogenesis of autoimmune cholangitis.

Abbreviations: PBC, primary biliary cholangitis; 2OA-BSA, 2-octynoic acid conjugated to bovine serum albumin; CX_3CR1, C-X3-C motif chemokine receptor 1; DC, dendritic cells; MoMF, monocyte-derived macrophages H&E, hematoxylin and eosin; IFN-γ, interferon gamma; IL-1β, interleukin 1 beta; IL-17, interleukin 17, IL-12, interleukin 12; IL-23, interleukin 23; Ccl2, chemokine (C-C motif) ligand 2; TNF-α, tumor necrosis factor alpha.

MATERIAL AND METHODS

Mice

This study included the following animals: Cx3cr1-cre mice (JAX stock no. 025524, B6J.B6N(Cg)-Cx3cr1tm1.1(cre)Jung/J) (16), CD11c-cre mice (17), Il23-flox mice (18) and heterozygote Cx3cr1-gfp/+ reporter mice (19). Only female mice were used. Cre-negative littermates were used as controls. Animals were maintained in the animal facility of the Tel-Aviv Sourasky Medical Center. Mice had unlimited access to food and water, were kept in temperature and humidity-controlled rooms, and were maintained in a 12-h light/dark cycle. Use of animals was in accordance with the National Institutes of Health policy on the care and use of laboratory animals and was approved by the Tel-Aviv Sourasky Medical Center Animal Use and Care Committee.

Preparation of Immunogen

2-octynoic acid (2OA) was purchased from Sigma-Aldrich (St Louis, MO, USA) and was conjugated with BSA (EMD Chemicals, Gibbstown, NJ, USA), as described previously (15). Briefly, 2OA was dissolved in dry dimethyl ether.

N-hydroxysuccinimide (NHS) was then added and the solution was cooled to 0°C and stirred for 20 minutes. Dicyclohexylcarbodimide was then added and the mixture was allowed to warm to ambient temperature overnight. The solution was filtered and concentrated. The product was then purified using flash chromatography (30% ethyl acetate/hexane). NHS-activated 2OA was dissolved in dimethyl sulphoxide and then coupled to the lysine residues of BSA. The solution was allowed to react for 3 hours followed by dialysis [phosphate-buffered saline (PBS)].

Immunization

Female mice were immunized at 8 weeks of age by an intraperitoneally (i.p) injection of 2OA conjugated to BSA (2OA-BSA) at 1mg/ml per animal in the presence of complete Freund's adjuvant (CFA) (Sigma-Aldrich) containing 10mg/ml of Mycobacterium tuberculosis strain H37Ra. Additionally, pertussis toxin (Sigma-Aldrich, 100ng/animal) was delivered i.p. on the day of immunization and 2 days after. A boost immunization was done 2 weeks following the initial immunization with 2OA-BSA in incomplete Freund's adjuvant (Sigma-Aldrich). End of experiments were carried out 8 weeks following initial immunization.

Histopathology

Mice livers were fixed in Formaldehyde 4% buffered (ph7.2), embedded in paraffin, cut into 4-µm sections, deparaffinized and stained with hematoxylin and eosin (H&E). A liver pathologist, blinded to treatment allocation, evaluated disease severity. 4 parameters were considered and each got a score between 0-2 (normal, moderate, or severe, respectively): 1.Portal infiltrate, 2.Bile duct damage and loss, 3. Granulomas formation and 4. Lobular inflammation, reaching a maximum score of 8.

Isolation of Hepatic Non-Parenchymal Cells for Flow Cytometry

Hepatic non-parenchymal cells were isolated as previously described (20). In brief, mice were anesthetized and the livers were perfused with cold PBS. Cervical dislocation was performed and the livers were excised. Small fragments of liver were incubated (37°C, 250 rpm for 45minutes) in the presence of 5ml digestion buffer [5% FBS, 0.5 mg/ml collagenase IV (Sigma-Aldrich, Rehovot, Israel, C5138-500MG), 0.1 mg/ml Deoxyribonuclease I from bovine pancreas (Sigma-Aldrich, USA) in $PBS^{+/+}$]. Following the incubation, the livers were filtered through 200µm wire mesh. To discard parenchymal cells, washings with $PBS^{-/-}$ at 400 rpm, 4°C for 5 minutes was done three times harvesting the supernatant and discarding the parenchymal cell pellet. Last, supernatant was centrifuged at 1500rpm, 4°C, 5 minutes followed by ACK Lysing buffer (0.15 M NH4Cl, 0.01 M KHCO3) to exclude erythrocytes and washed with $PBS^{-/-}$.

Stimulation of T Cells for IL-17A Detection

Hepatic non-parenchymal cells were stimulated with 20 ng/ml PMA and 1µg/ml Ionomycin in the presence of 10µg/ml Brefeldin A in RPMI 1640 medium (supplemented with 10% heat-inactivated fetal bovine serum, 2 mM L-glutamine, 100 units ml^{-1} penicillin and 100 mg ml^{-1} streptomycin) at 37°C in a humidified incubator with 5% CO2.

Following 4h of stimulation, cells were washed and stained for the T cells surface markers TCRβ, CD3, CD4 and CD8. Then, cells were washed and fixed with the Flow Cytometry Fixation and Permeabilization Buffer Kit I (R&D Systems) for 30 min in 4°C. Cells were washed with permeabilization buffer and stained for intracellular IL-17A.

Flow Cytometry Analysis and Sorting

Non-parenchymal liver cells were incubated with monoclonal antibody 2·4G2 for FcR blocking (BioLegend, San Diego, CA, USA) and then exposed at 4°C to a mixture of the following antibodies (dilutions are indicated):anti-mouse CD45 (clone 30-F11, 1:100), anti-mouse/human CD11b (clone M1/70, 1:300), anti-mouse Ly6C (clone HK1.4, 1:300), anti-mouse MHCII (clone M5/114.15.2, 1:200), anti-mouse CD11c (clone N418, 1:100), anti-mouse CD3ϵ (clone 145-2c11, 1:100), anti-mouse CD8a (clone 53-6.7, 1:100), anti-mouse CD4 (clone GK1.5, 1:100), anti-mouse TCRβ (clone 457-597, 1:100) all were purchased from BioLegend, San Diego, CA. Anti-mouse F4/80 (clone REA 126, 1:100) and anti-mouse Tim4 (clone REA999, 1:100) were purchased from Miltenyi Biotech.

For IL-17A staining, cells were first stained for surface markers, then the cells were fixed and permeabilized prior to intra-cellular staining with IL-17 (Clone TC11-18H10.1, 1:50, BioLegend). Cells were analyzed with BD FACS Canto™ II (BD Bioscience) or sorted with a FACSAria flow cytometer (BD Bioscience). Flow cytometry analysis was performed using FlowJo software (TreeStar, Ashland, OR).

Quantitative Real-Time PCR

RNeasy Micro kit (QIAGEN) was used to isolate RNA from the liver. cDNA was prepared using the High-Capacity cDNA Reversed transcription kit (Applied Biosystems) according to the manufacturer's instructions.

PCRs were performed with the SYBER green PCR Master Mix (Applied Biosystems) and with Taqman chemistry (Applied Biosystems) for IL-23p19 and IL-17A. Quantification was done with Step One software (V2.2). The Transcripts were tested, analyzed, and normalized relative to a housekeeping gene ribosomal protein, large P0 (RPLP0) and TATA-binding protein (TBP), for the genes IL-17A and IL-23p19 respectively.

Primer sequences were:

Gene	Forward primer	Reverse primer
RPLP0	TCCAGCAGGTGTTTGACAAC	CCATCTGCAGACACACACT
IFN-γ	GCGTCATTGAATCACACCTG	TGAGCTCATTGAATGCTTGG
TNF-α	CGAGTGACAAGCCTGTAGCC	CCTTGTCCCTTGAAGAGAACC
Ccl-2	AGGTCCCTGTCATGCTTCTG	GCTGCTGGTGATCCTCTTGT
IL-6	ACAGTGTGGGAAGCAAGTCC	TCGGTATCGAAGCTGGAACT
IL-12p40	GCAAAGAAACATGGACTTGAAGTTC	CACATGTCACTGCCCGAGAGT
IL-1β	GACCTTCCAGGATGAGGACA	AGCTCATATGGGTCCGACAG
CX_3CR1	AAGTTCCCTTCCCATCTGCT	CGAGGACCACCAACAGATTT
Ly6C	GCAGTGCTACGAGTGCTATGG	ACTGACGGGTCTTTAGTTTCCTT

Statistical Analysis

The results are presented as mean ± SEM. Statistical analysis was performed using Two-tailed Student *t* test; *p* values < 0.05 were considered as significant.

RESULTS

Monocyte and Monocyte-Derived Macrophages Become the Dominant Subsets of MNPs in the Liver Following Induction of Autoimmune Cholangitis

The healthy liver harbors a large population of immune cells, however, under inflammatory conditions, the cellular composition of this hepatic immune compartment changes rapidly and dramatically (5, 20, 21). The hepatic mononuclear phagocytes (MNPs) comprise of monocyte, dendritic cells (DCs) and monocyte derived macrophages (MoMF). We have recently demonstrated that infiltration of Ly6C^{hi} monocytes to the liver is crucial to the pathogenesis of PBC and inhibition of the recruitment of these cells ameliorated all aspects of the disease (5). To examine the dynamics in the distribution of hepatic immune cells during autoimmune cholangitis, we performed multiparameter flow cytometry analyses on purified non-parenchymal liver cells from 2OA-BSA immunized mice. As shown in **Figure 1A** and **Supplementary Figure 1**, we have detected six major populations: Kupffer cells (P1) defined as CD11b^{int}F4/80^{hi}Tim-4^{pos}, infiltrating classical monocytes (P2) defined as CD11b^{pos}Ly6c^{hi}MHC-II^{neg}, Neutrophils (P3) defined as CD11b^{hi}Ly6c^{int}MHC-II^{neg}, and another population we termed myeloid-APC (antigen presenting cells) (P4) defined as CD11b^{pos}Ly6c^{low}MHC-II^{pos}Tim-4^{neg} CD11c^{pos}CX$_3$CR1^{pos} cells. Taking advantage of the Cx3cr1-gfp

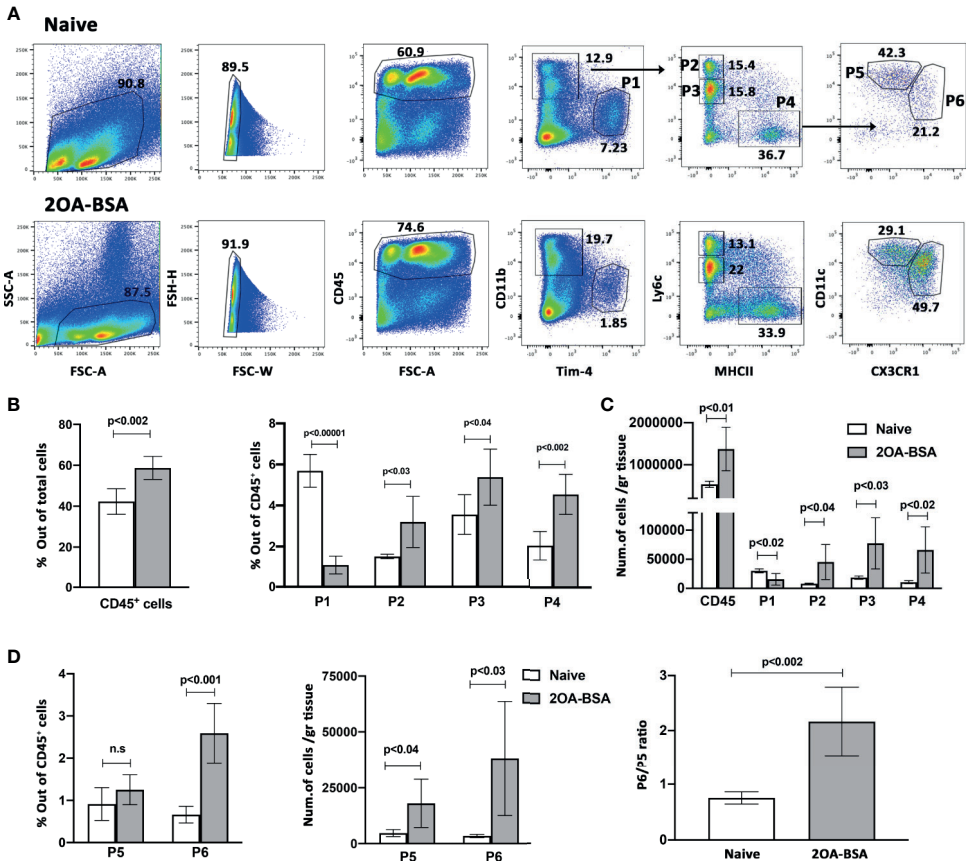

FIGURE 1 | Monocyte and monocyte-derived macrophages become the dominant subset of MNPs in the liver following induction of autoimmune cholangitis. **(A)** Representative flow cytometry analyses of purified non-parenchymal liver cells from naïve mice (upper panel) and 2OA-BSA immunized mice 8 weeks following immunization (lower panel). **(B)** Graphical summary of flow cytometry analysis of non-parenchymal liver cells; left graph summarizes the percentages of CD45-positive cells out of total cells and the right graph summarizes the percentages of each cell population out of CD45-positive cells. **(C)** Graphical summary of cells numbers normalized for liver tissue mass for CD45-positive cells and P1-P4 cell subsets. **(D)** Graphical summary of flow cytometry analysis showing the percentages of P5 and P6 cell populations out of CD45-positive cells (left panel), absolute cell numbers of P5 and P6 cell populations normalized for liver tissue mass (middle panel), and P6/P5 ratio (right panel), in naïve mice vs. 2OA-BSA immunized mice 8 weeks post immunization. Results presented as mean ± SEM (n≥5) for each group. Results are representative of two independent experiments. *p* values < 0.05 were considered as significant (unpaired Student's *t*-test).

reporter mice (19), the P4 population can be further segregated into $CD11c^{hi}CX_3CR1^{int}$ (P5) and $CD11c^{int}CX_3CR1^{hi}$ (P6) sub-populations, that represent myeloid dendritic cells and monocyte-derived macrophages (MoMF), respectively. During murine autoimmune cholangitis, a significant increase in neutrophils, $Ly6C^{hi}$ monocytes and myeloid-APCs population was found, whereas the KC population was significantly reduced (**Figures 1A, B**). Interestingly, focusing on myeloid-APCs (P4 population) under autoimmune cholangitis conditions, the $CD11c^{int}CX_3CR1^{hi}$ MoMF became the dominant subset (**Figure 1C**).

The IL-23-T_H-17 Pathway Is Activated in the 2OA-BSA Murine PBC Model

To address the involvement of IL-23-T_H-17 signaling pathway in experimental autoimmune cholangitis, we isolated non-parenchymal liver cells from naïve and 2OA-BSA immunized mice 8 weeks following immunization. Cells were stimulated with PMA and Ionomycin, as described in materials and methods, for detection of the intra-cellular cytokine IL-17A.

First, we looked at the T cell population in the liver and found that the percentage of T cells present in the liver following 2OA-BSA immunization were elevated and that the CD4/CD8 ratio was significantly decreased in the immunized mice, indicating massive infiltration of CD8 T cells (**Figures 2B, C**, respectively).

Flow cytometry analyses revealed a 4-fold increase in the incidence of hepatic IL-17A producing $CD4^+$ T cells in autoimmune cholangitis (**Figures 2A, D**). Moreover, these results were accompanied by a 3-fold and a 300-fold increase in IL23-p19 and IL17A expression levels in autoimmune cholangitis versus healthy controls, respectively (**Figure 2E**), as evaluated in the whole liver tissue by qPCR.

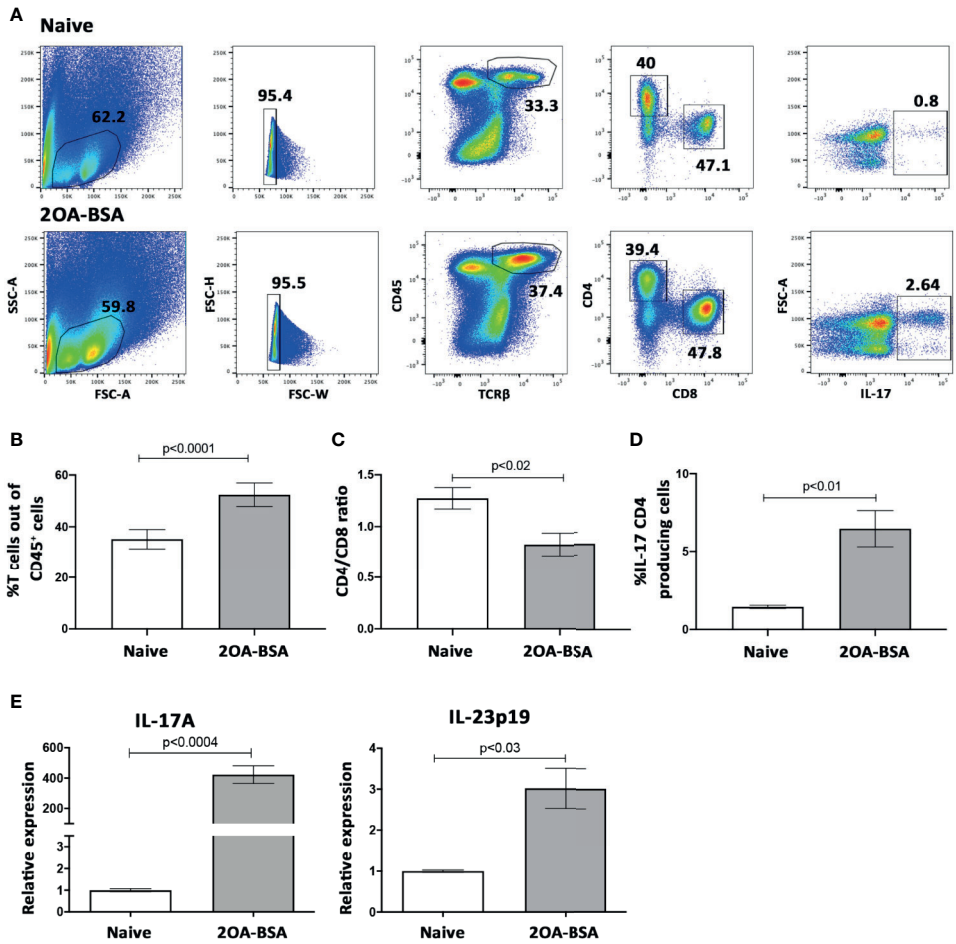

FIGURE 2 | IL-23-T_H-17 pathway is activated in the 2OA-BSA autoimmune cholangitis model. 2OA-BSA immunized mice and match-aged naïve mice were evaluated for: **(A)** Flow cytometry analyses of purified non-parenchymal liver cells, with a focus on intra hepatic T cells, from naïve mice (upper panel) and 2OA-BSA immunized mice (lower panel). **(B)** Graphical summary of the percentages of T cells out of CD45-positive cells. **(C)** Graphical summery of the CD4/CD8 T cell ratio. **(D)**. Graphical summery of the percentages of IL-17 CD4-positive producing cells. **(E)** Relative expression of hepatic IL-17A and IL-23p19 assessed by qPCR. Results presented as mean ± SEM (n≥5) for each group. Results are representative of two independent experiments. p values < 0.05 were considered as significant (unpaired Student's t-test).

MNPs-Restricted IL-23 Deficient Mice Display Attenuated Disease Severity in the 2OA-BSA Autoimmune Cholangitis Model

To evaluate the impact of MNPs restricted IL-23 deficiency on autoimmune cholangitis development we immunized CD11c^{cre}P19$^{fl/fl}$, CX$_3$CR1^{cre}P19$^{fl/fl}$ and their P19$^{fl/fl}$ littermates control mice with 2OA-BSA. A pronounced periportal infiltration of lymphocytes and mononuclear cells and bile ducts destruction was observed in P19$^{fl/fl}$ mice, whereas, in both MNPs restricted IL-23 deficient mice almost no irregularities were detected (**Figure 3A**). Histology score given by a blinded pathologist revealed a significant attenuation in disease severity in both MNPs restricted IL-23 deficient mice (**Figure 3B**).

To further investigate the effect of MNPs restricted IL-23 deficiency on liver inflammation, expression of pro-inflammatory cytokines and chemokines in liver tissue were examined by quantitative real time PCR. The levels of *Ifnγ*, *Tnfα*, *Il1β*, *Il6*, *Il12p40* and *Ccl2* were significantly increased in *P19$^{fl/fl}$* mice but not in CD11c^{cre}P19$^{fl/fl}$ and/or CX$_3$CR1^{cre}P19$^{fl/fl}$ mice immunized with 2OA-BSA. These results indicate that IL-23 derived from MNPs profoundly contributes to the development of pro-inflammatory response in experimental autoimmune cholangitis (**Figure 3C**).

MNPs Restricted IL-23 Deficient Mice Display a Significant Reduction in the Frequency of Hepatic IL-17A Producing CD4$^+$ T Cells and Diminished Activity of the IL-23-IL17 Axis in the Liver

We next attempted to determine the impact of specific MNPs-restricted IL-23 on the prevalence of hepatic IL-17A producing CD4$^+$ T cells and the overall activity of IL-23 and IL-17 in the liver. Thus, 8 weeks following 2OA-BSA immunization, non-parenchymal cells were isolated from MNPs restricted IL-23 deficiency mice and from P19$^{fl/fl}$ littermate controls and subjected

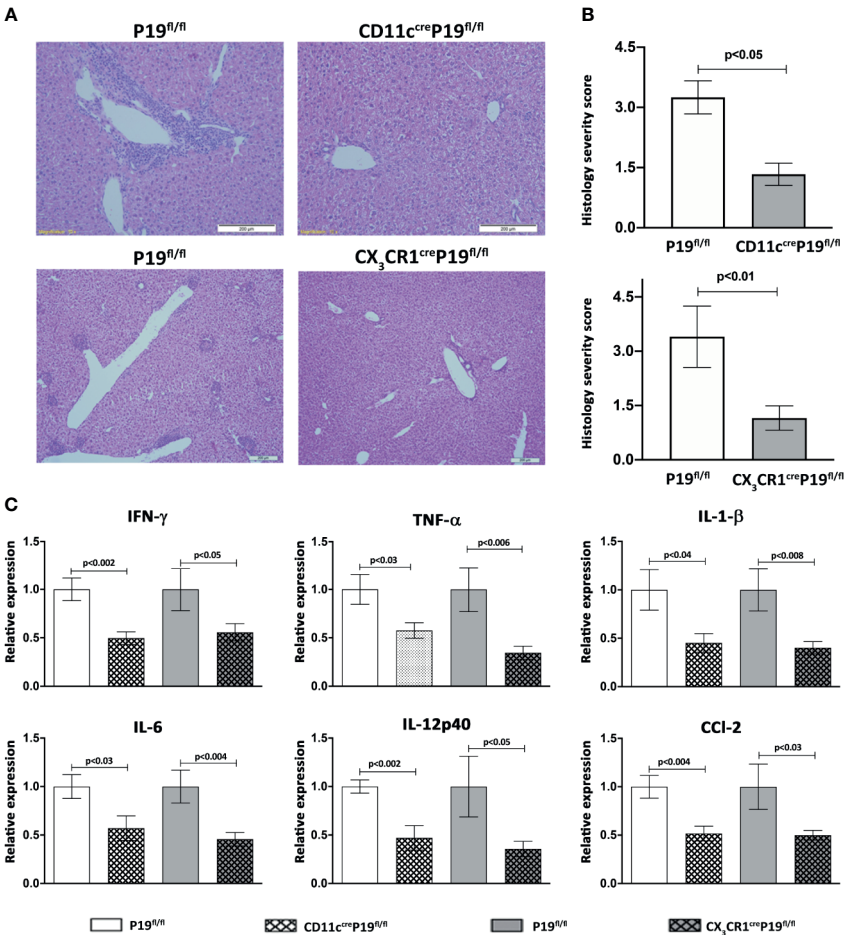

FIGURE 3 | MNPs-restricted IL-23 deficient mice display attenuated disease severity in the 2OA-BSA autoimmune cholangitis model. MNPs-restricted IL-23 deficient and littermate controls mice were immunized with 2OA-BSA. Disease severity was evaluated 8 weeks following immunization by histological assessment of liver sections stained for hematoxylin &eosin, original magnification 40X **(A)**, accompanied by graphical summary of histological severity score **(B)**. Graphical summary depicting expression levels of hepatic cytokines of indicated mice **(C)**. All data presented as mean ± SEM (n≥10) for each group. Results are representative of two independent experiments. p values < 0.05 were considered as significant (unpaired Student's t-test).

to flow cytometry analysis. We have found a notable and significant elevation in the CD4/CD8 ratio in both MNPs restricted IL-23 deficient mice, implying reduced infiltration of CD8 T cells to the liver (**Figure 4B**). In the $CX_3CR1^{cre}P19^{fl/l}$ mice, a significant reduction in hepatic IL-17A producing $CD4^+$ T cells as compared to $P19^{fl/fl}$ littermate controls was detected (**Figures 4A, C**). Moreover, qPCR analyses showed that the hepatic expression levels of IL-17A and IL-23p19 were significantly lower in $CX_3CR1^{cre}P19^{fl/l}$ mice whereas only hepatic levels of IL-23p19 were decreased in $CD11c^{cre}P19^{fl/fl}$ (**Figure 4D**). These could be due to a more robust protection from autoimmune induced cholangitis in $CX_3CR1^{cre}P19^{fl/l}$ mice, as was found also by liver histology assessment (**Figures 3A, B**).

High Expression Levels of IL-23 mRNA by Hepatic MNPs Population Expressing Both CD11c and CX_3CR1

To specifically identify the subset of cells responsible for IL-23 secretion in the liver during autoimmune cholangitis, we sorted 4 populations of non-parenchymal cells from 2OA-BSA immunized mice: Kupffer cells (P1), $Ly6C^{hi}$ Monocytes (P2) and the two subpopulations of myeloid APCs, P5 and P6 (see details in **Figures 1** and **5A**). This time, the sorting strategy to distinguish between myeloid DCs (P5) and MoMF (P6), was not based on CX_3CR1 expression (as depicted in **Figure 1A**) rather by CD11c and MHCII. To validate our sorted populations, we performed qPCR analysis of sorted cells first for Ly6C and confirmed that it is specifically expressed by classical monocyte-P2 as expected. Increased Ly6C expression levels were detected also in P5 and P6 subsets, supporting their origin from infiltrating monocytes (**Figure 5B**). Next, we performed qPCR analysis of sorted cells for CX_3CR1 expression levels and demonstrated higher levels in population P2 and P6, as expected from the flow cytometry analysis and strengthen P6 as the MoMF population (as described in **Figure 1A**). Of note, qPCR analysis of sorted cells from autoimmune cholangitis mice demonstrated unique high expression levels of IL-23 mRNA by P6 sub-population

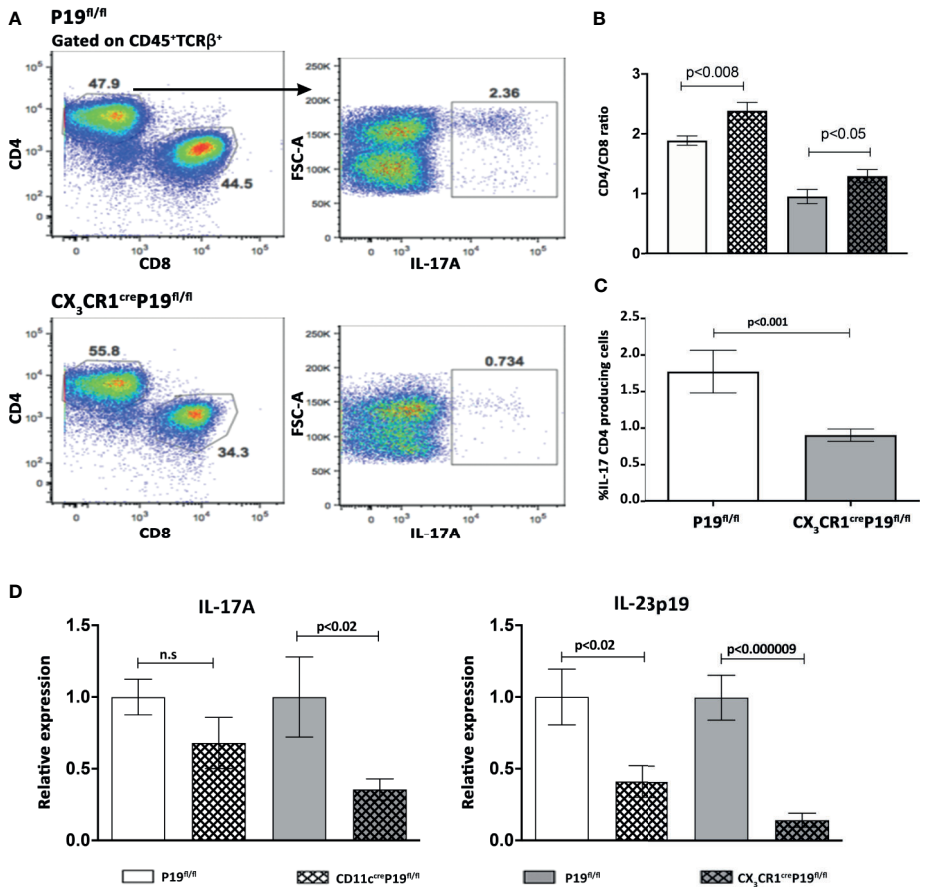

FIGURE 4 | MNPs restricted IL-23 deficient mice display a significant diminished activity of the IL-23-IL17 axis in the liver. **(A)** Flow cytometry analyses of purified non-parenchymal liver cells from indicated groups of mice, 8 weeks following 2OA-BSA immunization. **(B)** Graphical summary of the percentages of CD4/CD8 T cells ratio from $CD11c^{cre}P19^{fl/fl}$ and $CX_3CR1^{cre}P19^{fl/fl}$ immunized mice compared to their littermates' controls. **(C)** Graphical summary of the percentages of IL-17 $CD4^+$ producing cells in $CX_3CR1^{cre}P19^{fl/fl}$ immunized mice vs. $P19^{fl/fl}$ littermate controls. **(D)** Relative expression of hepatic IL-17A and IL-23p19 assessed by qPCR from indicated groups of mice, 8 weeks following 2OA-BSA immunization. Results presented as mean ± SEM (n≥10) for each group. Results are representative of two independent experiments p values < 0.05 were considered as significant (unpaired Student's t-test).

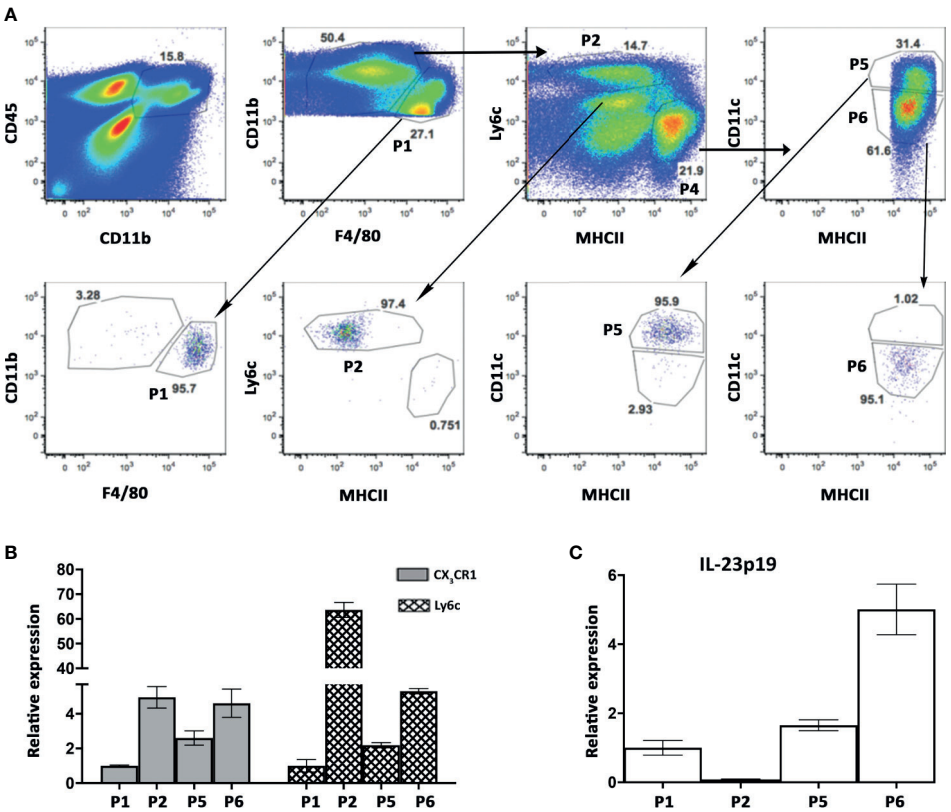

FIGURE 5 | High expression levels of IL-23 mRNA by hepatic MNPs population expressing both CD11c and CX_3CR1. **(A)** Flow cytometry sorting strategy of hepatic MNPs sub-populations from autoimmune cholangitis mice, 8 weeks following 2OA-BSA immunization (upper panel, and post-sorted cell populations (lower panel). **(B)** Graphical summary of qPCR analysis showing fold mRNA expression of CX_3CR1, Ly6C **(B)** and IL-23p19 **(C)** in sorted cell populations. Graph depicts means (SEM) of two independent experiments; each experiment comprised of pooled RNA from 5 mice.

(**Figure 5C**), a CX_3CR1^{hi} monocyte-derived macrophage that accumulate in the livers of animals with chronic autoimmune cholangitis (**Figure 1**).

DISCUSSION

In the current study we explored the importance of IL-23 expression by mononuclear phagocytes (MNPs) for the development of experimental autoimmune cholangitis. We showed that MNPs become the dominant cell subset in the liver during autoimmune cholangitis and that the IL-23-T_H-17 pathway is activated. MNPs-restricted IL-23 deficient mice displayed attenuated disease severity, that was accompanied by a significant decrease in the percentage of hepatic IL-17 producing CD4 T cells. Sorting of hepatic APCs sub-populations revealed high expression levels of IL-23p19 mRNA specifically by CX_3CR1^{hi} monocyte-derived macrophages, suggesting that IL-23 produced by these cells have a major role in the pathogenesis of PBC.

Interleukin 23 (IL-23) is a key pro-inflammatory cytokine important for the development of chronic inflammatory diseases. It is reported to be produced by various cellular sources including antigen-presenting cells as well as neutrophils, eosinophils and even non-immune cells (22–25). To specifically address the critical cell subset responsible for IL-23 production in experimental autoimmune cholangitis, we took advantage of two complementary conditional murine models. The $CD11c^{cre}$ strain targets classical dendritic cells and plasmacytoid DCs, as well as monocyte-derived cells. However, expression of CD11c has been demonstrated in other lineages including NK cells, NKT cells, IgA+ plasma cells as well as some CD11c+ B and T cells (26–29). The $Cx3cr1^{cre}$ strain is more specific to monocytes-derived cells, however resident tissue macrophages (e.g., hepatic Kupffer cells) and subsets of mast cells and DCs were shown to be targeted as well (16, 30). Our results demonstrating decrease in disease severity in both $CD11c^{cre}$IL-23p19$^{fl/fl}$ and $Cx3cr1^{cre}$IL-23p19$^{fl/fl}$ mice, overcome this limitation of non-specific targeting and prove that MNPs are the critical cellular source of IL-23 in autoimmune cholangitis. It should be noted that although both strains showed amelioration of disease severity, a more robust improvement in disease severity accompanied by decrease in IL-23-IL17A signaling was found in $Cx3cr1^{cre}$IL-23p19$^{fl/fl}$ mice (**Figures 3**, **4**), implying monocyte derived macrophages as the major source of IL-23 in this pathology. This was corroborated by the remarkable elevated expression levels of IL-23 mRNA found in CX_3CR1^{hi} monocyte-derived macrophages sorted from the livers of affected mice.

An important role of IL-23 in human PBC has been suggested as IL-23-positive cells were detected in livers of patients with advanced stage PBC and IL-23 serum levels were found to be in correlation with PBC disease severity (8, 9). Of note, Ustekinumab, an anti-IL-12/23 monoclonal antibody, has failed to achieve the alkaline phosphatase biochemistry endpoint in a phase 2 clinical trial (31). Nevertheless, modulation of the IL-12/23-related pathways was observed in a subset of patients with a decrease in alkaline phosphatase (31). Thus, assessment of other parameters, beside cholestatic liver enzymes is probably needed when evaluating response to biological treatments in PBC. Interestingly, in a transgenic murine model of PBC (dominant-negative form of transforming growth factor beta receptor type II) deletion of the p40 subunit, but not the p35 subunit resulted in amelioration of disease severity (32, 33), suggesting an important role for IL-23, but not IL-12 in this pathology. Moreover, it has been shown in other autoimmune disorders that IL-12 inhibition may even have a negative effect on disease course, a finding that has been attributed to a regulatory function of IL-12 *via* several mechanisms (34). Thus, specific IL-23 inhibition in a selected population of PBC patients with excessive inflammatory activity is worth an evaluation in a well-designed clinical trial.

In conclusion, we have recently revealed the critical role of hepatic monocyte infiltration for the development of experimental PBC; here, we have found that IL-23 production by these monocyte-derived cells drive this pathology. Our results support further evaluation of cell and cytokine specific therapeutic approaches in PBC patients not responding to current therapies.

DATA AVAILABILITY STATEMENT

The raw data supporting the conclusions of this article will be made available by the authors, without undue reservation.

ETHICS STATEMENT

The animal study was reviewed and approved by Tel-Aviv Sourasky Medical Center Animal Use and Care Committee.

AUTHOR CONTRIBUTIONS

EZ, MG, and DR designed and guided the research. DR and MRB performed the animal experiments and analyzed most of the experiments. PV, PL, and PT contributed to research design and/or conducted experiments. EB performed the histological disease severity assessment. EZ and DR wrote the manuscript. All authors contributed to the article and approved the submitted version.

FUNDING

This work was supported in part by the Israel Science Foundation (ISF) grant no. 2226/14, the United States–Israel Binational Science Foundation (BSF) grant no. 2013297, and by National Institutes of Health grant DK067003.

SUPPLEMENTARY MATERIAL

The Supplementary Material for this article can be found online at: https://www.frontiersin.org/articles/10.3389/fimmu.2021.718841/full#supplementary-material

Supplementary Figure 1 | Kupffer cells are CD11b^{int}Tim-4^{pos}F4/80$^{hi.}$ Flow cytometry strategy for KC identification by indicated Abs.

REFERENCES

1. Lleo A, Leung PSC, Hirschfield GM, Gershwin EM. The Pathogenesis of Primary Biliary Cholangitis: A Comprehensive Review. *Semin Liver Dis* (2020) 40(1):34–48. doi: 10.1055/s-0039-1697617
2. Miah M, Goh I, Haniffa M. Prenatal Development and Function of Human Mononuclear Phagocytes. *Front Cell Dev Biol* (2021) 9:649937. doi: 10.3389/fcell.2021.649937
3. Varol C, Mildner A, Jung S. Macrophages: Development and Tissue Specialization. *Annu Rev Immunol* (2015) 33:643–75. doi: 10.1146/annurev-immunol-032414-112220
4. Shimoda S, Harada K, Niiro H, Taketomi A, Maehara Y, Tsuneyama K, et al. CX3CL1 (Fractalkine): A Signpost for Biliary Inflammation in Primary Biliary Cirrhosis. *Hepatology* (2010) 51(2):567–75. doi: 10.1002/hep.23318
5. Reuveni D, Gore Y, Leung PSC, Lichter Y, Moshkovits I, Kaminitz A, et al. The Critical Role of Chemokine (C-C Motif) Receptor 2-Positive Monocytes in Autoimmune Cholangitis. *Front Immunol* (2018) 9:1852. doi: 10.3389/fimmu.2018.01852
6. Oppmann B, Lesley R, Blom B, Timans JC, Xu Y, Hunte B, et al. Novel P19 Protein Engages IL-12p40 to Form a Cytokine, IL-23, With Biological Activities Similar as Well as Distinct From IL-12. *Immunity* (2000) 13(5):715–25. doi: 10.1016/S1074-7613(00)00070-4
7. Croxford AL, Mair F, Becher B. IL-23: One Cytokine in Control of Autoimmunity. *Eur J Immunol* (2012) 42(9):2263–73. doi: 10.1002/eji.201242598
8. Qian C, Jiang T, Zhang W, Ren C, Wang Q, Qin Q, et al. Increased IL-23 and IL-17 Expression by Peripheral Blood Cells of Patients With Primary Biliary Cirrhosis. *Cytokine* (2013) 64(1):172–80. doi: 10.1016/j.cyto.2013.07.005
9. Yang CY, Ma X, Tsuneyama K, Huang S, Takahashi T, Chalasani NP, et al. IL-12/Th1 and IL-23/Th17 Biliary Microenvironment in Primary Biliary Cirrhosis: Implications for Therapy. *Hepatology* (2014) 59(5):1944–53. doi: 10.1002/hep.26979
10. Kawata K, Tsuda M, Yang GX, Zhang W, Tanaka H, Tsuneyama K, et al. Identification of Potential Cytokine Pathways for Therapeutic Intervention in Murine Primary Biliary Cirrhosis. *PloS One* (2013) 8(9):e74225. doi: 10.1371/journal.pone.0074225
11. Wang J, Yang G, Dubrovsky AM, Choi J, Leung PS. Xenobiotics and Loss of Tolerance in Primary Biliary Cholangitis. *World J Gastroenterol* (2016) 22(1):338–48. doi: 10.3748/wjg.v22.i1.338
12. Amano K, Leung PS, Rieger R, Quan C, Wang X, Marik J, et al. Chemical Xenobiotics and Mitochondrial Autoantigens in Primary Biliary Cirrhosis: Identification of Antibodies Against a Common Environmental, Cosmetic, and Food Additive, 2-Octynoic Acid. *J Immunol* (2005) 174(9):5874–83. doi: 10.4049/jimmunol.174.9.5874
13. Gershwin ME, Mackay IR. The Causes of Primary Biliary Cirrhosis: Convenient and Inconvenient Truths. *Hepatology* (2008) 47(2):737–45. doi: 10.1002/hep.22042
14. Long SA, Quan C, Van de Water J, Nantz MH, Kurth MJ, Barsky D, et al. Immunoreactivity of Organic Mimeotopes of the E2 Component of Pyruvate

Dehydrogenase: Connecting Xenobiotics With Primary Biliary Cirrhosis. *J Immunol* (2001) 167(5):2956–63. doi: 10.4049/jimmunol.167.5.2956
15. Wakabayashi K, Lian ZX, Leung PS, Moritoki Y, Tsuneyama K, Kurth MJ, et al. Loss of Tolerance in C57BL/6 Mice to the Autoantigen E2 Subunit of Pyruvate Dehydrogenase by a Xenobiotic With Ensuing Biliary Ductular Disease. *Hepatology* (2008) 48(2):531–40. doi: 10.1002/hep.22390
16. Yona S, Kim KW, Wolf Y, Mildner A, Varol D, Breker M, et al. Fate Mapping Reveals Origins and Dynamics of Monocytes and Tissue Macrophages Under Homeostasis. *Immunity* (2013) 38(1):79–91. doi: 10.1016/j.immuni.2012.12.001
17. Caton ML, Smith-Raska MR, Reizis B. Notch-RBP-J Signaling Controls the Homeostasis of CD8- Dendritic Cells in the Spleen. *J Exp Med* (2007) 204 (7):1653–64. doi: 10.1084/jem.20062648
18. Thakker P, Leach MW, Kuang W, Benoit SE, Leonard JP, Marusic S. IL-23 is Critical in the Induction But Not in the Effector Phase of Experimental Autoimmune Encephalomyelitis. *J Immunol* (2007) 178(4):2589–98. doi: 10.4049/jimmunol.178.4.2589
19. Jung S, Aliberti J, Graemmel P, Sunshine MJ, Kreutzberg GW, Sher A, et al. Analysis of Fractalkine Receptor CX(3)CR1 Function by Targeted Deletion and Green Fluorescent Protein Reporter Gene Insertion. *Mol Cell Biol* (2000) 20(11):4106–14. doi: 10.1128/MCB.20.11.4106-4114.2000
20. Zigmond E, Samia-Grinberg S, Pasmanik-Chor M, Brazowski E, Shibolet O, Halpern Z, et al. Infiltrating Monocyte-Derived Macrophages and Resident Kupffer Cells Display Different Ontogeny and Functions in Acute Liver Injury. *J Immunol* (2014) 193(1):344–53. doi: 10.4049/jimmunol.1400574
21. Kubes P, Jenne C. Immune Responses in the Liver. *Annu Rev Immunol* (2018) 36:247–77. doi: 10.1146/annurev-immunol-051116-052415
22. Arnold IC, Mathisen S, Schulthess J, Danne C, Hegazy AN, Powrie F. CD11c (+) Monocyte/Macrophages Promote Chronic Helicobacter Hepaticus-Induced Intestinal Inflammation Through the Production of IL-23. *Mucosal Immunol* (2016) 9(2):352–63. doi: 10.1038/mi.2015.65
23. Ehst B, Wang Z, Leitenberger J, McClanahan D, de la Torre R, Sawka E, et al. Synergistic Induction of IL-23 by TNFalpha, IL-17A, and EGF in Keratinocytes. *Cytokine* (2021) 138:155357. doi: 10.1016/j.cyto.2020.155357
24. Guerra ES, Lee CK, Specht CA, Yadav B, Huang H, Akalin A, et al. Central Role of IL-23 and IL-17 Producing Eosinophils as Immunomodulatory Effector Cells in Acute Pulmonary Aspergillosis and Allergic Asthma. *PloS Pathog* (2017) 13(1):e1006175. doi: 10.1371/journal.ppat.1006175
25. Kvedaraite E, Lourda M, Idestrom M, Chen P, Olsson-Akefeldt S, Forkel M, et al. Tissue-Infiltrating Neutrophils Represent the Main Source of IL-23 in the Colon of Patients With IBD. *Gut* (2016) 65(10):1632–41. doi: 10.1136/gutjnl-2014-309014
26. Bennett CL, Clausen BE. DC Ablation in Mice: Promises, Pitfalls, and Challenges. *Trends Immunol* (2007) 28(12):525–31. doi: 10.1016/j.it.2007.08.011
27. Hebel K, Griewank K, Inamine A, Chang HD, Muller-Hilke B, Fillatreau S, et al. Plasma Cell Differentiation in T-Independent Type 2 Immune Responses Is Independent of CD11c(high) Dendritic Cells. *Eur J Immunol* (2006) 36 (11):2912–9. doi: 10.1002/eji.200636356
28. Hume DA. Applications of Myeloid-Specific Promoters in Transgenic Mice Support In Vivo Imaging and Functional Genomics But Do Not Support the Concept of Distinct Macrophage and Dendritic Cell Lineages or Roles in Immunity. *J Leukoc Biol* (2011) 89(4):525–38. doi: 10.1189/jlb.0810472
29. van Rijt LS, Jung S, Kleinjan A, Vos N, Willart M, Duez C, et al. In Vivo Depletion of Lung CD11c+ Dendritic Cells During Allergen Challenge Abrogates the Characteristic Features of Asthma. *J Exp Med* (2005) 201 (6):981–91. doi: 10.1084/jem.20042311
30. Abram CL, Roberge GL, Hu Y, Lowell CA. Comparative Analysis of the Efficiency and Specificity of Myeloid-Cre Deleting Strains Using ROSA-EYFP Reporter Mice. *J Immunol Methods* (2014) 408:89–100. doi: 10.1016/j.jim.2014.05.009
31. Hirschfield GM, Gershwin ME, Strauss R, Mayo MJ, Levy C, Zou B, et al. Ustekinumab for Patients With Primary Biliary Cholangitis Who Have an Inadequate Response to Ursodeoxycholic Acid: A Proof-of-Concept Study. *Hepatology* (2016) 64(1):189–99. doi: 10.1002/hep.28359
32. Tsuda M, Zhang W, Yang GX, Tsuneyama K, Ando Y, Kawata K, et al. Deletion of Interleukin (IL)-12p35 Induces Liver Fibrosis in Dominant-Negative TGFbeta Receptor Type II Mice. *Hepatology* (2013) 57(2):806–16. doi: 10.1002/hep.25829
33. Yoshida K, Yang GX, Zhang W, Tsuda M, Tsuneyama K, Moritoki Y, et al. Deletion of Interleukin-12p40 Suppresses Autoimmune Cholangitis in Dominant Negative Transforming Growth Factor Beta Receptor Type II Mice. *Hepatology* (2009) 50(5):1494–500. doi: 10.1002/hep.23132
34. Torres T. Selective Interleukin-23 P19 Inhibition: Another Game Changer in Psoriasis? *Focus Risankizumab Drugs* (2017) 77(14):1493–503. doi: 10.1007/s40265-017-0794-1

Conflict of Interest: PT is employed by Regeneron Pharmaceuticals, Inc.

The remaining authors declare that the research was conducted in the absence of any commercial or financial relationships that could be construed as a potential conflict of interest.

Publisher's Note: All claims expressed in this article are solely those of the authors and do not necessarily represent those of their affiliated organizations, or those of the publisher, the editors and the reviewers. Any product that may be evaluated in this article, or claim that may be made by its manufacturer, is not guaranteed or endorsed by the publisher.

Copyright © 2021 Reuveni, Brezis, Brazowski, Vinestock, Leung, Thakker, Gershwin and Zigmond. This is an open-access article distributed under the terms of the Creative Commons Attribution License (CC BY). The use, distribution or reproduction in other forums is permitted, provided the original author(s) and the copyright owner(s) are credited and that the original publication in this journal is cited, in accordance with accepted academic practice. No use, distribution or reproduction is permitted which does not comply with these terms.

frontiers in Immunology

REVIEW
published: 13 August 2021
doi: 10.3389/fimmu.2021.724601

The Role of Retinal Pigment Epithelial Cells in Regulation of Macrophages/Microglial Cells in Retinal Immunobiology

Andrew W. Taylor, Samuel Hsu and Tat Fong Ng*

Department of Ophthalmology, Boston University School of Medicine, Boston, MA, United States

The ocular tissue microenvironment is immune privileged and uses several mechanisms of immunosuppression to prevent the induction of inflammation. Besides being a blood-barrier and source of photoreceptor nutrients, the retinal pigment epithelial cells (RPE) regulate the activity of immune cells within the retina. These mechanisms involve the expression of immunomodulating molecules that make macrophages and microglial cells suppress inflammation and promote immune tolerance. The RPE have an important role in ocular immune privilege to regulate the behavior of immune cells within the retina. Reviewed is the current understanding of how RPE mediate this regulation and the changes seen under pathological conditions.

Keywords: ocular immune privilege, immune tolerance, retinal pigment epithelial cells (RPE), retinal immunobiology, suppressor macrophages

OPEN ACCESS

Edited by:
Alexander Steinkasserer, University Hospital Erlangen, Germany

Reviewed by:
Chen Yu, Duke University, United States
Paul Gerard McMenamin, Monash University, Australia

****Correspondence:***
Andrew W. Taylor
awtaylor@bu.edu

Specialty section:
This article was submitted to Antigen Presenting Cell Biology, a section of the journal Frontiers in Immunology

Received: *13 June 2021*
Accepted: *28 July 2021*
Published: *13 August 2021*

Citation:
Taylor AW, Hsu S and Ng TF (2021) The Role of Retinal Pigment Epithelial Cells in Regulation of Macrophages/Microglial Cells in Retinal Immunobiology. Front. Immunol. 12:724601. doi: 10.3389/fimmu.2021.724601

INTRODUCTION

Ocular Immune Privilege

The eye is called immune privileged from the original observations of prolonged allograft survival within the anterior chamber even following immunization to alloantigens (1). This now includes immune regulation and immune tolerance to antigens and pathogens within the eye (2–4). The ocular microenvironment is delineated by blood barriers and the lack of direct lymphatic drainage. Within this microenvironment immune cells differentiate into cells that suppress inflammation and promote immune tolerance (5). The mediators of ocular immune regulation and tolerance are soluble, and membrane bound molecules. An important membrane bound molecule is membrane FasL (6, 7). Its expression by cells of the ocular blood-barriers, including the retinal pigment epithelial cells (RPE), mediates a contact dependent induction of apoptosis in monocytes and lymphocytes preventing their accumulation and infiltration. Also, the RPE release extracellular membranes expressing membrane-FasL that also induce apoptosis in macrophages potentially away from the RPE monolayer (8). Many of the soluble mediators of ocular immunosuppression can be found in aqueous humor and in the supernatant of cultured RPE. These mediators include a wide range immunoregulating cytokines, neuropeptides, and soluble ligands. These include Transforming Growth Factor-beta2 (TGF-β2) and alpha-Melanocyte Stimulating Hormone (α-MSH), which are highly conserved and potent regulators of immune cell activity and suppressors of inflammation (9–12). The current picture of ocular immune privilege is a tissue

microenvironment that actively manipulates immune cells to promote the health of the visual axis, and to prevent the activation of inflammation. These mechanisms of ocular immune privilege are for most of us highly effective in preventing inflammation, and the mediators of immune privilege have potential to be therapeutically adapted to suppress inflammation within the eye and in other tissues.

One of the experimental examples of ocular immune privilege is the phenomena of anterior chamber associated immune deviation (ACAID) (13, 14). ACAID is induced by placing foreign antigen within the anterior chamber of the eye. The antigen is picked up and processed for presentation by F4/80 positive macrophages that migrate to the spleen (15, 16). In the spleen with the help of recruited B-cells and NK T cells, there is an antigen-specific activation and expansion of both CD8 and CD4 regulatory T cells (17–20). This brings about systemic tolerance to the foreign antigen. Placing foreign antigen in the subretinal space (the temporary pocket that forms when the photoreceptors are detached from the RPE) also induces an ACAID-like response (21). This has defined immune privilege to include the retina.

RPE Regulation of Immune Activity

The placement of neonatal-retinal allografts into the retina are not immunologically rejected and moreover they differentiate (22). Also, there is induced tolerance to the alloantigen through an ACAID-like response. The induction of the ACAID-like response is mediated by TGF-β2 like in ACAID; however, it requires the expression of Thrombospondin-1 (TSP-1) (23). The TSP-1 is a known activator of latent TGF-β2 (24). In mice with TSP-1 knocked out the ACAID-like response cannot be induced; moreover, TSP-1 knock-out mice with experimental autoimmune disease (EAU) cannot self-resolve EAU like wild-type mice. The ACAID-like response cannot be induced when the integrity of the RPE monolayer is compromised through chemical or laser wounding (21, 25, 26). In addition, laser wounding not only causes the loss of immune privilege in the affected eye but also causes a loss of immune privilege in the untouched contralateral eye. This may be mediated by the release of Substance P by the retina (26). Together the results demonstrate the need for an intact RPE monolayer to maintain ocular immune privilege.

The ACAID-like response shows that the RPE directly affect the functionality of immune cells by maintaining the anti-inflammatory retinal microenvironment. One of the interesting findings is that the RPE soluble molecules induce and enhance regulatory activity in Treg cells (27–29). Also, the RPE release soluble factors that suppress the activation of effector T cells (23, 30). Of interest in this review is the ability of the RPE to regulate potential antigen presenting cells, the immune cells that sit at the interface of innate and adaptive immune response. The RPE have been found to suppress the activation of dendritic cells (31, 32), which would prevent naive T cell activation to antigen carried from the retina to a regional lymph node. In addition, the RPE promote the development and activation of myeloid suppressor cells from bone-marrow progenitor cells (33). These suppressor cells are highly capable of preventing and inhibiting adaptive immune responses. Interestingly, the RPE induction of these suppressor cells is mediated by IL-6, which is usually considered a proinflammatory cytokine and an anti-ACAID cytokine (34).

Using a technique of *in situ* RPE eyecup cultures, treating endotoxin-stimulated macrophages with the RPE eyecup conditioned culture-media suppresses proinflammatory cytokine production, while promoting anti-inflammatory activity (35–37). Moreover, the treatment of macrophages with the RPE soluble factors induces anti-inflammatory cytokine production and characteristics of myeloid suppressor cells (37). The mediators of this activity are the neuropeptides α-MSH, and Neuropeptide Y (NPY) produced by the RPE. The collective action of the soluble factors, constitutively produced by the RPE, induce macrophages, and resident microglial cells to be themselves mediators of anti-inflammatory activity and activators of Treg cells. These findings demonstrate the importance of the RPE monolayer in maintaining immune privilege.

RPE PHYSIOLOGY

RPE Function

The health and integrity of the RPE monolayer may very well be required for maintaining immune regulation along with maintaining a functional retina. The RPE is a cuboidal monolayer of hexagonal cells that lies between the photoreceptors and Bruch's membrane (38). On the apical side, the RPE has microvilli that envelop the distal-ends of the photoreceptors with each RPE cell projecting towards 20-55 photoreceptors (39–41). On the basal side lies Bruch's membrane a pentalaminar structure, which separates the RPE from the eye's fenestrated choroidal capillaries (42). The RPE maintains this polarity through a complex network of tight junctions near the apical side that create a barrier to paracellular diffusion (43). The tight junctions include occludins and claudins both of which play essential regulatory roles in maintenance of the function of the tight junctions. The composition of claudins expressed in the RPE varies by species (44). In the human RPE, claudin 19 is the most predominant and mutations of CLDN10 gene that encodes it can lead to dysfunction of the tight junctions along with severe ocular abnormalities (43, 45).

The RPE plays a variety of critical roles in maintaining the function of the retina including acting as the outer blood-retina barrier and regulating the transport of waste and nutrients (46, 47). In order to accomplish these functions, the RPE exhibits polarity with an asymmetric distribution of organelles, proteins, and functionality allowing it to create a unique microenvironment for the retina (48). For example, melanosomes are preferentially located near the apical cell membrane with Golgi and mitochondria preferentially localize to basal cytoplasm (38). The visual cycle is dependent on the conversion of 11-cis-retinol to 11-trans-retinol and the RPE plays a key role in re-isomerizing 11-cis-retinol from 11-trans-retinol (39, 49, 50). Many of the key metabolic enzymes involved in this re-isomerization process are expressed in the RPE (39). The photoreceptors have a delicate equilibrium between nutrient renewal and damaged component disposal which sheds up to 10% of their volume. The RPE

phagocytizes the end-processes allowing new end-processes to take their place (39).

RPE and the Retinal Blood Barrier

In the healthy retina, the RPE separates the choroidal blood supply from photoreceptors and manages the microenvironment of the retina by regulating the flow of water and ions between the two spaces (51). The RPE contains tight junctions that play a role in its ability to act as the outer part of the blood-retina barrier (47). In studies on chicken RPE, it was shown that the tight junctions of the RPE have increased complexities with P-face-associated tight junctions *vs* the tight junctions in choroid vessels (52). This increased complexity may be necessary for the formation of an effective blood-retina barrier. However, *in vitro* studies have indicated that the functional barrier for macromolecules, specifically serum albumin, is similar between the RPE and the iris pigment epithelium (53). This suggests that at the very least the general barrier function of the RPE is like other tight-junction epithelial layers. The regulation of what can enter the retina is apparent as the outer blood-retinal barrier formed by the RPE sometimes poses a problem in the use of some systemic drugs for the treatment of retinal diseases (54). However, even with the blood-retina barrier of the RPE and its tight junctions, the retina is still susceptible to damage, as in the case of some systemic medications lead to retinal dysfunction and degeneration (21, 55).

In disease states like AMD and Alzheimer's, the accumulation of Aβ in the RPE *via* RAGE/p38 MAPK-mediated endocytosis can lead to attenuation and disorganization of the tight junctions, and in some cases breakdown of the tight junctions (56, 57). In AMD the leading cause of visual impairment in western countries of people over 50 (58), damage to the RPE and RPE dysfunction are thought to be the initial insult in the atrophic variant which accounts for 85-90% of cases (40, 59). In the wet variant, while the choriocapillaris complex is thought to be the initial site of dysfunction, damage to the RPE soon follows and plays a key role in visual loss (59).

The breakdown of the blood-retina barrier created by the RPE has been shown to be one of the earliest pathologic changes that can be detected in some diseases like diabetes (60). In diabetic retinopathy, previous work has noted that the involvement of the inner blood-retina barrier due to endothelial cell dysfunction can lead to diabetic macular oedema and retinopathy (47). The dysfunction of the outer blood-retina barrier at the RPE may play a role in diabetic retinopathy in that the presence of cytokines, such as IL-6, have been shown to disrupt the outer blood-retina barrier through amplified recruitment of microglial cells and increased production of TNF- α (61). Additionally, high glucose states have been shown to lead to RPE cells downregulating GLUT-1 and a reduction in the levels of antioxidants potentially leading to retinal tissue damage (62). In some rodent studies the breakdown of the tight junctions in the RPE results in vascular leakage as visualized in diabetic and ischemic rodents (63). When the blood-retina barrier is compromised, it can lead to additional disease processes such as uveitic macular edema (64). Abnormal regulation of the RPE in mice lacking ATP-binding cassette transporters (ABCA1 and ABCG1) leads to discontinuities of the RPE and degeneration of the overlying photoreceptors (65). In some disease states like AMD and diabetic retinopathy the transplantation of RPE has even been explored as treatment options with some trials showing preliminary signs of success (66, 67). Interestingly in mice with degenerating photoreceptors, retinal microglia cells migrate from the inner retina to the subretinal space and undergo a transcriptional change to express homeostatic checkpoint and wound-responsive genes that protect the RPE (68). While it is not clear as to the signals that induced the migration, this does suggest that there is an initial attempt by the ocular microenvironment to preserve the functionality of the RPE and its blood-barrier under disease conditions. Therapeutic interventions that can maintain or restore RPE health could also maintain and restore immune privilege that would reduce the potential contribution of inflammation to many retinal degenerative diseases.

CHANGES IN THE RPE EXPERIMENTALLY INDUCED DISEASE

Laser Injury

The growing use of lasers in the military, healthcare, laboratories, and academia causes an increased in ocular injury by misdirected lasers (69). In general, lasers are classified as I, II, IIIa, IIIb and IV. The first two Classes of Class II and Class IIIa are relatively safe while the last two are hazardous. Laser light is visible between 400 and 700 nm, and other sources are infrared and ultraviolet lasers. Usually, transient exposure to Class II or Class IIIa laser may not result in eye injury. Handheld laser pointers are usually Class IIIa and have comparatively low energy that is insufficient to cause injury at the ocular surface, but the focusing power of the eye causes a powerful amplification of irradiance that makes the retina susceptible to laser injury. The prolonged exposure to this laser may cause severe, permanent, and irreversible damage accompanied with vision loss (70, 71).

The coagulative irradiation of laser causes an initial destruction and secondary tissue responses (**Figure 1**). The initial destruction occurs from the thermal degradation of the incident energy absorbed by RPE pigment and changes are seen almost immediately (72–75). Coagulation necrosis of the RPE and the photoreceptor cells happens at this acute stage. The inner-nuclear-layer (INL) is usually unharmed. The RPE barrier breaks down and cell debris is found within and between disrupted RPE and in the outer retina. Three days after laser burn, Bruch membrane is disrupted and the subretinal space and the inner retina are infiltrated with macrophages. The RPE and photoreceptors become necrotic (**Figure 1B**). Five days after laser burn, all photoreceptor cells around the burn area are gone, but most of the INL cells are still intact (**Figure 1C**). There is vacuoling of cells in the IP and the retinal ganglion cell (RGC) layers are seen. By day 14, the RPE show placoid and are found to cover the laser injury site partially. There were many clusters of pigment-filled macrophages around the injury site including in the INL (**Figure 1D**). By day 120, the RPE covers the injury site (75).

The RPE is not only a physical barrier but is also an important source of immune-suppressive molecules that contribute to the immune privileged status of the eye. In naive retinas, microglia are in the inner and outer plexiform layer and after laser injury they accumulate with macrophages and granulocytes at the site of the laser burn in the retina and choroid (76). Changes in retinal microglial cells can be seen 1 day after the laser injury with expression of MHC class II (75). In addition, co-stimulatory factors of CD40 and CD86 are found on these activated microglia. The condition media of cultured RPE eyecups from laser-wounded eyes contain significantly lower amounts of α-MSH (37). In the normal retina the microglia co-express NOS2 and Arginase1, but in laser wounded retinas co-expression of the two enzymes is not seen (37). Moreover, infiltrating the laser wound site are Arginase1-positive macrophages that are a source of VEGF to initiate choroidal neovascularization (37, 77). This corresponds with the loss of ACAID in both the eye with the laser injury and the unwounded counter-lateral eye (25, 26). This appears be mediated by the release of another neuropeptide Substance P. How this affects RPE regulation of immunity in the non-lasered eye is not understood; however, the laser wounded RPE monolayer does not induce the co-expression of NOS2 and Arginase 1 in macrophages (37). This further indicates the importance of an intact RPE monolayer for the RPE to regulate immune cells.

After the laser injury, the damage of the RPE and the surrounding neural retina and the underlying choroid, the retinal microglia and the choroidal inflammatory cells may mediate release of proinflammatory cytokines (78–80). These cytokines may exacerbate neuronal damage. Pro-angiogenic VEGF is the primary factor made and pro-inflammatory cytokines including IL-1β, IL-3, IL-6 and TNF-α would be necessary as a wound repair process following laser photocoagulation. In addition, production of chemokines including MCP-1 and MIP-2 are increased (75, 81). These show that physical damage of the RPE monolayer promotes the infiltration of immune cells and the induction of an inflammatory response. This has implications not only on laser wounding, but also on retinal degenerative diseases like age related macular degeneration as RPE cells die.

Experimental Autoimmune Uveitis

Autoimmune uveitis is one of the leading causes of blindness in developed countries. The retina is usually the target, but the RPE cells may also be killed as collateral damage due to inflammation (82, 83). The common rodent models of experimental

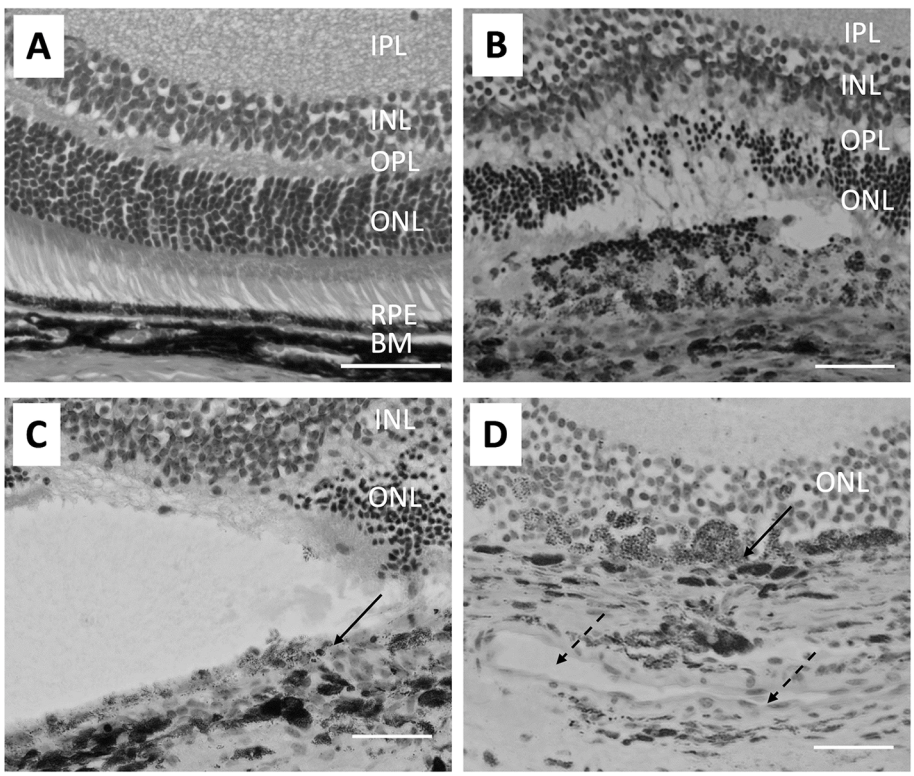

FIGURE 1 | Micrographs show the pathological changes of retina and choroid from day 0 to day 14 after laser injury. **(A)** shows a healthy naive retina. The RPE is a single cell layer. **(B)** shows the retina on day 3 after laser injury. Bruch's membrane is disrupted and RPE cells and most ONL cells are lost at the laser injury site. Also, arrangement of pigmented cells in the choroid is disrupted. **(C)** Similar histological structures are seen on day 5 after retinal laser-injury. Solid arrow points to the discontinued RPE cells. **(D)** shows the retina 14 days after laser injury. A large capillary (broken arrows) forms in the choroid adjacent to the laser injury site. Macrophages filled with pigment are found in the ONL and some RPE (solid arrow) are found covering the injured site with a disrupted Bruch's membrane. The size bar is 50 microns in length.

autoimmune uveitis (EAU) are induced with inter-photoreceptor retinoid-binding protein (IRBP) emulsified in adjuvant, and other models use retinal arrestin, rhodopsin and RPE-65 (84–86). The IRBP-model has a prodromal phase till day 14 and usually reaches a score of 1 on the clinical grading system and peaks on day 21 with a clinical score of 3. Then the disease progresses into a chronic phase of sustained clinical scores of 3 until day 70 where the disease begins to self-resolve (87, 88).

Histological evaluation of the eyes from rodents immunized to induce EAU show that the loss of the RPE monolayer is progressive along with the chronic nature of EAU (**Figure 2**) (89–91). Very little damage to the RPE is seen in the early stages of EAU (**Figures 2A–C**); however, As the disease progresses through the chronic phase, there is severe damage of both INL cells and photoreceptor cells, with the RPE shows damage with pigment-laden macrophages near the damaged RPE (**Figure 2D**).

The pathogenesis of inflammatory disorders of EAU is associated with autoreactive effector CD4+ T cells. In the early stages of IRBP-induced EAU the effector T cells are polarized to the Th1 phenotype and produce IFNγ (92, 93). These effector Th1 cells are highly active and mediate EAU in naive recipient animals. However, neutralizing IFNγ does not suppress EAU but worsen the disease because of the activation of Th17 cells (94–97). The Th17 cells target the RPE, and the disruption of the blood-retinal barrier causes the influx of serum antibodies, which exacerbate EAU (98). Mice with TSP-1 knocked-out also suffer with severe and prolonged EAU. To initiate a T cell response there needs to be present an APC expressing MHC class II. Normally the expression of MHC along with co-stimulatory molecules within the eye is low to undetectable, and while initially the microglia do not express MHC, they increase in MHC expression as EAU progresses (93, 99). In addition, there is need for the microglia in a non-MHC dependent manner to recruit effector T cells and MHC-expressing monocytes into the retina (99).

Since the course of EAU is self-limiting, it has suggested that while the RPE may be targeted and affected by the retinal inflammation there is still some immunosuppressive activity. It was found that EAU resolution is associated with the emergence of a specific type of APC within the spleen that in an antigen-specific manner counter-converts effector T cells into inducible Treg cells (88, 100). This process is dependent on the expression of the melanocortin 5-receptor (MC5r), one of the receptors of α-MSH. Moreover, expression of MC5r is necessary to modulate the severity of EAU and the functions of APC (91). The RPE is important to maintain the health of the retina not only by phagocytosis of photoreceptor outer segments, recycling retinol and maintaining the blood-retinal barrier, it also provides support to maintain immune privilege within the eye.

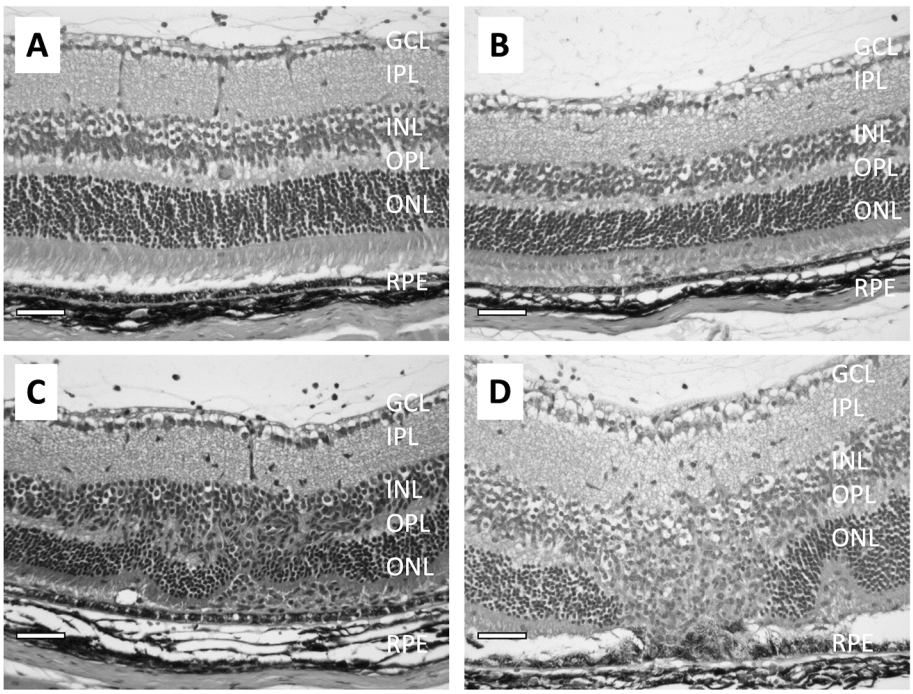

FIGURE 2 | Micrographs show the pathological changes of retina from mice with EAU clinical score ranging from 1 to 3. **(A)** shows a retina with EAU clinical score 1. The RPE is intact and there are no noted changes in the retina except for some inflammatory cells in the vitreous. **(B)** shows the retina with EAU clinical score 2. There are more infiltrating cells in the vitreous and the subretinal space. Both the retina and RPE are intact, with minor lesions found in the INL. **(C)** is the retina at early stage of chronic EAU, clinical score 3. The RPE is intact, and infiltration of inflammatory cells are found in the vitreous and in the retina with disruption of the INL and IPL with loss of the ONL cells. **(D)** shows the retina at a late stage of chronic EAU, sustained clinical score of 3. The RPE monolayer is disrupted and fused with the ONL and adjacent outer/inner segments of the photoreceptors gone. There are pigment-filled macrophages around sites of RPE cell loss. The size bar is 50 microns in length.

RPE AND REGULATION OF IMMUNITY

RPE Influenced Activity of Macrophages

ACAID demonstrates that macrophages with the potential of becoming antigen presenting cells (APC) are influenced by the ocular microenvironment to promote Treg cell activation. This has suggested that within the retina a similar influence should be seen with resident microglial cells. When assayed it is found that microglial cells are very much suppressed in immune activity; moreover, they co-express Nitric Oxide Synthase 2 (NOS2) with Arginase 1 (37). This co-expression of a M1 marker of inflammation-mediating cells and a M2 tissue repair/suppressor-mediating cells is characteristic of tumor associated myeloid cells that suppress immune attack of tumors (101, 102). Co-expression of NOS2 and Arginase 1 is induced by treating macrophages with the soluble factors of RPE. Specifically, it was found that the neuropeptides α-MSH and NPY produced by the RPE mediate this unique characterization of macrophages, which can enhance apoptosis in activated effector T cells (37). The soluble RPE factors also induce macrophages to produce anti-inflammatory cytokines even when the macrophages are treated with a pro-inflammatory signal such as endotoxin (35, 36, 103). This alternative activation of macrophages is mediated by α-MSH and provides for an anti-inflammatory response when there is an immune challenge within the ocular microenvironment (35). This potential for the retina to be a site of generating alternatively activated macrophages and myeloid-like suppressor cells makes the environment nor only anti-inflammatory but a site where immune cells are made to regulate other immune cells.

Phagocytizing materials is central for an APC to process antigen for presentation on MHC class II molecules (104). Recently we have found that the process of phagocytosis is also altered by the RPE through its release of α-MSH and NPY (105, 106). The neuropeptides mediate a differential regulation of phagocytic uptake of gram-negative and gram-positive bacteria (107). There is suppression in the number of gram-negative bacteria taken up and a suppression of the number of macrophages taking-up gram-positive bacteria. There is no change in the expression of scavenger receptors on the macrophages suggesting that this may be a change in how Toll-like receptor stimulation in the macrophages is suppressed (108, 109). If the bacteria are opsonized, there is no effect of the neuropeptide treatment on the up-take of opsonized-gram-negative and positive bacteria (107). However, activation of the phagolysosome is suppressed. The suppression is in part due to both downregulation of LAMP1, which is needed for phagolysosome acidification, and a blockade of the phagosome maturation pathway preventing the transition of phagosomes from early to intermediate (110). The suppression of phagocytosis and phagosome maturation by the RPE through the neuropeptides α-MSH and NPY would either prevent the processing of antigen within the retina or at least alter the processing of the antigen to unrecognizable amino-acid sequences that could be presented by APC in the retina (110). The RPE from eyes with autoimmune uveitis do not suppress the phagocytic pathway, and this may be associated with high levels of IL-6 expression (105). The regulation of phagolysosome activation is dependent also on the RPE maintaining an intact monolayer (106). Therefore, one potential contribution of the RPE to immune privilege is its suppression of the processing and presentation of self-antigens by retinal APC that would prevent the activation of autoimmune disease-mediating effector T cells. This importance of the RPE to mediate immune regulation and prevent induction of autoimmune disease indicates that changes to the RPE will have a corresponding change in the regulation of immune cells within the retina.

Recovery of RPE Mediated Immune Regulation

A key reason for understanding the molecular mechanisms of ocular immune privilege is to see whether these molecules that are normally regulating immune cell activity can be used to suppress uveitis and restore immune privilege. Since the neuropeptide α-MSH has its own immune regulating/anti-inflammatory properties as well as contributing to the mechanism of ocular immune privilege there is a strong potential of using α-MSH as a therapeutic approach to uveitis (111, 112). The neuropeptide is 13 amino acids long and is easily injected. When mice with EAU are treated with α-MSH at the beginning of the chronic phase the retinal inflammation begins to resolve within a week of the treatment (84, 91, 100). After 2 to 3 weeks EAU is fully resolved in comparison to another 8 weeks in the untreated EAU mice. In the spleen of the α-MSH-treated EAU mice are Treg cells specific for retinal autoantigen. These Treg cells provide the mice with protection from a memory immune response to the autoantigen. The same induction of Treg cell is found in the spleen of mice that have resolved EAU on their own (88, 113, 114). These Treg cells are derived from the population of effector T cells that are converted by APC into antigen-specific inducible Treg cells (88, 100). Under conditions of uveitis the RPE cannot suppress phagosome maturation and phagolysosome activation, and after α-MSH therapy the RPE recover their ability to suppress phagosome maturation and phagolysosome activation (91, 105). Therapeutic use of α-MSH in EAU suppresses uveitis, induces Treg cells to retinal autoantigen, and may very well reestablish RPE regulation of immune cell activity within the retina.

There is a dependency on MC5r for some of the EAU recovery. While MC5r-knockout mice recover on their own from EAU, like wild type mice, they lack the presence of the suppressor APC and the antigen-specific Treg cells within their spleens (100, 114, 115). While α-MSH treatment suppressed EAU in the knockout mice it does not protect the retina from the damage of inflammation, not did it promote recovery of RPE mediated suppression of phagolysosome activation (91). These results suggest that while the use of α-MSH in therapy to suppress inflammation is possible through its other receptors, it appears that the recovery of immune privilege is dependent on α-MSH working through MC5r. Also, by tailoring the therapy to specific melanocortin receptors different aspects of an immune response can be targeted for regulation (116). The experimental therapeutic use of α-MSH in EAU demonstrates that it is

possible to use the mechanisms of ocular immune privilege, and potentially other RPE generated molecules, to suppress inflammation and reestablish ocular immune privilege and tolerance (117, 118).

CONCLUSION

The RPE holds an important role in the maintenance of ocular immune privilege in being a blood-barrier and a producer of immune regulatory molecules. These molecules are not just anti-inflammatory, they promote immune regulatory and suppressive behaviors within immune cells they target. It makes these different for other forms of therapy that either suppress all immune activity or block specific key cytokines. The change in immune cells behavior by the RPE allows for immune cell activity to be supportive of the retina while immune cells regulate themselves and other immune cells that may migrate into the retina. While it is not fully understood as to whether in retinal diseases the change is first in the retina or in the RPE, but once the RPE layer is injured it is difficult for the retina to function and to prevent the activation of damaging immune activity.

AUTHOR CONTRIBUTIONS

All three authors were involved in the planning, writing and editing of this review and agree to be accountable for the content of this work. All authors contributed to the article and approved the submitted version.

FUNDING

This work is supported in part by a grant from the NIH/NEI EY025961 and the Massachusetts Lions Eye Research Fund.

REFERENCES

1. Medawar P. Immunity to Homologous Grafted Skin. III. The Fate of Skin Homografts Transplanted to the Brain to Subcutaneous Tissue, and to the Anterior Chamber of the Eye. *Br J Exp Pathol* (1948) 29:58–69.
2. Taylor AW, Kaplan HJ. Ocular Immune Privilege in the Year 2010: Ocular Immune Privilege and Uveitis. *Ocul Immunol Inflamm* (2010) 18(6):488–92. doi: 10.3109/09273948.2010.525730
3. Taylor AW. Ocular Immune Privilege. *Eye (Lond)* (2009) 23(10):1885–9. doi: 10.1038/eye.2008.382
4. Forrester JV, McMenamin PG, Dando SJ. CNS Infection and Immune Privilege. *Nat Rev Neurosci* (2018) 19(11):655–71. doi: 10.1038/s41583-018-0070-8
5. Taylor AW, Ng TF. Negative Regulators That Mediate Ocular Immune Privilege. *J Leukoc Biol* (2018) 103:1179–87. doi: 10.1002/JLB.3MIR0817-337R
6. Griffith TS, Brunner T, Fletcher SM, Green DR, Ferguson TA. Fas Ligand-Induced Apoptosis as a Mechanism of Immune Privilege. *Science* (1995) 270 (5239):1189–92. doi: 10.1126/science.270.5239.1189
7. Levy O, Calippe B, Lavalette S, Hu SJ, Raoul W, Dominguez E, et al. Apolipoprotein E Promotes Subretinal Mononuclear Phagocyte Survival and Chronic Inflammation in Age-Related Macular Degeneration. *EMBO Mol Med* (2015) 7(2):211–26. doi: 10.15252/emmm.201404524
8. Sanjiv N, Osathanugrah P, Fraser E, Ng TF, Taylor AW. Extracellular Soluble Membranes From Retinal Pigment Epithelial Cells Mediate Apoptosis in Macrophages. *Cells* (2021) 10(5):1193. doi: 10.3390/cells10051193
9. Taylor AW, Streilein JW, Cousins SW. Identification of Alpha-Melanocyte Stimulating Hormone as a Potential Immunosuppressive Factor in Aqueous-Humor. *Curr Eye Res* (1992) 11(12):1199–206. doi: 10.3109/02713689208999545
10. Cousins SW, Mccabe MM, Danielpour D, Streilein JW. Identification of Transforming Growth-Factor-Beta as an Immunosuppressive Factor in Aqueous-Humor. *Invest Ophth Vis Sci* (1991) 32(8):2201–11.
11. Granstein RD, Staszewski R, Knisely TL, Zeira E, Nazareno R, Latina M, et al. Aqueous-Humor Contains Transforming Growth-Factor-Beta and a Small (Less-Than 3500 Daltons) Inhibitor of Thymocyte Proliferation. *J Immunol* (1990) 144(8):3021–7.
12. Jampel HD, Roche N, Stark WJ, Roberts AB. Transforming Growth Factor-Beta in Human Aqueous Humor. *Curr Eye Res* (1990) 9(10):963–9. doi: 10.3109/02713689009069932
13. Streilein JW, Niederkorn JY. Induction of Anterior Chamber-Associated Immune Deviation Requires an Intact, Functional Spleen. *J Exp Med* (1981) 153(5):1058–67. doi: 10.1084/jem.153.5.1058
14. Kaplan HJ, Streilein JW. Do Immunologically Privileged Sites Require a Functioning Spleen? *Nature* (1974) 251(5475):553–4. doi: 10.1038/251553a0
15. Wilbanks GA, Streilein JW. Studies on the Induction of Anterior Chamber-Associated Immune Deviation (ACAID). 1. Evidence That an Antigen-Specific, ACAID-Inducing, Cell-Associated Signal Exists in the Peripheral Blood. *J Immunol* (1991) 146(8):2610–7.
16. Wilbanks GA, Streilein JW. Macrophages Capable of Inducing Anterior Chamber Associated Immune Deviation Demonstrate Spleen-Seeking Migratory Properties. *Reg Immunol* (1992) 4(3):130–7.
17. Faunce DE, Stein-Streilein J. NKT Cell-Derived RANTES Recruits APCs and CD8+ T Cells to the Spleen During the Generation of Regulatory T Cells in Tolerance. *J Immunol* (2002) 169(1):31–8. doi: 10.4049/jimmunol.169.1.31
18. D'Orazio TJ, Niederkorn JY. Splenic B Cells are Required for Tolerogenic Antigen Presentation in the Induction of Anterior Chamber-Associated Immune Deviation (ACAID). *Immunology* (1998) 95(1):47–55. doi: 10.1046/j.1365-2567.1998.00581.x
19. Sonoda KH, Sakamoto T, Qiao H, Hisatomi T, Oshima T, Tsutsumi-Miyahara C, et al. The Analysis of Systemic Tolerance Elicited by Antigen Inoculation Into the Vitreous Cavity: Vitreous Cavity-Associated Immune Deviation. *Immunology* (2005) 116(3):390–9. doi: 10.1111/j.1365-2567.2005.02239.x
20. Sonoda KH, Stein-Streilein J. Ocular Immune Privilege and CD1d-Reactive Natural Killer T Cells. *Cornea* (2002) 21(2 Suppl 1):S33–8. doi: 10.1097/00003226-200203001-00008
21. Wenkel H, Streilein JW. Analysis of Immune Deviation Elicited by Antigens Injected Into the Subretinal Space. *Invest Ophthalmol Vis Sci* (1998) 39 (10):1823–34.
22. Jiang LQ, Jorquera M, Streilein JW. Subretinal Space and Vitreous Cavity as Immunologically Privileged Sites for Retinal Allografts. *Invest Ophthalmol Vis Sci* (1993) 34(12):3347–54.
23. Zamiri P, Masli S, Kitaichi N, Taylor AW, Streilein JW. Thrombospondin Plays a Vital Role in the Immune Privilege of the Eye. *Invest Ophthalmol Vis Sci* (2005) 46(3):908–19. doi: 10.1167/iovs.04-0362
24. Taylor AW. Review of the Activation of TGF-Beta in Immunity. *J Leukoc Biol* (2009) 85(1):29–33. doi: 10.1189/jlb.0708415
25. Qiao H, Lucas K, Stein-Streilein J. Retinal Laser Burn Disrupts Immune Privilege in the Eye. *Am J Pathol* (2009) 174(2):414–22. doi: 10.2353/ajpath.2009.080766
26. Lucas K, Karamichos D, Mathew R, Zieske JD, Stein-Streilein J. Retinal Laser Burn-Induced Neuropathy Leads to Substance P-Dependent Loss of Ocular Immune Privilege. *J Immunol* (2012) 189(3):1237–42. doi: 10.4049/jimmunol.1103264

27. Sugita S, Horie S, Nakamura O, Futagami Y, Takase H, Keino H, et al. Retinal Pigment Epithelium-Derived CTLA-2alpha Induces TGFbeta-Producing T Regulatory Cells. *J Immunol* (2008) 181(11):7525–36. doi: 10.4049/jimmunol.181.11.7525
28. Kawazoe Y, Sugita S, Keino H, Yamada Y, Imai A, Horie S, et al. Retinoic Acid From Retinal Pigment Epithelium Induces T Regulatory Cells. *Exp Eye Res* (2012) 94(1):32–40. doi: 10.1016/j.exer.2011.11.002
29. Imai A, Sugita S, Kawazoe Y, Horie S, Yamada Y, Keino H, et al. Immunosuppressive Properties of Regulatory T Cells Generated by Incubation of Peripheral Blood Mononuclear Cells With Supernatants of Human RPE Cells. *Invest Ophthalmol Vis Sci* (2012) 53(11):7299–309. doi: 10.1167/iovs.12-10182
30. Aderem A, Underhill DM. Mechanisms of Phagocytosis in Macrophages. *Annu Rev Immunol* (1999) 17:593–623. doi: 10.1146/annurev.immunol.17.1.593
31. Sugita S, Kawazoe Y, Imai A, Usui Y, Iwakura Y, Isoda K, et al. Mature Dendritic Cell Suppression by IL-1 Receptor Antagonist on Retinal Pigment Epithelium Cells. *Invest Ophthalmol Vis Sci* (2013) 54(5):3240–9. doi: 10.1167/iovs.12-11483
32. Gregerson DS, Sam TN, McPherson SW. The Antigen-Presenting Activity of Fresh, Adult Parenchymal Microglia and Perivascular Cells From Retina. *J Immunol* (2004) 172(11):6587–97. doi: 10.4049/jimmunol.172.11.6587
33. Tu Z, Li Y, Smith D, Doller C, Sugita S, Chan CC, et al. Myeloid Suppressor Cells Induced by Retinal Pigment Epithelial Cells Inhibit Autoreactive T-Cell Responses That Lead to Experimental Autoimmune Uveitis. *Invest Ophthalmol Vis Sci* (2012) 53(2):959–66. doi: 10.1167/iovs.11-8377
34. Ohta K, Yamagami S, Taylor AW, Streilein JW. IL-6 Antagonizes TGF-Beta and Abolishes Immune Privilege in Eyes With Endotoxin-Induced Uveitis. *Invest Ophthalmol Vis Sci* (2000) 41(9):2591–9.
35. Lau CH, Taylor AW. The Immune Privileged Retina Mediates an Alternative Activation of J774A.1 Cells. *Ocul Immunol Inflamm* (2009) 17(6):380–9. doi: 10.3109/09273940903118642
36. Zamiri P, Masli S, Streilein JW, Taylor AW. Pigment Epithelial Growth Factor Suppresses Inflammation by Modulating Macrophage Activation. *Invest Ophthalmol Vis Sci* (2006) 47(9):3912–8. doi: 10.1167/iovs.05-1267
37. Kawanaka N, Taylor AW. Localized Retinal Neuropeptide Regulation of Macrophage and Microglial Cell Functionality. *J Neuroimmunol* (2011) 232 (1-2):17–25. doi: 10.1016/j.jneuroim.2010.09.025
38. Sparrow JR, Hicks D, Hamel CP. The Retinal Pigment Epithelium in Health and Disease. *Curr Mol Med* (2010) 10(9):802–23. doi: 10.2174/156652410793937813
39. Kiser PD, Golczak M, Palczewski K. Chemistry of the Retinoid (Visual) Cycle. *Chem Rev* (2014) 114(1):194–232. doi: 10.1021/cr400107q
40. Binder S, Stanzel BV, Krebs I, Glittenberg C. Transplantation of the RPE in AMD. *Prog Retin Eye Res* (2007) 26(5):516–54. doi: 10.1016/j.preteyeres.2007.02.002
41. Bairati AJr., Orzalesi N. The Ultrastructure of the Pigment Epithelium and of the Photoreceptor-Pigment Epithelium Junction in the Human Retina. *J Ultrastruct Res* (1963) 41:484–96. doi: 10.1016/S0022-5320(63)80080-5
42. Booij JC, Baas DC, Beisekeeva J, Gorgels TG, Bergen AA. The Dynamic Nature of Bruch's Membrane. *Prog Retin Eye Res* (2010) 29(1):1–18. doi: 10.1016/j.preteyeres.2009.08.003
43. Naylor A, Hopkins A, Hudson N, Campbell M. Tight Junctions of the Outer Blood Retina Barrier. *Int J Mol Sci* (2019) 21(1):211. doi: 10.3390/ijms21010211
44. Rizzolo LJ, Peng S, Luo Y, Xiao W. Integration of Tight Junctions and Claudins With the Barrier Functions of the Retinal Pigment Epithelium. *Prog Retin Eye Res* (2011) 30(5):296–323. doi: 10.1016/j.preteyeres.2011.06.002
45. Konrad M, Schaller A, Seelow D, Pandey AV, Waldegger S, Lesslauer A, et al. Mutations in the Tight-Junction Gene Claudin 19 (CLDN19) are Associated With Renal Magnesium Wasting, Renal Failure, and Severe Ocular Involvement. *Am J Hum Genet* (2006) 79(5):949–57. doi: 10.1086/508617
46. Lehmann GL, Benedicto I, Philp NJ, Rodriguez-Boulan E. Plasma Membrane Protein Polarity and Trafficking in RPE Cells: Past, Present and Future. *Exp Eye Res* (2014) 126:5–15. doi: 10.1016/j.exer.2014.04.021
47. Cunha-Vaz J, Bernardes R, Lobo C. Blood-Retinal Barrier. *Eur J Ophthalmol* (2011) 21:S3–9. doi: 10.5301/EJO.2010.6049
48. Burke JM. Epithelial Phenotype and the RPE: Is the Answer Blowing in the Wnt? *Prog Retin Eye Res* (2008) 27(6):579–95. doi: 10.1016/j.preteyeres.2008.08.002
49. Zhang J, Choi EH, Tworak A, Salom D, Leinonen H, Sander CL, et al. Photic Generation of 11-Cis-Retinal in Bovine Retinal Pigment Epithelium. *J Biol Chem* (2019) 294(50):19137–54. doi: 10.1074/jbc.RA119.011169
50. Jin M, Li S, Moghrabi WN, Sun H, Travis GH. Rpe65 is the Retinoid Isomerase in Bovine Retinal Pigment Epithelium. *Cell* (2005) 122(3):449–59. doi: 10.1016/j.cell.2005.06.042
51. Strauss O. The Retinal Pigment Epithelium. In: H Kolb, E Fernandez and R Nelson, editors. *Webvision: The Organization of the Retina and Visual System*. Salt Lake City (UT): Webvision John Moran Eye Center (1995).
52. Kniesel U, Wolburg H. Tight Junction Complexity in the Retinal Pigment Epithelium of the Chicken During Development. *Neurosci Lett* (1993) 149 (1):71–4. doi: 10.1016/0304-3940(93)90350-T
53. Rezai KA, Lappas A, Kohen L, Wiedemann P, Heimann K. Comparison of Tight Junction Permeability for Albumin in Iris Pigment Epithelium and Retinal Pigment Epithelium *In Vitro*. *Graefes Arch Clin Exp Ophthalmol* (1997) 235(1):48–55. doi: 10.1007/BF01007837
54. Liu L, Liu X. Roles of Drug Transporters in Blood-Retinal Barrier. *Adv Exp Med Biol* (2019) 1141:467–504. doi: 10.1007/978-981-13-7647-4_10
55. Tsang SH, Sharma T. Drug-Induced Retinal Toxicity. *Adv Exp Med Biol* (2018) 1085:227–32. doi: 10.1007/978-3-319-95046-4_48
56. Park SW, Kim JH, Mook-Jung I, Kim KW, Park WJ, Park KH, et al. Intracellular Amyloid Beta Alters the Tight Junction of Retinal Pigment Epithelium in 5XFAD Mice. *Neurobiol Aging* (2014) 35(9):2013–20. doi: 10.1016/j.neurobiolaging.2014.03.008
57. Park SW, Kim JH, Park SM, Moon M, Lee KH, Park KH, et al. RAGE Mediated Intracellular Abeta Uptake Contributes to the Breakdown of Tight Junction in Retinal Pigment Epithelium. *Oncotarget* (2015) 6(34):35263–73. doi: 10.18632/oncotarget.5894
58. Ambati J, Ambati BK, Yoo SH, Ianchulev S, Adamis AP. Age-Related Macular Degeneration: Etiology, Pathogenesis, and Therapeutic Strategies. *Surv Ophthalmol* (2003) 48(3):257–93. doi: 10.1016/S0039-6257(03)00030-4
59. Bhutto I, Lutty G. Understanding Age-Related Macular Degeneration (AMD): Relationships Between the Photoreceptor/Retinal Pigment Epithelium/Bruch's Membrane/Choriocapillaris Complex. *Mol Aspects Med* (2012) 33(4):295–317. doi: 10.1016/j.mam.2012.04.005
60. Cunha-Vaz J, Leite E, Sousa JC, de Abreu JR. Blood-Retinal Barrier Permeability and its Relation to Progression of Retinopathy in Patients With Type 2 Diabetes. A Four-Year Follow-Up Study. *Graefes Arch Clin Exp Ophthalmol* (1993) 231(3):141–5. doi: 10.1007/BF00920936
61. Jo DH, Yun JH, Cho CS, Kim JH, Kim JH, Cho CH. Interaction Between Microglia and Retinal Pigment Epithelial Cells Determines the Integrity of Outer Blood-Retinal Barrier in Diabetic Retinopathy. *Glia* (2019) 67(2):321–31. doi: 10.1002/glia.23542
62. Ponnalagu M, Subramani M, Jayadev C, Shetty R, Das D. Retinal Pigment Epithelium-Secretome: A Diabetic Retinopathy Perspective. *Cytokine* (2017) 95:126–35. doi: 10.1016/j.cyto.2017.02.013
63. Xu HZ, Le YZ. Significance of Outer Blood-Retina Barrier Breakdown in Diabetes and Ischemia. *Invest Ophthalmol Vis Sci* (2011) 52(5):2160–4. doi: 10.1167/iovs.10-6518
64. Sood G, Patel BC. Uveitic Macular Edema. In: *StatPearls [Internet]*. Treasure Island (FL): StatPearls Publishing (2021). Available at: https://www.ncbi.nlm.nih.gov/books/NBK562158/.
65. Storti F, Klee K, Todorova V, Steiner R, Othman A, van der Velde-Visser S, et al. Impaired ABCA1/ABCG1-Mediated Lipid Efflux in the Mouse Retinal Pigment Epithelium (RPE) Leads to Retinal Degeneration. *Elife* (2019) 8: e45100. doi: 10.7554/eLife.45100
66. Radtke ND, Aramant RB, Petry HM, Green PT, Pidwell DJ, Seiler MJ. Vision Improvement in Retinal Degeneration Patients by Implantation of Retina Together With Retinal Pigment Epithelium. *Am J Ophthalmol* (2008) 146 (2):172–82. doi: 10.1016/j.ajo.2008.04.009
67. Binder S, Krebs I, Hilgers RD, Abri A, Stolba U, Assadoulina A, et al. Outcome of Transplantation of Autologous Retinal Pigment Epithelium in Age-Related Macular Degeneration: A Prospective Trial. *Invest Ophthalmol Vis Sci* (2004) 45(11):4151–60. doi: 10.1167/iovs.04-0118
68. O'Koren EG, Yu C, Klingeborn M, Wong AYW, Prigge CL, Mathew R, et al. Microglial Function Is Distinct in Different Anatomical Locations During Retinal Homeostasis and Degeneration. *Immunity* (2019) 50(3):723–37e7. doi: 10.1016/j.immuni.2019.02.007

69. Barkana Y, Belkin M. Laser Eye Injuries. *Surv Ophthalmol* (2000) 44(6):459–78. doi: 10.1016/S0039-6257(00)00112-0
70. Ajudua S, Mello MJ. Shedding Some Light on Laser Pointer Eye Injuries. *Pediatr Emerg Care* (2007) 23(9):669–72. doi: 10.1097/PEC.0b013e31814b2dc4
71. Marshall J, O'Hagan JB, Tyrer JR. Eye Hazards of Laser 'Pointers' in Perspective. *Br J Ophthalmol* (2016) 100(5):583–4. doi: 10.1136/bjophthalmol-2016-308798
72. Marshall J, Bird AC. A Comparative Histopathological Study of Argon and Krypton Laser Irradiations of the Human Retina. *Br J Ophthalmol* (1979) 63 (10):657–68. doi: 10.1136/bjo.63.10.657
73. Wallow IH. Repair of the Pigment Epithelial Barrier Following Photocoagulation. *Arch Ophthalmol* (1984) 102(1):126–35. doi: 10.1001/archopht.1984.01040030104047
74. Takahashi K, Lam TT, Fu J, Tso MO. The Effect of High-Dose Methylprednisolone on Laser-Induced Retinal Injury in Primates: An Electron Microscopic Study. *Graefes Arch Clin Exp Ophthalmol* (1997) 235(11):723–32. doi: 10.1007/BF01880672
75. Ng TF, Turpie B, Masli S. Thrombospondin-1-Mediated Regulation of Microglia Activation After Retinal Injury. *Invest Ophthalmol Vis Sci* (2009) 50(11):5472–8. doi: 10.1167/iovs.08-2877
76. Eter N, Engel DR, Meyer L, Helb HM, Roth F, Maurer J, et al. In Vivo Visualization of Dendritic Cells, Macrophages, and Microglial Cells Responding to Laser-Induced Damage in the Fundus of the Eye. *Invest Ophthalmol Vis Sci* (2008) 49(8):3649–58. doi: 10.1167/iovs.07-1322
77. Liu J, Copland DA, Horie S, Wu WK, Chen M, Xu Y, et al. Myeloid Cells Expressing VEGF and Arginase-1 Following Uptake of Damaged Retinal Pigment Epithelium Suggests Potential Mechanism That Drives the Onset of Choroidal Angiogenesis in Mice. *PloS One* (2013) 8(8):e72935. doi: 10.1371/journal.pone.0072935
78. Richardson PR, Boulton ME, Duvall-Young J, McLeod D. Immunocytochemical Study of Retinal Diode Laser Photocoagulation in the Rat. *Br J Ophthalmol* (1996) 80(12):1092–8. doi: 10.1136/bjo.80.12.1092
79. Wittchen ES, Nishimura E, McCloskey M, Wang H, Quilliam LA, Chrzanowska-Wodnicka M, et al. Rap1 GTPase Activation and Barrier Enhancement in Rpe Inhibits Choroidal Neovascularization In Vivo. *PloS One* (2013) 8(9):e73070. doi: 10.1371/journal.pone.0073070
80. Krause TA, Alex AF, Engel DR, Kurts C, Eter N. VEGF-Production by CCR2-Dependent Macrophages Contributes to Laser-Induced Choroidal Neovascularization. *PloS One* (2014) 9(4):e94313. doi: 10.1371/journal.pone.0094313
81. Nagai N, Oike Y, Izumi-Nagai K, Koto T, Satofuka S, Shinoda H, et al. Suppression of Choroidal Neovascularization by Inhibiting Angiotensin-Converting Enzyme: Minimal Role of Bradykinin. *Invest Ophthalmol Vis Sci* (2007) 48(5):2321–6. doi: 10.1167/iovs.06-1296
82. Horai R, Caspi RR. Cytokines in Autoimmune Uveitis. *J Interferon Cytokine Res* (2011) 31(10):733–44. doi: 10.1089/jir.2011.0042
83. Zhong Z, Su G, Kijlstra A, Yang P. Activation of the Interleukin-23/Interleukin-17 Signalling Pathway in Autoinflammatory and Autoimmune Uveitis. *Prog Retin Eye Res* (2021) 80:100866. doi: 10.1016/j.preteyeres.2020.100866
84. Taylor AW, Yee DG, Nishida T, Namba K. Neuropeptide Regulation of Immunity. The Immunosuppressive Activity of Alpha-Melanocyte-Stimulating Hormone (Alpha-MSH). *Ann N Y Acad Sci* (2000) 917:239–47. doi: 10.1111/j.1749-6632.2000.tb05389.x
85. Nakamura H, Yamaki K, Kondo I, Sakuragi S. Experimental Autoimmune Uveitis Induced by Immunization With Retinal Pigment Epithelium-Specific 65-kDa Protein Peptides. *Curr Eye Res* (2005) 30(8):673–80. doi: 10.1080/02713680590968330
86. Caspi RR, Roberge FG, Chan CC, Wiggert B, Chader GJ, Rozenszajn LA, et al. A New Model of Autoimmune Disease. Experimental Autoimmune Uveoretinitis Induced in Mice With Two Different Retinal Antigens. *J Immunol* (1988) 140(5):1490–5.
87. Ohta K, Wiggert B, Yamagami S, Taylor AW, Streilein JW. Analysis of Immunomodulatory Activities of Aqueous Humor From Eyes of Mice With Experimental Autoimmune Uveitis. *J Immunol* (2000) 164(3):1185–92. doi: 10.4049/jimmunol.164.3.1185
88. Lee DJ, Taylor AW. Recovery From Experimental Autoimmune Uveitis Promotes Induction of Antiuveitic Inducible Tregs. *J Leukoc Biol* (2015) 97 (6):1101–9. doi: 10.1189/jlb.3A1014-466RR
89. McMenamin PG, Forrester JV, Steptoe R, Dua HS. Ultrastructural Pathology of Experimental Autoimmune Uveitis in the Rat. *Autoimmunity* (1993) 16 (2):83–93. doi: 10.3109/08916939308993315
90. Chen J, Caspi RR. Clinical and Functional Evaluation of Ocular Inflammatory Disease Using the Model of Experimental Autoimmune Uveitis. *Methods Mol Biol* (2019) 1899:211–27. doi: 10.1007/978-1-4939-8938-6_15
91. Ng TF, Manhapra A, Cluckey D, Choe Y, Vajram S, Taylor AW. Melanocortin 5 Receptor Expression and Recovery of Ocular Immune Privilege After Uveitis. *Ocul Immunol Inflamm* (2021) 22:1–11. doi: 10.1080/09273948.2020.1849735
92. Xu H, Rizzo LV, Silver PB, Caspi RR. Uveitogenicity is Associated With a Th1-Like Lymphokine Profile: Cytokine-Dependent Modulation of Early and Committed Effector T Cells in Experimental Autoimmune Uveitis. *Cell Immunol* (1997) 178(1):69–78. doi: 10.1006/cimm.1997.1121
93. Heng JS, Hackett SF, Stein-O'Brien GL, Winer BL, Williams J, Goff LA, et al. Comprehensive Analysis of a Mouse Model of Spontaneous Uveoretinitis Using Single-Cell RNA Sequencing. *Proc Natl Acad Sci USA* (2019) 116 (52):26734–44. doi: 10.1073/pnas.1915571116
94. Caspi RR, Chan CC, Grubbs BG, Silver PB, Wiggert B, Parsa CF, et al. Endogenous Systemic IFN-Gamma has a Protective Role Against Ocular Autoimmunity in Mice. *J Immunol* (1994) 152(2):890–9.
95. Jones LS, Rizzo LV, Agarwal RK, Tarrant TK, Chan CC, Wiggert B, et al. IFN-Gamma-Deficient Mice Develop Experimental Autoimmune Uveitis in the Context of a Deviant Effector Response. *J Immunol* (1997) 158(12):5997–6005.
96. Yoshimura T, Sonoda KH, Miyazaki Y, Iwakura Y, Ishibashi T, Yoshimura A, et al. Differential Roles for IFN-Gamma and IL-17 in Experimental Autoimmune Uveoretinitis. *Int Immunol* (2008) 20(2):209–14. doi: 10.1093/intimm/dxm135
97. Luger D, Silver PB, Tang J, Cua D, Chen Z, Iwakura Y, et al. Either a Th17 or a Th1 Effector Response can Drive Autoimmunity: Conditions of Disease Induction Affect Dominant Effector Category. *J Exp Med* (2008) 205(4):799–810. doi: 10.1084/jem.20071258
98. Pennesi G, Mattapallil MJ, Sun SH, Avichezer D, Silver PB, Karabekian Z, et al. A Humanized Model of Experimental Autoimmune Uveitis in HLA Class II Transgenic Mice. *J Clin Invest* (2003) 111(8):1171–80. doi: 10.1172/JCI15155
99. Okunuki Y, Mukai R, Nakao T, Tabor SJ, Butovsky O, Dana R, et al. Retinal Microglia Initiate Neuroinflammation in Ocular Autoimmunity. *Proc Natl Acad Sci U S A* (2019) 116(20):9989–98. doi: 10.1073/pnas.1820387116
100. Lee DJ, Taylor AW. Both MC5r and A2Ar are Required for Protective Regulatory Immunity in the Spleen of Post-Experimental Autoimmune Uveitis in Mice. *J Immunol* (2013) 191(8):4103–11. doi: 10.4049/jimmunol.1300182
101. Gordon S. The Macrophage: Past, Present and Future. *Eur J Immunol* (2007) 37:S9–17. doi: 10.1002/eji.200737638
102. Mantovani A, Sozzani S, Locati M, Schioppa T, Saccani A, Allavena P, et al. Infiltration of Tumours by Macrophages and Dendritic Cells: Tumour-Associated Macrophages as a Paradigm for Polarized M2 Mononuclear Phagocytes. *Novartis Found Symp* (2004) 256:137–45. discussion 46-8, 259-69.
103. Mo JS, Streilein JW. Immune Privilege Persists in Eyes With Extreme Inflammation Induced by Intravitreal LPS. *Eur J Immunol* (2001) 31 (12):3806–15. doi: 10.1002/1521-4141(200112)31:12<3806::AID-IMMU3806>3.0.CO;2-M
104. Mantegazza AR, Magalhaes JG, Amigorena S, Marks MS. Presentation of Phagocytosed Antigens by MHC Class I and II. *Traffic* (2013) 14(2):135–52. doi: 10.1111/tra.12026
105. Wang E, Choe Y, Ng TF, Taylor AW. Retinal Pigment Epithelial Cells Suppress Phagolysosome Activation in Macrophages. *Invest Ophthalmol Vis Sci* (2017) 58(2):1266–73. doi: 10.1167/iovs.16-21082
106. Taylor AW, Dixit S, Yu J. Retinal Pigment Epithelial Cell Line Suppression of Phagolysosome Activation. *Int J Ophthalmol Eye Sci* (2015) Suppl 2(1):1–6. doi: 10.19070/2332-290X-SI02001
107. Phan TA, Taylor AW. The Neuropeptides Alpha-MSH and NPY Modulate Phagocytosis and Phagolysosome Activation in RAW 264.7 Cells. *J Neuroimmunol* (2013) 260(1-2):9–16. doi: 10.1016/j.jneuroim.2013.04.019

108. Taylor AW. The Immunomodulating Neuropeptide Alpha-Melanocyte-Stimulating Hormone (Alpha-MSH) Suppresses LPS-Stimulated TLR4 With IRAK-M in Macrophages. *J Neuroimmunol* (2005) 162(1-2):43–50. doi: 10.1016/j.jneuroim.2005.01.008
109. Li D, Taylor AW. Diminishment of Alpha-MSH Anti-Inflammatory Activity in MC1r siRNA-Transfected RAW264.7 Macrophages. *J Leukoc Biol* (2008) 84(1):191–8. doi: 10.1189/jlb.0707463
110. Benque IJ, Xia P, Shannon R, Ng TF, Taylor AW. The Neuropeptides of Ocular Immune Privilege, Alpha-MSH and NPY, Suppress Phagosome Maturation in Macrophages. *Immunohorizons* (2018) 2(10):314–23. doi: 10.4049/immunohorizons.1800049
111. Taylor AW, Lee D. Applications of the Role of Alpha-MSH in Ocular Immune Privilege. *Adv Exp Med Biol* (2010) 2010:681:143–9. doi: 10.1007/978-1-4419-6354-3_12
112. Clemson CM, Yost J, Taylor AW. The Role of Alpha-MSH as a Modulator of Ocular Immunobiology Exemplifies Mechanistic Differences Between Melanocortins and Steroids. *Ocul Immunol Inflamm* (2017) 25(2):179–89. doi: 10.3109/09273948.2015.1092560
113. Kitaichi N, Namba K, Taylor AW. Inducible Immune Regulation Following Autoimmune Disease in the Immune-Privileged Eye. *J Leukoc Biol* (2005) 77 (4):496–502. doi: 10.1189/jlb.0204114
114. Lee DJ, Taylor AW. Following EAU Recovery There is an Associated MC5r-Dependent APC Induction of Regulatory Immunity in the Spleen. *Invest Ophthalmol Vis Sci* (2011) 52(12):8862–7. doi: 10.1167/iovs.11-8153
115. Lee DJ, Preble J, Lee S, Foster CS, Taylor AW. MC5r and A2Ar Deficiencies During Experimental Autoimmune Uveitis Identifies Distinct T Cell Polarization Programs and a Biphasic Regulatory Response. *Sci Rep* (2016) 6:37790. doi: 10.1038/srep37790
116. Spana C, Taylor AW, Yee DG, Makhlina M, Yang W, Dodd J. Probing the Role of Melanocortin Type 1 Receptor Agonists in Diverse Immunological Diseases. *Front Pharmacol* (2019) 9:1535. doi: 10.3389/fphar.2018.01535
117. Nelson WW, Lima AF, Kranyak J, Opong-Owusu B, Ciepielewska G, Gallagher JR, et al. Retrospective Medical Record Review to Describe Use of Repository Corticotropin Injection Among Patients With Uveitis in the United States. *J Ocul Pharmacol Ther* (2019) 35(3):182–8. doi: 10.1089/jop.2018.0090
118. Nguyen QD, Baughman RP, Chu DS, Mah FC, Sergott RC, Taylor AW. Melanocortin in the Pathogenesis of Inflammatory Eye Diseases: Considerations for Treatment. *Retina* (2018) 38(Suppl 1):1–12. doi: 10.1097/01.iae.0000547767.97133.45

Conflict of Interest: AT is a scientific advisor and recipient of a sponsored research agreement from Palatin Technologies Inc.

The remaining authors declare that the research was conducted in the absence of any commercial or financial relationships that could be construed as a potential conflict of interest.

Publisher's Note: All claims expressed in this article are solely those of the authors and do not necessarily represent those of their affiliated organizations, or those of the publisher, the editors and the reviewers. Any product that may be evaluated in this article, or claim that may be made by its manufacturer, is not guaranteed or endorsed by the publisher.

Copyright © 2021 Taylor, Hsu and Ng. This is an open-access article distributed under the terms of the Creative Commons Attribution License (CC BY). The use, distribution or reproduction in other forums is permitted, provided the original author(s) and the copyright owner(s) are credited and that the original publication in this journal is cited, in accordance with accepted academic practice. No use, distribution or reproduction is permitted which does not comply with these terms.

frontiers in Immunology

ORIGINAL RESEARCH
published: 23 September 2021
doi: 10.3389/fimmu.2021.757231

Ubiquitin Ligases CBL and CBL-B Maintain the Homeostasis and Immune Quiescence of Dendritic Cells

*Haijun Tong[1,2,3†], Xin Li[1,2,3†], Jinping Zhang[4†], Liying Gong[1,5], Weili Sun[1,5], Virginie Calderon[1], Xiaochen Zhang[1], Yue Li[1], Adeline Gadzinski[1], Wallace Y. Langdon[6], Boris Reizis[7,8], Yongrui Zou[9] and Hua Gu[1,2,3,5]**

[1] Molecular Immunology Research Unit, Montreal Clinic Research Institute, Montreal, QC, Canada, [2] Department of Microbiology and Immunology, University of Montreal, Montreal, QC, Canada, [3] Department of Biochemistry and Molecular Medicine, University of Montreal, Montreal, QC, Canada, [4] Institute of Biology and Medical Science, SooChow University, Jiangsu, China, [5] Division of Experimental Medicine, McGill University, Montreal, QC, Canada, [6] School of Biomedical Sciences, University of Western Australia, Crawley, WA, Australia, [7] Department of Pathology, New York University Langone Medical Center, New York, NY, United States, [8] Department of Medicine, New York University Langone Medical Center, New York, NY, United States, [9] The Feinstein Institute for Medical Research, Manhasset, New York, NY, United States

OPEN ACCESS

Edited by:
Alexander Steinkasserer,
University Hospital Erlangen, Germany

Reviewed by:
Manfred B. Lutz,
Julius Maximilian University of Würzburg, Germany
Satoshi Ishido,
Hyogo College of Medicine, Japan

***Correspondence:**
Hua Gu
hua.gu@ircm.qc.ca

†These authors have contributed equally to this work

Specialty section:
This article was submitted to Antigen Presenting Cell Biology, a section of the journal Frontiers in Immunology

Received: 11 August 2021
Accepted: 06 September 2021
Published: 23 September 2021

Citation:
Tong H, Li X, Zhang J, Gong L, Sun W, Calderon V, Zhang X, Li Y, Gadzinski A, Langdon WY, Reizis B, Zou Y and Gu H (2021) Ubiquitin Ligases CBL and CBL-B Maintain the Homeostasis and Immune Quiescence of Dendritic Cells. Front. Immunol. 12:757231. doi: 10.3389/fimmu.2021.757231

Dendritic cells (DCs) are composed of multiple lineages of hematopoietic cells and orchestrate immune responses upon detecting the danger and inflammatory signals associated with pathogen and damaged tissues. Under steady-state, DCs are maintained at limited numbers and the functionally quiescent status. While it is known that a fine balance in the DC homeostasis and activation status is also important to prevent autoimmune diseases and hyperinflammation, mechanisms that control DC development and activation under stead-state remain not fully understood. Here we show that DC-specific ablation of CBL and CBL-B ($CBL^{-/-}CBL\text{-}B^{-/-}$) leads to spontaneous liver inflammation and fibrosis and early death of the mice. The mutant mice have a marked expansion of classic $CD8\alpha^{+}/CD103^{+}$ DCs (cDC1s) in peripheral lymphoid organs and the liver. These DCs exhibit atypical activation phenotypes characterized by an increased production of inflammatory cytokines and chemokines but not the cell surface MHC-II and costimulatory ligands. While the mutant mice also have massive T cell activation, lymphocytes are not required for the disease development. The $CBL^{-/-}CBL\text{-}B^{-/-}$ mutation enhances FLT3-mTOR signaling, due to defective FLT3 ubiquitination and degradation. Blockade of FLT3-mTOR signaling normalizes the homeostasis of cDC1s and attenuates liver inflammation. Our result thus reveals a critical role of CBLs in the maintenance of DC homeostasis and immune quiescence. This regulation could be relevant to liver inflammatory diseases and fibrosis in humans.

Keywords: E3 ubiquitin ligase, dendritic cell (DC), FLT3, liver inflammation, homeostasis

INTRODUCTION

Dendritic cells (DCs) are not only special sentinels that orchestrate immune responses against various pathogens but also important regulators to control immune tolerance and inflammation (1–3). DCs detect pathogens and inflammation cues *via* pattern recognition receptors such as Toll-like (TLRs), NOD-like, and TNF family of receptors (4–7). In the absence of infectious and inflammatory stimuli, DCs are either maintained at the quiescent status or function as regulatory DCs that actively induce immune tolerance (8, 9). However, since the ligands for the pattern recognition receptors, such as commensal microbes and host metabolic or tissue damage products, are constantly present under steady-state, there must be mechanisms that refrain DCs from provoking unwanted immune responses (10, 11). The functional quiescence of DCs is known to depend on intracellular negative regulators for pattern recognition receptor signaling (12, 13). In addition, it has been reported that increased lifespan of DCs or depletion of DCs may exhibit a profound effect on the immune quiescence and the development of autoimmune and myeloid proliferative diseases (14, 15). These findings thus suggest that control of a fine balance in DC homeostasis can be another important dimension to maintain DC functional quiescence under steady-state.

DCs are composed of multiple lineages, including classical or conventional DC (cDC) and plasmacytoid DCs (pDC), and the former are further divided into the subsets of CD8α$^+$ cDC (cDC1), CD11b$^+$ cDC (cDC2), and tissue CD103$^+$ cDC1 (16, 17). CD8α$^+$ and CD103$^+$ cDC1s are functionally unique because they present antigens not only to CD4$^+$ but also to CD8$^+$ T cells by a mechanism termed cross presentation (18–20). Lineage specification of cDC1s is controlled by the transcription factor IRF8, which may coordinate with BATF family members (21–23). In addition, Notch signaling has been shown to be necessary for optimizing cDC1 genesis (24). Moreover, while development of both cDC1s and cDC2s requires FLT3 signaling, enhanced activity of PI3 kinase that acts at the downstream of FLT3 may selectively expand cDC1s (25). However, given that FLT3L is constantly present in periphery it is not fully understood how the homeostasis of cDC subsets in the periphery is maintained under steady state.

Chronic liver inflammation is a major cause for liver fibrosis and cirrhosis, a devastating disease that often leads to cancer or death. The pathologic process is usually associated with chronic liver injury as a result of virus infection, toxin stress, alcoholic, nonalcoholic steatohepatitis and fatty liver diseases, and autoimmune diseases (26). While inflammation developed following liver injury is complicated due to the diverse causes, it can be attributed mainly to the activation of liver macrophages, including Kupffer cells and migratory macrophages (27, 28). Activated macrophages may recruit other immune cells to the damage site and activate hepatic stellate cells which then initiate a cascade of extracellular matrix secretion and deposition (26). Although it is well known that DCs are the first line of players to detect the inflammatory alarm and danger signals, the role of DCs in liver inflammation and fibrosis remains largely unclear (29).

CBL and CBL-B (CBLs), two members of the CBL family of E3 ubiquitin ligases, are important in the prevention of autoimmune diseases mediated by T and B cells (30, 31). They regulate T and B cell development, tolerance, and function by modulating the signals delivered by the T and B cell antigen receptors and coreceptors (31, 32). However, in contrast to T and B cells we still know little about the roles of CBLs in DC biology, in particular in the context of inflammation and immune tolerance. In this report, we show that conditional ablation of CBLs, but not CBL nor CBL-B alone, in DCs is detrimental to mice, as the mutant mice manifest severe spontaneous inflammation predominantly in the liver and liver fibrosis. Although most CD4$^+$ and CD8$^+$ T cells in the mutant mice are activated, lymphocytes are not required for the development of the disease. The mutation significantly alters DC homeostasis, as the mutant mice possess markedly more CD8$^+$ cDC1s but not CD11b$^+$ cDC2s in peripheral lymphoid organs and CD103$^+$ DC1s in the liver. In addition, the mutant DCs exhibit a phenotype of atypical hyperactivation, characterized by high levels of IL-6 and inflammatory chemokines, but normal cell surface costimulatory molecules and MHC-II. Moreover, we show that ablation of CBLs impairs FLT3 ubiquitination, resulting in enhanced FLT3-AKT-mTOR signaling. Blockade of mTOR signaling in the mutant mice rebalances the homeostasis of cDC1s and attenuates the liver inflammation and fibrosis. Thus, our data demonstrate that CBL-mediated protein ubiquitination acts as a critical DC intrinsic regulatory mode to maintain the homeostasis and immune quiescence of peripheral cDCs under steady-state. These results also suggest a potential role of cDCs in human liver inflammation and fibrosis and that modulation of DC homeostasis could be an effective treatment for liver inflammation and fibrosis.

METHODS

Animals

C57BL/6 mice, B6.SJL mice, RAG1$^{-/-}$ mice were from The Jackson Laboratory. CBL$^{flox/flox}$ and CBL-B$^{-/-}$ mice were described previously (33, 34). CBL$^{-/-}$ CBL-B$^{-/-}$ mice were generated by crossing *Cbl*$^{flox/flox}$ and *Cbl-b*$^{-/-}$ mice to *CD11c-Cre* transgenic mice (24). RAG1.CBL tko mice were generated by breeding CBL$^{-/-}$ CBL-B$^{-/-}$ mice to RAG1$^{-/-}$ mice. CBL-B$^{C373A/C373A}$ mice were described previously (35). All animal experiments were performed in accordance with the Canadian Council of Animal Care and approved by The Institut de Recherches Cliniques de Montréal (IRCM) Animal Care Committee.

Antibodies and Flow Cytometry

Total splenic cells, bone marrow cells, or liver infiltrating cells were resuspended in FACS buffer [5% BSA in PBS (PH=7.2)] and stained with the corresponding antibodies on ice for 30 min. Cells were washed twice with FACS buffer and then subjected to analysis on a BD Fortessa or Cyan or to cell sorter purification on a FACS Aria or Moflo. The following antibodies were used for the staining: anti-B220, anti-CD11c, anti-MHCII, anti-CD11b, anti-CD8α, anti-CD4, anti-CD44, anti-CD62L, anti-CD3ε, anti-F4/80, anti-Gr1, anti-CD86, anti-CD80, anti-CD40, and anti-PD-L1 (eBioscience). For BrdU incorporation analysis, mice were injected intravenously with 1 mg of BrdU (BD

PharMingen) in DPBS. Cells were then surface stained with corresponding antibodies, and BrdU labeled cells were stained using an anti-BrdU kit according to the manufacturer's protocols (BD PharMingen).

Pathological Analysis

Tissues were harvested, fixed in paraffin, cut into 8 μM sections and then stained with Hematoxilin and Eosin (H&E). For liver fibrosis, collagenous components were revealed by Masson's trichrome staining.

Bone Marrow DC Culture

FLT3L conditioned medium was collected as the supernatant of FLT3L-secreting B16 melanoma cell culture. BM cells (10^6 cells/ml) were cultured in different doses of FLT3L conditioned medium at 37°C for 7-9 days, before being harvested for FACS analysis or subjected to cell sorting.

DC Activation and Cytokine Analysis

Purified DC (10^6 cells/ml) were cultured in 48-well plate in the presence or absence of 10 μg/ml LPS (Sigma) or 10 μM/ml CpG (Invivogen). After 1-3 days, DCs were harvested and subjected for flow cytometric analysis. Culture supernatants were collected, and cytokines in the supernatants were detected by Enzyme-Linked Immunosorbent Assay (ELISA) using a Ready-Set-Go ELISA kit (eBioscience). In brief, supernatant or serum samples were diluted and incubated in 96-well plates pre-coated with different capture antibodies at 4°C overnight. Plates were washed three times and incubated with horseradish peroxidase (HRP)-conjugated detection antibodies for at 37°C for one hour. After washing with PBS, HRP activity in each well was developed in tetramethylbenzidine (TMB) substrate solution.

Antigen Presentation and T Cell Proliferation Assay

OVA-specific $CD8^+$ (OT-I) or $CD4^+$ (OT-II) splenic T cells were purified by EasySepTM Mouse $CD8^+$ or $CD4^+$ T cell enrichment kit as described in manufacturer's manual (StemCell Technologies). Purified T cells were labeled with CFSE (ThermoFisher), cocultured with OVA (40 μg/ml) and graded ratios of purified splenic DC subsets in a 96-well plate for 3 days or 4 days. OT-I and OT-II T cells were stained with anti-TCR Vα2, and cell proliferation was determined based on the dilution of CFSE.

Biochemical Analysis

For FLT3, AKT, and ERK signaling, purified DC subsets were incubated at 37°C without serum and FLT3L for at least one hour. Cells were then stimulated with FLT3L at 37°C for the indicated time, lysed in TNE buffer (50 mM Tris; 140 mM NaCl; 5mM EDTA; 0.5% SDS), and immunoblotting was performed following standard procedures. For immunoprecipitation, proteins were immunoprecipitated by incubating cell lysate with the appropriate antibodies (1-2 μg/1 ml) at 4°C overnight, followed by precipitation of the protein-antibody complexes using protein G agarose (Cell Signaling) for another 1 hour at 4°C. Immunoprecipitates were washed four times with TNE buffer, boiled in 40 μl loading buffer and immunoblotted to a PVDF membrane for western blot analysis. The following antibodies were used for biochemical study: anti-CBL (SantaCruz); anti-CBL-B (Cell Signaling); anti-β Actin (abcam); anti-FLT3 (abcam); anti-pFLT3 (Cell Signaling); anti-pAKT (Cell Signaling); anti-pEKR1/2 (Cell Signaling); anti-HA, anti-IRF8, anti-IRF4, anti-ID2 (Santa Crutz). HRP-conjugated goat anti-rabbit, goat anti-mouse or donkey anti-goat antibody was used as a secondary antibody, respectively. HRP activity was detected using an enhanced chemiluminescence detection system (GE Healthcare).

For FLT3 ubiquitination and degradation assays, 2 μg pcDNA-FLT3 and pcDNA-Ub-HA was co-transfected with 2 μg pcDNA empty vector, pcDNA-CBL or pcDNA-CBL-B to HEK-293 cells by calcium transfection, respectively. Forty-eight hours later, transfected cells were treated with or without FLT3L (100 ng/ml) at 37°C for two hours. For protein degradation assay, new protein synthesis was blocked by Cycloheximide (100 μg/ml) (Cell Signaling). For ubiquitination assay, protein degradation was blocked with chloroquine (40 μg/ml) or MG132 (20 μg/ml) for 15 min before stimulation with FLT3L. FLT3 ubiquitination and expression were then analyzed by Imunoprecipitation and Western blot analysis.

RNAseq and qPCR

To study the gene expression profiling, $CD11b^+$ cDC2 and $CD8\alpha^+$ cDC1 from WT and $CBL^{-/-}CBL\text{-}B^{-/-}$ mice were purified by FACS sorting. Total RNAs from sorted cells (pooled from six mice) was extracted using an RNEasy Mini Kit (QIAGEN), and reversely transcribed into cDNA using a Reverse-Transcription kit (Invitrogen) according to manufacturer's instructions, respectively. RNA-seq was performed using the Illumina TruSeq Stranded mRNA Kit according to manufacturer's instructions on an Illumia HiSeq 2000 sequencer. Read quality was confirmed using FastQC v0.10.1. Read alignment was performed using TopHat v2.010 on the mouse GRCm38/mm10 genome. Differential expression analysis was performed with DESeq2 from the raw alignment counts calculated with featureCounts. For qPCR analysis, a SYBR Green PCR mix (Thermo Scientific) and gene-specific primers were used for quantitative RT-PCR analysis (20-50 ng cDNA per reaction). All reactions were done in triplicates with ViiA7-96 Real Time PCR System (Applied Biosystems). Results were analyzed by the change-in-threshold method, with β-Actin or GAPDH as 'housekeeping' reference genes.

Rapamycin Blockade Assay

For *in vitro* rapamycin blocking assay, BM FLT3L culture (1:10 dilution of FLT3 conditional medium) was treated with different doses of rapamycin (LC Laboratories) starting at day 3. Generations of DC subsets were analyzed at day 7. For short-term *in vivo* rapamycin blockage, 10-week-old WT and $CBL^{-/-}CBL\text{-}B^{-/-}$ mice were injected i.p. with rapamycin (30 mg/day) for seven consecutive days. Mice were then sacrificed and splenic cDC subsets were examined by FACS. For long-term *in vivo* rapamycin blockade assay, 3-month-old RAG1.CBL tko mice were injected i.p. with PBS or rapamycin (100 mg/2 days). Mice were then monitored for the manifestation of inflammatory diseases.

Statistical Analysis

Statistical analyses were performed with a two-tailed, unpaired Student's t test or Fisher's exact t test, with GraphPad Prism V7 software. A P value < 0.05 was considered statistically significant. For survival curve analysis, log-rank test was performed. A P value < 0.05 was considered statistically significant.

RESULTS

The CBL$^{-/-}$CBL-B$^{-/-}$ Mutation Alters the Homeostasis of Peripheral CD8α^{+} cDC1

In steady-state, peripheral DCs include cDC1s, cDC2s, and pDCs. To study the role of CBLs in DC development and function we generated DC specific CBL and CBL-B double null mutant mice by crossing *Cbl*$^{flox/flox}$ and *Cbl-b*$^{-/-}$ mice to *CD11c-Cre* transgenic (tg) mice in which DCs carried the *Cbl*$^{-/-}$ and *Cbl-b*$^{-/-}$ *alleles* (termed the CBL$^{-/-}$ CBL-B$^{-/-}$ mutation), whereas all other lineages of cells harbored the germline *Cbl-b*$^{-/-}$ mutation (33, 34). Deletion of CBL and CBL-B in DCs was confirmed by Western blot analysis (**Supplementary Figures 1A, B**). Flow cytometry analysis revealed that the percentage of CD11c^{+} MHC-II^{+} cDCs in the spleen was increased approximately two folds in CBL$^{-/-}$ CBL-B$^{-/-}$ mice compared to WT, CBL$^{-/-}$ or CBL-B$^{-/-}$ mice (**Figure 1A**). While the subset of CD11b^{+} cDC2s remained unaltered, the total number of CD8α^{+} cDC1s increased fivefold in CBL$^{-/-}$CBL-B$^{-/-}$ mice relative to other control groups (**Figure 1A**). Splenic cDC1s in the mutant mice phenotypically resembled the canonic CD8α^{+} cDC1 rather than the alternative lineage of CD8α^{+} DC, as they expressed similar levels of cell surface CD8α, CD86 and PD-L1 (**Supplementary Figures 2A, B**) (36, 37). In addition, they were functionally consistent with the canonic cDC1s because they secreted a higher amount of IL-12 upon TLR stimulation and were able to cross-present soluble ovalbumin (Ova) antigen to OT-I TCR transgenic CD8^{+} T cells as efficiently as WT cDC1s (**Figures 1B, C**) (19). The total number of CD11c^{low} PDCA1^{+} pDCs was not affected by the CBL$^{-/-}$CBL-B$^{-/-}$ mutation in the bone marrow; however, they were significantly reduced in the spleen (**Supplementary Figures 2C, D**). The mutant pDCs failed to downmodulate chemokine receptor CXCR4 and upregulate CCR5, thus suggesting that CBLs may promote pDC migration to the periphery (**Supplementary Figure 2E**) (38, 39). Together these results demonstrate that CBLs selectively control the homeostasis of peripheral cDC1s and pDCs. Given that the development of cDC1s and pDCs was neither significantly altered in CBL$^{-/-}$ nor in CBL-B$^{-/-}$ mice, we conclude that it is a redundant function between CBL and CBL-B.

CBL$^{-/-}$CBL-B$^{-/-}$ cDCs Exhibit an Altered Profile of Cytokine and Chemokine Expression

To study whether the CBL$^{-/-}$CBL-B$^{-/-}$ mutation affected the activation status of cDCs, we examined activation markers and gene transcription profiles of cDC1 and cDC2 subsets in young CBL$^{-/-}$CBL-B$^{-/-}$ mice before the onset of the inflammation. Both cDC1 and cDC2 from the mutant mice expressed similar amounts of MHC-II and conventional costimulatory ligands CD80, CD86, CD40 and PD-L1 compared to the corresponding subsets from WT, CBL$^{-/-}$ and CBL-B$^{-/-}$ mice (**Supplementary Figure 2B**). However, RNAseq analysis revealed that the mutant cDC1s constitutively produced higher amounts of IL-6, IL-18, and IL-21, and chemokines CCL2 and CXCL9, whereas mutant cDC2s expressed higher levels of IL-10, IL-12β, and IL-21 and chemokine CXCL9 relative to WT counterparts (**Figure 1D**, and **Supplementary Figure 3A**). The increased expression of IL-6 and CCL2 was further confirmed by the qPCR assay (**Supplementary Figure 3B**). To test whether mutant cDC1s were more potent at priming T cells, we co-cultured CFSE labeled OT-II CD4^{+} T cells with WT or CBL$^{-/-}$CBL-B$^{-/-}$ cDC1s in the presence of Ova antigen and then measured the proliferation of OT-II CD4^{+} T cells by FACS. The mutant cDC1s induced more vigorous proliferation of OT-II CD4^{+} T cells compared to WT cDC1s (**Figure 1E**). Together these results show that ablation of CBLs in DCs leads to the loss of the immune quiescent status of cDCs. However, the hyperactivation of the mutant cDCs appears to be atypical because it is not accompanied by the increased expression of conventional costimulatory ligands, but rather involves only the overexpression of several inflammatory cytokines and chemokines.

The CBL$^{-/-}$CBL-B$^{-/-}$ Mutation Enhances the Proliferation but Differentially Affects the Survival of cDC1s and cDC2s

Homeostasis of cDC1s is influenced by lineage commitment of DC precursors as well as proliferation and survival of peripheral mature cDC1s. Since CD11c-Cre was mainly expressed in committed and mature DCs, we hypothesized that the CBL$^{-/-}$CBL-B$^{-/-}$ mutation affected proliferation and survival rather than lineage commitment of cDC1s. To test this hypothesis, we first examined the rate of DC proliferation based on the cell proliferation marker Ki67. We found that approximately 60-70% of splenic CBL$^{-/-}$CBL-B$^{-/-}$ cDC1s and cDC2s expressed a high amount of Ki67 (Ki67^{hi}). In contrast, WT cDC1s and cDC2s contained only 40% of Ki67^{hi} cells (**Figure 2A**). The enhanced proliferation of the mutant cDC1s and cDC2s was confirmed by BrdU labeling as the mutant mice had approximately 50% more BrdU^{+} cDC1s and cDC2s relative to WT mice after overnight BrdU labeling (**Figure 2B**). In contrast to the increased proliferation, cDC1s in CBL$^{-/-}$CBL-B$^{-/-}$ mice appeared to have a slightly reduced population of cells expressing the active form of Caspase (Caspase^{hi}) compared to WT counterparts (**Figure 2C**). In contrast, the mutant mice contained more Caspase^{hi} cDC2s relative to WT mice (**Figure 2C**), suggesting that the CBL$^{-/-}$CBL-B$^{-/-}$ mutation leads to a more profound apoptosis of cDC2s relative to cDC1s. Thus, the altered homeostasis of cDC1s but not cDC2s in CBL$^{-/-}$CBL-B$^{-/-}$ mice could be explained by a combined effect of enhanced proliferation of both mutant cDC1s and cDC2s and increased apoptosis of cDC2s.

Development of cDCs is driven by FLT3 signaling as well as the balanced action of transcription factors IRF8, IRF4, and ID2 (23). To examine whether these molecules were involved in the altered homeostasis of cDC1s in CBL$^{-/-}$CBL-B$^{-/-}$ mice, we analyzed DC development in FLT3-dependent bone marrow

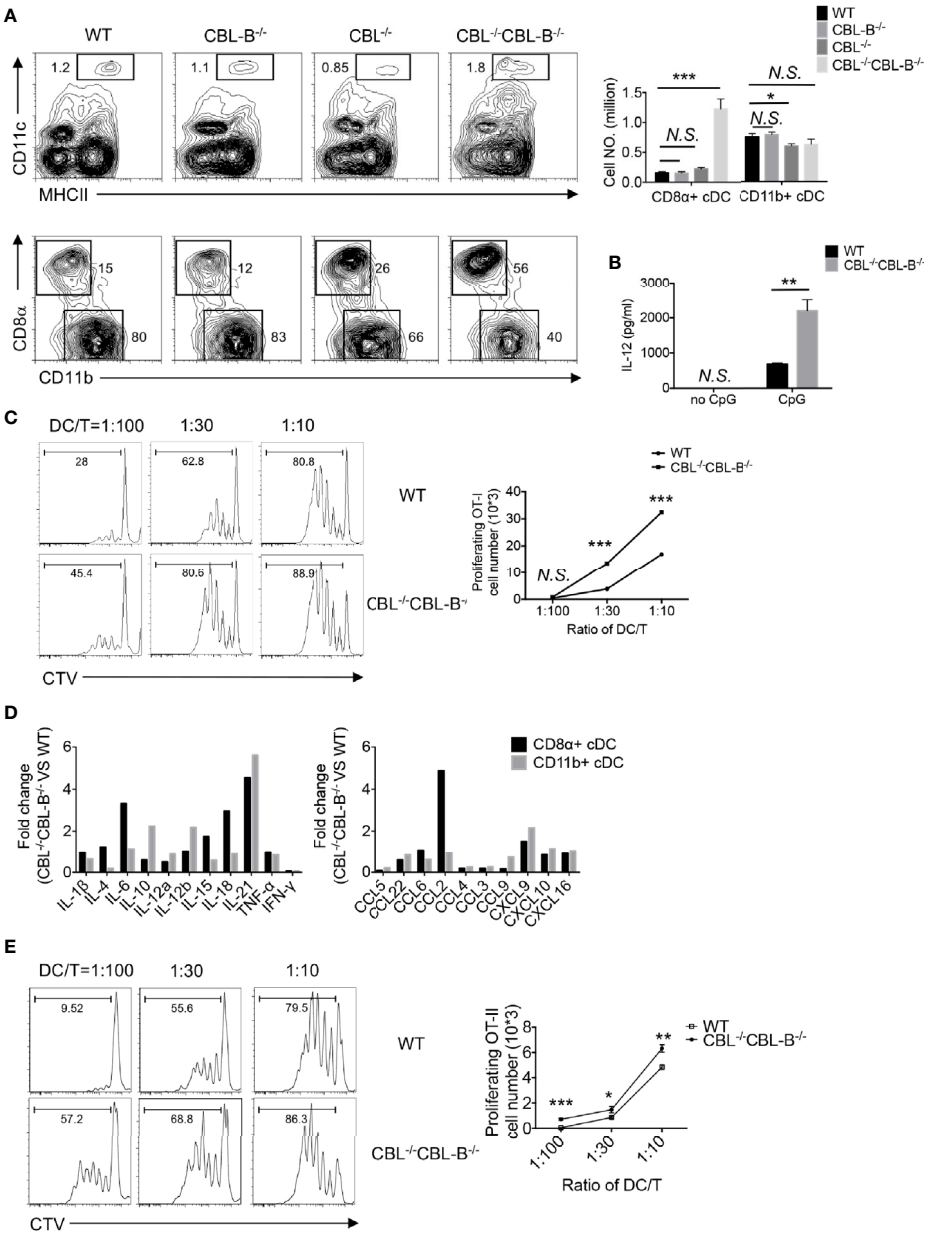

FIGURE 1 | Analyses of the DC development in WT and CBL$^{-/-}$CBLB$^{-/-}$ mice. **(A)** Flow cytometry and statistical analyses of splenic cDCs. CD11c *vs* MHC-II staining of total splenic cDCs (Top panel), CD8α *vs* CD11b staining of CD8α^{+} cDC1 and CD11b^{+} cDC2 (bottom panel), and statistics (right bars) (n = 5). **(B)** IL-12 production by WT and CBL$^{-/-}$CBL-B$^{-/-}$ cDC1 upon CpG stimulation (n = 3). **(C)** Antigen cross presentation to CD8^{+} T cells by WT and CBL$^{-/-}$CBL-B$^{-/-}$ CD8α^{+} cDC1. Histograms of OT-I CD8^{+} T cell proliferation (left). Statistics of OT-I CD8^{+} T cell proliferation (right) (n = 3). **(D)** RNAseq analyses of cytokine and chemokine profiles of CD8α^{+} cDC1s and CD11b^{+} cDC2s. **(E)** Comparison of the antigen presentation efficiency of WT and CBL$^{-/-}$CBL-B$^{-/-}$ cDC1s to CD4^{+} T cells (n=3). Data are mean ± SEM. of at least two independent experiments **(A–E)**. N.S., not significant; *p < 0.05; **p < 0.01; ***p < 0.001.

(BM) cell culture (40). CD8α^{+} cDC1-like cells and CD11b^{+} cDC2s were identified as MHC-II^{+} CD11c^{+} CD24^{hi} (CD24^{hi}) and MHC-II^{+} CD11c^{+} CD11b^{+} CD24^{low} (CD11b^{+}) cells, respectively. In the presence of a low concentration (0.8%) of FLT3L there were 50% more CD24^{hi} cDC1s derived from the CBL$^{-/-}$CBL-B$^{-/-}$ BM culture as compared to WT controls (**Figure 2D**). In contrast, the numbers of CD11b^{+} cDC2 generated in the mutant and WT BM cultures were comparable. The high concentration (20%) of FLT3L led to a more profound increase in CD24^{hi} DC1s in WT relative to the mutant BM cell culture, suggesting that the enhanced FLT3 signaling in WT cells may override the difference caused by the CBL$^{-/-}$CBL-B$^{-/-}$ mutation (**Figure 2D**). The increased generation of CD24^{hi} cDC1s in the mutant BM cell culture was likely a result

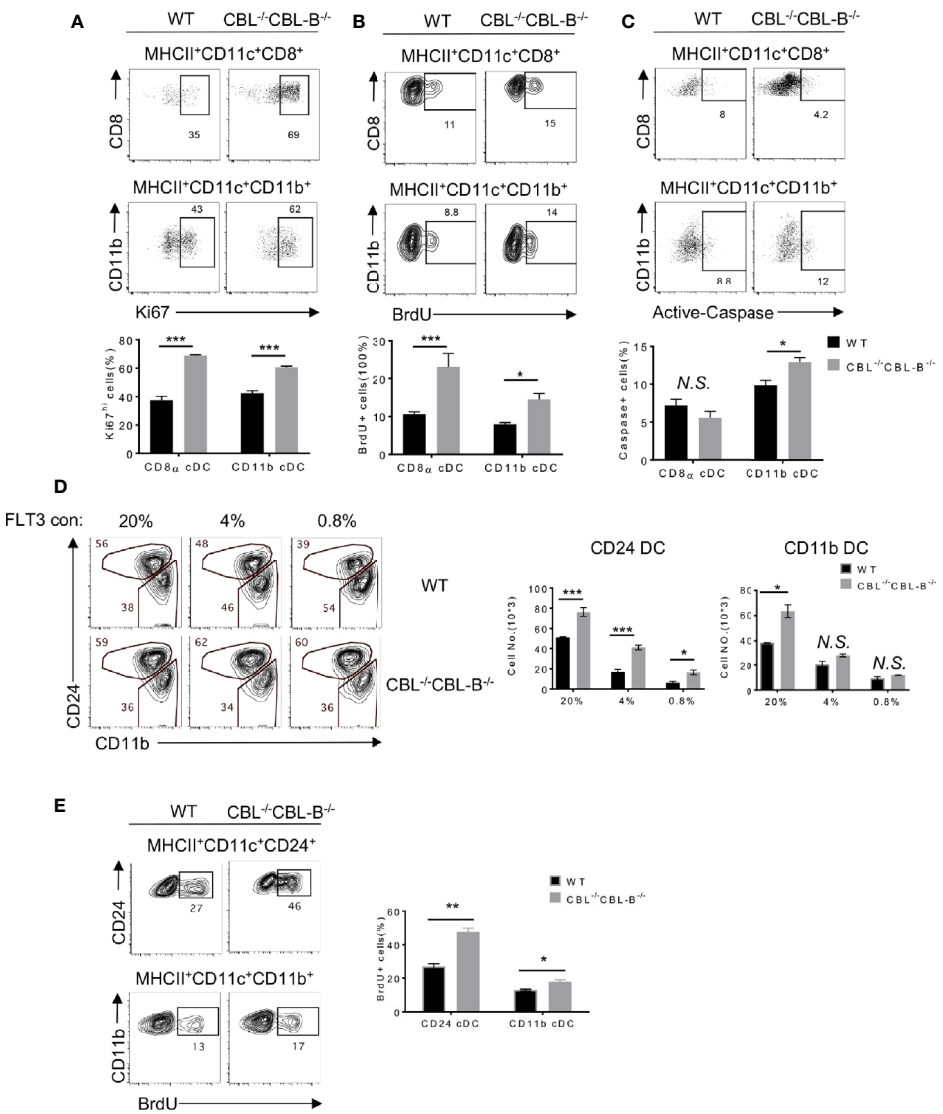

FIGURE 2 | Proliferation, death, and lineage commitment of WT and CBL$^{-/-}$CBL-B$^{-/-}$ cDCs. **(A–C)** Flow cytometry (top panels) and statistics (bottom panels) of splenic proliferating **(A, B)** and apoptotic **(C)** CD8α^{+} cDC1s and CD11b^{+} cDC2s, as determined respectively by anti-Ki67 (n = 3) **(A)**, BrdU (n = 6) **(B)**, and anti-Active Caspase (n = 3) **(C)** staining. **(D)** Comparison of WT and CBL$^{-/-}$CBL-B$^{-/-}$ CD24^{+} (CD8α^{+}-like) cDC1s and CD11b^{+} cDC2s in FLT3 dependent BM cell culture. Shown are the contour maps (left) and statistics (right) of CD24 *vs* CD11b staining of the gated CD11c^{+} cells (n = 3). **(E)** Proliferation of WT and CBL$^{-/-}$CBL-B$^{-/-}$ cDC generated in FLT3 dependent BM cell culture. Shown are FACS analyses (left) and statistics (right) of BrdU^{+} CD24^{hi}CD11b^{lo} and CD24^{lo}CD11b^{hi} cells (n = 3). Data are mean ± SEM. of at least two independent experiments. N.S., not significant; *p < 0.05; **p < 0.01; ***p < 0.001.

of enhanced proliferation, because BrdU labeling analysis revealed more BrdU^{+} CD24^{hi} cDC1s and CD11b^{+} cDC2s in CBL$^{-/-}$CBL-B$^{-/-}$ BM culture compared to WT controls (**Figure 2E**). To examine whether the CBL$^{-/-}$CBL-B$^{-/-}$ mutation affected the expression of cDC1 lineage commitment genes, we purified CD24^{hi} cDC1s and CD11b^{+} cDC2s from BM cell FLT3L culture and examined IRF4 and IRF8 expression by Western blot analysis. Consistent with RNAseq data, the expression of these transcription factors was comparable between the WT and mutant cDC subsets (**Supplementary Figures 3A, C**). These results together support that CBLs regulate the homeostasis of cDC1s by controlling the proliferation rather than the lineage commitment of cDC1s through modulating FLT3 signaling.

CBLs Control FLT3-AKT Signaling by Promoting FLT3 Ubiquitination

FLT3 is a receptor tyrosine kinase that transduces signals through both the MAP kinase and PI3 kinase pathways, the latter activating AKT-mTOR signaling. We therefore examined whether the CBL$^{-/-}$CBL-B$^{-/-}$ mutation enhanced PI3 kinase and MAP kinase signaling. Since we could not obtain enough splenic cDCs for a biochemical study, we used BM cell derived CD24^{hi}

cDC1s and CD11b$^+$ cDC2s in our experiments. In unstimulated WT CD24^{hi} cDC1s, the AKT activity was minimal and stimulation of FLT3 significantly increased AKT activity (**Figure 3A**). In contrast, CBL$^{-/-}$CBL-B$^{-/-}$ CD24^{hi} cDC1s showed a very high level of constitutive AKT activity that may be maximal since FLT3 stimulation did not further enhances the signal. Similar to AKT activation, unstimulated CBL$^{-/-}$CBL-B$^{-/-}$ CD24^{hi} cDC1s contained elevated active forms of ERK1/2 and stimulation of FLT3 elicited even greater ERK1/2 activity in the mutant cells compared to WT controls (**Figure 3B**). In CD11b$^+$ cDC2s, FLT3L stimulation elicited a comparable level of AKT activity between WT and the mutant cells, suggesting that CBLs exert little effect on FLT3 signaling in these cells (**Figure 3A**). These findings thus suggest that CBLs directly target FLT3 in CD24^{hi} cDC1s.

Since CBLs are E3 ubiquitin ligases, we next examined whether CBLs negatively regulate FLT3 signaling by promoting FLT3 ubiquitination and degradation. Flow cytometric analysis revealed that FLT3 expression was higher on WT CD24^{hi} cDC1s compared to that on cDC2s (**Figure 3C**). In CD24^{hi} cDC1s, both CBL and CBL-B were associated with FLT3 (**Figure 3D**). Ablation of CBLs markedly increased the active form of FLT3 (pFLT3 Tyr$^{589/591}$) in CD24^{hi} cDC1s (**Figure 3E**), supporting the idea that CBLs promote the clearance of the active form of FLT3. To determine whether CBLs promote FLT3 ubiquitination, we co-expressed FLT3 with CBL or CBL-B in 293T cells and examined FLT3 ubiquitination with or without FLT3L stimulation. Expression of either CBL or CBL-B promoted FLT3 ubiquitination upon FLT3L stimulation (**Figure 3F**). Consistent with this finding the expression of either CBL or CBL-B in 293T cells removed the active form of FLT3 (**Figure 3G**).

To determine whether the altered homeostasis of CD8α^+ cDC1 was related to CBL mediated ubiquitination, we examined CD8α^+ cDC1 and CD11b$^+$ cDC2 development in DC specific CBL$^{-/-}$ CBL-B$^{C373A/C373A}$ mice. The mutant CBL-B$^{C373A/C373A}$ mice carried a cysteine (373) to alanine mutation in CBL-B that inactivates only the ubiquitin ligase activity but does not affect the scaffolding function of CBL-B (35). Compared to WT mice, CBL$^{-/-}$ CBL-B$^{C373A/C373A}$ mice possessed a similarly increased number of cDC1s and a reduced number of pDCs as that found in CBL$^{-/-}$CBL-B$^{-/-}$ mice (**Figure 3H**). This finding indicates that inactivation of the ubiquitin ligase activity of CBLs is fully responsible for the altered DC homeostasis in CBL$^{-/-}$CBL-B$^{-/-}$ mice.

Together we propose that CBLs control the strength of FLT3 signaling by promoting FLT3 ubiquitination. The preferential expression of FLT3 in CD8α^+ cDC1s as compared to CD11b$^+$ cDC2s could explain why the CBL$^{-/-}$CBL-B$^{-/-}$ mutation exerts a more profound effect on the homeostasis of cDC1s relative to cDC2s.

Ablation of CBLs in DCs Leads to Manifestation of Severe Liver Inflammatory Disease and Early Fatality

Increased numbers and hyperactivation status of cDCs in CBL dko mice prompted us to examine whether the CBL$^{-/-}$CBL-B$^{-/-}$ mutation impaired immune tolerance and caused autoimmune diseases. Our inspection revealed that CBL$^{-/-}$CBL-B$^{-/-}$ mice were healthy at birth; however, they gradually lost bodyweight and became moribund before six months of age (**Figures 4A, B**). Pathological studies revealed that the mutant mice developed exclusively severe liver inflammatory diseases, characterized by serum and skin jaundice, massive liver infiltration of leukocytes, and liver infarct and fibrosis (**Figure 4C**). In a small number of mutant mice, widespread infiltration of leukocytes was also found in other tissues such as the lung and kidney (**Supplementary Figure 4A**). While spleen architecture of the mutant mice was significantly distorted, we did not detect serum auto-antibodies against double-strained DNA or nuclear antigens, suggesting that B cells are probably not involved in the manifestation of the tissue inflammation.

Given that the mutant mice developed severe liver inflammation, we examined the cellularity of liver infiltrating cells by flow cytometry and cytokine production by qPCR and ELISA. We found that livers from the diseased mutant mice contained markedly increased numbers of CD103$^+$ cDC1s, CD4$^+$ and CD8$^+$ T cells, and Ly6G$^+$ granulocytes (**Figure 4D**). Consistent with the severe liver inflammation, the mutant mice produced significantly higher amounts of serum cytokines IL-6, TNFα and inflammatory chemokines relative to WT controls (**Figure 4E**). Compared to WT counterparts the mutant liver also produced high levels of IL-6 and TNF-α, indicating that the liver has hyper inflammation (**Figure 4F**). In contrast, the total number of liver F4/80$^+$ macrophages was not increased (**Figure 4D**), suggesting that Kupffer cells and recruited macrophages are not the major players responsible for the disease.

DC Intrinsic CBLs Are Required for the Maintenance of T Cell Immune Quiescence in Steady-State

Development of spontaneous liver inflammation prompted us to examine whether CBL$^{-/-}$CBL-B$^{-/-}$ DCs elicited systemic hyperactivation of the immune system. We found that before the disease development CBL$^{-/-}$CBL-B$^{-/-}$ mice possessed similar numbers of splenic CD4$^+$ and CD8$^+$ T cells, Ly6G$^+$ granulocytes, and Ly6C$^+$ monocytes as compared to WT mice (**Figures 5A, B**). However, compared to WT mice, significantly increased numbers of CD4$^+$ and CD8$^+$ T cells in the mutant mice exhibited the phenotype of effector/memory T cells as they expressed a higher amount of CD44 and reduced CD62L (**Figure 5C**). In addition, a large proportion of activated CD4$^+$ T cells in the mutant mice adopted the T_{H1} cell fate as they secreted a higher amount of IFN-γ but not IL-4 nor IL-17 upon activation (**Figure 5D**). This finding thus indicates that under steady-state CBLs in CD11c$^+$ cells including cDCs are responsible for the maintenance of immune quiescence of CD4$^+$ and CD8$^+$ T cells.

Manifestation of Liver Inflammation in CBL $^{-/-}$CBL-B$^{-/-}$ Mice Is Independent of T and B Cells

Hyperactivation of T cells in CBL$^{-/-}$CBL-B$^{-/-}$ mice suggested that the observed liver inflammation was caused by T cells activated by CBL$^{-/-}$CBL-B$^{-/-}$ DCs. To assess the contribution of T cells and CBL$^{-/-}$CBL-B$^{-/-}$ DCs in disease development we monitored RAG1$^{-/-}$CBL$^{-/-}$CBL-B$^{-/-}$ triple knockout (RAG1.CBL tko) mice that lack T and B cells. The RAG1.CBL tko mice quickly lost

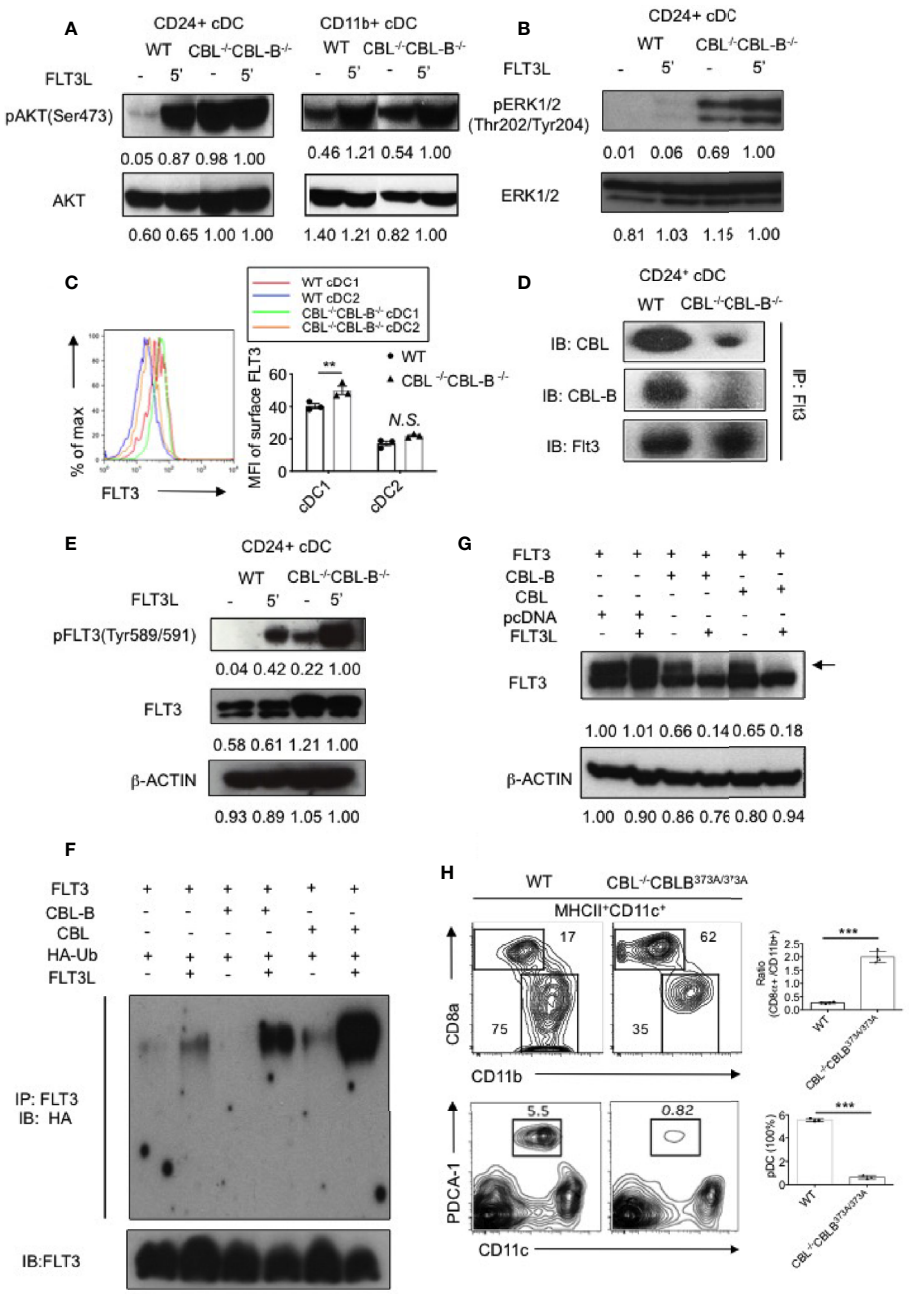

FIGURE 3 | Analyses of FLT3 ubiquitination and signaling by CBLs. **(A)** Western blot analysis of AKT activation in WT and CBL$^{-/-}$CBL-B$^{-/-}$ cDC1s and cDC2s (n = 2). **(B)** Western blot analysis of ERK1/2 activation in WT and CBL$^{-/-}$CBL-B$^{-/-}$ cDC1s (n = 2). **(C)** Cell surface expression of FLT3 in WT and CBL$^{-/-}$CBL-B$^{-/-}$ cDC1s and cDC2s (n = 3). **(D)** Association of FLT3 with CBL and CBL-B in BM derived CD11c^{+}CD24^{hi} cDC1s (n = 2). **(E)** Western blot analysis of FLT3 activation. pFLT3 (Tyr589/591): active form of FLT3 (n = 2). **(F)** Western blot analysis of FLT3 ubiquitination (n = 2). **(G)** Western blot analysis of phosphorylated FLT3 (pFLT3) (n = 2). **(H)** Dependence of CD8α^{+} cDC1 and pDC homeostasis on CBL ubiquitin ligase activity. Shown are contour maps (left) and statistics (right) of splenic cDC1s and cDC2s (top) and pDC (bottom) in WT and CBL$^{-/-}$CBL-B$^{C373A/C373A}$ mice (n = 3-4). Data are mean ± SEM. of at least two independent experiments **(A, B, D–H)**, and one experiment for **(C)** N.S., not significant; $^{**}p < 0.01$; $^{***}p < 0.001$.

body weight relative to RAG1$^{-/-}$ littermates and had a shorter lifespan even compared to CBL$^{-/-}$CBL-B$^{-/-}$ mice (**Figures 6A, B**). Analyses of cytokine and chemokine profiles showed that RAG1.CBL tko mice produced higher amounts of serum IL-6 and TNF-α and inflammatory chemokines such as CCL2, CXCL1, CXCL10, and CXCL13 compared to RAG1$^{-/-}$ controls (**Figures 6C, D**, and **Supplementary Figure 4B**). RAG1.CBL tko mice also manifested exclusively liver inflammation,

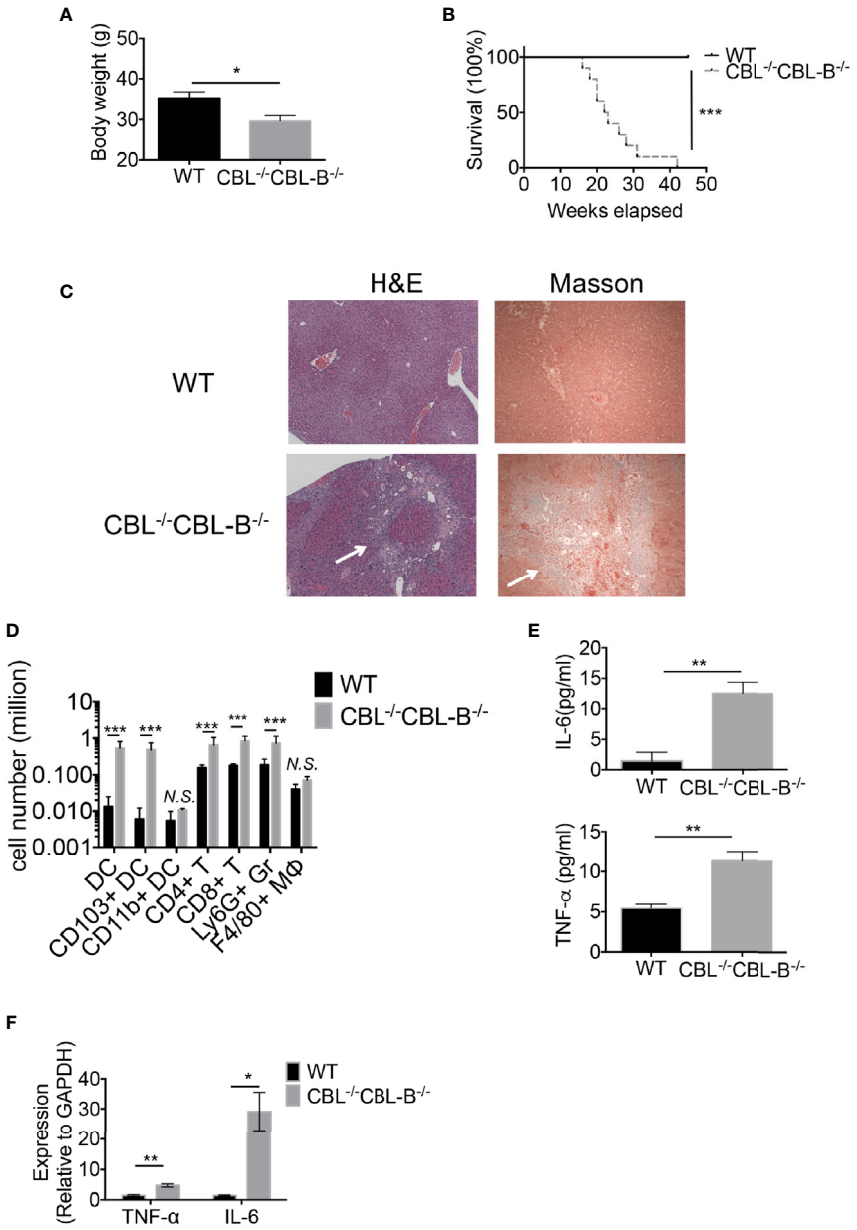

FIGURE 4 | CBL$^{-/-}$CBL-B$^{-/-}$ mice have a reduced lifespan and severe inflammation. **(A)** Body weight comparison between 12-week-old WT and CBL$^{-/-}$CBL-B$^{-/-}$ mice (n = 5). **(B)** Kaplan-Meier survival analysis of WT (n = 20) and CBL$^{-/-}$CBL-B$^{-/-}$ (n = 20) mice. **(C)** Pathological analysis WT and CBL$^{-/-}$CBL-B$^{-/-}$ mice. Shown are H-E staining and Masson staining of the liver. Infiltrating leukocytes and liver fibrosis are indicated by arrows. **(D)** Flow cytometric analysis of liver leukocyte subsets. Shown are the statistics of infiltrated cell subsets of the gated CD45$^+$ cells in livers from WT and CBL$^{-/-}$CBL-B$^{-/-}$ mice (n = 5). DC: CD11c$^+$MHC-II^{hi}; CD103$^+$ DC: CD11c$^+$MHC-II^{hi}CD103$^+$CD8α$^+$; CD11b$^+$ DC: CD11c$^+$MHC-II^{hi}CD11b$^+$; CD4$^+$ T: TCRβ$^+$CD4$^+$; CD8$^+$ T: TCRβ$^+$CD8$^+$; Ly6G$^+$ Gr: CD11b$^+$Ly6G$^+$; F4/80$^+$ MΦ: CD11b$^+$F4/80$^+$. **(E)** Cytokine IL-6 and TNF-α secretion in serum (n = 5-6). **(F)** qPCR analysis of cytokine IL-6 and TNF-α expression in the liver (n = 3). Data are mean ± SEM. of at least two independent experiments **(C–F)**. N.S., not significant; *p < 0.05; **p < 0.01; ***p < 0.001.

characterized by skin jaundice, massive liver infiltration of leukocytes and fibrosis (**Figure 6E**), similar to that found in CBL$^{-/-}$CBL-B$^{-/-}$ mice. Flow cytometric analysis of liver infiltrating cells showed a ten-fold increase in CD103$^+$ cDC1s, whereas numbers of liver infiltrating NK1.1$^+$ cells and F4/80 macrophages$^+$ were not increased or slightly reduced (**Supplementary Figure 4C**). Thus, in CBL$^{-/-}$CBL-B$^{-/-}$ mice while T cells are massively activated, manifestation of liver inflammation is positively correlated with the increased CD103$^+$ cDC1s but is not dependent on T and B cells.

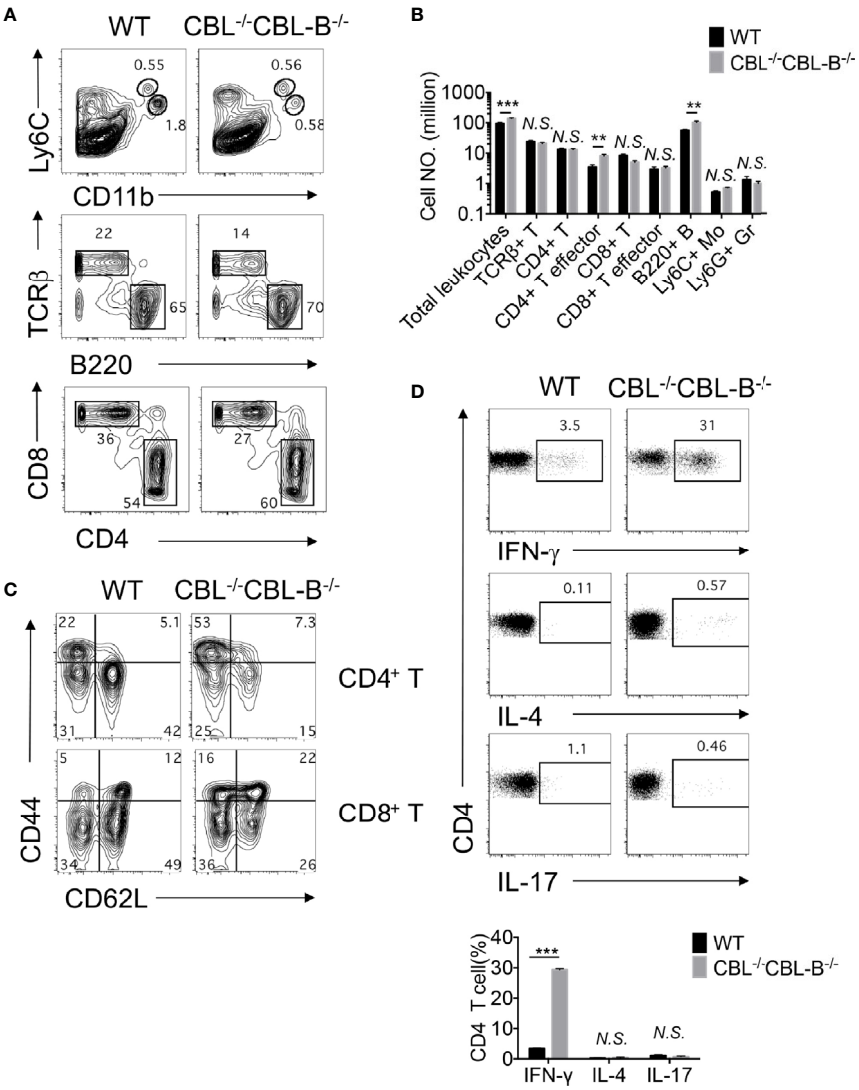

FIGURE 5 | Impaired immune quiescence in CBL$^{-/-}$CBL-B$^{-/-}$ mice. **(A, B)** Flow cytometry and statistical analyses of the spleen cellularity (n = 5). **(C)** Activation status of splenic CD4^{+} and CD8^{+} T cells. Shown are contour maps of CD44 *vs* CD62L staining of naïve (CD44^{lo}CD62L^{hi}), memory/effector (CD44^{hi}CD62L^{hi}), effector (CD44^{hi}CD62^{lo}) T cells (n = 5). **(D)** T effector T cell subsets in the spleen. Th1, Th2, and Th17 cell subsets were stained by anti-TCRβ, CD4, and intracellular IFN-γ, IL-4, and IL-17, respectively (n = 3). Data are mean ± SEM. of at least two independent experiments **(A–D)**. N.S., not significant; **p < 0.01; ***p < 0.001.

Blockade of mTOR Signaling in CBL$^{-/-}$ CBL-B$^{-/-}$ Mice Restores the Homeostasis of cDC1s and Immune Quiescence and Attenuates Liver Inflammation

Enhanced FLT3-AKT signaling in CBL$^{-/-}$ CBL-B$^{-/-}$ cDC1s suggests that attenuation of FLT3-AKT signaling may normalize cDC1 homeostasis and cure liver inflammatory disease in CBL$^{-/-}$CBL-B$^{-/-}$ mice. Since AKT activates mTORs, we examined whether blockade of mTOR signaling reduced the number of cDC1s to normality and restored immune quiescence in CBL$^{-/-}$CBL-B$^{-/-}$ mice. To do so, we pharmacologically blocked mTOR signaling using rapamycin both *in vitro* and in mice and then analyzed cDC development by flow cytometry. We found that rapamycin treatment significantly diminished the number of CD24^{hi} cDC1s in CBL$^{-/-}$CBL-B$^{-/-}$ BM cell FLT3L culture compared to WT controls (**Figure 7A**). Consistent with this finding, *in vivo* rapamycin treatment significantly reduced the number of cDC1s in CBL$^{-/-}$CBL-B$^{-/-}$ mice (**Figure 7B**). In contrast, the same rapamycin treatment exhibited little effect on the numbers of CD11b^{+} cDC2s in both BM cell FLT3L culture and mice, indicating that mTOR signaling selectively regulates the development of cDC1s. To examine whether blockade of mTOR signaling influenced immune quiescence and liver inflammation, we monitored the survival and pathological changes of rapamycin treated CBL$^{-/-}$CBL-B$^{-/-}$ mice. Compared to PBS treated CBL$^{-/-}$ CBL-B$^{-/-}$ mice, rapamycin treated mutant

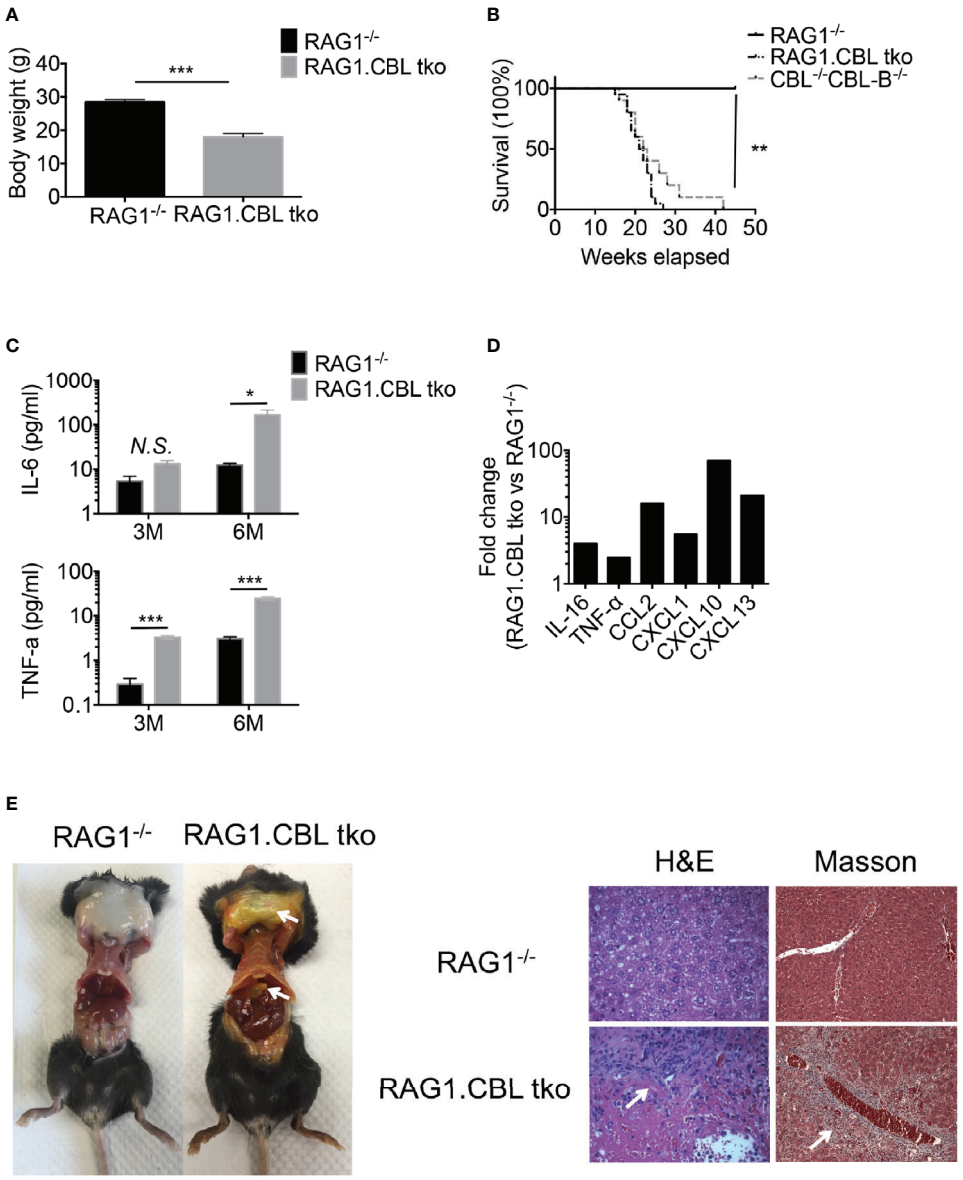

FIGURE 6 | Development of liver inflammation and fibrosis in CBL$^{-/-}$CBL-B$^{-/-}$ mice is independent of lymphocytes. **(A)** Body weight comparison between 12-week-old RAG1$^{-/-}$ and RAG1.CBL tko mice (n = 5). **(B)** Kaplan-Meier survival analysis of RAG1$^{-/-}$, CBL$^{-/-}$CBL-B$^{-/-}$, and RAG1$^{-/-}$CBL tko mice (n = 20). **(C)** Serum Cytokines IL-6 and TNF-α production in RAG1$^{-/-}$ and RAG1.CBL tko mice by ELISA (n = 3-4). **(D)** Serum inflammatory cytokines and chemokines in RAG1.CBL tko mice. **(E)** Images of skin jaundice (left) and histology analysis of liver fibrosis revealed by H-E staining (right panel) and Masson staining (right panel). Data are mean ± SEM. of at least two independent experiments **(C–E)**. N.S., not significant; *p < 0.05; **p < 0.01; ***p < 0.001.

mice had significant longer lifespans (**Figure 7C**). In addition, they had markedly reduced levels of TNF-α in the liver and absence of liver inflammation and fibrosis compared to the PBS treated cohort, possibly due to reduced infiltration of inflammatory cells (**Figures 7D, E**). These results thus support the notion that enhanced FLT3-mTOR signaling in CBL$^{-/-}$CBL-B$^{-/-}$ DCs is responsible for the altered homeostasis of cDC1s. In addition, they provide evidence that this signaling axis is at least partly responsible for the loss of immune quiescence and the development of lethal liver inflammation and fibrosis in the mutant mice.

DISCUSSION

Under steady-state, DC function is maintained quiescent. However, since microbial and immune danger signals are constantly present, there must be mechanisms that restrain DCs from overreaction.

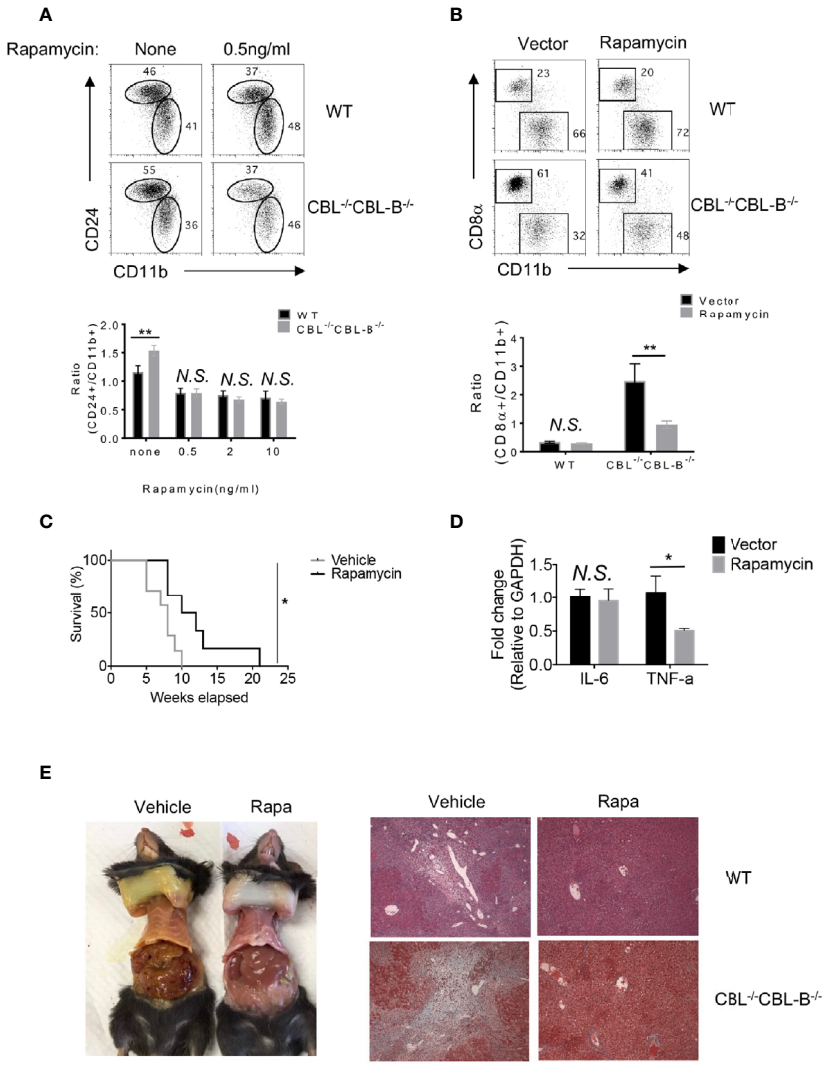

FIGURE 7 | Homeostasis of cDC1s and liver inflammation in mTOR treated CBL$^{-/-}$CBL-B$^{-/-}$ mice. **(A)** Flow cytometry analysis of CD24^{hi}CD11b^{lo} and CD24^{lo}CD11b^{hi} cDCs in FLT3-dependent BM culture treated with rapamycin (n = 3). **(B)** Flow cytometry analysis of CD8α^{+} cDC1s and CD11b^{+} cDC2s in WT and CBL$^{-/-}$ CBL-B$^{-/-}$ mice with or without rapamycin treatment (n = 3). **(C)** Kaplan-Meier survival analysis of CBL$^{-/-}$CBL-B$^{-/-}$ mice treated with rapamycin or vehicle (n = 6-7). **(D)** qPCR analysis of liver IL-6 and TNF-α in rapamycin treated CBL$^{-/-}$CBL-B$^{-/-}$ mice (n = 5). **(E)** Pathology analysis of CBL$^{-/-}$CBL-B$^{-/-}$ mice with rapamycin or vehicle treatment. Left: Image of skin jaundice. Right: H-E staining of liver sections. Data are mean ± SEM. of at least two independent experiments **(A**, **B**, **D**, **E)**. N.S., not significant; *p < 0.05; **p < 0.01.

Loss of DC immune quiescence has been found in the mutant mouse models such as those deficient in the negative regulators for TLRs, NFκB, and PI3 kinases (12, 13, 25). In addition, it has been shown that depletion of DCs or increase in DC lifespan leads to myeloid lineage expansion or autoimmunity (14, 15), suggesting that the homeostasis of DCs also influences the functional quiescence of DCs. In this report, we show that ablation of CBLs in DCs alters DC homeostasis, with a marked increase in the number of CD8α^{+} and liver CD103^{+} cDC1s, and a reduction in peripheral pDCs. CBL$^{-/-}$CBL-B$^{-/-}$ mice manifest spontaneous liver inflammatory diseases and fibrosis. Treatment of the mutant mice with rapamycin reduces the number of cDC1s and attenuates the liver inflammation. Our finding thus identifies CBLs as critical regulators to maintain peripheral DC homeostasis and supports that altered DC homeostasis may breakdown immune quiescence under steady-state. In addition, we also provide evidence that modulation of DC homeostasis can be an effective approach to treat liver inflammation.

How do CBLs in DCs regulate immune quiescence and prevent liver inflammation at steady-state? Our results reveal that CBL$^{-/-}$CBL-B$^{-/-}$ mice have a great expansion of the cDC1 population. While the mutant cDCs do not exhibit typical activation phenotypes, such as upregulation of cell surface costimulatory ligands CD80, CD86, and MHC-II, freshly

isolated mutant cCD1s and cDC2s produce slightly more IL-6 and significantly higher levels of inflammatory chemokines, even in the absence of stimulation. Since $CD103^+$ cDC1s are significantly increased in the liver, we propose that the increased number of cDC1s, and the amount of inflammatory cytokines and chemokines therein, create an inflammatory environment that recruits granulocytes and other inflammatory cells to the liver, leading to the development of liver inflammation. At present, it is not clear whether microbial and other danger signals such as those released by dead cells contribute to the activation of the liver $CD103^+$ cDC1s. However, since CpG stimulation enhances the production of IL-6 and chemokines in $CBL^{-/-}$CBL-$B^{-/-}$ cDCs relative to WT counterparts, we speculate that microbial products or self danger cues in the liver might also be involved in disease development by triggering DC activation *de novo via* TLRs. Consistent with this prediction, we have found that $CBL^{-/-}$ CBL-$B^{-/-}$ mice deficient in MyD88 (termed as $MyD88^{-/-}$.CBL tko mice), while still have a similarly increased number of $CD8\alpha^+$ cDC1s, exhibit much longer lifespan and less severe liver inflammation relative to $CBL^{-/-}$CBL-$B^{-/-}$ mice (**Supplementary Figures 5A, B**). Thus, in addition to the homeostasis of cDC1s, the $CBL^{-/-}$CBL-$B^{-/-}$ mutation might also alter MyD88 dependent signaling. It will be interesting to further elucidate which TLRs are regulated by CBLs. It will also be important to determine whether blockade of both mTOR and MyD88 completely prevents development liver inflammation.

The development of cDCs depends on FLT3 signaling and our finding that CBLs negatively regulate FLT3 signaling by promoting FLT3 ubiquitination and degradation is in agreement with the previous finding that enhanced FLT3-PI3K activity in DCs leads to increased number of cDC1s (25, 36). However, we have shown that the total number of cDC2 is not increased and the number of splenic pDCs is even reduced in the mutant mice, suggesting that other regulations may also exert a role in DC subset homeostasis. Indeed, our data shows that while cDC2s from $CBL^{-/-}$CBL-$B^{-/-}$ mice also proliferate more vigorously relative to WT counterparts, they are more prone to apoptosis than the mutant cDC1s. The reason behind such an alteration is not yet clear. One plausible explanation is that cDC2s are less competitive to access the limited amount of FLT3L available in periphery, because they express relatively lower amount of FLT3 as compared to cDC1s. As for the reduced number of pDCs, our data indicates that they are generated normally in the BM, however, markedly reduced in the periphery. Gene expression profile reveals that $CBL^{-/-}$CBL-$B^{-/-}$ pDCs fail to downmodulate CXCR4 and upregulate CCR5. Given that CXCR4 downmodulation and CCR5 upregulation have been linked to pDC migration from the BM to periphery (39), our finding thus suggests that CBLs regulate the exit of pDCs to periphery rather than the overall development of pDC in the BM.

Currently, cellular mechanisms leading to liver fibrosis are not fully understood. Inflammation following liver damage is considered to be one of the main causes triggering the cascade of hepatic stellate cell activation and liver fibrosis (26). Kupffer cells and recruited macrophages have been shown to play a major role in liver inflammation (29). While evidence implicates that Th17 cells could also be involved in promoting liver inflammation and fibrosis by stimulating Kupffer cells and macrophages to produce inflammatory cytokines and hepatic stellate cells to produce collagen type-I and differentiate to fibrogenic myofibroblasts (41, 42), liver DCs are generally considered tolerogenic and their role in the pathology of liver inflammation and fibrosis has not been extensively explored, despite the fact that extrahepatic DCs have been shown to affect liver inflammation (26, 43). While our data cannot completely exclude the possibility that CBLs were deleted in some macrophages/Kupffer cells or NK cells due to the potential leakiness of CD11c-Cre tg expression, the CBL mutant macrophages are less likely a major cause to induce liver inflammation because we have found that the number of liver macrophages is not increased and cytokine production of BM-derived CBL macrophages from $CBL^{-/-}$CBL-$B^{-/-}$ mice is not altered. In addition, ablation of CBL and CBL-B in monocytes and macrophages using the Lys-Cre allele does not cause liver inflammation in mice (44). In contrast, our data reveal a close correlation between the number and inflammatory cytokine and chemokine production of liver $CD103^+$ cDC1s and inflammation and fibrosis. Blockade of mTOR signaling by rapamycin in $CBL^{-/-}$ CBL-$B^{-/-}$ mice concomitantly reduces the number of liver $CD103^+$ cDC1s and the incidence of liver inflammation and fibrosis. In this regard, data from our mutant mice supports a further study to elucidate whether DCs are also involved in the liver inflammation and fibrosis in humans.

DATA AVAILABILITY STATEMENT

The datasets presented in this study can be found in online repositories. The names of the repository/repositories and accession number(s) can be found below: https://osf.io/2kst3/?view_only=53c4e1cc99e84069af0c7c6db21bcaf6.

ETHICS STATEMENT

The animal study was reviewed and approved by The Institut de Recherches Cliniques de Montréal (IRCM) Animal Care Committee.

AUTHOR CONTRIBUTIONS

HT, XL, and JZ did mouse, biochemical, and flow cytometric analyses. LG, WS, XZ, AG, and YL conducted some mouse and *in vitro* cell culture experiments. VC contributed to bioinformatics analysis. BR provided CD-11c Cre tg mice and B16-FLT3L cell line and contributed to manuscript preparation. WL provided $CBL^{C373A/C373A}$ mice. YZ contributed to the design of the experiments and manuscript preparation. HG is responsible for the overall designs of the experiment and manuscript writing. All authors contributed to the article and approved the submitted version.

FUNDING

This work was Supported by The A. Aisenstadt Chair Fund to HG; Chinese Scholarship Council Ph.D. training grants to HT and XL. Grants from The National Natural Science Foundation of China (31270939, 81471526, 81771667), Training Program of the Major Research Plan in regional immunology of the National Natural Science Foundation of China (91442110), and PCSIRT (IRT1075) to JZ; National Health and Medical Research Concil project grant (1101318) and the Medical and Health Infrastructure Fund to WL, and a NSHLIJ Institutional Fund to YZ.

ACKNOWLEDGMENTS

We thank F. Huang (Fudan University Medical College, Shanghai, China) for MSCV-IκB-GFP reporter, R. Chen (IRCM, Montreal, Canada) for HA-Ubiqutin vector.

SUPPLEMENTARY MATERIAL

The Supplementary Material for this article can be found online at: https://www.frontiersin.org/articles/10.3389/fimmu.2021.757231/full#supplementary-material

Supplementary Figure 1 | Expression of CBL and CBL-B in DC and lymphocyte subsets and pathological analysis of CBL-/-CBL-B-/- mice (A) FACS sorting strategy for purifying splenic pDCs, cDCs, T and B cells. (B) Western blot analysis of CBL and CBL-B expression in pDCs, cDCs, T and B cells. Data represents one of two experiments.

Supplementary Figure 2 | Characterization of CD8a+ cDC1s and pDCs **(A)** CD8a *vs* CD11b staining of gated CD11c+ MHC-II+ splenic cDCs in WT and CBL-/-CBL-B-/- mice. The experiment was repeated for more than three times. **(B)** Expression of costimulatory ligands on CD8a+ cDC1s and CD11b+ cDC2s. The experiment was repeated for more than three times. **(C, D)** FACS analysis of the bone marrow (BM) and splenic (SP) pDCs. Shown are PDCA-1 vs CD11c staining of BM and spleen cells **(C)** and statistics **(D)**. (n = 5). (E) qPCR analysis of CXCR4 and CCR5 expression in WT and CBL-/-CBL-B-/- pDCs. (n = 3). Data are means ± SEM of at least five mice or three independent experiments. *p < 0.01; **p < 0.001.

Supplementary Figure 3 | Gene and protein expression profiles in WT and CBL-/-CBL-B-/- cDC1s and cDC2s **(A)** Heatmap analysis of the chemokines, cytokines and genes related to DC development and function. Data represent pooled RNA samples from 6x WT and 6x CBL-/-CBL-B-/- mice. **(B)** qPCR analysis of TNF-a, IL-6 and CCL2 expression in WT and CBL-/-CBL-B-/- CD8a+ cDC1s. Shown are fold increases of the corresponding gene transcripts in the mutant cells relative to WT cells. (n = 3). Data are means ± SEM of at least three independent experiments. *p < 0.01. **(C)** Western blot analyses of IRF4 and IRF8 in WT and CBL-/-CBL-B-/- CD24hi cDCs.

Supplementary Figure 4 | Pathological analyses of CBL-/-CBL-B-/- mice and RAG1.CBL tko mice **(A)** H&E staining of lung and kidney sections of WT and sick CBL-/-CBL-B-/- mice. Data are from one of five mice. **(B)** Serum cytokine and chemokine titers. Shown are dot blot hybridization of serum cytokine and chemokine titers of pooled serum samples from WT RAG1-/- and sick RAG1.CBL tko mice. (n = 3). **(C)** Total numbers of inflammatory cell subsets in liver infiltrating leukocytes of RAG1-/- and sick RAG1.CBL tko mice. (n = 5). Data are means ± SEM of at least five mice. *p < 0.01; **p < 0.001.

Supplementary Figure 5 | Flow cytometric analysis of cDC subsets in and lifespan analysis of MyD88.CBL tko mice **(A)** FACS analysis (left) and statistics (right) of cDCs and CD8a+ cDC1s and CD11b+ cDC2s in WT (C57BL/6 or MyD88-/-) and MyD88.CBL tko mice. (n = 6). **(B)** Kaplan Meier survival analysis of WT (MyD88-/-), CBL-/-CBL-B-/- and MyD88.CBL tko mice. (n=10). Data are mean ± SEM of two independent experiments. *P < 0.01; **p < 0.001.

REFERENCES

1. Steinman RM. Decisions About Dendritic Cells: Past, Present, and Future. *Annu Rev Immunol* (2012) 30:1–22. doi: 10.1146/annurev-immunol-100311-102839
2. Audiger C, Rahman MJ, Yun TJ, Tarbell KV, Lesage S. The Importance of Dendritic Cells in Maintaining Immune Tolerance. *J Immunol* (2017) 198:2223–31. doi: 10.4049/jimmunol.1601629
3. Ganguly D, Haak S, Sisirak V, Reizis B. The Role of Dendritic Cells in Autoimmunity. *Nat Rev Immunol* (2013) 13:566–77. doi: 10.1038/nri3477
4. Rakoff-Nahoum S, Paglino J, Eslami-Varzaneh F, Edberg S, Medzhitov R. Recognition of Commensal Microflora by Toll-Like Receptors is Required for Intestinal Homeostasis. *Cell* (2004) 118:229–41. doi: 10.1016/j.cell.2004.07.002
5. Chen G, Shaw MH, Kim YG, Nunez G. NOD-Like Receptors: Role in Innate Immunity and Inflammatory Disease. *Annu Rev Pathol* (2009) 4:365–98. doi: 10.1146/annurev.pathol.4.110807.092239
6. Kawai T, Akira S. The Role of Pattern-Recognition Receptors in Innate Immunity: Update on Toll-Like Receptors. *Nat Immunol* (2010) 11:373–84. doi: 10.1038/ni.1863
7. Izcue A, Coombes JL, Powrie F. Regulatory Lymphocytes and Intestinal Inflammation. *Annu Rev Immunol* (2009) 27:313–38. doi: 10.1146/annurev.immunol.021908.132657
8. Steinman RM, Hawiger D, Nussenzweig MC. Tolerogenic Dendritic Cells. *Annu Rev Immunol* (2003) 21:685–711. doi: 10.1146/annurev.immunol.21.120601.141040
9. Darrasse-Jeze G, Deroubaix S, Mouquet H, Victora GD, Eisenreich T, Yao KH, et al. Feedback Control of Regulatory T Cell Homeostasis by Dendritic Cells *In Vivo*. *J Exp Med* (2009) 206:1853–62. doi: 10.1084/jem.20090746
10. Steinman RM, Nussenzweig MC. Avoiding Horror Autotoxicus: The Importance of Dendritic Cells in Peripheral T Cell Tolerance. *Proc Natl Acad Sci USA* (2002) 99:351–8. doi: 10.1073/pnas.231606698
11. Kurts C, Heath WR, Carbone FR, Allison J, Miller JF, Kosaka H. Constitutive Class I-Restricted Exogenous Presentation of Self Antigens *In Vivo*. *J Exp Med* (1996) 184:923–30. doi: 10.1084/jem.184.3.923
12. Hammer GE, Turer EE, Taylor KE, Fang CJ, Advincula R, Oshima S, et al. Expression of A20 by Dendritic Cells Preserves Immune Homeostasis and Prevents Colitis and Spondyloarthritis. *Nat Immunol* (2011) 12:1184–93. doi: 10.1038/ni.2135
13. Kool M, van Loo G, Waelput W, De Prijck S, Muskens F, Sze M, et al. The Ubiquitin-Editing Protein A20 Prevents Dendritic Cell Activation, Recognition of Apoptotic Cells, and Systemic Autoimmunity. *Immunity* (2011) 35:82–96. doi: 10.1016/j.immuni.2011.05.013
14. Chen M, Wang YH, Wang Y, Huang L, Sandoval H, Liu YJ, et al. Dendritic Cell Apoptosis in the Maintenance of Immune Tolerance. *Science* (2006) 311:1160–4. doi: 10.1126/science.1122545
15. Birnberg T, Bar-On L, Sapoznikov A, Caton ML, Cervantes-Barragan L, Makia D, et al. Lack of Conventional Dendritic Cells is Compatible With Normal Development and T Cell Homeostasis, But Causes Myeloid Proliferative Syndrome. *Immunity* (2008) 29:986–97. doi: 10.1016/j.immuni.2008.10.012
16. Naik SH, Sathe P, Park HY, Metcalf D, Proietto AI, Dakic A, et al. Development of Plasmacytoid and Conventional Dendritic Cell Subtypes From Single Precursor Cells Derived *In Vitro* and *In Vivo*. *Nat Immunol* (2007) 8:1217–26. doi: 10.1038/ni1522
17. Onai N, Obata-Onai A, Schmid MA, Ohteki T, Jarrossay D, Manz MG. Identification of Clonogenic Common Flt3+M-CSFR+ Plasmacytoid and Conventional Dendritic Cell Progenitors in Mouse Bone Marrow. *Nat Immunol* (2007) 8:1207–16. doi: 10.1038/ni1518
18. Merad M, Sathe P, Helft J, Miller J, Mortha A. The Dendritic Cell Lineage: Ontogeny and Function of Dendritic Cells and Their Subsets in the Steady State and the Inflamed Setting. *Annu Rev Immunol* (2013) 31:563–604. doi: 10.1146/annurev-immunol-020711-074950

19. Mildner A, Jung S. Development and Function of Dendritic Cell Subsets. *Immunity* (2014) 40:642–56. doi: 10.1016/j.immuni.2014.04.016
20. Schraml BU, Reis e Sousa C. Defining Dendritic Cells. *Curr Opin Immunol* (2015) 32:13–20. doi: 10.1016/j.coi.2014.11.001
21. Sichien D, Scott CL, Martens L, Vanderkerken M, Van Gassen S, Plantinga M, et al. IRF8 Transcription Factor Controls Survival and Function of Terminally Differentiated Conventional and Plasmacytoid Dendritic Cells, Respectively. *Immunity* (2016) 45:626–40. doi: 10.1016/j.immuni.2016.08.013
22. Hildner K, Edelson BT, Purtha WE, Diamond M, Matsushita H, Kohyama M, et al. Batf3 Deficiency Reveals a Critical Role for CD8alpha+ Dendritic Cells in Cytotoxic T Cell Immunity. *Science* (2008) 322:1097–100. doi: 10.1126/science.1164206
23. Murphy TL, Grajales-Reyes GE, Wu X, Tussiwand R, Briseno CG, Iwata A, et al. Transcriptional Control of Dendritic Cell Development. *Annu Rev Immunol* (2016) 34:93–119. doi: 10.1146/annurev-immunol-032713-120204
24. Caton ML, Smith-Raska MR, Reizis B. Notch-RBP-J Signaling Controls the Homeostasis of CD8- Dendritic Cells in the Spleen. *J Exp Med* (2007) 204:1653–64. doi: 10.1084/jem.20062648
25. Sathaliyawala T, O'Gorman WE, Greter M, Bogunovic M, Konjufca V, Hou ZE, et al. Mammalian Target of Rapamycin Controls Dendritic Cell Development Downstream of Flt3 Ligand Signaling. *Immunity* (2010) 33:597–606. doi: 10.1016/j.immuni.2010.09.012
26. Koyama Y, Brenner DA. Liver Inflammation and Fibrosis. *J Clin Invest* (2017) 127:55–64. doi: 10.1172/JCI88881
27. Wang M, You Q, Lor K, Chen F, Gao B, Ju C. Chronic Alcohol Ingestion Modulates Hepatic Macrophage Populations and Functions in Mice. *J Leukoc Biol* (2014) 96:657–65. doi: 10.1189/jlb.6A0114-004RR
28. Bouwens L, Baekeland M, De Zanger R, Wisse E. Quantitation, Tissue Distribution and Proliferation Kinetics of Kupffer Cells in Normal Rat Liver. *Hepatology* (1986) 6:718–22. doi: 10.1002/hep.1840060430
29. Pradere JP, Kluwe J, De Minicis S, Jiao JJ, Gwak GY, Dapito DH, et al. Hepatic Macrophages But Not Dendritic Cells Contribute to Liver Fibrosis by Promoting the Survival of Activated Hepatic Stellate Cells in Mice. *Hepatology* (2013) 58:1461–73. doi: 10.1002/hep.26429
30. Kitaura Y, Jang IK, Wang Y, Han YC, Inazu T, Cadera EJ, et al. Control of the B Cell-Intrinsic Tolerance Programs by Ubiquitin Ligases Cbl and Cbl-B. *Immunity* (2007) 26:567–78. doi: 10.1016/j.immuni.2007.03.015
31. Huang F, Gu H. Negative Regulation of Lymphocyte Development and Function by the Cbl Family of Proteins. *Immunol Rev* (2008) 224:229–38. doi: 10.1111/j.1600-065X.2008.00655.x
32. Liu YC, Gu H. Cbl and Cbl-b in T-Cell Regulation. *Trends Immunol* (2002) 23:140–3. doi: 10.1016/S1471-4906(01)02157-3
33. Naramura M, Jang IK, Kole H, Huang F, Haines D, Gu H. c-Cbl and Cbl-b Regulate T Cell Responsiveness by Promoting Ligand-Induced TCR Down-Modulation. *Nat Immunol* (2002) 3:1192–9. doi: 10.1038/ni855
34. Chiang YJ, Kole HK, Brown K, Naramura M, Fukuhara S, Hu RJ, et al. Cbl-B Regulates the CD28 Dependence of T-Cell Activation. *Nature* (2000) 403:216–20. doi: 10.1038/35003235
35. Oksvold MP, Dagger SA, Thien CB, Langdon WY. The Cbl-b RING Finger Domain has a Limited Role in Regulating Inflammatory Cytokine Production by IgE-Activated Mast Cells. *Mol Immunol* (2008) 45:925–36. doi: 10.1016/j.molimm.2007.08.002
36. Lau CM, Nish SA, Yogev N, Waisman A, Reiner SL, Reizis B. Leukemia-Associated Activating Mutation of Flt3 Expands Dendritic Cells and Alters T Cell Responses. *J Exp Med* (2016) 213:415–31. doi: 10.1084/jem.20150642
37. Bar-On L, Birnberg T, Lewis KL, Edelson BT, Bruder D, Hildner K, et al. CX3CR1+ CD8alpha+ Dendritic Cells are a Steady-State Population Related to Plasmacytoid Dendritic Cells. *Proc Natl Acad Sci USA* (2010) 107:14745–50. doi: 10.1073/pnas.1001562107
38. Sawai CM, Sisirak V, Ghosh HS, Hou EZ, Ceribelli M, Staudt LM, et al. Transcription Factor Runx2 Controls the Development and Migration of Plasmacytoid Dendritic Cells. *J Exp Med* (2013) 210:2151–9. doi: 10.1084/jem.20130443
39. Chopin M, Preston SP, Lun ATL, Tellier J, Smyth GK, Pellegrini M, et al. RUNX2 Mediates Plasmacytoid Dendritic Cell Egress From the Bone Marrow and Controls Viral Immunity. *Cell Rep* (2016) 15:866–78. doi: 10.1016/j.celrep.2016.03.066
40. Naik SH, Proietto AI, Wilson NS, Dakic A, Schnorrer P, Fuchsberger M, et al. Cutting Edge: Generation of Splenic CD8+ and CD8- Dendritic Cell Equivalents in Fms-Like Tyrosine Kinase 3 Ligand Bone Marrow Cultures. *J Immunol* (2005) 174:6592–7. doi: 10.4049/jimmunol.174.11.6592
41. Lemmers A, Moreno C, Gustot T, Marechal R, Degre D, Demetter P, et al. The Interleukin-17 Pathway is Involved in Human Alcoholic Liver Disease. *Hepatology* (2009) 49:646–57. doi: 10.1002/hep.22680
42. Meng F, Wang K, Aoyama T, Grivennikov SI, Paik Y, Scholten D, et al. Interleukin-17 Signaling in Inflammatory, Kupffer Cells, and Hepatic Stellate Cells Exacerbates Liver Fibrosis in Mice. *Gastroenterology* (2012) 143:765–76.e763. doi: 10.1053/j.gastro.2012.05.049
43. Goubier A, Dubois B, Gheit H, Joubert G, Villard-Truc F, Asselin-Paturel C, et al. Plasmacytoid Dendritic Cells Mediate Oral Tolerance. *Immunity* (2008) 29:464–75. doi: 10.1016/j.immuni.2008.06.017
44. Naramura M, Nadeau S, Mohapatra B, Ahmad G, Mukhopadhyay C, Sattler M, et al. Mutant Cbl Proteins as Oncogenic Drivers in Myeloproliferative Disorders. *Oncotarget* (2011) 2:245–50. doi: 10.18632/oncotarget.233

Conflict of Interest: The authors declare that the research was conducted in the absence of any commercial or financial relationships that could be construed as a potential conflict of interest.

Publisher's Note: All claims expressed in this article are solely those of the authors and do not necessarily represent those of their affiliated organizations, or those of the publisher, the editors and the reviewers. Any product that may be evaluated in this article, or claim that may be made by its manufacturer, is not guaranteed or endorsed by the publisher.

Copyright © 2021 Tong, Li, Zhang, Gong, Sun, Calderon, Zhang, Li, Gadzinski, Langdon, Reizis, Zou and Gu. This is an open-access article distributed under the terms of the Creative Commons Attribution License (CC BY). The use, distribution or reproduction in other forums is permitted, provided the original author(s) and the copyright owner(s) are credited and that the original publication in this journal is cited, in accordance with accepted academic practice. No use, distribution or reproduction is permitted which does not comply with these terms.

frontiers in Immunology

ORIGINAL RESEARCH
published: 26 October 2021
doi: 10.3389/fimmu.2021.746469

Identification of Two Subsets of Murine DC1 Dendritic Cells That Differ by Surface Phenotype, Gene Expression, and Function

*David Hongo[1], Pingping Zheng[2], Suparna Dutt[1], Rahul D. Pawar[1], Everett Meyer[2], Edgar G. Engleman[3] and Samuel Strober[1]**

[1] Department of Medicine, Division of Immunology and Rheumatology, Stanford University School of Medicine, Stanford, CA, United States, [2] Department of Medicine, Division of Blood and Marrow Transplantation, Stanford University School of Medicine, Stanford, CA, United States, [3] Department of Pathology, Stanford University School of Medicine, Stanford, CA, United States

Classical dendritic cells (cDCs) in mice have been divided into 2 major subsets based on the expression of nuclear transcription factors: a $CD8^+Irf8^+Batf3$ dependent (DC1) subset, and a $CD8^-Irf4^+$ (DC2) subset. We found that the $CD8^+$DC1 subset can be further divided into $CD8^+$DC1a and $CD8^+$DC1b subsets by differences in surface receptors, gene expression, and function. Whereas all 3 DC subsets can act alone to induce potent Th1 cytokine responses to class I and II MHC restricted peptides derived from ovalbumin (OVA) by OT-I and OT-II transgenic T cells, only the DC1b subset could effectively present glycolipid antigens to natural killer T (NKT) cells. Vaccination with OVA protein pulsed DC1b and DC2 cells were more effective in reducing the growth of the B16-OVA melanoma as compared to pulsed DC1a cells in wild type mice. In conclusion, the Batf3-/- dependent DC1 cells can be further divided into two subsets with different immune functional profiles *in vitro* and *in vivo*.

Keywords: dendritic cells, type I dendritic cells, type II dendritic cell, CD4 T cell, CD8 T cell, tumor vaccination

OPEN ACCESS

Edited by:
Daniel Saban,
Duke University, United States

Reviewed by:
Luc Van Kaer,
Vanderbilt University, United States
Joana Dias,
Vaccine Research Center (NIAID), United States

***Correspondence:**
Samuel Strober
sstrober@stanford.edu

Specialty section:
This article was submitted to Antigen Presenting Cell Biology, a section of the journal Frontiers in Immunology

Received: *23 July 2021*
Accepted: *17 September 2021*
Published: *26 October 2021*

Citation:
Hongo D, Zheng P, Dutt S, Pawar RD, Meyer E, Engleman EG and Strober S (2021) Identification of Two Subsets of Murine DC1 Dendritic Cells That Differ by Surface Phenotype, Gene Expression, and Function. Front. Immunol. 12:746469. doi: 10.3389/fimmu.2021.746469

HIGHLIGHTS

Two subsets of DC1 dendritic cells differ by surface phenotype, gene expression, and function.

INTRODUCTION

The subset of $CD8^+$dendritic cells (DCs) that is dependent on the Batf3 and Irf8 nuclear transcription factors for development and maturation in mouse lymphoid tissues has been extensively studied (1–5). This subset, that has been identified as DC1 by Murphy and co-workers (6, 7) plays a required role in the induction of $CD8^+$ T cell immunity to tumors and viruses (8–15). DC1 cells express the surface markers CD11c and MHCII associated with all classical myeloid DCs, and express high levels of CD24 and XCR1 and low levels of CD172 (SIRPα) surface markers (5–16). This surface phenotype has been used to distinguish the DC1 subset from the $CD8^-$

DC2 subset that expresses low levels of CD24 and XCR1 and high levels of CD172a (6, 7). Inactivation of the gene encoding Batf-3 results in the selective elimination of $CD8^+$ and $CD103^+$ DC1 DCs (17, 18). Both subsets express high levels of XCR1, low levels of CD172, and can stimulate CD8+ T cell immunity (19–21). In contrast to the DC1 subset, the DC2 subset is dependent on the Irf4 nuclear transcription factor and has been subdivided further into Notch2-dependent and KIf4-dependent populations (22, 23). Batf3 is expressed in both the $Irf8^+$ and $Irf4^+$ DCs (5). Nevertheless, the DC2 cells are predominantly Batf3 independent (20).

It is not clear whether the $CD8^+$ Batf-3 dependent DC1 subset is homogeneous or whether it can be divided further into additional subsets. Phenotypic and functional heterogeneity of the subset has been described previously with regard to the expression of CD103 in the spleen, skin draining lymph nodes, tumors, and intestines (24–28). DC1 cells in the skin draining lymph nodes, tumors, and intestines express high levels of CD103 whereas DC1 cells in the spleen have low or undetectable levels (24–28). The $CD8^+$ subset of DCs has been reported to be more potent than the $CD8^-$ subset in cross-presenting cell associated protein antigens to conventional $CD8^+$ T cells, and selective depletion of the CD8+ subset markedly attenuates CD8+ T cell immunity to tumors and viruses by virtue of cross antigen presentation (29–32). $CD8^+$ DCs take up proteins from exogenous cell sources that are the source of the antigens, such as tumor cells and viral infected cells, process the proteins such that the derived peptides are cross-presented to $CD8^+$ T cells after association with MHC receptors on the cell surface (1–11). In accordance with these observations, the ability of radiation therapy to induce T cell mediated durable complete remissions of solid and lymphoid tumors was dependent on the presence of $CD8^+$Batf3 dependent DCs, since remissions observed in wild type mice were abrogated in *Batf3*$^{-/-}$ mice (33, 34). Remissions were restored by injecting $CD8^+$ DCs into the tumors (33, 34).

Previous studies showed that after uptake of the soluble ovalbumin protein injected *in vivo*, the $CD8^+$ DCs were effective at presenting the antigen to ovalbumin specific TCR transgenic $CD8^+$T cells but not $CD4^+$ T cells, and $CD8^-$DCs were effective at presenting to transgenic $CD4^+$T cell (32). These observations are consistent with the dominant role of $CD8^+$DCs in the induction of $CD8^+$T cell immunity to cell bound viral and tumor antigens. However, vaccination with soluble ovalbumin protein linked to antibodies directed to the DCIR2 surface receptor of the $CD8^-$ subset of DCs induced effective $CD8^+$T cell immunity against the B16-OVA melanoma tumor after injection of the conjugate *in vivo* (35). Thus, $CD8^-$ DC2 cells can also induce $CD8^+$T cell immunity to an ovalbumin tumor antigen depending on the nature of the vaccination. However, it was not determined whether $CD8^+$DCs in the tumor microenvironment were also required for the $CD8^+$ T cell anti-tumor effect in addition to the systemic immune response induced by the DCIR2 targeted $CD8^-$ DCs.

The $CD8^+$DC1 and $CD8^-$DC2 subsets have also been compared for their efficacy in presenting glycolipid antigens to NKT cells (36, 37). The latter T cells recognize glycolipids in association with the CD1d antigen presenting molecule (38–40). The DC1 subset was effective and the DC2 subset was ineffective in the induction of NKT cell anti-glycolipid immune responses. It is not clear whether the ability of the $CD8^+$ DC1 subset to present soluble and cell associated protein antigens to $CD8^+$ T cells, on one hand, and glycolipid antigens to NKT cells, on the other, is a function of a single subset or of at least two subsets of $CD8^+$ DC1 cells.

The current study identified two major subsets of Batf3 dependent $CD8^+$ DCs (DC1a and DC1b) that differ from each other and from the $CD8^-$DC2 subset on the basis of clear differences in their surface receptors, and gene expression. The ability of all of the latter subsets to induce T cell immune responses to a variety of antigens was compared, and key differences were elucidated.

RESULTS

Identification of 2 Subsets of $CD8^+$ Batf3 Dependent DCs

Single cells were harvested from the spleen of adult wild type (WT) C57BL/6 mice, stained for surface receptors, and CD3-CD56-CD3-CD19-Gr-1- (Lin-) cells were analyzed by flow cytometry for CD11c vs MHC class II expression. As shown in (**Figure 1A**), 4.5% were contained in the box enclosing a discrete population of $CD11c^+MHCII^+$ cells that were identified as dendritic cells (DCs). Further study of the gated DCs in the spleen of WT mice for expression of CD8 vs CD172a showed that 3 populations of cells with discrete concentric contours were present (enclosed in ellipses in **Figure 1A**). Population 1 (identified as the DC1a subset in all subsequent Figures and Tables) contained $CD8^{hi}CD172^{lo}$ cells, population 2 (identified as the DC1b subset) contained $CD8^{int}CD172^{int}$ cells, and population 3 (identified as DC2 subset) contained $CD8^-CD172^{hi}$ cells. In order to determine whether populations 1 and 2 expressed the Irf8+/Irf4- nuclear factor expression pattern that characterizes DC1cells, all three populations were gated separately, and stained for intracellular Irf8 and Irf4. As shown in the histograms in **Figure 1A**, both the DC1a and DC1b populations expressed the Irf8+/Irf4- pattern. In contrast, the DC2 population, expressed the Irf8-Irf4+ pattern that has been shown previously to characterize the DC2 subset. The mean percentages of the 3 populations among gated $CD11c^+MHC^+$ cells enclosed in the ellipses in the spleen of C57BL/6 WT mice are shown in the panel of **Figure 1B**. DC1a, DC1b, and DC2 subsets made up about 12%,48%, and 40% of total DCs respectively. In additional experiments, the mean percentages of the 3 subsets among splenic DCs in C57BL/6 and BALB/c WT mice were compared. The DC1b cells represented the majority of DCs in both strains, and the mean percentage of DC2 cells was significantly higher in the BALB/c mice.

Abbreviations: DCs, Dendritic cells; DC1, Type I dendritic cell; DC2, Type II dendritic cell; Batf3, basic leucine zipper transcription factor, ATF-3; NKT cell, Natural killer T cell; MLR, Mixed leukocyte reaction.

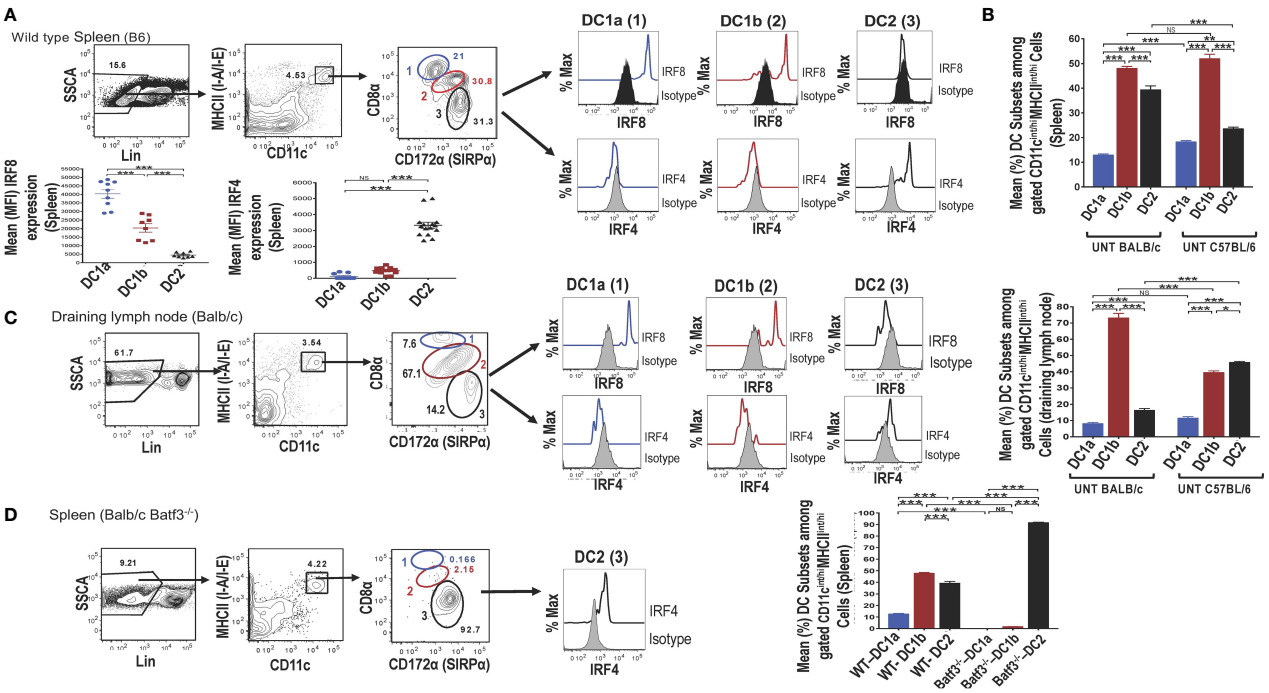

FIGURE 1 | Identification of 2 subsets of CD8$^+$ Batf3 dependent DCs. Spleen cells from untreated wild-type (WT) C57BL/6 or BALB/c mice were stained and analyzed by flow cytometry for DC susbsets. **(A)** Show representative two color FACS gating strategy to identify MHCII(I-A/I-E)$^+$ CD11+ total DCs after gating on lineage negative (CD3, B220, CD19, CD56, Gr-1) spleen cells. Boxes in panels show the percentages of cells enclosed. Gated total DCs cells were further analyzed for CD8 *versus* CD172a, and 3 discrete populations were observed; populations 1 (DC1a), 2 (DC1b), and 3 (DC2) (indicated by blue, red, and black ovals) respectively. The 3 populations were analyzed for intracellular staining of the Irf8 and Irf4 nuclear factors compared to isotype control staining. Representative histograms are shown as well as the mean (MFI) for Irf8 and Irf4 staining intensity among the gated DC populations (n = 8-10). One-way ANOVA (Holm-Sidak's multiple comparison test) was used for statistical analysis. *p < 0.05, **p < 0.01, ***p < 0.001, NS-not significant (p > 0.05). **(B)** Compares the mean (± SEM) percentages of populations 1 (DC1a), 2 (DC1b), and 3 (DC2) among total DCs from the spleens of untreated (UNT) WT C57BL/6 and BALB/c mice (n =18-20). **(C)** Shows staining for CD8α *versus* CD172 on gated CD11c$^+$MHCII$^+$ draining lymph node cells from WT BALB/c mice. The 3 gated populations of DCs were stained for Irf8 and Irf4, and representative histograms are shown. The bar graphs compare the mean percentages of DC1a, DC1b, and DC2 cells from draining lymph nodes of WT BALB/c and C57BL/6 mice **(D)** Shows representative two color FACS patterns of CD11c+ MHCII+ cells among spleen cells from *Batf3*$^{-/-}$ BALB/c mice. Gated cells from each box were further analyzed for CD8 *versus* CD172a. Too few populations 1 and 2 cells were available to stain for nuclear factors, and expression of Irf4 by population 3 is shown in a representative histogram. The mean percentages of the 3 DC populations are compared from WT *versus* Batf3-/- BALB/c mice in the bar graphs.

The mean fluorescence intensity (MFI) of staining for Irf8 and Irf4 among the 3 populations of gated splenic DCs is shown in **Figure 1A**. Mean intensity for Irf8 was highest in the DC1a cells, intermediate in DC1b cells and at background levels in DC2 cells. Differences in means were statistically significant for all 3 populations (p<0.001). As expected, the staining pattern for Irf4 showed the opposite pattern with the mean for Irf4 significantly increased (p<0.001) as compared to background staining levels for DC1a and DC1b cells.

Similar analysis of expression of CD8 vs CD172 on gated DCs from the draining lymph nodes of WT BALB/c mice showed that the same discrete contours for 3 populations was observed, and histograms of Irf8 and Irf4 staining followed the pattern observed in the spleen (**Figure 1C**). Although the mean percentage of DC1b cells in the draining nodes of BALB/c mice was about 70%, the DC2 cells constituted the majority of DCs in the draining nodes of C57BL/6 mice (**Figure 1C**).

Additional analysis of gated DCs from the spleen of Batf3-/- BALB/c mice showed a dramatic reduction of the DC1a and DC1b cells in representative histograms, and the DC2 cells with the Irf8-Irf4+ pattern accounted for about 93% of total DCs (**Figure 1D**). The DC1a and DC1b population each made up means of less than 3% of the gated DCs, and the DC2 cells made up a mean of over 90% (of **Figure 1D**). Mean percentages of each subset are compared for BALB/c WT *versus* Batf3-/- mice in the bar graph in **Figure 1D**. Mean percentages for DC1a and DC1b cells in the latter mice were below 2% and the mean for DC2 cells was above 90%. The loss of DC1a and DC1b subsets indicated that these were CD8$^+$Batf3 dependent DCs that have been previously identified as DC1 cells (6, 7). The DC2 subset was similar to the CD8$^-$CD172^{hi} subset previously identified as the DC2 subset (6, 7).

DC1a, DC1b and DC2 Cells Differ in Their Expression of Multiple Surface Markers

In an effort to further distinguish the DC populations from one another, we stained the 3 gated subsets of DCs in the WT BALB/c spleen for a variety of additional surface receptors including

those previously shown to identify DC1 cells such as XCR1 and CD24 (5–7). **Figure 2A** shows that XCR1, CD24, DEC205, Tim-3, Clec9A, BTLA, MHCII, and CD8 were highly expressed on DC1a cells as compared to other DC populations (MFI vs DC1b and DC2 cells p<0.001). In contrast, the MFI for CD1d, CD103, and Tim4 on DC1b cells was significantly increased as compared to that of DC1a and DC2 cells (**Figure 2B**). Surface receptors highly expressed on DC2 cells as compared to DC1a and DC1b cells were CD11b, CD40, CD172, and CD4 (p<0.001) (**Figure 2C**). **Figure 2D** summarizes the patterns of high levels of receptor expression that distinguishes each of the 3DC populations.

DC1a, DC1b and DC2 Cells Differ in Their Tissue Distributions

In further studies, we elucidated the distribution of the DC populations in the mesenteric lymph nodes (msLNs), intestines (gut), liver, and peripheral blood. Mononuclear cells were collected from the four tissue sources from WT BALB/c mice, and the percentages of these cells among total DCs were determined and compared to that in the spleen and draining lymph nodes. MHCII+CD11c+ total DCs from each tissue were gated as before and analyzed for the expression of CD8 *versus* CD172 as shown in **Figure 3A**. Three DC populations were clearly identified among the the msLN cells and peripheral blood mononuclear cells (PBMC) as shown in the representative two color stainings. In contrast, only one population of DCs that had the staining characteristics of DC1b cells was found among the gut mononuclear cells, and neither the DC1a nor the DC2 populations were identified (**Figure 3A**). Two DC populations with characteristics of the DC1a and DC1b cells were found among liver mononuclear cells, and the DC2 population was not observed (**Figure 3A**).

Figures 3B-E shows the mean percentages of each DC population among total DCs from the 4 tissues. Each population accounted for a mean of at least 10% among total DCs in the msLNs and PBMC, and the mean percentage of DC1a cells were significantly increased as compared to the other populations in these tissues (p<0.001) (**Figures 3B, E**). The mean percentage of DC1a and DC2 cells among total DCs in the gut accounted for less that 2%, and almost all were DC1b cells (**Figure 3C**). The mean percentage of DC2 cells was below 1% in the liver, and about 60% were DC1b cells and 30% DC1a (**Figure 3D**). In summary, three populations of DCs were found in the msLNs and PBMC as was observed in the spleen and draining lymph nodes. Whereas the dominant population in the latter two tissues was DC1b, the dominant population among the msLNs and the PBMC was DC1a. DC2 cells were not identified in the two non-lymphoid tissues (gut and liver), and were easily identified in the four lymphoid tissues.

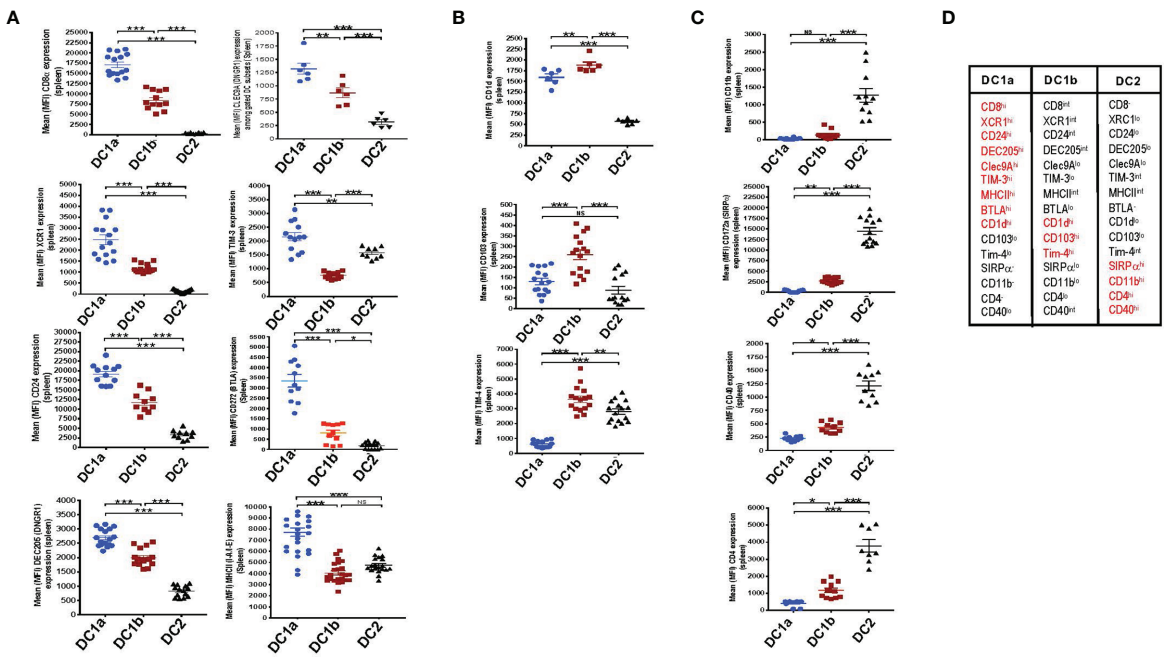

DC1a	DC1b	DC2
CD8^{hi}	CD8^{int}	CD8^{-}
XCR1^{hi}	XCR1^{int}	XRC1^{lo}
CD24^{hi}	CD24^{int}	CD24^{lo}
DEC205^{hi}	DEC205^{int}	DEC205^{lo}
Clec9A^{hi}	Clec9A^{lo}	Clec9A^{lo}
TIM-3^{hi}	TIM-3^{lo}	TIM-3^{int}
MHCII^{hi}	MHCII^{int}	MHCII^{int}
BTLA^{hi}	BTLA^{lo}	BTLA^{-}
CD1d^{lo}	CD1d^{hi}	CD1d^{lo}
CD103^{lo}	CD103^{hi}	CD103^{lo}
Tim-4^{lo}	Tim-4^{hi}	Tim-4^{int}
SIRPα^{-}	SIRPα^{lo}	SIRPα^{hi}
CD11b^{-}	CD11b^{lo}	CD11b^{hi}
CD4^{-}	CD4^{lo}	CD4^{hi}
CD40^{lo}	CD40^{int}	CD40^{hi}

FIGURE 2 | DC1a and DC1b cells in the spleen differ in their expression of multiple surface markers that also distinguish them from DC2 cells. **(A)** Shows individual and mean (MFI) levels of staining intensity of receptors that are most highly expressed on gated population 1(*DC1a*) cells including CD8a, XCR1, CD24, DEC205, Clec9A, TIM-3, MHCII, and BTLA (CD272) in WT BALB/c spleen cell samples. **(B)** Shows MFI levels of receptors most highly expressed on population 2 (*DC1b*) cells including CD1d, CD103, (DNGR1), and TIM-4. **(C)** Shows MFI levels of receptors most highly expressed on population 3 (*DC2*) cells including CD11b, CD172a (SIRP), CD40, and CD4. **(D)** Table shows the summary patterns of high expression of surface receptors on 3 DC subsets in the spleen. Receptors in red are those with MFIs that were significantly increased as compared to that of the two other DC populations. (N = 10-20). One-way ANOVA (Holm-Sidak's multiple comparison test) was used for statistical analysis. *p < 0.05, **p < 0.01, ***p < 0.001, NS, not significant (p > 0.05). MFI, mean fluorescence intensity.

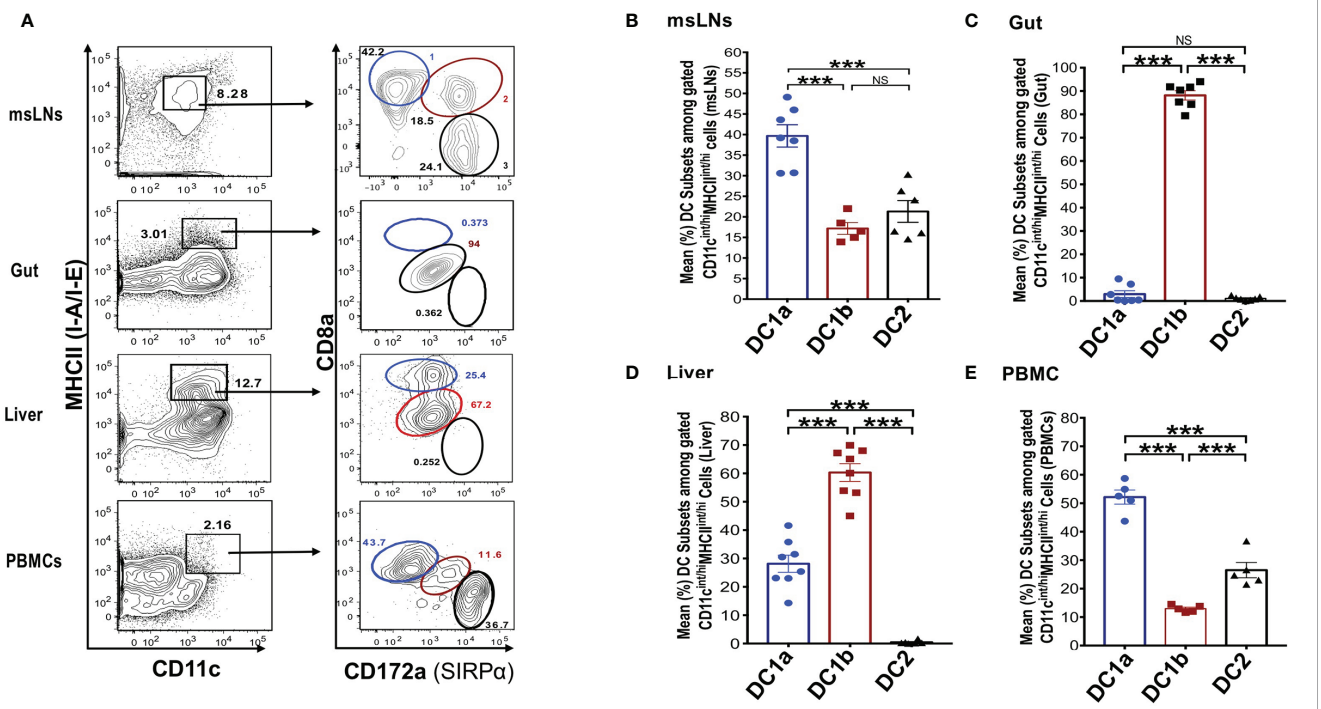

FIGURE 3 | Distribution of 3 DC subsets in different tissues (mesenteric LNs, gut, liver and PBMCs). **(A)** Shows representative FACS staining of gated MHCII+CD11c+ total DCs from mesenteric lymph nodes (msLNs), intestines (gut), liver and PBMCs of WT BALB/c mice. Total DCs were further analyzed for CD172a *versus* CD8a staining, and ellipses outline populations 1,2, and 3(DC1a, DC1b, DC2). Mean (SEM) percentages of 3 DC populations among total DCs in **(B)** msLNs, **(C)** gut, **(D)** liver, and **(E)** PBMCs cells. (N = 6-10). One-way ANOVA (Holm-Sidak's multiple comparison test) was used for statistical analysis. ***p < 0.001, NS, not significant.

Gene Expression Profiling Distinguishes the 3 DC Populations

In order to compare the gene expression pattern of the 3 DC populations in the spleen of WT BALB/c mice, the cells were sorted by flow cytometry according to the gates shown in **Figure 1A** for populations 1, 2, and 3, RNA was extracted from the sorted cells, and the gene expression profiles were compared using the RNAseq. **Figure 4A** shows the heat map comparison of gene expression for sorted DC1a vs DC1b cells, **Figure 4B** shows the comparison for DC1a vs DC2 cells, and **Figure 4C** shows the comparison for DC1b vs DC2 cells. The 3 heat maps clearly distinguished the gene expression patterns of the 3 sorted populations. Further quantitative analysis of differences in the immune response and signaling pathways encoded by the upregulated genes of the DC1b *versus* DC1a cells are shown in **Supplemental Figure 1**.

In particular, genes encoding pro-inflammatory and allograft rejection immune response pathways including upregulation of signaling pathways for TNFalpha and IL-2 were significantly increased in the DC1b *versus* DC1a cells as judged by normalized enrichment scores (NES)(**Supplementary Figure 1A**). Similar upregulation of genes encoding pro-inflammatory response pathways and cytokine signaling including interferon alpha and gamma, TNFalpha, or IL-2 were observed as judged by NES when DC2 cells were compared to DC1a cells or when DC2 cells were compared to DC1b cells (**Supplementary Figures 1B, C**). In contrast, expression of gene pathways encoding Myc targets and oxidative phosphorylation were reduced when comparing DC1b *versus* DC1a cells, and DC2 *versus* DC1a cells. Principal component analysis (**Supplementary Figure 1D**) also showed marked differences in gene expression patterns of the 3 DC populations with variances of 40% and 29% for PC1 and PC2 respectively. Duplicate experiments for purification of each of the 3 populations showed marked concordance of gene expression patterns within each population as compared to marked differences between populations (**Supplemental Figure 1E**).

Analysis of the upregulated genes shown in **Figures 4A-C** identified three surface proteins that were predicted to be upregulated in DC1b vs DC1a cells: CD324 (E-cadherin), DC1a vs DC2 cells CD207 (langerin), and DC1b vs DC2 cells (Ly6-D). Staining of the splenic DCs showed that the MFIs of the 3 receptors were increased the appropriate cell populations as predicted by the gene expression patterns (**Figures 4D–F**).

All 3 DC Subsets Present Class I and II MHC Restricted OVA Peptide Antigens to OT-I CD8$^+$ T Cells and OT-II CD4$^+$ T Cells Respectively

We tested the ability of the 3 DC subsets to present a class I MHC restricted ovalbumin (OVA) peptide antigen to OT-1 CD8$^+$T cells harvested from C57BL/6 mice bearing a transgenic TCR

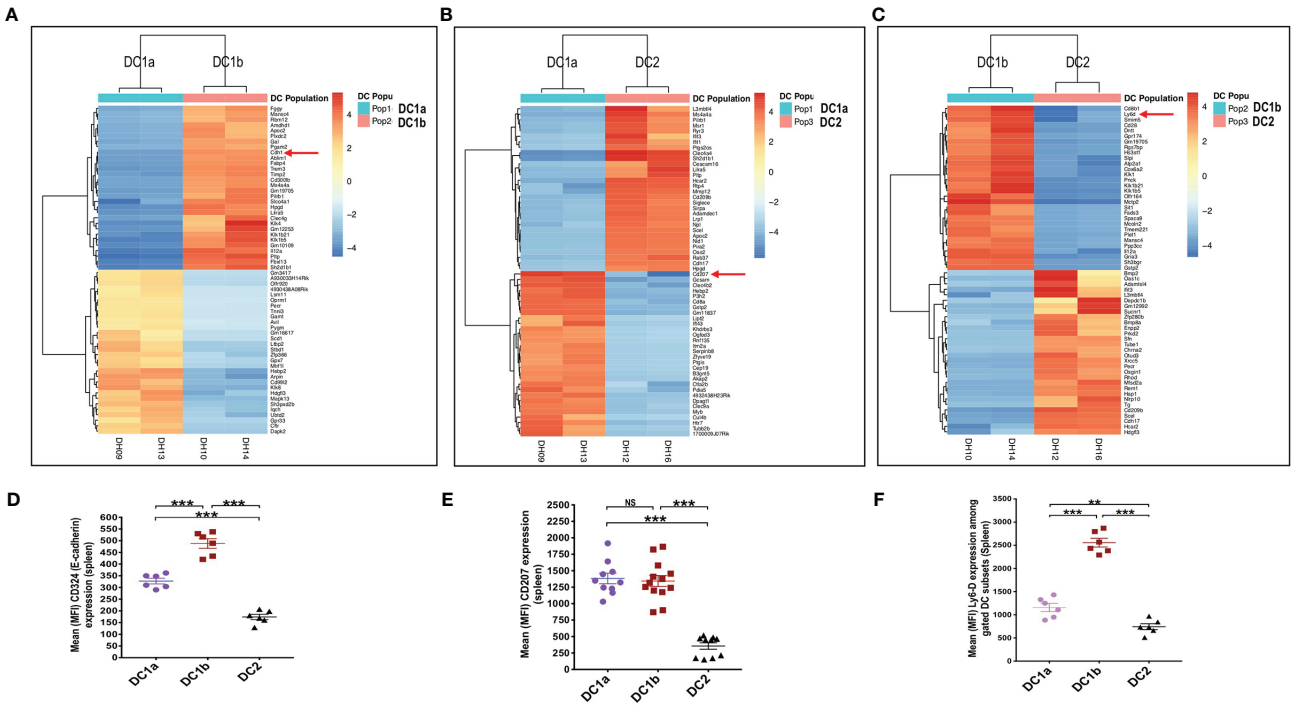

FIGURE 4 | Gene expression profiling reveals additional differences between the 3 DC subsets. **(A)** Heat map of genes with significantly increased or decreased expression levels (as determined by RNA-seq analysis) in sorted DC1a (Pop 1) *versus* DC1b (Pop 2) or **(B)** DC1a (Pop 1) *versus* DC2 (Pop 3) or **(C)** DC1b (Pop 2) *versus* DC2 (Pop 3) from the WT BALB/c spleen. Each row represents a gene identified on the right side of the map, and each column represents a result from a single sample. The color scale shown on the map shows the relative expression levels of the genes across all the samples. Red and yellow shades represent higher expression levels, while blue shades represent lower expression levels. **(D–F)** Representative staining intensities and MFI of upregulated receptors CD207 (langerin), CD324 (E-cadherin; *Cdh1*), and Ly6-D cells on DC subsets (n = 10-20). The genes of these three markers were identified by the RNAseq analysis and were stained to confirm their expression at the protein level. One-way ANOVA (Holm-Sidak's multiple comparison test) was used for statistical analysis of MFI. *p < 0.05, **p < 0.01, ***p < 0.001, NS, not significant (p > 0.05).

that recognizes this peptide antigen (41, 42). In addition, we tested the ability of the 3 DC subsets to present a class II MHC restricted peptide to OT-II $CD4^+$ T cells with the appropriate transgenic TCR (42). Since the 3 DC subsets described above expressed both class I and class II MHC on their cell surfaces, we hypothesized that each DC subset would be able to present both the class I and class II restricted peptides to the OT-I and OT-II T cells respectively when the peptides were added to cultures of each DC subset with the appropriate T cells. However, the lower levels of class II MHC on DC1b cells as compared to the DC1a and DC2 cells, could reduce the activity of the former as compared to the latter subsets with regard to presentation of the class II restricted peptide.

In order to test the antigen presenting activity of the 3 DC subsets independent of the need for antigen processing, OT-1 $CD8^+$ T cells were harvested from the spleens of C57BL/6 transgenic mice and cultured in the presence or absence of sorted C57BL/6 DC1a, DC1b, or DC2 cells in the presence or absence of the class I MHC restricted SIINFEKL peptide derived from ovalbumin. Culture supernatants were assayed for IL-4, IFN, IL-13, and IL-2. **Figure 5A** shows that all 3 subsets of DCs stimulated the robust secretion of IFN and IL-2 with little or no secretion of IL-4 (<100pg/ml) and modest secretion of IL-13 (<600pg/ml). The mean concentrations of IFN (about 9,000 pg/mL) in the cultures containing the combination of $CD8^+$T cells with each DC subset, and peptide were increased ($p<0.001$) as compared to the means in cultures containing the combination of $CD8^+$ T cells and peptide without the DCs. DC1a cells stimulated a mean concentration that was a few hundred pg/mL higher than that of the DC1b and DC2 cells ($p<0.05$). In contrast, the DC2 subset stimulated the highest secretion of IL-2 (mean about 12,5000pg/mL) that was about 10,000 pg/mL higher than that stimulated by the DC1a subset ($p<0.001$).

In further experiments, we tested the ability of the 3 DC subsets to present a class II MHC restricted peptide to $CD4^+$ OT-II T cells. **Figure 5B** shows that all 3 DC subsets stimulated robust secretion of IFN and IL-2 at levels that were comparable to those observed with OT-I cells (2,500-12,500pg/ml), and minimal secretion (<100pg/ml) of IL-4 or IL-13 (<300/pg/ml) consistent with the Th1 pattern observed with OT-I cells. The experiments with OT-II cells were repeated using ovalbumin protein instead of ovalbumin peptide. As shown in **Supplemental Figures 2A-D**, the Th1 pattern of OT-II cell immune response was similar when the protein was used instead of the peptide. In particular, the 3 DC subsets stimulated robust secretion of IFN gamma and IL-22

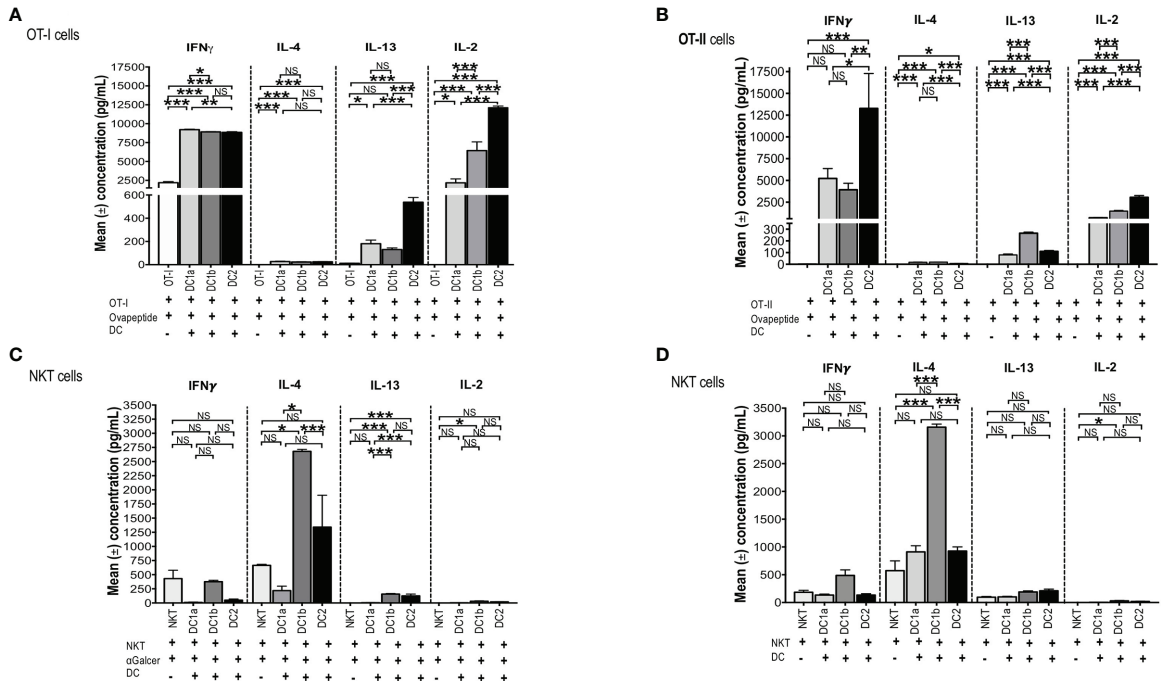

FIGURE 5 | All 3 DC subsets can present Class I, and II MHC restricted OVA peptide antigens, but only DC1b cells present glycolipid antigens. **(A)** Mean concentrations of IL-2 (Right), IL-13 (Right Middle), IL-4 (Left Middle), and IFNγ (Left) in culture supernatants of FACS-sorted DC subsets (DC1a, DC1b and DC2) ($1x10^4$ per well) from wild type untreated C57BL/6 mice that were cultured with OT-I restricted $OVA_{257-264}$ peptide (1g/mL) and with CFSE-labelled OT-I $CD8^+$ T-cells ($1x10^5$ cells per well). In control experiments, CFSE-labelled OT-I $CD8^+$ T-cells ($1x10^5$ cells per well) were incubated with $OVA_{257-264}$ peptide (1g/mL) but without DCs for 5 days. The concentrations of IL-4, IL-13, IL-2, IFN in culture supernatants was measured by Luminex. **(B)** Mean concentrations of IL-2 (Right), IL-13 (Right Middle), IL-4 (Left Middle), and IFNγ (Lef) in culture supernatants of FACS-sorted DC subsets (DC1a, DC1b and DC2) ($1x10^4$ per well) from wild type untreated C57BL/6 mice that were cultured with OT-II restricted $OVA_{323-339}$ peptide (10g/mL) with CFSE-labelled OT-II $CD4^+$ T-cells ($1x10^5$ cells per well). In control experiments, CFSE-labelled OT-II $CD4^+$ T-cells ($1x10^5$ cells per well) were incubated with $OVA_{323-339}$ peptide (10g/mL) without DCs for 5 days. The concentrations of IL-4, IL-13, IL-2, IFN in culture supernatants was measured by Luminex. All data are representative of three independent experiments (6 mice per experiment). **(C, D)** Mean concentrations of cytokines in cultures of sorted DC1a (Pop 1), DC1b (Pop 2) and DC2 (Pop 3) ($15x10^3$ cells/well) subsets incubated with sorted NKT cells ($5x10^5$ cells/well) from untreated wild type BALB/c spleen cells. AlphaGalcer (α-galactosylceramide) (100ng/mL) was added to all cultures in **(C)** but not in **(D)**. Control cultures contained NKT cells with **(C)** or without **(D)** glycolipid but without DCs. Supernatants were harvested after 5 days, and concentrations were measured by Luminex. Data pooled from 2 or more independent experiments for a total of at least 10-12 mice per group, represented as mean ± SEM. *$p < 0.05$, **$p < 0.01$, ***$p < 0.001$, NS, not significant ($p > 0.05$). One-way ANOVA (Holm-Sidak's multiple comparison test) was used for statistical analysis.

(>2,500pg/ml), and considerably less IL-2, IL-13, TNF alpha, and IL-17 (<1,000 pg/ml). The results indicate that all 3 DC subsets can process the protein for presentation to the OT-II T cells. Stimulation of the OT-I and OT-II cells by DCs pulsed with peptide or protein as measured by proliferation (CFSE dilution), indicated that all 3 subsets were effective inducers of proliferation (data not shown).

The DC1b, but Neither the DC1a nor DC2 Subset, Presents Glycolipid to NKT Cells and Induces a TH2 Response

A previous study, showed that Batf-3 dependent $CD8^+$ DCs were able to present a variety of glycolipids, including the potent activating Galcer glycolipid, to NKT cells *in vitro* and *in vivo*, but the Batf-3 independent DC2 cells could not (36). We hypothesized that the DC1b subset described above would be more potent than the DC1a and DC2 subsets in stimulating an immune response to the Galcer glycolipid after co-culture with purified NKT cells, since the DC1b subset expressed significantly higher levels of glycolipid antigen presenting molecule, CD1d, as compared to the DC1a and DC2 DC subsets (**Figure 2**).

To test this hypothesis, $CD1dtetramer^+$ NKT cells were harvested from the spleens of BALB/c mice and cultured in the presence or absence of sorted BALB/c DC1a, DC1b, or DC2 cells in the presence of Galcer. **Figure 5C** compares the mean concentrations of IFN, IL-4, IL-13 and IL-2 from cultures of NKT cells and Galcer without or without the purified DC subsets. Only DC1b cells induced IL-4 (about 2,500 pg/mL) as compared to cultures lacking DCs. DC1b cells induced significantly higher levels of IL-4 as compared to DC1a and DC2 cells. DC2 cells failed to stimulate significantly increased production of IL-4 as compared to control cultures without DCs. **Figure 5C** shows that DC1b cells (but not DC1a) stimulated low levels of secretion of IL-13 (mean <100pg/ml) and IL-2 (mean <50pg/ml *in vitro* that were increased as compared to the background controls, but 25-50-fold less than IL-4.

Since, DCs are able to present constitutively expressed endogenous glycolipid antigens to NKT cells (48), the above

experiments that tested the ability of DC subsets to stimulate cytokine secretion of purified NKT cells were repeated in the absence of Galcer. **Figure 5D** shows that the secretion of IL-4 induced by DC1b cells in the absence of Galcer was at least as robust as in the presence of Galcer. There was a highly significant increase in the mean concentration of IL-4 in NKT cell cultures with DC1b cells *versus* cultures with NKT cells alone ($p<0.001$). In addition, DC1a and DC2 cells failed to significantly increase IL-4 concentrations as compared to control cultures with NK T cells alone. A similar pattern was observed with IL-13 secretion; however, the concentrations were all below 200pg/ml. None of the 3 DC subsets induced robust NKT cell secretion of IFN or IL-2 (**Figures 5C, D**). In summary, only DC1b cells induced robust Th2 cytokine secretion by NKT cells that was predominantly polarized toward IL-4 in contrast to the TH1 pattern induced in OT-I and OT-II by all 3 DC subsets. The response of NKT cells induced by DC1b cells is likely due to endogenous glycolipid antigens.

Slowing the Growth of B16-OVA Melanoma After Vaccination With OVA Loaded DC Subsets

Batf3 dependent $CD8^+CD103^+$ DC1 cells, present in the microenvironment of tumors, cross-present tumor antigens to $CD8^+$ T cells in the regional lymph nodes, and are required to initiate an immune response to the tumor (9–11). It is unclear, whether the DC1 cells are also required to initiate an anti-tumor immune response when the tumor antigens are incorporated into a subcutaneous vaccination to treat a tumor. In order to determine whether tumor antigen pulsed DC1a, DC1b, and/or DC2 cells can be used as a vaccination to initiate an immune response and slow the growth of the subcutaneous B16-OVA melanoma tumor, the purified subsets were incubated with ovalbumin whole protein and injected subcutaneously twice into wild type BALB/c mice 4 and 2 weeks before injection of the tumor cells. **Figure 6** shows the growth of the subcutaneous tumors as measured by tumor volume on days 11, 15, 17 and 22 after tumor cell injection. Control wild type mice had no vaccination.

The tumor growth in control mice was rapid, and the mean tumor volume at day 22 was about $4500mm^3$. Experimental mice that were vaccinated with the 3 different subsets of DCs showed significant slowing of tumor growth with all 3 subsets as compared to control mice. When DC1a cells were used as the vaccination, the day 22 mean volume was reduced to 2500 mm^3 ($p<0.05$), and when DC1b and DC2 cells were used the volumes were further reduced to about 1,200 and 1,000 mm^3 respectively ($p<0.001$). The DC1b and DC2 cells were significantly ($p<0.01$) more effective in slowing tumor growth than the DC1a cells.

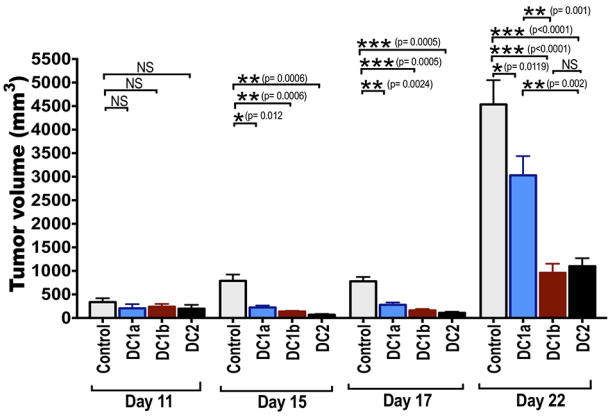

FIGURE 6 | Tumor antigen-pulsed DC1b and DC2 cells are more effective than tumor antigen-pulsed DC1a cells at reducing tumor growth. Bar graphs depicting mean (+/-SE) tumor volumes in wild type C57BL/6 hosts monitored for 22 days. FACS-sorted DC subsets from wild type C57BL/6 mice were pulsed with whole OVA protein (500g/mL) *in vitro* for 1 hour, and then injected *in vivo* into wild type C57BL/6 hosts twice subcutaneously with a 2-week interval between injections. Hosts were then challenged with B16F10-ova tumor cells ($5x10^4$ cells/mouse) injected subcutaneously on the flank of mouse 2 weeks after the second injection of OVA pulsed DCs, and the tumor volumes monitored over time. Control mice received tumor cells with no vaccination. Data are representative of two independent experiments. Each data point reflects data from 6-10 mice injected with FACS-sorted DC subsets pooled from 8-10 mice. One-way ANOVA (Holm-Sidak's multiple comparison test) results are indicated as *$P < 0.05$, **$p < 0.01$, ***$p < 0.001$, NS, not significant ($p > 0.05$).

DISCUSSION

Our findings show that Batf3 dependent $CD8^+$DC1 cells, which had been previously distinguished from DC2 cells by the expression of surface markers such as CD24 and XCR1 (6, 20) and the nuclear transcription factor Irf8 (4, 5), can be further divided by their surface phenotype, gene expression profile and function into two subsets that we have designated DC1a and DC1b. Both DC1a and DC1b cells expressed CD24, XCR1, CD8, and Irf8 but the levels of expression were significantly different, and the DC1b cells expressed significantly lower levels. DC1b cells expressed significantly higher levels of CD1d, CD103, and Tim-4 as compared to the DC1a cells. In contrast, the DC2 cells failed to express CD24, XCR1, CD8, and Irf8, but did express Irf4. The DC1a, DC1b, and DC2 subsets were clearly identified by flow cytometry in the lymphoid tissues including the spleen, skin draining lymph nodes, msLNs, and PBMC when MHCII +CD11c+ total DCs were further analyzed for the expression of CD8 *versus* CD172.

Interestingly, only the DC1b subset was clearly identified by flow cytometry among total DCs in the intestines. The results suggest a failure of the DC1a and DC2 subsets to migrate to the gut. Our continuing studies investigate the chemokine receptors and other trafficking molecules on all three subsets, and whether sorted DC1b cells from the intestines differ in their gene expression pattern and function from the sorted DC1b cells from the lymphoid tissues. It has been previously shown that almost all CD8+DCs in the intestines express CD103 (27). The latter is consistent with the current finding that only DC1b cells are present in the intestines, since DC1b cells expressed

significantly higher levels of CD103 than the DC1a or DC2 cells. E-Cadherin was also highly expressed along with CD103 on the DC1b cells, and this is likely to promote interactions between these cells since E-Cadherin binds to CD103, and the heterodimers can modulate their immune functions (48).

Sorted DC1a, DC1b and DC2 cells from the spleen were compared for their gene expression patterns using RNAseq analysis. Differences in gene expression patterns predicted that the expression of E-cadherin and Ly6-D surface receptors also could be used to distinguish the subsets, and this was confirmed by surface staining. Despite the capacity of all 3 DC subsets to present peptide and protein antigens to OT-II CD4 T cells and OT-I CD8 T cells, only the DC1b subset with the highest level of expression of the CD1d was able to effectively present the Galcer or endogenous glycolipid antigens to NKT cells. This finding is consistent with the previously reported ability of $CD8^+$DCs to present a variety of glycolipid antigens to NKT cells *in vitro*, whereas the $CD8^-$DCs were ineffective (36, 37). Interestingly, the NKT cell response elicited by the DC1b cells showed a Th2 skewing made up predominantly of IL-4 with minimal IFN or IL-2 (27). This polarization is likely due to the low level of CD40 on the DC1b subset, since blocking of the CD40/CD40L interaction has been shown to result in a Th2 polarization of NKT cells (49).

The DC2 cells were also more effective than DC1 cells in eliciting immune responses after vaccination with OVA pulsed DC subsets to control the growth of the OVA-B16 melanoma tumor cells. DC1 cells have been studied extensively for their capacity to cross-present intracellular tumor antigens and viral antigens to $CD8^+$ T cells in local lymph nodes to subsequently induce systemic immune responses (9). However, the role of DC1 *versus* DC2 cells in the context of the induction of immune responses after subcutaneous vaccination with tumor or viral antigens remains to be elucidated, since the antigens in vaccines can be taken up directly by DCs in local lymph nodes without the need for cross-presentation. In addition, DCs can be pulsed *in vitro* with these antigens. Previous studies showed that DC2 cells can be at least as effective as DC1 cells in the induction of anti-tumor immune responses after vaccination, and can generate anti-tumor $CD4^+$ and $CD8^+$ memory T cells (35).

In the current study, we found that vaccination with OVA pulsed DC1b and DC2 cells were more effective than the pulsed DC1a cells in controlling the growth of the OVA-B16 melanoma. The results suggest that the DC1b cells are more effective in generating memory T cells to OVA tumor antigen than DC1a cells in the context of vaccination. However, further studies are needed to compare the efficacy of the two subsets for antigen cross-presentation of tumor antigens in the tumor microenvironment. Tumor control is likely to involve DCs in the generation of memory T cells from the vaccination as well as cross-presentation of antigen by DCs in the tumor microenvironment. In conclusion, our studies showed that $CD8^+$Batf3 dependent DC1 cells are comprised of DC1a and DC1b subsets that differ in their surface marker phenotype, gene expression patterns, and function from each other as well as from DC2 cells.

MATERIALS AND METHODS

Mice

Adult 8- to 10-week-old male *Batf3*$^{-/-}$ BALB/c (H-2K^d)[1] mice, wild type C57BL/6 (H-2K^b), and (C57BL/6-Transgenic (*TcraTcrb*)1100Mj) OT-I ($CD8^+$ TCR-Tag specific for ovalbumin (OVA) derived SIINFEKL peptide) mice (41) were used for the studies. Transgenic C57BL/6-OT-II mice (B6. Cg *(TcraTcrb)* 425Cbn/J) with a $CD4^+$TCR-Tag specific for OVA $_{323\text{-}339}$ peptide, were used also. All mice were obtained from the Jackson Laboratory (Bar Harbor, ME) (42). *Ja18*$^{-/-}$ BALB/c mice were originally obtained through a material transfer agreement with Dr. Taniguchi of RIKEN Research, Japan. Wild type BALB/c (H-2K^d), *Cd1*$^{-/-}$ BALB/c mice and *Ja18*$^{-/-}$ BALB/c mice (39) were bred in the Department of Comparative Medicine, Stanford University (Stanford, CA), and all mice were maintained in the Department according to institutional guidelines approved by the National Institutes of Health.

Immunofluorescent Staining and Fluorescent Activated Cell Sorter Analysis

Staining procedures and flow cytometry analysis performed on FACS LSRII or Aria machines (Becton Dickinson, San Jose, CA) and have previously been described in detail (43). The Fluorochrome conjugated mAbs used for staining were purchased from Invitrogen (San Diego, CA), Biolegend (San Diego, CA), BD biosciences (San Jose, CA), Novus Biologicals (Littleton, CA), Bio-Rad (Hercules, CA) and R&D Systems, (Minneapolis, MN). The following reagents and antibodies were used for flow cytometry:

CD11c (clone: N418; HL3); CD8a (clone: 53-6.7); CD205 (DEC205)(clone: NLDC-145); MHCII (I-A/I-E)(clone: M5/144.15.2); TLR3 (clone: 40C1285.6); TLR3 (clone: 40C1285.6); TLR4 (clone: MTs510); CD16 (FcγRIIIA)(clone: 5B11); CD32B (FcγRIIB); CD11b (clone: M1/70); CD172a (SIRPa) (clone: P84); CD45R/B220 (clone: RA3-6B2); CD370 (CLEC9A, DNGR1, clone: 7H11), CD103 (clone: 2E7), Treml4 (clone: 16E5), TIM-4 (clone: RMT4-54); CD40 (3/23); Rae-1; CD69 (clone: H1.2F3); TCRb (clone: H57-597); CD24 (clone: M1/69); XCR1 (clone: ZET); TIM-3 (CD366, clone: RMT3-32); CD1d (clone: 1B1); Clec9A (DNGR1, clone: 7H11); CD4 (clone: GK1.5); CD207 (clone: 929F3.01); CD324 (E-cadherin, clone: DECMA); Ly6-D (clone: 49-H4); PDL-2 (clone: TY25) and PDL-1 (clone: MIH5). Cells were stained with monoclonal antibodies and aqua dye (Zombie Aqua, Biolegend, San Diego, CA), a dead cell exclusion dye prior to flow cytometry analysis as per the manufacturer's protocol (eBioscience, BD biosciences). Phycoerythrin and allophycocyanin conjugated CD1d-tetramers were obtained from the National Institutes of Health (NIH) Tetramer Facility, Rockville, MD. FACS analysis used FlowJo Software.

Isolation, Purification, and Co-Culture of OT-I, and OT-II T Cells

The C57BL/6 spleen cells from either OT-I or OT-II transgenic mice (Jackson Laboratory) were harvested, and the single cell suspensions lysed with ACK lysis buffer (0.15M NH_4Cl, 1mM

KHCO3, and 0.1mM Na_2EDTA {pH 7.4]) for 2 min at room temperature. Subsequently, cells were purified using conventional $CD8^+$ T cell or $CD4^+$ T cell isolation kit by negative selection on MACS LS columns, and then CFSE-labeled (labeled with 2.5μM CFSE) (Molecular Probe, Invitrogen, Eugene, OR). The DC subsets were co-cultured with enriched CFSE-labeled $CD8^+$ T or $CD4^+$ T cells from OT-I or OT-II mice spleen respectively with or without Ovalbumin peptides ($OVA_{257-264}$ (1g/mL), $OVA_{323-339}$ (10g/mL) or whole OVA protein (1g/mL) in 96-well round bottom plates at a ratio of 1:10 (DCs: T cells) at 37C, 5% CO_2 in Complete (10% FCS) RPMI medium for 5 days. After co-culture the culture supernatants were collected for cytokine analysis using Luminex, and the cells were stained for OT-I or OT-II proliferation analysis by flow cytometry. OVA peptides and whole OVA protein were purchased from Sigma-Aldrich (St. Louis, MO).

Isolation and Purification of NKT Cells

Invariant NKT (iNKT) cells were isolated using a gating strategy as described in detail before (44). Briefly splenocytes from wild-type BALB/c mice were stained with glycolipid loaded PE-conjugated CD1d tetramers (National Institutes of Health, Tetramer Facility, Emory-Atlanta, GA), and PE-conjugated-Galcer loaded CD1d dimer-mouse IgG fusion protein (BD Biosciences, San Jose, CA). iNKT cells were enriched subsequently by incubating with anti-PE microbeads (Miltenyi Biotech, Auburn, CA), and passing through a magnetic column (Miltenyi Biotech). The cells were then stained with anti-TCR-FITC and sorted by FACS Aria II (Becton Dickinson). The purity of sorted iNKT cells ($TCR^+CD1d\text{-}tet^+$) was more than 97%. Sorted iNKT cells were then cocultured *in vitro* with DC subsets from untreated wild type BALB/c mice.

Isolation, Purification, and *In Vitro* Irradiation of DC Subsets

The C5BL/6 spleen cells from wild type untreated mice were cut into pieces with scalpel blades, and then digested with collagenase solution at 37C for 30 min on a shaker. The digested spleen cells were filtered with a cell strainer (70μm), and then RBCs were lysed with lysis buffer. For sorting, Miltenyi Mouse Pan-DC enrichment kit was used to enriched $CD11c^+$ cells by magnetic beads labeling and purification on a LS column. For sorting DC cell subsets, the enriched $CD11c^+$ cells were stained with the following monoclonal antibodies; CD11c, B220, MHCII, CD8a, and CD172a. The sorted DC subsets (DC1a (Pop 1), DC1b (Pop 2), DC2 (Pop 3) used for antigen (Ova) presentation to OT-I T cells, were irradiated (3,000 rads) from a ^{137}Cs source (J.L. Shephard & Associates, San Fernando; CA).

Cytokine Quantification of Supernatants From Cultures of NKT Cells, OT-I and OT-II Cells

To determine cytokine production in culture supernatants, NKT cells were cultured (at $5x10^4$ cells/well) with DC subsets (at $1x10^4$ cells/well), or alone. In another study of antigen presentation, OT-I cells ($CD8^+$ T cells; $1x10^5$ cells/well), or OT-II cells or were cocultured with DC subsets (at $1.5x10^4$ cells/well) or alone for 4 days at 37 °C under 5% CO_2 in 96-well flat-bottomed plates (Falcon, Becton Dickinson, Franklin Lakes, NJ) in a volume of 0.2 ml in Complete (10% FCS) RPMI medium for 4 days. Cell-free supernatants were collected after centrifugation for protein analysis, while cell pellets were resuspended and stained for flow cytometric analysis. Supernatants were assayed for IL-4, IL-13, IL-2 and IFN protein amounts using Multiplex magnetic Bead Array kit (ThermoFisher Scientific, Waltham, MA), quantified using a MAGPIX instrument (Luminex Corporation, TX).

In Vitro Stimulation of NKT Cells by Splenic DC Subsets

To assess the efficacy of the 3 DC subsets to stimulate NKT cell cytokine production, sorted iNKT cells from untreated BALB/c mice, and sorted DC subsets (DC1a, DC1b, DC2) obtained from untreated wild type BALB/c spleen cells were cultured alone or together or in some cultures, α-galactosylceramide (100ng/mL) was added. iNKT cells ($5x10^4$ cells/well) and DC subsets ($1.5x10^4$ cells/well) were cultured at 37C, 5% CO_2 in Complete (10% FCS) RPMI medium for 4 days. After culture, the supernatants were harvested, and the concentrations of cytokines in supernatants were quantified using a MAGPIX instrument (Luminex Corporation, TX).

In Vitro Stimulation OT-I $CD8^+$ T Cells, and OT-II $CD4^+$ T Cells by Splenic DC Subsets

To evaluate antigen presentation capabilities of sorted DCs, irradiated DC subsets (DC1a, DC1b, and DC2) were plated in a round bottom 96-well plate at concentration of $1x10^4$ per/well. Purified OT-I $CD8^+$ T cells, or OT-II^+CD4^+ T cells were mixed with DC subsets at a ratio of 1:10 and cocultured for 4 days at 37C in 5% CO_2 in Complete (10% FCS) RPMI media. In some wells, MHCI restricted ovalbumin specific peptide SIINFEKL (OVA peptide $_{257-64}$), or MHCII restricted ISQAVHAAHAEINEAGR (OVA peptide $_{323-339}$, recognized by transgene encoded TCR of OT-II^+CD4^+ T cells), or whole OVA protein were added to the cell cultures. DC subsets were cultured either alone or with OVA or with OT-I T cells or OT-II cells. OT-I T, OT-II or were also either cultured alone or with OVA peptides or with whole OVA protein in control cultures.

In Vivo Immunization of Mice With OVA Protein Pulsed DC Subsets Prior to Tumor (B16F10-OVA Cell Line) Challenge

The ability of DC subsets to process and present antigen to naïve T cells *in vivo* to control OVA-specific tumor (B16F10-Ova) was compared. Sorted DC subsets were pulsed *in vitro* with whole OVA protein (500g/mL) for 1hr in 37C, 5%CO_2 incubator. Pulsed DCs were then used to vaccinate naïve wild type C57BL/6 hosts 2 times in a 2-week interval at a dose of $2x10^5$ cells per mouse by intravenous injection of the tail vein.

Two weeks after the last vaccination with primed DC subsets, C57BL/6 hosts were injected subcutaneously into the flank with $5x10^4$ B16F10-OVA cells/mouse and monitored for tumor growth. B16F10-OVA cells were kindly provided by Dr. Darrell Irvine (Massachusetts Institute of Technology MIT (Cambridge, MA). The equation used to calculate tumor volume was as follows: tumor volume = length x width^2 x 0.52. Mice were euthanized when the tumor diameter of the tumor mass reached 2 cm.

RNA Sequencing Analysis

Total RNA was prepared by sorting enriched CD11c$^+$ subsets; DC1a (Pop 1), DC1b (Pop 2) and DC2 (Pop 3) from spleen cells (1,000 cells per sample) into RLT Plus lysis buffer (Qiagen) and stored at –80 °C, and then processed using RNeasy Micro Plus kit (Qiagen) per the manufacturer's protocol. Two biological replicates were used for DC1a, DC1b and DC2 RNA-seq. The RNA quality was assessed by Agilent 2100 Bioanalyzer (Agilent Technologies). cDNA synthesis and amplification were prepared using SMARTseq v4 UltraLow Input RNA kit (Takara Inc.). The cDNA library was further processed for bulk RNASeq using a KAPA HyperPlus library kit (Roche Inc.) followed by ligation of Illumina Adaptor tags (Illumina Inc.). Library were quantified and sequenced at Human Immune monitoring Core Center and Genomics/ Microarray Core Facility at Stanford University on Illumina Hiseq 4000.

Sequencing yielded 76 bp paired-end reads with a mean sequencing depth of 24.8 million paired-end reads/sample. Trimmomatic (version 0.36) (45) was used to remove adaptors from reads. Clean reads were then aligned to the *Mus musculus* transcriptome (GRCm38) using histat2(version 2.1.0) (46) and gene count matrix of those mapped uniquely to known mRNAs (GRCm38.84.gtf) were generated by stringtie (version 1.3.1c, prepDE.py function) (47). DESeq2 was used to carry out differential gene expression of pairwise comparisons between tissues with the same genotype and between genotypes in the same tissue.

Statistical Analysis

Results from independent experiments were pooled, and all data were analyzed using Prism (GraphPad Software; VERSION 7) by comparison of means using unpaired two-tailed Student's *t* tests. A difference of 0.05 was accepted as statistically significant. The data in all figures represent mean ± SEM to indicate variation within each experiment. One-way ANOVA (Holm-Sidak's multiple comparison test) was used for statistical analysis. *-p<0.05; **-p<0.01; ***-p<0.001; NS-not significant (p>0.05). Statistical analysis for RNA-seq data is described above.

DATA AVAILABILITY STATEMENT

The original contributions presented in the study are publicly available. This data can be found here: https://www.ncbi.nlm.nih.gov/geo/GSE181475.

ETHICS STATEMENT

The animal study was reviewed and approved by Stanford University IACUC and APLAC committee according to institutional guidelines approved by the National Institutes of Health.

AUTHOR CONTRIBUTIONS

DH designed and performed research, contributed vital analytical methods, collected, analyzed and interpreted data, and wrote manuscript. PZ helped perform RNA sequencing and gene expression analysis. SD helped perform tumor experiment. RP helped with Luminex analysis. EM helped design experiments. EE helped design experiments, and helped write manuscript. SS provided overall research supervision and wrote manuscript. All authors contributed to the article and approved the submitted version.

FUNDING

This work was supported by grants from the National Institutes of Allergy and Infectious Diseases (R01CA23395801), and National Heart, Lung, and Blood Institute (PO1HL- 075462).

SUPPLEMENTARY MATERIAL

The Supplementary Material for this article can be found online at: https://www.frontiersin.org/articles/10.3389/fimmu.2021.746469/full#supplementary-material

Supplementary Figure 1 | DC1a, DC1b and DC2 cells shows differences in expression of genes encoding immune response and cytokine signaling pathways. **(A–C)** GSEA (gene set enrichment analysis) of the most significantly ($p < 0.1$) upregulated and downregulated genes was compared using NES (normalized enrichment scores) of gene transcripts obtained by RNAseq analysis of sorted DC1a (Pop 1), DC1b (Pop 2) and DC2 (Pop 3) cells from WT BALB/c spleens. GSEA was used to determine NES as follows: - NES = actual ES/mean (ESs against all permutations of the data set). A small normal p value and a high FDR value indicates not significant. FDR is adjusted for gene set size and multiple hypothesis testing but not p value. **(D, E)**. Shows the PCA of the three DC subsets, and the distance among the samples respectively. The information for gene set analysis were obtained from the following websites. GSEA website: https://www.gseamsigdb.org/gsea/doc/GSEAUserGuideTEXT.htm#_Enrichment_Score_(ES) Hallmark gene sets were downloaded from website: http://bioinf.wehi.edu.au/MSigDB/v7.1/Mm.h.all.v7.1.entrez.rds: H hallmark gene sets.

Supplementary Figure 2 | All 3 DC subsets pulsed with OVA protein stimulated robust secretion of Th1 cytokines by OT-II CD4$^+$ T-cells. **(A–D)** Mean concentrations of IFN, IL-4, IL-13, IL-2, IL-22, TNF, and IL-17a in culture supernatants. FACS-sorted enriched DC subsets (DC1a, DC1b and DC2) ($1x10^4$ per well) from wild type untreated C57Bl/6 mice cultured alone or with CFSE-labelled OT-II CD4$^+$ T-cells from ($1x10^5$ cells per well) in the presence of whole OVA protein (1g/mL). Cytokines in culture supernatants were measured by Luminex. Control cultures contained OT-II cells alone. Data was pooled from 2 or more independent experiments for a total of at least 10-12 mice per group. One-way ANOVA (Holm-Sidak's multiple comparison test) results are indicated.

REFERENCES

1. Hildner K, Edelson BT, Purtha WE, Diamond M, Matsushita H, Kohyama M, et al. Batf3 Deficiency Reveals a Critical Role for CD8alpha+ Dendritic Cells in Cytotoxic T Cell Immunity. *Science* (2008) 322:1097–100. doi: 10.1126/science.1164206
2. Edelson BT, Kc W, Juang R, Kohyama M, Benoit LA, Klekotka PA, et al. Peripheral CD103+ Dendritic Cells Form a Unified Subset Developmentally Related to CD8alpha+ Conventional Dendritic Cells. *J Exp Med* (2010) 207:823–36. doi: 10.1084/jem.20091627
3. Aliberti J, Schulz O, Pennington DJ, Tsujimura H, Reis e Sousa C, Ozato K, et al. Essential Role for ICSBP in the *In Vivo* Development of Murine CD8alpha + Dendritic Cells. *Blood* (2003) 101:305–10. doi: 10.1182/blood-2002-04-1088
4. Grajales-Reyes GE, Iwata A, Albring J, Wu X, Tussiwand R, Kc W, et al. Batf3 Maintains Autoactivation of Irf8 for Commitment of a CD8alpha(+) Conventional DC Clonogenic Progenitor. *Nat Immunol* (2015) 16:708–17. doi: 10.1038/ni.3197
5. Murphy TL, Grajales-Reyes GE, Wu X, Tussiwand R, Briseno CG, Iwata A, et al. Transcriptional Control of Dendritic Cell Development. *Annu Rev Immunol* (2016) 34:93–119. doi: 10.1146/annurev-immunol-032713-120204
6. Satpathy AT, Wu X, Albring JC, Murphy KM. Re(de)fining the Dendritic Cell Lineage. *Nat Immunol* (2012) 13:1145–54. doi: 10.1038/ni.2467
7. Briseno CG, Haldar M, Kretzer NM, Wu X, Theisen DJ, Kc W, et al. Distinct Transcriptional Programs Control Cross-Priming in Classical and Monocyte-Derived Dendritic Cells. *Cell Rep* (2016) 15:2462–74. doi: 10.1016/j.celrep.2016.05.025
8. Broz ML, Binnewies M, Boldajipour B, Nelson AE, Pollack JL, Erle DJ, et al. Dissecting the Tumor Myeloid Compartment Reveals Rare Activating Antigen-Presenting Cells Critical for T Cell Immunity. *Cancer Cell* (2014) 26:638–52. doi: 10.1016/j.ccell.2014.09.007
9. Engelhardt JJ, Boldajipour B, Beemiller P, Pandurangi P, Sorensen C, Werb Z, et al. Marginating Dendritic Cells of the Tumor Microenvironment Cross-Present Tumor Antigens and Stably Engage Tumor-Specific T Cells. *Cancer Cell* (2012) 21:402–17. doi: 10.1016/j.ccr.2012.01.008
10. Krueger PD, Kim TS, Sung SS, Braciale TJ, Hahn YS. Liver-Resident CD103+ Dendritic Cells Prime Antiviral CD8+ T Cells in Situ. *J Immunol* (2015) 194:3213–22. doi: 10.4049/jimmunol.1402622
11. Roberts EW, Broz ML, Binnewies M, Headley MB, Nelson AE, Wolf DM, et al. Critical Role for CD103(+)/CD141(+) Dendritic Cells Bearing CCR7 for Tumor Antigen Trafficking and Priming of T Cell Immunity in Melanoma. *Cancer Cell* (2016) 30:324–36. doi: 10.1016/j.ccell.2016.06.003
12. Pascual DW, Wang X, Kochetkova I, Callis G, Riccardi C. The Absence of Lymphoid CD8+ Dendritic Cell Maturation in L-Selectin-/- Respiratory Compartment Attenuates Antiviral Immunity. *J Immunol* (2008) 181:1345–56. doi: 10.4049/jimmunol.181.2.1345
13. Sun T, Rojas OL, Li C, Ward LA, Philpott DJ, Gommerman JL. Intestinal Batf3-Dependent Dendritic Cells are Required for Optimal Antiviral T-Cell Responses in Adult and Neonatal Mice. *Mucosal Immunol* (2017) 10:775–88. doi: 10.1038/mi.2016.79
14. Desai P, Tahiliani V, Abboud G, Stanfield J, Salek-Ardakani S. Batf3-Dependent Dendritic Cells Promote Optimal CD8 T Cell Responses Against Respiratory Poxvirus Infection. *J Virol* (2018) 92. doi: 10.1128/JVI.00495-18
15. GeurtsvanKessel CH, Willart MA, van Rijt LS, Muskens F, Kool M, Baas C, et al. Clearance of Influenza Virus From the Lung Depends on Migratory Langerin+CD11b- But Not Plasmacytoid Dendritic Cells. *J Exp Med* (2008) 205:1621–34. doi: 10.1084/jem.20071365
16. Anderson DA3rd, Murphy KM, Briseno CG. Development, Diversity, and Function of Dendritic Cells in Mouse and Human. *Cold Spring Harb Perspect Biol* (2018) 10. doi: 10.1101/cshperspect.a028613
17. Sutherland RM, Londrigan SL, Brady JL, Azher H, Carrington EM, Zhan Y, et al. Shutdown of Immunological Priming and Presentation After *In Vivo* Administration of Adenovirus. *Gene Ther* (2012) 19:1095–100. doi: 10.1038/gt.2011.187
18. Murillo O, Dubrot J, Palazon A, Arina A, Azpilikueta A, Alfaro C, et al. In Vivo Depletion of DC Impairs the Anti-Tumor Effect of Agonistic Anti-CD137 mAb. *Eur J Immunol* (2009) 39:2424–36. doi: 10.1002/eji.200838958
19. Kamphorst AO, Guermonprez P, Dudziak D, Nussenzweig MC. Route of Antigen Uptake Differentially Impacts Presentation by Dendritic Cells and Activated Monocytes. *J Immunol* (2010) 185:3426–35. doi: 10.4049/jimmunol.1001205
20. Gurka S, Hartung E, Becker M, Kroczek RA. Mouse Conventional Dendritic Cells Can be Universally Classified Based on the Mutually Exclusive Expression of XCR1 and SIRPalpha. *Front Immunol* (2015) 6:35. doi: 10.3389/fimmu.2015.00035
21. Vanders RL, Murphy VE, Gibson PG, Hansbro PM, Wark PA. CD8 T Cells and Dendritic Cells: Key Players in the Attenuated Maternal Immune Response to Influenza Infection. *J Reprod Immunol* (2015) 107:1–9. doi: 10.1016/j.jri.2014.09.051
22. Satpathy AT, Briseno CG, Lee JS, Ng D, Manieri NA, Kc W, et al. Notch2-Dependent Classical Dendritic Cells Orchestrate Intestinal Immunity to Attaching-and-Effacing Bacterial Pathogens. *Nat Immunol* (2013) 14:937–48. doi: 10.1038/ni.2679
23. Tussiwand R, Everts B, Grajales-Reyes GE, Kretzer NM, Iwata A, Bagaitkar J, et al. Klf4 Expression in Conventional Dendritic Cells is Required for T Helper 2 Cell Responses. *Immunity* (2015) 42:916–28. doi: 10.1016/j.immuni.2015.04.017
24. Bachem A, Hartung E, Guttler S, Mora A, Zhou X, Hegemann A, et al. Expression of XCR1 Characterizes the Batf3-Dependent Lineage of Dendritic Cells Capable of Antigen Cross-Presentation. *Front Immunol* (2012) 3:214. doi: 10.3389/fimmu.2012.00214
25. Beavis PA, Henderson MA, Giuffrida L, Davenport AJ, Petley EV, House IG, et al. Dual PD-1 and CTLA-4 Checkpoint Blockade Promotes Antitumor Immune Responses Through CD4(+)Foxp3(-) Cell-Mediated Modulation of CD103(+) Dendritic Cells. *Cancer Immunol Res* (2018) 6:1069–81. doi: 10.1158/2326-6066.CIR-18-0291
26. Crozat K, Tamoutounour S, Vu Manh TP, Fossum E, Luche H, Ardouin L, et al. Cutting Edge: Expression of XCR1 Defines Mouse Lymphoid-Tissue Resident and Migratory Dendritic Cells of the CD8alpha+ Type. *J Immunol* (2011) 187:4411–5. doi: 10.4049/jimmunol.1101717
27. Jaensson E, Uronen-Hansson H, Pabst O, Eksteen B, Tian J, Coombes JL, et al. Small Intestinal CD103+ Dendritic Cells Display Unique Functional Properties That are Conserved Between Mice and Humans. *J Exp Med* (2008) 205:2139–49. doi: 10.1084/jem.20080414
28. Tomura M, Hata A, Matsuoka S, Shand FH, Nakanishi Y, Ikebuchi R, et al. Tracking and Quantification of Dendritic Cell Migration and Antigen Trafficking Between the Skin and Lymph Nodes. *Sci Rep* (2014) 4:6030. doi: 10.1038/srep06030
29. Torti N, Walton SM, Murphy KM, Oxenius A. Batf3 Transcription Factor-Dependent DC Subsets in Murine CMV Infection: Differential Impact on T-Cell Priming and Memory Inflation. *Eur J Immunol* (2011) 41:2612–8. doi: 10.1002/eji.201041075
30. Grees M, Sharbi-Yunger A, Evangelou C, Baumann D, Cafri G, Tzehoval E, et al. Optimized Dendritic Cell Vaccination Induces Potent CD8 T Cell Responses and Anti-Tumor Effects in Transgenic Mouse Melanoma Models. *Oncoimmunology* (2018) 7:e1445457. doi: 10.1080/2162402X.2018.1445457
31. Behboudi S, Moore A, Hill AV. Splenic Dendritic Cell Subsets Prime and Boost CD8 T Cells and are Involved in the Generation of Effector CD8 T Cells. *Cell Immunol* (2004) 228:15–9. doi: 10.1016/j.cellimm.2004.03.010
32. Pooley JL, Heath WR, Shortman K. Cutting Edge: Intravenous Soluble Antigen is Presented to CD4 T Cells by CD8- Dendritic Cells, But Cross-Presented to CD8 T Cells by CD8+ Dendritic Cells. *J Immunol* (2001) 166:5327–30. doi: 10.4049/jimmunol.166.9.5327
33. Dutt S, Atallah MB, Minamida Y, Filatenkov A, Jensen KP, Iliopoulou BP, et al. Accelerated, But Not Conventional, Radiotherapy of Murine B-Cell Lymphoma Induces Potent T Cell-Mediated Remissions. *Blood Adv* (2018) 2:2568–80. doi: 10.1182/bloodadvances.2018023119
34. Filatenkov A, Baker J, Mueller AM, Kenkel J, Ahn GO, Dutt S, et al. Ablative Tumor Radiation Can Change the Tumor Immune Cell Microenvironment to Induce Durable Complete Remissions. *Clin Cancer Res* (2015) 21:3727–39. doi: 10.1158/1078-0432.CCR-14-2824
35. Neubert K, Lehmann CH, Heger L, Baranska A, Staedtler AM, Buchholz VR, et al. Antigen Delivery to CD11c+CD8- Dendritic Cells Induces Protective Immune Responses Against Experimental Melanoma in Mice *in Vivo*. *J Immunol* (2014) 192:5830–8. doi: 10.4049/jimmunol.1300975

36. Arora P, Baena A, Yu KO, Saini NK, Kharkwal SS, Goldberg MF, et al. A Single Subset of Dendritic Cells Controls the Cytokine Bias of Natural Killer T Cell Responses to Diverse Glycolipid Antigens. *Immunity* (2014) 40:105–16. doi: 10.1016/j.immuni.2013.12.004
37. Venkataswamy MM, Porcelli SA. Lipid and Glycolipid Antigens of CD1d-Restricted Natural Killer T Cells. *Semin Immunol* (2010) 22:68–78. doi: 10.1016/j.smim.2009.10.003
38. Smiley ST, Kaplan MH, Grusby MJ. Immunoglobulin E Production in the Absence of Interleukin-4-Secreting CD1-Dependent Cells. *Science* (1997) 275:977–9. doi: 10.1126/science.275.5302.977
39. Cui J, Shin T, Kawano T, Sato H, Kondo E, Toura I, et al. Requirement for Valpha14 NKT Cells in IL-12-Mediated Rejection of Tumors. *Science* (1997) 278:1623–6. doi: 10.1126/science.278.5343.1623
40. Borg NA, Wun KS, Kjer-Nielsen L, Wilce MC, Pellicci DG, Koh R, et al. CD1d-Lipid-Antigen Recognition by the Semi-Invariant NKT T-Cell Receptor. *Nature* (2007) 448:44–9. doi: 10.1038/nature05907
41. Hogquist KA, Jameson SC, Heath WR, Howard JL, Bevan MJ, Carbone FR. T Cell Receptor Antagonist Peptides Induce Positive Selection. *Cell* (1994) 76:17–27. doi: 10.1016/0092-8674(94)90169-4
42. Robertson JM, Jensen PE, Evavold BD. DO11.10 and OT-II T Cells Recognize a C-Terminal Ovalbumin 323-339 Epitope. *J Immunol* (2000) 164:4706–12. doi: 10.4049/jimmunol.164.9.4706
43. Hongo D, Tang X, Dutt S, Nador RG, Strober S. Interactions Between NKT Cells and Tregs are Required for Tolerance to Combined Bone Marrow and Organ Transplants. *Blood* (2012) 119:1581–9. doi: 10.1182/blood-2011-08-371948
44. Tang X, Zhang B, Jarrell JA, Price JV, Dai H, Utz PJ, et al. Ly108 Expression Distinguishes Subsets of Invariant NKT Cells That Help Autoantibody Production and Secrete IL-21 From Those That Secrete IL-17 in Lupus Prone NZB/W Mice. *J Autoimmun* (2014) 50:87–98. doi: 10.1016/j.jaut.2014.01.002
45. Kim D, et al. TopHat2: Accurate Alignment of Transcriptomes in the Presence of Insertions, Deletions and Gene Fusions. *Genome Biol* (2013) 14:R36. doi: 10.1186/gb-2013-14-4-r36
46. Robinson PN, Krawitz P, Mundlos S. Strategies for Exome and Genome Sequence Data Analysis in Disease-Gene Discovery Projects. *Clin Genet* (2011) 80:127–32. doi: 10.1111/j.1399-0004.2011.01713.x
47. Anders S, Pyl PT, Huber W. HTSeq–a Python Framework to Work With High-Throughput Sequencing Data. *Bioinformatics* (2015) 31:166–9. doi: 10.1093/bioinformatics/btu638
48. Van den Bossche J, Laoui D, Naessens T, Smits HH, Hokke CH, Stijlemans B, et al. E-Cadherin Expression in Macrophages Dampens Their Inflammatory Responsiveness *In Vitro*, But Does Not Modulate M2-Regulated Pathologies *In Vivo*. *Sci Rep* (2015) 5:12599. doi: 10.1038/srep12599
49. Hirai T, Ishii Y, Ikemiyagi M, Fukuda E, Omoto K, Namiki M, et al. A Novel Approach Inducing Transplant Tolerance by Activated Invariant Natural Killer T Cells With Costimulatory Blockade. *Am J Transplant* (2014) 14:554–67. doi: 10.1111/ajt.12606

Conflict of Interest: The authors declare that the research was conducted in the absence of any commercial or financial relationships that could be construed as a potential conflict of interest.

Publisher's Note: All claims expressed in this article are solely those of the authors and do not necessarily represent those of their affiliated organizations, or those of the publisher, the editors and the reviewers. Any product that may be evaluated in this article, or claim that may be made by its manufacturer, is not guaranteed or endorsed by the publisher.

Copyright © 2021 Hongo, Zheng, Dutt, Pawar, Meyer, Engleman and Strober. This is an open-access article distributed under the terms of the Creative Commons Attribution License (CC BY). The use, distribution or reproduction in other forums is permitted, provided the original author(s) and the copyright owner(s) are credited and that the original publication in this journal is cited, in accordance with accepted academic practice. No use, distribution or reproduction is permitted which does not comply with these terms.

frontiers in Immunology

ORIGINAL RESEARCH
published: 16 November 2021
doi: 10.3389/fimmu.2021.742154

Combined Deficiency of the Melanocortin 5 Receptor and Adenosine 2A Receptor Unexpectedly Provides Resistance to Autoimmune Disease in a CD8$^+$ T Cell-Dependent Manner

Trisha McDonald[1], *Fauziyya Muhammad*[2], *Kayleigh Peters*[1] *and Darren J. Lee*[1,2*]

[1] Dean McGee Eye Institute, Department of Ophthalmology, University of Oklahoma Health Sciences Center, Oklahoma City, OK, United States, [2] Department of Microbiology and Immunology, University of Oklahoma Health Sciences Center, Oklahoma City, OK, United States

OPEN ACCESS

Edited by:
Daniel Saban,
Duke University, United States

Reviewed by:
Luc Van Kaer,
Vanderbilt University, United States
Chander Raman,
University of Alabama at Birmingham, United States

***Correspondence:**
Darren J. Lee
darren-lee@ouhsc.edu

Specialty section:
This article was submitted to Antigen Presenting Cell Biology, a section of the journal Frontiers in Immunology

Received: *15 July 2021*
Accepted: *28 October 2021*
Published: *16 November 2021*

Citation:
McDonald T, Muhammad F, Peters K and Lee DJ (2021) Combined Deficiency of the Melanocortin 5 Receptor and Adenosine 2A Receptor Unexpectedly Provides Resistance to Autoimmune Disease in a CD8$^+$ T Cell-Dependent Manner. Front. Immunol. 12:742154. doi: 10.3389/fimmu.2021.742154

Regulatory immunity that provides resistance to relapse emerges during resolution of experimental autoimmune uveitis (EAU). This post-EAU regulatory immunity requires a melanocortin 5 receptor (MC5r)-dependent suppressor antigen presenting cell (APC), as shown using a MC5r single knock-out mouse. The MC5r-dependent APC activates an adenosine 2A receptor (A2Ar)-dependent regulatory Treg cell, as shown using an A2Ar single knock-out mouse. Unexpectedly, when MC5r$^{-/-}$ post-EAU APC were used to activate A2Ar$^{-/-}$ post-EAU T cells the combination of cells significantly suppressed EAU, when transferred to EAU mice. In contrast, transfer of the reciprocal activation scheme did not suppress EAU. In order to explain this finding, MC5r$^{-/-}$A2Ar$^{-/-}$ double knock-out (DKO) mice were bred. Naïve DKO mice had no differences in the APC populations, or inflammatory T cell subsets, but did have significantly more Treg cells. When we examined the number of CD4 and CD8 T cell subsets, we found significantly fewer CD8 T cells in the DKO mice compared to WT and both single knock-out mice. DKO mice also had significantly reduced EAU severity and accelerated resolution. In order to determine if the CD8 T cell deficiency contributed to the resistance to EAU in the DKO mice, we transferred naïve CD8 T cells from WT mice, that were immunized for EAU. Susceptibility to EAU was restored in DKO mice that received a CD8 T cell transfer. While the mechanism that contributed to the CD8 T cell deficiency in the DKO mice remains to be determined, these observations indicate an importance of CD8 T cells in the initiation of EAU. The involvement of CD4 and CD8 T cells suggests that both class I and class II antigen presentation can trigger an autoimmune response, suggesting a much wider range of antigens may trigger autoimmune disease.

Keywords: autoimmune uveitis, A2a adenosine receptor (A2Ar), melanocortin 5 receptor, Treg - regulatory T cell, CD8 T cell

INTRODUCTION

Ocular inflammation, uveitis, can cause permanent damage to the light-gathering structures of the eye, resulting in permanent blindness. Uveitis is the third leading cause of blindness in countries with access to cataract surgery, with an incidence between 25.6 – 122 cases per 100,000 a year, and a prevalence of 69 - 623 cases per 100,000 (1–3). Active uveitis patients experience transient or permanent vision loss occurs with an estimated 12.5% going on to develop glaucoma (4). Autoimmune uveitis patients experience relapsing and remitting inflammation, with 33% of anterior uveitis cases becoming chronic (5). A better understanding of the immunobiology that contributes to relapsing and remitting intraocular inflammation has the potential to develop novel more effective treatments for autoimmune uveitis.

Experimental autoimmune uveitis (EAU) is the most widely used mouse model of human autoimmune uveitis (6). In C57BL/6J mice, resolution of EAU occurs at 75-90 days following immunization for EAU without further relapse (7–9), and at this point (post-EAU) regulatory immunity is found in the spleen (10). This post-EAU regulatory immunity provides resistance to relapse and suppresses EAU when transferred to recipient EAU mice (10–13). A critical component of post-EAU regulatory immunity is expression of the adenosine 2A receptor (A2Ar) for activation and differentiation of Treg cells, and expression of the melanocortin 5 receptor (MC5r) on the post-EAU suppressor antigen presenting cell (APC) (11, 12). While A2Ar-expressing post-EAU Tregs and MC5r-expressing APC are not required for resolution of EAU (11, 14), it has been shown that depletion of all Foxp3$^+$ Treg cells before resolution of EAU prevents resolution (15). Therefore, the resolution of EAU and induction of regulatory immunity that provides resistance to relapse occur independently of one another. As such, a better understanding of the melanocortin-adenosinergic pathway is needed.

It is well documented that CD8$^+$ T cells have a role in uveitis through observations in rodent models of EAU (16–19), and analysis of aqueous humor from uveitis patients (20, 21). MC5r transcript expression has been reported in CD8$^+$ T cells from human PBMCs (22) but protein expression was not confirmed and the role of MC5r in this cell subset has not been further examined. A2Ar has been extensively studied in the field of cancer biology, and has a suppressive role on CD8$^+$ T cells, as tumor evasion by the immune system is observed with blockade of A2Ar on CD8$^+$ T cells (23, 24). However, the role of MC5r and A2Ar have not been examined on CD8$^+$ T cells in the context of autoimmune uveitis.

In this report, we demonstrate that the melanocortin-adenosinergic pathway is more nuanced than was previously understood and involves more cell types than previously reported. In addition to the involvement in the induction and activation of post-EAU regulatory immunity, the melanocortin-adenosinergic pathway has an additional role in the disease phase of EAU that requires CD8$^+$ T cells for the induction of EAU.

METHODS

Mice

All mouse procedures described in this study were approved by the University of Oklahoma Health Sciences Center Institutional Animal Care and Use Committee (OUHSC IACUC) and all mouse study methods were carried out in accordance with the relevant guidelines approved by the OUHSC IACUC. C57BL/6J mice and adenosine 2A receptor knock-out (A2Ar$^{-/-}$) mice were purchased from Jackson Laboratories. Melanocortin 5 receptor knockout mice (MC5r$^{-/-}$) mice on a C57BL/6J background were a generous gift from Roger D. Cone (Oregon Health Sciences, Portland, Oregon). A2Ar$^{-/-}$ MC5r$^{-/-}$ double knock-out (DKO) mice were bred in the Dean McGee Eye Institute vivarium, and the genotype was confirmed by PCR in the DMEI Genotyping Core.

Experimental Autoimmune Uveoretinitis

EAU was induced in mice according to the previously described immunization protocol (13). An emulsion of complete Freund's adjuvant (CFA) with 5 mg/mL desiccated *M. tuberculosis* (Difco Laboratories, Detroit, MI) and 2 mg/ml interphotoreceptor retinoid binding protein (peptides 1-20) (IRBP) (Genscript, Piscataway, NJ) was used to immunize mice for EAU. A volume of 100 µl was injected subcutaneously at two separate sites in the lower back along with an intraperitoneal injection of 0.3 µg pertussis toxin. Fundus examinations using a slit lamp microscope occurred every 3-4 days to monitor the severity of retinal inflammation over the course of EAU. To examine the retina, the iris was dilated using 1% tropicamide, the cornea was numbed with 0.5% proparacaine, and the cornea was flattened with a glass coverslip in order to examine the retina. The severity of EAU was scored on a 5-point scale, as previously described (25), using the clinical signs of observable infiltration and vasculitis in the retina. Both eyes were scored and the higher score was taken to represent that mouse for that day, and the average score for the group was calculated.

In Vitro Stimulation

Spleens were collected into 5% FBS in RPMI supplemented with 10 µg/ml Gentamycin (Sigma), 10 mM HEPES, 1 mM Sodium Pyruvate (BioWhittaker), Nonessential Amino Acids 0.2% (BioWhittaker) and made into a single cell suspension that was depleted of red blood cells using RBC lysis buffer (Sigma, St Louis, MO). The spleen cells were resuspended in serum free media (SFM) and IRBP was added at 50 µg/mL for 48 hours at 37°C and 5% CO_2 to reactivate antigen specific T cells. SFM consisted of RPMI-1640 with 1% ITS+1 solution (Sigma) and 0.1% BSA (Sigma). Following the reactivation, supernatants were collected and analyzed and/or cells were collected for adoptive transfer into recipient mice.

In some experiments antigen presenting cells (APC) and T cells were cultured from different strains. APC were collected by incubating splenocytes in SFM at 37°C and 5% CO_2 for 90 minutes in tissue culture plates, washed twice, and adherent cells were scraped off of the plastic in ice cold SFM, and plated at 4 x

10^5 cells per well. CD3 enriched T cells were obtained from post-EAU spleens using a CD3 enrichment column (R&D Systems), added to the sorted APC at 8 x 10^5 cells per well with 50 μg IRBP peptide, and cultured at 37°C 5% CO_2 for 48 hours. After 48 hours, T cells and APC were collected, and washed in PBS. Following the reactivation, cells were collected for adoptive transfer into recipient mice.

Adoptive Transfer

Cultured cells described above were collected under sterile conditions washed with sterile PBS, and resuspended in sterile PBS. Mice were injected with 1 x 10^6 activated post-EAU cells in PBS into the tail vein. Following the adoptive transfer, the mice were immunized for EAU as described above.

Cytokine Analysis

Cell culture supernatants were assayed using the mouse Th1/Th2/Th17/Th22/Treg 18-multiplex procartaplex kit, (Invitrogen, Vienna, Austria) to assay the culture supernatants. The Multiplex plate was analyzed with Bio-Rad plate reader (Bioplex system, Hercules, CA). The assay was performed according to manufacturer's instructions.

Flow Cytometry

Mouse spleen cells were washed with PBS with 1% BSA (staining buffer), blocked with mouse IgG in staining buffer, then stained with conjugated antibodies. Antibodies used were anti-CD11b (clone M1/70, Biolegend, San Diego, CA), anti-Ly-6C (clone HK1.4, Biolegend), anti-Ly-6G (clone 1A8, Biolegend), anti-F4/80 (clone BM8, eBiosciences, San Diego, CA), anti-MHCII (clone M5/114.15.2, Biolegend), anti-CD4 (clone RM4-5, Biolegend), anti-PD-1 (clone 29F.1A12, Biolegend), anti-Foxp3 (clone FJK-16s, eBiosciences), anti-Tbet (clone 4B10, Biolegend), and anti-RORγt (clone AFKJS-9, Biolegend). Prior to anti-Foxp3, anti-Tbet, and anti-RORγt staining, the cells were fixed and permeabilized.

Stained cells were analyzed in the Oklahoma Medical Research Facility (OMRF) Flow Cytometry Core Facility on a BD LSRII (BD Biosciences) or the DMEI Ocular Immunobiology Core on a 4-laser Aurora (Cytek Biosciences, Fremont, CA). When the Aurora was used, unmixing was done using SpectroFlo Software (Cytek) and data was analyzed using FlowJo Software (Tree Star, Inc., Ashland, OR).

Statistics

Statistical significance between maximum EAU scores was determined using nonparametric Mann-Whitney U test between groups of mice. Two-way ANOVA was also used to assess significant changes in the tempo of disease between the groups of treated EAU mice with post-test Bonferroni comparison analysis. Statistical significance was determined when $P \leq 0.05$ (two-sided). All statistical tests were conducted in R v3.5.1 and statistical analysis for mouse experiments were analyzed with Graphpad Prism software.

RESULTS

The Melanocortin-Adenosinergic Pathway Is More Complicated Than Previously Observed

The aim of this study is to further understand the role of the melanocortin-adenosinergic pathway in the induction of autoimmune uveitis. We have previously reported that the melanocortin-adenosinergic pathway is necessary for the induction of post-EAU regulatory immunity that provides resistance to relapse (11, 14, 26, 27). Our previous work specifically showed that expression of the melanocortin 5 receptor (MC5r) on the post-EAU antigen presenting cell (APC) is required for activation of post-EAU regulatory T cells that express the adenosine 2A receptor (A2Ar). We therefore reasoned that a post-EAU MC5r$^{-/-}$ APC would be unable to activate a post-EAU A2Ar$^{-/-}$ T cell. However, when transferred to a recipient mouse immunized for EAU we observed a significant suppression of disease compared to EAU mice that received no cell transfer (**Figure 1A**). When the reciprocal activation scheme was used, we found that post-EAU A2Ar$^{-/-}$ APC used to activated post-EAU MC5r$^{-/-}$ T cells were unable to suppress disease in recipient mice (**Figure 1B**). These unexpected observations suggested the interplay between APC and T cells through the melanocortin-adenosinergic pathway is more complicated than previously understood. We next asked what the role of this pathway is during the induction of disease using a double knockout (DKO) mouse with the MC5r$^{-/-}$ A2Ar$^{-/-}$ genotype.

The DKO Mice Have No Difference in Suppressor APCs, More Tregs, and Are Resistant to Disease

We first asked if the APC compartment is different in DKO mice compared to the single knockout (SKO) mice. Spleens from naïve WT, DKO, MC5r$^{-/-}$, and A2Ar$^{-/-}$ were collected and stained for CD11b, F4/80, Ly6G, and Ly6C as we have done before (14). We observed a similar number of CD11b$^+$F4/80$^+$ macrophages between each of the four strains of mice (**Figure 2A**). However, we did observe significantly more CD11b$^+$ F4/80$^+$ Ly6G$^+$ Ly6C^{lo} macrophages in DKO mice compared to WT, MC5r$^{-/-}$, and A2Ar$^{-/-}$ mice (**Figure 2B**), but did not observe a significant difference in the abundance of CD11b$^+$ F4/80$^+$ Ly6G$^+$ MHCII$^+$ macrophages between the WT, DKO, MC5r$^{-/-}$, and A2Ar$^{-/-}$ mice (**Supplementary Figure 1**). Because the CD11b$^+$ F4/80$^+$ Ly6G$^+$ Ly6C^{lo} macrophages have previously been demonstrated to be the suppressor macrophage population at the resolution of disease that activates post-EAU Tregs (11, 14), we asked if there were more PD-1$^+$ Foxp3$^+$ Tregs, the Tregs we previously identified as post-EAU Tregs that suppress disease (27). Comparison of the Treg compartment between WT, DKO, MC5r$^{-/-}$, and A2Ar$^{-/-}$ mice revealed that DKO mice had significantly more PD-1$^+$Foxp3$^+$ Tregs than the WT, MC5r$^{-/-}$, and A2Ar$^{-/-}$ mice (**Figure 2C**).

We next asked what the effect of the MC5r and A2Ar deficiency in DKO mice has on EAU. WT, DKO, MC5r$^{-/-}$, and A2Ar$^{-/-}$mice were immunized for EAU and monitored through

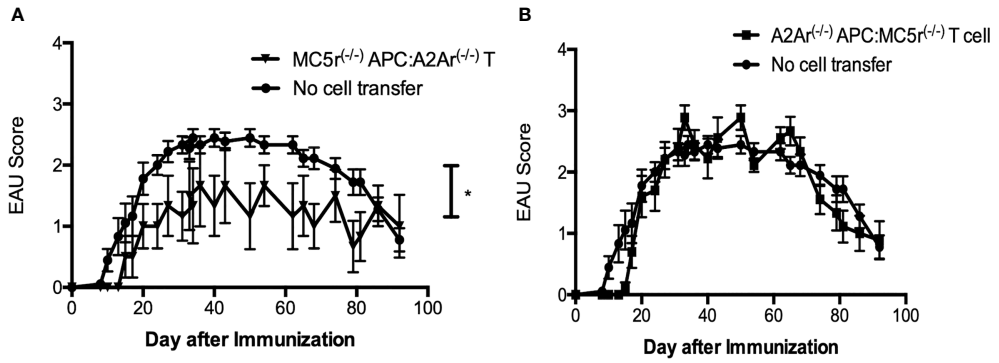

FIGURE 1 | Activation requirements of post-EAU regulatory macrophages and T cells in MC5r$^{-/-}$ and A2Ar$^{-/-}$ mice. APC and T cells from post-EAU MC5r$^{-/-}$ and A2Ar$^{-/-}$ mice were collected. APC and T cells were cultured *in vitro* with IRBP and adoptively transferred to recipient mice immunized for EAU. The solid line with closed circles are EAU control mice that did not receive an adoptive transfer of spleen cells (no cell transfer, n = 18). Post-EAU MC5r$^{-/-}$ APC were used to activate post-EAU A2Ar$^{-/-}$ T cells and transferred to a recipient mouse and immunized for EAU (**A**, solid line with inverted triangles, n = 6). Post-EAU A2Ar$^{-/-}$ APC were used to activate post-EAU MC5r$^{-/-}$ T cells and transferred to a recipient mouse and immunized for EAU (**B**, solid line with squares, n = 10). Disease was monitored every 3-4 days from the time of immunization through resolution. Each experiment consisted of 4-5 mice, and each experiment was repeated 2-4 times. Significant suppression of disease was observed compared to EAU mice that received no cell transfer (*P< 0.05), determined by two-way ANOVA with Bonferroni post-test.

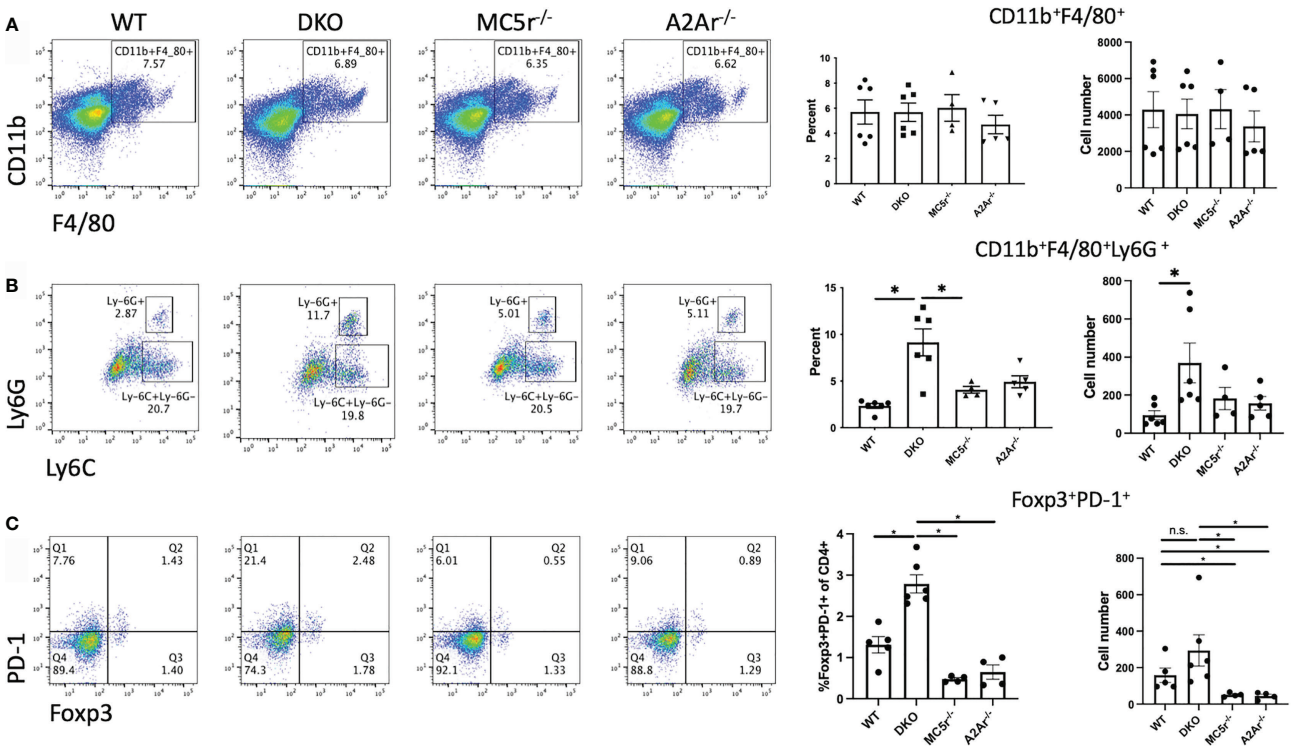

FIGURE 2 | Comparison of APC and Tregs in naïve DKO with WT, MC5r$^{-/-}$, and A2Ar$^{-/-}$ mice. Spleens from naïve WT (N=6), DKO (N=6), MC5r-/- (N= 4), and A2Ar-/- (N = 5) were collected and stained for CD11b, F4/80, Ly6G, Ly6C, CD4, PD-1, and Foxp3. Representative pseudocolor dot plots and the mean ± SEM for each mouse are shown for CD11b and F4/80 **(A)**, Ly6G and Ly6C **(B)**, and PD-1 and Foxp3 **(C)**. The Ly-6G and Ly6C panels are gated on CD11b^{+}F4/80^{+} cells, and PD-1 and Foxp3 panels are gated on CD4^{+} cells. Each experiment consisted of 1-2 mice, and each experiment was repeated 2-3 times. Significance was assessed by nonparametric Mann-Whitney U test. Statistical significance (P ≤ 0.05) is designated by *, or not significant (n.s.).

the course of disease. As we previously observed, MC5r$^{-/-}$ and A2Ar$^{-/-}$ mice showed no significant change in EAU tempo and severity (**Figures 3A, B, D**). However, we observed a significant reduction in the severity and course of disease in DKO mice (**Figures 3C, D**). These observations reveal an unexpected role of these receptors on the induction of disease that is in contrast with what we have observed in relation to the induction of regulatory immunity that provides resistance to disease.

DKO Mice Have More Tregs and Th1 Cells During the Disease Phase

We next sought to understand the mechanism providing resistance to disease in the DKO mice. We first asked if the APC compartment is different in DKO mice compared to the single knockout (SKO) mice at the onset of disease. Spleens from naïve WT, DKO, MC5r$^{-/-}$, and A2Ar$^{-/-}$ were collected and stained for CD11b, F4/80, Ly6G, and Ly6C as we have done before (14). We observed a significant decrease in the abundance of CD11b^{+}F4/80^{+} macrophages in MC5r$^{-/-}$ mice compared to DKO mice (**Figures 4A–E**). We also observed a significant decrease in the abundance of CD11b^{+} F4/80^{+} Ly6G^{+} Ly6C^{lo} macrophages in DKO mice compared to MC5r$^{-/-}$ mice (**Figures 4F–J**). However, we did not observe a significant difference in the abundance of CD11b^{+} F4/80^{+} Ly6G^{+} MHCII^{+} macrophages between the WT, DKO, MC5r$^{-/-}$, and A2Ar$^{-/-}$ mice (**Supplementary Figure 1**).

We next asked what the T cell response was at the onset of disease. Spleens were collected, restimulated, and assayed for Treg, Th17, and Th1 profiles. Flow cytometry staining revealed more Foxp3^{+}PD-1^{+} Tregs (**Figures 4K–O**) and Rorγt^{+} T cells (**Figures 5A–E**) in DKO mice compared to A2Ar$^{-/-}$ mice in the CD4^{+} compartment. However, the Th17-associated cytokines, IL-17A, IL-22, and IL-6 were not significantly different between the four genotypes (**Figures 5E–H**). The transfer of post-EAU splenocytes to EAU mice resulted in a significant suppression of EAU in recipient mice (**Supplementary Figure 2**), suggesting a dominant regulatory phenotype in the DKO mice. We observed a significant increase in the number of Tbet^{+} T cells in DKO mice compared to WT, MC5r$^{-/-}$, and A2Ar$^{-/-}$ mice among CD4^{+} T cells (**Figure 5I**). However, DKO mice compared to WT, MC5r$^{-/-}$, and A2Ar$^{-/-}$ mice, produced significantly less IFN-γ and production of TNF-α was not significantly different (**Figures 5J, K**). These observations demonstrate that T cell polarization is disrupted in DKO mice, such that the characteristic Treg, Th1, and Th17 transcription factors are expressed, but the characteristic inflammatory cytokine is not significantly elevated.

DKO Mice Have a Reduced CD8 T Cell Compartment

We next pursued an explanation for the observation that DKO had a significantly greater abundance of Tbet^{+} cells but significantly reduced IFN-γ production. Because CD8^{+} T cells can also produce IFN-γ (28, 29), we asked if there was a reduced number of CD8^{+} T cells in the DKO mice. We observed a significant reduction in CD8^{+} T cells in the spleen and thymus of DKO mice compared to WT, MC5r$^{-/-}$, and A2Ar$^{-/-}$ mice (**Figures 6A–H, J, L**). In contrast, the number of CD4^{+} T cells between all four genotypes was not significantly different (**Figures 6A–H, I, K**). These observations suggest that a defect in the development of CD8^{+} T cells occurs in the DKO mice and could explain why these mice are resistant to EAU.

CD8 T Cells From WT Mice Allow for EAU Susceptibility in DKO Mice

We next tested if restoring the CD8^{+} T cell compartment in DKO mice is sufficient to eliminate resistance to EAU. EAU scores of mice that received a transfer of WT CD8 T cells before immunization for EAU were significantly elevated compared to DKO mice immunized for EAU that did not receive a cell transfer (**Figure 7A**). Additionally, the maximum EAU scores were not significantly different between the DKO EAU mice that received a CD8 T cell transfer and DKO EAU mice that received no cell transfer (**Figure 7B**). These observations demonstrate that a WT CD8^{+} T cell compartment is necessary to overcome the resistance to EAU observed in DKO mice.

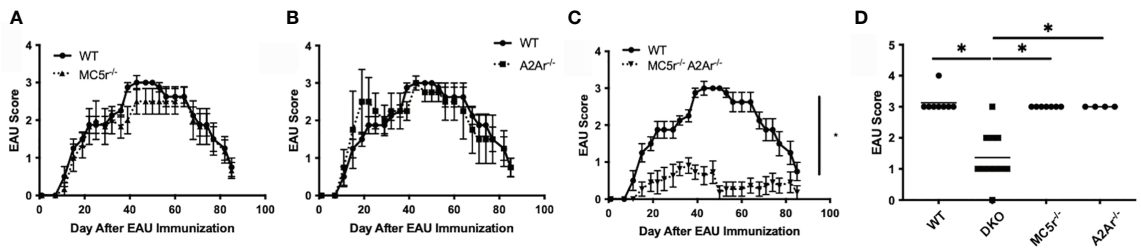

FIGURE 3 | The course of EAU in WT, MC5r$^{-/-}$, A2Ar$^{-/-}$, and DKO mice. WT mice (n = 8), MC5r$^{-/-}$ (n = 7), A2Ar$^{-/-}$ (n = 4), and DKO (n = 11) mice were immunized for EAU and evaluated from the time of immunization every 3 - 4 days for clinical signs of uveitis. The course of disease MC5r$^{-/-}$ (**A**, dashed line with triangles), A2Ar$^{-/-}$ (**B**, dashed line with squares), and DKO (**C**, dashed line with inverted triangles) is shown with WT mice (solid line with circles). The severity of disease is indicated by the maximum score of each mouse over the entire course of disease **(D)**. Each experiment consisted of 1-4 mice, and each experiment was repeated 2-3 times. Significance was assessed by two-way ANOVA with Bonferroni post-test for EAU scores over the course of disease and nonparametric Mann-Whitney U test for maximum scores. Statistical significance ($P \leq 0.05$) is designated by *.

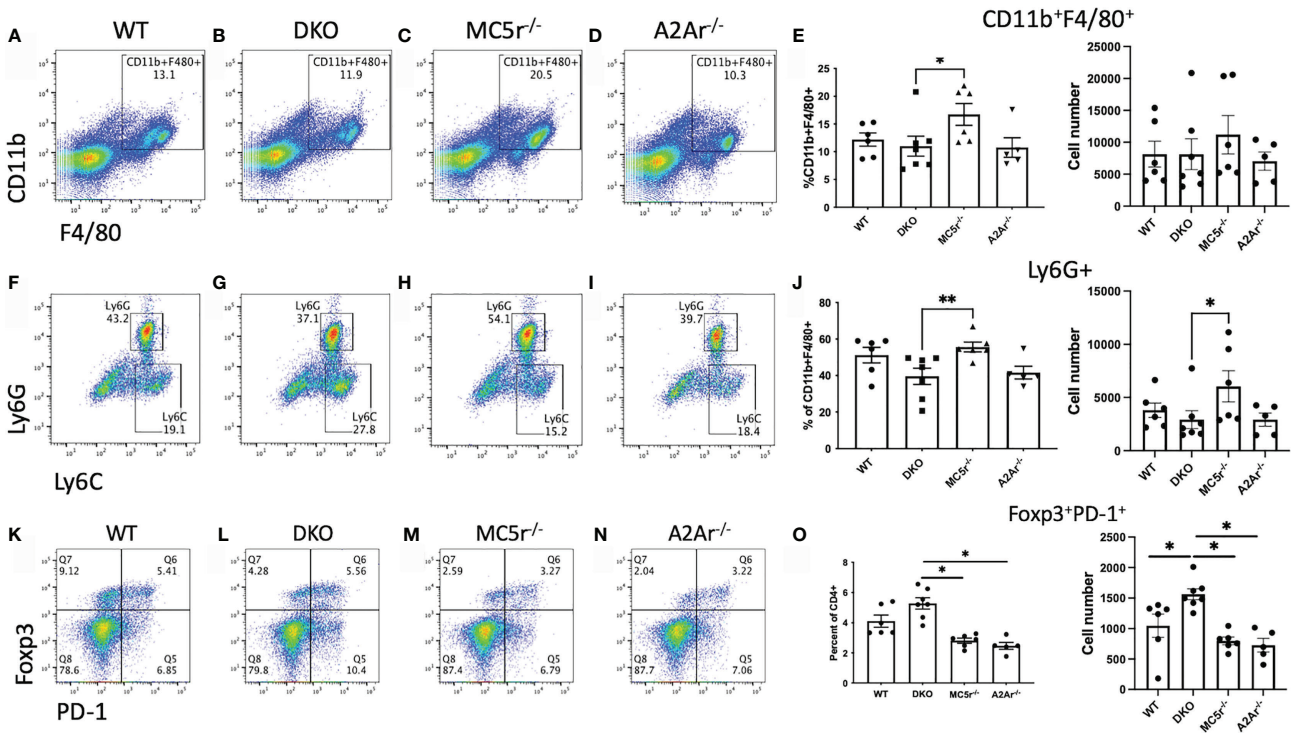

FIGURE 4 | Comparison of APC and Tregs at the onset of EAU in DKO with WT, MC5r$^{-/-}$, and A2Ar$^{-/-}$ mice. Spleens from EAU onset (day 24) WT (n=6), DKO (n=7), MC5r$^{-/-}$ (n= 6), and A2Ar$^{-/-}$ (n= 5) were collected and stained for CD11b, F4/80, Ly6G, Ly6C, CD4, PD-1, and Foxp3. Representative pseudocolor dot plots and the mean ± SEM for each mouse are shown for CD11b and F4/80 **(A–E)**, Ly6G and Ly6C **(F–J)**, and PD-1 and Foxp3 **(K–O)**. The Ly-6G and Ly6C panels are gated on CD11b+F4/80+ cells, and PD-1 and Foxp3 panels are gated on CD4+ cells. Each experiment consisted of 1-2 mice, and each experiment was repeated 2-3 times. Significance was assessed by nonparametric Mann-Whitney U test. Statistical significance (*P ≤ 0.05 or **P ≤ 0.01) is designated by * and **.

DISCUSSION

In this report, we sought to further define the role of MC5r and A2Ar in the induction of post-EAU regulatory immunity and determine the role of MC5r and A2Ar during the course of disease. Our observations reveal a more complicated role for MC5r expression of APC and A2Ar on Treg cells in the induction of post-EAU regulatory immunity that remains to be investigated. This observation drove us to create a DKO mouse to investigate the role of a deficiency of both MC5r and A2Ar in the same mouse. We unexpectedly found that DKO mice were resistant to disease. The DKO mice had a similar APC compartment, but elevated Tregs, and reduced CD8$^+$ T cells. We found that a transfer of CD8$^+$ T cells from WT mice was sufficient to overcome the disease resistance in DKO mice. These observations demonstrate the complexity of MC5r and A2Ar on the pathogenesis of EAU and in the induction of regulatory immunity, and shows the importance of CD8$^+$ T cells in susceptibility to autoimmune disease. Based on this work we suggest that CD8$^+$ T cells that are dependent on MC5r and A2Ar expression suppress Tregs and are necessary to induce autoimmune uveitis (**Supplementary Figure 3**).

The RORγt T cell transcription factor expression in DKO mice was elevated in the DKO compared to A2Ar$^{-/-}$ mice. However, the observation that cytokine production was no different for IL-17A, IL-22, IL-6, or TNF-α suggests that while the transcriptional profile was altered, there was no polarization towards Th17 in the DKO mice. We did observe a significantly increased number of Tregs in the DKO compared to MC5r$^{-/-}$ and A2Ar$^{-/-}$ mice, which suggests the resistance to disease may be due to an increased abundance of Tregs. This is not unexpected, given previous observations that Tregs are necessary for resolution of disease (15). We further observed the Tregs in the DKO mice did suppress EAU when transferred to WT EAU mice, which showed the DKO Tregs are functionally suppressive.

The observation that the Th1 transcription factor, Tbet, was expressed in significantly more CD4$^+$ T cells in DKO mice compared to WT, MC5r$^{-/-}$, and A2Ar$^{-/-}$ mice suggested DKO mice were skewed to a Th1 polarization. However, the significant reduction of IFN-γ production suggested the DKO mice were not skewed toward a Th1 phenotype. We further explored this possibility by quantifying the CD8$^+$ T cells in the spleen and thymus and found DKO mice had significantly less CD8$^+$ T cells

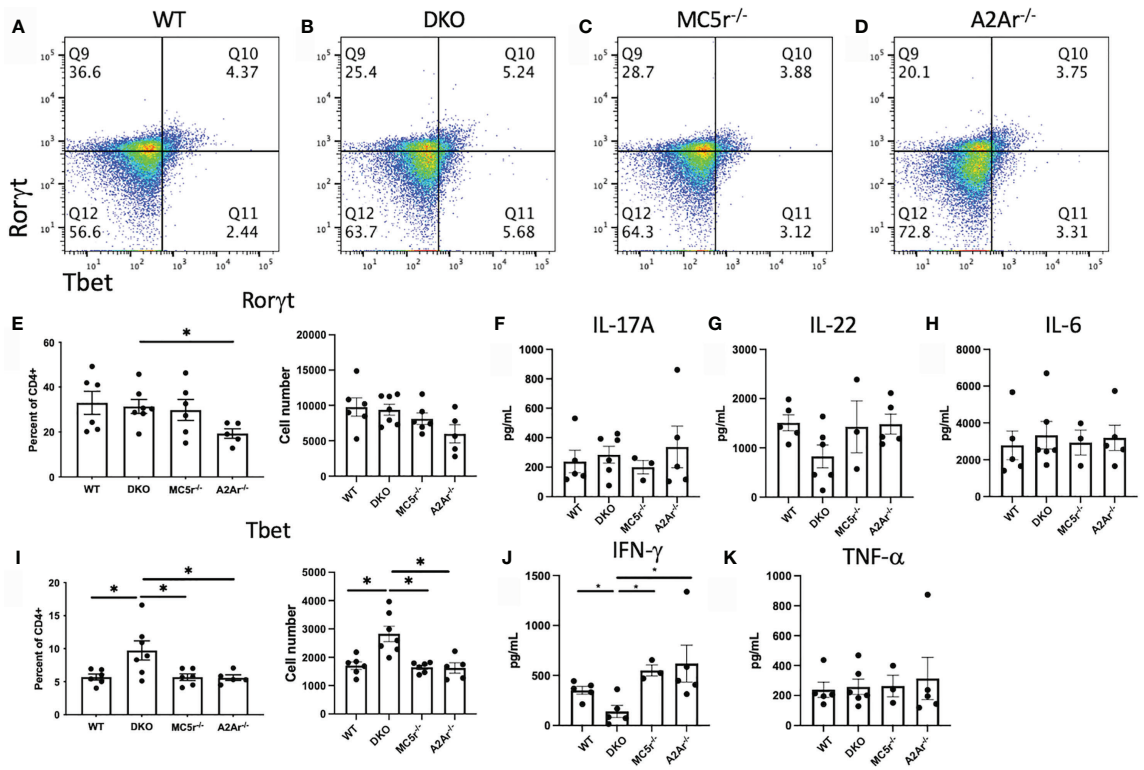

FIGURE 5 | T cell response at the onset of EAU in WT, MC5r$^{-/-}$, A2Ar$^{-/-}$, and DKO mice. Spleens from WT (n = 4-6), DKO (n = 6-7), MC5r-/- (n = 3-6) and A2Ar$^{-/-}$ (n = 5) were collected, restimulated with IRBP, and assayed for Treg, Th17, and Th1 profiles from at the onset (day 24) of disease. Representative pseudocolor flow cytometry dot plots are shown for Rorgt and Tbet expression from the spleen **(A–D)** with the mean ± SEM for all mice. The mean ± SEM is shown for Rorgt **(E)** IL-17A **(F)**, IL-22 **(G)**, IL-6 **(H)**, Tbet **(I)**, IFN-g **(J)**, and TNF-a **(K)**. Significance was determined by Mann-Whitney U test. Statistical significance (P ≤ 0.05) is designated by *.

in both tissues. In order to determine if the lack of CD8$^+$ T cells in DKO mice was the cause of disease resistance, CD8$^+$ T cells were transferred from WT mice, and we observed disease in mice that received the transfer. These observations demonstrate the resistance to EAU in the DKO mice is dependent on CD8$^+$ T cells. However, further investigation of the role of the melanocortin-adenosinergic pathway in CD8$^+$ T cells is needed to understand the melanocortin-adenosinergic role in CD8$^+$ T cells during the induction of EAU. A potential mechanism that could explain the requirement for A2Ar and MC5r on CD8$^+$ T cells to induce EAU could be that the limited number CD8$^+$ T cells from these mice are deficient in their effector functions. Since significantly fewer CD8$^+$ T cells were observed in the thymus of DKO mice, this suggests there is a defect in thymic development of the CD8$^+$ cells in the DKO mice. There may be an insufficient activation signal that allows for CD8$^+$ T cells to undergo positive selection, a defect with negative selection in CD8$^+$ T cells, or the deficiency in A2Ar and MC5r blocks expression of the CD8 co-receptor. This possibility will be investigated in future studies. However, if this is the mechanism for the reduction of CD8$^+$ T cells in DKO mice, this would be a novel mechanism that highlights a nuance between CD4 and CD8 T cell development.

Others have demonstrated the importance of minimally activated CD8$^+$ T cells in uveitis in rats and mice (16–19), and CD8$^+$ T cells are present in eyes of uveitis patients (20, 21). While it is clear that effector CD8$^+$ T cells are involved in the inflammatory immune response, the connection with activation of these cells with the melanocortin-adenosinergic pathway is paradoxical. CD8$^+$ regulatory T cells are an essential component of anterior chamber associated immune deviation (ACAID) (30, 31), and minimally activated CD8$^+$ T cells in EAU are suppressive (32). These observations suggest there may be some overlap between the induction of post-EAU regulatory immunity and the ACAID response, and provides some possible insight into the paradoxical observation that a MC5r and A2Ar deficiency results in reduced susceptibility to EAU. While additional work is needed to better understand this observation, it suggests that MC5r and A2Ar have a role in the development of CD8$^+$ T cells, and this population may have a role in the induction of post-EAU regulatory immunity. A future question to address is if the defect is intrinsic to bone-marrow derived cells, which could be addressed with bone marrow chimeras.

These observations also illustrate the disconnect between the induction of post-EAU regulatory immunity that provides

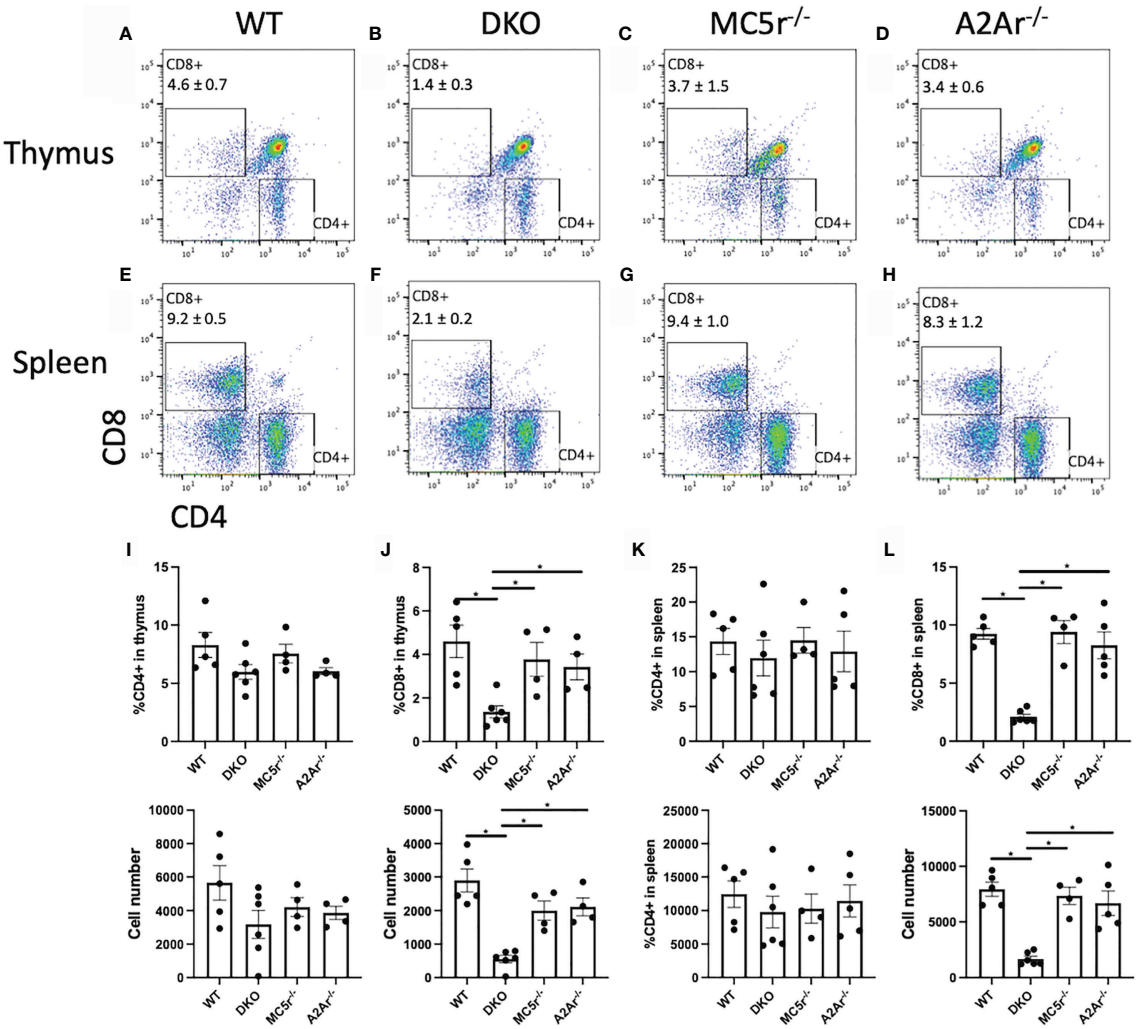

FIGURE 6 | Comparison of CD4 and CD8 T cells in WT, MC5r$^{-/-}$, A2Ar$^{-/-}$, and DKO mice. The spleens and thymus of naïve WT (n = 4-5), DKO (n = 6), MC5r$^{-/-}$ (n = 4) and A2Ar$^{-/-}$ (n = 4-5) mice were harvested and stained for CD8 and CD4. Representative pseudocolor flow cytometry dot plots are shown for CD8 and CD4 expression from the thymus **(A–D)** and spleen **(E–H)** with the mean ± SEM for all mice for thymic cells **(I, J)** and spleen cells **(K, L)**. Each experiment consisted of 1-2 mice, and each experiment was repeated 2-3 times. Significance was assessed by nonparametric Mann-Whitney U test. Statistical significance (*P ≤ 0.05) is designated by *.

resistance to relapse and resolution of disease with resolution of EAU. A mechanism of ocular immune privilege is the induction of systemic regulatory immunity against ocular antigen. We and others have found this regulatory immunity to emerge at resolution of uveitis (10, 26, 27, 33). However, we have found that resolution of uveitis can occur without induction of post-EAU regulatory immunity (12, 14). Therefore, this report adds to the body of evidence that resolution of uveitis does not necessarily provide the regulatory immunity that provides resistance to relapse. The unfortunate consequence of the independent induction of this regulatory immunity and resolution is that patients may experience remission, but are susceptible to relapse. It is possible that the 33% of uveitis patients that become chronic (5) do so because of the lack of regulatory immunity that provides resistance to relapse. Our previous observations that stimulation of the melanocortin-adenosinergic pathway only induces regulatory T cells in a subset of patients (14, 26, 34), supports this hypothesis based on our animal model observations.

While ocular immune privilege may have evolved to protect the delicate light-gathering tissues of the eye, it is not perfect. It is thought the selection pressure to maintain vision had a selective evolutionary advantage in the gathering of food and detection of predators (35–37). In the context of evolutionary pressure, elimination of lethal pathogens would have taken precedence over preservation of vision. Therefore, another

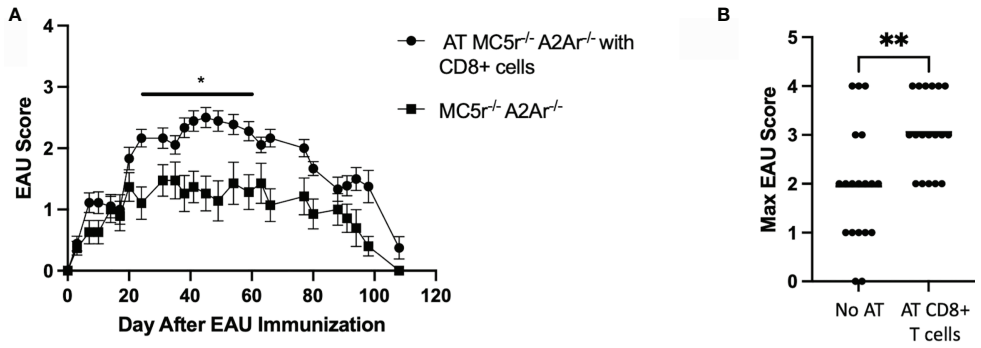

FIGURE 7 | The course of EAU in DKO mice following transfer of WT CD8$^+$ T cells. EAU was induced in DKO mice that received an adoptive transfer of WT CD8$^+$ T cells two days before immunization (solid line with circles, n = 18) or EAU DKO mice that did not receive a cell transfer (solid line with squares, n = 19). Mice were immunized for EAU and evaluated from the time of immunization every 3 - 4 days for clinical signs of uveitis **(A)**. The severity of disease is indicated by the maximum score of each mouse over the entire course of disease **(B)**. Each experiment consisted of 4-7 mice, and each experiment was repeated 3-4 times. Significance was assessed by two-way ANOVA with Bonferroni post-test for EAU scores over the course of disease and nonparametric Mann-Whitney U test for maximum scores. Statistical significance (*P ≤ 0.05 or **P ≤ 0.01) is designated by * and **.

explanation for our paradoxical results could be that a compensatory mechanism for survival exists in the DKO mice that also provides resistance to EAU. As such, in some cases the evolutionary pressure for survival comes at the cost of loss of ocular immune privilege, followed by the loss of vision.

DATA AVAILABILITY STATEMENT

The raw data supporting the conclusions of this article will be made available by the authors, without undue reservation.

AUTHOR CONTRIBUTIONS

All experiments, analysis, and experimental design of this work was done by DL, FM, and TM. The conceptual design of this work and the writing of this manuscript was a collaborative effort between DL and KP. All authors contributed to the article and approved the submitted version.

FUNDING

This work was supported by National Institutes of Health/ National Eye Institute grants EY021725 (P30), EY024951 (DL), and in part by an unrestricted Research to Prevent Blindness grant (New York, NY, USA).

ACKNOWLEDGMENTS

We would like to thank the Oklahoma Medical Research Foundation Core facility. We would like to thank Ryan E. Lee for contributing the artwork for **Supplementary Figure 3**.

SUPPLEMENTARY MATERIAL

The Supplementary Material for this article can be found online at: https://www.frontiersin.org/articles/10.3389/fimmu.2021.742154/full#supplementary-material

REFERENCES

1. Darrell RW, Wagener HP, Kurland LT. Epidemiology of Uveitis. Incidence and Prevalence in a Small Urban Community. *Arch Ophthalmol* (1962) 68:502–14. doi: 10.1001/archopht.1962.00960030506014
2. Hwang DK, Chou YJ, Pu CY, Chou P. Epidemiology of Uveitis Among the Chinese Population in Taiwan: A Population-Based Study. *Ophthalmology* (2012) 119(11):2371–6. doi: 10.1016/j.ophtha.2012.05.026
3. Suhler EB, Lloyd MJ, Choi D, Rosenbaum JT, Austin DF. Incidence and Prevalence of Uveitis in Veterans Affairs Medical Centers of the Pacific Northwest. *Am J Ophthalmol* (2008) 146(6):890–6 e8. doi: 10.1016/j.ajo.2008.09.014
4. Gritz DC, Wong IG. Incidence and Prevalence of Uveitis in Northern California; the Northern California Epidemiology of Uveitis Study. *Ophthalmology* (2004) 111(3):491–500; discussion. doi: 10.1016/j.ophtha.2003.06.014
5. Natkunarajah M, Kaptoge S, Edelsten C. Risks of Relapse in Patients With Acute Anterior Uveitis. *Br J Ophthalmol* (2007) 91(3):330–4. doi: 10.1136/bjo.2005.083725
6. Agarwal RK, Silver PB, Caspi RR. Rodent Models of Experimental Autoimmune Uveitis. *Methods Mol Biol* (2012) 900:443–69. doi: 10.1007/978-1-60761-720-4_22
7. Caspi RR, Roberge FG, Chan CC, Wiggert B, Chader GJ, Rozenszajn LA, et al. A New Model of Autoimmune Disease. Experimental Autoimmune Uveoretinitis Induced in Mice With Two Different Retinal Antigens. *J Immunol* (1988) 140(5):1490–5.
8. Chen J, Qian H, Horai R, Chan CC, Caspi RR. Mouse Models of Experimental Autoimmune Uveitis: Comparative Analysis of Adjuvant-Induced vs Spontaneous Models of Uveitis. *Curr Mol Med* (2015) 15(6):550–7. doi: 10.2174/1566524015666150731100318

9. Caspi RR, Silver PB, Luger D, Tang J, Cortes LM, Pennesi G, et al. Mouse Models of Experimental Autoimmune Uveitis. *Ophthalmic Res* (2008) 40(3-4):169–74. doi: 10.1159/000119871
10. Kitaichi N, Namba K, Taylor AW. Inducible Immune Regulation Following Autoimmune Disease in the Immune-Privileged Eye. *J Leukoc Biol* (2005) 77 (4):496–502. doi: 10.1189/jlb.0204114
11. Lee DJ, Taylor AW. Following EAU Recovery There is an Associated MC5r-Dependent APC Induction of Regulatory Immunity in the Spleen. *Invest Ophthalmol Vis Sci* (2011) 52(12):8862–7. doi: 10.1167/iovs.11-8153
12. Lee DJ, Taylor AW. Both MC5r and A2Ar Are Required for Protective Regulatory Immunity in the Spleen of Post-Experimental Autoimmune Uveitis in Mice. *J Immunol* (2013) 191(8):4103–11. doi: 10.4049/jimmunol.1300182
13. Lee DJ, Taylor AW. Recovery From Experimental Autoimmune Uveitis Promotes Induction of Antiuveitic Inducible Tregs. *J Leukoc Biol* (2015) 97 (6):1101–9. doi: 10.1189/jlb.3A1014-466RR
14. Lee DJ, Preble J, Lee S, Foster CS, Taylor AW. MC5r and A2Ar Deficiencies During Experimental Autoimmune Uveitis Identifies Distinct T Cell Polarization Programs and a Biphasic Regulatory Response. *Sci Rep* (2016) 6:37790. doi: 10.1038/srep37790
15. Silver PB, Horai R, Chen J, Jittayasothorn Y, Chan CC, Villasmil R, et al. Retina-Specific T Regulatory Cells Bring About Resolution and Maintain Remission of Autoimmune Uveitis. *J Immunol* (2015) 194(7):3011–9. doi: 10.4049/jimmunol.1402650
16. Boldison J, Khera TK, Copland DA, Stimpson ML, Crawford GL, Dick AD, et al. A Novel Pathogenic RBP-3 Peptide Reveals Epitope Spreading in Persistent Experimental Autoimmune Uveoretinitis. *Immunology* (2015) 146(2):301–11. doi: 10.1111/imm.12503
17. Cortes LM, Mattapallil MJ, Silver PB, Donoso LA, Liou GI, Zhu W, et al. Repertoire Analysis and New Pathogenic Epitopes of IRBP in C57BL/6 (H-2b) and B10.RIII (H-2r) Mice. *Invest Ophthalmol Vis Sci* (2008) 49(5):1946–56. doi: 10.1167/iovs.07-0868
18. Heuss ND, Lehmann U, Norbury CC, McPherson SW, Gregerson DS. Local Activation of Dendritic Cells Alters the Pathogenesis of Autoimmune Disease in the Retina. *J Immunol* (2012) 188(3):1191–200. doi: 10.4049/jimmunol.1101621
19. Pepple KL, Wilson L, Van Gelder RN. Comparison of Aqueous and Vitreous Lymphocyte Populations From Two Rat Models of Experimental Uveitis. *Invest Ophthalmol Vis Sci* (2018) 59(6):2504–11. doi: 10.1167/iovs.18-24192
20. Dave N, Chevour P, Mahendradas P, Venkatesh A, Kawali A, Shetty R, et al. Increased Aqueous Humor CD4+/CD8+ Lymphocyte Ratio in Sarcoid Uveitis. *Ocul Immunol Inflammation* (2019) 27(7):1033–40. doi: 10.1080/09273948.2017.1421232
21. Maruyama K, Inaba T, Sugita S, Ichinohasama R, Nagata K, Kinoshita S, et al. Comprehensive Analysis of Vitreous Specimens for Uveitis Classification: A Prospective Multicentre Observational Study. *BMJ Open* (2017) 7(11): e014549. doi: 10.1136/bmjopen-2016-014549
22. Andersen GN, Hagglund M, Nagaeva O, Frangsmyr L, Petrovska R, Mincheva-Nilsson L, et al. Quantitative Measurement of the Levels of Melanocortin Receptor Subtype 1, 2, 3 and 5 and Pro-Opio-Melanocortin Peptide Gene Expression in Subsets of Human Peripheral Blood Leucocytes. *Scand J Immunol* (2005) 61(3):279–84. doi: 10.1111/j.1365-3083.2005.01565.x
23. Newton HS, Chimote AA, Arnold MJ, Wise-Draper TM, Conforti L. Targeted Knockdown of the Adenosine A2A Receptor by Lipid NPs Rescues the Chemotaxis of Head and Neck Cancer Memory T Cells. *Mol Ther Methods Clin Dev* (2021) 21:133–43. doi: 10.1016/j.omtm.2021.03.001
24. Kjaergaard J, Hatfield S, Jones G, Ohta A, Sitkovsky M. A2A Adenosine Receptor Gene Deletion or Synthetic A2A Antagonist Liberate Tumor-Reactive CD8(+) T Cells From Tumor-Induced Immunosuppression. *J Immunol* (2018) 201(2):782–91. doi: 10.4049/jimmunol.1700850
25. Namba K, Kitaichi N, Nishida T, Taylor AW. Induction of Regulatory T Cells by the Immunomodulating Cytokines Alpha-Melanocyte-Stimulating Hormone and Transforming Growth Factor-Beta2. *J Leukoc Biol* (2002) 72 (5):946–52. doi: 10.1189/jlb.72.5.946
26. Muhammad F, Wang D, McDonald T, Walsh M, Drenen K, Montieth A, et al. TIGIT(+) A2Ar-Dependent Anti-Uveitic Treg Cells are a Novel Subset of Tregs Associated With Resolution of Autoimmune Uveitis. *J Autoimmun* (2020) 111:102441. doi: 10.1016/j.jaut.2020.102441
27. Muhammad F, Wang D, Montieth A, Lee S, Preble J, Foster CS, et al. PD-1+ Melanocortin Receptor Dependent-Treg Cells Prevent Autoimmune Disease. *Sci Rep* (2019) 9(1):16941. doi: 10.1038/s41598-019-53297-w
28. Alspach E, Lussier DM, Schreiber RD. Interferon Gamma and Its Important Roles in Promoting and Inhibiting Spontaneous and Therapeutic Cancer Immunity. *Cold Spring Harb Perspect Biol* (2019) 11(3):1–20. doi: 10.1101/cshperspect.a028480
29. Kim TS, Shin EC. The Activation of Bystander CD8(+) T Cells and Their Roles in Viral Infection. *Exp Mol Med* (2019) 51(12):1–9. doi: 10.1038/s12276-019-0316-1
30. Jiang L, Yang P, He H, Li B, Lin X, Hou S, et al. Increased Expression of Foxp3 in Splenic CD8+ T Cells From Mice With Anterior Chamber-Associated Immune Deviation. *Mol Vision* (2007) 13:968–74.
31. Stein-Streilein J, Taylor AW. An Eye's View of T Regulatory Cells. *J leukocyte Biol* (2007) 81(3):593–8. doi: 10.1189/jlb.0606383
32. Peng Y, Shao H, Ke Y, Zhang P, Han G, Kaplan HJ, et al. Minimally Activated CD8 Autoreactive T Cells Specific for IRBP Express a High Level of Foxp3 and are Functionally Suppressive. *Invest Ophthalmol Vis Sci* (2007) 48(5):2178–84. doi: 10.1167/iovs.06-1189
33. Uchio E, Kijima M, Ishioka M, Tanaka S, Ohno S. Suppression of Actively Induced Experimental Autoimmune Uveoretinitis by CD4+ T Cells. *Graefe's Arch Clin Exp Ophthalmol = Albrecht von Graefes Archiv fur klinische und experimentelle Ophthalmologie* (1997) 235(2):97–102. doi: 10.1007/BF00941737
34. Muhammad FY, Peters K, Wang D, Lee DJ. Exacerbation of Autoimmune Uveitis by Obesity Occurs Through the Melanocortin 5 Receptor. *J Leukoc Biol* (2019) 106(4):879–87. doi: 10.1002/JLB.MA0119-030RR
35. Streilein JW. Ocular Immune Privilege: The Eye Takes a Dim But Practical View of Immunity and Inflammation. *J Leukoc Biol* (2003) 74(2):179–85. doi: 10.1189/jlb.1102574
36. Streilein JW. Ocular Immune Privilege: Therapeutic Opportunities From an Experiment of Nature. *Nat Rev Immunol* (2003) 3(11):879–89. doi: 10.1038/nri1224
37. Streilein JW, Ohta K, Mo JS, Taylor AW. Ocular Immune Privilege and the Impact of Intraocular Inflammation. *DNA Cell Biol* (2002) 21(5-6):453–9. doi: 10.1089/10445490260099746

Conflict of Interest: The authors declare that the research was conducted in the absence of any commercial or financial relationships that could be construed as a potential conflict of interest.

Publisher's Note: All claims expressed in this article are solely those of the authors and do not necessarily represent those of their affiliated organizations, or those of the publisher, the editors and the reviewers. Any product that may be evaluated in this article, or claim that may be made by its manufacturer, is not guaranteed or endorsed by the publisher.

Copyright © 2021 McDonald, Muhammad, Peters and Lee. This is an open-access article distributed under the terms of the Creative Commons Attribution License (CC BY). The use, distribution or reproduction in other forums is permitted, provided the original author(s) and the copyright owner(s) are credited and that the original publication in this journal is cited, in accordance with accepted academic practice. No use, distribution or reproduction is permitted which does not comply with these terms.

frontiers in Immunology

ORIGINAL RESEARCH
published: 16 March 2022
doi: 10.3389/fimmu.2022.839502

ATF3 Positively Regulates Antibacterial Immunity by Modulating Macrophage Killing and Migration Functions

*Yuzhang Du[1], Zhihui Ma[1], Juanjuan Zheng[1], Shu Huang[1], Xiaobao Yang[1], Yue Song[1], Danfeng Dong[1], Liyun Shi[2] and Dakang Xu[1]**

[1] Department of Laboratory Medicine, Ruijin Hospital, Shanghai Jiao Tong University School of Medicine, Shanghai, China, [2] Department of Immunology and Medical Microbiology, Nanjing University of Chinese Medicine, Nanjing, China

The clinical severity of *Staphylococcus aureus* (*S. aureus*) respiratory infection correlates with antibacterial gene signature. *S. aureus* infection induces the expression of an antibacterial gene, as well as a central stress response gene, thus activating transcription factor 3 (ATF3). ATF3-deficient mice have attenuated protection against lethal *S. aureus* pneumonia and have a higher bacterial load. We tested the hypothesis that ATF3-related protection is based on the increased function of macrophages. Primary marrow-derived macrophages (BMDM) were used *in vitro* to determine the mechanism through which ATF3 alters the bacterial-killing ability. The expression of ATF3 correlated with the expression of antibacterial genes. Mechanistic studies showed that ATF3 upregulated antibacterial genes, while ATF3-deficient cells and lung tissues had a reduced level of antibacterial genes, which was accompanied by changes in the antibacterial process. We identified multiple ATF3 regulatory elements in the antibacterial gene promoters by chromatin immunoprecipitation analysis. In addition, Wild type (WT) mice had higher F4/80 macrophage migration in the lungs compared to ATF3-null mice, which may correlate with actin filament severing through ATF3-targeted actin-modifying protein gelsolin (GSN) for the macrophage cellular motility. Furthermore, ATF3 positively regulated inflammatory cytokines IL-6 and IL-12p40 might be able to contribute to the infection resolution. These data demonstrate a mechanism utilized by *S. aureus* to induce ATF3 to regulate antibacterial genes for antimicrobial processes within the cell, and to specifically regulate the actin cytoskeleton of F4/80 macrophages for their migration.

Keywords: *Staphylococcus aureus*, activating transcription factor 3 (ATF3), antibacterial, macrophages, migration

OPEN ACCESS

Edited by:
Alexander Steinkasserer, University Hospital Erlangen, Germany

Reviewed by:
Ka Man Law, Kaiser Permanente Bernard J Tyson School of Medicine, United States
Sarang Tartey, IGM Biosciences, United States

****Correspondence:***
Dakang Xu
dakang_xu@163.com

Specialty section:
This article was submitted to Antigen Presenting Cell Biology, a section of the journal Frontiers in Immunology

Received: *20 December 2021*
Accepted: *28 February 2022*
Published: *16 March 2022*

Citation:
Du Y, Ma Z, Zheng J, Huang S, Yang X, Song Y, Dong D, Shi L and Xu D (2022) ATF3 Positively Regulates Antibacterial Immunity by Modulating Macrophage Killing and Migration Functions. Front. Immunol. 13:839502. doi: 10.3389/fimmu.2022.839502

INTRODUCTION

Staphylococcus aureus (*S. aureus*) is a major human pathogen that causes severe respiratory infections (1). Innate immune cells, mainly macrophages and neutrophils, act as gatekeepers in their interactions with *S. aureus*, killing the strain by phagocytosis to clear the infection (2). The important role of macrophages in protecting from *S. aureus* infection by using a wide range of

killing mechanisms has attracted increasing attention. *S. aureus* has evolved multiple strategies to survive, such as manipulating and evading macrophages (2, 3). Macrophages and *S. aureus* affect the outcome of infection through various direct interactions. In addition, *S. aureus* has developed resistance to a variety of antibiotics; thus, effective treatment strategies for these bacteria are limited (4). *S. aureus* can exploit the immune system to evade the host's defense system. Therefore, *S. aureus* is a serious threat to human health, and new treatment strategies are needed.

Although neutrophils are important antibacterial cells, their capability to produce inflammatory cytokines/chemokines is more limited than that of macrophages. Depletion of macrophages has been reported to significantly affect the host's defense response and impede bacterial clearance, suggesting that control of infection is dependent on innate subpopulations of cells rather than on adaptive immune cells (5). In addition, adoptive transfer experiments have shown that macrophages primarily mediate the prevention of staphylococcal reinfection. Macrophages release large amounts of proinflammatory cytokines, chemokines, and antimicrobial peptides (AMPs), and by recruiting immune cells to coordinately fight against pathogens (6).

Macrophages sense and clear the invading microbial pathogens. *S. aureus* initial Toll-like receptor (TLR)-2 mediates local production of soluble mediators, including cytokines, chemokines, and AMPs (7). Such an inflammatory response can also promote the production of IL-17 to orchestrate the host immune response. Recent findings have suggested that IL-17 and IL-22/IL-23 regulate the function of macrophages, thereby inducing the expression of AMPs, such as regenerated islet-derived protein 3 (Reg3) and defensins, which can kill or inactivate microorganisms (8, 9). Therefore, inactivation of IL17, IL-22, and IL-23 leads to an increased bacterial load in the lungs, exacerbation of *S. aureus* pneumonia, and higher mortality (8, 10). Given the critical role of TLR2 and IL-17/IL-22/IL-23 pathways in host defense responses, it is important to elucidate the mechanisms involved and search for factors with regulatory potential.

Activating transcription factor 3 (ATF3) is a hub cellular stress response gene in the pathogenesis of the disease. For modulation of infection and inflammation, ATF3 encodes a member of the ATF/cyclic adenosine monophosphate (cAMP) response element (CRE) binding (CREB) transcription factor family (11). ATF3 plays an important role in the negative feedback loop response by suppressing TLR-mediated cytokine expression (12). This implies that ATF3 is a key regulator of host resistance to invasive pathogens and inflammatory diseases, including *S. aureus* infection (13). However, the exact mechanisms involved in ATF3-related regulation of proinflammatory cytokines, chemokines, and AMPs for the antimicrobial effects in *S. aureus* infection are still unclear. Furthermore, the role of ATF3 in *S. aureus* infection and the mechanism of its action remain to be determined.

In the present study, we demonstrated that ATF3 can promote bacterial clearance through the regulation of the host's defense response and thus alleviate lethal *S. aureus* pneumonia. During *S. aureus* infection, the expression level of ATF3 closely correlated with the level of the host's AMPs. We found that ATF3-deficient mice or cells had a higher bactericidal loading. Furthermore, we found that ATF3 positively correlated with AMPs gene expression (e.g., Reg3 that ATF3 transcription factors directly regulated AMPs genes *via* chromatin immunoprecipitation analysis of putative binding sites, consistent with macrophage bactericidal and migratory functions. ATF3 also affected the migration of F4/80 macrophages in the lungs, which correlated with actin filament severing through ATF3 regulation. Our data suggested that ATF3 plays an important role in early Staphylococcus aureus. infection through positive regulation of the host immunity against bacterial infection by regulating macrophage Reg3 expression, AMPs gene-mediated bacterial clearance, and F4/80 macrophage recruitment.

MATERIALS AND METHODS

Mice

ATF3 -/- mice were reported by us previously (14). Sex- and age-matched (8–10 weeks) WT and ATF3 KO mice were used during the whole experiments. The mice were bred and kept on a 12 h reverse light/dark cycle and were provided with adequate water and food under specific pathogen-free conditions. The animals were transferred and housed in an animal facility for 3 d of stable housing prior to any experiments. The experiments were conducted in strict accordance with the National Institutes of Health Guide for the Care and Use of Laboratory Animals, approved by the Ethics Committee of Ruijin Hospital, Shanghai Jiao Tong University School of Medicine.

Cell Culture

RAW 264.7 murine macrophages were maintained in Dulbecco's modified Eagle's medium (DMEM) containing 10% fetal calf serum at 37°C in a 5% CO_2-humidified incubator. For bone marrow-derived macrophages (BMDMs), isolation and differentiation were performed in line with our published procedure with minor changes (15). Briefly, we flushed the tibias and femurs with precooled phosphate-buffered saline (PBS) using a 25-gauge needle and a 5 mL syringe. Then, the collected bone marrow was gently resuspended into single-cell suspension, and sometimes it was necessary to use red blood cell lysis solution (Sangon Biotech, Shanghai, China) to lyse the red blood cells in it. The cells were centrifuged at 700*g* for 4 min at room temperature. Then, they were resuspended using a 10 mL conditioned medium (DMEM + 10% fetal bovine serum (FBS) 1% penicillin/streptomycin, and 30% L929) and transferred into a 10-cm cell culture dish. Three days later, 10 mL of fresh conditioned medium was used to replace the old medium in the Petri dishes, and most of the cells were found to be stuck to the Petri dishes. After 7 d of cultivation, fresh medium was replaced, and the cells were used for experiments.

S. aureus Growth and Labeling Conditions

The MRSA strain (USA300) reported by our previous study (16) was cultured in Luria Bertani broth at 37°C until its stable growth phase, and then collected by centrifugation at 8,000 rpm for 5 min. The bacteria were washed three times with PBS and resuspended to an optical density of 0.8 at 600 nm. Then, 500 μL of the bacterial suspension was incubated with an equal volume of 5.0 μM solution of 5(-and 6) carboxyfluorescein diacetate succinimidyl ester (CFDA/SE, Selleck) for 30 min in the dark at 37°C. Subsequently, the stained bacteria were washed three times with PBS and the resuspended bacteria were used for later experiments.

Pneumonia Model

For lung bacterial infections, a total volume of 40 μL of PBS containing *S. aureus* (5×10^6 CFU/mouse) was injected into the trachea of mice. For survival experiments, we used 2×10^8 CFU/mouse of *S. aureus* and observed their survival 48 h after the infection. The survival rate of the mice was monitored every 3 h.

Bronchoalveolar Lavage Fluid (BALF) Collection

BALF collection was performed in line with our published procedure with minor modifications (16). Briefly, we sacrificed the mice by cervical dislocation and exposed the trachea. A 20-gauge catheter was used, and 0.8 mL of PBS was dripped into the lungs and gathered into clean tubes. This process was repeated four times to collect about 3 mL of BALF from each mouse. We used a cell counting plate to count the total number of cells in the alveolar lavage fluid and a flow cytometer to count the number of macrophages and neutrophils in BALF. The remaining BALF was then centrifuged at 700 g for 5 min, and supernatants were stored at −80°C until cytokine analysis.

Internalization and Killing of Bacteria

To evaluate the phagocytic capability, macrophages were incubated with CFSE-labeled *S. aureus* (MOI 10) for the indicated time periods. Then, the infected cells were washed using PBS, and extracellular bacteria were eliminated by treatment with lysostaphin (20 μg/mL) for 30 min. Macrophages were then collected, and intracellular bacterial loads were quantified by flow cytometry. To determine the bactericidal capability of macrophages, the cells were seeded on coverslips for 24 h and incubated with CFSE-labeled *S. aureus* (MOI 10) for 2 h. The cells were then washed and further cultured in a fresh medium containing lysostaphin (2 μg/mL) for the indicated time periods. Thereafter, the cells were fixed, and the nuclei were counterstained with DAPI, and then they were observed by fluorescence microscopy.

Macrophage Killing Assay

The intracellular killing assay was conducted following a previously described procedure with slight modifications (17). BMDM cells from WT and ATF3 KO mice were infected with *S. aureus* (MOI 10) for 2 h. The cells were then washed and treated with a medium containing gentamicin (300 μg/mL) for 30 min to kill the extracellular bacteria. Then, the cells were further cultured in a fresh medium containing gentamicin (100 μg/mL) for the indicated time periods (2 h, 6 h, 12 h, and 18 h). Subsequently, the cells were washed several times with PBS and then lysed with 0.1% Triton X-100 to release the bacteria inside the cells. To estimate the number of bacteria, the lysate was serially diluted with sterile PBS, applied to LB plates, and incubated overnight in a dedicated bacterial incubator.

Quantitative PCR

Total RNA was extracted using TRIzol reagent (Thermo Fisher Scientific, Waltham, MA, USA) in accordance with the manufacturer's guidelines. One microgram of total RNA was reverse-transcribed to cDNA using SuperScript II (Invitrogen, Carlsbad, CA), and qRT-PCR was performed using SYBR Green technology (Takara, Tokyo, Japan). β-actin was used for normalization, and data were analyzed through the ΔΔCt method. The primers used for the detection in the study were synthesized by GENEWIZ (Suzhou, China), and sequences are shown in **Supplementary Table 1**.

Myeloperoxidase (MPO) Activity Assay

MPO activity was assessed as an indicator of neutrophil accumulation in lung tissues by using Myeloperoxidase (MPO) Activity Fluorometric Assay Kit (#K745-100, BioVision, California, USA) in accordance with its instruction.

Immunofluorescence Microscopy

WT and ATF3 KO BMDM cells were seeded on glass slides and stimulated with *S. aureus* for the indicated time. The cells were washed twice with prewarmed PBS and fixed with 4% paraformaldehyde solution for 15 min at room temperature. We washed the samples and permeabilized them in 0.1% Triton X-100 for 20 min. After washing the samples three times with PBS, we added the fluorescent phalloidin staining solution to each coverslip and incubated them in a covered container for 50 min at room temperature. We again washed the samples three times with PBS, and recorded immunofluorescence images by laser scanning confocal microscopy.

Histological Analysis of Lung Tissues

For histological analysis, mouse lung samples were thoroughly washed in PBS, fixed in 4% (wt/vol) paraformaldehyde for 24 h, embedded in paraffin, and sliced into 5-μm-thick sections. Hematoxylin and eosin staining was performed in line with standard procedures. For immunostaining, the lung sections were deparaffinized, hydrated, and blocked in Dulbecco's phosphate-buffered saline (DPBS)containing 2% normal goat serum. The slides were then stained with the indicated primary antibody and biotin-conjugated secondary antibody and then incubated with streptavidin-conjugated horseradish peroxidase (HRP). Finally, the slides were incubated with DAB reagent and counterstained with hematoxylin for observation.

Cytokine Measurement

The levels of TNFα, IL-6, IL-1β, and IL-12 in the cell culture supernatants and BALF were measured by ELISA kits

(R&D Systems, Minneapolis, MN) in accordance with the manufacturers' guidelines.

Transwell Migration Assay

BMDMs (1×10^5 cells) were seeded onto the top chamber of an 8-μm pore transwell insert (Corning, NY, USA) in a 24-well plate with media containing 2% FBS. After 36 h, the media within the transwell inserts were carefully removed, and the cells were fixed with 2% paraformaldehyde and stained with 0.2% crystal violet. Cells that did not migrate across the transwell membrane were wiped from the top of the chamber. The migrated cells were viewed using a Nikon DS-F2 microscope. The inserts were then incubated with 30% acetic acid, and the absorbance was read at 570 nm. The experiment was repeated three times.

Western Blot

The cell lysate was prepared with SDS-lysis buffer (Beyotime, Shanghai, China). Total protein concentration was measured by Nano-100 Micro-Spectrophotometer. Protein was then separated by 10% SDS-polyacrylamide microgel and transferred to 0.45-μm polyvinylidene difluoride membranes (Invitrogen). The PVDF membranes were then blocked in Tris-buffered saline containing 5% nonfat dry milk (w/v) (Sangon Biotech) in Tween-20 (TBST) for 1 h at room temperature. After that, the membranes were incubated with the indicated primary antibodies overnight. Then, they were incubated with a secondary antibody conjugated with HRP. We used Tanton™ Chemistar High-sig ECL Western Blotting Substrate (ECL) to display the signal. Full blots of images cropped for presentation are presented in **Supplementary Material**.

Chromatin Immunoprecipitation Assay

The ChIP assay was performed using the ChIP-IT Express Magnetic Chromatin Immunoprecipitation kit (53008, Active Motif, Carlsbad, CA, USA) according to the manufacturer's instructions. The chromatin solution was immunoprecipitated using either an anti-ATF3 antibody (CST, USA) or normal anti-IgG antibody (CST, USA) and then incubated with magnetic beads overnight at 4°C with rotation. Next, the DNA-Antibody complexes were washed sequentially by CHIP buffer1 and CHIP buffer2 and then eluted with elution buffer AM2. Then, RT-PCR was performed using purified DNA fragments and primers directed to the specific area spanning the putative ATF3-binding motif. Primer pairs used for ChIP are shown in **Supplementary Table 2**.

Generation of Stable Cell Lines

The plasmids pLVX-flag-REG3β-IRES-Puro and pLVX-flag-REG3γ-IRES-Puro were purchesed from Shanghai Xitubio biotechnology Co., Ltd. To generate stable cell lines expressing REG3β or REG3γ, pLVX-flag-REG3β-IRES-Puro or pLVX-flag-REG3γ-IRES-Puro plasmid together with the packaging plasmids (psPAX2+pMD2.G) were transfected into human embryonic kidney 293T (HEK293T) cells using EZ Trans transfection resgents (Life iLab Bio-Technology, China). The supernatants containing the virus were harvested after 48 h post–transfection and filtered using a 0.45-μm filter. Cells were incubated with viral supernatants plus equal complete medium in the presence of 5 μg/mL polybrene (Sigma) for 24 h. After infection, positive clones were selected by puromycin selection and infection efficacy were validated by immunoblotting assays.

Statistical Analyses

Unless otherwise stated, all data are expressed as the mean ± SD of three independent experiments. Student's *t* test or one-way analysis of variance was used for comparison between groups. *P* values < 0.05 were considered statistically significant. Kaplan–Meier survival analysis with log-rank test was used to evaluate the survival curve. All calculations were performed using the Prism 8 software program (GraphPad Software).

RESULTS

ATF3 Plays a Host Protective Role in Pneumonia Caused by *S. aureus*

To explore the potential role of ATF3 in the host's lung defense against *S. aureus* infection, we used a lethal dose of *S. aureus* (US 300) (2×10^8 CFUs/mouse) to infect WT and ATF3 KO mice intratracheally and observed survival patterns for 48 h. Although all ATF3 KO mice died within 24 h, 60% of WT mice survived more than two days after infection (**Figure 1A**). To determine whether the difference in survival was due to the difference in bacterial load in various organs, we measured the bacterial load in the lungs, BALF, and extrapulmonary organs after infecting mice with a sublethal inoculum (5×10^7 CFU) of *S. aureus*. Compared with WT mice, ATF3 KO mice had a higher bacterial load in the lungs and BALF, while there was no significant difference in spleen and blood bacterial load at 6 and 18 h after infection (**Figures 1B–E**). Meanwhile, the total protein (a measure of lung leakage) in the BALF of ATF3 KO mice was higher than that in the WT mice (**Figure 1F**). This suggests that ATF3 has a protective function against lethal *S. aureus* pneumonia and limits the host bacterial load.

ATF3 Promotes Macrophage Recruitment and Enhances Resistance to *S. aureus*

Macrophages and neutrophils are necessary to control *S. aureus* infection in the lungs (18). Since macrophages and neutrophils are critical to the survival of pneumonia, we investigated whether the loss of ATF3 affects the recruitment of macrophages or neutrophils to the alveolar space during *S. aureus* pneumonia. ATF3 KO mice displayed profound lung pathology during the infection **(Figures 2A, B**). To further analyze the neutrophil accumulation in the lung parenchyma, we performed MPO assay and showed that the MPO activity was similar between the two genotypes (**Figure 2C**). We also found that WT and ATF3 KO mice had a comparable neutrophil number as reflected by s100a9 staining and Ly6G+/CD11b+ population in the FACS analysis in post-infection lung tissue sections (**Figures 2D, E**). In addition, the total number of infiltrating cells was very similar between the WT and ATF3 KO mice from BALF samples (**Figure 2F**).

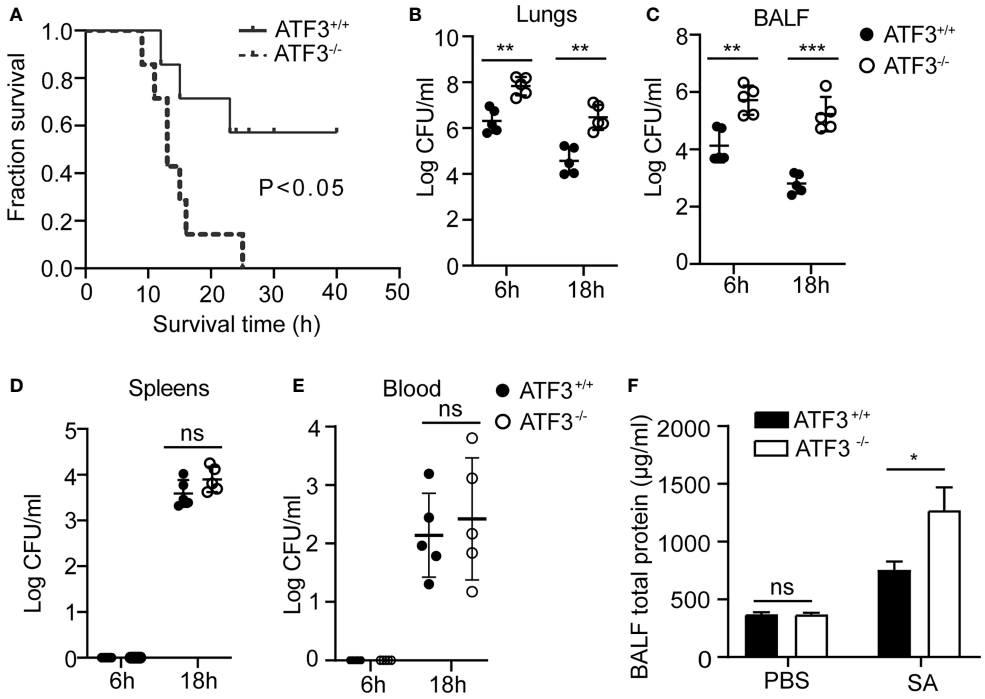

FIGURE 1 | ATF3 provides protection against *S. aureus* infections. **(A)** WT and ATF3 KO mice were challenged intratracheally with 2×10^8 CFU/mouse of a lethal inoculum of *S. aureus* (USA 300) and then observed to survive for 48 h. For the functional analysis, WT and ATF3 KO mice were infected intratracheally with a sublethal *S. aureus* inoculum (5×10^7 CFU/mouse) and then euthanized at 6h and 18hafter infection to quantify the bacterial load in the lungs **(B)**, BALF **(C)**, spleens **(D)**, and blood **(E)**. **(F)** Total protein in BALF was measured. ns, $P > 0.05$, $^*P < 0.05$, $^{**}P < 0.01$, $^{***}P < 0.001$.

Interestingly, we noticed that, compared to WT mice, ATF3 KO mice had fewer macrophages recruited into alveolar spaces, as revealed by F/80 staining for the macrophages (**Figure 2G**). We further confirmed ATF3 controls F4/80 macrophage cell recruitment to the lung with histologic observations, the increased F4/80 macrophage cell in the WT mice lung through time-dependent manner during the S. aureus infection (added **Figure 1 Supplementary Data**). ATF3 KO mice also had a lower macrophage infiltration from BALF samples the FACS analysis and absolute cell counts (**Figures 2H, I**), which indicated that ATF3 had a host protective effect on survival through macrophage-mediated anti-*S. aureus* immunity. Collectively, in *S. aureus* infection, ATF3 exerts host protection by increasing the number of macrophages in the alveolar lavage fluid.

ATF3 Enhances Macrophage Bacterial Clearance Ability

We next examined the effect of ATF3 on the ability of macrophages to clear bacteria. The phagocytic activity of macrophages was initially assessed by carboxyfluorescein succinimidyl ester (CFSE)-labeled *S. aureus*. There was no significant difference in the number of internalized bacteria between the WT and ATF3 KO macrophages (**Figures 3A, B**), indicating that ATF3 had no significant effect on macrophage phagocytosis. However, the count of bacterial colony-forming units (CFU) showed that the bacterial load was significantly reduced in WT, while ATF3 KO had less reduction during the 6-18 h infection process (**Figure 3C**). To further evaluate the bactericidal ability of macrophages, we conducted a lysostaphin protection test, in which the survival of internalized bacteria was observed with a fluorescence microscope (19). Remarkably, the number of living bacteria was increased in ATF3 KO macrophages compared to WT macrophages and lungs (**Figures 3D, E**), indicating that ATF3 enhanced the ability of macrophages to eliminate invading bacteria.

ATF3 Enhances Macrophage Bacterial Clearance Independent of Lung Released Pro Inflammatory Cytokines

Given the importance of macrophages in host defense against bacterial infections (5, 20), we next evaluated the effect of ATF3 on macrophages during staphylococcal infection. First, we noticed that ATF3 was induced in BMDM cells and RAW264.7 macrophages in a time-dependent manner after *S. aureus* infection (**Figures 4A, B**). Our previous study has reported that ATF3 is a crucial response gene in the lipid/cholesterol mediated inflammatory responses (14). The other study also showed that the transcriptional response suggests that the cholesterol *de novo* synthesis increases considerably in

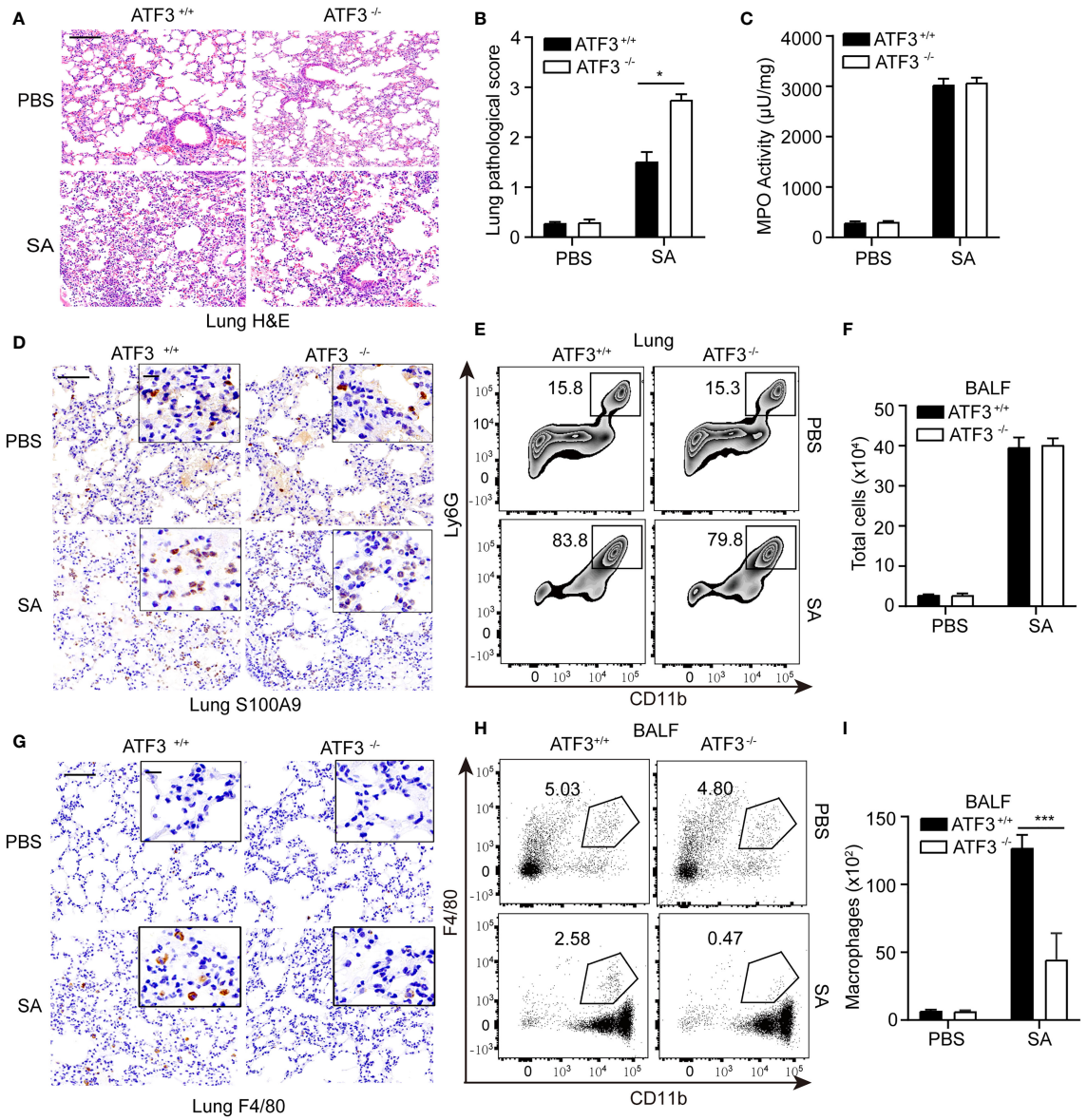

FIGURE 2 | Macrophages confer host protection in WT mice compared with the ATF3 KO. **(A)** Tissue sections of lung tissues stained with hematoxylin and eosin. **(B)** Pathological damage scores of lung tissues. **(C)** Measures of MPO activity as quantified by ELISA in lung extracts from WT or ATF3 KO mouse after S. aureus infection. **(D)** Representative images of WT and ATF3 KO mice lung tissues were assessed for neutrophils (S100A9) after S. aureus infection. **(E)** Representative zebra plot showing CD11b+ Ly6G+ cells from WT or ATF3 KO mice lung tissues after S. aureus infection. **(F)** Mice BALF was collected; counts of total cells are shown. WT and ATF3 KO mice were infected intratracheally with S. aureus (5 X 10^7 CFU/mouse). After 6h, the mice were euthanized and their BALF was collected, stained and subjected to flow cytometry. **(G)** Representative images of WT and ATF3 KO mice lung tissues were assessed for macrophage (F4/80) after S. aureus infection. **(H)** Representative dot plot showing CD11b+ F4/80 + cells. **(I)** Quantification of **(H)** Data are shown as the mean ± SD. *$P < 0.05$; ***$P < 0.001$ by Student's t test.

RAW264.7 cells to compare other macrophage cells, by those ATF3 was the top list of upregulated genes (21). It is indicated that ATF3 appears to have differing effects in immune response and is related to the metabolic regulation. Such an altered expression was also observed in the lungs from staphylococcal infection mice (**Figure 4C**). Indeed, the similar regulatory effect between WT and ATF3 KO significantly increased the expression of M1 proinflammatory cytokines, such as IL-1β, TNF-α (**Figures 4D, E**), with the exception of IL-6 and IL-12p40 being more significantly elevated in BMDM of WT (**Figures 4F, G**), while there were no differences in BALF among the major proinflammatory agents involved in the antimicrobial response *in vivo* (**Figures 4H–K**). In conclusion, our data suggest that ATF3 promotes the inflammatory response of macrophages in the early stages of staphylococcal infection regardless of lung released pro inflammatory cytokines.

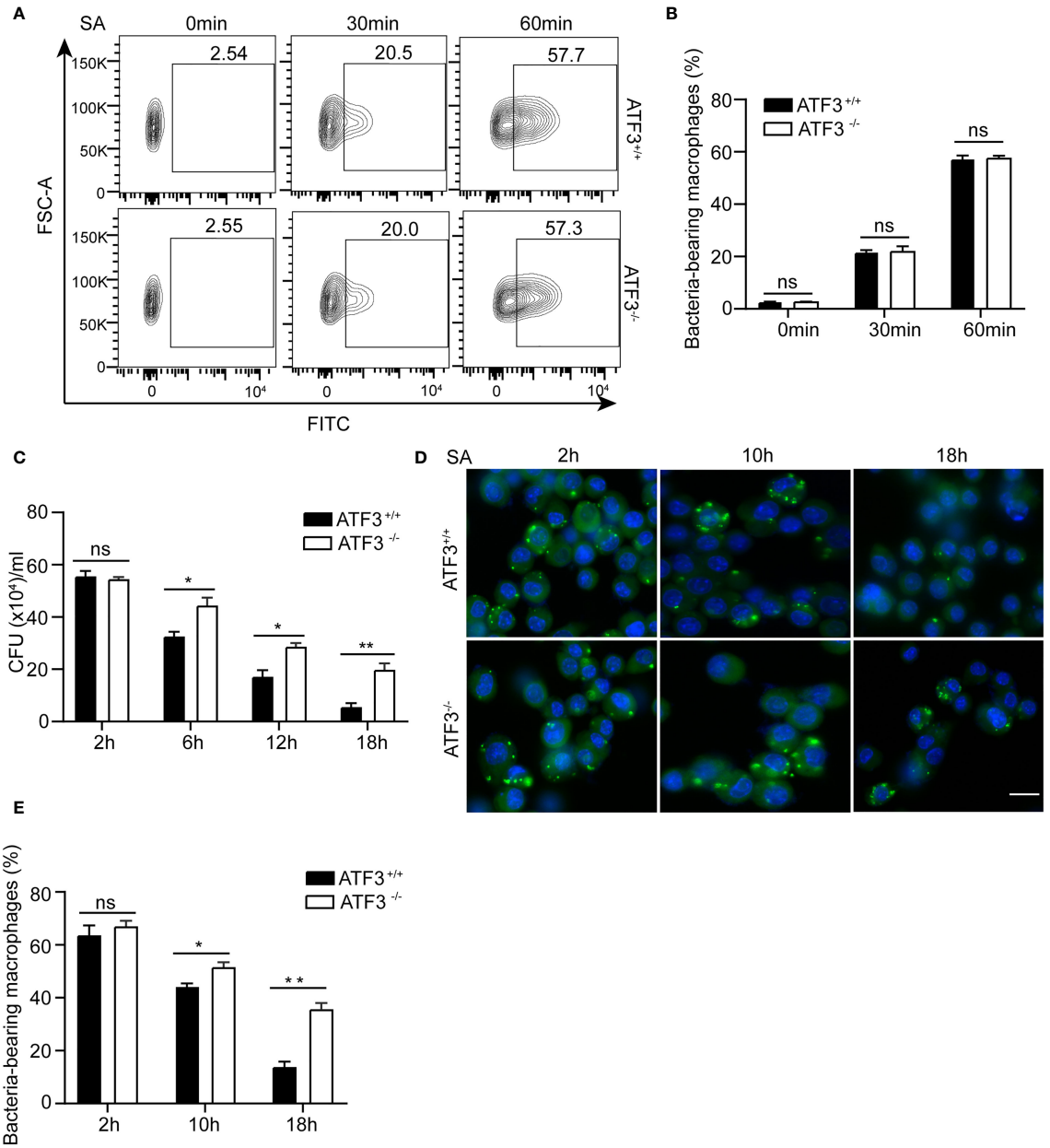

FIGURE 3 | ATF3 enhances macrophage bacterial clearance ability. WT and ATF3 KO BMDM cells were infected with *S. aureus* (MOI = 1) for the indicated time periods. **(A, B)** The phagocytic ability was evaluated by taking up the percentage of macrophages with CFSE-labeled *S. aureus*. Representative plots and quantification by bar graphs from five independent experiments of flow cytometry are shown. **(C)** The bacterial load was measured and calculated in BMDM cells within the indicated time period after infection. **(D, E)** Intracellular bacteria measured by immunofluorescence microscopy. At 2, 10, and 18 h after infection, the uptake of *S. aureus* in BMDM cells is marked by CFSE (green). The nuclei are stained with DAPI (blue). Five representative images of each group were analyzed. Scale bar, 30 μm. ns, $P > 0.05$, $^{*}P < 0.05$, $^{**}P < 0.01$.

ATF3 Enhances Macrophage Bacterial Clearance Dependent on Antimicrobial Signature

There is increasing evidence that antimicrobial peptides (AMP) play a central role in restricting bacterial replication and preventing tissue damage (22). The AMP such as Regenerating islet-derived protein type 3 [Reg3] was regulated by the IL-17, IL-22/23 through stat3 signaling (23). First, we experimentally found no significant difference in STAT3 signaling between WT and ATF3 KO cells with respect to the expression of phosphorylated STAT3 and its target gene SOCS3 (**Figures 5A, B**). Given that IL-22 can mediate the expression

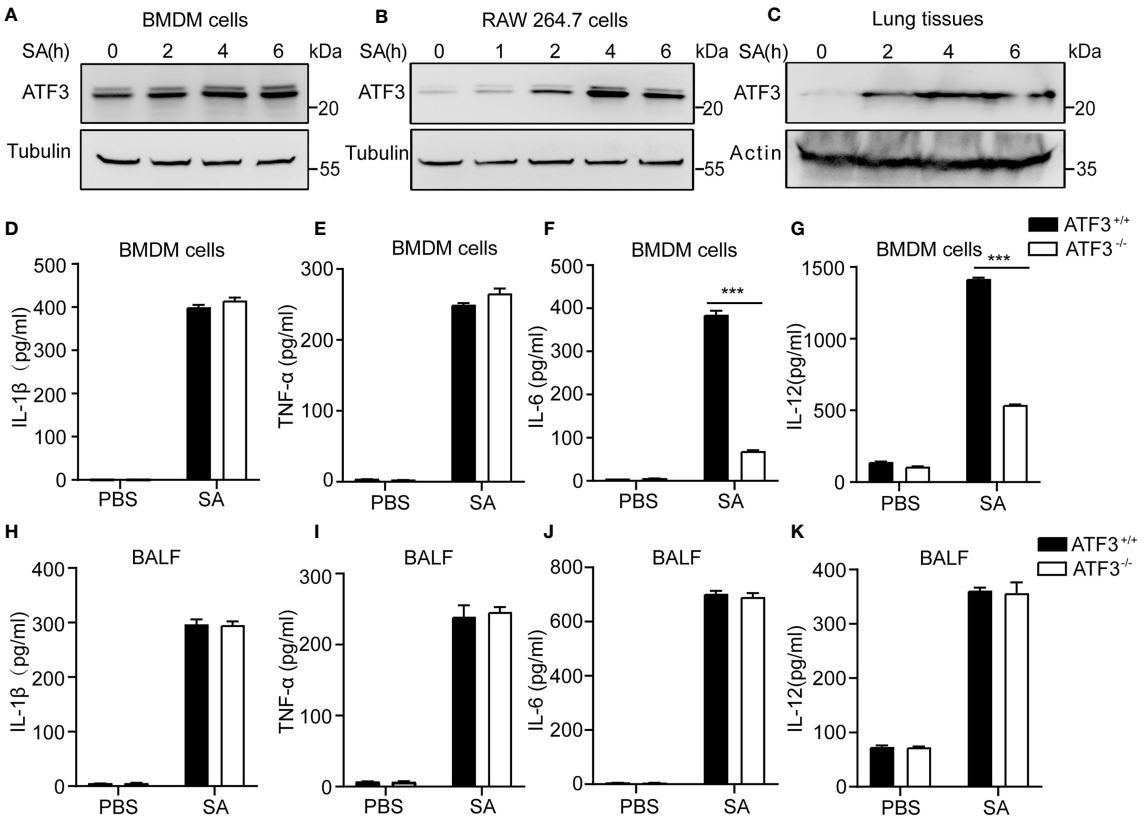

FIGURE 4 | ATF3 enhances macrophage bacterial clearance independent of M1/M2 macrophages. WT and ATF3 KO mice were challenged with 5×10^6 *S. aureus* colony forming units (CFU) and sacrificed 12 h later for subsequent functional analysis. **(A, B)** BMDM cells and RAW264.7 cells were infected with *S. aureus* for the indicated time periods. The cells were then lysed, and ATF3 protein levels were examined by immunoblotting. **(C)** Lungs obtained from *S. aureus*-infected mice for indicated time points were homogenized and ATF3 protein expression were measured by immunoblotting. **(D–G)** Macrophages derived from WT and ATF3 KO mice were infected with *S. aureus* for the indicated time periods, and cytokine levels in the cell supernatants were determined by ELISA. **(H-K)** WT and ATF3 KO mice were challenged with 5×10^6 CFUs of *S. aureus* and sacrificed 6 h later for the subsequent functional analysis. The levels of BALF cytokines (IL-1β, TNF-α, IL-6, and IL-12) were detected by ELISA. ***$P < 0.001$.

of many AMPs, including Reg3 family and S100A8,9 (24), we examined whether ATF3 has an effect on AMP and analyzed the changes in IL-22 levels. Notably, increased levels of IL-22 and the related cytokines IL-17 and IL-23 were observed in macrophages infected by *S. aureus*, but no differences in induction of IL-17, IL-22, and IL-23 were observed between WT and ATF3 KO cells (**Figure 5C**). Interestingly, the expression levels of the molecules with antibacterial properties, such as S100A8 and Reg3 family genes were increased in WT macrophages but decreased in ATF3-null cells (**Figures 5D, E**). Further we found that WT and ATF3 KO BMDM cells had a comparable induced expression of cytokines, chemokines after S. aureus infection (**Figures 5F, G**). Collectively, our data suggest that ATF3 enhances the production of its antimicrobial effector molecules, thereby potentially enhancing the ability of macrophages to clear bacteria.

ATF3 Directly Regulates the Antimicrobial Genes Through the ATF3 Binding Sites

We next investigated the functional relevance of ATF3 induction by *S. aureus* infection with respect to AMP expression. We studied the regulatory role of the transcription factor ATF3 in AMP transcription. To explore whether ATF3 could regulate AMP expression, CiiiDER, a tool for predicting and analyzing transcription factor binding sites was used to analyze the potential ATF3 binding site in these AMP genes (25). In our computational prediction results, those AMP genes had at least one predicted ATF3-binding site (**Figure 6A**). Consistent with Reg3β and Reg3γ as a direct target, chromatin immunoprecipitation analysis revealed that endogenous ATF3 bound to different regions of Reg3β and Reg3γ regulatory elements containing ATF3 or ATF/CREB binding sites; such binding was abolished by ATF3 KO BMDM (**Figures 6B, C**). Hence, ATF3 seems to regulate the levels of Reg3β and Reg3γ *via* direct transcription control. To evaluate a role for antimicrobial protein Reg3, we overexpressed Reg3β and Reg3γ in macrophages. Immunoblotting of BMDM cell lysates showed the exogenous Reg3β and Reg3γ proteins (**Figures 6D, E**). Reg3β and Reg3γ have potent growth-inhibitory activity against S. aureus (**Figures 6F, G**). These data are consistent with the finding that Reg3 has selective bactericidal activity against pulmonary S. aureus infections (9).

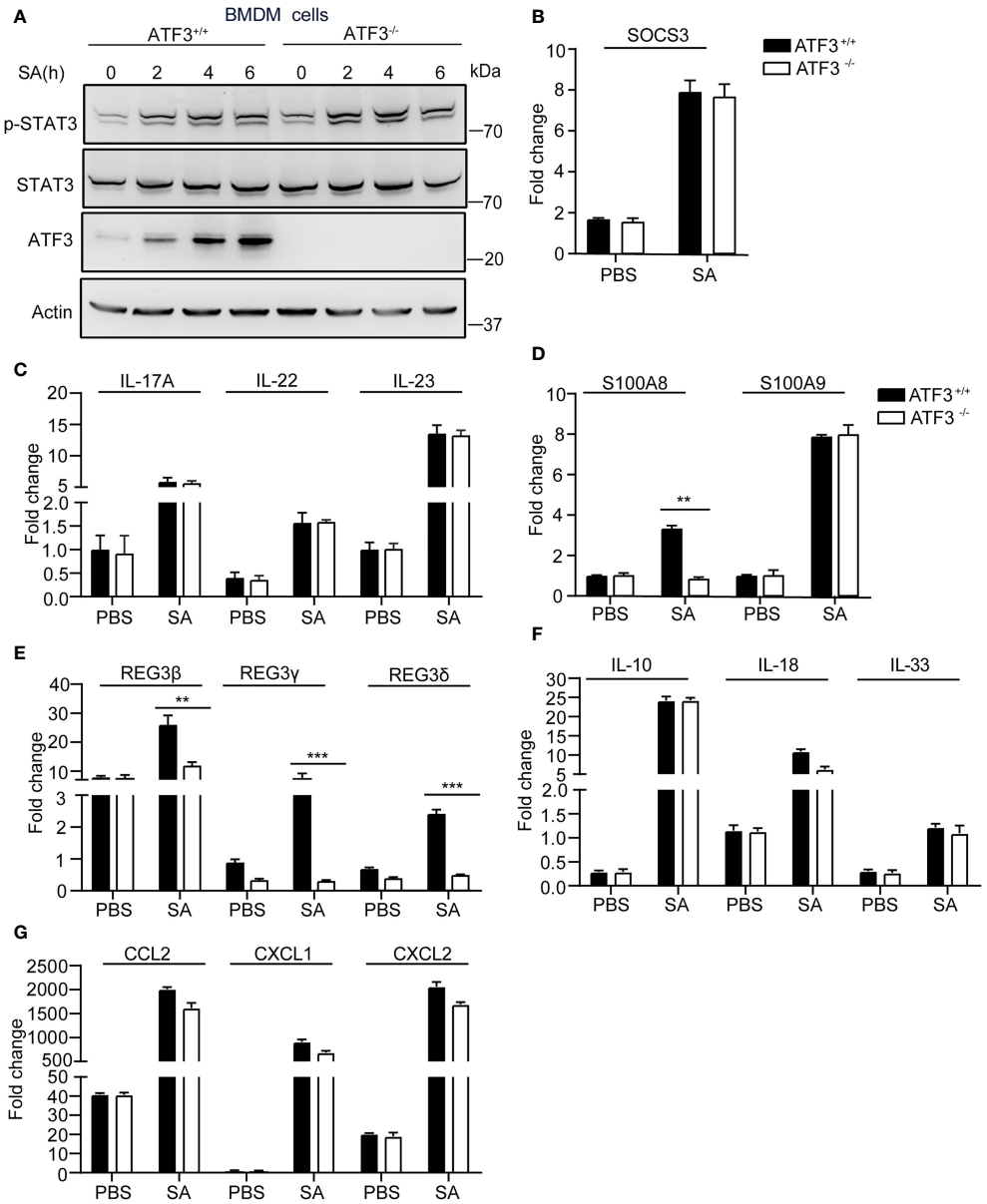

FIGURE 5 | ATF3 enhances macrophage bacterial clearance dependent on an antimicrobial signature. WT and ATF3 KO BMDM cells or mice were infected with *S. aureus* (MOI = 1) for the indicated time periods. **(A, B)** The cells were lysed; the protein levels of STAT3 and p-STAT3 were analyzed, and the amount of SOCS3 mRNA was detected using quantitative PCR (qPCR). **(C–G)** qPCR analysis of the indicated cytokines (IL-17, IL-22, and IL-23), AMPs (S100A8,S100A9,REG3β, REG3γ, REG3δ), and other cytokines (IL-10, IL-18, and IL-33), chemokines (CCL2, CXCL1, and CXCL2) associated with bactericidal activity. All results are from three independent experiments and are expressed as mean ± SD. $^{*}P < 0.05$, $^{**}P < 0.01$, $^{***}P < 0.001$ by the Student's *t* test.

ATF3 Exerts its Effect on Macrophage Migration and Recruitment in Acute Lung Infection by Regulating F-Actin

Figure 2H shows that ATF3 KO mice had a lower macrophage infiltration after *S. aureus* infection. To further investigate how ATF3 controls cell recruitment through motility, we studied the effect of ATF3 on the actin cytoskeleton. The polymerization and depolymerization of filamentous (F) actin have been reported to control the reorganization of the cytoskeleton, which is essential for cell movement through morphological changes (26). We next investigated whether ATF3 may regulate cellular recruitment by altering the actin cytoskeleton. We performed staining for F-actin in WT and ATF3 KO BMDM, revealing that there was no significant difference in actin stress fibers between WT and KO cells. Interestingly, in the case of S. aureus infection, we found that WT cells had significantly more actin stress fibers (**Figures 7A, B**).In addition, this impacted F-actin correlated with actin-modifying protein gelsolin (GSN) expression, which

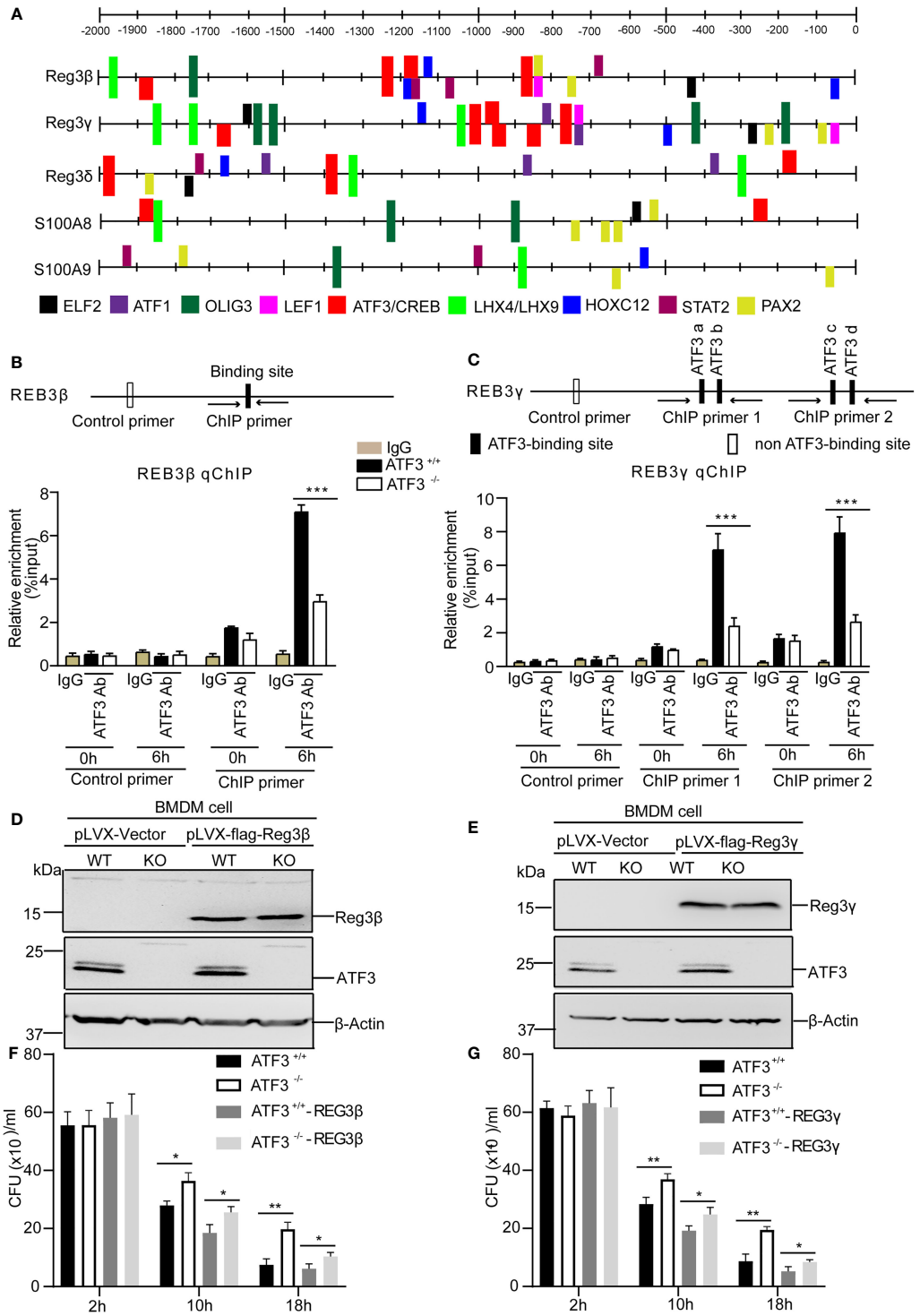

FIGURE 6 | ATF3 directly regulates the antimicrobial genes through the ATF3-binding sites. **(A)** Schematic linear map shows the putative binding sites of ATF3 and other transcription factors of the AMP genes. **(B, C)** The diagram shows the regulatory regions of the AMP gene that contain or lack the high-affinity ATF3-binding site (black and white boxes on the map). ChIP assays was performed in WT and ATF3 KO cells using either anti-IgG or an anti-ATF3 antibody to assess binding ability at the putative ATF3 binding site in Reg3β and Reg3γ promoter pretreated with PBS or S. aureus. **(D, E)** The efficiency of WT and ATF3 KO BMDM cells stably over-expressing REG3β or REG3γ was assessed by immunoblotting. **(F, G)** WT and ATF3 KO BMDM cells and cells stably over-expressing REG3β or REG3γ were infected with *S. aureus* (MOI = 1) for the indicated time periods and then the bacterial load was measured and calculated in BMDM cells after infection. ns, $P > 0.05$, $^{*}P < 0.05$, $^{**}P < 0.01$, $^{***}p < 0.001$.

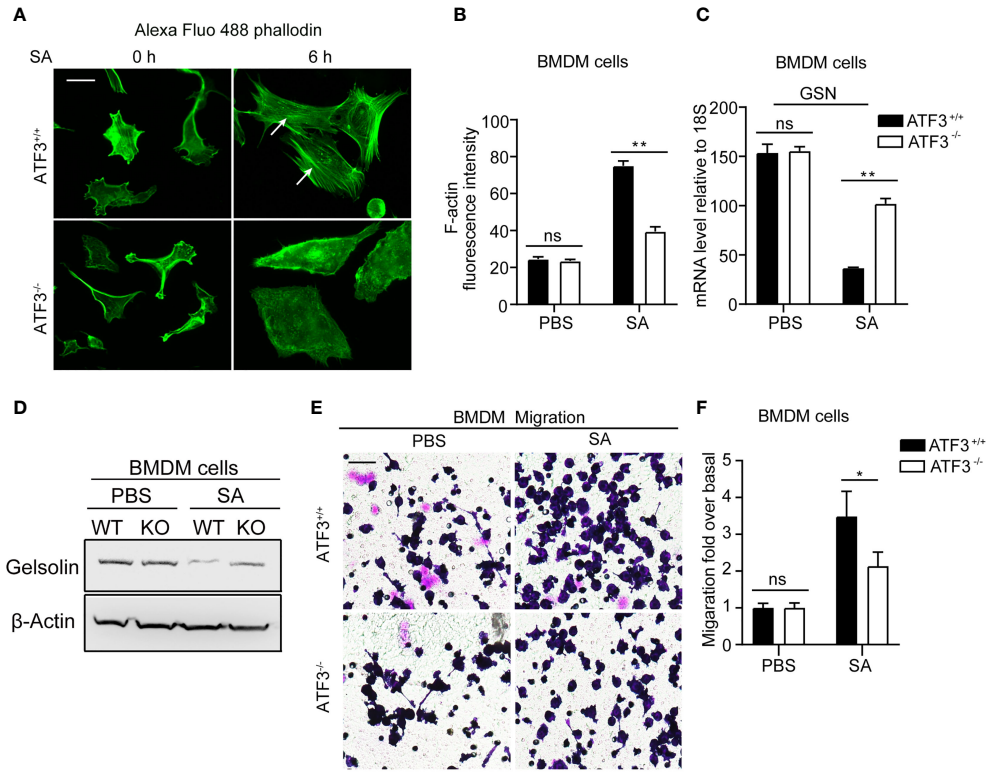

FIGURE 7 | ATF3 regulates GSN and cytoskeleton remodeling for macrophage motility and recruitment. **(A)** Representative images of the actin cytoskeleton stained with phalloidin in WT and ATF3 KO BMDM cells and cells infected with *S. aureus* (MOI = 1). The white arrow indicates F-actin. **(B)** The intensity of F-actin is quantified on the right (*$P < 0.05$). **(C, D)** The GSN expression was analysis by the qPCR analysis and immunoblotting assay between WT and ATF3 KO BMDM cells with or without S. aureus infection. **(E)** The effect of S. aureus infection on WT and ATF3 KO BMDM cells migration was evaluated by trans-well assay in 24h. **(F)** Quantitative analysis of the cell migration ratio in **(E)**. ns, $P > 0.05$, *$P < 0.05$, **$P < 0.01$.

was regulated by ATF3, as described in our previous study (27). Positive or negative regulation of GSN by ATF3 is dependent on cofactors, such as different histone deacetylases (HDACs) in a context-dependent manner. Results showed that ATF3 negatively regulated the GSN mRNA and proteins expression in BMDM and GSN expression was higher in ATF3 KO cells compared to WT cells after S. aureus infection (**Figure 7C, D**). We further examined the role of ATF3 in cell motility and found no significant difference in the degree of migration of WT BMDM and ATF3 KO BMDM in the unstimulated conditions; however, WT BMDM were significantly more migratory than ATF3 KO cells in *S. aureus*-stimulated conditions (**Figures 7E, F**). These data show that ATF3 regulates cell motility *in vitro* and may drive macrophage recruitment in lung tissues.

DISCUSSION

Macrophages, like neutrophils, are important immune sentinels that contribute significantly to innate defense but are also involved in adaptive immunity. However, despite their ability to control microbial infections, they fail to eradicate *S. aureus*, leading to immune evasion and causing chronic persistent infections (28). Despite significant progress in understanding the molecular details of the interaction between *S. aureus* and macrophages, which play an important role in the clearance of bacteria, many questions remain to be answered. In this study, we showed that infection with *S. aureus* significantly increased ATF3 expression, which accelerated bacterial clearance and could reduce the symptoms of pneumonia in mice. Meanwhile, ATF3 KO mice were more susceptible to *S. aureus* infection, had a higher bacterial load, and experienced exacerbated pneumonia tissue damages. Importantly, we also found that ATF3 expression correlated with antimicrobial gene expression, which corresponded to bacterial killing. ATF3-deficient cells and lung tissues had reduced expression levels of antibacterial genes, which in turn resulted in altered antimicrobial capacity. Our further studies showed that the antimicrobial genes upregulated during the antimicrobial process were direct targets of the transcription factor ATF3 as confirmed by chromatin immunoprecipitation analysis. Furthermore, anti-*S. aureus* infection was primarily mediated by macrophages, which were regulated by ATF3-mediated chemokines and antimicrobial peptides to recruit macrophages to synergistically combat pathogens. The immune regulation of ATF3 against *S. aureus* infection primarily involved proinflammatory cytokines, but it

was independent of the local release of cytokines, and also independent of STAT3 activation, leading to IL-17 and IL-22 expression.

One of the most important findings of this study is that ATF3 contributes to *S. aureus*-induced AMPs production. First, *S. aureus* infection induced the accumulation of ATF3, which in turn upregulated AMPs, and we also identified the increased AMPs genes containing the putative ATF3/CREB consensus pattern by ChIP analysis. Second, ATF3 regulated the expression of antimicrobial genes that correspond to bacterial killing, rather than those affecting phagocytosis. Third, ATF3 exerted a cell motility-dependent effect on macrophage recruitment by regulating the expression of the actin GSN.

The original study has reported that ATF3 functions to suppress TLR-mediated cytokine expression through a negative feedback loop. Subsequently, the function of ATF3 was applied to the study of multiple bacterial infection responses. During bacterial sepsis, hosts responded to infection by upregulating or inhibiting cytokines through ATF3 (29, 30). In the case of Gram-negative bacterial infection, ATF3 acted as a negative regulator to inhibit the production of inflammatory cytokines during the invasion of *Escherichia coli* and *Neisseria gonorrhoeae* (31, 32). Therefore, ATF3 KO mice showed longer survival times than WT controls after infection with Gram-negative bacteria due to the induction of ATF3-mediated sepsis-related immunosuppression on the major reactive oxygen species (ROS) condition (29). In contrast, in Gram-positive bacterial infections, ATF3 acted as a positive regulator to enhance the production of proinflammatory cytokines against pathogens such as *Streptococcus pneumoniae*, *Listeria monocytogenes*, and *S. aureus* (13). In the present study, we found that during *S. aureus* infection, ATF3 promoted the antimicrobial response, as well as macrophage infiltration, increasing the production of inflammatory cytokines. Proinflammatory cytokines, such as IL-6, TNF-α, and IL-1β, have been shown to play a guiding role in the production of antimicrobial cytokines or other effector molecules and contribute to resolving infections. For example, TNF-α induced by recruited monocytes is necessary for IL-17 production, macrophage phagocytosis, and bacterial clearance, and therefore, for facilitating recovery from pneumonia (33). To date, *S. aureus* remains one of the leading causes of iatrogenic and community-associated infections, with high mortality and with limited therapeutic options, while the functional significance of ATF3 in Gram-positive infections remains poorly understood. ATF3 KO mice are sometimes more susceptible and sometimes more resistant to bacterial infections, regardless of Gram-negative or positive strain or the action of inflammatory cytokines. It is more dependent on the antimicrobial response *via* AMPs.

It has been reported that IL-17 and IL-22 can induce the expression of AMPs that can kill or inactivate microorganisms by regenerated islet-derived protein 3 (Reg3) and defensins (34). Accordingly, the loss of IL-17 or IL-22 leads to a higher lung bacterial load and severe staphylococcal pneumonia (35). The production of IL-17 and IL-22 is regulated by a key signal event from STAT3 activation (36). In our study, the loss of ATF3 did not alter the STAT3 phosphorylation; subsequently, we also analyzed the downstream target genes of STAT3, such as IL-17 and IL-22, or AMPs; we only found a decrease in Reg3 and S100A8, but no difference in IL-17 and IL-22 between WT and ATF3 KO BMDM after *S. aureus* infection. These data indicated that ATF3 may be downstream of STAT3 and IL-17/IL-22 signaling, and some studies have indicated Toll-like receptor (TLR)-induced ATF3 by c-Src (30), which may pass STAT3 or crosstalk to STAT3 downstream signaling, such as AMPs genes. Whether those kinases can regulate ATF3-mediated cellular antimicrobial and migration needs further characterization. Our current study elucidated a regulatory mechanism mediated by the ATF3/AMPs axis, which plays a key role in modulating macrophage antibacterial responses. However, since ATF3-driven antimicrobial signaling is also triggered by other immune cell subpopulations, such as innate lymphocytes and T cells (37), we think that the early response and macrophage-mediated antibacterial infection may exclude the effect of other immune cells' response. In addition, Alveolar macrophages (AMs) are a lung-specific type of Tissue-resident macrophages (TRM). They play a central role in maintaining alveolar homeostasis by removing cellular debris, excess surfactant, and inhaled bacteria. Still, they are also crucial in preserving lung function during pulmonary infections. Two alveolar epithelial cell types surround AMs. alveolar type 2 cells (AT2s) produce surfactant, act as facultative progenitors in case of alveolar injury, and activate the immune system in response to pathogen-related stimuli. Granulocyte-macrophage colony-stimulating factor (CSF), also known as CSF2, and granulocyte CSF, also known as CSF3, are important survival and proliferation factors for neutrophils and macrophages. AT2-derived GM-CSF continues to be a critical niche factor for the maintenance of AM in the adult alveoli (38). In our case, CSF2 and CSF3 were significantly induced by S. aureus infection at WT lung, which may support long term macrophages survival, but not for short term (few hours) macrophages migration (added **Figure 2 Supplementary Data**). ATF3 mediated macrophages recruitment finding was supported by the mechanical of ATF3 regulates the actin cytoskeleton of F4/80 macrophages within the cell for their migration, rather than cytokines and chemokine mediated the cell recruitment.

Our data indicate that ATF3 plays a role in repressing the ability of GSN to sever actin stress filaments (depolymerization) and trigger macrophage migration consistent with the recent report that lipopolysaccharide (LPS) induced the expression of microRNA miR-21, which downregulated GSN expression and reversed the high-density phenotype, indicating the high motility of macrophages (39). Epigenetic repression of the tumor suppressor GSN is frequently observed in cancers, and chronic inflammation can promote tumor progression *via* aberrant DNA methylation (40). Downregulated GSN leads to increased cell mobility through actin stress filaments, which can promote cancer metastasis (27). We propose here that the low level of GSN in macrophages may be due to the increased expression of ATF3, and that ATF3 is directly bound to GSN regulatory elements. Other reports have indicated that epigenetic silencing

plays a role in the regulation of GSN, and histone deacetylase (HDAC) and DNA methylation inhibitors both increase GSN levels. Others have previously reported that ATF3 interacts with HDAC1 (31), which may be one of the reasons why ATF3 negatively regulates GSN. Our current findings that *S. aureus* induces ATF3 and regulates GSN-mediated F-actin polymerization fill a gap in the molecular regulatory mechanism of macrophage motility function, which is consistent with recent reports that TLR2 or LPS induces macrophages by enhancing actin polymerization and cell migration (41, 42).

In conclusion, this study revealed that the role of ATF3 in innate immunity involves the regulation of macrophage recruitment and function during early *S. aureus* infection. Furthermore, ATF3 contributes to bacterial killing in both lung tissues and BMDM cells, which is related to the regulation of AMPs gene promoter and their expression. ATF3 also triggers filamentous (F-actin) to control cytoskeletal reorganization in macrophages, thereby leading to morphological changes critical to cell motility in the intra infection sites of the lung, which may lead to antimicrobial processes within the cells.

DATA AVAILABILITY STATEMENT

The raw data supporting the conclusions of this article will be made available by the authors, without undue reservation.

ETHICS STATEMENT

The animal study was reviewed and approved by Ruijin Hospital, Shanghai Jiao Tong University School of Medicine.

AUTHOR CONTRIBUTIONS

DX contributed to the design and implementation of the research. YD performed most of the *in vitro* and *in vivo* experiments. ZM performed *in vivo* experiments. JZ, SH, and YS performed *in vitro* experiments. XY performed data acquisition and analysis. YD and DX drafted the article. LS supervised the study and provided critical reagents. All authors contributed to the article and approved the submitted version.

FUNDING

This work was supported by project grants from the National Natural Science Foundation of China (NSFC) (81871274, 82071811, and 31670905).

SUPPLEMENTARY MATERIAL

The Supplementary Material for this article can be found online at: https://www.frontiersin.org/articles/10.3389/fimmu.2022.839502/full#supplementary-material

REFERENCES

1. Sakr A, Bregeon F, Mege JL, Rolain JM, Blin O. Staphylococcus Aureus Nasal Colonization: An Update on Mechanisms, Epidemiology, Risk Factors, and Subsequent Infections. *Front Microbiol* (2018) 9:2419. doi: 10.3389/fmicb.2018.02419
2. Flannagan RS, Heit B, Heinrichs DE. Antimicrobial Mechanisms of Macrophages and the Immune Evasion Strategies of Staphylococcus Aureus. *Pathogens* (2015) 4(4):826–68. doi: 10.3390/pathogens4040826
3. Cole J, Aberdein J, Jubrail J, Dockrell DH. The Role of Macrophages in the Innate Immune Response to Streptococcus Pneumoniae and Staphylococcus Aureus: Mechanisms and Contrasts. *Adv Microbial Physiol* (2014) 65:125–202. doi: 10.1016/bs.ampbs.2014.08.004
4. Rodvold KA, McConeghy KW. Methicillin-Resistant Staphylococcus Aureus Therapy: Past, Present, and Future. *Clin Infect Dis: Off Publ Infect Dis Soc America* (2014) 58 Suppl 1:S20–7. doi: 10.1093/cid/cit614
5. Chan LC, Rossetti M, Miller LS, Filler SG, Johnson CW, Lee HK, et al. Protective Immunity in Recurrent Staphylococcus Aureus Infection Reflects Localized Immune Signatures and Macrophage-Conferred Memory. *Proc Natl Acad Sci USA* (2018) 115(47):E11111–E9. doi: 10.1073/pnas.1808353115
6. Vaishnava S, Yamamoto M, Severson KM, Ruhn KA, Yu X, Koren O, et al. The Antibacterial Lectin RegIIIgamma Promotes the Spatial Segregation of Microbiota and Host in the Intestine. *Science* (2011) 334(6053):255–8. doi: 10.1126/science.1209791
7. Bekeredjian-Ding I, Stein C, Uebele J. The Innate Immune Response Against Staphylococcus Aureus. *Curr Topics Microbiol Immunol* (2017) 409:385–418. doi: 10.1007/82_2015_5004
8. De Luca A, Pariano M, Cellini B, Costantini C, Villella VR, Jose SS, et al. The IL-17f/IL-17rc Axis Promotes Respiratory Allergy in the Proximal Airways. *Cell Rep* (2017) 20(7):1667–80. doi: 10.1016/j.celrep.2017.07.063
9. Choi SM, McAleer JP, Zheng M, Pociask DA, Kaplan MH, Qin S, et al. Innate Stat3-Mediated Induction of the Antimicrobial Protein Reg3gamma Is Required for Host Defense Against MRSA Pneumonia. *J Exp Med* (2013) 210(3):551–61. doi: 10.1084/jem.20120260
10. Robinson KM, Choi SM, McHugh KJ, Mandalapu S, Enelow RI, Kolls JK, et al. Influenza A Exacerbates Staphylococcus Aureus Pneumonia by Attenuating IL-1beta Production in Mice. *J Immunol* (2013) 191(10):5153–9. doi: 10.4049/jimmunol.1301237
11. Hai T, Wolford CC, Chang YS. ATF3, a Hub of the Cellular Adaptive-Response Network, in the Pathogenesis of Diseases: Is Modulation of Inflammation a Unifying Component? *Gene Expression* (2010) 15(1):1–11. doi: 10.3727/105221610x12819686555015
12. Thompson MR, Xu D, Williams BR. ATF3 Transcription Factor and Its Emerging Roles in Immunity and Cancer. *J Mol Med* (2009) 87(11):1053–60. doi: 10.1007/s00109-009-0520-x
13. Nguyen CT, Luong TT, Lee S, Kim GL, Pyo S, Rhee DK. ATF3 Provides Protection From Staphylococcus Aureus and Listeria Monocytogenes Infections. *FEMS Microbiol Lett* (2016) 363(8):fnw062. doi: 10.1093/femsle/fnw062
14. De Nardo D, Labzin LI, Kono H, Seki R, Schmidt SV, Beyer M, et al. High-Density Lipoprotein Mediates Anti-Inflammatory Reprogramming of Macrophages *via* the Transcriptional Regulator ATF3. *Nat Immunol* (2014) 15(2):152–60. doi: 10.1038/ni.2784
15. Sadler AJ, Rossello FJ, Yu L, Deane JA, Yuan X, Wang D, et al. BTB-ZF Transcriptional Regulator PLZF Modifies Chromatin to Restrain Inflammatory Signaling Programs. *Proc Natl Acad Sci USA* (2015) 112(5):1535–40. doi: 10.1073/pnas.1409728112
16. Liu X, Mao Y, Kang Y, He L, Zhu B, Zhang W, et al. MicroRNA-127 Promotes Anti-Microbial Host Defense Through Restricting A20-Mediated De-Ubiquitination of STAT3. *iScience* (2020) 23(1):100763. doi: 10.1016/j.isci.2019.100763
17. Batra S, Cai S, Balamayooran G, Jeyaseelan S. Intrapulmonary Administration of Leukotriene B(4) Augments Neutrophil Accumulation and Responses in the Lung to Klebsiella Infection in CXCL1 Knockout Mice. *J Immunol* (2012) 188(7):3458–68. doi: 10.4049/jimmunol.1101985

18. Fournier B, Philpott DJ. Recognition of Staphylococcus Aureus by the Innate Immune System. *Clin Microbiol Rev* (2005) 18(3):521–40. doi: 10.1128/CMR.18.3.521-540.2005
19. West AP, Brodsky IE, Rahner C, Woo DK, Erdjument-Bromage H, Tempst P, et al. TLR Signalling Augments Macrophage Bactericidal Activity Through Mitochondrial ROS. *Nature* (2011) 472(7344):476–80. doi: 10.1038/nature09973
20. Schmaler M, Jann NJ, Ferracin F, Landmann R. T and B Cells Are Not Required for Clearing Staphylococcus Aureus in Systemic Infection Despite a Strong TLR2-MyD88-Dependent T Cell Activation. *J Immunol* (2011) 186 (1):443–52. doi: 10.4049/jimmunol.1001407
21. Maurya MR, Gupta S, Li X, Fahy E, Dinasarapu AR, Sud M, et al. Analysis of Inflammatory and Lipid Metabolic Networks Across RAW264.7 and Thioglycolate-Elicited Macrophages. *J Lipid Res* (2013) 54(9):2525–42. doi: 10.1194/jlr.M040212
22. Berger CN, Crepin VF, Roumeliotis TI, Wright JC, Serafini N, Pevsner-Fischer M, et al. The Citrobacter Rodentium Type III Secretion System Effector EspO Affects Mucosal Damage Repair and Antimicrobial Responses. *PloS Pathog* (2018) 14(10):e1007406. doi: 10.1371/journal.ppat.1007406
23. Ratsimandresey RA, Indramohan M, Dorfleutner A, Stehlik C. The AIM2 Inflammasome Is a Central Regulator of Intestinal Homeostasis Through the IL-18/IL-22/STAT3 Pathway. *Cell Mol Immunol* (2017) 14(1):127–42. doi: 10.1038/cmi.2016.35
24. Mulcahy ME, Leech JM, Renauld JC, Mills KH, McLoughlin RM. Interleukin-22 Regulates Antimicrobial Peptide Expression and Keratinocyte Differentiation to Control Staphylococcus Aureus Colonization of the Nasal Mucosa. *Mucosal Immunol* (2016) 9(6):1429–41. doi: 10.1038/mi.2016.24
25. Gearing LJ, Cumming HE, Chapman R, Finkel AM, Woodhouse IB, Luu K, et al. CiiiDER: A Tool for Predicting and Analysing Transcription Factor Binding Sites. *PloS One* (2019) 14(9):e0215495. doi: 10.1371/journal.pone.0215495
26. Fletcher DA, Mullins RD. Cell Mechanics and the Cytoskeleton. *Nature* (2010) 463(7280):485–92. doi: 10.1038/nature08908
27. Yuan X, Yu L, Li J, Xie G, Rong T, Zhang L, et al. ATF3 Suppresses Metastasis of Bladder Cancer by Regulating Gelsolin-Mediated Remodeling of the Actin Cytoskeleton. *Cancer Res* (2013) 73(12):3625–37. doi: 10.1158/0008-5472.CAN-12-3879
28. Horn J, Stelzner K, Rudel T, Fraunholz M. Inside Job: Staphylococcus Aureus Host-Pathogen Interactions. *Int J Med Microbiol: IJMM* (2018) 308(6):607–24. doi: 10.1016/j.ijmm.2017.11.009
29. Hoetzenecker W, Echtenacher B, Guenova E, Hoetzenecker K, Woelbing F, Bruck J, et al. ROS-Induced ATF3 Causes Susceptibility to Secondary Infections During Sepsis-Associated Immunosuppression. *Nat Med* (2011) 18(1):128–34. doi: 10.1038/nm.2557
30. Nguyen CT, Kim EH, Luong TT, Pyo S, Rhee DK. ATF3 Confers Resistance to Pneumococcal Infection Through Positive Regulation of Cytokine Production. *J Infect Dis* (2014) 210(11):1745–54. doi: 10.1093/infdis/jiu352
31. Gilchrist M, Thorsson V, Li B, Rust AG, Korb M, Roach JC, et al. Systems Biology Approaches Identify ATF3 as a Negative Regulator of Toll-Like Receptor 4. *Nature* (2006) 441(7090):173–8. doi: 10.1038/nature04768
32. Whitmore MM, Iparraguirre A, Kubelka L, Weninger W, Hai T, Williams BR. Negative Regulation of TLR-Signaling Pathways by Activating Transcription Factor-3. *J Immunol* (2007) 179(6):3622–30. doi: 10.4049/jimmunol.179.6.3622
33. Xiong H, Keith JW, Samilo DW, Carter RA, Leiner IM, Pamer EG. Innate Lymphocyte/Ly6C(hi) Monocyte Crosstalk Promotes Klebsiella Pneumoniae Clearance. *Cell* (2016) 165(3):679–89. doi: 10.1016/j.cell.2016.03.017
34. Loonen LM, Stolte EH, Jaklofsky MT, Meijerink M, Dekker J, van Baarlen P, et al. REG3gamma-Deficient Mice Have Altered Mucus Distribution and Increased Mucosal Inflammatory Responses to the Microbiota and Enteric Pathogens in the Ileum. *Mucosal Immunol* (2014) 7(4):939–47. doi: 10.1038/mi.2013.109
35. Treerat P, Prince O, Cruz-Lagunas A, Munoz-Torrico M, Salazar-Lezama MA, Selman M, et al. Novel Role for IL-22 in Protection During Chronic Mycobacterium Tuberculosis HN878 Infection. *Mucosal Immunol* (2017) 10 (4):1069–81. doi: 10.1038/mi.2017.15
36. Villarino AV, Kanno Y, O'Shea JJ. Mechanisms and Consequences of Jak-STAT Signaling in the Immune System. *Nat Immunol* (2017) 18(4):374–84. doi: 10.1038/ni.3691
37. Lee S, Kim GL, Kim NY, Kim SJ, Ghosh P, Rhee DK. ATF3 Stimulates IL-17A by Regulating Intracellular Ca(2+)/ROS-Dependent IL-1beta Activation During Streptococcus Pneumoniae Infection. *Front Immunol* (2018) 9:1954. doi: 10.3389/fimmu.2018.01954
38. Gschwend J, Sherman SPM, Ridder F, Feng X, Liang HE, Locksley RM, et al. Alveolar Macrophages Rely on GM-CSF From Alveolar Epithelial Type 2 Cells Before and After Birth. *J Exp Med* (2021) 218(10):e20210745. doi: 10.1084/jem.20210745
39. Sharma RK, Goswami B, Das Mandal S, Guha A, Willard B, Ray PS. Quorum Sensing by Gelsolin Regulates Programmed Cell Death 4 Expression and a Density-Dependent Phenotype in Macrophages. *J Immunol* (2021) 207 (5):1250–64. doi: 10.4049/jimmunol.2001392
40. Wang HC, Chen CW, Yang CL, Tsai IM, Hou YC, Chen CJ, et al. Tumor-Associated Macrophages Promote Epigenetic Silencing of Gelsolin Through DNA Methyltransferase 1 in Gastric Cancer Cells. *Cancer Immunol Res* (2017) 5(10):885–97. doi: 10.1158/2326-6066.CIR-16-0295
41. Tu Y, Zhang L, Tong L, Wang Y, Zhang S, Wang R, et al. EFhd2/swiprosin-1 Regulates LPS-Induced Macrophage Recruitment *via* Enhancing Actin Polymerization and Cell Migration. *Int Immunopharmacol* (2018) 55:263–71. doi: 10.1016/j.intimp.2017.12.030
42. Wang G, Zhao H, Zheng B, Li D, Yuan Y, Han Q, et al. TLR2 Promotes Monocyte/Macrophage Recruitment Into the Liver and Microabscess Formation to Limit the Spread of Listeria Monocytogenes. *Front Immunol* (2019) 10:1388. doi: 10.3389/fimmu.2019.01388

Conflict of Interest: The authors declare that the research was conducted in the absence of any commercial or financial relationships that could be construed as a potential conflict of interest.

Publisher's Note: All claims expressed in this article are solely those of the authors and do not necessarily represent those of their affiliated organizations, or those of the publisher, the editors and the reviewers. Any product that may be evaluated in this article, or claim that may be made by its manufacturer, is not guaranteed or endorsed by the publisher.

Copyright © 2022 Du, Ma, Zheng, Huang, Yang, Song, Dong, Shi and Xu. This is an open-access article distributed under the terms of the Creative Commons Attribution License (CC BY). The use, distribution or reproduction in other forums is permitted, provided the original author(s) and the copyright owner(s) are credited and that the original publication in this journal is cited, in accordance with accepted academic practice. No use, distribution or reproduction is permitted which does not comply with these terms.

frontiers | Frontiers in Immunology

ORIGINAL RESEARCH
published: 14 April 2022
doi: 10.3389/fimmu.2022.789366

Acidic Microenvironments Found in Cutaneous *Leishmania* Lesions Curtail NO-Dependent Antiparasitic Macrophage Activity

Linus Frick[1†], Linda Hinterland[1†], Kathrin Renner[2,3], Marion Vogl[1], Nathalie Babl[2,3], Simon Heckscher[4], Anna Weigert[1], Susanne Weiß[1], Joachim Gläsner[1], Raffaela Berger[4], Peter J. Oefner[4], Katja Dettmer[4], Marina Kreutz[2,3‡], Valentin Schatz[1‡] and Jonathan Jantsch[1‡]*

[1] Institute of Clinical Microbiology and Hygiene, University Hospital of Regensburg and University of Regensburg, Regensburg, Germany, [2] Department of Internal Medicine III, University Hospital Regensburg, Regensburg, Germany, [3] Leibniz Institute for Immunotherapy, Regensburg, Germany, [4] Institute of Functional Genomics, University of Regensburg, Regensburg, Germany

Local tissue acidosis affects anti-tumor immunity. In contrast, data on tissue pH levels in infected tissues and their impact on antimicrobial activity is sparse. In this study, we assessed the pH levels in cutaneous *Leishmania* lesions. *Leishmania major*-infected skin tissue displayed pH levels of 6.7 indicating that lesional pH is acidic. Next, we tested the effect of low extracellular pH on the ability of macrophages to produce leishmanicidal NO and to fight the protozoan parasite *Leishmania major*. Extracellular acidification led to a marked decrease in both NO production and leishmanicidal activity of lipopolysaccharide (LPS) and interferon γ (IFN-γ)-coactivated macrophages. This was not directly caused by a disruption of NOS2 expression, a shortage of reducing equivalents (NAPDH) or substrate (L-arginine), but by a direct, pH-mediated inhibition of NOS2 enzyme activity. Normalization of intracellular pH significantly increased NO production and antiparasitic activity of macrophages even in an acidic microenvironment. Overall, these findings indicate that low local tissue pH can curtail NO production and leishmanicidal activity of macrophages.

Keywords: pH, *Leishmania*, macrophages, NO, NOS2

OPEN ACCESS

Edited by:
Alexander Steinkasserer, University Hospital Erlangen, Germany

Reviewed by:
Juliana Perrone Bezerra De Menezes, Gonçalo Moniz Institute (IGM), Brazil
Heitor Affonso Paula Neto, Federal University of Rio de Janeiro, Brazil

***Correspondence:**
Jonathan Jantsch
Jonathan.Jantsch@ukr.de

[†]These authors have contributed equally to this work

[‡]These authors have contributed equally to this work

Specialty section:
This article was submitted to Antigen Presenting Cell Biology, a section of the journal Frontiers in Immunology

Received: *04 October 2021*
Accepted: *14 March 2022*
Published: *14 April 2022*

Citation:
Frick L, Hinterland L, Renner K, Vogl M, Babl N, Heckscher S, Weigert A, Weiß S, Gläsner J, Berger R, Oefner PJ, Dettmer K, Kreutz M, Schatz V and Jantsch J (2022) Acidic Microenvironments Found in Cutaneous Leishmania Lesions Curtail NO-Dependent Antiparasitic Macrophage Activity. Front. Immunol. 13:789366. doi: 10.3389/fimmu.2022.789366

INTRODUCTION

Immune responses in infected tissues are not only driven by inflammatory cytokines and mediators, but also by local ionic composition [reviewed in: (1)], metabolism (2–5), and oxygen availability [reviewed in: (6–8)]. Hypoxia is a hallmark of infected tissue [reviewed in: (6–9)]. It triggers anaerobic glycolysis which ultimately contributes to lactic acid production [reviewed in: (10, 11)]. Moreover, infection and inflammation can trigger excess metabolic breakdown of glucose to pyruvate, which surpasses the cell's capability to fuel it into the mitochondrial respiration [reviewed in: (11, 12)]. Both factors ultimately contribute to accumulation of lactic acid and, thus, induce

tissue acidosis [reviewed in: (10, 13)] and in case of systemic infection (sepsis), lactic acidosis [reviewed in: (11)].

The role of lactic acidosis especially in the diagnosis and treatment of septic patients has been studied intensively (reviewed in: [11, 14)]. The influence of local tissue pH, however, on antimicrobial immunity has received less attention. Therefore, to assess the role of an acidic microenvironment, we used a mouse model of cutaneous leishmaniasis, which is induced by the protozoan parasite *Leishmania* (*L.*) *major* (15–17). Control of *L. major* in this model critically depends on the ability of macrophages to produce high levels of leishmanicidal nitric oxide [NO; reviewed in: (18–20)]. The production of NO during cutaneous *L. major* infection not only ensures direct killing of the protozoan parasite [reviewed in: (21–23)], but NO also curtails the parasite's metabolic activity (24) Moreover, NO impairs the recruitment of monocyte-derived phagocytes to the infectious lesions (25). This mechanism significantly contributes to antimicrobial control as recruited monocyte-derived phagocytes provide an important cellular niche that favor *Leishmania* replication (25–27).

Low extracellular pH levels can reportedly inhibit the activity of the enzyme NOS2 (28–30), which is required for NO production in macrophages. Therefore, we set out to quantify the pH levels in infected cutaneous *Leishmania* lesions and to assess the role of extracellular acidification on the ability of macrophages to fight intracellular *Leishmania*.

MATERIALS AND METHODS

Reagents and Antibodies

Lipopolysaccharide (LPS) from *Escherichia coli* O111:B4, lactic acid (LA), sodium lactate (NaL), L-arginine hydrochloride (Arg-HCl), and L-arginine methyl ester dihydrochloride (Arg-ME) were purchased from Sigma Aldrich (Taufkirchen, Germany), whereas interferon γ (IFN-γ) and 1-[N-(2-aminoethyl)-N-(2-aminoethyl)amino] diazen-1-ium-1,2-iolate (DETA-NO) were obtained from Invitrogen (Darmstadt, Germany) and Cayman Chemical (Ann Harbor, MI), respectively. Hydrochloric acid (HCl) was purchased from Fisher Chemical (Schwerte, Germany). RPMI 1640, DMEM and PBS were purchased from Gibco (Darmstadt, Germany). Immunoblotting was carried out using the following antibodies: rabbit anti-Actin (A2066; Sigma Aldrich), mouse anti-HSP90α/β (sc-7947; Santa Cruz Biotechnology, Heidelberg, Germany), rabbit anti-NOS2 (ADI-KAS-NO001; Enzo Life Sciences, Lörrach, Germany) and mouse anti-Arginase 1 (sc-166920; Santa Cruz). Either swine anti-rabbit HRP (P0399, Dako, Hamburg, Germany) or goat anti-mouse HRP (P0447, Agilent) were used as secondary antibodies.

Cultivation of *L. major*

L. major promastigote strain MHOM/IL/81/FEBNI was propagated in RPMI 1640 (10% fetal calf serum) on Novy-MacNeal-Nicolle blood agar slants for a maximum of five passages and used as described earlier (31, 32). *L. major* promastigotes were collected from blood agar slants. After washing with phosphate-buffered saline (PBS), 3 x 10^6 parasites were used for infection. For *in vitro* infection of bone marrow-derived macrophages (BMDM), *L. major* were propagated in Schneider's insect medium (Sigma Aldrich) for a maximum of five passages, washed with PBS and resuspended in RPMI microscopically 1640 complete medium.

In Vitro Infection of Macrophages

BMDM were generated from wildtype C57BL/6NCrl (Charles River Breeding Laboratories, Sulzfeld, Germany) as described earlier (33). Briefly, BMDM were harvested from Teflon bags (FT FEP 100 C; Dupont; purchased *via* APSOparts, Fellbach, Germany) and infected with *L. major* promastigotes with a multiplicity of infection of 30 for 4 h in RPMI 1640 medium, as described earlier (32). Thereafter, cells were washed with PBS and *Leishmania*-infected BMDM were costimulated with 20 ng/mL LPS/IFN-γ each (unless indicated otherwise) in the presence or absence of 10 mM LA in RPMI 1640 medium for indicated period of time. After 72 h, infected BMDM were stained with Diff-Quik (Eberhard Lehmann, Berlin, Germany) and analyzed for determination of the percentage of infected cells. Per high power field up to 34 cells were counted.

Immunoblotting

Preparation of cell lysates, extraction of proteins, and immunoblotting were carried out as described earlier (32, 34). Proteins were separated on TRIS-glycine gels (7.5% for NOS2 and 12% for Arginase 1) and transferred to PVDF membranes. Staining with appropriate primary and secondary antibodies was followed by signal visualization using the Chemo Star Imager (Intas Science Imaging Instruments, Göttingen, Germany). Densitometry of signals was done using ImageJ (Version 1.52a; Rasband, W., ImageJ, National Institutes of Health, USA, https://imagej.nih.gov/ij/).

Nitrite Production

Accumulation of nitrite in cell supernatants was quantified by the Griess reaction, as described earlier (32). In brief, supernatants of infected and/or stimulated BMDM were mixed with equal amounts of Griess reagent 1 (1% sulfonamide in 5% phosphorous acid) and Griess reagent 2 (0.1% N-1-naphtyletylenediamine in H_2O). Sodium nitrite (Sigma) was used as standard. Absorbance was recorded at 540 nm using an iMark™ microplate absorbance reader (Bio-Rad, Feldkirchen, Germany).

Gene Expression Analysis

As described earlier (32), total RNA was extracted from stimulated cells after 24 h with TriFAST reagent (VWR International, Ismaning, Germany) and subjected to reverse transcription (high-capacity cDNA reverse transcription kit, Applied Biosystems, Darmstadt, Germany). Quantitative real-time PCR was performed on ABI Prism 7900 sequence detector (Applied Biosystems) using FastSTart Universal Probe Master (Rox) (Roche Diagnostics, Mannheim, Germany) and the following TaqMan probes: Hypoxanthine phosphoribosyltransferase 1 (*Hprt1*; Mm03024075_m1), *Nos2* (Mm00440502_m1), and *Arg1* (Mm00475988_m1). These probes were purchased from Applied Biosystems. The ΔΔcCT method was used for quantification. The ratio of target mRNA to control *Hprt1* in non-stimulated (ns) specimen was set to 1.

NADPH/NADP$^+$ Quantification

NADPH/NADP$^+$-ratio was determined according to manufacturer's instruction using the NADP/NADPH-Glo^{TM} Assay (Promega GmbH, Walldorf, Germany) which allows for quantification of NADP/NADPH using a single-reagent. Briefly, BMDM were costimulated with LPS/IFNγ in absence or presence of lactic acid for 24 h and then mixed with NADP/NADPH-Glo^{TM} reagent which quantifies NADP/NADPH in a single-step. Cells were incubated for 30 min at room temperature and luminescence was recorded on a Viktor3^{TM} multilabel plate reader (PerkinElmer, Rodgau, Germany).

Arginine Quantification

BMDM were washed three times with PBS to remove remaining traces of cell culture medium. Then, 80% of cold aqueous methanol was added and samples were immediately frozen at −80°C. As described earlier for amino acid analysis (35), samples were thawed and 10 µL of an internal standard mix containing uniformly ^{13}C- and ^{15}N-labeled amino acids (MSK-CAA-1, Euriso-Top GmbH, Saarbrücken, Germany) and deuterated ornithine and deuterated hippuric acid were added. The samples were vortexed, and centrifuged at 9,560 x g for 5 min at 4°C. The supernatants were collected, followed by addition of 200 µL 80% methanol, vortexing and centrifugation to wash the pellets. The wash steps were repeated, but the samples were centrifuged at a higher speed (13,800 g). All supernatants were combined and dried in a vacuum evaporator (CombiDancer, Hettich AG, Bach, Switzerland) followed by reconstitution in 100 µL pure water. Amino acid analysis by HPLC-ESI-MS/MS (HPLC 1200 (Agilent, Waldbronn, Germany) with API 4000 QTRAP (AB SCIEX, Darmstadt, Germany) or ExionLC AD with Triple Quad 6500+, AB SCIEX) after derivatization with propyl chloroformate/propanol was performed using a 10 µL aliquot of the sample extract as described (36).

Intracellular amino acid amounts were normalized to total protein content, which was determined using an assay based on the fluorescent dye SERVA Purple (Serva, Heidelberg, Germany) as recently described (37). The relative arginine content was calculated in relation to the mean value of the LPS/IFN-γ costimulated cells of the respective experiment.

Recombinant NOS2 Enzyme Activity

For determination of recombinant NOS2 enzyme activity, 2 units of recombinant enzyme (Biomol, Hamburg, Germany) were incubated in appropriate buffer following the manufacturer's protocol. In short, 50 mM HEPES (Carl Roth, Karlsruhe, Germany) and 1 mM magnesium acetate (Sigma Aldrich) were adjusted to pH 7.4 or 6.0 by addition of hydrochloric acid (Carl Roth). Prior to buffer use, 0.15 mM NADPH (Sigma Aldrich), 4.5 µM oxyhemoglobin (Sigma Aldrich), 18 µM tetrahydrobiopterin (Sigma Aldrich), and 180 µM dithiothreitol (Sigma Aldrich) were freshly added. 1 mM Arg-HCl (Sigma Aldrich) was also freshly added where indicated. After incubation at 37°C, nitrite accumulation was quantified at distinct time points between 1 h and 8.5 h using the Griess assay (32).

Measurement of Extracellular pH Levels *In Vitro*

pH levels in culture medium were measured non-invasively by using the PreSens technology (PreSens Precision Sensing GmbH, Regensburg, Germany), as described earlier (38). 0.5x10^6 BMDM were seeded in 24-well Hydrodish HD24 plates in 1 mL RPMI 1640 medium under cell culture conditions for the indicated period of time. pH levels were continuously monitored using the SDR SensorDish® Reader. Data were analyzed with SDR_v38 software package (Presens Precision Sensing GmbH, Regensburg, Germany).

Quantification of Intracellular pH in BMDM

Essentially, quantification of intracellular pH in BMDM followed an earlier published protocol (39). BMDM were incubated with indicated treatments for 24 h in RPMI 1640 medium. Afterwards, cells were loaded with 10 µM carboxy SNARF-1 AM acetate (Thermo Fisher Scientific, #C1272) in 1 mL Hank's balanced salt solution (HBSS, containing 2 g/L NaHCO3) for 30 min and subsequently incubated with or without 10 mM lactic acid for 10 min in the presence or absence of increasing concentrations of Arg-HCl. For calibration curves, an intracellular pH calibration buffer kit (Thermo Fisher Scientific, #P35379) was used. In brief, BMDM were incubated with a mix of pH-controlled buffers and valinomycin/nigericin according to the manufacturer's instructions. Intracellular pH was assessed by flow cytometry. In detail, pH-dependent spectral shifts of SNARF-1 were recorded and the ratios of the emission wavelength at λ1, transmitted by a 585/42 BP filter, to the wavelength at λ2, transmitted by a 670 LP filter were calculated, as described earlier (39). Treatment induced changes were delineated from the calibration curve, performed for each experiment. FlowJo software version 10.7.1 was used for data analysis.

Measurement of Lesional pH

All animal experiments followed a protocol that had been approved by the Animal Welfare Committee of the local governmental authority (Regierung von Unterfranken, Würzburg, Germany). Mice were infected subcutaneously with 3 x 10^6 stationary-phase *L. major* promastigotes (of low *in vitro* passage [≤ 5] in the right hind footpad in 50 µL PBS), as described earlier (32). 14 days post infection, mice were sacrificed and, immediately thereafter, footpad pH was determined by a micro fiber optic pH meter with needle-type housed pH microsensors (20/0.4) using a manual micromanipulator (PreSens Precision Sensing GmbH) essentially as described earlier (38). After overnight calibration according to the manufacturer's protocol, the microsensor was inserted 3 - 4 mm into the footpad and pH values were recorded over a period of 1 - 3 min after insertion of the pH sensor with the software pH1-View (PreSens Precision Sensing GmbH).

Statistical Analysis

Data is expressed as mean ± SEM (unless indicated otherwise). Statistical analysis was carried out using Prism v6.0 or v8.0 software (GraphPad). Outliers were identified using the ROUT test (**Figures 4A, D**). Comparing two groups, unpaired Student's t-*test* ± Welch correction (if unequal variances were detected by the F-Test) was applied for datasets where the Kolmogorov-Smirnow test indicated normal distribution. Otherwise, the Mann-Whitney test was used. Multiple groups were tested either with Kruskal-Wallis test in combination with Dunn multiple-comparison test for not normally distributed data

points or ANOVA followed by Bonferroni's multiple-comparison test for normally distributed data. Unless indicated otherwise, p-values <0.05 were considered as significant.

RESULTS

Leishmanial Skin Lesions Are Acidic

In our experimental setup, C57BL/6 mice usually develop a clear clinical lesion at day 14 after infection. At this point, the cutaneous lesion has reached its maximum or it barely enlarges thereafter, before it heals over several weeks (32, 40). Lesional pH was determined 14 days after infection with *L. major* in cutaneous lesions and contralateral uninfected healthy skin tissue. The pH of uninfected tissue was 7.1, while the pH of *Leishmania*-infected lesions dropped to 6.7, indicating that lesional pH is acidic (**Figure 1A**).

In vitro, addition of 10 mM lactic acid to LPS/IFN-γ-costimulated macrophages resulted in an immediate steep decrease in extracellular pH. Compared with LPS/IFN-γ-costimulated macrophages, pH remained lower in cells additionally treated with lactic acid throughout the 72 hour observation period. At 24 hours after the addition of lactic acid, this simulated quite well the situation *in vivo*. (**Figure 1B**).

Extracellular Acidification Impairs NO Production and Leishmanicidal Macrophage Activity

Macrophages play a critical role in fighting *Leishmania* [reviewed in: (20, 41)]. Therefore, we tested whether acidification of the extracellular microenvironment would influence the ability of LPS/IFN-γ-cotreated macrophages to produce leishmanicidal NO and to ward off *Leishmania*. Addition of 10 mM lactic acid to LPS/IFN-γ-costimulated macrophages curtailed their ability to produce NO (**Figure 2A**). Its sodium salt [sodium lactate (NaL)], in contrast, did not impact the release of NO from macrophages (**Figure 2B**). Extracellular acidification with hydrochloric acid (HCl) also impaired NO production of LPS/IFN-γ-coactivated macrophages (**Figure 2C**). Decreased NO release under acidic conditions was accompanied by a reduced ability of the macrophages to clear *Leishmania* (**Figures 2D, E**). Addition of NO donor 1-[N-(2-aminoethyl)-N-(2-aminoethyl) amino] diazen-1-ium-1,2-iolate (DETA-NO) restored not only NO levels (**Figure 2F**) but also leishmanicidal activity (**Figure 2G**) of activated macrophages exposed to 10 mM lactic acid.

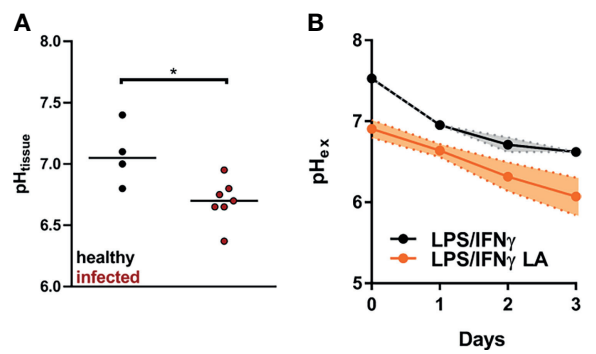

FIGURE 1 | pH levels found in *L. major* infected lesions can be simulated by addition of 10 mM lactic acid to LPS/IFN-γ-coactivated macrophages. **(A)** C57BL/6 mice were infected with *L. major* in their hind footpads. At day 14 post infection tissue pH (pH_{tissue}) was determined in healthy and infected tissue (median, n = 4-7 animals from two independent experiments). *$p < 0.05$, Mann-Whitney test. **(B)** BMDM were stimulated with LPS (10 ng/mL)/IFN-γ (20 ng/mL) for 24 h. Where indicated, cells were exposed to 10 mM lactic acid (LA). Determination of extracellular pH (pH_{ex}; mean + SEM, n = 3-5 from three independent experiments).

Induction of *Nos2* mRNA and Protein Expression Is Maintained Upon Exposure to Lactic Acid

Next, we wanted to elucidate the mechanism that underlies the reduced ability of macrophages to produce NO. Production of high-level NO in macrophages hinges on the ability of macrophages to induce the expression of the type 2 NO synthase (NOS2) [reviewed in: (19, 20)]. In contrast to only LPS-stimulated macrophages (28, 30), addition of lactic acid to LPS/IFN-γ-costimulated macrophages did not interfere with *Nos2* expression at both the mRNA (**Figure 3A**) and protein (**Figure 3B**) level. From these findings we concluded that reduced NO production was not caused by impaired *Nos2* expression.

NADPH- and L-Arginine Availability Do Not Explain Reduced NO Production of Acid-Exposed Macrophages

Alternatively, addition of lactic acid might affect the availability of L-arginine and NADPH, both of which are required for NO production by NOS2 [reviewed in: (42)]. Extracellular acidification increased the NADPH/$NADP^+$-ratio compared to controls suggesting that reduced NO production is not due to lack of NADPH (**Figure 4A**). Acidic conditions can induce the expression of arginases (43) and, thereby, limit the availability of L-arginine. Here, addition of lactic acid to LPS/IFN-γ-costimulated macrophages led to a minor, non-significant increase in Arginase 1 (Arg1) expression at both the mRNA (**Figure 4B**) and protein levels (**Figure 4C**), which nonetheless resulted in a significantly reduced intracellular pool of L-arginine (**Figure 4D**). Next, we tested the impact of L-arginine shortage on NO release from activated macrophages exposed to acidic conditions. For that purpose, we used cell permeable L-arginine methyl ester dihydrochloride (Arg-ME) to replenish the intracellular L-arginine pool (**Figure 4D**). In contrast to Nω-nitro-L-arginine methyl ester hydrochloride [reviewed in: (44)], Arg-ME did not inhibit NO production (**Figure 4E**). Of note, addition of Arg-ME to infected macrophages did not restore NO production by LPS/IFN-γ-costimulated macrophages exposed to acidic conditions (**Figure 4E**). This suggests that the reduced L-arginine availability is not limiting NO production under acidic conditions.

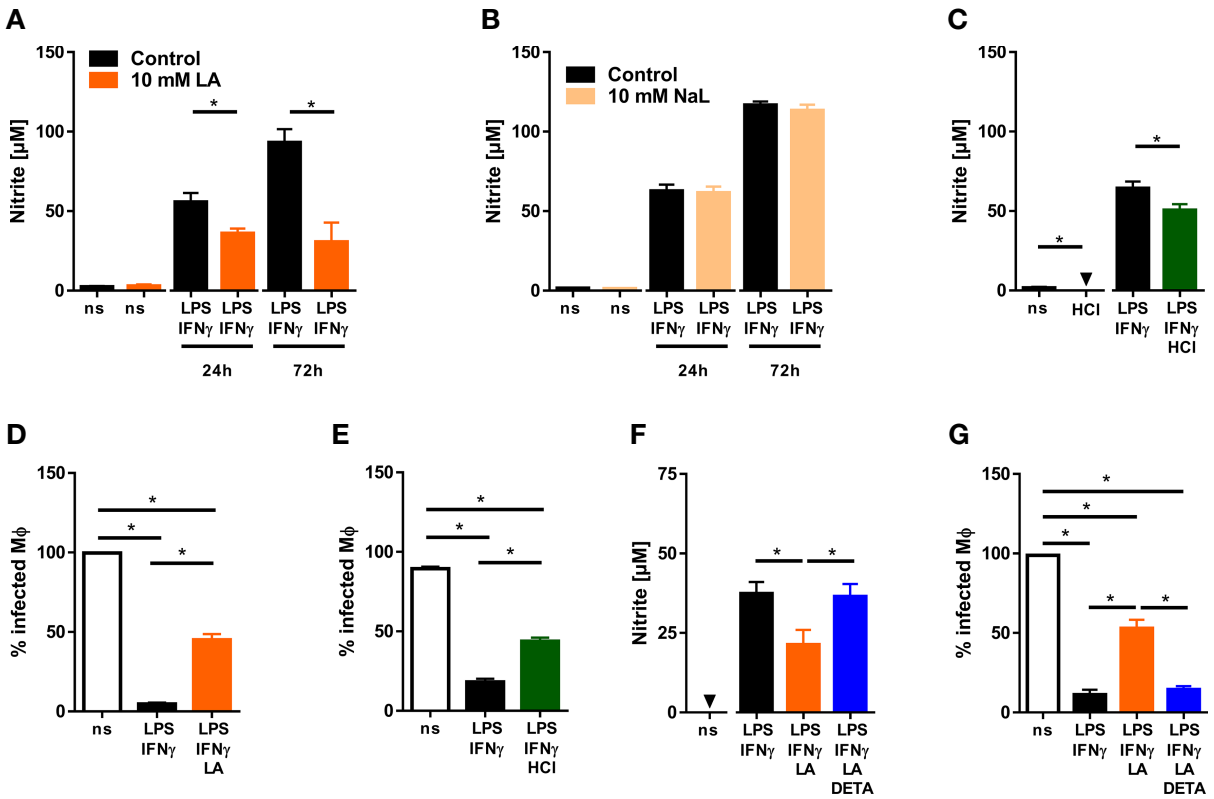

FIGURE 2 | Low pH reduces NO production and impairs anti-leishmanial defenses of LPS/IFN-γ-coactivated macrophages. **(A, B)** BMDM were stimulated with LPS (10 ng/mL)/IFN-γ (20 ng/mL) or left unstimulated (ns) for 24 - 72 h. Where indicated, 10 mM lactic acid (LA) or 10 mM sodium lactate (NaL) were added. **(A)** Nitrite levels were determined at indicated time points (means + SEM, n = 10-29 samples from at least four independent experiments; *$p < 0.01$, Student's t-test + Welch correction or Mann-Whitney test). **(B)** Nitrite levels were determined at indicated time points (mean + SEM, n = 16-40 samples from ten independent experiments; *$p < 0.01$, Mann-Whitney test). **(C)** As in **(A)**, but cells were stimulated with 10 mM HCl for 24 h (means + SEM; n = 12-16 from at least two independent experiments; *$p < 0.05$, Student's t-test or Mann-Whitney test). **(D–G)** BMDM were infected with *L. major* and costimulated with LPS (20ng/mL)/IFN-γ (20 ng/mL) or left unstimulated (ns) for 72 h. Where indicated cells were additionally exposed to 10 mM HCl or 10 mM LA and/or 25 µM DETA-NO (DETA). **(D)** Infection rate (mean + SEM, n = 29-30 high power fields from three independent experiments; *$p < 0.05$, Kruskal-Wallis test and Dunn *post hoc* test). **(E)** Infection rate (mean + SEM, n = 16 high power fields from two independent experiments; *$p < 0.05$, ANOVA with Bonferroni's test). **(F)** Nitrite content of supernatants (mean + SEM, n = 14 from three independent experiments; *$p < 0.05$, Kruskal-Wallis test and Dunn *post hoc* test. **(G)** Infection rate (mean + SEM, n = 18 high power fields from three independent experiments; *$p < 0.05$, Kruskal-Wallis test and Dunn *post hoc* test).

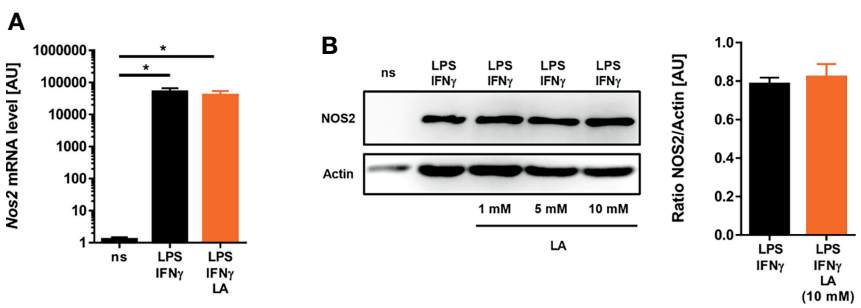

FIGURE 3 | Induction of *Nos2* on mRNA and protein level is preserved upon exposure to lactic acid in LPS/IFN-γ-coactivated macrophages. **(A, B)** BMDM were costimulated with LPS (10 ng/mL)/IFN-γ (20 ng/mL) or left unstimulated (ns) for 24 h. Cells were treated with 10 mM lactic acid (LA), unless indicated otherwise. **(A)** *Nos2* mRNA levels (mean + SEM, n = 14-15 samples from five independent experiments; *$p < 0.05$, Kruskal-Wallis test and Dunn *post hoc* test). **(B)** Left panel: NOS2 and Actin protein levels (representative out of six similar independent experiments). Right panel: Densitometry of NOS2 normalized to Actin protein levels after treatment with 10 mM LA (mean + SEM, n = 6 from six independent experiments; Student's *t*-test).

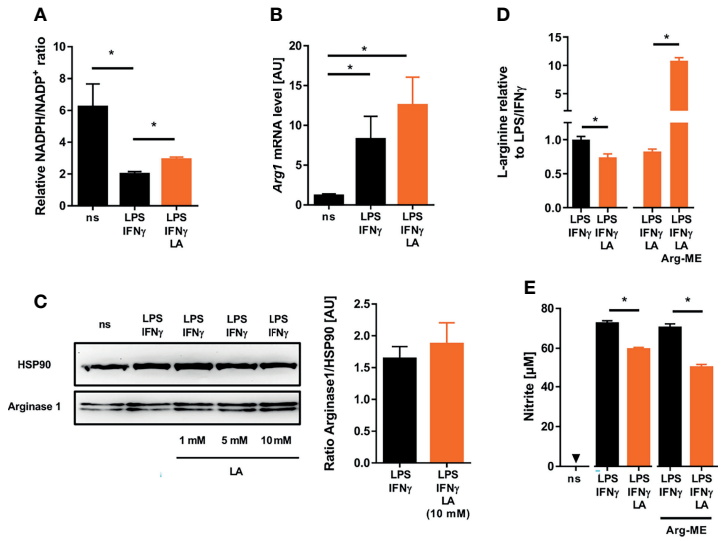

FIGURE 4 | Lactic acid-induced changes in cosubstrate availability do not underlie impaired NO production in LPS/IFN-γ coactivated macrophages. **(A–E)** BMDM were costimulated with LPS (10 ng/mL)/IFN-γ (20 ng/mL) or left untreated (ns) for 24 h. Cells were treated with 10 mM lactic acid (LA), unless indicated otherwise. **(A)** Relative NADPH/$NADP^+$-ratio (mean + SEM, n = 11-12 from three independent experiments; *$p < 0.05$, Kruskal-Wallis test and Dunn *post hoc* test). **(B)** *Arg1* mRNA levels (mean + SEM, n = 14-15 from five independent experiments; *$p < 0.05$, Kruskal-Wallis test and the Dunn *post hoc* test). **(C)** Left panel: Arginase 1 and HSP90 protein levels (representative of six similar independent experiments). Right panel: Densitometry of Arginase 1 normalized to HSP90 protein levels after treatment with 10 mM LA (mean + SEM, n = 6 from six independent experiments; Mann-Whitney test). **(D)** Relative L-arginine levels (mean + SEM, n = 9-28 from at least two independent experiments; *$p < 0.05$, Student's *t*-test or Mann-Whitney test). **(E)** LPS/IFN-γ stimulated BMDM ± LA were treated with 10 mM L-arginine methyl ester dihydrochloride (Arg-ME) for 24 h. Nitrite accumulation in supernatants (mean + SEM, n = 16 from two independent experiments; *$p < 0.05$, Mann-Whitney test).

Low pH Levels Directly Inhibit Enzymatic NOS2 Activity

Extracellular acidification can trigger intracellular acidification (45). Therefore, we used the pH-sensitive dye SNARF-1 to monitor intracellular pH levels (46). In line with earlier findings in mouse dendritic cells (47), we found that coactivation of macrophages with LPS/IFN-γ resulted in a drop in intracellular pH (**Figure 5A**). More importantly, exposure of LPS/IFN-γ costimulated macrophages to acidic conditions resulted in a further significant decrease in intracellular pH (**Figures 5A, B**). Acidic pH is known to affect the activity of various enzymes [reviewed in: (48)] including NOS2 (29). Therefore, we tested whether the pH (pH 5.81 ± 0.19) encountered within LPS/IFN-γ-costimulated macrophages upon exposure to lactic acid (**Figure 5A**) was able to inhibit the enzymatic activity of recombinant NOS2 directly. These experiments showed that enzymatic NOS2 activity at pH 6.0 was substantially diminished compared to its activity at pH 7.4 (**Figure 5C**).

Increasing Intracellular pH Restores Leishmanicidal Activity of Macrophages in an Acidic Microenvironment

Infusion of arginine hydrochloride (Arg-HCl) lowers extracellular pH in rats, but increases intracellular pH levels (49). In line with this, we found that Arg-HCl treatment significantly elevated the intracellular pH levels in LA-exposed macrophages *in vitro* (**Figure 5D**). This was accompanied by a significant increase in NO production (**Figure 5E**) and leishmanicidal activity (**Figure 5F**) of LPS/IFN-γ-cotreated macrophages exposed to lactic acid. Taken together, these findings demonstrate that normalization of intracellular pH is able to restore NO production and leishmanicidal macrophage activity in acidic microenvironments.

DISCUSSION

In this report, we provide evidence that extracellular acidification resulted in direct inhibition of NOS2 enzyme activity and subsequent reduced production of leishmanicidal NO in macrophages, which ultimately impeded their antimicrobial activity. In addition to cancerous tissues [reviewed in: (50, 51)], increased proton concentrations and tissue acidosis are found in inflamed, infected, and ischemic tissues [reviewed in: (10, 13, 52)]. We reported earlier that *Leishmania* skin lesions displayed low oxygen levels when the skin lesions reached their maximum size around 14 days post infection (40). Our findings of low lesional tissue pH at day 14 after infection conforms with this, because low tissue oxygenation is paralleled by increased proton levels in afflicted tissues [reviewed in: (10, 11)]. Healing of *Leishmania* lesions was accompanied by normalization of tissue oxygenation (40). It is tempting to speculate that resolution of disease is associated with restoration of lesional pH to normal as well.

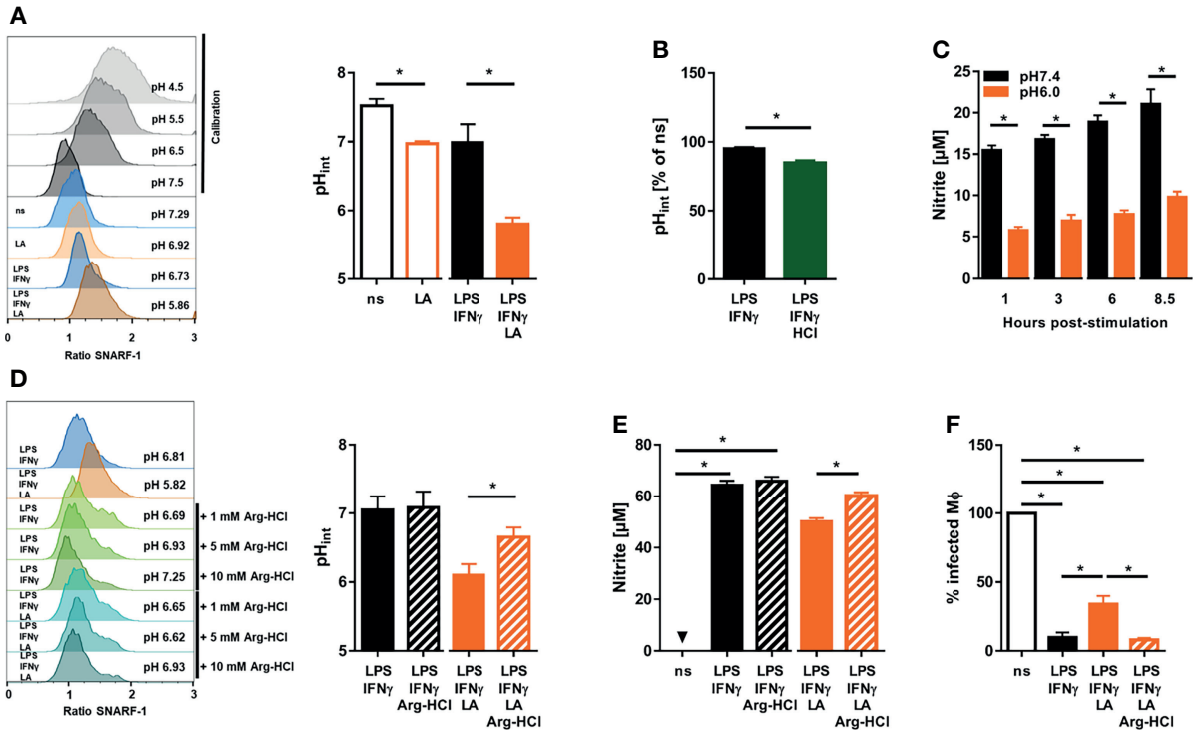

FIGURE 5 | Exposure to lactic acid triggers low intracellular pH levels which directly impair NOS2 enzyme activity in LPS/IFN-γ coactivated macrophages **(A)** BMDM were costimulated with LPS (10 ng/mL)/IFN-γ (20 ng/mL) or left unstimulated (ns) for 24 h. Where indicated, cells were treated with 10 mM lactic acid (LA). Determination of intracellular pH. Left panel: representative histograms out of four similar independent experiments upon exposure to calibration buffers (in grey), unstimulated (ns), 10 mM lactic acid (LA), and LPS/IFN-γ ± LA treated BMDM. Right panel: intracellular pH (mean + SEM, n = 4 samples from four independent experiments; *$p < 0.05$, Mann-Whitney test. **(B)** BMDM were costimulated with LPS (10 ng/mL)/IFN-γ (20 ng/mL) for 24 h. Where indicated, cells were treated with additional 10 mM hydrochloric acid (HCl). Determination of intracellular pH in percent of unstimulated (ns) cells (mean + SEM, n = 4 samples from four experiments; *$p < 0.05$, Mann-Whitney test). **(C)** *In vitro* activity of recombinant NOS2 at different pH values over time. Nitrite accumulation (mean + SEM, n = 9 from four independent experiments; *$p < 0.05$, Student's *t*-test or Mann-Whitney test). **(D)** As in **(A)**, but 1, 5 or 10 mM L-arginine monohydrochloride (Arg-HCl) were added where indicated. Left panel: histogram of LPS/IFN-γ ± LA stimulated BMDM cotreated with Arg-HCl (representative out of five similar independent experiments). Right panel: intracellular pH of LPS/IFN-γ ± LA stimulated BMDM exposed to 10 mM Arg-HCl (mean + SEM, n = 5 samples from five independent experiments; *$p < 0.05$, Student's *t*-test). **(E)** As in **(A)**, but 10 mM Arg-HCl was added, where indicated. Nitrite accumulation (mean + SEM, n = 29-38 from seven independent experiments; *$p < 0.05$, Kruskal-Wallis test and Dunn *post hoc* test or Mann-Whitney test). **(F)** BMDM were infected with *L. major* and costimulated with LPS (20 ng/mL)/IFN-γ (20 ng/mL) ± 10 mM Arg-HCl for 72 h. Infection rate (mean + SEM, n = 26 high power fields from five independent experiments; *$p < 0.05$, Kruskal-Wallis test and Dunn *post hoc* test).

The mechanisms that trigger low tissue pH warrant further investigation. For instance, following and extending earlier reasoning [reviewed in: (10)], it is possible that infection-associated cell death [reviewed in: (53)], infection-induced increases in glycolysis and metabolic reprogramming [reviewed in: (12)] and/or infection-triggered induction of low tissue oxygen [reviewed in: (6)] contribute to low tissue pH.

Increases in extracellular proton concentrations are able to impact the function of immune cells [reviewed in: (54, 55)]. For instance, acidic microenvironments are able to activate immature dendritic cells (56) and to promote the phagocytic capacity of neutrophils (57). Moreover, acidosis can trigger inflammasome activation in human macrophages (58). Acidic conditions can increase the production of interleukin-1β by murine macrophages in response to *Pseudomonas aeruginosa* infection (59). Based on these findings, extracellular acidosis has been proposed as a "danger signal" (58).

In tumor environments, low pH potentiates the immunosuppressive function of macrophages and thereby promotes tumor growth (43, 60). Although many antimicrobial peptides require low pH for their optimal activity [reviewed in: (61)], to the best of our knowledge, data on the impact of low pH on antimicrobial macrophage activity is limited. Extracellular acidosis reportedly enhances Zika virus replication in various cells including human monocytes (62). Enhanced viral replication in this study was linked to increased viral attachment to heparan sulphate, which is expressed on the surface of host cells (62). In a porcine model of cystic fibrosis, airway surface liquid was more acidic compared to healthy lungs (63). This pH reduction in the airway surface liquid inhibited the antimicrobial activity (63). Interestingly, the airway mucosal microenvironment undergoes large excursions in pH during breathing (64). Transient alkalinization seems to be important for host defense (64).

Here, we demonstrate that increases in extracellular protons curtail LPS/IFN-γ-triggered NO production, which is critical for anti-leishmanial control in macrophages (21–23). Our findings are in line with others who have found decreased NO production in macrophages (28) and mesangial cells (29) cultivated under acidic conditions. However, the opposite observation of increased NO production by macrophages upon exposure to increased extracellular proton availability has also been reported (30, 65). A comprehensive model that reconciles these disparate findings into a unified concept does not exist yet. Differences in the experimental setup might explain the divergent findings. For instance, using HCl to adjust pH, exposure of the LPS-stimulated mouse macrophage-like cell line RAW 264.7 to mild acidic conditions increased NO release, while harsh acidic conditions resulted in suppressed NO production (30). Of note, in the same study lactic acid inhibited NO production in a dose dependent manner (30). In this situation, reduced NO production upon exposure to acidic conditions was correlated with impaired binding of the nuclear factor (NF)-κB to DNA and reduced *Nos2* expression (30). In line with this, acidic conditions are able to impair *Nos2* gene expression in renal kidney cells directly (66). When we compared cells costimulated with LPS and IFN-γ and tested the impact of increased proton concentrations on the expression of *Nos2*, we did not detect a significant difference. This suggests that in our experimental setup transcriptional regulation of *Nos2* was not linked to a decrease in NO production. It is possible that costimulation with LPS and IFN-γ overrode the effect of low pH on NF-κB-dependent transcriptional responses in cells which were only stimulated with LPS.

Further, our experimental data does not suggest that the sole lack of L-arginine and/or $NADPH/H^+$ caused the observed decrease in NO production by LPS/IFN-γ-costimulated macrophages exposed to lactic acid. Rather, intracellular acidification impairs enzymatic activity of NOS2 directly. This notion is supported by at least partial rescue of both, NO production and leishmanicidal activity in macrophages upon treatment with arginine hydrochloride, which was paralleled by a partial normalization of intracellular pH. This very much recapitulates earlier findings in mesangial cells, where low pH levels directly interfered with NOS2 enzyme activity (29). Intracellular acidification has also been shown to impair superoxide and hydrogen peroxide production of neutrophils, which could further diminish antimicrobial control and support microbial proliferation (67).

Since administration of bicarbonate promoted cancer immunotherapy (68, 69), buffering might represent a strategy to reduce the suppressive effects of acidification on immune cell activation and, ultimately, on their antimicrobial potential. In the case of *Leishmania* infection, it is tempting to speculate that buffering might increase local NO production in leishmanial lesions. This could enhance direct leishmanicidal activity (22) and, in addition, might inhibit the excess influx of mononuclear cells, which in turn serve as cellular niches for *Leishmania* replication (25). Whether bicarbonate and/or Arg-HCl treatment are useful for this purpose will require additional experimentation, which, for instance, may include monitoring of lesional pH, tissue NO levels and parasite burden.

In addition, the mechanisms that facilitate entry of protons into macrophages that ultimately result in intracellular acidosis are unclear and warrant further investigation. For instance, the transient receptor potential cation channel subfamily V member (TRPV) 1 is able to sense increased availability of protons and to increase proton concentrations in neurons (70). TRPV1 is also expressed on macrophages (71). Moreover, other transporters, channels, and exchangers such as Na^+/H^+ exchangers or monocarboxylate transporters (39, 47, 72–75) may play a role as well. Finally, the cellular mechanism that results in at least partial normalization of intracellular pH by addition of Arg-HCl is unclear and warrants further investigation.

In summary, our findings demonstrate that leishmanial lesions displayed low pH and that acidic conditions impaired the leishmanicidal activity of macrophages *via* inhibition of NOS2 enzyme activity. Of note, normalization of the intracellular pH largely restored NO production and leishmanicidal activity even in an acidic microenvironment.

DATA AVAILABILITY STATEMENT

The raw data supporting the conclusions of this article will be made available by the authors, without undue reservation.

ETHICS STATEMENT

The animal study was reviewed and approved by Animal Welfare Committee of the local governmental authority (Regierung von Unterfranken Würzburg, Germany).

AUTHOR CONTRIBUTIONS

LF, LH, KR, MV, NB, AW, SW, SH, and VS acquired, analyzed and interpreted data. JG, PO, RB, KD, and KR interpreted data and contributed to the design of experiments. LF, LH, VS, MK, and JJ interpreted data and designed and conceptualized experiments. JJ and MK oversaw the study. JJ, VS, and MK provided the first draft of the manuscript. All authors read and approved the final version of the manuscript.

ACKNOWLEDGMENTS

KD and JJ were supported by DFG (Deutsche Forschungsgemeinschaft, German Research Foundation) Research Training Group 2740 Immunomicrotope and by the Bavarian Ministry of Science and the Arts in the framework of the Bavarian Research Network 'New Strategies Against Multi-Resistant Pathogens by Means of Digital Networking–bayresq.net'. We are very grateful to Monika Nowottny, Elke Perthen and Christine Lindner for excellent technical assistance.

REFERENCES

1. Jobin K, Muller DN, Jantsch J, Kurts C. Sodium and Its Manifold Impact on Our Immune System. *Trends Immunol* (2021) 42:469–79. doi: 10.1016/j.it.2021.04.002
2. Balmer ML, Ma EH, Thompson AJ, Epple R, Unterstab G, Lotscher J, et al. Memory CD8(+) T Cells Balance Pro- and Anti-Inflammatory Activity by Reprogramming Cellular Acetate Handling at Sites of Infection. *Cell Metab* (2020) 32:457–67.e5. doi: 10.1016/j.cmet.2020.07.004
3. Fernandez-Veledo S, Ceperuelo-Mallafre V, Vendrell J. Rethinking Succinate: An Unexpected Hormone-Like Metabolite in Energy Homeostasis. *Trends Endocrinol Metab* (2021) 32:680–92. doi: 10.1016/j.tem.2021.06.003
4. Medina CB, Mehrotra P, Arandjelovic S, Perry JSA, Guo Y, Morioka S, et al. Metabolites Released From Apoptotic Cells Act as Tissue Messengers. *Nature* (2020) 580:130–5. doi: 10.1038/s41586-020-2121-3
5. Dudek M, Pfister D, Donakonda S, Filpe P, Schneider A, Laschinger M, et al. Auto-Aggressive CXCR6(+) CD8 T Cells Cause Liver Immune Pathology in NASH. *Nature* (2021) 592:444–9. doi: 10.1038/s41586-021-03233-8
6. Hayek I, Schatz V, Bogdan C, Jantsch J, Luhrmann A. Mechanisms Controlling Bacterial Infection in Myeloid Cells Under Hypoxic Conditions. *Cell Mol Life Sci* (2021) 78:1887–907. doi: 10.1007/s00018-020-03684-8
7. Jantsch J, Schodel J. Hypoxia and Hypoxia-Inducible Factors in Myeloid Cell-Driven Host Defense and Tissue Homeostasis. *Immunobiology* (2015) 220:305–14. doi: 10.1016/j.imbio.2014.09.009
8. Schatz V, Neubert P, Rieger F, Jantsch J. Hypoxia, Hypoxia-Inducible Factor-1alpha, and Innate Antileishmanial Immune Responses. *Front Immunol* (2018) 9:216. doi: 10.3389/fimmu.2018.00216
9. Colgan SP, Campbell EL, Kominsky DJ. Hypoxia and Mucosal Inflammation. *Annu Rev Pathol* (2016) 11:77–100. doi: 10.1146/annurev-pathol-012615-044231
10. von Ardenne M, Kruger W. Local Tissue Hyperacidification and Lysosomes. *Front Biol* (1979) 48:161–94.
11. Suetrong B, Walley KR. Lactic Acidosis in Sepsis: It's Not All Anaerobic: Implications for Diagnosis and Management. *Chest* (2016) 149:252–61. doi: 10.1378/chest.15-1703
12. O'Neill LA, Hardie DG. Metabolism of Inflammation Limited by AMPK and Pseudo-Starvation. *Nature* (2013) 493:346–55. doi: 10.1038/nature11862
13. Reeh PW, Steen KH. Chapter 8. Tissue Acidosis in Nociception and Pain. *Prog Brain Res* (1996) 113:143–51. doi: 10.1016/S0079-6123(08)61085-7
14. Maciel AT, Noritomi DT, Park M. Metabolic Acidosis in Sepsis. *Endocr Metab Immune Disord Drug Targets* (2010) 10:252–7. doi: 10.2174/187153010791936900
15. Sacks D, Noben-Trauth N. The Immunology of Susceptibility and Resistance to Leishmania Major in Mice. *Nat Rev Immunol* (2002) 2:845–58. doi: 10.1038/nri933
16. Mougneau E, Bihl F, Glaichenhaus N. Cell Biology and Immunology of Leishmania. *Immunol Rev* (2011) 240:286–96. doi: 10.1111/j.1600-065X.2010.00983.x
17. Burza S, Croft SL, Boelaert M. Leishmaniasis. *Lancet* (2018) 392:951–70. doi: 10.1016/S0140-6736(18)31204-2
18. Olekhnovitch R, Bousso P. Induction, Propagation, and Activity of Host Nitric Oxide: Lessons From Leishmania Infection. *Trends Parasitol* (2015) 31:653–64. doi: 10.1016/j.pt.2015.08.001
19. Bogdan C. Nitric Oxide Synthase in Innate and Adaptive Immunity: An Update. *Trends Immunol* (2015) 36:161–78. doi: 10.1016/j.it.2015.01.003
20. Bogdan C. Macrophages as Host, Effector and Immunoregulatory Cells in Leishmaniasis: Impact of Tissue Micro-Environment and Metabolism. *Cytokine X* (2020) 2:100041. doi: 10.1016/j.cytox.2020.100041
21. Liew FY, Millott S, Parkinson C, Palmer RM, Moncada S. Macrophage Killing of Leishmania Parasite *In Vivo* Is Mediated by Nitric Oxide From L-Arginine. *J Immunol* (1990) 144:4794–7.
22. Olekhnovitch R, Ryffel B, Muller AJ, Bousso P. Collective Nitric Oxide Production Provides Tissue-Wide Immunity During Leishmania Infection. *J Clin Invest* (2014) 124:1711–22. doi: 10.1172/JCI72058
23. Diefenbach A, Schindler H, Donhauser N, Lorenz E, Laskay T, MacMicking J, et al. Type 1 Interferon (IFNalpha/beta) and Type 2 Nitric Oxide Synthase Regulate the Innate Immune Response to a Protozoan Parasite. *Immunity* (1998) 8:77–87. doi: 10.1016/S1074-7613(00)80460-4
24. Muller AJ, Aeschlimann S, Olekhnovitch R, Dacher M, Spath GF, Bousso P. Photoconvertible Pathogen Labeling Reveals Nitric Oxide Control of Leishmania Major Infection *In Vivo via* Dampening of Parasite Metabolism. *Cell Host Microbe* (2013) 14:460–7. doi: 10.1016/j.chom.2013.09.008
25. Formaglio P, Alabdullah M, Siokis A, Handschuh J, Sauerland I, Fu Y, et al. Nitric Oxide Controls Proliferation of Leishmania Major by Inhibiting the Recruitment of Permissive Host Cells. *Immunity* (2021) 54:2724–39.e10. doi: 10.1016/j.immuni.2021.09.021
26. Romano A, Carneiro MBH, Doria NA, Roma EH, Ribeiro-Gomes FL, Inbar E, et al. Divergent Roles for Ly6C+CCR2+CX3CR1+ Inflammatory Monocytes During Primary or Secondary Infection of the Skin With the Intra-Phagosomal Pathogen Leishmania Major. *PloS Pathog* (2017) 13:e1006479. doi: 10.1371/journal.ppat.1006479
27. Heyde S, Philipsen L, Formaglio P, Fu Y, Baars I, Hobbel G, et al. CD11c-Expressing Ly6C+CCR2+ Monocytes Constitute a Reservoir for Efficient Leishmania Proliferation and Cell-to-Cell Transmission. *PloS Pathog* (2018) 14:e1007374. doi: 10.1371/journal.ppat.1007374
28. Huang C-J, Slovin PN, Skimming JW. Effects of pH on Inducible Nitric Oxide Synthase Expression in Cultured Murine Machrophages. *Crit Care Med* (1999) 27:A96. doi: 10.1097/00003246-199912001-00252
29. Prabhakar SS. Inhibition of Mesangial iNOS by Reduced Extracellular pH Is Associated With Uncoupling of NADPH Oxidation. *Kidney Int* (2002) 61:2015–24. doi: 10.1046/j.1523-1755.2002.00368.x
30. Kellum JA, Song M, Li J. Lactic and Hydrochloric Acids Induce Different Patterns of Inflammatory Response in LPS-Stimulated RAW 264.7 Cells. *Am J Physiol Regul Integr Comp Physiol* (2004) 286:R686–92. doi: 10.1152/ajpregu.00564.2003
31. Bogdan C, Debus A, Sebald H, Rai B, Schafer J, Obermeyer S, et al. Experimental Cutaneous Leishmaniasis: Mouse Models for Resolution of Inflammation Versus Chronicity of Disease. *Methods Mol Biol* (2019) 1971:315–49. doi: 10.1007/978-1-4939-9210-2_18
32. Schatz V, Strussmann Y, Mahnke A, Schley G, Waldner M, Ritter U, et al. Myeloid Cell-Derived HIF-1alpha Promotes Control of Leishmania Major. *J Immunol* (2016) 197:4034–41. doi: 10.4049/jimmunol.1601080
33. Schleicher U, Bogdan C. Generation, Culture and Flow-Cytometric Characterization of Primary Mouse Macrophages. *Methods Mol Biol* (2009) 531:203–24. doi: 10.1007/978-1-59745-396-7_14
34. Siegert I, Schodel J, Nairz M, Schatz V, Dettmer K, Dick C, et al. Ferritin-Mediated Iron Sequestration Stabilizes Hypoxia-Inducible Factor-1alpha Upon LPS Activation in the Presence of Ample Oxygen. *Cell Rep* (2015) 13:2048–55. doi: 10.1016/j.celrep.2015.11.005
35. Feist M, Schwarzfischer P, Heinrich P, Sun X, Kemper J, von Bonin F, et al. Cooperative STAT/NF-kappaB Signaling Regulates Lymphoma Metabolic Reprogramming and Aberrant GOT2 Expression. *Nat Commun* (2018) 9:1514. doi: 10.1038/s41467-018-03803-x
36. van der Goot AT, Zhu W, Vazquez-Manrique RP, Seinstra RI, Dettmer K, Michels H, et al. Delaying Aging and the Aging-Associated Decline in Protein Homeostasis by Inhibition of Tryptophan Degradation. *Proc Natl Acad Sci USA* (2012) 109:14912–7. doi: 10.1073/pnas.1203083109.
37. Berger RS, Wachsmuth CJ, Waldhier MC, Renner-Sattler K, Thomas S, Chaturvedi A, et al. Lactonization of the Oncometabolite D-2-Hydroxyglutarate Produces a Novel Endogenous Metabolite. *Cancers (Basel)* (2021) 13(8):1756. doi: 10.3390/cancers13081756
38. Renner K, Bruss C, Schnell A, Koehl G, Becker HM, Fante M, et al. Restricting Glycolysis Preserves T Cell Effector Functions and Augments Checkpoint Therapy. *Cell Rep* (2019) 29:135–50.e9. doi: 10.1016/j.celrep.2019.08.068
39. Brand A, Singer K, Koehl GE, Kolitzus M, Schoenhammer G, Thiel A, et al. LDHA-Associated Lactic Acid Production Blunts Tumor Immunosurveillance by T and NK Cells. *Cell Metab* (2016) 24:657–71. doi: 10.1016/j.cmet.2016.08.011
40. Mahnke A, Meier RJ, Schatz V, Hofmann J, Castiglione K, Schleicher U, et al. Hypoxia in Leishmania Major Skin Lesions Impairs the NO-Dependent Leishmanicidal Activity of Macrophages. *J Invest Dermatol* (2014) 134:2339–46. doi: 10.1038/jid.2014.121
41. Tomiotto-Pellissier F, Bortoleti B, Assolini JP, Goncalves MD, Carloto ACM, Miranda-Sapla MM, et al. Macrophage Polarization in Leishmaniasis: Broadening Horizons. *Front Immunol* (2018) 9:2529. doi: 10.3389/fimmu.2018.02529

42. Andrew PJ, Mayer B. Enzymatic Function of Nitric Oxide Synthases. *Cardiovasc Res* (1999) 43:521–31. doi: 10.1016/S0008-6363(99)00115-7
43. Colegio OR, Chu NQ, Szabo AL, Chu T, Rhebergen AM, Jairam V, et al. Functional Polarization of Tumour-Associated Macrophages by Tumour-Derived Lactic Acid. *Nature* (2014) 513:559–63. doi: 10.1038/nature13490
44. Vitecek J, Lojek A, Valacchi G, Kubala L. Arginine-Based Inhibitors of Nitric Oxide Synthase: Therapeutic Potential and Challenges. *Mediators Inflamm* (2012) 2012:318087. doi: 10.1155/2012/318087
45. Coss RA, Storck CW, Wachsberger PR, Reilly J, Leeper DB, Berd D, et al. Acute Extracellular Acidification Reduces Intracellular Ph, 42 Degrees C-Induction of Heat Shock Proteins and Clonal Survival of Human Melanoma Cells Grown at pH 6.7. *Int J Hyperthermia* (2004) 20:93–106. doi: 10.1080/02656730310001605519
46. Buckler KJ, Vaughan-Jones RD. Application of a New pH-Sensitive Fluoroprobe (Carboxy-SNARF-1) for Intracellular pH Measurement in Small, Isolated Cells. *Pflugers Arch* (1990) 417:234–9. doi: 10.1007/BF00370705
47. Rotte A, Pasham V, Eichenmuller M, Mahmud H, Xuan NT, Shumilina E, et al. Effect of Bacterial Lipopolysaccharide on Na(+)/H(+) Exchanger Activity in Dendritic Cells. *Cell Physiol Biochem* (2010) 26:553–62. doi: 10.1159/000322323
48. Talley K, Alexov E. On the pH-Optimum of Activity and Stability of Proteins. *Proteins* (2010) 78:2699–706. doi: 10.1002/prot.22786
49. Rothe KF, Fluchter SH, Schorer R. Studies on Therapy of Metabolic Alkalosis During Experimental Uremia. Influences of Arginine-Hydrochloride on the Intra- and Extracellular Acid-Base Status of the Rat. *Urol Int* (1986) 41:161–6. doi: 10.1159/000281189
50. Erra Diaz F, Dantas E, Geffner J. Unravelling the Interplay Between Extracellular Acidosis and Immune Cells. *Mediators Inflamm* (2018) 2018:1218297. doi: 10.1155/2018/1218297
51. Siska PJ, Singer K, Evert K, Renner K, Kreutz M. The Immunological Warburg Effect: Can a Metabolic-Tumor-Stroma Score (MeTS) Guide Cancer Immunotherapy? *Immunol Rev* (2020) 295:187–202. doi: 10.1111/imr.12846
52. Vermeulen ME, Gamberale R, Trevani AS, Martinez D, Ceballos A, Sabatte J, et al. The Impact of Extracellular Acidosis on Dendritic Cell Function. *Crit Rev Immunol* (2004) 24:363–84. doi: 10.1615/CritRevImmunol.v24.i5.40
53. Pasparakis M, Vandenabeele P. Necroptosis and its Role in Inflammation. *Nature* (2015) 517:311–20. doi: 10.1038/nature14191
54. Lardner A. The Effects of Extracellular pH on Immune Function. *J Leukoc Biol* (2001) 69:522–30.
55. Kellum JA, Song M, Li J. Science Review: Extracellular Acidosis and the Immune Response: Clinical and Physiologic Implications. *Crit Care* (2004) 8:331–6. doi: 10.1186/cc2900
56. Vermeulen M, Giordano M, Trevani AS, Sedlik C, Gamberale R, Fernandez-Calotti P, et al. Acidosis Improves Uptake of Antigens and MHC Class I-Restricted Presentation by Dendritic Cells. *J Immunol* (2004) 172:3196–204. doi: 10.4049/jimmunol.172.5.3196
57. Pliyev BK, Sumarokov AB, Buriachkovskaia LI, Menshikov M. Extracellular Acidosis Promotes Neutrophil Transdifferentiation to MHC Class II-Expressing Cells. *Cell Immunol* (2011) 271:214–8. doi: 10.1016/j.cellimm.2011.08.020
58. Rajamaki K, Nordstrom T, Nurmi K, Akerman KE, Kovanen PT, Oorni K, et al. Extracellular Acidosis Is a Novel Danger Signal Alerting Innate Immunity *via* the NLRP3 Inflammasome. *J Biol Chem* (2013) 288:13410–9. doi: 10.1074/jbc.M112.426254
59. Torres IM, Patankar YR, Shabaneh TB, Dolben E, Hogan DA, Leib DA, et al. Acidosis Potentiates the Host Proinflammatory Interleukin-1beta Response to Pseudomonas Aeruginosa Infection. *Infect Immun* (2014) 82:4689–97. doi: 10.1128/IAI.02024-14
60. Bohn T, Rapp S, Luther N, Klein M, Bruehl TJ, Kojima N, et al. Tumor Immunoevasion *via* Acidosis-Dependent Induction of Regulatory Tumor-Associated Macrophages. *Nat Immunol* (2018) 19:1319–29. doi: 10.1038/s41590-018-0226-8
61. Malik E, Dennison SR, Harris F, Phoenix DA. pH Dependent Antimicrobial Peptides and Proteins, Their Mechanisms of Action and Potential as Therapeutic Agents. *Pharmaceut (Basel)* (2016) 9(4):67. doi: 10.3390/ph9040067
62. Varese A, Dantas E, Paletta A, Fitzgerald W, Di Diego Garcia F, Cabrerizo G, et al. Extracellular Acidosis Enhances Zika Virus Infection Both in Human Cells and *Ex-Vivo* Tissue Cultures From Female Reproductive Tract. *Emerg Microbes Infect* (2021) 10:1169–79. doi: 10.1080/22221751.2021.1932606
63. Pezzulo AA, Tang XX, Hoegger MJ, Abou Alaiwa MH, Ramachandran S, Moninger TO, et al. Reduced Airway Surface pH Impairs Bacterial Killing in the Porcine Cystic Fibrosis Lung. *Nature* (2012) 487:109–13. doi: 10.1038/nature11130
64. Kim D, Liao J, Scales NB, Martini C, Luan X, Abu-Arish A, et al. Large pH Oscillations Promote Host Defense Against Human Airways Infection. *J Exp Med* (2021) 218(4):e20201831. doi: 10.1084/jem.20201831
65. Bellocq A, Suberville S, Philippe C, Bertrand F, Perez J, Fouqueray B, et al. Low Environmental pH Is Responsible for the Induction of Nitric-Oxide Synthase in Macrophages. Evidence for Involvement of Nuclear factor-kappaB Activation. *J Biol Chem* (1998) 273:5086–92. doi: 10.1074/jbc.273.9.5086
66. Riemann A, Reime S, Giesselmann M, Thews O. Extracellular Acidosis Regulates the Expression of Inflammatory Mediators in Rat Epithelial Cells. *Adv Exp Med Biol* (2020) 1232:277–82. doi: 10.1007/978-3-030-34461-0_35
67. Rotstein OD, Nasmith PE, Grinstein S. The Bacteroides by-Product Succinic Acid Inhibits Neutrophil Respiratory Burst by Reducing Intracellular Ph. *Infect Immun* (1987) 55:864–70. doi: 10.1128/iai.55.4.864-870.1987
68. Potzl J, Roser D, Bankel L, Homberg N, Geishauser A, Brenner CD, et al. Reversal of Tumor Acidosis by Systemic Buffering Reactivates NK Cells to Express IFN-Gamma and Induces NK Cell-Dependent Lymphoma Control Without Other Immunotherapies. *Int J Cancer* (2017) 140:2125–33. doi: 10.1002/ijc.30646
69. Robey IF, Baggett BK, Kirkpatrick ND, Roe DJ, Dosescu J, Sloane BF, et al. Bicarbonate Increases Tumor pH and Inhibits Spontaneous Metastases. *Cancer Res* (2009) 69:2260–8. doi: 10.1158/0008-5472.CAN-07-5575
70. Hellwig N, Plant TD, Janson W, Schafer M, Schultz G, Schaefer M. TRPV1 Acts as Proton Channel to Induce Acidification in Nociceptive Neurons. *J Biol Chem* (2004) 279:34553–61. doi: 10.1074/jbc.M402966200
71. Sanjai Kumar P, Nayak TK, Mahish C, Sahoo SS, Radhakrishnan A, De S, et al. Inhibition of Transient Receptor Potential Vanilloid 1 (TRPV1) Channel Regulates Chikungunya Virus Infection in Macrophages. *Arch Virol* (2021) 166:139–55. doi: 10.1007/s00705-020-04852-8
72. Hahn EL, Halestrap AP, Gamelli RL. Expression of the Lactate Transporter MCT1 in Macrophages. *Shock* (2000) 13:253–60. doi: 10.1097/00024382-200004000-00001
73. Rich IN, Worthington-White D, Garden OA, Musk P. Apoptosis of Leukemic Cells Accompanies Reduction in Intracellular pH After Targeted Inhibition of the Na(+)/H(+) Exchanger. *Blood* (2000) 95:1427–34. doi: 10.1182/blood.V95.4.1427.004k48_1427_1434
74. Yang W, Bhandaru M, Pasham V, Bobbala D, Zelenak C, Jilani K, et al. Effect of Thymoquinone on Cytosolic pH and Na+/H+ Exchanger Activity in Mouse Dendritic Cells. *Cell Physiol Biochem* (2012) 29:21–30. doi: 10.1159/000337583
75. Tan Z, Xie N, Banerjee S, Cui H, Fu M, Thannickal VJ, et al. The Monocarboxylate Transporter 4 Is Required for Glycolytic Reprogramming and Inflammatory Response in Macrophages. *J Biol Chem* (2015) 290:46–55. doi: 10.1074/jbc.M114.603589

Conflict of Interest: The authors declare that the research was conducted in the absence of any commercial or financial relationships that could be construed as a potential conflict of interest.

Publisher's Note: All claims expressed in this article are solely those of the authors and do not necessarily represent those of their affiliated organizations, or those of the publisher, the editors and the reviewers. Any product that may be evaluated in this article, or claim that may be made by its manufacturer, is not guaranteed or endorsed by the publisher.

Copyright © 2022 Frick, Hinterland, Renner, Vogl, Babl, Heckscher, Weigert, Weiß, Gläsner, Berger, Oefner, Dettmer, Kreutz, Schatz and Jantsch. This is an open-access article distributed under the terms of the Creative Commons Attribution License (CC BY). The use, distribution or reproduction in other forums is permitted, provided the original author(s) and the copyright owner(s) are credited and that the original publication in this journal is cited, in accordance with accepted academic practice. No use, distribution or reproduction is permitted which does not comply with these terms.

Advantages of publishing in Frontiers

OPEN ACCESS
Articles are free to read for greatest visibility and readership

FAST PUBLICATION
Around 90 days from submission to decision

HIGH QUALITY PEER-REVIEW
Rigorous, collaborative, and constructive peer-review

TRANSPARENT PEER-REVIEW
Editors and reviewers acknowledged by name on published articles

Frontiers
Avenue du Tribunal-Fédéral 34
1005 Lausanne | Switzerland

Visit us: www.frontiersin.org
Contact us: frontiersin.org/about/contact

REPRODUCIBILITY OF RESEARCH
Support open data and methods to enhance research reproducibility

DIGITAL PUBLISHING
Articles designed for optimal readership across devices

FOLLOW US
@frontiersin

IMPACT METRICS
Advanced article metrics track visibility across digital media

EXTENSIVE PROMOTION
Marketing and promotion of impactful research

LOOP RESEARCH NETWORK
Our network increases your article's readership